

## University of Wollongong - Research Online

### Thesis Collection

Title: Organic petrology and geochemistry of the tertiary formations at Meulaboh area, west Aceh Basin, Sumatra, Indonesia

Author: Hadiyanto

Year: 1992

Repository DOI:

#### Copyright Warning

You may print or download ONE copy of this document for the purpose of your own research or study. The University does not authorise you to copy, communicate or otherwise make available electronically to any other person any copyright material contained on this site.

You are reminded of the following: This work is copyright. Apart from any use permitted under the Copyright Act 1968, no part of this work may be reproduced by any process, nor may any other exclusive right be exercised, without the permission of the author. Copyright owners are entitled to take legal action against persons who infringe their copyright. A reproduction of material that is protected by copyright may be a copyright infringement. A court may impose penalties and award damages in relation to offences and infringements relating to copyright material.

Higher penalties may apply, and higher damages may be awarded, for offences and infringements involving the conversion of material into digital or electronic form.

**Unless otherwise indicated, the views expressed in this thesis are those of the author and do not necessarily represent the views of the University of Wollongong.**

Research Online is the open access repository for the University of Wollongong. For further information contact the UOW Library: [research-pubs@uow.edu.au](mailto:research-pubs@uow.edu.au)

*University of Wollongong Thesis Collections*

*University of Wollongong Thesis Collection*

---

*University of Wollongong*

*Year 1992*

---

Organic petrology and geochemistry of  
the tertiary formations at Meulaboh area,  
west Aceh Basin, Sumatra, Indonesia

Hadiyanto  
University of Wollongong

Hadiyanto, Organic petrology and geochemistry of the tertiary formations at Meulaboh area, west Aceh Basin, Sumatra, Indonesia, Doctor of Philosophy thesis, Department of Geology, University of Wollongong, 1992. <http://ro.uow.edu.au/theses/1397>

This paper is posted at Research Online.

## **NOTE**

This online version of the thesis may have different page formatting and pagination from the paper copy held in the University of Wollongong Library.

## **UNIVERSITY OF WOLLONGONG**

### **COPYRIGHT WARNING**

You may print or download ONE copy of this document for the purpose of your own research or study. The University does not authorise you to copy, communicate or otherwise make available electronically to any other person any copyright material contained on this site. You are reminded of the following:

Copyright owners are entitled to take legal action against persons who infringe their copyright. A reproduction of material that is protected by copyright may be a copyright infringement. A court may impose penalties and award damages in relation to offences and infringements relating to copyright material. Higher penalties may apply, and higher damages may be awarded, for offences and infringements involving the conversion of material into digital or electronic form.

**ORGANIC PETROLOGY AND GEOCHEMISTRY OF THE TERTIARY  
FORMATIONS AT MEULABOH AREA, WEST ACEH BASIN,  
SUMATRA, INDONESIA**

A thesis submitted in (partial) fulfillment of the requirements for the award of  
the degree of

**DOCTOR OF PHILOSOPHY**

from



**THE UNIVERSITY OF WOLLONGONG**

by

**HADIYANTO**

B.Sc. , Akademi Geologi dan Pertambangan-Bandung,  
Ir., Universitas Pembangunan Nasional "Veteran"- Yogyakarta  
M.Sc., The University of Wollongong- Australia

Department of Geology  
1992

Except where otherwise acknowledged in the text, the contents of this thesis are the result of original research by the author. The work has not been previously submitted for a degree to any other university or similar institution.

## ABSTRACT

The West Aceh Basin is one of several Indonesian Tertiary forearc basins which contain a thick sedimentary succession of coal-bearing rocks that were deposited during the Oligocene to Pliocene. The continued subduction of the Indo-Australian Plate under continental Sundaland was responsible for the development of this asymmetrical, tectonically-active forearc basin which is located along the west coast of the Aceh region of northwestern Sumatra. Significant petroleum discoveries have not been found in any Indonesian forearc basin and this study was initiated to assess the hydrocarbon generation potential of the West Aceh Basin and to formulate a model to aid future exploration in this and other forearc basins.

The type, abundance and maturity of organic matter in the Tertiary sequence was determined using optical microscopy and geochemical techniques. The organic matter in both coals and clastic rocks is derived from land plants with a minor algal component in some of the claystones and shales. The coals, ranging in age from Oligocene to Pliocene, are dominated by vitrinite with lesser liptinite and only very minor inertinite. A distinctive feature of the coals is the abundance of exsudatinite, resinite, suberinite and cutinite. Using optical properties and textural features, exsudatinite can be divided into two groups and much of this secondary maceral is derived from resinite and suberinite. The significance of exsudatinite as an indicator of petroleum generation is discussed.

Dispersed organic matter (DOM) in the clastic rocks comprises mostly liptinite with lesser vitrinite and only minor inertinite. The rocks contain small but significant quantities of bitumen which indicate migration of hydrocarbons through the rocks or *in situ* generation of hydrocarbons.

The coal and clastic rocks are potential source rocks but most are immature and have not produced significant liquid hydrocarbons. Use of a modified petrographic scoring system shows that of the clastic rocks, the Tangla Formation shales and to a lesser extent, the Kueh Formation, are the best source rocks. The Oligocene coal, and possibly the Miocene coal, have very good hydrocarbon generation potential. The onshore vitrinite

reflectance gradients are greater than those offshore and thus the oil window is predicted to be shallower in the onshore areas.

Geochemical data confirms the source rock potential of the rocks although the organic matter is mostly Type III or transitional Type II/III using the 1984 classification of Tissot and Welte. The shale contain 1 to 5% Total Organic Carbon (TOC) and Rock Eval data show that the organic matter in the shale and coal is oil to gas prone with Hydrogen Indices (HI) of less than 200 to 465. S<sub>2</sub> values are highest in the Tangla Formation but lowest in the Tutut Formation. Samples from the Tangla Formation contain the highest extractable hydrocarbons (mgHC/gTOC) although petrographic data suggest that this is due to bitumen impregnation. Pyrolysis-GC traces of these Oligocene and Miocene coals are characterised by a high abundance of normal alkane hydrocarbons. In many respects, the pyrograms are similar to those of the Talang Akar coal which are known source rocks.

Future exploration should be directed towards the onshore areas or those offshore areas where the sequence is thick and the potential for intersecting the oil window is greater. Areas of greatest interest would those which contain coal and carbonaceous shale as these lithologies have the greatest source rock potential.

## ACKNOWLEDGMENTS

The work reported in this thesis was supported by many people and institutions through a grant from the Australian International Development Assistance Bureau under a bilateral relationship program with the Indonesian Government.

Special thanks go to my supervisors, Dr A C Hutton and Associate Professor B G Jones, for their guidance and assistance during my study. I am also grateful to my earlier supervisor, Dr A C Cook, for his suggestion regarding the earlier work of this thesis. Dr C J Boreham of Bureau Mineral Resources (BMR) provided invaluable assistance with organic geochemistry and give constructive criticisms on the text. I thank Mrs J Hope and Mr P Fletcher of BMR for their kindness in teaching me how to process and analyse the samples for Rock-Eval, Gas Chromatography and Pyrolysis-GC. Thanks are also due to Dr J S Esterle of CSIRO Geomechanics Division for her criticism of this work and for permission to use some of her polished peat samples from Indonesian and Malaysia. Mr M M Faiz and Mr A Mazaheri give me insight on heat transfer and mechanisms in coal and sedimentary rocks.

I appreciate the help of all other academic staff and technical officers of the Department of Geology, University of Wollongong, for their assistance during my study especially Mr D Martin who prepared several figures. My thanks also go to my colleagues Hery Heryanto, Hakim Sutarwan and Augustinus Probo Driyakara for their help using Macintosh computers.

Samples for this study were given by the Directorate of Mineral Resources (DMR) of



Indonesia and Pertamina (Indonesia). I wish to thank the former Director of DMR, Mr Salman Padmanagara, former Chief of the Coal and Peat Division of DMR, Mr Hardjono and former Chief of the Exploration Division of Pertamina, Dr Pulunggono, for their permission to use the samples. Mr Kingking Alkantri, Director of DMR and Mr Ii Syarifuddin, Chief of the Coal and Peat Division, DMR, gave valuable suggestions during my study.

Finally, I gratefully acknowledge the spiritual encouragement and advice given to me by my wife, Evina Widyantini and my parents Mr and Mrs Sapardi and parents-in-law Mr and Mrs Eddy Soehardjo. I also thank my sons, Prasojo Widiyanto and Prakoso Adinugroho, for their patience and support during my study.

# TABLE OF CONTENTS

	Page
CHAPTER 1 INTRODUCTION	1
1.1 Geographic Location	2
1.2 Background and Objectives of the Research	2
1.3 Previous Work and Exploration History	5
CHAPTER 2 GEOLOGY OF WEST ACEH BASIN	8
2.1 INTRODUCTION	8
2.2 REGIONAL GEOLOGICAL SETTING	8
2.3 GENERAL STRATIGRAPHIC FRAMEWORK	10
2.3.1 Pre-Tertiary	11
2.3.2 Tertiary Succession	13
2.3.2.1 Brueh Formation	14
2.3.2.2 Tangla Formation	14
2.3.2.3 Kueh Formation	15
2.3.2.4 Calang Volcanic Formation	16
2.3.2.5 Tutut Formation	18
2.3.2.6 Meulaboh Formation	19
2.4 IGNEOUS ROCKS	19
2.4.1 Intrusive Rocks	20
2.4.2 Volcanic Rocks	20
2.5 GEOLOGICAL STRUCTURE	21
2.6 GEOLOGICAL HISTORY OF THE WEST ACEH BASIN DURING THE TERTIARY PERIOD	24
CHAPTER 3 ANALYTICAL METHODS	28
3.1 ORGANIC PETROLOGICAL ANALYSIS	28
3.1.1 Sampling	29
3.1.2 Sample Preparation	30
3.1.2.1 Polished Block	31
3.1.2.2 Polished Grain Mounts	31
3.1.3 Microscopic Examination	32
3.1.3.1 Reflectance Measurements	32
3.1.3.2 Maceral Analyses	34
3.1.3.3. Fluorescence Observation	35
3.1.3.4. Maceral Analysis Results	35
3.2 ORGANIC GEOCHEMISTRY ANALYSES	36
3.2.1 Rock-Eval and T.O.C Analyses	37
3.2.2 Column Gas-Chromatography	38
3.2.3 Pyrolysis-Gas Chromatography	39
CHAPTER 4 ORGANIC PETROLOGY	40
4.1 NOMENCLATURE	40
4.2 MACERAL COMPOSITION AND ABUNDANCE	
4.2.1 Maceral Composition of Tertiary Coals	44

4.2.1.1	Oligocene Coal	45
4.2.1.2	Miocene Coal	49
4.2.1.3	Pliocene Coal	52
4.3	MINERAL MATTER OF THE TERTIARY COALS	
4.3.1	Mineral Matter in Oligocene Coal	57
4.3.2	Mineral Matter in Miocene Coal	58
4.3.3	Mineral Matter in Pliocene Coal	58
4.4	ORGANIC MATTER ABUNDANCE IN OFFSHORE SAMPLES	59
4.4.1	Tangla Formation	60
4.4.2	Kueh Formation	62
4.4.3	Tutut Formation	65
4.4	VITRINITE REFLECTANCE AND COAL RANK	68
4.4.1	Oligocene Coal	68
4.4.2	Miocene Coal	69
4.4.3	Pliocene Coal	69
4.6	DISCUSSION	70
4.6.1	The Origin and Occurrence of Exsudatinite and Bitumen	70
4.6.1.1	Exsudatinite	70
4.6.1.2	Bitumen	76
4.6.2	Maceral Distribution and Coalification	80
CHAPTER 5	MATURITY OF THE WEST ACEH BASIN SEQUENCE	92
5.1	INTRODUCTION	92
5.2	RANK-DEPTH RELATIONS	93
5.3	MATURATION LEVEL	97
5.4	VITRINITE REFLECTANCE GRADIENT	99
5.5	VERTICAL AND LATERAL RANK VARIATIONS	102
5.5.1	Onshore Rank Variations	103
5.5.2	Offshore Rank Variations	105
5.6	DISCUSSION	106
CHAPTER 6	THERMAL HISTORY	114
6.1	INTRODUCTION	114
6.2	GEO THERMAL GRADIENTS	115
6.3	PALAEOTEMPERATURES	118
6.4	BURIAL HISTORY AND THE TIMING OF HYDROCARBON GENERATION	123
6.4.1	Burial History	124
6.4.2	Timing of Hydrocarbon Generation	126
6.5	DISCUSSION	127

CHAPTER 7	SOURCE ROCK AND PETROLEUM	
	GENERATION	133
7.1	INTRODUCTION	133
7.2	SCORING SYSTEMS AND SOURCE ROCK	
	POTENTIAL	133
7.3	SOURCE ROCK EVALUATION	136
7.3.1	Tutut Formation	137
7.3.2	Kueh Formation	137
7.3.3	Tangla Formation	137
7.3.4	Summary	138
7.4	SOURCE ROCK GEOCHEMISTRY	139
7.4.1	Rock-Eval/TOC	139
7.4.1.1	Clastic Sediment Samples	142
7.4.1.2	Coal Samples	146
7.4.2	Gas Chromatography and Source Rock	
	Characteristics	149
7.4.2.1	Extractable Organic Matter	149
7.4.2.2	N-Alkane Distribution	151
7.4.2.3	Isoprenoid Hydrocarbons	156
7.4.3	Pyrolysis Gas Chromatography	159
7.5	RELATIONSHIP BETWEEN MACERALS AND	
	PYROLYSIS HYDROCARBONS	164
7.6	MIGRATED HYDROCARBONS	167
7.7	SUMMARY	168
CHAPTER 8	GENERAL DISCUSSION	170
8.1	INTRODUCTION	170
8.2	MATURITY CONSIDERATIONS	172
8.3	SOURCE ROCK RICHNESS	178
8.4	EXSUDATINITE AND BITUMEN IN PETROLEUM	
	GENERATION IN THE WEST ACEH BASIN	183
8.5	CONCEPTUAL MODEL FOR HYDROCARBON	
	GENERATION AND ACCUMULATION IN THE	
	WEST ACEH BASIN	190
CHAPTER 9	CONCLUSIONS	195
9.1	CONCLUSIONS	196
9.2	FUTURE WORK AND EXPLORATION	
	STRATEGIES	201
REFERENCES		203

LIST OF FIGURES	
LIST OF TABLES	
LIST OF PLATES	
LIST OF APPENDICES	

VOLUME II
VOLUME II
VOLUME II
VOLUME II

## CHAPTER 1

### INTRODUCTION

The West Aceh Basin is one of the Indonesian Tertiary basins containing a thick sedimentary succession in which coal-bearing sequences were deposited during the Oligocene to Pliocene. The continued subduction of the Indo-Australian Plate under continental Sundaland was responsible for the development of this an asymmetrical tectonically-active forearc basin along the west coast of the Aceh region in northwestern Sumatra.

Although various attempts have been made to evaluate this basin for petroleum potential, exploration to date has proven unsuccessful in locating economically viable liquid hydrocarbons. However, studies in organic petrology and geochemistry offer an opportunity to understand and establish the origin, distribution and character of hydrocarbon source rocks in the basin. Such data would be useful in interpreting the thermal history and timing of the generation of any hydrocarbons within this basin; this has not been determined previously. The integration and evaluation of such interpretations are needed for improving the petroleum exploration potential and success ratio in this area of Indonesia and it is for this reason that the present study was undertaken.

### 1.1. Geographic Location

The research area for this study is situated in the northern part of Sumatra on the west coast of the Special Province of Aceh, Indonesia (Figure 1.1). It includes onshore areas and a small portion of the offshore area bounded to the north and south by latitudes  $4^{\circ} 30'$  and  $5^{\circ}$  N and bounded to the west and east by longitudes  $95^{\circ} 30'E$  and  $97^{\circ}$  E respectively. It covers parts of the three geological maps of the Calang, Meulaboh and Takengon Quadrangles (Bennet *et al.*, 1981; Cameron *et al.*, 1982; Cameron *et al.*, 1983) and covers an area of approximately 8,000 km<sup>2</sup>. The main drainage pattern flows southwestward from the Barisan Mountains into the Indian Ocean and is mostly dendritic with some minor structural control. The main rivers in this area are Kr. Teunom, Kr. Woyla, Kr. Merbau, Kr. Seunagan and Kr. Tripa. These rivers have meandering patterns on the coastal plain. (Note: "Kr" the abbreviation for Krueng, the local Indonesian word for River)

Meulaboh, the capital city of the West Aceh district, is the main centre for economic activities of this area.

### 1.2. Background and Objectives of the Research

Ideally, coal develops in a basin where the rate of subsidence is neither very fast nor very slow. Subsidence should be matched by the rate of accumulation of plant debris in the basin and, hence, many major coal-bearing basins are on craton margins in retroarc

(backarc) basins (Koesoemadinata and Hardjono, 1976). In more tectonically active areas differential subsidence, caused by plate collision during and after deposition, has a significant influence in terms of the geometry of coal seams and the type and rank of the coal.

Coal in western Indonesia was deposited not only in relatively stable retroarc basins in the intracratonic depressions and areas such as the Sunda Platform, but was also deposited in narrow tectonically active forearc basins such as the West Aceh, West Sumatra and Bengkulu Basins. However, the West Aceh Basin has a more widespread distribution of Tertiary coal-bearing sequences than the West Sumatra and Bengkulu Basins (Hadiyanto and Faiz, 1990). Thus the West Aceh Basin is more prospective both for a commercial coal industry and for petroleum accumulations derived from terrestrial organic matter.

Studies regarding the hydrocarbon generation potential of coal and dispersed organic matter have been conducted in various parts of several Tertiary backarc basins in Indonesia (e.g. Roe and Polite, 1977; Sutton, 1977; Gordon, 1985; Kelly *et al.*, 1985) but not in forearc basins such as the West Aceh Basin. The coal-bearing sequences in the West Aceh Basin, and other forearc basins, show considerable petroleum source potential, but the discovery of liquid hydrocarbons has proven to be unsuccessful. As a consequence, there has developed a general opinion that forearc basins are not the ideal place for hydrocarbons to be generated because within this type of basins:

- (i) the heat flow is low;
- (ii) the hydrocarbon source rocks are immature;
- (iii) the sequence lacks the coarse, quartz-rich sediment necessary for clastic reservoir

formation;

- (iv) the organic matter is diluted by an abundance of volcanic detritus; and
- (v) there is a reduction in the porosity and permeability of the sediment as a result of decomposition of unstable volcanoclastic components (Katili, 1984; Barber, 1985).

However, such arguments are based on a general point of view without supporting data, such as organic petrology and geochemistry, that may be very useful for assessing why hydrocarbons are not generated within this type of basin.

Hence, the primary objectives of this study were to obtain an understanding of the petroleum generation potential in the West Aceh Basin, with special reference to the organic petrology and geochemistry of coal and dispersed organic matter in the clastic interseam units. The main aspects of coal geology that have been studied from the West Aceh Basin include the following.

1. Determination of regional variation in coal type and rank within the basin in order to assess the origin of the coal and the thermal history of the basin.
2. Comparison and integration of organic petrographic and organic geochemical data to determine the characteristics of the organic matter in coal and clastic interseam sedimentary rocks, as well as to determine the maturation patterns and petroleum source rock potential.
3. Formulation of a model for liquid hydrocarbon generation in the West Aceh Basin that may be applicable to other Indonesian forearc basins.



### 1.3. Previous Work and Exploration History.

Although numerous geological surveys have been conducted over various parts of the Tertiary West Aceh Basin, the organic petrology and geochemistry has not been studied in detail and very few relevant publications are available. Most geological information on the basin is based on pre-World War II Dutch mapping. The regional geology and tectonic development of the Aceh Region was interpreted by Zwierzycki (1922), Oppenoorth and Zwierzycki (1918) and Jansen *et al.* (1922) provided information on the mineral potential especially in the Woyla River area. The regional geological data was compiled much later by van Bemmelen (1970). A joint geological and geochemical research program was undertaken between 1975 and 1979 by the Directorate of Mineral Resources of Indonesia and the Institute of Geological Science of the United Kingdom. This study resulted in the production of a geological map of the northern Sumatra area with special interest on the location of mineralised zones (Bennet *et al.*, 1981). Cameron *et al.* (1980) formulated the geological evolution of northern Sumatra on the basis of data collected from that joint research program. He established the geological nomenclature, the geological history and the basin boundaries in northern Sumatra and noted that the West Aceh Basin lies in a forearc basin setting (Cameron *et al.*, 1980).

Oil exploration in the West Aceh Basin started during the 1960's. Kurash (1967) conducted a general geological investigation on Nias Island as part of the Union Oil Company activities in the area surrounding Meulaboh. Burrough and Power (1968) carried out field surveys for Union Oil Company in the southern part of the northwest Sumatra contract area.

In the years 1968-1969, the Union Oil Company (as a contractor to Pertamina (Indonesian State Oil Company)) undertook geophysical investigations prior to their drilling programs. The main emphasis was on air-gun seismic surveys in offshore areas near Meulaboh where water depths were less than 200 m. Onshore seismic surveys were undertaken only on Nias Island which is located southeast and oceanward of the Meulaboh district (Rose, 1983).

Drilling programs were carried out between 1970 and 1978 in the Meulaboh area and primarily targeted the carbonate build-ups suspected to be reservoir rocks. During this period, Union Oil Company drilled eight exploratory wells of which two penetrated pre-Tertiary rocks and two showed methane gas but were considered uneconomic at that time (Rose, 1983). The Meulaboh and Tuba wells were abandoned in Mesozoic rock at depths of approximately 3000 m. The Meulaboh well also penetrated a significant methane reservoir with excellent flow characteristics over the period of the drill stem test (Anon, 1971). Methane gas was also reported in the upper Miocene reef section in the Keudapasi well but the quality and the quantity were uncertain. The geographic locations of the offshore wells are shown in Figure 1.2.

Coal exploration in the West Aceh Basin commenced in 1984, beginning with a preliminary survey conducted by the Coal and Peat Exploration Division of the Directorate of Mineral Resources of Indonesia. Of special interest in this survey was the delineation and distribution of Pliocene coal seams (Hanif *et al.*, 1984). The results indicated good potential resources, especially in the Kawai block.

In the period 1985-1986, exploratory cored holes were drilled at 24 widespread locations in the Meulaboh district, with total depths of the holes averaging 200 m. This program was part of the activities of a Coal Inventory and Exploration Project by the Directorate of Mineral Resources of Indonesia and it emphasised the evaluation of Pliocene coal resources in the West Aceh Basin. This project resulted in the discovery of more than 500 million tonnes of lignite resources in the Kawai field (Hadiyanto and Amarullah, 1985; Hadiyanto *et al.*, 1986). During exploration, work focused on the measurement of physical and chemical properties of the coal seams which provided information on the depth, thickness and coal to non-coal ratios. Cores of coal seam intervals were analysed for moisture content, calorific value, fixed carbon, volatile matter, ash and sulphur contents. Coal petrology of the Pliocene lignite was also studied in detail, with special regard to the type and rank (Hadiyanto, 1988; Hadiyanto and Cook, 1991; Hadiyanto *et al.*, 1992).

## CHAPTER 2

### GEOLOGY OF WEST ACEH BASIN

#### 2.1. Introduction

The West Aceh Basin is a typical Tertiary tectonically-active, forearc basin resulting from the collision between the Indo-Australian and Asian plates. The basin lies between Sumatra and the adjacent outer arc ridge to the west. It trends northwest-southeast, is 100 km long and is approximately 80 km wide (Figure 2.1). The northern edge is bounded by an extension of the Batee Fault Zone (shown as the Ann Batee Fault Zone on several older publications). The southern margin terminates against the outer arc ridge.

A geological map of the West Aceh Basin (at a scale 1:250,000) has been compiled by Cameron *et al.* (1980) from existing maps of the Directorate of Mineral Resources of Indonesia. The geological features and stratigraphic nomenclature described herein follow the terminology of Cameron *et al.* (1980). A geological map of the West Aceh Basin is given in Figure 2.2.

#### 2.2. Regional Geological Setting

The main morphological features of the Aceh region of the island of Sumatra are the Barisan Mountain Chain with volcanoes in the magmatic belt, some of which erupted as

recently as in the Holocene, and a broad Tertiary and Quaternary sedimentary basin to the southwest of the Barisan Mountains. The Tertiary West Aceh Basin is situated along the western coast of the Aceh area which extends from Teunom in the northwest to the Tapaktuan border in the southeast. This basin is a symmetrical, thickens to the southwest with upwards of 6100 m of Neogene sediment adjacent to the outer-arc ridge (Rose, 1983). Davies (1987) suggested that the basin was once continuous with the North Sumatra Basin but was separated from it by the Barisan geanticline after Plio-Pleistocene uplift.

The present structural features in the West Aceh Basin are dominated in the northeast by the Barisan Mountains which formed Middle Miocene to Recent time (Cameron *et al.*, 1980). The latter consist of uplifted, highly folded Mesozoic and Palaeozoic rock complexes, with remnants of Early Tertiary volcanoes that were covered with a widespread volcanic mantle of andesitic, dacitic and rhyolitic lava, agglomerate and tuff. A major right lateral transcurrent fault runs along the north-northwest trending axis of the mountain range. The Batee Fault Zone is a northwest-trending expression of this fault.

Tectonic events during the Tertiary may represent a continuation of Mesozoic movements, as shown by obvious faults seen on seismic lines and by the juxtaposition of differing tectonic and sedimentary regimes (Rose, 1983).

Various studies in the West Aceh Basin and surrounding regions concluded that large lateral fault movements occurred during the Tertiary (Haile, 1979; Karig *et al.*, 1979, 1980; Page *et al.*, 1979; Cameron *et al.*, 1980; Bennet *et al.*, 1981). Evidence for the

lateral movement is based on the palaeomagnetic dating of diorite intrusions in the Brueh volcanic suite (northwest of Meulaboh) which show that palaeolatitudes were located two degrees north of their present positions. Therefore, the diorite and intruded Brueh volcanic rocks must have moved southeastward along the prominent lateral fault (Haile, 1979; Bennet *et al.*, 1981). Lateral movement was also suggested by Karig *et al.* (1980) on the basis of their interpretation of the abrupt offsets of the palaeoshelf break, especially in the Banyak area. These breaks were considered to represent right-lateral-slip faults which had a lateral displacement of about 100 km (Rose, 1983).

### **2.3. General Stratigraphic Framework**

The development of the Tertiary stratigraphic succession in the West Aceh Basin follows the same general development as in other Tertiary sedimentary basins in western Indonesia.

In general, Tertiary sediments in Indonesia can be categorised into two major depositional periods (Koesoemadinata and Hardjono, 1976). The first was associated with the Paleogene transgression which took place in the Eocene-Oligocene, and the second one with a period of post-Paleogene regression during the Miocene to Pleistocene.

The West Aceh Basin comprises Tertiary sediments unconformably overlying a pre-Tertiary metasedimentary complex. Cameron *et al.* (1980) recognised four major volcano-sedimentary sequences of Paleogene to Late Neogene age in the West Aceh Basin, each of which was separated by an unconformity (Figure 2.3). On the basis of

volcanic activity, he divided the Tertiary sequence in the West Aceh Basin into three periods of sedimentation: Tertiary 1, 2 and 3. Tertiary 2 was subdivided into Tertiary 2a and 2b on the basis of transgressive and regressive sequence boundaries.

Tertiary 1 represents the volcanic sediment deposited in the northwest Banda Aceh (the Brueh volcanic suite) ranging in age from Eocene to Early Oligocene. Tertiary 2a represents deposition of the Late Oligocene to Early Miocene Tangla Formation during a regional marine transgression. Tertiary 2b represents deposition of the Kueh Formation in the Early Miocene to late Middle or Late Miocene. This widespread transgression was at its peak in the Middle Miocene and resulted in marine sedimentation over most of northern Sumatra.

Tertiary 3 represents a period of regression resulting from the late Middle Miocene to Early Pleistocene Barisan uplift. In the backarc region, sedimentation was continuous. However, in the West Aceh forearc region, sedimentation only recommenced at the beginning of the Pliocene when the Tutut Formation was deposited.

### **2.3.1. Pre-Tertiary**

Cameron *et al.* (1983) divided the pre-Tertiary succession in northern Sumatra into three groups. The Late Palaeozoic Tapanuli Group represents the lowest unit and consists of argillite and arenite which have undergone low grade regional and higher grade dynamothermal metamorphism. The second group is the Late Permian-Late Triassic Peusangan Group of interbedded fossiliferous limestone and mafic volcanic rocks which

represent a palaeovolcanic arc-fringing reef environment.

The youngest unit is the Late Jurassic-Early Cretaceous Woyla Group which is composed of low grade metasedimentary and metavolcanic rocks deposited mainly in the West Aceh Basin (Cameron *et al.*, 1982). This group was divided into two facies or successions - one to the northwest and the other to the northeast of the Geumpang Line (Figure 2.2). Low-grade metavolcanic rocks and recrystallised limestone in the western succession were considered to represent a palaeovolcanic arc-fringing reef environment like the older Peusangan Group (Cameron *et al.*, 1980). The eastern succession has undergone more complex tectonism, most of which is associated spatially with serpentinite. Metabasalt, red chert and silicified volcanogenic rocks represent a lower sequence, which was intruded by minor gabbro and overlain by an upper sequence of slate, metavolcanic and volcanogenic metasedimentary rocks. The lower units may have formed during the generation of Cretaceous oceanic crust. They were incorporated, with the overlying sedimentary sequence, as ophiolitic material into the continental margin during a Late Mesozoic deformation episode (Bennet *et al.*, 1981; Cameron *et al.*, 1983). The Woyla Group includes, and is underlain by, portions of a dismembered Late Mesozoic ophiolite in which some of the ophiolitic rocks were remobilised and tectonically emplaced into the Tertiary successions, resulting in the serpentinite association.

Offshore, the complete succession of pre-Tertiary strata is uncertain although both the Meulaboh and Tuba wells penetrated the pre-Tertiary succession at depths below 2957 m in the Meulaboh well and below 2609 m in the Tuba well (Rose, 1983). The appearance of recrystallised belemnites at depth in the above wells suggests rocks of Mesozoic age.



However, the pre-Tertiary succession was recorded in the Lakota well located southeast of the present study near Singkel, which is off the west coast of Sumatra (Karig *et al.*, 1978). This sequence was interpreted as bathyal turbidites and structurally disrupted oceanic crust.

### 2.3.2. Tertiary succession

The Tertiary stratigraphy discussed in this section is restricted to the sedimentary rocks or formations deposited west of the Geumpang Line, which acts as the northeastern boundary of the West Aceh Basin (Cameron *et al.*, 1980, 1982).

As mentioned earlier, the Tertiary succession can be divided into three groups on the basis of three major tectonic events, i.e. Tertiary 1, 2, and 3. Tertiary 2 has been divided into 2a and 2b on the basis of transgressive and regressive sequence boundaries interpreted from seismic profiles (Cameron *et al.*, 1980; Beaudry and Moore, 1985).

In general, the Tertiary West Aceh Basin is filled with Paleogene and Neogene sequences, both of which show angular relationships with the underlying units. The Paleogene rocks consist of strongly folded sedimentary and volcanic sequences and are separated from the Neogene succession by an angular unconformity. In the onshore area, the Hulu Masen Group was deposited between the Eocene-Early Oligocene and Pleistocene and comprises six formations: Brueh Volcanic Formation, Tangla Formation, Kueh Formation, Calang Volcanic Formation, Tutut Formation and Meulaboh Formation (Figure 2.3). The following sections summarise the basic attributes of the Tertiary sequences within the

West Aceh Basin.

#### **2.3.2.1. Brueh Volcanic Formation**

This formation consists of basaltic volcanic rocks deposited in Tertiary 1 (Eocene-Early Oligocene) in the northern part of Banda Aceh. This formation was intruded by diorite at 29 Ma (according to K/Ar dating; Cameron *et al.*, 1980). In the offshore area this formation is correlated with the Late Eocene and Early Oligocene dolomitic limestone and calcareous mudstone penetrated in the Meulaboh and Tuba offshore wells (Beaudry and Moore, 1985).

#### **2.3.2.2. Tangla Formation**

The Tangla Formation is exposed in the northern portion of the study area and consists mainly of mudstone, siltstone, sandstone, basalt breccia-conglomerate, coal and some local andesitic volcanic rocks. It was deposited mainly in paralic to fluviatile environments in the Late Oligocene-Early Miocene (Tertiary 2a). This formation has an average thickness of 1000 m in the onshore area; it grades offshore into turbiditic marine Eocene-Oligocene sediment comprising interbedded siltstone and shale with several thin coal seams. The shale is grey, firm, slightly carbonaceous and calcareous, whereas the siltstone is grey, firm, calcareous and carbonaceous and slightly pyritic (Rose, 1983). This formation was penetrated by the Meulaboh and Tuba offshore drill holes.

Foraminiferal assemblages from the Meulaboh well indicated a Late Eocene age.

However, many of the specimens were poorly preserved and did not permit positive identification (Rose, 1983; Beaudry and Moore, 1985).

#### 2.3.2.3. Kueh Formation

After a period of uplift and erosion, sedimentary rocks belonging to the Tertiary 2b Kueh Formation were deposited disconformably over the Tangla Formation during the Middle Miocene. This unit consists of calcareous clastic sediment, mudstone, sandstone, siltstone and coal, laid down in an open marine to sublittoral environment passing downwards into paralic and fluviatile deposits (Cameron *et al.*, 1980). The formation has an average thickness of 1500 m. Offshore, this sequence has been penetrated in the Meulaboh, Tuba and Seunagan wells where it comprises chiefly nearshore marine and non-marine mudstone, sandstone, siltstone and coal ranging in age from Early to Middle Miocene age (Rose, 1983). Sandstone is a minor component in the Meulaboh and Tuba wells but it was more than 30 m thick in the Meulaboh East well. The sandstone is grey and has a fine to medium grain size. Quartz is dominant with common multi- or varicoloured lithic grains and some calcareous detritus. The mudstone and siltstone are dark in colour, calcareous to non-calcareous, firm and commonly interbedded (Rose, 1983). On the inner shelf, the Meulaboh, Meulaboh East, Tuba, Tripa and Bubon wells penetrated limestone reefs of Middle Miocene age. Rose (1983) suggested that the carbonate unit was deposited during an eastward-moving transgressive sedimentary phase. Middle Miocene carbonate was penetrated in the Meulaboh well and is thought to be an isolated carbonate build-up.

The position of the carbonate sequence suggests that sedimentation began west of the present day shelf-edge. The lower part of the Middle Miocene carbonate unit is characterised by light coloured, recrystallised, chalky to microcrystalline limestone with remnant features of bioclastic sand and intraclasts. The upper portion of this carbonate unit consists of intercalations of micrite and packstone. The packstone has a varying percentage of micrite matrix. Larger detritus in the packstone consists of sand to pebble-sized framework grains of broken coral, algae, foraminifers, brachiopods and bryozoans. Several elongate barrier reefs developed in the Bubon area as the maximum transgression moved eastward. The limestone is characterised by recrystallised micrite and minor packstone at the bottom of the sequence, succeeded by increasing amounts of packstone and reefal debris (Rose, 1983). It is suggested that the barrier reefs developed from northwest to southeast with time and were limited eastward by transgression onto the outer shelf and deep water Middle Miocene clay-mudstone-siltstone sequences. The southeastern edge of reef deposition is located near the Palumat well where a line of non-deposition probably represents a low subaerially exposed landmass.

The Middle Miocene carbonate unit gradationally changes into clastic inner shelf deposits to the east and north, and is correlated onshore with the upper Kueh Formation. The latter comprises interbedded fossiliferous calcareous sandstone, siltstone and the limestone (Cameron *et al.*, 1980).

#### **2.3.2.4. Calang Volcanic Formation**

The Calang Volcanic Formation is a product of coastal volcanism which occurred during

the Middle and Late Miocene. The resultant volcanic rocks comprise extrusive and subvolcanic intrusive porphyritic hornblendic andesite, subordinate basalt, microgabbroid rocks, breccia and agglomerate. Lavas were mainly intermediate in composition, but minor basalt was extruded locally in the Teunom Area. This formation is sandwiched unconformably between the Kueh and Tutut Formations and crops out in the northwest portion of the study area.

Karig *et al.* (1979) suggested that the Calang volcanism was triggered by a trench-trench ridge triple junction migrating northwestwards along the Tertiary trench. This argument was proposed because of the unusual position of the Calang volcanic facies, and the earlier Tangla Formation volcanic facies, which lie on the trench side of the main arc of Tertiary and present day magmatism.

In contrast, the offshore area of the basin contains Late Miocene carbonate, developed in a shelf environment, together with claystone, sandstone and mudstone (Rose, 1983). The Late Miocene carbonate was penetrated in the Meulaboh, Meulaboh East, Keudapasi and Teunom wells and was found to be composed of calcarenite and micrite. The calcarenite ranges from very fine-to coarse-grained with varying quantities of micritic matrix (Rose, 1983). Mudstone, with sandstone and limestone intercalations, was deposited as a lateral equivalent of this carbonate formation. Some Late Miocene carbonate build-ups developed in the Teunom area are interpreted as shelf-edge accumulations (Rose, 1983).

#### 2.3.2.5. Tutut Formation

The Tutut Formation represents a series of regressive sequences consisting chiefly of alternations of conglomerate, sandstone, siltstone, mudstone and coal deposited in a fluvio-deltaic setting during the Pliocene (Cameron *et al.*, 1980; Beaudry and Moore, 1985; Hadiyanto and Amarullah, 1985; Hadiyanto, 1988). This formation can be divided into two units - the Lower and Upper Tutut Formation (Hadiyanto and Amarullah, 1985; Hadiyanto *et al.*, 1986; Hadiyanto and Cook, 1991). The Lower Tutut Formation is dominantly composed of coarse-grained sedimentary rocks such as conglomerate and sandstone with intercalations of siltstone and mudstone. Thin inferior coal beds (less than 0.5 m thick) are present as intercalations within the clastic rocks. The clastic rocks are generally poorly sorted and are commonly associated with plant debris. Planar cross-bedding, graded bedding, parallel and ripple laminations are the most common sedimentary structure developed in this part of the sequence.

The Upper Tutut Formation mainly comprises fine-grained clastic mudstone, siltstone and sandstone with thick coal intercalations. Graded bedding, parallel lamination, ripple marks and convolute bedding are structures common in this unit. Coal seams in this sequence range from 0.5-10 m thick. Plant remains and coal debris are also often associated with the clastic rocks. In some parts of the section glauconite and gastropods are present in the clastic rocks.

Offshore this formation is interbedded with reefal limestone (Cameron *et al.*, 1980). Rose (1983) described this formation, in the offshore area, as interbedded claystone, siltstone,

sandstone and limestone. The sandstone is composed predominantly of quartz with minor lithic grains. These beds show a decrease in grain size and thickness in an onshore direction. Coal beds (up to 3 m thick) were deposited in a deltaic setting (Rose, 1983).

#### **2.3.2.6. Meulaboh Formation**

The Meulaboh Formation was deposited unconformably on the Tutut Formation as a result of the Pleistocene uplift of the Barisan Geanticline (Cameron *et al.*, 1982). Onshore, this formation consists of sandstone and conglomerate deposited in a fluvial to paralic environment (Cameron *et al.*, 1980, 1982). Offshore, it consists of coarse-grained sandstone and conglomerate. Lithic fragments in the rocks, derived from plutonic and volcanic detritus, indicate unroofing and exposure of batholithic rocks during this time (Beaudry and Moore, 1985).

According to the offshore seismic data, the boundary between the Pliocene and Pleistocene sequences is partly erosional. This evidence can be recognised in the Singkel area where a large channel was eroded into Pliocene shelf strata and filled with Pleistocene sand and gravel (Beaudry and Moore, 1985).

### **2.4. Igneous Rocks**

Igneous rocks of various ages are found in the West Aceh Basin but some of them are speculative in terms of their age due to the absence of radiometric data. Discussion of the igneous rocks is restricted to those in the West Aceh Basin, west or northwest of the

Geumpang Line.

#### 2.4.1. Intrusive rocks

The Sikuleh Batholith dominates the northwest part of the West Aceh Basin and consists of relatively mafic and foliated rocks which pre-date rocks of Late Mesozoic age. The batholith also pre-dates younger relatively felsic and foliated rocks that were speculated to be Late Cretaceous or Paleocene in age (Cameron *et al.*, 1982). Several intrusive bodies are also associated with the Calang Volcanic Formation, and Pleistocene mafic dykes occur in the coastal area of Calang. Pleistocene basaltic dykes also occur in the Tutut area, and have resulted in upgrading of the rank of some Miocene coals in the Kueh Formation.

#### 2.4.2. Volcanic rocks

Volcanic rocks ranging in age from Late Mesozoic to Late Miocene were deposited in the West Aceh Basin. In general, three main periods of volcanic activity occurred in the basin. The first was associated with Late Mesozoic volcanic activity which resulted in the formation of pyritic epidotised massive to schistose mafic volcanic rocks, basalt and pillow basalt, green metatuff and mass-flow lithic cobble metabreccia of the Geumpang Formation. This formation occurs locally in the Teunom area of the West Aceh Basin, but a more widespread development is found east of the Geumpang Line in the North Sumatra Basin (Cameron *et al.*, 1982).



The second volcanic sequence was related to Late Oligocene-Early Miocene volcanic activity and resulted in the development of the Sapi Formation and Tangla volcanic facies. The Sapi Formation consists of felsic, intermediate and mafic lava and pyroclastic rocks deposited in the southeast part of the study area (Kr. Tripa and Kr. Seunagan). In the northwestern West Aceh Basin volcanic facies of the Tangla Formation are associated with sedimentary facies consisting in part of volcanic and conglomeratic sandstone, siltstone, and mudstone. Intermediate volcanic and amygdaloidal basalt was developed locally (Cameron *et al.*; 1982). Coal lenses, derived from floating material, are also associated with this facies in restricted locations.

The third volcanic sequence is related to the Middle-Late Miocene volcanic activity and resulted in the development of the Calang Volcanic Formation. The sequence comprises interbedded rhyodacite, pyroxene andesite, basalt and agglomerate. Propylisation has occurred in some rocks (Cameron *et al.*, 1983). This sequence was deposited in the western part of the West Aceh Basin, especially in the Calang district.

## 2.5. Geological Structure

The structural geology of the Tertiary strata in the West Aceh Basin (Figure 2.4) is mainly controlled by the continued oblique approach and subduction of the Indo-Australian Plate under continental Sunda land. This plate motion caused dextral strike-slip displacement which is represented in the basin by the dextral strike faults in the Ann Batee Fault Zone which trends northwest-southeast (Cameron *et al.*, 1980). In general, the

sequence has been involved in faulting and thrusting rather than folding. The main phase of Tertiary folding occurred outside the West Aceh Basin and is restricted to the Kieme Formation, which is unconformably overlain by the Late Oligocene Sipopok Formation.

Transcurrent faults have had some impact on the variety of regional geologic structures. However, the effect has only resulted in gentle folding and tilting of the Hulu Masen Group west of the Geumpang Line. The unconformably overlying Tutut Formation is, in the main, flat-lying except for some sharp monoclinical flexures which occur near the Ann Batee Fault Zone (Bennet *et al.*, 1981; Cameron *et al.*, 1982). In the northeastern portion of the basin the Tertiary structures are more simple than those in other areas. Most are related to differential uplift; however, a local zone of disruption related to magmatic events during the Middle to Late Miocene are present in the coastal zone (Bennet *et al.*, 1981).

The Tertiary deformation events which characterise northern Sumatra did not occur in the West Aceh region because the Sikuleh Batholith had a shielding effect and the entire West Coast Range of the Barisan Geanticline was a stable epirogenic block during the Tertiary (Bennet *et al.*, 1981). A fracture pattern developed around the Sikuleh Batholith along a set of bounding ring faults which resulted from differential movement. The general trends of the faults are northeast to east-northeast and northwest to north-northwest. A series of southwesterly-directed over-thrusts, involving the Geumpang Formation and Tangse Serpentinite that are expressed as the Geumpang Line, occur northeast of the Sikuleh Batholith and suggest maximum movement at the beginning of the Pliocene (Cameron *et al.*, 1982). A major compound zone of dextral transcurrent faulting, which

axially bisects Sumatra, is expressed by the Banda Aceh-Ann Normal Fault, which is located northeast of the Geumpang Thrust. This is believed to be a segment of the Sumatra Fault System (Katili and Hehuwat, 1967; Tjia, 1977).

In the easternmost portion of the West Aceh Basin the structural geology tends to be more complex, especially in regions occupied by the Woyla Group. Cameron *et al.* (1983) suggested that at least four seismically active northwest-trending fault segments, belonging to the Sumatra Fault System, are responsible for the present topographic configuration. This fault system is still active and axially bisects the island of Sumatra (Katili and Hehuwat, 1967; Tjia, 1977). The Banda Aceh-Ann Fault, which is the principal fault segment within the system, splits at Ann to form the Ann Batee and Reungeut-Blangkejeren Faults which lie in the northeastern part of the basin.

The Ann-Batee Fault throws westward and defines the eastern boundary of the Meulaboh Embayment (Cameron *et al.*, 1983). A northwesterly culmination of major reactivated faults in the lower Kr. Tripa is responsible for the development of the present topography and structure in the eastern portion of this area and it appears to terminate in a sinistral west-northwest-trending fault system in the middle part of Kr. Geumpang (Cameron *et al.*, 1983). The Ann-Batee Fault in this region represents the onshore continuation of an offshore fault which is shown on seismic profiles in the forearc region and offsets the Paleogene shelf margin by approximately 100 km dextrally (Karig *et al.*, 1978, 1980; Beaudry and Moore, 1985). The appearance of ultrabasic and serpentinitic rocks and detritus in this part of the basin is interpreted to indicate that such rocks were exposed at the surface by thrust movement along the Geumpang Line, then eroded extensively and

the detritus was incorporated into the Plio-Pleistocene sediments. Cameron *et al.* (1983) further interpreted the serpentinite rocks in this area to result from the generation of Late Mesozoic back-arc or intra-arc melting of the oceanic crust beneath the Cenozoic rocks.

The development of the geological structure in the offshore area has not been studied in detail. This is because of restricted palaeontological data from the offshore wells. Union Oil Company, as a contractor to Pertamina, interpreted the limited palaeontological data from the Meulaboh and Tuba wells. It was concluded that at least two thrusting events occurred within the Miocene and Plio-Pleistocene. In contrast, Jamas (1973) concluded that there was no evidence for thrusting. Her conclusion was based on the continuity of age data from her observations of samples from the same holes used by the Union Oil Company. Some useful information regarding the tectonic development in the offshore area was given by Beaudry and Moore (1985). They interpreted seismic reflection profiles from well compilation reports for the Union Oil Company and concluded that three major uplifts occurred during the Tertiary period. The first was the Eocene-Oligocene uplift which resulted in the unconformity between Eocene and Oligocene strata. A Miocene uplift was interpreted from the Meulaboh and Tuba wells but was believed to have had a restricted influence. The third uplift was a regional event related to the Plio-Pleistocene orogenesis that effected in the entire basin.

## **2.6. Geological History of the West Aceh Basin during the Tertiary Period**

The Tertiary geological history of the West Aceh Basin has been summarised from the work of Cameron *et al.* (1980), Bennet *et al.* (1981), Rose (1983) and Beaudry and

Moore (1985). In general, the development of Tertiary stratigraphic sequences in Sumatra was mainly controlled by two regional cycles of transgressive and regressive events (Figure 2.5)

In the onshore part of the West Aceh Basin a major break in the stratigraphy occurred before any Tertiary sediment was deposited. The Brueh Volcanic Formation may be the only representative unit that accumulated in the West Aceh Basin during this break, although the only outcrop of the unit is located in the northwestern part of the basin. This break resulted in a regional angular unconformity between the Paleogene strata and the Neogene sequences in the western part of Indonesia. A marine transgression between the Late Oligocene and Early Miocene led to the deposition of fluviatile to paralic sequences constituting the Tangla Formation, where several coal beds developed especially within the lower part of the formation.

In the offshore area, however, this same period is represented by shallow water marine strata consisting of calcareous, prograded mudstone and shallow-water detrital limestone, deposited as alternating sequences during the Tertiary 2a and 2b times (Beaudry and Moore, 1985).

The development of Oligocene coal has also been reported from West Sumatra Basin, North Sumatra Basin and Central Sumatra Basin.

The second transgression occurred in the Early to Middle Miocene resulting in the development of the proximal fluviatile conglomerate and breccia of the Kueh Formation.

As the transgression continued, the environment changed gradually through paralic to open marine-inner sublittoral and the sediment changed from arkosic to calcareous sandstone and limestone. Coal beds are interbedded with mudstone and were deposited in the lower fluvial and paralic environments. In the offshore area the transgressive marine succession consists of thin beds of lignite, shallow-water sandstone and siltstone passing upward into detrital limestone and limy mudstone (Beaudry and Moore, 1985).

Volcanic activity recommenced onshore in the Early Miocene and resulted in the formation of mafic, intermediate and felsic rocks of the Sapi Formation, especially in the eastern part of the basin. Coastal volcanism in the Middle to Late Miocene resulted in the development of the Calang Volcanic Formation. Deposition of the Tangla volcanic facies also recommenced.

Following the Miocene transgression, a regression in the Late Tertiary resulted from subduction related regional uplift and minor deformation in the coastal zone (Cameron *et al.*, 1982; Beaudry and Moore, 1985). The greatest uplift occurred in the northeast portion of the West Aceh Basin and was probably related to the over-thrusting and transcurrent movements along the Geumpang Line at the beginning of the Pliocene. Emplacement of the Tangle Serpentinite, with its associated relict Late Mesozoic sequence also occurred at this time (Bennet *et al.*, 1981).

Sedimentation continued in the Plio-Pleistocene during the regression and resulted in the development of the thick wedge of shallow-water deltaic and fluvial to paralic deposits of the Tutut Formation, which comprise conglomerate, sandstone, siltstone and several

lignite beds. This formation prograded basinward and buried Late Miocene and Early Pliocene offshore reefs as the rate of subsidence exceeded the rate of reef sedimentation. As a consequence, the lateral accretion and aggradation during relative highs and or still stands and of sea level resulted in the basinward migration of a shelf-slope break (Beaudry and Moore, 1985). Basaltic dykes were emplaced at this time as a result of the differential uplift and faulting.

The Meulaboh Formation represents deposition near present base level and probably accumulated during a short-lived Pleistocene marine transgression associated with the continued uplift of the interior regions up to present time as indicated by the seismically active movement on the Banda Aceh-Ann Fault (Bennet *et al.*, 1981).

## CHAPTER 3

### ANALYTICAL METHODS

The analytical methods employed in this study include organic petrology and organic geochemistry. The organic petrological techniques used comprise maceral analysis and vitrinite reflectance measurements for both coal and dispersed organic matter (DOM) whereas the organic geochemical methods consist of total organic carbon, Rock-Eval, column gas-chromatography and pyrolysis-gas chromatography of both coal and clastic rock samples.

#### 3.1. Organic Petrological Analysis

The main objective of the organic petrological analysis is to provide information about the maceral composition, vitrinite reflectance and fluorescence characteristic of the coal macerals and dispersed organic matter in order to assess the type and abundance of organic matter within the Tertiary sequences. Regional rank variations within the basin, both vertical and lateral, were also assessed by employing vitrinite reflectance measurements.



### 3.1.1. Sampling

Rock specimens examined in this study were taken from several sources: outcrops, drill cores and cuttings. Coal samples were collected from outcrop using either channelling or grab methods. Channel samples taken from the coal seams were oriented normal to the bedding and these represent composite samples of the seam from the roof to the floor. In cases where the seam thickness was uncertain, grab samples were used. Although the grab samples are not representative of the whole coal thickness or all the seam macerals, they provide useful rank data for the coal.

In the case of non-coal samples from outcrop, such as siltstone, mudstone and carbonaceous rocks, a grab sampling method was used because most of the clastic rocks have undergone extensive weathering. Most samples were only used for assessing vitrinite reflectance of the dispersed organic matter. Ply samples were taken where a coal seam contained a dirt band more than 5 cm thick.

Core samples for this study came from the HQ-series diamond drill core collected during the onshore shallow drilling program undertaken by the Directorate of Mineral Resources of Indonesia during preliminary coal exploration activities in this area. Most of core recovery was 100% for the coal samples and therefore, the samples used in this study from those cores are representative.

Samples were taken from 18 of the 24 drill holes and comprise coal seams as well as some carbonaceous rocks. Coal seam samples were collected as full seam samples

prepared for proximate and ultimate analysis on an "as received" basis. Parts of the composite samples were taken for both petrographic and geochemical analysis. Non-coal chip samples were selected from some holes for additional reflectance data for additional evaluation of vertical rank profiles within the holes.

Cuttings samples were collected from offshore drill holes which were part of the Union Oil Company exploration program in western offshore Sumatra. The drilling program was designed mostly to delineate reservoir rocks within the basin. Samples were chosen from 8 holes which all intersected the coal-bearing sequences. Samples were assessed in regard to the evaluation of organic matter abundance and rank or maturity.

Selection of samples for this study depended on the available cuttings and permission to collect from Pertamina (Indonesian State Oil Company). Visual examination using a binocular microscope was carried out in order to select the samples containing organic matter. In the case of samples containing coal fragments, hand-picking of the coal fragments was undertaken. Core samples and wild-cat samples were not available for this purpose. In general the condition of the samples was good, however, minor caving has been reported in some holes. Therefore, sample selection was undertaken using the well completion report and the electric log report in order to gain samples as representative of the intervals as possible.

### **3.1.2. Sample Preparation**

Organic petrological analysis was carried out in both reflected white light and fluorescence

modes. Reflected white light was used to identify the vitrinite and inertinite components and to estimate the volumetric abundance of coal and/or dispersed organic matter either during point count analyses or visual estimations. The type and abundance of liptinite macerals was determined using fluorescence mode.

The samples were prepared as polished blocks for both the core and cuttings samples. The method of sample preparation is outlined in Figure 3.1.

#### **3.1.2.1. Polished Blocks**

Each polished block consists of a columnar sample, approximately 3 x 3 cm in size, cut perpendicular to the bedding plane. All of the samples prepared in this manner were collected from outcrops of coal, carbonaceous shale, siltstone, mudstone or shale. Polished blocks were used to determine coal rank by measuring the reflectance of dispersed organic matter. Each sample was placed in a plastic container that was filled with a mixture of epoxy resin and hardener (in a ratio of 100 ml: 3 ml) then labelled with the Department of Geology catalogue number. It was then evacuated in a vacuum oven in order to eliminate all bubbles. After evacuation the samples were left for 24 hours to harden before grinding.

#### **3.1.2.2. Polished Grain Mounts**

Coal samples were prepared by crushing the coal to a grain size of approximately 0.5 mm. The sample was then placed in a 2 cm cube-shaped plastic mould and stirred into

a mixture of resin and hardener (in a ratio of 100 ml: 4 ml) before being placed in a vacuum oven to eliminate all bubbles. The face for polishing was cut in a vertical plane to counteract the sedimentation effect during setting of the sample in the resin media and thus maintain a representative sample. Further procedures followed the steps illustrated in Figure 3.1 (Hutton, 1984).

### 3.1.3. Microscopic Examination

The microscopic examination method used in this study involves rank determination by measuring vitrinite reflectance and maceral analysis. The latter analysis enables identification of vitrinite and inertinite components and allows an estimate of the volumetric amount of these macerals using reflected light microscopy. The type and abundance of liptinite macerals can be determined by employing fluorescence mode microscopy.

The examination of blocks was conducted under controlled temperature and humidity conditions in the research microscope laboratory of the Department of Geology, University of Wollongong, using a Leitz MPV-1 microscope for reflectance measurements and a Leitz MPV-2 microscope for maceral analysis and photomicroscopy.

#### 3.1.3.1. Reflectance Measurements

Reflectance measurements were carried out in oil immersion using an Ortholux I microscope fitted with an MPV-1 microphotometer system where the output was sent to

a galvanometer.

Calibration of the equipment was conducted before measuring vitrinite reflectance in order to check linearity of the equipment. The known reflectance standards were a synthetic spinel standard with a reflectance of 0.416%, an yttrium garnet standard with a reflectance of 0.916% and a gallium garnet standard with 1.710% reflectance.

During measurement of reflectance, the temperature was maintained at  $23 \pm 1^\circ\text{C}$ . The immersion oil had a refractive index of 1.518 in green light of 546 nm wave length at  $23^\circ\text{C}$ .

The measurement procedure follows the Australian Standard AS 2486 (Standard Association of Australia, 1989). Reflectance measurements were made using an oil objective lens of nominal magnification x60. The area over which reflectance was measured was set at 2 microns dimensions.

The reflectance measurements were made on telovitrinite where possible as recommended by AS 2486. In samples with limited telovitrinite, measurements were also conducted on detrovitrinite and noted as such.

Maximum and minimum reflectance measurements were made by rotating the stage of the microscope through  $360^\circ$  in order to read both the first and second maxima. The number of measurements per sample for coal was thirty, but for dom the number of measurements varied according to the availability of suitable vitrinite.

### 3.1.3.2. Maceral Analyses

The maceral analysis procedure followed the Australian Standard for coal maceral analysis, AS 2856 (Standard Association of Australia, 1986). These analyses were carried out in reflected white light and fluorescence mode using 32x and 50x oil-immersion objectives at a total magnification of approximately 400-500x. A minimum of 500 points were counted using a electric point counter over a 2 x 2 cm surface area of the polished block where the density of grains was approximately 90%.

Semiquantitative analysis was carried out to estimate maceral abundance in dispersed organic matter in cutting samples. The volumetric composition of macerals in each sample was made by visual estimation methods established at the Department of Geology, University of Wollongong, as shown in Appendix 1.

In this scheme the maceral abundance is categorised into:

dominant	>40%
major	10-40%
abundant	2-10%
common	0.5-2%
sparse	0.1-0.5%
rare	<0.1%
absent	0%.

The number of visual estimations of maceral abundance was set at 50 grains per block from several traverses.

### 3.1.3.3. Fluorescence Observations

Fluorescence microscopy was carried out using a Leitz Orthoplan microscope fitted with a 100 watt mercury lamp for fluorescence mode and a 100 watt quartz iodide lamp for reflected light. The fluorescence filters were a 3 mm BG 3 (blue light) excitation filter and a 4 mm BG 38 excitation filter with a TK 400 dichroic beam splitting mirror and a K490 barrier filter.

Photomicrographs were taken using a Leitz Vario-orthomat camera and Ektachrome 400 film.

### 3.1.3.4. Maceral Analysis Results

The results of maceral analyses were expressed using a mineral counted basis, with the mineral matter determined by point count.

The formula used for maceral abundance in dom was that of Panggabean (1990):

$$\text{OMAv (\%)} = \frac{(\text{Vm.Am}) + (\text{Va.Aa}) + (\text{Vc.Ac}) + (\text{Vs.As}) + (\text{Vr.Ar})}{N}$$

where:

OMAv = total organic matter abundance for vitrinite (%)

Vm = % of grains with vitrinite in the major category

Va = % of grains with vitrinite in the abundant category

Vc = % of grains with vitrinite in the common category

$V_s$  = % of grains with vitrinite in the sparse category

$V_r$  = % of grains with vitrinite in the rare category

$A_m$  = % mid-point value for the major category - 25%

$A_a$  = % mid-point value for the abundant category - 6%

$A_c$  = % mid-point value for the common category - 1.3%

$A_s$  = % mid-point value for the sparse category - 0.3%

$A_r$  = % value for the rare category - 0.1%

$N$  = total clastic grains counted in the sample

The proportions of liptinite and inertinite macerals were also calculated using this formula with liptinite and inertinite replacing vitrinite where necessary. For the clastic and carbonate rocks containing coal grains, the amount of each maceral was visually estimated then the average was calculated by dividing summed percentages by the total number of grains (Panggabean, 1990).

### 3.2. Organic Geochemistry Analyses

Organic geochemistry techniques included total organic carbon (TOC), Rock-Eval, column-gas chromatography and pyrolysis-GC. The aim of these analyses was to determine the type of organic matter, source rock richness and maturation characteristics of the samples. All of the analyses were undertaken in the Organic Geochemistry Laboratory, Bureau of Mineral Resources, Canberra, under the supervision of Dr C.J. Boreham.



### 3.2.1. Rock-Eval and TOC (Total Organic Carbon) Analyses

The principles of Rock-Eval analyses have been discussed by Durand and Espitalie, (1973), Espitalie *et al.*, (1973, 1977, 1985), Peters, (1986), Hartman and Stroup, (1987) and Langford and Valleron, (1988). This method provides information such as type, quantity and thermal maturity of organic matter.

The equipment used in this study was Rock-Eval II equipment fitted with a flame ionisation detector (FID) which detected the hydrocarbons generated. The samples analysed comprised 100 mg of powder for clastic rock or 15 mg of powder for coal.

A series of samples were placed into stainless steel crucibles and run following a known standard sample. The first peak (S1) of a pyrogram was recorded after the sample was heated at 300°C for 5 minutes. The emissions represent the quantity of free hydrocarbon, in mg/g, in a sample.

The second peak (S2) was recorded after additional heating, at 25°C/minute, up to 550°C. This peak represents the amount of hydrocarbon (mg/g) produced during this cycle as organic matter in the rock sample is converted by thermal cracking and from the volatilisation and cracking of heavy extractible compounds (> C<sub>40</sub>) such as resins and asphaltenes (Espitalie *et al.*, 1985).

The third peak (S3) represents the amount of carbon dioxide (CO<sub>2</sub>) produced (in mg/g rock) whilst the sample is at a temperature of 300-390°C.

A thermocouple monitors the oven temperature and the temperature, at which the maximum amount of hydrocarbons is generated, is expressed as a  $T_{\max}$  ( $^{\circ}\text{C}$ ) value (Espitalie *et al.*, 1985).

S2 and S3 can be used to estimate the Hydrogen Index (HI) and Oxygen Index (OI) respectively with both expressed in mg of HC per gram of TOC (Espitalie *et al.*, 1985).

The proportion of free hydrocarbons in relation to the total hydrocarbon compounds present during pyrolysis [ $S1/(S1 + S2)$ ] is expressed as the Production Index or PI (Espitalie *et al.*, 1985).

Total organic carbon (TOC) was measured using a Leco DC 12 analyser. Approximately 200 mg of clastic rock powder or 30 mg of coal powder (added as a mixture of 50:50 coal to HCl and distilled water) was held until all bubbles disappeared and then heated at  $60^{\circ}\text{C}$  for one hour and allow to cool. After this the sample was filtered, washed with distilled water until neutral, and dried at  $60^{\circ}\text{C}$  for 12 hours.

### 3.2.2. Column Gas-chromatography

Samples were first demineralised using firstly hydrochloric acid (HCl) and then hydrofluoric acid (HF) to remove silicate minerals. The procedure for demineralisation is given in Appendix 2.

The demineralised samples were then extracted using the Soxhlet method for 24 hours.

Chromatography on silica gel was conducted in order to produce saturated, aromatic and polar hydrocarbon fractions (Appendix 3).

In this study the saturated hydrocarbon fraction was analysed using a Varian 3400 GC machine fitted with a fused silica capillary column (0.50 x 0.25 mm) coated with crosslinked HP ultra-1 methylsilicon (Boreham, pers. comm. 1991). The samples were injected into the column at 60°C, with hexane as a solvent, and held isothermally for 2 minutes. The chromatogram was developed by temperature-oven programming at 4°C/min to 300°C, and held for a period of 30 minutes until all peaks had been eluted (Boreham and Powell, 1991). The carrier gas was hydrogen at a linear flow rate of 30 cm/s. A DAPA GC software package was used to produce the chromatograms.

### 3.2.3. Pyrolysis-Gas Chromatography

The quantitative pyrolysis-GC method established at the Bureau of Mineral Resources Laboratory, Canberra (Boreham and Powell, 1987, 1991; Boreham *et al.*, 1988; Powell *et al.*, 1991) was used to analyse the relative proportions of hydrocarbons. One to four milligrams of washed, demineralised sample was doped with an internal standard of poly- $\alpha$ -methylstyrene, placed in a quartz tube and pyrolysed using the coil probe of a CDS Model 122 pyroprobe at 700°C for 1 min. This machine was connected to an HP 5700 gas chromatograph equipped with a SGE injector inlet splitter and a 25 m x 0.25 mm fused silica capillary column (HP ultra-1). The quantities of normal hydrocarbons (ranging from C7 to C30), low molecular weight aromatic compounds (C7 to C9) and phenols (C6 to C8) were detected as described in Powell *et al.* (1991).

## CHAPTER 4

### ORGANIC PETROLOGY

#### 4.1. Nomenclature

The petrographic terms for macerals used in this study follows those described by the Australian Standard AS 2856 (1986) as shown in Table 4.1. Although the Australian classification was based on the maceral terminology as defined by the International Committee for Coal and Organic Petrology ((ICCP) 1963, 1971, 1975), the distinction between brown coal and bituminous coal terminology was eliminated and modification were made to include terms for both brown coal and bituminous coal in the one system. Thus the complex terminologies of the ICCP for coals of different ranks were simplified into the one scheme. This scheme is more applicable for the present study where most of the coal samples are of brown coal rank but textural features are commonly those of bituminous coal rank. In some drill holes, coals show increasing rank with depth and pass from brown coal rank to bituminous coal rank (at  $R_v$  max of 0.4%) without significant changes in textural properties because of increased thermal gradients resulting from localised intrusions.

Based on the different petrographic properties such as morphology relief, internal structure, reflectance, fluorescence colour and intensity, as well as maceral associations, the "secondary" liptinite maceral exsudatinite, as defined by Teichmuller (1973; 1974; 1982), needs discussion. In sub-bituminous to high volatile bituminous coals from

northwest Germany, Illinois (USA), Rumania and Japan, the secondary macerals which represents bitumen produced during late diagenesis and early catagenesis is termed exsudatinite. She found that exsudatinite is a coalification exudate product which is formed from other macerals, such as resinite, cutinite and fluorinite, during the sub-bituminous and high volatile bituminous stages and is closely related to the formation of petroleum (Teichmuller, 1973; 1974; 1982). Jones and Murchison (1963) and Murchison (1976) reported resinite migrated into cleats and stated that such migrated matter in bituminous coal is of secondary origin. Shibaoka (1978) stated that the occurrence of the exsudatinite could be in a much wider range of coals ranging from brown coal to bituminous. His statement resulted from his investigation of brown coals from different countries in which he found that exsudatinite exuded from a continuous body of resinite, alginite, and sporinite and had filled cleats and other cavities. Zhao *et al.* (1989) reported that exsudatinite was an expulsion and migrated material mainly from resinite which was found in the low rank coal (between 0.36% and 0.40 % vitrinite reflectance) of the Baise Basin, South China.

In general, the term exsudatinite has been used for non-reflective transparent organic matter that fluorescences greenish-yellow to orange with moderate to high intensities and occurs in veins, wedge-shaped cracks, perpendicular or parallel to the bedding plane joints or empty cell lumens, pores and interstices between macerals (Plate I, 1a to 3b). Relief is low to moderate and commonly equal to vitrinite. Exsudatinite is commonly associated with telocollinite, desmocollinite, liptinite macerals in detrovitrinite groundmass, resinite, sporinite, cutinite and suberinite and has a reflectance ranging from 0.05% to 0.1%. It is in this sense that the term exsudatinite for organic matter in samples from the West Aceh Basin. One major difference is that although it is a significant component, many samples only have a rank

equivalent to a vitrinite reflectance of 0.25%.

Samples also contain a second fluorescing "se which would be designated by the term solid bitumen (migrabitumen) as proposed by Jacob (1976, 1981). Jacob stated that bitumen is a secondary amorphous maceral often dispersed in rocks as a filling of intercrystalline spaces, small (hair-like) cracks, microfossils and other microcavities. It can be found in samples with a rank ranging from from brown coal to the graphite. ICCP (1990) defined migrabitumen as a solid bitumen occurring in sedimentary rocks but not including coal; exsudatinite was used for the similar material in coal.

In many cases there is no optical difference between solid bitumen and exsudatinite although there is chemical or compositional difference (Jacob, 1976). Bitumen has a passive behaviour with respect to form, that is, the different morphological forms result from the entry of the bitumen into voids. Common shapes include flat bodies in crystal aggregates of carbonate and quartz, microplates in fine fissures, complex forms confined in microfossils such as foraminifera, diffuse masses in siltstones, marlstones and claystone rocks and rarely, but typically, globular bodies have been recorded (Jacob, 1989). Although contrary to the ICCP definition, the term bitumen has been for organic matter in coal and carbonaceous shale as well as clastic rocks and limestone.

The reflectance of bitumen ranges from almost 0% to 10%. Reflectance is one of the properties that is used to distinguish the various types of liptinite. However, reflectance values are not the only parameter to distinguish the type of bitumen (Jacob 1967, 1983); bitumen type also can be differentiated using parameters such as intensity of fluorescence and

microsolubility (Jacob, 1989). A revision of the Jacob (1989) classification of bitumen is beyond the scope of this study. However, it is considered that comment should be made on the occurrence and properties of exsudatinite and bitumen. The properties of the two in samples from the West Aceh Basin are sufficiently different and distinctive to be recognised as separate macerals in this study - the term exsudatinite is used only for secondary liptinite, whether it be referable to what is called either exsudatinite or bitumen in other publications, in coal and coaly materials whereas the term of bitumen used for secondary liptinite in clastic rocks, irrespective of origin.

The principle features that distinguish bitumen from exsudatinite, apart from their genesis, are optical properties and maceral associations in which the two occur. (Table 4.2).

The common morphology of the bitumen in samples from the study area are globular, rounded, oval and cauliflower shapes or irregular bodies, cavity and fracture fillings, especially in sandstone and carbonate rocks. The size varies from less than 5 microns to 80 microns. Relief is moderate to high but commonly higher than vitrinite. It is common in porous sandstone and carbonate rocks and envelops mineral grains. Shrinkage cracks and vesicles are common features for the globular, rounded, oval and cauliflower bitumens (Plate I, 4a to 6b). The colour varies from grey to brown with fluorescence ranging from low to moderate, brownish-yellow to yellow. Reflectance ranges from 0.08% to 0.2%.

The mechanism for the mode of formation of both exsudatinite and bitumen is discussed latter in this Chapter.

## **4.2. Maceral Composition and Abundance**

A total of 278 samples of coal, carbonaceous shale and clastic sedimentary rocks from the Tangla, Kueh and Tutut Formations were analysed petrographically. Of the samples, 151 comprised cuttings from 8 offshore oil wells, 60 were core samples from 12 of the 26 shallow onshore wells and 67 were from outcrop. The cutting samples were collected from the following wells: Teunom, Bubon, Keudapasi, Tuba, Meulaboh, Tripa, Meulaboh East and Palumat. The core samples were taken from the M series onshore wells, M1, M2, M3, M4, M10, M11, M12, M13, M15, M18, M21 and M22 .

The location of the samples used in this study was shown in Figure 1.2.

### **4.2.1. Maceral Composition of Tertiary Coals**

One hundred and twenty seven coal samples from the offshore wells, onshore wells and outcrop were examined to provide data on the organic matter type and maceral compositions of the coals. The average maceral compositions of the Tertiary coals are shown in Table 4.3 and detailed maceral compositions are given in Appendices 4, 5 and 6.

In general, most of coals are rich in vitrinite with vitrinite content generally in the range of 43% to 98%. Liptinite is the next most abundant maceral group ranging from 2 to 50%.

Inertinite is usually present but seldom comprises more than 10% of the coals. Mineral



matter does not exceed 3%. Figure 4.1 shows the general maceral composition of the Tertiary Coals.

#### 4.2.1.1. Oligocene Coal

Oligocene coal in the West Aceh Basin is of brown coal rank, except where adjacent to intrusions, and is only found in the Tangla Formation where the coal seams form a minor proportion of the sequence and are typically less than 1 m thick, generally within the range of 0.5 m - 1 m. The seams do not split and contain only minor mineral matter, ash contents are generally less than 1%. The seams generally lens out over short distances of less than 2 km. The seams consist of thick banded bright coal, intercalated with thinner banded dull coal. However, the uppermost seam is mostly dominated by dull coal.

Petrographically, the majority of coals are rich in vitrinite with the vitrinite content generally within the range 64% to 92% and with an average of 77% for all samples. Liptinite usually comprises in excess of 17% whereas inertinite generally does not exceed 6% on average.

The vitrinite macerals are dominated by detrovitrinite and telovitrinite subgroups with the detrovitrinite more abundant than the telovitrinite. Telovitrinite macerals generally occur as thin bands not more than 10 microns thick and interbedded with thicker bands of detrovitrinite (Plate II, 1a). Among the telovitrinite macerals, telocollinite is the most abundant, whereas eu-ulminite and textu-ulminite occur in lesser amounts. Telocollinite and eu-ulminite occur within the same sample in some cases (Plate II, 1b).

The detrovitrinite macerals mostly consist of desmocollinite (average of 31 % for all Oligocene coals) and densinite (average of 12%) with lesser amounts of attrinite (less than 1 % on average). Attrinite and densinite bands generally form the groundmass for the telovitrinite, liptinite, gelovitrinite and inertinite. Desmocollinite usually occurs in bands thicker than 10 microns.

Gelovitrinite constitutes not more than 4 % on average and mostly comprises corpogelinite with porigelinite and eugelinite (both less than 1 % of the total).

With reflected light, all the above mentioned macerals are grey to dark grey, with the desmocollinite showing brown to brownish-yellow fluorescence. The vitrinite composition of Oligocene coals is illustrated in Figure 4.2.a.

Cutinite, suberinite and liptodetrinite are the dominant liptinite macerals and occur with minor sporinite, resinite, alginite, fluorinite and exsudatinite. Cutinite (mostly tenuicutinite) is prominent in most of the Oligocene coals and usually occurs in association with vitrite layers as well-preserved, thin rims. This maceral exhibits brownish-orange and brownish-yellow fluorescence of varying intensity. The average amount of this maceral is 5% with a few samples containing as much as 10%. In samples which contain a lot of liptodetrinite and detrovitrinite groundmass, fragments of crassicutinite occur (Plate III, 1a).

Liptodetrinite is more abundant than suberinite, ranging from 0 to 9 % but typically does not exceed 4 %. Liptodetrinite is frequently associated with the desmocollinite groundmass.

Some samples have liptodetrinite-rich clarite intercalated with desmocollinite-rich vitrite. The fluorescence of liptodetrinite varies from brownish-yellow to orange with the intensity lower than that of cutinite.

Suberinite, derived from thick-walled cork tissue, is common and is commonly associated with vitrinite in bands of clarite, as fragments in the detrovitrinite groundmass or is associated with tabular phlobaphinite (Plate III, 1b). The fluorescence is variable with brownish-orange common. The average suberinite content is 2.3% but some counts of more than 13% were recorded in a small number of samples, for example GM 24583.

The average content of sporinite in the Oligocene coal for individual blocks ranges from 0.4% to 3.3%. Sporinite fluorescence varies from orangish-yellow to brownish-orange with most occurring as flattened exines with many of the central cavities filled with framboidal pyrite. In general sporinite is found mostly in clarite where it is associated with vitrinite mostly. Some of the sporinite also occurs in samples associated with resinite where the microlithotype is also clarite. Sporangia were recognised in a few samples, for example, GM 23234 where it commonly occurs in liptite, which in turn occurs in clarite.

Resinite content in individual samples ranges from 0 to 7.5% with the average value for all samples 1.8%. In general, resinite occurs in vitrinite, especially telovitrinite, with lesser amounts associated with detrovitrinite. Resinite is rounded or globular in shape with fluorescence ranging from yellow to brown to orangish-brown.

Fluorinite is generally rare in Oligocene coal, ranging from 0 to 1.8% with an average for all samples of 0.2%. Fluorinite occurs as globular bodies or thick lensoidal bodies in clarite.

It is grey under normal reflected light but the fluorescence is more intense than that of resinite and varies from bright yellow to bright orange.

Alginite is generally rare in the Oligocene coal and is associated with thin bands of clarite.

As can be seen in Plate III (1c), the alginite consists of *Botryococcus*-derived telalginite with strong orangish-yellow intensity fluorescence.

Exsudatinite was found in small amounts of normally less than 2% of although 9% was recorded in GM 22825. Exsudatinite typically fills fissures or cleats in telovitrinite or desmocollinite. Exsudatinite filled fractures are commonly perpendicular to bedding. It is transparent to grey in reflected light and fluorescence is greenish-yellow to orange with moderate to medium intensity. Oil hazes are associated with exsudatinite but are less abundant than in the Miocene coal

The average total liptinite composition of Oligocene coal samples is shown in Figure 4.2.b.

Although inertinite is relatively sparse (average 5.9%) some samples contain up to 24%, for example, GM 23237. Semifusinite is dominant over sclerotinite and is derived from thick-walled woody tissue although it appears degraded and detrital when associated with detrovitrinite. Sclerotinite comprises mostly sclerotite spores, associated with detrovitrinite, and sparse plectenchyme tissue. Fusinite occurs in clarite, associated with a detrovitrinite

groundmass, or as thin inertite bands associated with vitrite. Trace macrinite was found in clarite. The average inertinite composition of Oligocene coals is shown in Figure 4.2.c.

#### 4.2.1.2. Miocene Coal

The Miocene coal occurs as several thin seams, 0.4 to 0.8 m thick with most seams lensoidal bodies within the fine-grained siltstone and claystone of the Kueh Formation which was deposited in paralic and fluvial environments. Megascopically, the coals are characterised by dull to banded bright coal and are commonly interbedded with the thin dirt bands. In outcrop the colour of the coal varies from dark brown for the dull seams to black for the banded bright seams.

Microscopically, vitrinite is the dominant maceral group with abundances within the range of 60% to 98% (average of 75%); liptinite content varies between 0% and 18% with an average of 16% and, although inertinite is a minor component in all samples (average of 6%), one sample contains 22% (GM 23233).

Vitrinite macerals are dominated by detrovitrinite and telovitrinite with detrovitrinite more abundant than telovitrinite. Telovitrinite which mostly consists of eu-ulminite and telocollinite with minor amount of texto-ulminite, constitutes 5% to 38% of most samples, averaging 10%. Fine-grained mineral matter and sporadic liptinite, commonly resinite and liptodetrinite, are associated with texto-ulminite and eu-ulminite, usually in open cell lumen.

Overall, detrovitrinite constitutes more than 40% of the total macerals in these coals and with individual samples containing up to 60%. Desmocollinite is dominant over densinite and attrinite (Plate II, 2a).

Gelovitrinite content ranges from 2% to 20% with an average value of 6%. It comprises mostly corpogelinite with lesser amounts of porigelinite and eugelinite. Most of the gelovitrinite fills cell lumen in telovitrinite but is also associated with detrovitrinite, where it occurs in the densinite groundmass (Plate II, 2b).

The vitrinite composition of Miocene coals is shown in Figure 4.3.a.

Of the liptinite macerals cutinite and liptodetrinite are most abundant. Cutinite consists mostly of well-preserved, thin tenuicutinite associated with clarite bands where the cutinite rims vitrite layers (Plate III, 2a). Fragments of cutinite are also distributed sparsely in detrovitrinite layers. Cutinite has medium to strong, yellow to brownish-yellow fluorescence.

Liptodetrinite is commonly associated with detrovitrinite where it occurs as isolated fragments in the detrovitrinite groundmass and in desmocollinite. Some samples have liptodetrinite-rich clarite layers alternating with vitrite. Liptodetrinite has the widest range of fluorescence intensity and colour (dark brown to yellow) of any liptinite maceral.

Sporinite consists of miospores (tenuisporinite) in which the exines have not been fully compressed. Sporangia occur in clarite in some samples. Fluorescence intensity is moderate

and colours are mostly yellow.

In the Miocene coals resinite has similar modes of occurrence as in the Oligocene coals. Resinite mostly occurs in telovitrinite but some of resinite is associated with clarite layers (Plate III, 2b). Fluorescence varies from dark brown to yellow with low to strong intensity. Fluorinite with grey to greenish-grey autofluorescence in white light and strong greenish-yellow fluorescence is a minor component.

Suberinite occurs in thin-walled cork tissue where it is associated with tabular phlobaphinite. Fluorescence ranges from brownish-yellow to yellow with moderate intensity.

*Botryococcus*-related telalginite occurs in clarite layers or occurs in liptite layers associated with a finely divided densinite groundmass. Some samples contain up to 7% alginite, for example GM 23233, but the average is only 1.7% . Fluorescence is commonly yellow with moderate to strong intensity.

Exsudatinite is rare in most of the Miocene coal and occurs in cracks or fissures, commonly perpendicular to the bedding plane, in telovitrinite and desmocollinite macerals. In reflected light, it is transparent to grey but has medium to strong yellow fluorescence. Oil hazes are commonly expelled from exsudatinite; these have stronger fluorescence intensity than the exsudatinite and brighter yellow and greenish-yellow colours (Plate III, 2c).

The general abundance of liptinite macerals in the Miocene coal is given in Figure 4.3.b.

Inertinite is more abundant in the Miocene coal than in the Oligocene and Pliocene coals. Some samples have more than 20% inertinite, for example GM 23233. Semifusinite is most abundant, with sclerotinite and inertodetrinite next most abundant. Some semifusinite and inertodetrinite often occur as inertite layers associated with detrovitrinite bands. Sclerotinite is derived from various types of fungal sclerotia such as single-celled, twin-celled and multicellular teleutospores (Plate II, 2c).

Macrinite is rare in Miocene coal but is more abundant than in either the Oligocene or Pliocene coals. It occurs as small to large, oval to rounded bodies usually associated with desmocollinite and well-preserved cutinite (Plate II, 2d).

Fusinite is the least abundant inertinite in samples examined and comprises well-preserved woody tissue with generally open cell-lumen, some of which are filled with gelinite.

The abundance of inertinite macerals is given in Figure 4.3.c.

#### **4.2.1.3. Pliocene Coal**

Compared with Oligocene and Miocene coals, Pliocene coal is the most widely distributed in the study area with more than 10 seams ranging from 0.3 to 10 metres thick.

Macroscopically, most of the seams contain dull-brown coal with intercalated thin black layers vitrain. Clay bands and pyrite ribbons are common inclusions in the seams. In some of the



bottom seams, lenses of very dull, earthy coals occur at the top of a sequence comprising carbonaceous shale grading up to the very dull, earthy coal. These lenses have a maximum thickness of 40 cm and in drill logs these coals have been referred to as canneloid coals.

Microscopically, except for the canneloid coal, the Pliocene coal is vitrinite-rich with the average vitrinite content varying from seam to seam. The overall average vitrinite content for all Pliocene samples is 71% with a range in samples between 43% to 91%.

Compared with the Oligocene and Miocene coals, the Pliocene coal has a higher liptinite content, ranging from 6.6% to 50%, with an average of 20.4%. On the other hand, Pliocene coal has the lowest inertinite content, generally less than 3% but ranging up to a maximum of 11%, for example GM 22030.

Vitrinite chiefly comprises detrovitrinite, telovitrinite with lesser amounts of gelovitrinite. Detrovitrinite is dominant over telovitrinite ranging from 21 % to 60% (average 37%) with desmocolinite dominant over densinite and attrinite but relatively less abundant than in the Oligocene and Miocene coals as is densinite. In contrast, attrinite is more abundant in Pliocene coal than in Oligocene and Miocene coals (Plate II, 1c). Desmocolinite is generally intercalated with telocollinite layers. In a few samples, the desmocolinite has quite a wide range of reflectance values. In these samples, the colour of desmocolinite varies from grey to dark brown.

Telocollinite is the most abundant telovitrinite maceral with eu-ulminite the next abundant

telovitrinite maceral. The latter occurs as thin layers of woody material associated with telocollinite and desmocollinite layers. Texto-ulminite, a minor component, is usually associated with textinite or is associated with the attrinite groundmass.

Textinite, also a minor component, is well-preserved with both thin and thick walls and either ellipsoid or semi-rounded cell lumens, many of which have been filled with corpogelinite, porigelinite and clay-sized mineral matter (Plate II, 3b). Some of the cell walls are partly oxidized around the edges. In reflected light, textinite is reddish in the uppermost seams and gradually changes to the grey in the deeper seams.

Gelovitrinite is more abundant in the Pliocene coals than in the Oligocene and Miocene coals and in most samples it is dark grey-brown with low reflectance and brownish-yellow fluorescence with low to medium intensity. It chiefly consists of corpogelinite and porigelinite with minor amounts of eugelinite.

Figure 4.4.a shows the vitrinite content of Pliocene coals.

The average liptinite content of the Pliocene coals is 20.4% although some samples have up to 50% (for example, GM 22543).

Liptinite is predominantly cutinite, liptodetrinite, resinite, sporinite and suberinite and all occur in most samples.

The average cutinite abundance is 7.5% but some samples contain up to 24% (for example,

GM 21983). Both thick crassicutinite and thin tenuicutinite are common in clarite. In the detrovitrinite groundmass, the cutinite is fragmented. Cutinite has strong bright greenish-yellow fluorescence and some oil hazes are expelled from cutinite (Plate III, 1a).

Liptodetrinite is the second most abundant liptinite with an average value 4.5% and up to 14% in some samples (GM 22035). Liptodetrinite-rich clarite is commonly interbedded with Vitrite (desmocollinite) bands (Plate III, 1b). Fluorescence colours varies from dull brown, greenish yellow, green and yellow with medium to strong fluorescence intensities.

Resinite content is generally low (average 3%) but ranges up to 13%, for example GM 22850, and usually is a cell filling in telovitrinite and to a lesser extent, in sclerotinite and fusinite lumens. Resinite has moderate to strong fluorescence with brown to bright yellow colour. Some oil hazes are expelled from resinite.

Although the average sporinite content is 1%, several samples have more than 4% sporinite which is generally microspores (only partly compacted), sporangia and megaspores. Sporinite is usually in clarite bands and liptite layers or disseminated in the detrovitrinite groundmass (Plate III, 3c). Sporinite usually has moderate greenish-yellow to green fluorescence. Some oil hazes are associated with sporinite.

Suberinite is commonly associated with the phlobaphinite in clarite which is intercalated with vitrite layers. Rootlets with a cortex consisting of suberinite are also common. Suberinite commonly has moderate green fluorescence. Some oil haze are also expelled from suberinite.

Telalginite, fluorinite and exsudatinite occur in trace amounts.

Fluorinite content averages 0.8%, but in some samples, fluorinite constitutes more than 12% (GM 22000) where it is usually clustered along bedding planes or in vitrinite. Fluorinite has a globular to lensoidal form, is grey but has strong bright green fluorescence with much stronger intensity than that for resinite (Plate III, 3d).

*Botryococcus*-derived telalginite occurs in clarite, clay-rich layers or in detrovitrinite. Although the telalginite content is commonly less than 2% in most samples, some samples contain up to 5%. Telalginite fluorescence is commonly moderate to strong, bright yellow intensity.

Exsudatinite comprises up to 5% (GM 22017) of Pliocene coal and occurs mostly as fissure fillings in telocollinite and desmocollinite. Oil hazes are associated with exsudatinite. The fluorescence is commonly strong greenish-yellow.

Figure 4.4.b shows the liptinite content of Pliocene coals.

Compared to Oligocene and Miocene coals, the Pliocene coal has a lower inertinite contents which is less than 3% on average although individual samples contain more than 10%. Semifusinite is the dominant maceral and generally occurs in thick inertite layers which are intercalated with clarite and vitrite bands. Fusinite is very rare but some samples have up to 1%; it is usually associated with semifusinite. Compared to the Oligocene and Miocene coals, sclerotinite is less abundant in the Pliocene coal. However, Pliocene coals have a

greater variety of fungal tissue, especially fungal spores; bilocular and multilocular teuleutospore are common (Plate II, 3c). Sclerotinite is also associated with the vitrinite especially detrovitrinite, sporinite, suberinite, cutinite and inertodetrinite.

### **4.3. Mineral Matter of the Tertiary Coals**

The discussion of mineral matter in the samples from this study is restricted to that which can be recognised with the reflected light microscope and as such, discrete mineral matter of clay size is regarded as undifferentiated mineral matter. The use of X-ray diffraction techniques (XRD) for detailed clay mineral identification is beyond the scope and needs of this study. Undifferentiated mineral matter in many coals is commonly various species of clay minerals and this is likely in the samples from the West Aceh Basin.

The general mineral content for West Aceh samples is given in Appendix 7.

#### **4.3.1. Mineral Matter in Oligocene Coal**

The Oligocene coal samples have a lower mineral content compared to the Miocene and Pliocene coals and in general, contain less than 1% of mineral matter, most of which is undifferentiated mineral matter and pyrite. Undifferentiated mineral matter occurs as dispersed inclusions in vitrinite and inertinite and as thin laminae interbedded with vitrite layers. Pyrite occurs as discrete disseminated particles in vitrinite macerals and as infillings in sporinite and cell lumens of textured vitrinite or inertinite. Quartz is a traces component

in the Oligocene coal.

#### **4.3.2. Mineral Matter in Miocene Coal**

Miocene coal has a slightly higher mineral content than Oligocene coal but is lower than that in Pliocene coal. The average value is 0.7% but some samples have up to 2%. Miocene coal contains dominantly undifferentiated mineral matter and lesser amounts of pyrite and quartz. Undifferentiated mineral matter commonly occurs as infillings in cell lumens of vitrinite and inertinite and as dispersed inclusions in vitrite and clarite and as thin clay layers intercalated with vitrite bands. Pyrite is rare and consists of finely disseminated aggregates in vitrinite and in layers of undifferentiated mineral matter. Trace quartz is found as detrital grains in detrovitrinite associated with undifferentiated mineral matter.

#### **4.3.3. Mineral Matter in Pliocene Coal**

The Pliocene coal has the greatest quantity and diversity of mineral matter, ranging from 0% to 19.5% of the bulk rock with an average value 3.6%. The mineral assemblages in the Pliocene coal are dominated by undifferentiated mineral matter and pyrite with lesser amounts of carbonate and quartz. The undifferentiated mineral matter is the most abundant constituent and occurs as cavity infillings in the vitrinite and inertinite or as lenses intercalated with vitrite and clarite bands.

Where mineral matter is relatively abundant, it occurs in the microlithotypes carbargilite and

carbopyrite which commonly alternate with clarite bands. Pyrite commonly occurs as framboids, nodules, discrete grains or cleat infillings in vitrinite. Pyrite-rich coals in the study area are generally associated with the overlying marine strata (Hadiyanto, *et al.*, 1986). Such associations have been recognised elsewhere (Newman and Newman, 1982; Williams and Keith, 1983; Diessel, 1986).

Quartz occurs in minor amounts as sub-angular detrital grains associated with undifferentiated mineral matter.

Carbonate nodules, mostly calcite, are associated with pyrite-rich clarite.

#### **4.4. Organic Matter Abundance in Offshore Samples**

A total 151 of Tertiary cuttings samples from eight offshore oil wells were analysed petrographically. Detailed descriptions of the type and the relative abundance of the organic matter in the cuttings samples are enclosed as Appendix 8. All maceral percentages given for DOM refer to the calculated percentages as determined by the method given in Chapter 3.

In general, the type and abundance of organic matter varies from hole to hole and from one stratigraphic interval to another. In shales, claystones and sandstone, liptinite content is dominant over vitrinite and inertinite in almost all stratigraphic intervals. This is in contrast to both coal and shaly coal where vitrinite content is more abundant than liptinite and

inertinite. The average maceral composition for each formation is given in Tables 4.4, 4.5 and 4.6.

#### **4.4.1. Tangla Formation**

Eight samples of the Tangla Formation from Tuba well and 10 samples from Meulaboh well were examined. In general, organic matter in the Tangla Formation varies between common to major (0.8% to 10%) for dispersed organic matter (DOM), common for shaly coal (0.8% to 1%) and abundant for coal (2% to 9%). The average composition of each organic matter type is given in Table 4.4. Liptinite DOM is dominant over vitrinite in the offshore samples whereas vitrinite is the most abundant maceral in both the onshore shaly coal and coal.

In the Tangla Formation samples, coal grains constitute between of 2% to 9% of the total grains. Vitrinite mostly consist of detrovitrinite and telovitrinite with detrovitrinite dominant over telovitrinite. Detrovitrinite chiefly consists of desmocollinite layers whereas telovitrinite mostly comprises telocollinite layers.

Liptinite comprises cutinite, sporinite and suberinite, which are commonly associated with vitrinite in clarite. However, cutinite and sporinite fragments are common in detrovitrinite bands. Bitumen is associated with detrovitrinite whereas exsudatinite is found in vitrinite cleats.

The fluorescence intensity of the liptinite macerals ranges from low to medium with the



dominant fluorescence colour orangish-yellow. Inertinite is rare and mostly consists of sclerotinite and inertodetrinite.

Vitrite and clarite are the most common microlithotypes in the coal grains with vitrite dominant over clarite. Vitrite mostly comprises detrovitrinite bands whereas bands of clarite are mostly composed of detrovitrinite, cutinite, sporinite and liptodetrinite.

Shaly coal grains constitute up to 1 % of the Tangla Formation. Vitrinite is the most common maceral over the liptinite and inertinite. Detrovitrinite is more common than vitrinite. Liptinite consists of cutinite, sporinite and liptodetrinite. Some oil-hazes are commonly expelled from the cutinite and sporinite in fluorescence mode.

Inertinite is very rare in shaly coal grains and mostly consists of inertodetrinite in clay bands. Clarite is more abundant over vitrite and commonly intercalated with shaly layers.

Dispersed organic matter (DOM) of the Tangla Formation mostly occurs in siltstone and claystone (0.8 to 14%) and is rare to trace in the sandstone and limestone. Liptinite is dominant over vitrinite with inertinite occurring in trace amounts.

Vitrinite content ranges from common to abundant (0.8% to 3.3%) and is chiefly composed of telovitrinite and detrovitrinite with telovitrinite dominant over detrovitrinite. Telovitrinite usually occurs as thin layers of telocollinite, less than 5 micron thick, whereas detrovitrinite commonly shows oxidation rims that may indicate that this form is reworked vitrinite. This

oxidised vitrinite commonly occurs in the sandstone.

Liptinite content in the DOM varies from abundant to major (2.1 to 14%) with an average value of 2.4%. Cutinite, sporinite, liptodetrinite, resinite, suberinite and bitumen are the dominant macerals, with cutinite and liptodetrinite the most abundant. Fragments of cutinite occur in some sandstone grains. Some of the cutinite is associated with oil-cuts which have orangish-yellow fluorescence. The fluorescence intensity of cutinite is moderate to strong with the colour ranging from yellow to brownish-yellow.

Liptodetrinite has fluorescence intensities from low to moderate with the colours ranging from brownish-yellow to orangish-yellow. Where liptodetrinite occurs in sandstone grains it is black to brown in reflected light and appears to have been reworked.

Sporinite is sparse and mostly found in siltstone and sandstone occurring as well-preserved flattened exines of miospores in fine-grained siltstone and sandstone. Some oxidised sporinite occurs in sandstone grains. Most of the sporinite has brownish-orange fluorescence of medium to low intensity.

Suberinite and resinite are rare in general and are mostly associated with liptodetrinite. Some bitumen, orangish-yellow fluorescence with shrinkage cracks, is usually in the sandstone pores but seldom in claystone or siltstone.

#### **4.4.2. Kueh Formation**

Sixty two samples of the Kueh Formation, from eight offshore wells, were analysed petrographically. The average abundance and maceral group composition are illustrated in Table 4.5. In general, most of the holes have dispersed organic matter (DOM), shaly coal and coal although neither shaly coal nor coal was recorded in Keudapasi and Palumat wells and in Tuba well shaly coal was found. The abundance and maceral composition of the Kueh Formation varies from hole to hole and from stratigraphical interval to stratigraphic interval.

Coal grains constitute from 2% to 42% (average 5%) of samples. The most abundant maceral is vitrinite, ranging from 37% to 93%, with liptinite ranging between 1% and 55%. Inertinite on the other hand, ranges between <1% to 19%. Vitrite, clarite and duroclarite are the main microlithotypes in the coals with vitrite dominant over clarite and duroclarite.

Shaly coal is abundant, comprising 0% to 2% of the total grains. In general, the shaly coal contains higher liptinite than coal and has a greater variation in the liptinite content.

Detrovitrinite and telovitrinite are the dominant vitrinite subgroups in both coal and shaly coal with detrovitrinite generally more abundant than telovitrinite except in some shaly coal samples. Most detrovitrinite comprises thin to thick layers of desmocollinite which are generally intercalated with telocolinite layers. Telovitrinite generally occurs as thin layers or as lenses in the detrovitrinite groundmass.

Liptinite in coal and shaly coal comprises sporinite (tenuisporites), resinite, liptodetrinite, suberinite, cutinite and exsudatinites. Sporinite and liptodetrinite are the dominant liptinite

macerals and usually occur in detrovitrinite. Resinite is rare and is usually present as small to large elongated bodies, parallel to the bedding, or as cell lumen fillings in vitrinite. Exsudatinites occur in cleats or cracks of telocollinite or desmocollinite.

Inertinite is rare in coal or shaly coal and mostly consists of sclerotinite, semifusinite and inertodetrinite.

Vitrinite and clarite are the typical microlithotypes in most shaly coal samples but clarite is dominant over vitrinite.

Dispersed organic matter is sparse to abundant in the Kueh Formation ranging from approximately in claystone and siltstone. In sandstone, DOM commonly is fragmented and oxidised. Liptinite is dominant over vitrinite and inertinite.

Vitrinite is rare to abundant and mostly consists of telovitrinite or detrovitrinite. Most of the inertinite is inertodetrinite.

Liptinitic DOM comprises cutinite, sporinite, liptodetrinite, telalginite and lamalginite. Cutinite is more abundant than sporinite and mainly consists of tenuicutinite, with cuticular ledges, in liptodetrinite-rich shale grains. Sporinite commonly has partially open and megaspore fragments are common in sandstone grains.

Oxidised liptodetrinite is common in sandstone grains. Poorly-preserved telalginite derived

from *Botryococcus* is present in several samples but is rare to sparse and mostly in claystone and siltstone grains.

Lamalginites were found in samples 22356, 22435 and 22442 which can be classified as lamosite oil shale. Rare to sparse lamalginites derived from acritarch cysts occur in several claystone grains.

Bitumen was found in some carbonate and sandstone pores. Most of the bitumen has shrinkage cracks and some have oils in the fractures.

#### 4.4.3. Tutut Formation

Fifty five samples from the Tutut Formation, from eight exploration oil wells, were examined and found to contain shaly coal, coal and clastic lithologies with dispersed organic matter (DOM). Shaly coal was not found in the Keudapasi, Meulaboh-East and Palumat wells.

The average abundance and maceral group composition of organic matter in the Tutut Formation are given in Table 4.6.

In general, coal is common to major whereas shaly coal is absent to common. Vitrinite is dominant over liptinite with inertinite a minor component in both coal and shaly coal. Vitrinite abundance ranges between 67% to 90% and 70% to 90% in the coal and shaly coal respectively. Vitrinite is mainly detrovitrinite and telovitrinite and lesser amounts of

gelovitrinite. Detrovitrinite is dominant over telovitrinite in both coal and shaly coal; it mostly consists of desmocollinite with minor attrinite and densinite which occur as intercalated layers. Desmocollinite is commonly darker in reflected light compared to the other vitrinite macerals. Desmocollinite has weak brownish-yellow fluorescence.

Telocollinite is the most abundance telovitrinite maceral in both coal and shaly coal. Textinite, texto-ulminite and eu-ulminite are common in almost all samples examined. In some of the samples, textinite has a reddish colour in reflected light with most of the cell walls thickened. The cell lumens are collapsed and filled with gelovitrinite and liptodetrinite as well as mineral matrix. Resinous vitrinite is commonly associated with framboidal pyrite.

Inertinite is generally not abundant in either coal or shaly coal and consists mostly of inertodetrinite with trace semifusinite.

Vitrite is the dominant microlithotype over clarite in coal but in shaly coal clarite is dominant.

The average abundance of dispersed organic matter in the Tutut Formation varies between 0.7% and 6% (common to abundant categories) and is dominated by liptinite except in the Tuba and Tripa wells where vitrinite is dominant over liptinite and inertinite. Inertinite content does not exceed 3% in the Teunom, Bubon and Meulaboh wells and is absent in the Keudapasi, Meulaboh East, Tuba, Tripa and Palumat wells. Vitrinite commonly consists of grains of less than 10 micron and it is difficult to distinguish into submaceral. Detrovitrinite is dominant over telovitrinite with some sandstone grains containing oxidized detrovitrinite.

Telovitrinite mostly consists of telovitrinite bands in claystone and siltstone grain. Inertinite is rare to sparse and consists of inertodetrinite.

Except in the Tuba and Tripa wells, liptinite is rare to major in the Tutut Formation and consists of cutinite, sporinite, liptodetrinite, resinite, and suberinite. Alginite, fluorinite, exsudatinite and bitumen are minor but significant components in some samples. Cutinite with cuticular ledges is crassicutinite derived from leaf tissue. Thin cutinite (tenuicutinite) is a minor component.

Sporinite is usually open (tenuispores) and several samples contain sporangium which are found in liptite bands and usually occur in the shaly coal. Liptodetrinite occurs in clarite in coal and shaly coal but is scattered in DOM. Suberinite mostly occurs in the coal and is associated with phlobaphinite. Resinite is usually small to large elongated or ellipsoid bodies in vitrinite and inertinite in clarite bands.

Fluorinite commonly occurs as small to large rounded bodies in the vitrinite maceral with some filling vitrinite lumens. Exsudatinite mostly fills fractures in telocollinite or desmocollinite bands. Bitumen mostly occurs in the detrovitrinite matrix as globular, elongated or cauliflower forms. Telalginite, derived from *Botryococcus*, occurs mostly in the detrovitrinite groundmass and in mineral-rich grains. Telalginite fragments are commonly associated with liptodetrinite in shaly coal.

Trace lamalginite, derived from acritarch cysts, was recognized in the shaly coal and also in fine-grained siltstone, claystone and limestone grains.

#### 4.4. Vitrinite Reflectance and Rank of Coal Samples

Vitrinite reflectance ( $R_v$ , max) data were obtained to determine the rank of coal and shaly coal and the maturity of potential source rocks in the West Aceh basin. The use of vitrinite reflectance as an indicator of rank has been applied elsewhere (Stach, 1982; Teichmuller, 1950; Diessel, 1973; Kantsler, *et al.*, 1978; Bostick, 1979; Smith and Cook, 1980; Hunt, 1979; Tissot, 1974). Using mean maximum vitrinite reflectance, an assessment of coal rank is possible because vitrinite undergoes changes at a consistent rate in time in response to the general trend of organic metamorphism (Smith and Cook, 1980; Smith, 1981 and Bostick, 1974). It is believed that coal rank is a sensitive indicator of low temperature-low pressure burial metamorphism below greenschist facies in sedimentary sequences (Diessel, 1973; Teichmuller, 1974; Smith, 1982). Rank classification using several parameters, including vitrinite reflectance, is given in Table 4.7 (Heroux, *et al.*, 1979).

Vitrinite reflectance data obtained for this study are listed in Appendices 8 and 9. The data indicate a brown coal stage for most of the Miocene and Pliocene samples from the West Aceh Basin and brown coal to sub-bituminous stage for the Oligocene samples. However, Pliocene coal has a fairly wide scatter of reflectance values ranging from the peat stage to brown coal stage. A detailed discussion of the vitrinite reflectance and the implications for maturation patterns, and petroleum generation potential, of the West Aceh Basin sequences



is given in Chapter 5.

#### **4.4.1. Oligocene Coal**

The vitrinite reflectance data for outcrop coal samples, show that the Oligocene coal has reached the sub-bituminous stage, with reflectance values ranging between 0.50% to 0.60% (ACH Figure 4) with a small number with readings up to 0.80% and thus falling within the high volatile bituminous stage.

In contrast, the limited number of coal cuttings from offshore-drill holes tend to have vitrinite reflectances lower than those from the onshore area. The highest reflectance value in examined samples in the offshore area did not exceed than 60%.

#### **4.4.2. Miocene Coal**

The reflectance values obtained for the onshore Miocene coal mostly indicate a coalification stage of brown coal with the highest frequency of values falling in the 0.35% to 0.40% range (ACH Figure ). A few values within the sub-bituminous stage, ranging from 0.41% to 0.50%, were obtained and one sample gave a reflectance of 1.15% (GM 23243). The reason for this abnormal reflectance is thought to be a function of thermal elevation due to the occurrence of a dyke in the area where the sample is located.

Compared to the onshore samples, the offshore samples have lower reflectance values

indicating a lower rank, that of brown coal with the range of values lying between 0.30 and 0.35%.

#### **4.4.3. Pliocene Coal**

The onshore Pliocene coal has a fairly wide scatter of reflectance values indicating a coalification stage from peat to brown coal. Most of the Pliocene coal has a reflectance in the range of 0.26% to 0.35% ACH Figure ), thus falling in to brown coal stage, with a few of the samples having lower vitrinite reflectance between 0.20%-.25% and a smaller number of samples with very low values lying between 0.15% and 0.19%.

Th vitrinite reflectance values for offshore Pliocene coal range between 0.15 to 0.30% or generally below those of the onshore samples. It is of note that the rank trends of the offshore versus onshore samples for the Oligocene, Miocene and Pliocene coals is similar, suggesting similar coalification paths for each.

### **4.6. Discussion**

#### **4.6.1. The Origin and Occurrence of Exsudatinite and Bitumen**

The occurrence of exsudatinite and bitumen in coal and carbonaceous shale samples from the West Aceh Basin has not been reported until the present study. Although the general characteristics of these macerals has been mentioned in this chapter previously, a discussion

in relation to the possible origin and mode of occurrence of both is needed.

#### 4.6.1.1. Exsudatinitite

Exsudatinitite has been recognized in Oligocene, Miocene and Pliocene coal and carbonaceous shales which vary in rank from peat/marginal brown coal to sub-bituminous coal (0.25 % to 0.65 %  $R_{\text{max}}$ ). A summary and detailed, sample by sample, percentage of exsudatinitite are given in ACH Table 4 and Appendices 4, 5 and 6 respectively.

Although the average abundance of exsudatinitite is less than 1.5%, most samples contain exsudatinitite in trace quantities with some samples containing up to 5% (GM 22017 and GM 23232). Based on mode of occurrence (Plate IV), exsudatinitite can be categorized into two types. Type I consists of exsudatinitite which fills cracks, cleats or cavities at the edges of the parent or precursor maceral. Some of this "exsudatinitite" is at least partly soluble as witnessed by its solubility in immersion oil but it is still regarded as exsudatinitite.

For Type I, the shape varies depending on the size of the unfilled pore, cleat or crack. This exsudatinitite is mostly derived from resinite and cutinite (Plate IV-1 and IV-6). In some situations, this exsudatinitite occurs at the edge of grains, usually as globular or spherical because it is thermoplastic and expands into the polyester resin before the latter sets and it is thus able to assume such shapes because it solidifies in relatively free space. It is usually derived from resinite bodies which are parallel to the bedding planes (Plate IV-2) or resinite\sporinite-rich clarite (Plate IV-3). Exsudatinitite derived from liptodetrinite-rich clarite generally occurs as globular forms in the detrovitinite groundmass (Plate IV-4); exsudatinitite

derived from suberinite mostly occurs in the Pliocene coal and it is commonly parallel to the suberinite layers (Plate IV-5). Soluble exsudatinites are commonly associated with sporinite (Plate IV-6), cutinite, exsudatinites (Plate IV-7) and desmocollinites (Plate IV-8).

In general, Type I exsudatinites have lower relief than vitrinite, are transparent in reflected light, have moderate fluorescence ranging from greenish-yellow to yellow. The fluorescence intensity of the nonsoluble forms is commonly weaker than that of the parent maceral and also shows a cloudy appearance. By contrast, the soluble exsudatinites have stronger fluorescence intensity than that of the parent maceral and commonly are associated with oil smears. Reflectance ranges from 0.05% to 0.1%.

Type II exsudatinites occur either in the cleats of vitrinite macerals, such as telocollinites or desmocollinites, which contain mineral matter, including, commonly, framboidal pyrite (Plate V-1), or as isolated rounded, oval or cauliflower-shaped bodies associated with detrovitrinite macerals, such as densinites, and porigelinites (Plate V-3 to V-5). The parent maceral for the Type II exsudatinites is uncertain although, like Type I, it is of secondary origin.

For Type II, relief is moderate, commonly equal to that of vitrinite and it is grey in reflected light. Fluorescence colours are yellow to orangish-yellow with moderate to high intensity. Most of this type of exsudatinites has varying fluorescence colours and intensities in the one grain. Colours commonly appear paler and intensities weaker toward the centre of the exsudatinites where they occur in fractures (Figure V-1). However, in oval or cauliflower forms (Plate V-2 and V-3), the colours appear to be brighter, with stronger intensity toward the edges. These edge effects may simply be a function of volume or thickness of the

exsudatinite entity. The reflectance of Type II exsudatinite is commonly less than 0.1%.

The most distinguishing features between the two types of exsudatinite are the shrinkage cracks and vesicles that are found in Type II. These are most abundant in Pliocene coal.

A mechanism for the occurrence of exsudatinite in the brown coal from the Baise Basin, South China, has been proposed recently by Zhao, *et al.*, (1989) after a study involving spectral fluorescence techniques. They stated that the fluorescence intensity and colour of exsudatinite varies from type to type depending on the precursor of the exsudatinite and suggested that fluorescence colour normally shifts towards longer wavelengths, from greenish-yellow to yellowish-orange, after irradiation for thirty minutes.

Zhao *et al.* (1989) argued that the weaker fluorescence intensity and the longer wavelength of the exsudatinite, compared to the precursor maceral, is caused by the removal of lighter (lower molecular weight) component or fractions as a result of differentiation during primary migration. Therefore, the heavier components, with a higher aromaticity, remain in the non-migrated exsudatinite. They also found that the change in fluorescence intensity at 546 nm is accompanied by positive alteration.

Teichmuller and Wolf (1977) also suggested that shifts in the wavelength of macerals, irradiated for various periods of time, is a result of decreasing hydrogen content due to the escape of more volatile components.

Although the quantitative measurements were not conducted to examine the variation and

alteration of the fluorescence intensity in the West Aceh Basin samples, the hypothesis for the mechanism of exsudatinite formation is assumed to be the same as for the exsudatinite observed by Zhao *et al.* (1989), given that the same colour changes can be observed in the West Aceh basin samples, although only qualitatively.

As stated earlier, Type I exsudatinite is suggested to be an exudate material from parent macerals such as resinite, cutinite suberinite and sporinite and occurs in microlithotypes such as resinite-rich clarite and liptodetrinite-rich clarite. Evidence indicates, as can be seen in Plate V-1 to V-6, that most of the fluorescence intensity of the exsudatinite is lower and the colour is lighter than the corresponding features of the parent maceral. This may indicate, as suggested by Zhao *et al.* (1989), that the lighter component migrated away from the solid exsudatinite and resulted in the weaker fluorescence intensity because of changes in the molecular composition of the exsudatinite. If this is the case, it is likely that there are two generations of exsudatinite or at least two stages in the evolution of exsudatinite. The first generation exsudatinite migrates from the parent maceral and is trapped either in cracks, cleats or at the edge of the parent maceral as seen in Figure V-2 and V-3 (where the exsudatinite is shown to be expelled from the resinite and suberinite, respectively) and is trapped near the parent maceral. Some time later, the mobile exsudatinite molecules migrate away leaving a higher molecular weight fraction. The different fluorescence characteristics within the exsudatinite, especially the stronger intensity phase, indicate the second generation exsudatinite is a more labile or soluble form that migrated towards the margins and away from the first generation exsudatinite before, or after, it solidified. This argument is supported by the evidence of soluble exudates as illustrated in Plate V-7 and V-5.

Another possibility for such bimodal occurrences of exsudatinite may be related to differentiation of the exsudatinite that is produced from the parent maceral. If two phases of exsudatinite are formed at once, the more viscous and less soluble, heavier fraction, will form a core during the relatively short migration\expulsion. However, lighter, more mobile components would accumulate near the outer margins of the exsudatinite on the outside of the heavier component, resulting in differing fluorescence characteristics within the exsudatinite.

Plate V-7 shows an oil expulsion from sporinite after irradiated with UV-blue light excitation for several minutes. Two fluorescence intensities can be seen - a weaker fluorescence intensity adjacent to the outer spore exine and a second, stronger fluorescence intensity further away; this is interpreted as indicating two phases of organic matter.

A similar situation, but with different effects, is seen with desmocollinite in Figure V-8 which was irradiated for 5 minutes. The weaker fluorescence intensity occurs near the centre of the field with stronger fluorescence away from the centre. This is interpreted as follows. It is likely that the lighter, more volatile and less viscous components migrate away from the parent macerals which are more aromatic, heavier and more viscous components which are unlikely to migrate long distances. Given that this is a suitable explanation for the "artificial" differentiation of exsudatinite, it is not unreasonable to suggest that similar processes take place during natural coalification and that the natural petrographic associations of exsudatinite as discussed above have resulted from the same types of processes as observed under the microscope during irradiation with UV-blue excitation and shown in Plate V-7 and V-8.

As mentioned previously that the main features distinguishing the two types of exsudatinite are the shrinkage cracks and vesicle associated with the Type II. Both characteristics mostly occur in globular, rounded or cauliflower forms where fluorescence intensities are weaker toward to the boundary of the vesicles or near the shrinkage cracks (Plate I, 1a-2b). In many cases the immersion oil is cloudy and a "smeary" fluorescence covers the shrinkage cracks and vesicles. This implies that the soluble phase releases some of the volatile or labile components which may only be partly miscible.

During coalification, the release of volatile components results in a decreased volume for the residual exsudatinite and shrinkage cracks form when solidification has been completed. If the volatile components are unable to escape, vesicles form.

#### **4.6.1.2. Bitumen**

The occurrence of solid bitumen in clastic rocks is considered to be a secondary product that migrated into pores, fractures or shells of fossils (Jacob, 1976, 1981, 1989). Teichmüller (1974, 1982) suggested that the occurrence of the secondary maceral bitumen is related to the thermal transformation of the primary constituent or maceral during coalification and is equivalent to organic matter termed exsudatinite in coal.

Robert (1981) defined bitumen as a polycondensed hydrocarbon, which is either solid and insoluble in organic solvents and mostly has been deposited in a liquid form which has condensed and consolidated. The occurrence can either be syngenetic as in inclusions,



segregation in petroliferous facies, filling fissures, microorganism chambers and interstratified beds or epigenetic, such as in the pores of reservoir-rocks where they have been deposited during hydrocarbon migration (Robert, 1981).

Jacob (1989) classified bitumen into types as is given in Table 4.6. The classification is based on parameters such as reflectance, intensity of fluorescence, microsolubility and micro-flowpoint and calibrated to the macrosystem proposed by Abraham (1960). Jacob (1989) related between vitrinite reflectance (%) against bitumen reflectance (%) from various part of the countries as is given in Figure 4.10.

Using Jacob's diagram as shown in Figure 4.10, it is likely that most bitumen in the West Aceh Basin samples falls into the asphalt/asphaltites categories since most of the vitrinite reflectance less than 0.6%.

Using morphology, reflectance, fluorescence colour and intensity and the association of bitumen within the clastic rocks, two forms of bitumen can be recognised as was the case for exsudatinite. In general, the globular, rounded, oval and cauliflower shapes or irregular forms are associated with fine-grained sedimentary rocks such as shale, claystone and siltstone. This type of bitumen occurs as inclusions, isolated bodies or diffuse masses (Plate, VI-1 to VI4). The size varies from 10 microns to 80 microns with relief commonly higher than vitrinite. The reflectance ranges from 0.08% to 0.1%. Fluorescence colours vary from greenish-yellow to yellow, however, some bitumen in the Oligocene Tangla Formation has orangish-yellow fluorescence. The fluorescence intensity is commonly weak. Shrinkage

fractures are common in these forms. Fluorescence colour and intensity do not vary within the same grain.

Under UV-blue light excitation for approximately 30 minutes, the fluorescence colour and fluorescence intensities mostly remain constant. However, in a small number of cases, the bitumen has slightly different colours in some parts of the same entity and expels soluble fractions to the surrounding area (Plate VI-4).

The second type of bitumen is generally found in cavities, fractures or pores in coarse-grained sandstone, carbonate rocks and microfossil shells (Plate VI-5 to VI-8). Relief is commonly lower than for vitrinite. The reflectance values mostly range from 0.1% to 0.2%. Fluorescence colour varies ranging from green to yellow but is generally paler, although the intensity is stronger, than for the previous forms. Evidence indicates that most fluorescence intensity and colour varies within one grain and many of the soluble bitumen were expelled after irradiated using UV-blue light for approximately 30 minutes (Plate VI-6 and VI-7).

If it is accepted that the mechanism and mode of occurrence of the bitumen is similar to those of the exsudatinite and the parent material was the same, as stated by Teichmüller, it is likely that two different groups of bitumen formed in much the same way as exsudatinite and the two forms, although having different optical properties, are differentiation products.

The optical properties suggest that the bitumen shown in Plate VI-1 to VI-4 has a relatively high viscosity and is mostly insoluble. The shrinkage cracks may have formed as a result of

devolatilisation during the solidification process (Plate VI-1 to VI-3). It is interesting to note that this type of bitumen is commonly associated with fine-grained sedimentary rocks such as shale, claystone and siltstone which usually have abundant liptinite macerals. This, in turn, leads to the assumption that the source of the bitumen could be the liptinite macerals. This argument is supported by the evidence in Plate VI-4 where soluble bitumen is expelled from cutinite in shale after being irradiated using UV-blue light for approximately 15 minutes. If the same process, namely thermal heating, is the major factor expelling bitumen from the primary maceral in the natural coalification processes, as suggested by many researchers, it would be reasonable to assume that the bitumen associated with the fine-grained clastic rocks originated from the macerals in the those rocks.

It is likely that migration pathway from the source material was short because of the high viscosity and low solubility of the bitumen. Since the porosity and permeability of fine-grained sediment are low, the sediment will act as a barrier or cap for the further migration. Only gas or volatile matter will move any significant distance from the parent maceral and this would result in a decreased volume for the bitumen. This subsequent loss of soluble matter leads to the development of shrinkage cracks. Some of the bitumen may also contain significantly different chemical compounds whereby the lighter components migrate farther from the source and/or from the heavier components (as shown by the different fluorescence colours and intensities within the one grain).

Zhao *et al.* (1989) argued that differences in fluorescence colour is due to the different aromatic content of the liquid-derived bitumen or exsudatinite. Hence, it is may reasonable

to assume that this type of bitumen contains a more homogeneous chemical composition and the fluorescence colour and intensity are therefore more constant.

More labile and less viscous liquid components may continue to migrate after the bitumen was trapped in sandstone pores (Plate, VI-5 and Plate, VI-6), foraminiferal shells (Plate VI-7) and cavities in carbonate grains (Plate VI-8). Fluorescence colours and intensities of bitumen in sandstone are more variable than in the finer grained rocks. This evidence supports the argument that more mobile and lighter components occur in this type of bitumen than in the first group. It is likely that this type of bitumen migrated farther away from the source before finally being trapped in the pores or fossil chambers as illustrated (Plate VI-4 to VI-8). The labile component are able to migrate further as the bitumen undergoes additional thermal heating. This argument is supported by the evidence in Plate VI-6 and VI-7 in which the soluble components were expelled after irradiating the bitumen for approximately 15 minutes. This suggests that some labile components may still be associated with stable components in this bitumen, as indicated by the different fluorescence intensity and colour after UV-blue irradiation.

Plate VI-5 and VI-8 shows a field that was irradiated for 60 minutes. During this time, there was no indication of additional colour alteration in the bitumen apart from a slight change that occurred during the first minute of irradiation. The bitumen has variable fluorescence colour and intensity. The photographs are believed to show that the lighter and stronger fluorescence reflect areas where the labile component had migrated away whereas the paler colour and weaker intensity show bitumen that contains more aromatic components (which

remain in the sandstone pore and carbonate rocks respectively). This suggestion is similar to the explanation given for exsudatinite formation in the South China brown coal (Zhao *et al.*, 1989).

#### 4.6.2. Maceral Distribution and Coalification

Numerous studies on the organic petrology of the coals in Indonesian Tertiary basins have been conducted (Daulay, 1986; Esterle *et al.*, 1986; Daulay and Cook, 1988; Hadiyanto, 1988; Esterle, 1990; Panggabean, 1990; Hadiyanto and Cook, 1991; Hadiyanto *et al.*, 1986; Amir, 1991; Sutrisman, 1991; Hadiyanto *et al.*, 1992). In general, it can be concluded that most of the Indonesian Tertiary coals are rich in vitrinite and show little variation in maceral composition from basin to basin as well as within the basin itself. Compared to other overseas Tertiary coals, Indonesian coals are most like those of West Germany, Taiwan, New Zealand, Victoria and some South Korea deposits (Daulay and Cook, 1988). It is quite different from the Turkish, Indian and Canadian coal deposits (Mishra, 1986; Panggabean, 1990).

The most abundant maceral group in Indonesian coals is vitrinite which ranges between 50% and 90% with the most important subgroups being telovitrinite and detrovitrinite. Telovitrinite mostly consists of telocollinite although textinite, texto-ulminite and eu-ulminite are more dominant in the Pliocene coal than in either the Miocene and Oligocene coals. In contrast, the Oligocene coal contains more telocollinite than the Miocene and Pliocene coals.

Among the detrovitrinite macerals, desmocollinite is dominant over attrinite and densinite in the Miocene and Oligocene coals . In contrast, attrinite is the most abundant detrovitrinite maceral in the Pliocene coal.

Although gelovitrinite is a minor vitrinite maceral in West Aceh Basin coals, corpogelinite and porigelinite are more abundant in the Pliocene coal than in either the Miocene and Oligocene coal.

Although the maceral compositions of Tertiary coals in Indonesia are not very diverse, closer examination indicates that liptinite is more abundant in West Aceh Basin coals than in coals from other Tertiary basins of Indonesia and is similar to that in South Korean coals (Figures 4.6 to 4.8).

Studies of maceral composition, especially vitrinite, in Indonesian Tertiary coals has not been conducted yet in detail. Most of the early investigations have only focused on the general maceral composition without any detailed observation of the optical characteristics of the specific vitrinite macerals such the telovitrinite and detrovitrinite subgroups. Such a study may offer a better understanding of the coalification processes, which involve the effects of biogenic and geochemical influences (Teichmüller, 1982), within the sedimentary basins.

The West Aceh Basin, where the rank of the coal ranges from transitional peat-lignite to the bituminous stage, offers a good opportunity to study coalification processes and to assess the maceral products petrographically.

Texturally, the telovitrinite subgroup in most of the Pliocene coal exhibits an open cell structure, with the cell walls swollen and some of the lumens filled with corpogelinite, porigelinite and to a lesser extent resinite. The cell walls of the woody tissue in both Miocene and Oligocene coals are commonly more compressed and cemented resulting in the appearance of a more homogenised maceral which is recognised as telocollinite. In a few of the samples, however, gelification and liptinite macerals are enclosed within the compressed cell lumens.

Another feature of the West Aceh Basin coals is the high proportion of detrovitrinite macerals, reflected by the different proportions of attrinite, densinite and desmocollinite. As mentioned earlier, the Pliocene coal has more detrital macerals than the Miocene and Oligocene coals.

Microscopically, the ratio of coarse detrovitrinite (framework) to the finer detrovitrinite (matrix) in the Pliocene coal is greater than the same ratio in Miocene and Oligocene coals. The Pliocene coal also exhibits a looser packing of the larger macerals as well as within the framework detrovitrinite matrix. In contrast, the Oligocene and Miocene coals have more collapsed structures and more compacted gelified matter than Pliocene coal. These differences in the petrographic features may reflect different coalification processes during peat accumulation as outlined by Stach (1982) and Diessel (1985) who stated coalification processes which involve humification and gelification produce distinct maceral assemblages within the peat swamp.

The products formed first during the biochemical stage of coalification, that is, during deposition and early diagenesis, are related to the type of plant material in the peat, the extent of biochemical and chemical alteration as well as the climate and edaphic conditions in the mire (Cook, 1982; Hunt, *et al.*, 1986). During humification processes, plant tissues are transformed into humic acids as a result of slow partial oxidation as well as micro-organism activity; this usually occurs at or near the peat surface (Liu *et al.*, 1982). Further, the humic material becomes capable of passing at least partially into true or colloidal aqueous solution due to the oxidative changes, including the formation of the acidic carboxyl group (Liu *et al.*, 1982; Stach, 1982). On the other hand, gelification process may not be entirely distinguishable from the humification process and it may be a continuation of the humification process that leads to the formation of vitrinite in the sub-bituminous stage (Stach, 1982).

Teichmüller (1954) suggested that during gelification the changes appear to be predominantly of a physio-colloidal nature which can be recognised under the microscope by the swollen appearance of the highly homogenised cell walls which are the latest product of compression and cementation processes. In addition, gelification occurs throughout the desiccation stage of humified material, whether that humified material has remained in situ or has been transported and redistributed as colloidal humic matter (Liu *et al.*, 1982). In the case where the humified matter remains in situ, the morphology of the original plant tissue is preserved resulting in the transformation from textinite to texto-ulminite to eu-ulminite with telocollinite as the latest product.

In contrast, transported colloidal humic matter produces a gelified material which is



morphologically unrelated to the parent plant material. This will change attrinite to densinite and finally desmocolinite through a process of cementing colloidal gels (Stach, 1982; Liu *et al.*, 1982).

In addition, gelification can be related to the rank of the coal and is a function of biochemical and geochemical gelification. The first stage occurs in the peat and soft brown coal stages and is influenced by the original plant material, plant ecology, water, ion supply, degree of alkalinity and oxidation conditions (Teichmüller, 1954; Stach, 1982; Liu *et al.*, 1982). The second stage is related to raised temperatures and possibly pressure (due to burial) and occurs in the boundary between brown coal and bituminous coal stages.

The Pliocene coal, and to a lesser extent in the Miocene coal, contains well-preserved, often cellular botanical structures in textinite and textolinite macerals. The well-preserved cellular botanical structures suggest that the coal has undergone minimal change after the peat stage and that it has been subjected to less intensive change by either by bacterial activity or the degree of oxidation in the peat swamp.

In contrast, Oligocene coal has more telovitrinite than either the Miocene and Pliocene coal, probably as a result of more intensive compaction during coalification. In this case, most of the cell walls are compressed and flattened and many lumens have coalesced together to form massive and structureless telocollinite, something that may have occurred during geochemical gelification (Teichmüller, 1982).

With reference to attrinite, densinite and desmocolinite, the Pliocene coal tends to have more unpacked detrital attrinite than the Oligocene and Miocene coals. Conversely, desmocolinite, which is a product of compressed colloidal humic matter, is more dominant in the Oligocene coal. This suggests that the Oligocene coal has undergone more intensive coalification than the Miocene and Pliocene coals. Therefore, the Oligocene coal is likely to have reached the geochemical coalification stage whereas the Pliocene coal, and the Miocene coal to a lesser extent, have only reached the biochemical coalification stage.

Maceral composition, especially telovitrinite and detrovitrinite, is partly rank related (ACH Figure 4.5.4) which is common for many low rank coals. As rank increases the combined percentage of textinite, textu-ulminite and attrinite decreases although the plot shows a considerably scattered data population. Some of the Pliocene coals do not follow the general trend of this relationship. In these apparently anomalous samples the environment of deposition rather than coalification may have been of greater importance. However, it is clear that rank is also partly related to the age of coal and thus probably depth of burial. The Oligocene coal has the highest rank and all samples fall into one group; the lower rank Miocene coal subset partly overlaps the Pliocene coal. This suggests that the degree of gelification is both rank and age related. From the two relationships cited above, it can be assumed that, as coalification progressed, the role of compaction and gelification became more important and produced closed cell lumen in the woody tissue during the transformation of textinite to the telocollinite.

The influence of palaeo-environmental conditions on the occurrence of telocollinite and

desmocollinite may also be a possible factor. Rimmer and Davis (1988) suggested that the occurrence of telocollinite and desmocollinite macerals is correlated with the pH/Eh of water in the peat swamps, as well as the rate of subsidence. In basins where rapid subsidence and acidic conditions are dominant, telocollinite macerals will be well preserved but in areas with lower subsidence rates and more natural or oxidising conditions, possibly within areas that experienced fluctuating water levels, tissues are less well preserved because of partial subaerial exposure (Rimmer and Davis, 1988). In addition, the compaction process is likely to have been more intense in the Oligocene coal compared to both Miocene and Pliocene coal due to the depth of burial influence.

Similar studies in relating the coal rank to the amount of textinite, texto-ulminite and attrinite have also been conducted on Greek Brown coals. Cameron *et al.* (1984) concluded that as rank, as measured by vitrinite reflectance ( $R_{vmax}$ ), increased, the open textured and porous ulminite macerals decreased.

The West Aceh Basin coals do not have a diverse liptinite or inertinite content. Iertinite fragments are associated with the fragments of cutinite and sporinite that are embedded in the detrovitrinite groundmass. This suggests physical breakdown of inertinite and liptinite to form allochthonous products that are not necessarily transported long distances. Although some individual samples show substantial inertinite and liptinite contents, the general trends indicate that such apparently anomalous percentages may be caused by local influences within the swamp during peat deposition rather than global climatic changes or plant evolution during the Tertiary period. The various amounts of inertinite may reflect different intensities

of oxidative decomposition in the peat swamp, as well as sub-aerial oxidation due to drying out of the peat surface or lowering of the water table. Different periods of inundation by oxygenated water may also influence to the inertinite content (Stach *et al.*, 1982).

The Pliocene coal has more liptinite than the Oligocene and Miocene coals and are canneloid in part (for example, samples 21988, 22845, 22034, 22850, 22843, 22009, 22019 (Pliocene coal), 23240, 22820 (Miocene coal) and 23232 (Oligocene coal)).

The occurrence of the canneloid coal represents aquatic or sub-aquatic conditions, or possibly more herbaceous vegetation was incorporated into existing peat accumulations. Thus, the different composition within the Tertiary coal may also be due to facies related coal environments.

Diessel (1984) proposed a correlation between coal facies and depositional environment to assess the prevailing swamp type, the height of the water tables, the preservation of cell-tissues and the degree of oxidation and degradation due to transport. He used facies-critical macerals such as telocollinite, tellinite, desmocollinite, fusinite, semifusinite, inertodetrinite and macrinite to construct "Petrographic Indices" such as the Tissue Preservation Index and the Gelification Index. Based on Diessel's facies diagram, a forest moor depositional environment is suggested for samples from the West Aceh Basin (ACH Figure 4.5.6).

In general, most of the Tertiary coals have gelification indices of greater than 5. However, the Pliocene coal has a more variable tree preservation index than Oligocene and Miocene

coals. The Pliocene coal, therefore, was deposited in wet conditions in a forest swamp which gradually shifted toward dryer conditions. These conditions may reflect a range of environments deposition from lower delta plain to the upper delta plain and alluvial valley (Diessel, 1986; Kalkreuth *et al.*, 1990).

Fen-like depositional environments probably occurred during most of the Oligocene, and some Pliocene coals were deposited in areas resulting in high gelification indices and somewhat moderate tree preservation indices. This type of coal is commonly characterised by a large input of aquatic plants such as reeds and sedges (Kalkreuth *et al.*, 1990).

Recent studies have cast some doubt on the validity of maceral ratios as indicators of environments of deposition. For example, Crosdale (1992) studied late Early Miocene coal from the Maryville Coal Measures of New Zealand and argued that current coal maceral interpretations are inconsistent with modern tropical ombrogenous mires and difficulty is encountered if the principles are used for ancient systems. These problems may lead to erroneous interpretations of environments of deposition.

In addition to the maceral composition of the coal and shaly coal, the relative abundance and distribution of the dispersed organic matter of the Tertiary sequences varies from formation to formation, as well as within each the formation. A summary of the average abundance and maceral group composition of organic matter in the Tertiary formations from the eight offshore drill-holes in the West Aceh Basin is given in ACH Table 4... and illustrated in Figure 4.... to Figure 4.....

In general, most of the dispersed organic matter contained in the Tangla, Kueh and Tutut Formations is of land plant origin. However, liptinite macerals are derived from a wide range of organisms including marine acritarchs, non-marine algae and higher plants of non marine origin.

Unlike coal and shaly coal, the dispersed organic matter is composed mainly of liptinite which is dominant over vitrinite and inertinite in almost all of the Tertiary formations examined with the exception of the Kueh and Tutut Formations in the Meulaboh, Tuba and Tripa wells; these have slightly more vitrinite macerals than liptinite.

Liptinite macerals comprising dispersed organic matter consists of a wide range of structured and nonstructured liptinite. Structured liptinite consists of cutinite, sporinite, suberinite, liptodetrinite, telalginite, lamalginite and acritarchs. Unstructured liptinite comprises resinite, fluorinite and bitumen. The unstructured liptinite commonly occurs associated with the structured liptinite.

Most of the liptinite macerals are disseminated in claystone, siltstone and carbonaceous claystone which were deposited in terrestrial, deltaic and marine environments. However, in general the quantity of dispersed organic matter decreases away from the land, except for the some structured liptinite such as acritarch and lamalginite macerals. The average abundance of liptinite macerals in the Tangla Formation is about 0.2% to 1.8% (average 0.8%) of the total rock whereas the Kueh and Tutut Formations have liptinite abundances between 0.5% to 1% (average 0.6%) and 0.5% to 2.1% (average 1.6%) respectively .

The most abundant liptinite maceral is cutinite and sporinite. Some liptinite, both structured or unstructured liptinite, has a distinctive degraded appearance. Cutinite mostly occurs in the fine-grained sediments such as siltstone, claystone and carbonaceous mudstone either as well-preserved or degraded leaf cuticle. Fragmented cutinite, some with oxidised rims, occurs in the coarse-grained rocks such as sandstone. Thick-walled crassicutinite mostly occurs in the Tutut Formation whereas thin-walled tenuicutinite is the common cutinite in both the Tangla and Kueh Formations.

As with cutinite, sporinite commonly occurs in the fine-grained clastic sediments but is mostly associated with carbonaceous mudstone. Sporinite that occurs in sandstone shows some evidence of physical degradation and oxidation. Microspores are the common sporinite in the Tertiary formations but some megaspore are also present.

In the Tangla Formation, most of the sporinite is flattened and most of the sporinite have mineral matter which infills the central cavities. In contrast, most of the sporinite in the Kueh and Tutut Formations lack this mineral matter. However, most of the exine in the Kueh Formation is more compacted than that in the Tutut Formation but it is not as flattened as that in the Tangla Formation. In addition, pollen grains are common in the Tutut Formation but rare in both Kueh and Tangla Formations. Sporinite content decreases downward in the Tangla Formation and, as well, decreases towards the offshore areas in all formations.

## CHAPTER 5

### MATURITY OF THE WEST ACEH BASIN SEQUENCE

#### 5.1. Introduction

The rank or maturity of sedimentary rocks containing organic matter can be determined by various methods and is used as one parametric in the determination of the hydrocarbon potential of sedimentary basins. The use of vitrinite reflectance as a maturity indicator is a reliable indicator because changes are rectilinear and can be correlated with coalification. Vitrinite is usually present, although small quantities in many cases, in sedimentary rocks, occurring either as dispersed organic matter or as component of coaly lenses. a rank stage It is more sensitive than other minerals to changes in temperature but is not very sensitive to pressure changes (Teichmuller and Teichmuller, 1968; Kisch, 1969; Burgess, 1974; Kanstler *et al.*, 1978; Murchison *et al.*, 1985). Kanstler *et al.* (1978) suggested that the alteration of organic matter in sedimentary rocks resulted in the expulsion of oil and gas due to geothermal heating over long periods of time. Temperature is the critical factor affecting chemical reactions during the alteration of organic matter, while the effect of pressure is confined to compression and consolidation accompanied by losses of volume and moisture from the organic matter in the rock (Teichmuller and Teichmuller, 1968; Murchison *et al.*, 1985).

Many attempts have been made to correlate physical and chemical rank parameters in order



to established a reliable and predictive maturation indicator in relation to the generation of hydrocarbon. Heroux *et al.* (1979) compiled a rank stage classification based on physical and chemical parameters, such as vitrinite reflectance ( $R_v$ max), Tmax (rock-eval), T.A.I. (Thermal Alteration Index) and spore colour, and related the stages to the maturation of hydrocarbons (Figure 5.1).

Although vitrinite reflectance was found to be the most useful parameter obtained for this study, the maturation indices resulting from Rock-Eval analyses (Tmax) were also employed to some extent for comparison with the vitrinite reflectance data in order to evaluate the organic maturation level within the West Aceh Basin.

## 5.2. Rank-Depth Relations

Reflectance values for organic matter in the West Aceh Basin obtained from eight offshore wells and twelve onshore wells are given in Appendices 9 and 10 respectively, whereas Tmax values from seven offshore wells are presented in Appendix 11.

A general figure showing vitrinite reflectance versus depth profiles for the eight offshore wells was constructed (Figure 5.11), as well as reflectance versus depth profiles for each individual well using both arithmetic and semi-logarithmic scales. Although the use of a semi-logarithmic scale often creates problems in curve-fitting, information related to the maturation history and tectonic development of the basin (such as the presence of unconformities and faults) is usually more reliable (Dow, 1977).

In general, a good positive correlation exists between rank, expressed as vitrinite reflectance, and depth in the West Aceh Basin (Figure 5.2) and the trend is similar to those that have been demonstrated elsewhere by numerous authors (e.g. Bostick, 1979; Middleton, 1982; Russel and Baillie, 1989). Although the trends vary from well to well, the general pattern reveals that the rank increases gradually from about 0.15% to 0.6% with increasing depth. Most of the individual offshore boreholes, however, show significant changes within their reflectance versus depth profiles. The most obvious feature is the striking difference in slope of the reflectance profiles from below and above the boundary between the Tutut and Kueh Formations. In most cases the curves are flatter above the boundary and steeper below the boundary. This situation was recorded in the Teunom, Bubon, Keudapasi, Tuba, Meulaboh, Tripa, Meulaboh East and Palumat wells as shown in Figures 5.3 to 5.10. The semi-log plots in Figures 5.3 to 5.10 reveal that the reflectance profiles are offset at the Tutut-Kueh boundary to form two segments.

The offset could be interpreted as an erosional unconformity at or near the boundary between the Tutut and Kueh Formations. If this is the case, the sediment loss caused by erosion could be estimated using the simple equation proposed by Dow (1977) which extrapolates the maturation line from below the unconformity upward until it reaches the reflectance value immediately above the unconformity. The amount of upward extrapolation required represents the amount of sedimentary section lost (Waples, 1985). Using this formula it can be assumed that sediment loss in the area penetrated by these drill holes ranged from 250 m to 350 m, with the largest losses occurring in the Palumat well. Similarly, at the boundary between the Kueh and Tangla Formations, the increment of slope of the reflectance values is lower above the formation boundary, as can be seen in Figures

5.6 and 5.7. Sediment losses of 250 m and 300 m can be calculated for the Tuba and Meulaboh wells respectively.

Exceptions to the trend of upward decreasing slope in the reflectance profiles were observed in the Teunom and Meulaboh wells (Figures 5.3 to 5.7). The reflectance profiles show an offset toward lower reflectance at a depth of about 300 m in the Teunom well and at about 750 m in Meulaboh well. In addition, the reflectance profile in the Meulaboh well is also offset toward a lower reflectance at a depth of about 2500 m. Dow (1977) suggested that such offsets are typical of sequences that have undergone reverse faulting. However, care must be taken when interpreting such structures and it is necessary to consider several other factors such as the presence of cavings, type variation of the vitrinite, vitrinite reflectance suppression and palaeontological evidence as well as geophysical records.

Taking these factors into consideration, several explanations are possible for the offset in the Meulaboh and Teunom wells. In Meulaboh well the vitrinite population in the Kueh Formation samples generally covers the upper part of the reflectance range measured in samples taken from the overlying section. This situation indicates that much of the organic matter in the upper part of the Kueh Formation is contaminated by cavings from the middle and lower Tutut Formation. The occurrence of cavings in this interval was reported during drilling activities. Also palaeontological data and wireline logs indicate no repetition of the sedimentary sequences (Jamas, 1973) and this the offset is probably apparent rather than real.

Similar conditions were recorded for the reflectance offset at the top of the Tangla

Formation in the Meulaboh well. It can be suggested, therefore, that the offsets towards lower reflectance values in the Meulaboh well are probably not related to any structural features such as faults, or erosional breaks but rather they reflect caving problems during drilling.

A different situation was encountered in the Teunom well (Figure 5.3) where the offset towards a lower reflectance profile at a depth of about 300 m is most likely due to the presence of a different type of vitrinite. Most of the samples examined from the upper part of the Kueh Formation contain detrovitrinite and desmocolinite associated with coal fragments. This may account for the lower reflectance values than those obtained from the overlying sequences where the vitrinite consists of telocollinite. In addition, the offset toward the lower reflectance is only about 0.05%  $R_{\text{vmax}}$  which is too low to be related to typical sequences that have undergone reverse faulting and but is well within experimental error. Thus, the offset that occurs in the upper part of the Kueh Formation in the Teunom well is probably not a structural or erosional feature.

In the onshore area, vitrinite reflectance was also employed to analyse maturation profiles in the Tutut Formation from twelve shallow wells. Representative plots of vitrinite reflectance versus depth (Figure 5.11) show a slight scatter in terms of reflectance values. However, the general trend reveals that vitrinite reflectance increases with depth but the reflectance profiles commonly show a low angle of slope. Individual drill holes, however, show differences in the slope as shown in Figures 5.12 and 5.17. The reflectance profiles show offsets toward lower reflectance values at depths of 70 m and 140 m in the M13 and M11 wells respectively. Since the vitrinite reflectance values were obtained from core, a

decrease in the reflectance value due to the caving contamination can be discounted. Although the difference in the value of vitrinite reflectance across the offset was small, it could be due to suppression caused by the high content of liptinite macerals in these samples. The influence of the liptinite maceral in suppressing vitrinite reflectance has been reported elsewhere (Hutton and Cook, 1980; Raymond and Murchison, 1991; Wilkins *et al.*, 1991).

### 5.3. Maturation Level

As discussed in Chapter 4 the maturation level of organic matter can be determined by measuring both physical and chemical properties of organic matter contained in sedimentary rocks. Some common maturation indicators, and their relationships to hydrocarbon generation, are presented in Figure 5.1 (Heroux *et al.*, 1979). However, vitrinite reflectance is accepted as the best and most widely used measure of maturity (Tissot and Welte, 1978; Hunt, 1979; Durand, 1980; Teichmuller and Teichmuller, 1981). Following the scheme outlined in Figure 5.1, sedimentary rocks are classified as immature if they have not begun to generate oil, that is, have a vitrinite reflectance of less than 0.5%. The mature category is indicated by a reflectance level between 0.5% to 2.0% when the organic matter is currently generating oil and/or gas. The post-mature category is indicated by the cessation of oil generation but the generation of high temperature gas; reflectance values are greater than 2.0%.

Referring to the vitrinite reflectance profiles in Figures 5.3 to 5.10 and Figures 5.12 to 5.17, it is possible to assume that the great majority of the section drilled lies in the

immature zone ( $< 0.5\% R_{v,max}$ ). The depth to the zone of initial organic maturity ( $R_{v,max} = 0.5\%$ ) was penetrated in the Meulaboh and Tuba wells at depths of 2600 m and 2500 m respectively. From these figures, it can be suggested that the Tangla Formation is marginally mature to mature in the Meulaboh and Tuba wells below 2600 and 2500 m respectively whereas the Kueh and Tutut Formations lie entirely within the immature zone. The range of vitrinite reflectance levels and the maturity zones for the Tertiary sequences in the West Aceh Basin is given in Table 5.1:

Tmax values can also be used to determine the maturation level of organic matter. Espitalie *et al.* (1985) suggested that Tmax values of about 400-435°C represent the maximum yield temperature for the immature zone; 435-460°C represent the more yield temperature of the mature zone; and above 460°C represents the zone more yield temperature of the mature gas. The general trend for Tmax values versus depth in the West Aceh Basin is presented in Figure 5.18a whereas the individual data from every offshore well examined are enclosed in Appendix 11. From Figure 5.18, it is also clear that the majority of samples lie in the immature zone ( $< 400^{\circ}\text{C}$ ). The depth to the top of the mature zone appears to be generally in the range of 2000 m to 2800 m. Depths are of this magnitude restricted to the Tangla Formation. However, several factors must be considered when assessing maturation levels using Tmax values as they are affected by the type of organic matter in the rocks because different types of organic matter have different bond energy spectra. The range in variation of Tmax is 435-450°C, 420-460°C and 400-600° C for Type I, II and III kerogen respectively (Espitalie *et al.*, 1985). Other factors that effect the Tmax value are the presence of migrated hydrocarbons, a low pyrolysis yield ( $< 0.2$  kg/tonne) and a high mineral matrix content. Samples containing migrated hydrocarbons will have a suppressed

Tmax value, due to the poor separation of the S1 and S2 peaks whereas samples low pyrolysis yields ( $<0.2$  kg/tonne) will result in unreliable Tmax values (Clementz *et al.*, 1979). In addition, the Tmax value will increase as the quantity of mineral matrix increases (Espitalie *et al.*, 1980).

Tmax data is plotted against vitrinite reflectance in Figure 5.18b for representative samples from seven offshore drill-holes. Although the relationship shows a slight scatter, the general trend is for Tmax values to increase as the vitrinite reflectance increases. The mature zone as determined from Tmax values, appears to fall at a reflectance value of around 0.45% rather than 0.5%.

These Tmax data clearly show that the maturity level in the West Aceh Basin ranges from immature to marginally mature with a small portion extending into the mature zone. Because the deepest samples examined were only obtained from the upper part of the Tangla Formation in the Meulaboh and Tuba wells, the mature zone is expected to be present in the deeper sections of these holes. In addition, since the maturity pattern in this basin follows the general trend of increasing maturity with depth, it is likely that the mature zone was penetrated at greater depth in other drill holes examined.

#### 5.4. Vitrinite Reflectance Gradient

The coalification gradient, expressed as the reflectance increase per kilometre of overburden, has been assessed for five given reflectance levels for the twelve shallow onshore wells and the eight deeper offshore wells. Since an increase in vitrinite reflectance

follows increases in depth of burial of the sediment, the rate of coalification at any given vitrinite reflectance level can be assessed. The resultant vitrinite reflectance gradients at given levels of vitrinite reflectance for West Aceh samples are given in Table 5.2. The vitrinite reflectance levels used were 0.20%, 0.30%, 0.40%, 0.50% and 0.60%. However, for the Tripa, Bubon and Teunom wells, a reflectance level of 0.25% was used instead of 0.20% since the latter level was not encountered in these wells. The 0.20% reflectance level was not recorded in the onshore wells because vitrinite reflectance values for these wells started about this value and it been removed by erosion sediment. Most of the reflectance gradients were obtained by the best fit reconstruction and thus the accuracy varies from well to well. The values tend to be more diverse for the cuttings samples from offshore wells and more confidence can be placed on the onshore data since the measurements were conducted on core material. Most of the data indicate that the reflectance gradients increase for any given reflectance level from 0.30% downward. However, except for the Teunom well, the gradient decreases from the 0.20% reflectance level down to the 0.30% reflectance level. It is interesting to note that the reflectance gradient in the onshore area is much higher than in the offshore area but the values show wider differences and are more variable from well to well. In contrast, the reflectance gradients in the offshore area reveal no significant difference in values from well to well for any given reflectance level.

Broadly speaking, the reflectance gradients at the 0.20% reflectance level are low to moderate, ranging from 0.08%/km to 0.37%/km at depths between 54 m to 434 m. Reflectance gradients in the onshore area range from low (0.17%/km) to high (0.76%/km) at the reflectance level of 0.30% which lies at depths ranging from 13 m to 210 m. At the



same reflectance level, the reflectance gradients are lower in the offshore area, falling between 0.05 %/km to 0.15 %/km for most wells except the Teunom where the value was 0.25 %/km. This reflectance level occurs at a depth of 412 m to 1085 m. Moderate to high reflectance gradients occur at the 0.40% reflectance level in the onshore area (ranging from 0.47%/km to 0.85%/km) but the gradients are again generally lower in the offshore area (within the range 0.14%/km to 0.27%/km). The 0.40% reflectance level lies at depths of 112 m to 127 m and 803 m to 1779 m in the onshore and offshore areas respectively. The reflectance gradient at the 0.50% and 0.60% reflectance levels was only determined from the offshore Tuba and Meulaboh wells. Values of 0.18%/km were recorded for the 0.50% reflectance level in both wells at depths of about 2100 m and 2300 m respectively. The 0.21%/km to 0.24%/km reflectance gradient found at the 0.60% reflectance level occurred at a depth of approximately 2500 m in the Tuba well and at 2700 m in the Meulaboh well.

Compared to other Indonesian Tertiary basins, the vitrinite reflectance gradients in the West Aceh Basin are generally higher in the onshore area but lower in the offshore area. For example, vitrinite reflectance gradient in the Southeastern Kalimantan Basin was reported to range from 0.20%/km to 0.25%/km at the reflectance level of 0.50%, and between 0.30%/km to 0.35%/km at the same reflectance level in the Kutai Basin (Panggabean, 1990). In the Ombilin Basin in central Sumatra, however, the reflectance gradients are generally higher, up to 1.7%/km at a vitrinite reflectance level of 0.7% (Sukardjo, 1989). In the offshore area of the West Aceh Basin the low vitrinite gradients show no obvious comparison with either the onshore area of the basin or with the other Tertiary basins of Indonesia such as South Sumatra and Northwest Java Basin (Amir, 1991; Sutrisman, 1991). The low vitrinite gradient in the offshore area of West Aceh Basin may due to low

geothermal and/or palaeothermal gradients which were responsible for coalification.

In addition, most reflectance versus depth curves display a variety of different shapes depending on the reflectance gradients. In most cases the curves are steep in the upper stratigraphic levels and flatten out in the lower sequences in the offshore sections. The curves tend to remain steep in the onshore part of the basin (Figures 5.15 and 5.16). This implies that reflectance increments were small during the early coalification stage, but were followed by some later acceleration which resulted in a downward increase in reflectance gradient (Bustin *et al.*, 1983; Diessel, 1973; Stach *et al.*, 1982).

### 5.5. Vertical and Lateral Rank Variations

Rank variations, as measured by vitrinite reflectance, were also examined on a regional scale both vertically and horizontally through the Tertiary formations in the Meulaboh region of the West Aceh Basin. It is widely accepted that vitrinite reflectance can be related to various factors such as depth and duration of burial at specific temperatures during the coalification process (Hacquebard and Donaldson, 1974; Cook, 1982; Cameron, 1991). The most important factor in coalification is the gradual increase in geothermal energy with burial. It can increase rapidly as a result of anomalously high heat flows, which may be associated with intrusions or tectonic processes (Teichmuller and Teichmuller, 1968; Bostick, 1979). Since coalification is a function of temperature and time, an increase in coal rank and vitrinite reflectance can be related to an increase in depth. Wilson (1976) argued that the relationship between coal rank and depth is strongest in young continental basins, whereas intracratonic basins with a lower heat flow only show a minor increase in

coal rank with depth. Therefore, in a forearc basin setting, such as the West Aceh Basin where most of the basin has a low heat flow, the rate of coal rank increase with depth is expected to be low.

The most obvious feature in the West Aceh Basin data is the overall increase in  $R_{\text{vmax}}$  with depth. However, the largest variations in rank with depth, and the largest reflectance gradient variations at any given vitrinite reflectance level, mostly occur in the onshore area. This has resulted in a major difference in the maturation patterns between the offshore and onshore areas.

#### 5.5.1. Onshore Rank Variations

Vitrinite data from the onshore area mostly were taken from coal seams, with additional data from carbonaceous siltstone in some in seams wells where insufficient coal seams were present to construct a vitrinite reflectance profile. Although most wells only penetrated part of the Tutut Formation, the general trend from the maturity pattern should be useful since no great geological disturbances occur within the sections intersected. Most of the drill hole were sunk to an average depth of 250 m, but a few of them only penetrated to a depth of 150 m.

In addition to the drill hole data, outcrop data from coal ranging in age from Oligocene to Pliocene were also analysed to delineate the general lateral rank distribution. However, since the stratigraphic position and characteristics of the outcrop seams are hard to recognise, such data is rather generalised and must be used with great caution.

Furthermore, since no subsurface geological data for the other Tertiary sequences is available within the onshore area, severe limitations are placed on the geological interpretation of rank variations in relation to stratigraphy or depth. The latter can only be based on a regional geological synthesis for a broad area of the West Aceh Basin. The pronounced Tertiary deformation, commonly present elsewhere in northern Sumatra, did not occur in the West Aceh Basin because the Sikuleh Batholith provided a shielding effect and the entire West Coastal Range of the Barisan Mountains acted throughout the Tertiary as a stable epirogenic block (Cameron *et al.*, 1980; Bennet *et al.*, 1981).

Isoreflectance contours for the Tertiary sequence in the onshore area is presented in Figure 5.19. Although most coal outcrops belong to the Tutut Formation, with restricted coal outcrops of the Tangla and Kueh Formations, the general trend of rank shows a clear increase towards the older sequences, i.e. from the Plio-Pleistocene to the Oligocene. In a general sense this increase is toward the magmatic arc which is parallel to the length of Sumatra.

The highest vitrinite reflectance values (0.5% to 0.8%) generally occur in the Tangla Formation with the overlying Kueh Formation having vitrinite reflectance values ranging from 0.40% to 0.50%. The Tutut Formation generally shows an immature organic maturation with reflectance values between 0.20%-0.35%. Rank anomalies are shown as a northward projection of iso-reflectance lines in the area north of Tutut. Some Kueh Formation samples from this area reveal a reflectance value of up to 1.15% (sample GM 22824) resulting from rank upgrading adjacent to basaltic intrusions. Several intrusions and Pleistocene mafic dykes occur in the coastal area north of Calang where vitrinite reflectance

values are up to 0.85%. The existence of this westernmost anomaly is supported by the data from northern Calang which exhibits an increase in reflectance from less than 0.40% to over 0.70%  $R_{\text{vmax}}$ . A rank anomaly was also recorded on the western side of the Batee Fault zone in the Gunung Alem area. The rank of the Tutut Formation in this area generally ranges from 0.38% to 0.40% and is higher than the values from the Kawai and Bubon areas. An increase in anisotropic reflectance was also recorded at location T66 near Gunung Alem.

In addition to the information from outcrop, reflectance profiles from various well in the onshore area have been constructed. Significant rank changes can be substantiated both vertically and laterally where individual seams are followed through the region. Key marker beds are very useful for correlating seams within the basin. In general, the three principal coal seams in the Tutut Formation can be identified by the presence of thin bands of tuffaceous sandstone in seams 1 and 2. Using these key horizons in the Tutut Formation, correlation between the drill holes can be realised (Figure 5.20). The plot of rank versus depth shows a wide variation for any given depth interval. The northwest-southeast cross-section (Figure 5.20) clearly shows that the same rank, as measured by vitrinite reflectance, occurs at different stratigraphic levels. The rank drops downward drastically in wells M1 and M2. In contrast, higher rank values lie at shallower stratigraphic levels in M11, M12, M15, M18 and M21.

### 5.5.2. Offshore Rank Variations

An isoreflectance profile (Figure 5.21) was constructed for the eight offshore wells in order

to delineate vertical and lateral rank variations and to locate the mature stage of maturation within this basin. A deviation from the generally accepted maturation pattern for sedimentary basins occurs in the West Aceh Basin offshore area. Isoreflectance profiles, based on reflectance values ranging from 0.20% to 0.60%, show a regional trend with rank increasing at any given stratigraphic level from southeast to northwest. This maturation pattern is relatively smooth, although several high rank anomalies occur toward the northwest as indicated by the Teunom, Bubon and Keudapasi wells.

In contrast, reflectance gradients tend to become lower southeastward, except in Tripa well where the reflectance gradient increases in the upper portion of the sequence. In this well the 0.30% and 0.35% isoreflectance lines lie at deeper stratigraphic intervals compared to the other wells but the gradient increases for the 0.20% and 0.25% reflectance levels. Overall, most of the stratigraphic sequence intersected is immature. Marginally mature to mature zones were only intersected in the Tuba and Meulaboh wells at depths of 2000 m and 2200 m respectively. The deepest sections of these holes lie at a vitrinite level reflectance of 0.60% and are mature.

## 5.6. DISCUSSION

Several limitations of this study were taken into consideration when determining maturation patterns and rank variations in the Tertiary sequences of the West Aceh Basin. One obvious limitation is the relatively small number of coal and carbonaceous samples available for use in this study when considering an area as large as the West Aceh Basin. This limitation is entirely due to the lack of suitable outcrop in the field; most outcrop is highly oxidised and

weathered and only a few of the Miocene and Oligocene coal seams crop out. Another equally important limitation is the availability of subsurface data, both offshore and onshore, since the amount of drilling was limited and the wells only penetrated a restricted stratigraphic level, especially in the onshore area. The absence of subsurface structural geological data for the onshore and to some extent for the offshore area, was also a factor that had to be considered during interpretation. Consequently, the following interpretations of trends are somewhat limited but can be compared with general geological trends established by various authors, especially for the northern Sumatra basins (Cameron *et al.*, 1980, 1982, 1983; Bennet *et al.*, 1981; Rose, 1983; Beaudry and Moore, 1985; Hadiyanto and Amarullah, 1985; Hadiyanto *et al.*, 1986; Hamilton, 1988; Katili, 1989).

As mentioned previously, regional vitrinite reflectance variations in the study area show that maturation decreases from a maximum near the northeast limit of the basin towards the southeastern offshore area. The gradual northward increase in rank seems to be related directly to the geological age of the units, as well as to the relative position of the sample location with respect to the magmatic arc beneath central Sumatra. The increase in rank with age of the strata has been recognised from both the onshore and offshore areas. For example, the rank of most of the Tutut Formation is lower than that of the Kueh Formation (Figure 5.19). Within each formation, the rank also increases from south to north. However, some anomalies occur in the Tangla Formation near the Calang area where the rank increases towards the west. Some of the Tutut Formation, which has been affected by intense folding and thrust faulting when emplaced on top of the Mesozoic sequence west of the Batee Fault Zone (locations T54 and T55), has a similar rank too west of the Batee Fault Zone. Influence of tectonic deformation on rank is indicated in sample GM 22053,

where shearing effects along the Batee Fault resulted in an increase in rank at that location. Although such influence is not generally significant, the increase in anisotropic reflectance toward the fault zone reflects the influence of stress on the coal and organic materials. Many authors have suggested that tectonism does not produce a significant increase in rank (Teichmuller, 1982; Murchison *et al.*, 1985), but rather it causes physical changes, such as loss of moisture content and an increase in density, which play an important role in the metamorphic upgrading of lignite and sub-bituminous coal (Teichmuller and Teichmuller, 1966; Murchison *et al.*, 1985). In bituminous coals, however, the influence of tectonic stress on organic alteration usually occurs only in the immediate vicinity of thrust faults (Teichmuller and Teichmuller, 1966).

Coal rank in the West Aceh Basin is related to the relative position of the sample with respect to the magmatic arc; this is especially apparent when comparing the offshore and onshore rank data. The general trend reveals that isorank values, occurs at shallower stratigraphic depths in a shoreward direction. For example, reflectance value of 0.30% lie at depths ranging from approximately 10 m to 200 m in the onshore area, but the same rank is at a depth of 100 m to 400 m in the offshore area. In addition, most strata with a rank of 0.20% vitrinite reflectance lie at a depth of generally more than 100 m in the offshore area but they crop out or have been removed by erosion from the onshore area. Similar situations are also recorded at other rank levels (see Table 5.2).

Studies of coalification patterns have been conducted by many authors (Diessel, 1973; Damberger, 1974; Hacquebard and Donaldson, 1974; Costano and Sparks, 1974; Kanstler *et al.*, 1978; Smith, 1982). In general they concluded that the primary factor controlling



increase in rank is an increase in temperature. The pressure caused by the overburden or by tectonic deformation were considered to be less significant. Such influences will only result in physical changes such as density and moisture content rather than chemical alteration (Teichmuller and Teichmuller, 1982; Murchison *et al.*, 1985). Thus, heat is the most important factor involved in the coalification process and variations in temperature gradient and heat flow would cause significant rank variation. On the other hand, the different thermal conductivities of clastic rocks, as well as differences in the geothermal gradient, will affect the heat flow and temperature gradient and are also important in determining the maturation level of the rock (Damberger, 1968; Ammosov and Gorshkov, 1969).

The trends in reflectance gradient at specified maturation levels in the offshore and onshore parts of the West Aceh Basin is given in Figure 5.22. The difference in vitrinite reflectance gradient between the two areas is very significant. In the onshore area, the reflectance gradient at a reflectance level of 0.30% to 0.40% increases very sharply in most of the wells except M3 and M21. In contrast, the reflectance gradient decreases gradually and systematically in most offshore wells between the reflectance levels of 0.20% to 0.30%, and increases again slowly above a reflectance level of 0.30%. Anomalous values are found in Bubon and Teunom wells where the reflectance gradient lies between 0.20% and 0.30%; reflectance levels decrease in the Bubon well and increases markedly in the Teunom well.

Reflectance gradients in all offshore wells increase smoothly from the 0.30% to 0.40% reflectance levels but the gradients are lower than for the equivalent reflectance interval in

the onshore sequences. The reflectance gradient trends between vitrinite reflectance levels of 0.20% and 0.30% in the onshore area was unable to be assessed due to unavailability of suitable data.

Vitrinite reflectance gradients also increase as depth increases for various reflectance levels (Figure 5.23). Anomalies in the onshore area were recorded in wells M3 and M21 where the reflectance gradient between 0.30% and 0.40%  $R_{v,max}$  increased gradually as depth increased. If changes in the temperature gradient and heat flow due to regional and local variation in the geothermal energy flux and because of substantial differences in the thermal conductivity of the sedimentary rocks were responsible for the different rank gradients, it can be assumed that two separate thermal systems operated in the onshore and offshore areas respectively. If this is the case, the heat flow responsible for the rank gradient at and above a 0.30% vitrinite reflectance level in the onshore area was higher, at least at some stage in the basin's thermal history, than that in the offshore area. Any inflections in the onshore area (as shown in wells 31 and M21 at vitrinite reflectance levels of 0.30% to 0.40%) may be due to the superposition of higher local heat-flow systems resulting from intrusions. Comparing the rank gradient at the reflectance level of 0.20%-0.30% to the reflectance level of 0.30% upward, it is interesting to note that different thermal systems might have operated and affected coalification of the strata between these two reflectance intervals. The upper sequence shows a rank gradient decreasing downward whereas the lower sequence shows a smooth and consistent increase in gradient downward to the deeper sections. The anomaly shown in the Teunom well at a 0.20% to 0.30% reflectance level is probably due to a local geothermal system in this area.

Since heat is the prime agent involved in the organic maturation process, the temperature gradient, which is mainly controlled by the depth and temperature of the heat source beneath the basin, will be one of the most important factors influencing maturation gradients. Internal thermal events such as intrusions and diapirism will be the main heat source that effect temperatures in the sedimentary basins on a large scale (Blackwell and Steele, 1989). Such events, however, are not the only variable controlling the temperature in the sedimentary basin. Other heat sources such as initial and external heat flow, thermal conductivity, radioactivity, fluid flow, and thermal properties of the basin sequence will also influence the basin temperature, although the effect may be less dominant than the previous one (Blackwell and Steele, 1989).

The significance of these factors varies depending on the relative tectonic position of the basin to the heat source. In a cratonic basin, for example, internal thermal events are generally not significant but they will be dominant in active tectonic settings such as a rift zone or forearc basin (Roy *et al.*, 1968).

Assuming that such factors controlled coalification temperatures in the study area, which is located in a tectonically active forearc basin, then the heat source should increase towards the magmatic arc. Thus the sedimentary sequences beneath the onshore area will be governed by a higher heat flow and be closer to the heat source than those in the offshore area. If this is the case, the difference in rank gradient between the onshore and offshore areas may have resulted from the different heat flow patterns operating in the two areas.

Thamrin (1985) showed that in the Tertiary sedimentary basins of Sumatra, the heat flow

increases towards the magmatic arc. In the backarc region of Sumatra the heat flow is much higher than it is in the forearc basins. In the forearc basins, however, the shelf region has a higher heat flow than that in the outer arc.

Another factor controlling rank gradient in the study area may be the relative position and depth of the magma to the basin sequences undergoing coalification. Taking these conditions into consideration it is assumed that any maturity level in the sedimentary sequence may be related or partly controlled by the position of the sequence relative to the magmatic arc. This proposition accounts for the more variable and higher rank gradients in the onshore area than those observed in the offshore area. The shallow depths of magmatic diapirism in central Sumatra were suggested as the main factor controlling the very high heat flow in that area (Eubank and Makki, 1981). Carvalho *et al.* (1980) also conducted research on terrestrial heat flow in the Tertiary basins of central Sumatra and concluded that the heat flow density follows the trend of the Barisan Mountains with the heat flow intensity rising steeply toward the magmatic arc.

Considering the relationship between rank gradient and heat flow in the West Aceh Basin it is important to note the lateral variation in rank gradient in the offshore area. Figure 5.24 show the trend of rank gradient at the 0.25% reflectance level whereas Figures 5.25 and 5.26 illustrate the trend of the rank gradient at reflectance levels of 0.30% and 0.40% respectively. Although the data points are too sparse to delineate gradient rank contours they can give a general picture of different trend patterns at different reflectance levels. It is quite clear that at the reflectance level of 0.20% (Figure 5.24) the contours follow the trend of the Barisan Mountains with the reflectance gradient rising gradually toward the

magmatic arc (shoreward). Inflections in the trend of rank gradient occur at reflectance levels of 0.30% and 0.40% (Figures 5.25 and 5.26) where the rank increases towards the west with the highest reflectance gradient in the Teunom well. A similar situation also occurs in the onshore area with the general trend rising westward (Figure 5.19).

## CHAPTER 6

### THERMAL HISTORY

#### 6.1. INTRODUCTION

Thermal heating of organic matter through burial metamorphism within a sedimentary basin is the fundamental factor responsible for generating oil and gas from petroleum source rocks. The organic matter contained in sedimentary rocks is heated as the basin subsides and the degree of heating depends on the amount of heat (controlled by the geothermal gradient) and the effective time or duration of heating, as controlled by the rate of the subsidence (Tissot *et al.*, 1974; Hunt, 1979). As heating of the organic matter progresses first carbon dioxide, then methane, then ethane and then successively larger hydrocarbon molecules are given off in gradually increasing volume (Tissot and Welte, 1978). Thus the hydrocarbon product-mix depends on the degree of maturity of the organic matter which is influenced by the thermal heating.

Maturity of organic matter is one of the most sensitive natural recorders of the relatively low temperature thermal metamorphism that occurs in sedimentary basins (Feinstein *et al.*, 1989). Since the generation of oil and gas and the rank of coal are directly dependent on the time and temperature achieved in the host rock, estimation of the thermal history and palaeotemperature of the sedimentary rock is essential to evaluate the extent and timing of petroleum generation.

Many attempts have been made to predict maturity of sedimentary rocks, palaeotemperatures and timing of hydrocarbon generation by assuming that oil generation depends upon both temperature and time (Karweil, 1956; Tissot, 1969; Lopatin, 1971; Connan, 1974; Hood *et al.*, 1975; Waples, 1980). The palaeothermal history modelling used in this study follows the models formulated by Kanstler *et al.* (1978) and Smith and Cook (1984), whereas the timing of hydrocarbon generation is predicted using the Lopatin (1971) model as modified by Waples (1980).

## 6.2. GEOTHERMAL GRADIENT

Lateral and vertical variation of vitrinite reflectance is primarily temperature related, although this relationship is complicated by differences in the burial history (Kanstler *et al.* (1978). Therefore, it is necessary to establish the present-day pattern of geothermal gradient variation in order to assess the role of temperature variation in coalification and hydrocarbon generation.

An estimate of the present geothermal gradient was obtained in this study by using the formula:

$$dt/dx = (T - T_0)/X$$

where T is the bottom hole temperature (°C);

T<sub>0</sub> is temperature at zero depth (surface temperature);

X is the well depth at which the temperature (T) was measured

In this calculation, a value of 27°C has been used as the ambient temperature for offshore wells, as suggested by Aadland and Phoa (1981) for calculating the geothermal gradient

of other Indonesian Tertiary basins.

The lack of bottom hole temperatures for the shallow onshore wells meant that geothermal gradients could not be determined for the onshore area.

The present geothermal gradients for the eight offshore wells are presented in Table 6.1. For comparison, additional geothermal gradient data for other wells situated around the West Aceh Basin were obtained from Aadland and Phoa (1981) and are included in this table. The geothermal gradients in the study area are typically low, in the range of 17°C/km to 39°C/km. The lowest gradient occurs in the Tripa well whereas the highest value was recorded in the Teunom well. In general, the geothermal gradient increases towards the northwest but some inflections occur near the Bubon well.

Comparison of the pattern of geothermal gradients with maturation patterns for the West Aceh Basin suggests that generally high geothermal gradients are associated with high linear reflectance gradients and low geothermal gradients are related to low linear reflectance gradients. Data from other sources show that the geothermal gradient decreases from northwest to southeast through and beyond the study area (Aadland and Phoa, 1981; Thamrin, 1985); this is consistent with the observations for the West Aceh Basin.

However, compared with other basins in Sumatra most of the study area has a lower geothermal gradient (see Table 6.1); the higher values occur mostly in the backarc basins such as the North Sumatra, Northwest Aceh and Central Sumatra Basins. For example,



the average value in the Central Sumatra Basin is  $59.8^{\circ}\text{C}/\text{km}$  but individual readings of more than  $80^{\circ}\text{C}/\text{km}$  have been reported and these are suggested to be the highest geothermal gradients recorded anywhere in the world (Carvalho *et al.*, 1980). In other Sumatran backarc basins, such as the Northwest Aceh and North Sumatra Basins, the geothermal gradient ranges from moderate to high.

The geothermal gradient in Sumatra tends to increase toward the magmatic arc and this is the same as the heat flow pattern which also indicates an increasing gradient as the magmatic arc is approached (Thamrin, 1985).

This pattern of different geothermal gradients for relatively closely-spaced areas is not restricted to Sumatra but is also a feature of the whole Indonesian Archipelago. Thus, although the geothermal gradient in the study area is lower than those located in the Sumatran backarc basins, the value is relatively higher than the geothermal gradients recorded in some other forearc basins in Indonesia, such as the Bengkulu and South Java Basins. Compared to the Indonesian backarc basins, such as the Southeast Kalimantan, North Java and South Sumatra Basins, the average geothermal gradient in the West Aceh Basin is much lower. For example, the geothermal gradient in the Southeast Kalimantan Basin is approximately  $33^{\circ}\text{C}/\text{km}$  (Panggabean, 1990) whereas in the North Java and South Sumatra Basins it ranges from  $44.4^{\circ}\text{C}/\text{km}$  to  $49^{\circ}\text{C}/\text{km}$  (Remington and Pranyoto, 1985) and  $52.2^{\circ}\text{C}$  to  $56^{\circ}\text{C}$  (Thamrin, 1979), respectively.

### 6.3. PALAEOTEMPERATURES

Palaeotemperatures of sedimentary basins can be assessed using combined data such as the age of the sedimentary units (Ma) based on biostratigraphic correlation, the vitrinite reflectance ( $R_v$ max) and the theoretical mathematical models developed by Kanstler *et al.* (1978); the later are based on the T unit-Temperature- $R_v$ max Karweil monogram modified from Bostick (1973). Kanstler *et al.* (1978) suggested that the palaeothermal history of a formation should approximate either the isothermal or gradthermal model; the model can be tested against present temperatures to establish the relative palaeothermal history of a formation. The approximation of  $T_{\text{present}}$  ( $T_{\text{pres}}$ ), which is the present formation temperature, to either  $T_{\text{iso}}$  (isothermal) or  $T_{\text{grad}}$  (gradthermal) can be estimated by the following ratio given in Smith and Cook (1984):

$$\text{Grad:Iso} = (T_{\text{pres}} - T_{\text{iso}})/(T_{\text{grad}} - T_{\text{iso}})$$

where,  $T_{\text{iso}}$  is determined from the vitrinite reflectance data using the scale in Figure 6.1, and then it is converted to  $T_{\text{grad}}$  by using the conversion factor  $(T_{\text{iso}} - 10^\circ\text{C}) \times 1.6 + 10^\circ\text{C}$  as suggested by Kanstler *et al.* (1978) and Cook (1982).

Kanstler *et al.* (1978) defined  $T_{\text{iso}}$  as the temperature needed to give the observed reflectance assuming that this temperature has operated since the time of deposition.  $T_{\text{grad}}$  was defined as the temperature needed to give the observed reflectance, derived from  $T_{\text{iso}}$ , but assuming a history of uniformly rising temperature since the time of deposition. Smith (1981) suggested that if  $\text{Grad:Iso} > 1$  or close to 1 the present geothermal gradient ( $T_{\text{pres}}$ ) is higher than in the past and the formation history would approach the gradthermal

model. If the Grad:Iso ratio is lower than 1, the present geothermal gradient is assumed to be lower than in the past and the formation history approaches the isothermal model. If the present temperature is lower than the isothermal temperature, the Grad:Iso ratio will be negative which indicates that the palaeotemperatures were significantly higher than the present temperature.

The temperature history data for the study area (Table 6.2) were obtained using the calculation method for the temperature models proposed by Kanstler and Cook (1979) and Smith and Cook (1984). The ( $T_{\text{pres}}$ ) values were obtained from well completion reports produced by the Union Oil Company (1975-1979) following their drilling program in the West Aceh Basin, and from the compilation of geothermal data for Tertiary basins of Indonesia by Aadland and Phoa (1981). Age data were assessed from the palaeontological investigations of well sections by Jamas (1973) and the Union Oil Company (1975-1979). Where palaeontological data were not available, ages were estimated using the Indonesian Cenozoic Correlation Chart established by Billman (1975). This chart is commonly used in Indonesia for sequences which do not contain fossils but for which it is possible to date two or more parts of the section from other data or where recognised geological boundaries, such as widespread unconformities, can be established. The dates are tied to the relevant dates on the chart and ages of the unknown units in the sequence extrapolated from the chart. Thus although there is a possibility of a small error in the age given here for units less than 10 million years old, the ages are the best available estimate and would therefore provide the "minimum" case scenario.

Because the Karweil diagram does not provide a time scale for less than 10 Ma, the age

of any stratigraphic interval examined that was younger than 10 Ma was estimated using an extrapolated timeline between 0 and 10 Ma. However, the use of a timeline scale of less than 10 Ma may be less precise, and consequently, the  $T_{iso}$  resulting from the calculation is likely to have a wider range and greater degree of uncertainty.

In general, Grad:Iso ratios for the study area range from 0.98 to -0.31 but ratios are negative in most of the wells except for Tuba well at depths of 2184 and 2394 m and Meulaboh well at depths of 2373 and 2640 m. Negative Grad:Iso values indicate that the palaeotemperature gradients were considerably higher than the temperatures at present, that is,  $T_{pres} < T_{grad}$ . In some stratigraphic intervals, some of the Grad:Iso values are positive but the ratios are still than 1. This also implies that the present geothermal gradients are probably lower than in the past.

It is interesting to note that although most of the formations have negative Grad:Iso ratios, most of the Tutut Formation has a higher negative Grad:Iso ratio than the Kueh and Tangla Formations and, therefore, the palaeotemperatures were higher in the latter unit than in the former. Thus although the negative values of this ratio indicate a significantly higher palaeotemperature than present temperature for all formations, it can be assumed that there was a significant change in palaeotemperature between the deposition of Tangla Formation and the Tutut Formation.

As noted in Chapter 5, the Pliocene units have steeper reflectance profiles than the older strata. This suggests that the palaeotemperatures operating during the deposition of the Pliocene units were higher than those operating earlier. Thus there is good agreement

between the reflectance profiles and the palaeotemperature data. The rise in palaeotemperatures from the Oligocene to the Pliocene is probably related to the gradual and extensive magma doming responsible for the development of Sumatra since the Middle Miocene (the first phase of the Barisan Mountain uplift). This culminated in the Plio-Pleistocene period when proximal orogenesis influenced all of the western Indonesia basins (Cameron *et al.*, 1980).

Model-derived ( $T_{grad}$ ) temperatures in the study area were compared with the present well temperatures ( $T_{pres}$ ) and the results are shown in Figure 6.2. In general, the trends observed indicate that most of the data is spread below the tie-line ( $T_{pres} = T_{grad}$ ) but several data points from the Tuba and Meulaboh wells plot near the tie-line. For any given reflectance level,  $T_{grad}$  is greater than  $T_{pres}$  and with increasing rank the  $T_{grad}$  generally approaches  $T_{pres}$ .

Comparison of the data for Oligocene and Miocene sequences in all wells show that Tuba and Meulaboh wells plot near the tie-line whereas data for the other holes plot farther away. Consequently, for the Oligocene and Miocene in the Tuba and Meulaboh wells,  $T_{pres}$  is nearly equal to  $T_{grad}$ . This implies that relatively rapid coalification occurred during the Oligocene and Miocene in these wells and the thermal regime responsible for coalification is likely to have been almost the same as that experienced by the area now. For the Miocene and Pliocene sequences in Teunom, Bubon, Meulaboh East, Keudapasi, Tripa, Palumat wells, the data plot well below the tie-line and  $T_{pres} < T_{grad}$ . This indicates that a more rapid phase of coalification affected the Miocene and Pliocene sequences.

Overall, most of the sequences approximate the gradthermal model from which it can be assumed that coalification occurred during a phase of constant rapid burial, prior to a period of uplift and erosion. Struckmyer (1988) found a similar relationship for the Otway Basin of Australia.

The palaeothermal model in the study area is similar to models proposed for the other Tertiary Indonesian basins, such as the Southeast Kalimantan, Northwest Java, and South and Central Sumatra Basins (Daulay 1986; Panggabean, 1990; Amir, 1991 and Sutrisman, 1991). The latter basins also approach the gradthermal model ( $T_{\text{pres}} > T_{\text{grad}}$ ) and almost all of the palaeothermal data are spread below the tie-line except in the West Java Basin and some locations in the Northwest Java Basin. The Southeast Kalimantan Basin has  $T_{\text{pres}} > T_{\text{grad}}$  and Grad:Iso ranges from -1.04 to +0.75 (Panggabean, 1990). In the South Sumatra Basin, the Grad:Iso ratio was reported to range from -0.03 to +0.20 and  $T_{\text{pres}} > T_{\text{grad}}$  (Amir, 1991). The Talang Akar Formation in the Northwest Java Basin has  $T_{\text{pres}} > T_{\text{grad}}$  and the Grad:Iso ranges from -0.06 to +1.02 (Sutrisman, 1991). In the latter study, details for other formations were not given. An average Grad:Iso = 1 was reported to occur in the West Java Basin (Daulay, 1986).

Based on the data above, it can be assumed that during the Tertiary period most of the thermal regimes operating in western Indonesia were higher than the present thermal regime and probably rapid early coalification occurred in these basins. However, the degree and extent of thermal heating varied from one basin to another. Data suggest that, of the basins mentioned above, the highest palaeothermal conditions occurred in the West Aceh Basin. Slow coalification may have occurred in the Oligocene, as indicated by

palaeothermal patterns in the West Aceh and West Java Basins, and in some areas of the Northwest Java Basin.

#### 6.4. BURIAL HISTORY AND THE TIMING OF HYDROCARBON GENERATION

The burial history and timing of hydrocarbon generation in the study area using the method of Lopatin (1971), as modified by Waples (1980, 1985) requires estimates of time and temperature to calculate the thermal maturity of organic matter in sedimentary rocks and it is often called the time-temperature index of maturity (Connan, 1974; Hood *et al.*, 1975; Waples, 1985). Time and temperature are closely interchangeable (Lopatin, 1971; Connan, 1974; Bustin *et al.*, 1983; Ejedawe and Cohen, 1984; Waples, 1985). Thus a high temperature acting for a short time can have the same effect on maturation as a lower temperature acting over a longer time. It is suggested that there is a linear relationship between maturity and time. It is also assumed that the rate of maturation increases by a factor (R) for each 10°C interval. Therefore, for any other interval the temperature factor  $R = 2^n$ , where n is an index of temperature and increases by a factor of 1 for every 10°C change; for example, R is equal to -1 for the 90° to 100°C interval, 0 for the 100° to 110°C interval, 1 for the 110° to 120°C, etc.

The increase in maturity in any temperature interval is given by  $\Delta \text{maturity}_i = (\Delta t_i)(r_i^n)$  where  $t_i$  is the length of time spent by the sediment in the temperature interval i. Because maturation effects are additive and irreversible, total maturity for a given sediment is calculated by summing the incremental increase in maturity acquired in each interval by using the formula:

$$TTI = \sum_{n_{\min}}^{n_{\max}} (tn) (r^n)$$

where  $n_{\max}$  and  $n_{\min}$  are the highest and lowest temperature intervals, respectively; thus the TTI for a given unit is the sum of the product of the weighting factor and residence time for the unit in every 10°C interval (Lopatin, 1971).

Implementation of the Lopatin method begins with the construction of a burial-history curve from the deposition of the oldest rock layer of interest. This construction is best accomplished by plotting burial depth versus geological age. The value of TTI is obtained from the subsurface temperature data for every depth throughout the burial history using the present day geothermal gradients. However, the evaluated TTI should correlate with the value of vitrinite reflectance which provides useful information on the burial history and timing of organic maturity (Waples, 1980; Tissot and Welte, 1984). The correlation of vitrinite reflectance values with TTI value is given in Table 6.3.

#### 6.4.1. Burial History

Burial history models for the eight offshore wells from the study area (Figures 6.3 to 6.10) were reconstructed using the simple back stripping technique, without considering compaction factors for the sedimentary rocks, as suggested by Van Hinte (1978), Sclater and Christie (1980) and Guidish *et al.* (1980). This model requires the use of a constant gradient equal to that of the present day gradient rather than the variable geothermal gradients determined for this study. The ambient temperature at the surface was assumed to be 27°C as suggested by Aadland and Phoa (1981).



The time-stratigraphic data used for this study were obtained from the biostratigraphic zonation given in the Union Oil Company well completion reports that were re-assessed by Jamas (1973). An estimation of the amount of overburden removed by erosion has been attempted by using the method proposed by Dow (1977) which extrapolates the vitrinite reflectance profile plotted on a semi-log scale to a vitrinite reflectance intercept of 0.20%.

An unconformity was assumed to occur at the boundary between the Oligocene and Miocene, that is, between the Tangla and Kueh Formations. This assumption is based on palaeontological evidence supported by the offset on the reflectance profiles for the Tuba and Meulaboh wells. The thickness of cover lost at the unconformity was approximately 250 m in the Meulaboh well and 230 m in the Tuba well respectively. Because only Tuba and Meulaboh wells penetrated basement, the burial history interpretation of the other six wells is restricted to the younger units.

As shown in Figures 6.3 and 6.4, the burial curves show slow sedimentation and burial between 62 and 40 Ma. Sedimentation was continuous from then on, including a moderate increase in burial due to the relatively fast deposition of the Tangla Formation (between 38 Ma and 5 Ma). Rapid sedimentation and burial occurred from 5 Ma to approximately 1.8 Ma when the Kueh Formation was deposited. From approximately 1.8 Ma to present time, sedimentation and burial was slow giving rise to the undifferentiated Meulaboh Formation and recent deposits. A noticeable feature in Figures 6.3 to 6.10 is the similarity in the burial history profiles from 5 Ma to 1.8 Ma when sedimentation and burial changed from the previous moderate rate to a rapid rate for almost all of the wells

examined. However, an exception to this scenario is in the Bubon and Teunom areas where the rate of sedimentation and burial may have remained constant from approximately the Middle Miocene to Pleistocene. There has been considerable uplift in the last 40 Ma in these areas.

#### **6.4.2. Timing of Hydrocarbon Generation**

The oldest formation (Tangla) entered the oil generation zone at approximately 5 Ma as indicated in Tuba and Meulaboh wells. This occurred during the major phase of Miocene subsidence when the Kueh Formation was deposited. It is generally accepted that the generation of hydrocarbons or the oil window commences at  $TTI=3$ . In this study a vitrinite reflectance of 0.50% has been shown to be equivalent to  $TTI=3$  and is considered to represent the start of oil generation; a vitrinite reflectance of 0.60% (equivalent to  $TTI=10$ ) was reached in the lower parts of the Tuba and Meulaboh wells. The probability of the basal formations and the deeper parts of the Tangla Formation reaching the onset of oil generation can be expected since the vitrinite reflectance data increase as depth increases and the palaeothermal gradient was higher than the present geothermal gradient.

#### **6.5. DISCUSSION**

Examination of West Aceh Basin geothermal gradients from exploration wells in the offshore area show a lateral change in present gradients from 17°C/km to 39°C/km. However, gradients are below the average for the other Tertiary basins of Indonesia, especially the backarc basins. The lower geothermal gradients in forearc basins and this basin in particular, compared to the backarc basins, may have been caused by several different geological processes operating during and after deposition of the Tertiary sequences. Heat flow is one factor that is responsible for the geothermal gradient within this basin. Plate tectonic movement and regional tectonics caused by plate motion directly control the heat input into, and the simultaneous heat transfer within, the sedimentary basin (Yalcin and Welte, 1988).

Regionally, West Aceh Basin formed as a result of the collision between the Indo-Australian and Asian Plates but more specifically, on a local scale, the collision between the western margin of Sundaland (Curry *et al.*, 1979) and the Asian Plate. Magma generation associated with subduction has given rise to the Tertiary to Recent Sumatra Volcanic Arc (Cameron *et al.*, 1982). Consequently, the heatflow distribution in the backarc basins in this area should be higher than in forearc basins due to the deep magma bodies seated below the backarc basins. Relatively slower sedimentation and subsidence in the backarc basins resulted in more texturally compact sedimentary basin fill sequences and hence produced rocks with lower thermal conductivity than the forearc basins.

More rapid sedimentation in forearc basins, results in very inhomogeneous rocks in both vertical and lateral directions, which raises the thermal conductivity in the sediment deposited in this type of basin. Structural deformation due to plate movement results in

more intensive flexuring, folding, faulting and thrusting, particularly in the arcward region. These structural developments enhance magma doming, which is recognised elsewhere in Sumatra by the distribution of volcanic and igneous rocks and suggests an increased geothermal gradient in the arcward regions (Eubank and Makki, 1981; Thamrin, 1985). In addition, high geothermal gradients are often related to areas of shallow basement or areas adjacent to a major fault or igneous intrusion (Bennet *et al.*, 1981). This is the case for the anomalous gradient found in the area in which Teunom well is located; this gradient is the highest geothermal gradient in the West Aceh Basin. Bennet *et al.* (1981) suggested that in the Teunom area, coastal volcanism occurred in the Middle to Late Miocene and produced basaltic eruptions and the intrusion of microdiorite. Pleistocene basaltic dykes emplaced in this area may also have contributed to the high value of the geothermal gradient in this area.

Although geothermal gradient data in the onshore area are not available, the vitrinite reflectance gradients, which are higher than those in the offshore area, can give an indication of geothermal gradients because vitrinite reflectance is directly related to the geothermal gradient. Based on this assumption, the geothermal gradient is, and also probably was during the Tertiary, higher in the onshore area than in the offshore area. This interpretation is supported by geological data that suggest diapirism in the Pameue area and possibly in the Seunagan area. Higher heat flows could be interpreted for these areas because of the intrusions of ultramafic rocks during the Mio-Pliocene and Pleistocene (Cameron *et al.*, 1983).

Coal seams in the onshore area may have contributed to the higher geothermal

gradient here compared to the offshore area due to the low thermal conductivity of the coal. Such evidence has been reported in Rifle, Colorado, where the geothermal gradient is as high as 180°C/km within the coal interval whilst it is only 20 to 40°C/km in the associated sandstone and siltstone (Blackwell and Steele, 1989). Rapid changes in the vitrinite reflectance are also associated with rapid changes in temperature due to the low thermal conductivity of organic matter (Blackwell and Steele, 1989). Given the coals seams in the onshore area, and their influence on the geothermal gradients, it is likely that the geothermal gradient in the West Aceh Basin decreases in an offshore direction. Notwithstanding this, the influence of the intrusions in the area are the most likely cause of the geothermal gradients.

The sedimentation and burial history of the West Aceh Basin varies slightly from one locality to another. In general, a major break occurs before the onset of Tertiary sedimentation which began in the Early Eocene with the deposition of the Tangla Formation (Figures 6.3 and 6.4). Slow subsidence during the Early Eocene resulted in a relatively thin sequence of the basal Tangla Formation. Uplift, erosion and probably an episode of deformation took place in the Late Eocene followed by deposition of the Tangla Formation during the following transgression. However, compared to the previous period, sedimentation was more rapid.

In the Middle Miocene, uplift of the Barisan Mountains began and this resulted in a marine regression in the nearshore area but sedimentation probably continued in the area in which Tuba and Meulaboh wells are located (Figures 6.3 and 6.4). The regional reconstruction suggests that the uplift was a consequence of renewed magma intrusion and

tectonism related to movements on the main northwest-striking, re-activated arcuate dextral transcurrent fault through Sumatra, complex intersections of which have split the Barisan Mountains into a series of lenticular wedges (Cameron *et al.*, 1982). These structures have probably been active periodically since at least the Oligocene but movement appears to have climaxed at about the beginning of the Pliocene (Cameron *et al.*, 1980; Katili, 1973).

After the period of uplift and erosion, the Kueh Formation was deposited disconformably on the earlier sequence with the environment changing with continuing transgression from continental to open marine sublittoral by the Middle Miocene. The rate of sedimentation during Kueh Formation deposition varied considerably from place to place and this can easily be seen in the wells. For example, in the Meulaboh, Tuba, Teunom and Bubon and Meulaboh East well areas, the rate of subsidence and sedimentation was relatively rapid but constant (Figures 6.3 to 6.6). The sedimentation rates increased rapidly during the Pliocene in some areas but remained constant in the Teunom and Bubon well areas from the Miocene to the Late Pliocene.

Rapid changes in the rate of sedimentation and burial in the Late Pliocene/Early Pleistocene may be related to renewed uplift and tectonism which again affected the Barisan Mountains. Since the Barisan uplift (Middle Miocene), the palaeotemperature rose in the West Aceh Basin reaching a maximum at the Plio-Pleistocene boundary. The orogeny, which affected the whole western Indonesia region, has ensured rapid concurrent sedimentation since the Pliocene and consequently greater burial was achieved in the Plio-Pleistocene period. This resulted in the thick deposits of the Tutut Formation. The same

thermal events may also have been responsible for higher palaeothermal gradients than the present geothermal gradients, not only in the Tertiary West Aceh Basin but also in most of the other Tertiary basins of western Indonesia.

Intensive uplift on the arc side of the West Aceh Basin and concurrent rapid subsidence in the main part of the basin during the Plio-Pleistocene resulted in thick sedimentary packages and may have given sufficient burial for the thermal generation of hydrocarbons. For example, models for the Tuba and Meulaboh wells indicate that the Tangla Formation reached the top of oil window during the Plio-Pleistocene period (Figures 6.3 and 6.4). The fact that the bottom of the oil window has not been recognised in the West Aceh Basin, is probably because of the limited data available rather than the geological conditions within the basin.

Because increasing depth of burial is followed by an increase in maturation, as indicated by all wells examined, the bottom of the oil window may be expected to occur in the deeper sections below the base of the wells. In some cases, modelling the time of oil generation using present geothermal data, may underestimate the possibility of higher palaeothermal conditions operating in this basin in the past. This is the case for the Tuba and Meulaboh wells (Figures 6.3 and 6.4) where modelling used the highest geothermal gradient for any part of the basin (with a value of 39°C) instead of the regional geothermal gradient. Vitrinite reflectance data indicate that the mature zone was encountered in these wells.

The oil window has not been encountered in the other wells but this does not mean that

hydrocarbons have not been generated in these wells. As discussed in Chapter 5, the mature zone is almost certainly present in the deeper sections, which yet have not been intersected by drilling, of wells such as Keudapasi, Bubon and Teunom. The lack of data from greater depths in most of the wells is one of the major obstacles in evaluating the timing of hydrocarbon generation in the West Aceh Basin using the Lopatin model. Therefore, any interpretation concerning oil generation in this study has to rely on vitrinite reflectance data in combination with geochemical data.

In summary, the subsidence and maturation histories of the Tertiary sequences in the West Aceh Basin suggest that the timing of any hydrocarbon generation (such as the oil shows noticed during drilling if they are indigenous to the sequence) is probably related to the subsidence and sedimentation rate during Plio-Pleistocene. Using the Lopatin (1971) model, the general trend is hydrocarbon generation to occur in the upper Tangla Formation as it intersects the oil window. However, hydrocarbon generation may have also occurred in the onshore area since geothermal gradients are postulated to be higher than those in the offshore area.



## **CHAPTER 7**

### **SOURCE ROCK AND PETROLEUM GENERATION**

#### **7.1. INTRODUCTION**

Cutting samples taken from the eight offshore wells in the West Aceh Basin were studied to assess their potential as source rocks for hydrocarbon generation. Organic petrography was used to identify and characterise the type and abundance of organic matter and to determine the rank or maturation levels of the coals and shales, respectively. For this part of the study it was assumed that, although the degree and generation capacity of the various macerals are different, macerals are capable of generating liquid hydrocarbons and/or gas although inertinite produces gas and only small amounts compared to other macerals. The characterisation of both gas-prone and oil-prone source rocks is needed as the discovery of either, or both commodities is important for the future development of Indonesia.

Organic geochemistry analyses were used in conjunction with the petrographic data to provide additional information on the petroleum potential of Tertiary formations in the West Aceh Basin. The geochemical and optical methods used were discussed in Chapter 3.

#### **7.2. SCORING SYSTEMS AND SOURCE ROCK POTENTIAL**

Petrographic source rock assessment was originally based on qualitative estimates of maceral

abundance combined with vitrinite reflectance measurements to assess maturity. In later studies, attempts were made to quantify maceral abundance and scoring systems were introduced. Scoring systems are used for semiquantitative assessment of DOM in source rocks and replace time-consuming and expensive point counts which, because of the small amount of organic matter in many samples, do not give valid results unless an extremely large number of counts are made. For example, in a point count of 500 points, a maceral constituting 0.2% of the bulk rock is represented by 1 count. Where organic matter constitutes less than 5% of a rock (which is common for many source shales) and several macerals are present, the total number of points counted per maceral needs to be at least 5 and probably 10 before any significant discrimination between maceral abundances are valid.

It is a basic premise of a scoring system that by using selected parameters, commonly maceral abundance, and weighting these according to an assumed capacity to generate oil and/or gas, an accurate assessment of oil generation potential of a sequence can be made. Using such petrographic assessment of rocks, the focus and direction of exploration programs can be influenced, hopefully to achieve greater success.

Smyth *et al.* (1984) proposed a petrographic scoring system to assess the hydrocarbon generating potential of the Birkhead Formation (Cooper Basin, Australia), in which measured variables such as thickness of shale units, volume and type of DOM, volume and type of coal, and coal rank were used to assess to source potential and maturation. They suggested that the highest probabilities for the generation of commercial quantities of petroleum occur where favourable source and maturation characteristics are combined with a relatively thick section. A major aspect of their hypothesis was based on the assumption of Tissot and Welte

(1978, 1984) that liptinite is the best source material for oil but vitrinite also has some potential, but to a lesser extent. Consequently, they used the ratio of liptinite to vitrinite in both DOM and coals as one variable to assess the Birkhead Formation, with additional variables such as maturation (as measured by vitrinite reflectance), volume of both DOM and coal, and thickness of shale in the Birkhead Formation (Smyth *et al.*, 1984). On the basis of these variables (with coal thickness incorporated within the shale section) they developed a score-scale, with a maximum of 10 for each sample. It was assumed the score indicated the relative potential of the formation at the locations sampled.

Over the thickness of the unit or formation the average score could be calculated using each sample with the unit or formation. This process is outlined in Table 7.1.

After reviewing the scoring systems of Smyth *et al.* (1984), Struckmyer (1988) and Panggabean (1990), it was decided to use the scoring system of Smyth *et al.* as it offers some advantages, especially in new exploration areas such the West Aceh Basin, where petroleum has not been discovered. For example, the number of drill holes in the West Aceh Basin is relatively small. Thus comprehensive examination of this limited sample set should allow ranking of the most prospective stratigraphic units, thus facilitating exploration and enhancing the prospects of the discovery of oil and/or gas.

The scoring system of Smyth *et al.* (1984) was thought to be more applicable for the present study, where the number of cuttings samples in each well was limited, than the later methods of Struckmyer (1988) and Panggabean (1990). However, modifications had to be made for the thickness of the shale units and the immaturity of the sequence. To overcome the latter problem, it is proposed that the maturation score, as indicated by vitrinite reflectance, is

extended to a lower value than the minimum 0.50% vitrinite reflectance proposed by Smyth *et al.* (1984). The shale thickness had to be neglected from the analysis because the thicknesses of the shale units in the West Aceh Basin sequence were not known.

The weighting factors for this study are given in Table 7.2 and the volume, type and rank of DOM and coal in the Tertiary formations are given in Tables 7.3 to 7.5. The lowest score for DOM is 0.5 which is equivalent to a DOM volume of 0.50%; the highest score is 10 which is equivalent to a DOM volume of >4%. The lowest score for coal is 0.25 equivalent to a coal volume of 0.50%, whereas the highest score for coal is 5 which is equivalent to a coal volume of >4%. The lowest score for maturation level (measured by vitrinite reflectance) is 0.20 which is equivalent to a 0.20% vitrinite reflectance, whilst the highest score in this study is 1.00 which is equivalent to a vitrinite reflectance range of 0.50 to 0.60%.

### 7.3. SOURCE ROCK EVALUATION

In general, the highest score for both DOM and coal is attained in the Tangla Formation, followed in succession by the Kueh and Tutut Formations. The Kueh Formation contains the highest ratio of liptinite to vitrinite, as DOM, with a ratio of 2.16 whereas the Tutut Formation has the lowest ratio of DOM liptinite to vitrinite with a ratio of 1.38 (Table 7.6). A similar ratio of liptinite to vitrinite was recorded in coal where the Kueh Formation has a ratio of 1.27 whilst the Tutut Formation has a ratio of 0.18. The Tangla Formation has liptinite to vitrinite ratios of 1.45 (DOM) and 0.35 (coal).

### 7.3.1. Tutut Formation

Scores for the hydrocarbon potential of DOM in the Tutut Formation (Table 7.7) indicate that the source potential is highest in the Teunom well and lowest in the Tripa well, with most wells having values of  $> 3$ . However, when the score values for DOM and coal are summed, the Teunom well also has the highest calculated average value while the lowest score is in the Tripa well (Table 7.8). The ratio of liptinite to vitrinite, as DOM, in the Tutut Formation varies from 0.61 to 2.03; Keudapasi well has the highest value whereas the lowest value occurs in the Tuba well. The ratio of liptinite to vitrinite in coal for the Tutut Formation is within the range of 0.08 to 0.29.

### 7.3.2. Kueh Formation

Scores for hydrocarbon generation potential indicate that the source potential of DOM is mostly  $> 3$ , although lower values of 0.89 and 1.84 are found in the Palumat and Meulaboh wells respectively (Table 7.9). The ratio of liptinite to vitrinite in DOM is highest in the Teunom well with a ratio of 5.33 whilst the lowest ratio is found in the Meulaboh well with a value of 0.92. The highest combined score for DOM and coal is found in the Teunom well and the lowest combined score in the Palumat well; the scores were 18.35 and 0.89 respectively (Table 7.10).

### 7.3.3. Tangla Formation

Hydrocarbon generation scores of DOM for the Tangla Formation (Table 7.11) indicate that

the score potential of this formation is  $>7$  in the two wells examined. The Meulaboh well contains the better maceral assemblage, as DOM, for oil generation in this formation with a ratio of liptinite to vitrinite of 1.70. The combined DOM and coal score values range from 8.40 to 10.49 (Table 7.12). In addition the ratio of liptinite to vitrinite in coal ranges from 0.19 to 0.52.

#### 7.3.4. Summary

Although the Tangla Formation has a higher hydrocarbon potential score than both the Kueh and Tutut Formations, the observations are based on only a small number of samples. When assessing the hydrocarbon generating potential using the score values from two wells (Meulaboh and Tuba) the reliability of the conclusions should be considered within this context. Furthermore assessments of lateral variations in the abundance and nature of the organic matter, as well as maturity, are highly speculative at present.

The highest level of maturity in the West Aceh Basin is attained in the Tangla Formation. It is likely that, on a regional scale, the Tangla Formation is the most prospective source rock because it has probably reached maturities within the 'oil window'. Comparable data for the Tangla Formation in the onshore area also suggests that it is the most prospective stratigraphic unit there as well.

In summary, the petrographic scoring system is not the only method for assessing hydrocarbon generation potential but it does at least (as stated by Smyth *et al.*, 1984) provide basic information on which to select areas for more detailed study. Therefore, an organic

geochemical evaluation has been used in conjunction with organic petrography to provide more information for assessing hydrocarbon potential in the West Aceh Basin.

#### **7.4. SOURCE ROCK GEOCHEMISTRY**

A potential hydrocarbon source rock can be characterised by a combination of several different geochemical techniques (Tissot and Welte, 1978, 1984). The data presented here are used to assess source rock richness, type of organic matter and maturity, and to predict actual petroleum composition within the samples. A total of 56 offshore samples and 28 onshore coals were analysed by TOC/Rock-Eval and these data are summarised in Tables 7.13 to 7.14 and Table 7.16 respectively. Rock-Eval data for each offshore well is given in Appendix 11.

In addition, eleven cuttings samples and twelve onshore coal samples were soxhlet-extracted with solvent ( $\text{CHCl}_3$ :MeOH:87:13) for forty-eight hours and the saturated, aromatic and polar (NSO) fractions were obtained from column chromatography of the extract using silica (Table 7.17 and 7.18). The saturated hydrocarbon fraction was then analysed for a variety of straight-chained alkanes and acyclic isoprenoid hydrocarbons by gas chromatography.

##### **7.4.1. Rock-Eval/TOC**

Composite cuttings samples for Rock-Eval pyrolysis analyses were obtained by mixing consecutive samples on which petrographic data were available. This method was needed because the individual samples supplied to the researcher were too small to allow both

petrography and geochemistry in many cases. All components of the composite samples used in the organic geochemical study had previously been examined for the type and abundance of organic matter and the level of thermal maturity. In addition the TOC of 56 offshore samples and onshore coal samples were determined by the direct combustion method using a LECO carbon analyser.

$T_{\max}$  values for samples with  $S_2$  less than 0.2 mg HC/g rock are often unreliable, and were discarded. In addition, clastic rocks containing TOC < 0.5% and carbonate rocks containing < 0.3% TOC, or  $S_2$  < 0.2, were considered to have no hydrocarbon potential. These are accepted as the minimum lower source richness limits for commercial oil generation (Thomas, 1979; Smyth *et al.*, 1984; Peters, 1986).

Reference to Table 7.13 shows that the average TOC content in offshore samples is highest in the Tangla Formation (average value 14.13%) with the Kueh Formation containing the second highest TOC (average of 8.59%); the Tutut Formation has the lowest TOC (average value of 6.92%). The individual TOC values and Rock-Eval results for offshore samples are given in Appendix 12 and the average TOC/Rock-Eval results for each well are presented in Table 7.14.

The Tutut Formation is represented in all of the wells for which data are available and most of the shale samples contain TOC of more than 0.5%, except for some samples from the Bubon (GM 22456), Keudapasi (GM 22384 and GM 22385) and Tripa (GM 22423) wells. The highest TOC in any shale sample is in the Palumat well (GM 22397) where the TOC value was 5%. For coal and carbonaceous shale samples, the highest TOC value was found



in the Bubon well (GM 22352) with values of up to 48% and an average of 35%.

Kueh Formation was also represented in all wells examined. The average TOC content is greater than 0.5% in shale samples and more than 40% in coal samples. The highest value in shale was found in the Bubon well (GM 22461) with a value of 17.5% whilst the highest TOC in a coal sample was also found in the Bubon well (GM 22469) with a value of 51%. Overall, Meulaboh East contains the highest combined coal and shale average TOC with a value of 27% whilst the lowest combined value is found in the Palumat well where the average value is only 0.87%.

The average TOC for the Tangla Formation (4 data points, including carbonaceous shale) is 14.13%. These data may be misleading as three of the four samples were shale and the TOC ranged from 2.68% to 10.22%. The fourth sample was a coaly shale sample (GM 22367) and contained 40% TOC.

TOC content for onshore coal (Table 7.16) ranges from 11.90% (coal with dirt bands) to 78.0%. The highest values of TOC are found in the Oligocene coal where they range from 44.60% to 73.60% and average 62.48%. The TOC content of Miocene coals ranges from 12.40 (coal with dirt bands) to 78.0%, with an average of 53.40%. Pliocene coal has the lowest TOC values ranging from 11.90% to 52.0% with an average of 36.40%. There is a tendency for the TOC to increase as rank increases in both offshore and onshore areas, but the general trends show that the values are higher in the onshore area than in the offshore area for any stratigraphic interval. This is in agreement with the lateral and vertical rank pattern in this basin in which rank increases with depth and in an onshore direction for any

stratigraphic interval.

TOC values tend to increase with increasing maturity level and this is similar to the trend for Fixed Carbon analysed on air dried basis (Hadiyanto and Amarullah, 1985). These trends may only be valid for the clean coal seams in which dirt bands are not found in the seam. The possible explanation in relation to the different TOC content between offshore and onshore areas is due to the facies control on sediment input which in turn is caused by the different palaeoenvironments within the peat swamps. If this is the case the relative abundance of mineral partings in the coals from the offshore area, in which clastic sediment supply is more dominant than those of onshore area, may also responsible for the lower TOC value in this area.

For Rock-Eval data,  $T_{max}$  is recorded in degrees Celsius and corresponds to the temperature at which maximum hydrocarbon generation (S2) occurs during kerogen pyrolysis.  $T_{max}$  is also used as a maturation indicator where a temperature below 435°C is considered immature, temperatures between 435°C to 465°C are indicative of oil generation and temperatures above 465°C are considered to be post-mature and, therefore, only gas prone (Espitalie *et al.*, 1985). However, for Type III kerogen and coal slightly higher  $T_{max}$  values, 435°-455°C are required before the onset of significant hydrocarbon generation.

#### 7.4.1.1. Clastic Sediment Samples

Based on the data presented in Table 7.13, it is clear that most of the samples lie in the immature zone with  $T_{max}$  values lower than 430°C. The highest  $T_{max}$  values are in the Tangla

Formation where the average value is 426°C; the average  $T_{\max}$  values for the Kueh and Tutut Formations are 404°C and 394°C respectively. Although the average value of  $T_{\max}$  in the three formations is lower than 435°C, regarded as the lower limit for the onset of oil generation, some individual samples have  $T_{\max}$  values greater than 435°C. For example, sample GM 223525 from the Kueh Formation in Bubon well has  $T_{\max}$  values at 438°C and a sample from the Tangla Formation in the Meulaboh well (GM 22475; Appendix 11) has a  $T_{\max}$  of 436°C. However, it is considered that these samples have not yet reached sufficient maturity for hydrocarbon generation to have been produced by kerogen breakdown.

The S1 value is a measure of the amount of free hydrocarbon released at 300°C during temperature programmed pyrolysis. At higher temperatures of 300°C to 600°C kerogen pyrolysis, which generates hydrocarbon compounds, occurs and this is given as S2. S3 is the quantity of CO<sub>2</sub> formed by pyrolysis of the organic matter. S1 and S2 are expressed in milligrams of hydrocarbon per gram of rock (mg HC/g of rock) whereas S3 is expressed in milligram of CO<sub>2</sub> per gram of rock (mg CO<sub>2</sub>/g of rock).

The hydrogen Index (HI) and oxygen index (OI) are calculated from the S2 and S3 peaks respectively ( $HI = 100 \times S2/TOC$  and  $OI = 100 \times S3/TOC$ ) and are expressed as mg/g of TOC. For the values of HI expressed on a per-carbon basis,  $HI > 300$  indicates hydrogen-rich organic matter and is regarded as oil prone, whereas  $HI < 200$  characterises hydrogen-poor organic matter and is gas prone. Intermediate HI values (200-300) have both gas and oil potential.

The Production Index (PI) is calculated from the formula  $S1/(S1+S2)$ . The latter indicates the level of maturation and also the presence of epigenetic hydrocarbons (Espitalie *et al.*,

1985; Peters, 1986).  $S_2/S_3$  values between 0 and 3 indicate gas prone conditions;  $S_2/S_3$  values between 3 and 5 are considered to have both gas and oil potential and values greater than 5 are oil prone (Peters, 1986).

The Rock-Eval results show that the free hydrocarbon yield ( $S_1$ ) of the offshore West Aceh Basin samples ranges from 0.01 to 15.20 mg HC/g with the highest average  $S_1$  value in samples from the Kueh Formation (2.22 mg HC/g). Lower values were obtained for the Tutut Formation (1.96 mg HC/g) and Tangla Formation (1.69 mg HC/G; Table 7.13).

Except for the Tangla Formation, where samples were taken from only one drill hole, the highest average  $S_1$  value was in the Meulaboh East well (7.56 mg HC/g) and the Bubon well (6.69 mg HC/g) for the Kueh and Tutut Formations respectively (Table 7.14). Overall, individual samples had  $S_1$  values mostly less than 2% for shale and between 4.0 and 15.20 mg HC/g for coal samples (Appendix 12).

The average  $S_2$  value was highest in the Tangla Formation (26.87 mg HC/g) and lowest in the Tutut Formation (2.86 mg HC/g); the Kueh Formation has an average  $S_2$  value of 14.32 mg HC/g (Table 7.14). For individual wells, the highest  $S_2$  values are in the Meulaboh well (26.87 mg HC/g) for the Tangla Formation and in the Bubon (35.34 mg HC/g) and Teunom (8.91 mg HC/g) wells for the Kueh and Tutut Formations respectively.  $S_2$  values are mostly less than 8 mg HC/g for shale samples and between 31 to 92 mg HC/g for the coal samples (Appendix 12).

The HI and OI data for West Aceh Basin samples (Figure 7.1a) plot in the region occupied

by Type III kerogen using the Tissot and Welte (1984) diagram. This is in agreement with the petrographic data which show that the macerals are derived mostly from land plants and the samples have a high vitrinite content and can be best assigned to Type III organic matter. Although the Tangla Formation was only represented by four samples, the HI values ranged from 79 to 241; the latter value came from a sample from the Meulaboh well (GM 22475) which contained 14% liptinite macerals, whereas other samples contained less than 4% liptinite. The average HI for the Tangla Formation was higher than corresponding values for the Kueh and Tutut Formations. These Tangla Formation data span the Type II/III region of the Tissot and Welte plot. Most Tutut Formation samples have HI values lower than 100 and the OI values range from 60 to 227. The reason for the high OI values is not known, however, elsewhere it has been reported that high oxygen contents are due to reworking, oxidation or reaction with CO<sub>2</sub> liberated from carbonate minerals (Boreham *et al.*, 1988).

Although some Kueh Formation samples contain relatively higher proportions of liptinite (GM 223525, GM 22388, GM 22393, GM 22414, GM 22417) than other samples, the HI values of these samples are very low and almost near the base line in the HI/OI crossplot. In addition the OI values are relatively high. It is likely that the low HI values are due to a mineral matrix effect because these samples have abundant mineral matter. Mineral matrix content, especially clay minerals, may retain some pyrolysate. It has been shown that samples with <4% organic carbon can record very low values because of this clay matrix effect (Orr, 1981; Boreham, 1988).

Another possible reason for the low HI values is increased oxidation of the organic matter during deposition and diagenetic processes (Boreham, 1988). Although a high inertinite

content in samples decreases the HI value, the West Aceh Basin samples contain almost no inertinite and thus this cannot be a contributing factor. However, many samples show oxidation rims around liptinite and detrovitrinite and this suggests that the macerals are secondary components and that oxidation occurred during transportation. Hence, this may be the cause of the low HI and increased OI values.

The highest vitrinite reflectance value of 0.54% falls in the marginally mature zone and was recorded from the Tangla Formation (GM 22475). However, a  $HI/T_{max}$  crossplot indicates that this sample also contains predominantly Type II kerogen (Figure 7.2). All other samples have  $R_{v,max} < 0.54\%$  (up to marginally mature) and their type of organic matter is as for the HI/OI assignment.

The wide range in  $T_{max}$  values (390-430°C) is most likely due to contributions of high molecular weight organic molecules associated with the unbound organic matter (S1) being evolved with the kerogen. The relative contributions of each to the S2 profile will have a marked effect on the measured  $T_{max}$  value. Indeed Rock-Eval analyses of the extracted rock show consistently higher  $T_{max}$  values (Table 7.15) reflecting the sole contribution from the breakdown of kerogen.

#### 7.4.1.2. Coal Samples

Rock-Eval data (Table 7.16) of onshore coals vary considerably. Although Pliocene coal Rock-Eval values show less pyrolytic products than those of Miocene and Oligocene coals, the S1 values are relatively higher in some samples. S1 for the Pliocene coal ranges from

3.19 to 21.19 mg HC/g, and S2 ranges from 6.33 mg HC/g to 123.55 mg HC/g. HI values are mostly less than 150 mg HC/g of TOC, indicating that the Pliocene coal is characteristically hydrogen-poor. Although  $R_{\text{max}}$  data indicate that most Pliocene coal samples are immature,  $T_{\text{max}}$  and PI values range from 397-421°C and 0.18-0.34 respectively. These wide ranges may also be due to contributions of high molecular weight organic molecules associated with unbound organic matter (S1) being evolved with the kerogen (Boreham, pers. comm.). If this is the case, the presence of high molecular weight molecules in these Pliocene coal samples may be associated with the petrographic observation of exsudatinite. In addition the relatively high value of PI is related to the occurrence of free hydrocarbons in the Pliocene coal. Since exsudatinite is a product of hydrocarbon release from the coal, the high value of PI in the Pliocene coal may also be attributed to this secondary maceral.

The Miocene coal samples have a wide range of S1 and S2 values from 0.19 (coal with dirt bands) to 20.33 mg HC/g and 11.89 to 264.10 mg HC/g respectively. The lowest S1 and S2 values are found in sample GM 22053 and are probably due to the absence of liptinite macerals in this sample. On the other hand, the huge amount of liptinite macerals, especially exsudatinite and resinite, in sample GM 22825 probably accounts for the highest S1 and S2 values occurring in this sample. The HI of the Miocene coal varies considerable between 22 and 454 mg HC/g of TOC. The lowest value is found in the vitrinite-rich sample (GM 22053) whilst the highest value occurs in the liptinite-rich sample (GM 22825).  $T_{\text{max}}$  values of 404° to 462°C and PI values of 0.02 to 0.12 indicate that the Miocene coal ranges from a low to high maturity level. However, the highest  $T_{\text{max}}$  value (462°C, consistent with  $R_{\text{max}}$  of 1.15%) is associated with sample (GM 22824) which underwent thermal upgrading due

to an igneous intrusion.

Oligocene coals have a range of S1 and S2 values. S1 ranges from 4.25 to 27.08 mg HC/g of rock whereas S2 values range from 130 to 282 mg HC/g of rock. The highest S1 value is associated with a sample rich in exsudatinite (GM 22825) whereas the highest S2 value is found in a sample rich in desmocollinite (GM 23234). The HI is generally more than 250 mg HC/g of TOC.  $T_{\max}$  and PI values vary between 425°-450°C and 0.02-0.14 respectively.

A diagram of HI vs OI (Figure 7.2a) shows most of the onshore coal samples from the West Aceh Basin plot in the regions occupied by Type II and Type III kerogens (Tissot and Welte, 1984). All Oligocene coal have a HI value between 200-400 indicating high liquid generating potential. For most of the Miocene coal, HI value are between 200-300 suggesting both oil and gas potential. The Miocene coal show both extremes; sample GM 22825 has highest HI and this is consistent with a predominantly liptinite content (50%), suggesting a significant liquid potential. On the other hand the Miocene coal (GM 22053) has a HI of 22 indicating little or no hydrocarbon potential. This is in agreement with the petrographic data which show that the macerals mostly consists of vitrinite and the liptinite maceral was absent. Although Miocene sample (GM 22826) is currently gas prone (HI=129), the high  $T_{\max}$  (462°C) and  $R_{\max} = 1.15\%$  indicate that significant hydrocarbon generation has most likely occurred (this sample underwent localised thermal upgrading due to an igneous intrusion). Rock Eval data alone is unable to estimate its original potential and pyrolysis-gc analysis is required (see below).

Where  $T_{\max}$  values are plotted against HI (Figure 7.2b), it is clear that most Pliocene coal



samples plot closer to the Type III curve and fall in the immature zone whereas most Oligocene and some Miocene coal samples plot near the Type II curve and lie in the mature zone. This is in agreement with vitrinite reflectance data that indicate most Pliocene coal samples are immature (around 0.30%) and that Miocene and Oligocene coal samples are marginally mature and mature respectively. The highest vitrinite reflectance value from sample GM 22826 plots within the mature zone. However, the  $HI/T_{max}$  crossplot indicates that this sample also contains predominantly Type III kerogen and, therefore, the type of organic matter is as for the HI/OI assignment.

#### **7.4.2. Gas Chromatography and Source Rock Characteristics**

Eleven offshore samples and twelve onshore coal samples, selected on the basis of formation and rank, were extracted following initial screening by Rock-Eval and TOC analyses. The hydrocarbon composition of the extracted fraction consisted of saturated, aromatic and polar fractions. The saturated fractions from each sample were analysed using capillary gas chromatography.

##### **7.4.2.1. Extractable Organic Matter**

The composition of the extractable organic matter of both offshore and onshore samples is given in Table 7.17 and Table 7.18 respectively. The total extractable organic matter (EOM) of offshore samples varies widely from 0.8 to 239.5 mg, whilst onshore samples range from 7.5 to 462 mg. Although most Tutut samples have higher EOM than both Kueh and Tangla samples, the TOC content is mostly lower than for the Kueh and Tangla samples. In most

cases the higher EOM values for both offshore and onshore samples are related to the amount rock extracted and, therefore, no relationship is expected between EOM and TOC values.

Normalised HC on a per organic carbon basis indicate that the hydrocarbon content of both offshore and onshore samples ranges from 13.30 to > 500 mg HC/g TOC and 2.30 to 27.40 mg HC/g TOC respectively. In addition most of the onshore coal samples yielded lower HC than those of offshore shale samples (Figure 7.3a and 7.3b). Although there is evidence elsewhere that the yield of HC/gTOC from extracted coal is lower than those of conventional source-rocks (Espitalie *et al.*, 1985; Hunt, 1991), the reason for this is uncertain. It may be due to HC being more easily expelled from the coal during coalification or more likely due to the inability of the solvent extraction method to release the maximum HC from the coal (Given, 1984) or a bias in the published data towards coals with lower liquid potential than the shales. When the shale samples with low hydrocarbon potential (< 1% TOC) are excluded there is little differentiation between coal and shale (Figure 7.3c).

It is also evident that HC yields (mg HC/g TOC) do not correlate well with the rank ( $R_{\text{max}}$ ; Figure 7.4a and 7.4b). This is consistent with the low maturity of the samples. However, the higher rank samples (GM 22825 and GM 22824, Figure 7.4b) show higher HC yields compared to all the other coals respectively. Values around 30 mg HC/gTOC are considered to be a lower limit for hydrocarbon retention in a source rock and above this expulsion can occur (Powell, 1988). Thus, it can be suggested that these coals have generated sufficient hydrocarbons to presently support future expulsion or they are in the process of active expulsion and the hydrocarbons are retained within the coal at a constant level.

Only during petroleum generation ( $R_{\text{vmax}} > 0.5\%$ ) will any consistent trend of increasing yield be seen (Espitalie *et al.*, 1985). Powell (1978) and Crick *et al.* (1988) suggested that the lower limit for an excellent source rock is equivalent to 80 mg HC/g TOC whilst the lower limits of good and marginal source rocks are equivalent to 50 and 30 mg HC/g TOC respectively for the samples having TOC content  $> 1\%$ . Poor effective source rocks, which may be gas prone or immature, are considered to be rocks yielding less than 30 mg HC/g TOC. The high mg HC/gTOC for samples with TOC content  $< 0.5\%$  (for example GM 22456 and GM 22466) are considered not to be effective source rocks but indicate hydrocarbon migration or suffer from contamination and or staining.

Extracted HC yield from both offshore and onshore samples indicate that most of the samples are immature. The high ratio of the polar fraction to aromatic and/or saturated fraction further indicates the immaturity of these samples. However, some onshore coal samples show a low ratio between polar to aromatic or saturated fractions as evident in the mature samples (GM 22824 and GM 22825). The evidence from both offshore and onshore samples indicates that the saturated/aromatic ratio is negatively related to the rank of the coal ( $R_{\text{vmax}}$ ), as shown in Figure 7.5. As rank increases the ratio decreases, which corresponds to the release of short chain hydrocarbons and less complex aromatic molecules through disproportionation reactions (Korth, pers. comm.).

#### 7.4.2.2. N-Alkane Distribution

Gas chromatography (GC) analyses of saturated extracts from offshore samples show homologous series of straight-chained alkanes ranging from  $n\text{-C}_{14}$  to  $n\text{-C}_{33}$  (Figures 7.6 to

7.16). In general, most of the GC profiles indicate immature samples with relatively low amounts of n-alkane although some samples do show a major contribution of indigenous extractable organic matter. Samples with non-representative GC profiles in the Bubon (GM 22456, GM 22460, GM 223525), Tripa (GM 22428, GM 22433, GM 22441), Meulaboh (GM 22353, GM 22359) and Teunom (GM 22370, GM 22441) wells are considered to indicate background material that has been either contaminated from outside (well site or laboratory) or altered by oxidation/weathering. Saturated HC yields are extremely low, further exaggerating any non-indigenous contribution. Sample GM 22475 indicates a marginally mature sample with a relatively high amount of n-alkane. Background materials also occurred in this sample but in a small amount.

Samples from Bubon well (Figures 7.6 to 7.8) show a unimodal n-alkane distribution with n-alkane predominance in the range n-C<sub>16</sub> to n-C<sub>20</sub> with maximum peak height at n-C<sub>18</sub>. Similar distributions were also recorded in samples from the Tripa well (Figures 7.9 to 7.11).

The concentration of the carbon numbers n-C<sub>16</sub> to n-C<sub>20</sub> has been discussed in several papers. Powell and McKirdy (1973) and Hunt (1979) believed that the concentration of these carbon numbers is due to the influence of marine organic matter or bacterial affinities. However, in a later study on the pyrolysis of extracted sporinite, Winans and Crelling (1984) concluded that sporinite yields mostly normal alkanes and alkenes up to C<sub>19</sub> with C<sub>16</sub> being the most abundant product. Petrographic data for samples from the Bubon and Tripa wells, except sample GM 22428, shows that sporinite and, to a lesser extend cutinite, are the most abundant macerals indicating that the organic matter was derived from land plants. The distribution of n-alkanes in these samples is similar to the distribution of these compounds

given by Winans *et al.* (1984). Therefore, terrestrial-derived organic matter is the most likely component in these samples although bacterial origin can not be discounted. In contrast, the low proportion of higher molecular weight n-alkanes in GM 22428 (Figure 7.9) would appear to indicate that there was no contribution, or only a small one if any, from terrestrial plants and thus the organic matter was lacustrine, at least in part. Since EOM represents only a small fraction of the total organic matter, there exists the real possibility that the composition of the EOM does not reflect that of the whole kerogen. Petrographic data show that lamalginite is common in this sample with minor cutinite. The n-alkane profile of lamalginite-dominated rocks is generally associated with low to moderately high molecular weight n-alkanes. Thus the appearance of low molecular weight n-alkanes most likely represents a strong bias of the bacteria contribution in the extractable organic matter. Since fragmented cutinite is associated with this sample, it is possible therefore to assume that this sample may represent a lacustrine environment with some input of terrestrial plants.

The n-alkane distributions in the Meulaboh well are presented in Figures 7.12 to 7.14. In general, a bimodal distribution is indicated with one maxima in the range n-C<sub>15</sub> to n-C<sub>21</sub> and the second maxima from n-C<sub>24</sub> to n-C<sub>31</sub>. Sample GM 22475 shows a more prominent bimodal distribution than samples GM 22360 and GM 22353. A terrestrial waxy input may be present in all samples, within the range of n-C<sub>22</sub> to n-C<sub>33</sub> with maximum peak heights at n-C<sub>29</sub> for both GM 22475 and GM 22353. In GM 22363, the waxy input is less pronounced and the maximum peak height is at n-C<sub>27</sub>. The bimodal n-alkane distribution has been reported to indicate respective contributions from algal/bacterial (or marine) and terrestrial-derived alkanes (Hunt, 1979). In sample GM 22353, for example, *Botryococcus*-type telalginite probably contributed compounds over the whole molecular weight range whereas

the cutinite component would contribute waxy hydrocarbons. Since there was no petrographic evidence of a marine input in these samples, the low molecular weight n-alkane maxima is due to the algal or bacterial inputs. The small quantity of sporinite in these samples would also contribute to the lower carbon number fraction if the results reported by Winans *et al.* (1984) apply in this context.

The n-alkane distributions of the two samples (GM 22367 and GM 22370) from the Teunom well (Figures 7.15 and 7.16) are very similar and have high peak intensities in the range n-C<sub>16</sub> to n-C<sub>20</sub> with a shift toward smaller peak intensities for the higher n-alkanes. An odd-even carbon number predominance occurs in both samples in the region of n-C<sub>24</sub> to n-C<sub>32</sub> with a shift toward lower carbon numbers and a maximum peak at n-C<sub>18</sub>. The terrestrial-waxy input may be contributed from the cutinite maceral as supported by petrographic data from this sample.

The n-alkane distribution of onshore coal samples varies widely but mostly ranges from n-C<sub>14</sub> to n-C<sub>33</sub>; a few samples contain linear alkanes beyond C<sub>33</sub>. The GC profile indicates immature to mature samples with a low to high amounts of n-alkanes (Figures 7.17 to 7.28). Samples representative of the GC profile in Pliocene coal (GM 23319, GM 22843, GM 22352), Miocene coal (GM 22448, GM 22469, GM 22826) and Oligocene coal (GM 22367) are considered to contain high background material. This background material may have resulted from alteration processes due to weathering since most of these samples were taken from outcrop. In contrast, most of the Oligocene coal samples (except GM 22367) and one Miocene coal sample (GM 22824) show very little influence of background material and, are dominated by the n-alkane envelope. The general trend indicates that the amount of n-alkane

increases as rank increases and also increases from Pliocene coal towards the Oligocene coal samples.

The Pliocene (Tutut Formation) coal is represented by samples GM 23319, GM 22843 and GM 22352 (Figure 7.17 to 7.19). The GC profile indicates that all of the samples are immature with very low amounts of n-alkanes. This is in agreement with the maturity measured by vitrinite reflectance where all of the samples attained a vitrinite reflectance of about 0.30% ( $R_{v,max}$ ).

Although these samples are immature and contain relatively high background material, the biomarker signature can be recognised in the area between n-C<sub>29</sub> and n-C<sub>31</sub>. This may represent the hopanoid biomarker which is relatively resistant to biodegradation (Boreham, pers. comm.).

Figures 7.20 to 7.23 represent more mature Miocene coal samples from the Kueh Formation. Although the amount of n-alkane is higher than for the Pliocene coal samples, background material contributed to the peak distribution of the pyrogram. This should be taken into consideration when assessing the n-alkane distribution. Roughly, bimodal patterns are evident from these samples and include one maxima in the range n-C<sub>14</sub> to n-C<sub>20</sub> and the second maxima in the range n-C<sub>23</sub> to n-C<sub>33</sub>. It is interesting to note that although sample GM 22824 is mature ( $R_{v,max}=1.15\%$ ) the chromatogram shows a degree of immaturity indicated in the higher molecular weight range from n-C<sub>25</sub> to n-C<sub>33</sub> (an odd carbon predominant). This sample underwent rapid thermal heating due to an igneous intrusion and highlight the different time/temperature on the maturation of vitrinite and the kinetics of hydrocarbon generation.

The evidence from the Oligocene (Tangla Formation) coal sample GM 22825) is in contrast with the evidence in GM 22824 cited above. This mature ( $R_{vmax}=0.65$ ) sample underwent normal coalification processes in which there was no influence of igneous thermal heating. This sample is characteristic of slightly more mature n-alkane distribution with a higher content of lighter molecular hydrocarbons and a lower odd-even carbon predominance in the  $> C_{22}$  waxy n-alkanes, although only having a  $R_{vmax}$  of 0.65%. This again reflects the different responses of the two processes (vitrinite reflectance and petroleum generation) to the temperature history.

In general, most of the Oligocene coal samples are marginally mature in the range of  $R_{vmax}$  between 0.50% to 0.65%. They contain a relatively high amount of n-alkanes, which are characterised (except in sample GM 22825) by an odd-even predominance, and may contain terrestrial waxy compounds as indicated by the maxima in the range n- $C_{25}$  to n- $C_{33}$ . The long chain predominance at the rank of these samples may indicate decarboxylation of the higher molecular weight fatty acids rather than polymerisation products of short chain hydrocarbons (Given, 1984).

#### 7.4.2.3. Isoprenoid Hydrocarbons

Overall, pristane (Pr) and phytane (Ph) are the most common isoprenoids in both offshore and onshore samples. These isoprenoids have been assumed to be diagenetic products of the phytol side chain of chlorophyll (ten Haven *et al.*, 1987). Didyk *et al.* (1978) stated that pristane is formed through an oxidative pathway, for example, through phytanic and/or phytenic acids and subsequent defunctionalisation, while phytane is generated via various



reductive paths. Thus, the presence of oxic or anoxic conditions during or just after deposition will have the greatest influence on intimate pristane and phytane concentrations in sedimentary rocks. Although there is no exact value of the Pr/Ph ratio for assessing the palaeoenvironment during deposition, general acceptance indicates that values  $< 1$  are related to anoxic or hypersaline environments whilst values  $> 3$  are found in terrestrial oxic conditions. However, the use of Pr/Ph ratio is not recommended as an environmental indicator for immature samples (Powell, 1988).

Pristane and phytane data for offshore and onshore samples are given in Tables 7.19 and 7.20 respectively. The Pr/Ph ratio of offshore samples ranges from 0.57 to 5.4, whilst onshore samples have a Pr/Ph ratio mostly greater than 2 with maximum value of 9.23. The relationship between the Pr/Ph ratio to the rank parameter measured by vitrinite reflectance for both offshore and onshore samples is plotted in Figure 7.29. The offshore data show a relatively high degree of scatter with almost no relationship between the variables (Figure 7.29a). This may indicate that several variables, rather than just rank, controlled the development of pristane and phytane. Independent sources for the 2 isoprenoids, other than from phytol, are known. In immature samples unsaturated precursor to the isoprenoid hydrocarbons will be present. If the separate hydrogenation reactions leading to the 2 isoprenoids occur at different rates then variable reactions will be obtained. A similar situation occurs for the onshore samples where all of the samples are coal. Here there is delicate balance between the conversion of the isoprenoid hydrocarbon precursors to their fully saturated products (Pr and Ph) and generation from kerogen. The increase in Pr/Ph ratio up to  $R_v$  max of 0.65% being associated with the former process while a decrease in the ratio for GM 22824 ( $R_v$  max 1.15) may be associated with thermal catagenic processes. Such

variations are common within a maturity sequence (Powell, 1988). The relationship between the Pr/Ph ratio of coal to the vitrinite reflectance is given in Figure 7.29b.

The maturation parameters, Pr/C<sub>17</sub> and the vitrinite reflectance of both offshore and onshore samples are plotted in Figures 7.30 and 7.31 respectively. Although the data plots are scattered, especially for the reflectance level below 0.5%, the highest value of 1.0 for the Pr/C<sub>17</sub> ratio occur above R<sub>v</sub>max 0.4% for the offshore samples (Figure 7.30a) and values > 2.0 for the onshore samples (Figure 7.30b) occur above R<sub>v</sub>max 0.50%. The wide range of Pr/C<sub>17</sub> values of the immature samples (R<sub>v</sub>max < 0.5%) may be due to variations in the organofacies, variation in the depositional environment (Leythaeuser and Schwarzkopf, 1986) as well as incomplete conversion of precursor isoprenoid to pristane. With increasing maturity, especially beyond 0.8%, this range of variation is diminished sharply (Leythaeuser and Schwarzkopf, 1986). This may be the case for the onshore coal samples (Figure 7.35b) where increasing vitrinite reflectance level up to 0.65% show an increase in Pr/C<sub>17</sub> most likely due to conversion of pristane precursor to C<sub>17</sub>. At higher maturities preferential generation of n-alkanes from kerogen decomposition leads to a lower value of Pr/C<sub>17</sub>.

A similar comparison with the rank was attempted for the Ph/C<sub>18</sub> ratio for both offshore and onshore samples as shown in Figures 7.30b and 7.31b respectively. The relationship with rank is more linear than for the Pr/C<sub>17</sub>. This smooth linear relationship may indicate that phytane is formed at a higher rate than C<sub>18</sub> during the main phase of hydrocarbon generation. This is especially the case for onshore coal samples in which most of the coal contains a lower amount of phytane than C<sub>18</sub> in the lower rank coal (Pliocene and Miocene) and it increases in the higher rank coal (Oligocene). In the offshore samples the relationship was

quite good, but due to the limited number of high rank samples assumptions regarding the phytane ratio distribution should be restricted to the data available. However, sample GM 22475 with a higher rank than other samples plotted in Figure 7.30b, also shows a higher ratio of phytane to  $C_{18}$ . If this evidence can be generalised at least in the West Aceh Basin, although the reason is still uncertain, the  $Ph/C_{18}$  may provide a better rank parameter in assessing organic maturation level than the  $Pr/C_{17}$  ratio.

#### 7.4.3. Pyrolysis Gas Chromatography

Pyrolysis gas chromatography (Py-GC) has been used to analyse the hydrocarbon generation potential of the Tertiary coals from the West Aceh Basin. Py-GC provides basic information on the petroleum composition and quantitative distribution of petroleum components such as the gas/oil ratio, waxy content, aliphatic and aromatic hydrocarbons, phenols and other hydrocarbon compounds (Horsfield *et al.*, 1987; Horsfield, 1988; Boreham and Powell, 1991).

Fourteen coal samples from the West Aceh Basin, for which the maceral composition had been determined and which ranged from immature to mature ( $R_{\text{max}}$  between 0.30% to 1.15%), were analysed using the Py-GC technique. Each sample was also analysed using the Rock-Eval technique as discussed earlier. The Py-GC data and maceral compositions are presented in Table 7.21, whilst Rock-Eval data are given in Table 7.16. Although the hydrocarbon generation potential is best determined on immature samples, in some instances the composition of the pyrolysate from the mature residual kerogen can be used to infer original hydrocarbon potential of the immature equivalent.

The Py-GC traces (Figures 7.32 to 7.45) reveal that the samples have varying yields of homologous series of straight-chain alkanes and alk-1-enes. The low rank Pliocene coals have a significant wax content. Pliocene samples (GM 22039 and GM 21989) show that odd-numbered hydrocarbons predominant at C25 and between C27 and C29. Similar distributions were also recorded in a Miocene sample (GM 220391, Figure 7.38) and in Oligocene samples (GM 24584, Figure 7.41; and GM 24585, Figure 7.45).

The occurrence of a significant wax content in the pyrolysate of low rank coals has been reported elsewhere from suberinite-rich and cutinite-rich coal (Powell *et al.*, 1991). A recent study on the Kings Bay coal by Khorasani and Michelsen (1991) concluded that suberinite was the primary coal maceral contributing significant amounts of hydrocarbons, especially with a high wax content and that natural petroleum generation had occurred at a low thermal stress ( $R_{\text{max}} < 0.60\%$ ). The authors noted different distributions of waxy hydrocarbons produced from suberin than from cuticle. In the former there was a strong, odd-carbon predominance around C21 to C25, whilst the latter showed a strong odd-carbon predominance occurring at higher molecular weight of C25 to C27 (Khorasani and Murchison, 1988; Khorasani and Michelsen, 1991).

Given the data by the above authors, a similar relationship is predicted for the West Aceh Basin coals. The coals which have normal hydrocarbons distributions extending up to the high molecular weight wax range also have abundant suberinite and cutinite and these macerals are most likely associated with generation of the high molecular weight compounds. It is interesting to note sample GM 22424 (Figure 7.38), although it is mature ( $R_{\text{max}} = 1.15\%$ ), still generates appreciable amounts of waxy straight-chained hydrocarbons.

It is also clear from Figure 7.38 that the carbon number distribution is shifted towards a lower molecular weight, characteristic of a mature sample. Thus, the occurrence of linear hydrocarbons and relatively low aromatic contents suggests that the originally coal had a much higher HI and had a significant liquid potential, a large proportion of which has already been generated.

When total hydrocarbons are plotted against the ratio of normal hydrocarbons to aromatic compounds (Figure 7.46a) the data show quite a large scatter, although a weak positive correlation is apparent. The Pliocene coal tends to be in one group located in the lower portion of the graph. In contrast Miocene and Oligocene coal samples are widely spread without any such grouping as for the Pliocene coal. This relationship may be influenced by several factors such as organic matter type and rank, together with external factors such as weathering and oxidation of the samples. However, when rank is compared to the ratio of normal hydrocarbons to aromatic compounds (Figure 7.46b) the relationship is scattered and no correlation is evident.

It is widely accepted that aromaticity of a coal increases with increasing rank while the O/C ratio and the aromatic content decreases (Stach *et al.*, 1982; Zhou *et al.*, 1984). Following this concept, it is clear that some anomalies occur in the case of Figure 7.46b. The extreme anomaly is for sample GM 220391 which is supported by the previous evidence from the Py-GC traces. The anomaly can be attributed to the rapid heating caused by an igneous intrusion, where the short time for thermal cracking left unbroken aliphatic bonds. The high aromaticity is usually partly contributed by suberinite (Given, 1984) but this is not the case for sample GM 220391. It is likely that the maximum yield of normal hydrocarbons in the

West Aceh Basin, except for sample GM 220391, is at approximately 0.50 to 0.65 %  $R_{\text{vmax}}$  and may follow normal coalification (Teichmuller, 1982).

Although the peak distribution of hydrocarbons produced from the Py-Gc is not greatly different within the one group of coal samples, different trends are evidence for the different age groups of coal. The Pliocene coal is placed in one group with the least liquid hydrocarbon content (Figure 7.47a). The composition of the pyrolysis product is quite different for the Miocene and Oligocene groups which yielded more liquid hydrocarbons than the Pliocene coals. However, the Miocene and Oligocene coal samples plot in one group. This implies that the distribution of the  $C_6+$  component in both coals is not greatly different. Since the macerals in both coals do not show a great contrast, the similarity in the hydrocarbons may be related to the same or similar geological factors, such palaeoenvironmental conditions that controlled maceral composition and also the thermal effects during the coalification process. Similar trends occur when hydrocarbon compounds such as phenol, n-octane+oct-1-ene ( $C_8$ ) and m+p xylene are plotted in a triangular diagram (Figure 7.47b). It is again evident that the Pliocene group is distinct whereas the Miocene and Oligocene samples form another group.

The Pliocene coals are deficient in aromatic compounds whilst the Oligocene and Miocene coals contain less phenol than the Pliocene coal. This may reflect the maceral composition and rank of the coal. As the Pliocene samples are rich in vitrinite, the high phenol content may be contributed from the vitrinite maceral (Teichmuller, 1982; Given, 1984). On the other hand, the higher aromatic components in the Miocene and Oligocene coal may due to the higher rank of both coals in comparison to the Pliocene coal. However, other factors,

such as the conditions in the palaeoenvironment may also contribute to the different petroleum compositions of the coals.

A study of the Talang Akar coal in Indonesia, with special reference to petroleum generation, indicated that palaeoenvironmental conditions are more effective with respect to the petroleum composition than simple decarboxylation during peat accumulation (Noble *et al.*, 1991). Coal from a lower delta plain environment gives different hydrocarbon compounds from coal deposited in the upper delta plain. Peat formed in an environment adjacent to a marine environment (i.e. lower delta plain) will give more hydrogen than peat deposited in terrestrial conditions (Diessel, 1992). If this case can be generalised, it is possible that the palaeoenvironmental conditions during the deposition of the Pliocene coal may differ from those for both the Miocene and Oligocene coals. This suggestion is supported by the maceral composition of the Pliocene coal which is significantly different from both the Miocene and Oligocene coals.

Another plot was made to illustrate the change in pyrolysis composition within the samples examined (Figure 7.48a). The hydrogen deficiency of the Pliocene coal is evident in this figure but the gas fraction in the Pliocene coal is higher than in both the Miocene and Oligocene coals. Since the Pliocene coal has only attained a brown coal rank, any higher gas content in this coal is entirely related to diagenetic gas. In addition the hydrogen content also increases as the rank increases (from Pliocene to Oligocene samples) but there is no clear differentiation in trend between the Miocene and Oligocene coals which may imply that both coals contain similar organic entities or at least were formed under similar geological conditions and processes during peat accumulation.

A similar situation is also indicated in Figure 7.48b. It is again clear that the Pliocene coal is hydrocarbon deficient compared to the Miocene and Oligocene coals. In this respect it is likely that type and rank of organic matter is the most important factor controlling the hydrogen and normal hydrocarbon content in these coals because the relationship between both is excellent. From the last two figures, it can be concluded that the Oligocene coal, and to some extent the Miocene coal, have the best petroleum generation potential whereas the Pliocene coal has a lower petroleum potential.

## 7.5. RELATIONSHIP BETWEEN MACERALS AND PYROLYSIS HYDROCARBONS

Since the hydrocarbon content in the West Aceh Basin is influenced by several factors, and the fact that coal is a complex mixture with a heteroatomic framework, it is not possible to described precisely which component has the greatest control on the hydrocarbon products. Assuming that macerals composition and rank are the most important variables controlling the distribution and characteristics of the pyrolysis hydrocarbon products, a relationship between maceral composition and the hydrocarbons produced from the pyrolysis can be expected, at least in a general manner.

For this purpose, R-mode analysis using the product moment correlation coefficient has been used to correlate rank, maceral composition and pyrolysis products from Rock-Eval and Py-Gc determinations. A software package developed by Dr B. G. Jones at the University of Wollongong (Jones and Facer, 1982) was used.

The R-mode cluster analysis dendrogram for the maceral composition and Rock-Eval data sets



(Table 7.16) and their correlation coefficient matrices are given in Figure 7.49, Table 21 and Appendix 13.  $T_{\max}$  is the only variable showing a very significant correlation with vitrinite reflectance ( $R_v\max$ ). However, the relationships between exsudatinite and free hydrocarbon ( $S_1$ ) and the hydrogen index are significant at the 99% confidence level. This maceral is also correlated with resinite at the 99% confidence level. Among the pyrolysis products TOC is correlated with  $S_2$  at the 99% confidence level. In addition, vitrinite reflectance is also correlated at the 99% confidence level with TOC,  $S_2$  and HI.

An R-mode cluster analysis dendrogram for maceral composition, vitrinite reflectance and Py-GC data (Table 7.22) and their correlation coefficient matrices are given in Figure 7.50 and Appendix 14 respectively. Figure 7.50 shows strong correlations between a number of variables, for example, telovitrinite and  $R_v\max$ ; detrovitrinite and C6-C16; C15+ and C7+/aromatic; C1-C5 and A3 (m+p xylene)/C8(octene). Among the macerals, only detrovitrinite (including desmocolinite) is strongly correlated with light carbon components (C6-C14) at the 99% confidence level (Table 7.23).

Although the product moment correlation coefficient between exsudatinite and lower molecular weight hydrocarbons (C6-C14) is low a positive correlation is evident. In contrast, vitrinite reflectance shows a strong correlation at the 95% and 99% confidence levels with C6 to C14 and the C7/aromatic ratio respectively. From the two cluster analyses it is interesting to note that exsudatinite and detrovitrinite have good correlations with the pyrolysis products. It is likely that exsudatinite was exuded from other organic matter and it occurs as a free hydrocarbon substance in the cleats and fissures in the macerals, especially vitrinite. When it is pyrolysed, it will be recorded, together with unbound free hydrocarbon fractions,

as the S1 peak. It is possible that because exsudatinite is generated from labile components, as was discussed in Chapter 4, they will react faster than other macerals at lower temperatures using the Rock-Eval technique. Consequently the exsudatinite will contribute more to the S1 than the S2 value, as indicated by the product moment correlation coefficients. If this case can be referred back to natural coalification, it is possible to assume that the occurrence of exsudatinite is related to hydrocarbon generation or at least related to the migrated oils, whether migrated in or migrated out, in the coal. The fact that exsudatinite has been found in the low rank coal of the West Aceh Basin, may imply that it was not related to the main phase of oil generation but it may be generated from the fatty acid break-up which occurs in the diagenetic stage. This evidence is supported by the Py-GC data in which appreciable amounts of lighter molecular weight hydrocarbons are found in some low rank coal samples; exsudatinite in one coal sample comprise 18% of the total rock as has been discussed previously. An appreciable amount of waxy compounds are also found in the low rank samples. This component is thought to be contributed from fatty acid or ester linkage (Boreham, pers. comm.).

Cluster analysis also indicates a good correlation between exsudatinite and resinite. Evidence from petrographic analyses, support this result and it was clear that much of the exsudatinite was expelled from resinite bodies, as also suggested by several other authors (Teichmuller, 1973; Murchison, 1975; Zhao *et al.*, 1989; Misra and Cook, 1992). Thus the exsudatinite in the coals from the study area was mostly derived from resinite although a minor proportion was expelled from cutinite, sporinite and suberinite.

Good relationships between detrovitrinite and the lighter hydrocarbon components (C6 to

C14) may be due to the contribution of aliphatic hydrocarbons derived from liptinitic matrices, which commonly occur in coal with abundant desmocollinite.

From the two R-mode analyses it is concluded that the best correlations are obtained for data obtained by the same experimental technique rather than different techniques. For example, vitrinite reflectance is generally better correlated with aspects of maceral composition than to the pyrolysis products. This could imply that pyrolysis products are more dependant on rank of the precursor rock than maceral composition, particularly for the range of coal used in this study.

## 7.6. MIGRATED HYDROCARBONS

The Production Index (PI) is a sensitive variable which is used to estimate hydrocarbon migration. Any anomaly, either positive or negative, in the PI value can be assumed to be related to the accumulation or drainage of hydrocarbons (Espitalie *et al.*, 1985). Several studies on the migration of hydrocarbons have also been conducted elsewhere (Clementz *et al.*, 1979; Espitalie *et al.*, 1984; Whelan *et al.*, 1986). Plots of  $T_{\max}$ , PI and vitrinite reflectance are the most common methods used in the study of migration phenomena. A study by Boreham *et al.* (1988) used the hydrocarbon yield and TOC from extracted samples in addition to the maturation parameters cited above.

In the samples from the West Aceh Basin, migration phenomena were interpreted using the method of Boreham *et al.* (1988). Migration is thought to have occurred in samples from Bubon, Tripa and Meulaboh wells. The maturation parameters  $T_{\max}$ , vitrinite reflectance and

PI were plotted against depth for the eight offshore wells and the results are presenting in Figure 7.51.

In general, the trend of  $T_{\max}$  against depth (Figure 7.51a) and  $R_v$ max against depth (Figure 7.51b) follow the normal maturation pattern, that is as depth increases the value increases. The inverse situation occurs where PI is plotted against depth (Figure 7.51c). This latter figure may imply that migration has occurred in this basin. Similar plots for the Bubon, Tripa and Meulaboh wells (Figures 7.52 to 7.54) clearly indicate some inflection in the PI value at almost the same depth level in each well. In addition, TOC, extracted hydrocarbon yield (mg HC/g TOC) and the saturated/aromatic ratio (Table 7.19) was added for each drill hole. Although these data are very limited, the general pattern indicates that migration may have occurred in these three drill holes; it is perhaps better to say that some bitumen impregnation or enrichment was found at certain stratigraphic levels. The fact that the PI inflection point occurs at a similar stratigraphic level may not be accidental and, therefore, should reflect actual conditions. Petrographic data support this evidence since most bitumen is found in samples from near the inflection point.

If it is assumed that bitumen is a product of petroleum migration as stated by Jacob (1975, 1989), the combined petrographic and pyrolysis data, it follows that in the West Aceh Basin, hydrocarbon migration may have occurred at least in the three wells cited above.

## 7.7. SUMMARY

Organic petrographic data indicate that most of the offshore samples contain land-plant

derived organic matter with liptinite dominant over vitrinite. The scoring system (modified from Smyth *et al.*, 1984) shows that the highest score is associated with samples from the Tangla Formation and the lowest score is for samples from the Tutut Formation. The average hydrocarbon potential, using the liptinite to vitrinite ratio, also indicates that the Tangla Formation has the best source rock potential. Although some individual samples from the Kueh and Tutut Formations have a high ratio of liptinite to vitrinite, the fact that these formations lie in the immature zone is a major obstacle to them being classed as having good source rock potential at present. The offshore area is in a tectonically active basin, and sedimentation and tectonic processes are still developing. Thus petroleum generation may be possible in the future but at the moment, finding prospective source rocks in the Kueh and Tutut Formation depends on finding areas where higher maturity levels have been available because of local geological processes.

As the vitrinite and geothermal gradients tend to increase shoreward, mature zones for the Kueh and Tutut Formations may be found in the onshore region and any similarity in organic matter type and abundance in the onshore region would constitute a prospective area for these units in that region.

Organic geochemistry also suggests that the best hydrocarbon potential in the West Aceh Basin is confined to the Tangla Formation and to some extent, the Kueh Formation. Pyrolysis products of coals, as measured by Rock Eval and Pyrolysis-GC, clearly indicate that the Oligocene and some Miocene coals have reached the main oil window and have better hydrocarbon potential than Pliocene coal.

## CHAPTER 8

### GENERAL DISCUSSION

#### 8.1. INTRODUCTION

It is a feature of Indonesian petroleum geology that although petroleum resources are widely distributed throughout the Indonesian Tertiary basins, the economically significant resources are confined to the backarc and intracratonic basins, such as the North Sumatra, Central Sumatra, South Sumatra and North Java Basins, together with some Tertiary basins in the eastern part of Kalimantan and Irian Jaya (Figure 8.1). Recoverable petroleum resources have not been discovered in the more tectonically active forearc basins such as the South Java, Bengkulu, West Sumatra and West Aceh Basins.

Although preliminary petroleum exploration has been conducted in the forearc basins of Indonesia, only rare oil shows and uneconomical methane gas accumulations have been reported so far from the Bengkulu, West Sumatra and West Aceh Basins and there has been a tendency to conclude that forearc basins are not suitable for petroleum generation (Dickinson, 1970; Dickinson and Seely, 1978; Barber, 1985). The lack of economic petroleum has mainly been attributed to the immaturity of the clastic sedimentary sequences rather than a consideration of the type and distribution of the organic matter which also is a most critical factor for assessing petroleum generation. The until-now-believed predominance of immature sedimentary rocks and the paucity of reservoir rocks

in forearc basins has been ascribed to the rapid deposition of deep water sediments, to the diagenesis of the volcanic components and to the discontinuity of reservoir rocks due to tectonic instability.

Clearly these assumptions have not been correct and on the positive side there is a wide variety of types of potential reservoirs and traps in shallow water and terrestrial facies in the forearc basins. This is well illustrated by the range of shelf facies in the West Aceh Basin and the known minor occurrences of hydrocarbons.

At least two other factors have been considered to limit the generation of hydrocarbons in forearc basins according to petroleum companies. The first is believed to be the low geothermal gradients in forearc basins and the second is the distribution of oxidised organic matter. Evidence for the latter opinion has not been studied in detail in the forearc basins of Indonesia. A summary of the geological factors that need to be assessed when considering the possibility of petroleum occurrences in forearc basins are summarised in Table 8.1. This study has attempted to assess whether some of these requirements are met in forearc basins, especially the West Aceh Basin.

There is a wide variation in the type and rank of organic matter in the West Aceh Basin, as shown by organic petrography and geochemistry, and the conventional requirements for hydrocarbon generation have been reached, at least, in the Tangla Formation. These are positive features that have to be assessed during the evaluation of hydrocarbon generation in the West Aceh Basin and both offer challenges that need to be confronted in future exploration programs. Combining these data, and integrating them with

structural and sedimentological data, it should be possible to make an assessment of favourable conditions and the potential for generating and accumulating petroleum in this basin. Furthermore, it should be possible to predict the better areas for exploration and thus reduce the risk and increase the petroleum exploration success ratio.

For example, using similar reasoning economical petroleum resources have been found in the previously "barren" Bengal forearc basin of Bangladesh. It was suggested that the petroleum was derived from terrestrial source rocks or coals. Using this example as a possible model and taking the local geological factors into consideration, it is possible to consider factors that may give some insight as to the potential for generating hydrocarbons in the forearc West Aceh Basin.

## 8.2. MATURITY CONSIDERATIONS

One of the main factors to be considered when determining the potential of forearc basins as the suitable places for the generation and the accumulation of hydrocarbons is the geothermal gradient. In Indonesia, most of the Tertiary basins that are oil producing have geothermal gradients greater than  $35^{\circ}\text{C}/\text{km}$ . On the other hand, the average geothermal gradient in the West Aceh Basin is  $25^{\circ}\text{C}$  and this is lower than those of the backarc basins. The lateral trend of the geothermal gradient in offshore areas of the basin shows an increase towards the northwest, that is, toward the Teunom and Calang area, and a decrease towards the southeast, or towards the Palumat area.

Discoveries of economical hydrocarbon in areas with relatively low geothermal gradients,



that is lower than  $20^{\circ}\text{C}/\text{km}$  elsewhere in the world should reopen an appraisal of Indonesian forearc basins in general, and the West Aceh forearc basin in particular, as potential economical hydrocarbon source areas.

The low geothermal gradient associated with oil-producing forearc basins reported elsewhere indicate that the main oil generation zones are at depths of greater than 3500 m (Handique and Bharali, 1981; Price, 1982; Leonard, 1983; Ismail and Shamsuddin, 1991). A recent study on the maturity of organic matter in the Bengal forearc basin concluded that the economical oil-producing regions in this area are associated with geothermal gradient of  $20^{\circ}\text{C}$  to  $26^{\circ}\text{C}$  (Ismail and Syamsuddin, 1991; Ahmed *et al.* (1991). The oil generation windows in this area are confined to depths of 3,000 to 10,000 m with present temperatures and vitrinite reflectance ranging from 116 to  $275^{\circ}\text{C}$  and 0.65% to 1.3% respectively (Ismail and Syamsuddin, 1991). Using this as a tentative model, it is not impossible to say that such conditions might be expected to occur in the West Aceh Basin since the latter basin was formed within the same tectonically framework and regime as the Bengal forearc basin. In a similar case, the economical oil-producing forearc basin of Trinidad the oil window was reported at a depth of 5800 m and at a temperature of  $140^{\circ}\text{C}$  (Leonard, 1983).

From the above two examples, it is obviously that the role of the palaeotemperatures operating in the forearc basin, rather than present temperatures, has to be considered when assessing basins as oil producers. Ismail and Syamsuddin (1991) considered that palaeotemperatures of  $160^{\circ}\text{C}$  to  $275^{\circ}\text{C}$  correspond to an oil generation window equivalent to a vitrinite reflectance 0.65% to 1.30% respectively. Thus the conventional acceptance

that the oil generation window corresponds to a temperature of approximately 65°C to 150°C should not be used in a broad-brush approach for all basins but should be re-evaluated for each local area or geological framework that may in turn be influenced by its respective tectonic regime and development. Thus, although the majority of the sequence examined from the offshore portion of the West Aceh Basin is immature, as indicated by the vitrinite reflectance values of less than 0.5%, this should not be taken as the over-riding consideration. At present, a vitrinite reflectance lower than 0.5% is believed to be below the oil generating window and 1.35% to be the upper boundary of the oil window. The limited number of samples available for this study from this part of the basin may not have given the complete picture and parts of the sequence, in areas not studied, may have maturation levels equivalent to greater than 0.50% vitrinite reflectance, which based on present data is confined to the Tangla Formation.

Evidence from seismic data clearly indicate that the Tangla Formation and equivalent units occur not only in the West Aceh Basin but also in surrounding areas and are continuous with little variation in thickness or tectonic history (Seely, 1978; Rose, 1983; Beaudry and Moore, 1985). In addition, a thick Oligocene sequence, equivalent to the Tangla Formation in West Aceh Basin was penetrated in the Raja offshore well, which is located northwest of the study area (Figure 8.1). This thick Oligocene sequence is very important for future study because it is thick and has an obvious boundary with the underlying (Pre Tertiary) and overlying (Miocene) sequences.

Although the Tangla Formation was only penetrated in Tuba and Meulaboh wells (Figure 8.2), the general trends clearly indicate that rank increases to the northwest in all

stratigraphic intervals. This is opposite to the conventionally held opinion that rank increases toward the thicker parts of the units. This situation may be related to the basement high associated with the volcanic and tectonic activities in the northwestern part of the area (surrounding Teunom well) as volcanic and igneous rocks occur in this area. In contrast the rank appears to be decrease in the southeast direction (in Palumat well) in all stratigraphic intervals. This may imply, as suggested by Cameron *et al.* (1983), that this area has been a subareal land mass since the Miocene and has been characterised by a period of slow subsidence but rapid sedimentation followed by more rapid subsidence and sedimentation in Pliocene period. The rapid subsidence and sedimentation occurred near the depocentre of the basin (Meulaboh, Tuba and Tripa area) with units thickening toward this area. However, reflectance data reveals that although increasing burial is confined to this area, maturation rates are slower compared to the shoreward areas. This may be due to rapid sedimentation over a short time interval, without any additional heat flux, as it appeared to happen shoreward during the uplifted tectonic movements associated with the generation of the Barisan mountain chain which in turn resulted from the basement high in the surrounding shoreward area.

It is possible to generalise and imply that any rank associated with the stratigraphic interval equivalent to the Tangla Formation will be higher and shallower to the northwest and the mature zone will also be shallower to the northwest.

General trends show that vitrinite gradients are higher in the onshore area than in the offshore. This may due to higher geothermal/palaeogeothermal gradients in the onshore than in the offshore area as already discussed earlier in Chapters 5 and 6. Local

variations in vitrinite gradients occur both in the offshore and onshore areas and may due to the variation in the different thermal regime operating in this basin. For example, a high apparently anomalous vitrinite gradient was recorded in Teunom well; the vitrinite reflectance gradient increases sharply at any given vitrinite reflectance level. It is possible to conclude that the higher ranks that are associated with various stratigraphic intervals are located in the onshore area but also, locally, in the offshore area. This trend has a northwesterly pattern and is associated with the basement high.

Geochemical results also support the petrographic data; mature samples with  $T_{\max}$  greater than  $435^{\circ}\text{C}$  are confined to the Tangla Formation or equivalent Oligocene samples with some from the onshore Keuh Formation. The  $T_{\max}$  values are higher in samples from the onshore area for any given stratigraphic level and thus the oil window, using this parameter, is located within the Tangla Formation and partly in the Kueh Formation. Therefore, geochemical data also indicates that at present maturation requirements for oil generation in the West Aceh Basin has been achieved only in the Tangla Formation and parts of the onshore Kueh Formation.

It is interesting to note that the Production Index (PI) in the offshore area of West Aceh Basin decreases down section. If this pattern is assumed to be a migration phenomena, as suggested by Espitalie *et al.* (1985), it indicates some bitumen enrichment in the uppermost of the sequences. This observation is supported by the petrographic and chemical data for the extracted samples which also shows some bitumen enrichment in the uppermost sequences. However, due to the limited number of the extracted samples examined, the migration phenomena indicated should be viewed with care. However, the

fact that bitumen impregnations was recognised in the similar stratigraphic sequences, should promote further detailed investigation of the migration phenomena in this basin.

The occurrence of methane gas in the Miocene carbonates of Keudapasi and Meulaboh wells should be taken as additional indications of hydrocarbon generation within the West Aceh Basin although there is a possibility that this gas may be biogenic.

The general trends for maturation patterns in Indonesian forearc basins, as measured by vitrinite reflectance, indicate that the rank increases shoreward not only in the West Aceh Basin but also in other basins such as the Bengkulu and West Sumatra Basins (Hadiyanto, 1988). If this rank pattern is a generalisation for the forearc basins in Sumatra, it follows that for any strata the more mature parts of the units will be in onshore areas rather than in the offshore areas.

Thus the future prospects of most other forearc basins, in terms of the rank, will likely be confined to the Oligocene sequences since the regional geothermal and rank gradients pattern follow the pattern of the West Aceh basin. This is true for the Bengkulu and West Sumatra Basins in which the more mature strata, and therefore organic matter of higher rank, are associated with the onshore Oligocene sequences (Hadiyanto, 1988). However, local geological conditions and phenomena such as tectonic activity and sedimentology should produce rank variations within individual basins. As palaeothermal gradients in West Aceh Basin have been postulated to be higher than the present geothermal gradient, any rank evaluation within this basin should not overestimate the importance of the present low geothermal gradients.

### 8.3. SOURCE ROCK RICHNESS

The petrographic composition of DOM varies from well to well and ranges from sparse to abundant. Liptinite is the predominant maceral in all units with vitrinite the second most abundant; inertinite rarely exceeds 2% by volume. It is generally accepted that liptinite is the best source rock for oil with vitrinite considered has some liquid potential (Tissot and Welte, 1984; Cook, 1982; Smyth and Mastalerz, 1991).

Based on this assumption, for any given volume or weight of organic matter per unit sediment, the ratio of liptinite to vitrinite should be an indicator of hydrocarbon source potential (Smyth *et al.*, 1984). For the West Aceh Basin, it is likely that the Kueh Formation has the greatest oil generation potential because the average ratios of liptinite to vitrinite in DOM and coal are 2.16 and 1.27 respectively; in the Tangla and Tutut Formations the same ratios are 1.45 and 0.35, and 1.38 and 0.18, respectively. However, using the scoring system discussed in Chapter 7 the highest generation potential for DOM is in the Tangla Formation whilst the lowest potential is associated with Tutut Formation. The highest score for coal occurs in the Kueh Formation with the Tangla and Tutut Formations having lower values, with the Tangla Formation having the lowest.

On a well for well basis, excluding the Tangla Formation because it was only penetrated in two wells, the highest DOM and coal ratios for all other units occur in Bubon and Palumat wells whereas the lowest values are found in Palumat well. For the Tangla Formation the highest ratio for DOM occurs in Meulaboh well but the highest ratio for coal is in the Tuba well. Thus using liptinite to vitrinite ratios only, these data would

suggest that the Kueh Formation in the area around Bubon and Palumat wells has the highest generation potential.

In the offshore area the low maturity level of the Kueh Formation suggests that hydrocarbon generation has been insignificant so far and future prospects for finding economic hydrocarbons depends on finding areas where the maturity levels are significantly higher which, given the vitrinite reflectance patterns, this is likely to be in the onshore area as discussed above.

For the Tutut and Kueh Formation, there is relative high potential for hydrocarbon generation in the area centred on Bubon and Teunom wells whereas the lowest potential is in the southeast area centred on Palumat well.

Combining these data with the maturation pattern of the offshore area as discussed above it is likely that the best prospects for hydrocarbon generation are in the northwest area and the weakest prospects are in the southeast area near Palumat well. In the depocentre areas (located near Meulaboh, Tuba, Tripa, Keudapasi, Meulaboh East wells), good hydrocarbon generation prospects are likely but the fact that the mature zone occurs at greater depths than in Bubon and Teunom area is the main obstacle encouraging exploration.

In addition, since the lateral distribution pattern of rank and thickness of the Tangla Formation follows those of the Kueh and Tutut Formations, as projected from the seismic data of Beaudry and Moore (1985), and the maceral abundance is at least the same as

found in the Meulaboh and Tuba wells, better prospects for hydrocarbon generation probably also occur in the Bubon and Teunom wells area, or in more general sense, the onshore area. However, as discussed by Smyth and Mastalerz (1991), the type and abundance of organic matter, especially liptinite, are controlled by local development of the palaeodepositional environments and therefore any evaluation of maceral distribution and abundance, both vertically and laterally, would be better related to the facies development that operated within the basin at the time of deposition. If this is the case a detailed facies analysis throughout this basin is necessary in order to provide a better understanding of the organic facies distribution which in turn, would give a clearer understanding of the types of organic matter and their distribution in relation with palaeoenvironment deposition.

Total organic carbon data from the Tertiary samples in the offshore area reveal that the Tangla, Kueh, and Tutut Formations have higher than the generally accepted minimum levels of TOC (1.0%) for the formation of sufficient hydrocarbons to permit migration and accumulation. The highest TOC values occur in the Tangla Formation and the lowest values are in the Tutut Formation. Based on Rock Eval determination, most of the organic matter in these formations is Type III although one Tangla sample lies on the transition Type III/II organic matter boundary of Tissot and Welte (1984). This is an agreement with petrographic data that shows terrestrially-derived organic material is dominant, especially vitrinite, although *Botryococcus*-derived telalginite and lacustrine lamalginite occur in a small number of samples; the contribution of the latter macerals to the total organic matter is not significant.



Hydrogen Index (HI) of the Tangla formation indicates that this Formation has both oil and gas potential ( $HI > 200$ ) whereas Tutut and Kueh Formations, characterise by hydrogen-poor organic matter, is only gas prone. The  $S_2$  values are highest in the Tangla Formation but lowest in the Tutut Formation. Consequently, based on the Rock Eval data alone, the best source rock potential for hydrocarbons in West Aceh Basin is the Tangla Formation.

Extracted shale samples from these formations also indicate that Tangla samples contain the highest extractable hydrocarbons (mgHC/gTOC) although some samples from the Kueh and Tutut Formations also have appreciable extractable hydrocarbons; petrographic data suggest that this is due to bitumen impregnation and therefore may not be a true indication of source potential.

Pyrolysis data from the Tertiary coals show that the Oligocene Tangla Formation coal has the best oil potential in terms of organic maturity and organic matter type. The organic matter is mostly the Type II as would be expected from the maceral composition. The HI indicates that this coal is oil-prone and it contains the most extractable hydrocarbons.

Gas chromatography data indicate that mature samples are the Oligocene coal and to a lesser extent the Miocene coal. Some samples of the former have similar normal hydrocarbon distributions as the Talang Akar delta plain coal, which is a proven oil source rock in the Northwest Java Basin, South Sumatra Basin and the Ardjuna Sub-Basin, offshore northwest Java, and the Mahakam coal, a proven source rock in the East Kalimantan Basin (Gordon, 1985; Monthioux *et al.*, 1985; Wu, 1987; Horstfield *et al.*,

1988; Noble and Wu, 1990; Pramono *et al.*, 1990; Noble *et al.*, 1991; Sutrisman, 1991; Amir, 1991). These traces also show some similarities with some crude oils from Gippsland Basin (Boreham, pers. comm.).

Pyrolysis-GC data indicate that the Oligocene coal and some of the Miocene coals have the best liquid generation potential. Pyrolysis-GC traces of these Oligocene and Miocene coals are characterised by a high abundance of normal hydrocarbons. In many respects, the pyrograms are similar to those of the Talang Akar coal. The Pliocene coal is the most immature and the chemistry indicates it has the least hydrocarbon potential although appreciable amounts of waxy compounds were found in this coal.

In summary and looking at only the non-coal rocks from a combined maturation, petrographic and geochemical view, the shale of Tangla Formation has the most potential as a source rock in the West Aceh Basin. However, the uncertainty of unit thickness within this formation requires special attention during future assessment programs. The source rock potential of the Kueh Formation also requires further investigation especially in the onshore area because the mature sequences are most likely to occur in this region as evidenced by the rank of Miocene coal.

The role of Oligocene and Miocene coal as source rock in the West Aceh Basin are still open to discussion despite the fact that coals are known source rocks for oil in backarc basins of Indonesia such as in South Sumatra, North West Java and East Kalimantan Basins and other basins of the world (Brooks, 1970; Durand and Paratte, 1983; Cook and Struckmeyer, 1986; Powell *et al.*, 1991; Powell and Boreham, 1991; Boreham and

Powell, 1991; Hunt, 1991; Binjie *et al.*, 1991; Clayton *et al.*, 1991; Mukhopadhyay *et al.*, 1991). Based on petrographic and geochemical data obtained during this study, the Oligocene and to a lesser extent, the Miocene coal, have the best hydrocarbon potential.

Using maturity and both petrographic and geochemical characteristics of the organic matter, the Tutut Formation is unlikely to be a source rock within the West Aceh Basin and this Formation should be ruled out as a possible source rock in future exploration programs. An understanding of the depositional settings and palaeogeography of the formations has to receive more emphasis in future work in order to clarify vertical and lateral organic facies distributions.

#### **8.4. EXSUDATINITE AND BITUMEN IN PETROLEUM GENERATION IN THE WEST ACEH BASIN.**

It is clear from the literature that there is some uncertainty regarding the significance and importance of exsudatinite in relation to the generation of petroleum. The main reason for this uncertainty is the lack of direct measurements of both petrographical and chemical data for either pure exsudatinite or the samples in which it occurs. The difficulty in separating exsudatinite from the other macerals, especially other liptinite macerals, is a major factor.

Although several papers have related exsudatinite formation to the generation of the petroleum, some contradiction occurs, especially regarding the rank at which exsudatinite formation occurs and the precursors of exsudatinite. Jones and Murchison (1963) were

amongst the first researchers to suggest that the migration of "secondary resinite", later called exsudatinite, was due to a combination of temperature-time and pressure under the normal coalification processes. They suggested that the migration took place early in the high-volatile bituminous stage. Such migration was also reported by Larter (1966) who studied secondary resinite using infrared spectral patterns of the coal and suggested that migration occurred at the boundary between sub-bituminous coal and bituminous coals.

Teichmuller (1973) first used the term "exsudatinite" for the secondary migrated maceral in coals of sub-bituminous rank. Exsudatinite was reported to be related to the petroleum generation. Currently, opinions have been reported elsewhere that exsudatinite occurs in coals of lower rank than sub-bituminous. This is contrary to Teichmuller's interpretation (1973; 1974; 1982), which stated that exsudatinite is generated by liptinite macerals during coalification at a rank of sub-bituminous to high volatile bituminous coal.

Teichmuller stated that exsudatinite can migrate into cracks, especially shrinkage cracks, and believed that such cracks formed after the geochemical gelification of vitrinite which does not occur earlier than sub-bituminous ranks. She concluded, therefore that the exsudatinite did not form earlier than the sub-bituminous stage and suggested that it is evidence of *in situ* generation of a petroleum-type substance, forming at about the same stage of diagenesis at which petroleum is formed in oil source rocks. She supported her argument by referring to the hypothesis of geochemical oil generation in coal made by previous workers such as Jacob (1966); Leythaeuser and Welte (1969); Brook and Smith (1969); Hood and Gutjahr (1972); Vahrmann and Watts (1972). In those studies, the maximum ratio of saturated to aromatic fractions, as well as the maximum C content, was

attained in high volatile bituminous coals as was equivalent to the oil generation in the source rocks; for example, the CPI (carbon preference index) of crude oils is less than 1.2 to 1.3 and this is reached in high volatile bituminous C coals.

Teichmüller summarised work done by Brooks (1970) and stated that petroleum-type hydrocarbons are formed in the sub-bituminous to high volatile bituminous coals stage from components of waxy leaf cuticles, pollen and spores by chemical reactions in which oxygen groups are removed from long-chain acids, alcohols and esters. She pointed out that work done by Jacob (1966) showed that extracts from bituminous coals have similar properties as crude oils but that crude oil is dissimilar to extracts from brown coals.

Murchison (1976) suggested that much of the resinite in bituminous coal is of secondary origin and is formed during the bituminous rank stage, which in turn is related to the zone of maximum petroleum generation. However, Shiboaka (1978) argued that the formation of exsudatinite does not necessarily indicate the generation of hydrocarbons and stated that exsudatinite can be formed during the brown coal stage. He concluded that the formation of exsudatinite is not directly related to chemical changes in lipids, but relates to the movement of mobile material into cleats as a result of a force such as compaction pressure on the coal seam. His argument was based on a study of the occurrence of exsudatinite in the Gippsland Basin. Although the overburden of the Tertiary coals in this basin is thick, the sediments in the basin were deposited in a very short period of geological time and, thus, the rank of the coal is lower than the normal rank needed to generate petroleum. Therefore Shiboaka concluded that the occurrence of exsudatinite in the Gippsland Tertiary coals may be due to migrated oils from the deeper parts of the basin.

Exsudatinitite from such oils was retained in the cavities or cracks of the coals since the sample examined was located below the reservoir rock.

Supporting Shiboaka *et al.* (1984) stated that exsudatinitite can be generated at a very early stage of coalification (equivalent to rank of  $<0.30\% R_{vmax}$ ). Teichmuller and Durand (1983) defined exsudatinitite as neo-formed solid bitumen occurring in samples with a rank ranging between  $0.38\%$  and  $0.96\% R_{vmax}$  and also stated that it is related to the generation of petroleum. Their suggestion was based on a comparative study using fluorescence microscopy and Rock-Eval data.

Cook and Struckmeyer (1986) suggested that the occurrence of exsudatinitite is related to petroleum generation and stated that formation could be during the brown coal stage at a rank of approximately  $0.40\% R_{vmax}$ . They concluded that early generation of petroleum probably results from the breakdown of compounds such as fatty acids, esters and alcohols.

Zhao *et al.* (1989) proposed that the occurrence of exsudatinitite in South China brown coal ( $0.36\%$  to  $0.40\% R_{vmax}$ ) is evidence for immature oil generation and primary migration. Their proposal was based on the combination of a fluorescence spectral study of the exsudatinitite and parent resinitite and a biomarker study of extracts from resin samples. They found that hydrocarbon abundance in the South China brown coal ( $0.36\%$  to  $0.40\% R_{vmax}$ ) fits the "commonly-accepted source rock criterion" and that the presence of various predominantly saturated and aromatic resin-derived biomarkers, such as retene, simonellite, fichtelite, dehydroabietin, was consistent with the origin of exsudatinitite from

resinite in the coal. Zhao *et al.* (1989) concluded, therefore, that both exudatinite and resinite-derived biomarker are evidence for oil generation and fluorescence alteration in the brown coal. There appeared to be a contradiction in the petrographic observations. They resolved this by stating that the reflectance data indicated a thermal immaturity for oil generation although the occurrence of exsudatinite supported the generation of immature oil.

Zhao *et al.* supported their conclusions by referring to the work of Snowdon and Powell (1982) who used biomarker data to correlate light crude oil and resinite from brown coal of the Mackenzie Delta Basin of Canada. These authors suggested that resinite is a potential source for immature petroleum in that basin.

The occurrence of exsudatinite as an indicator of hydrocarbon generation has been reported elsewhere from Tertiary sedimentary basin of Indonesia (Panggabean, 1990; Amir, 1991; Sutrisman, 1991). The range of equivalent vitrinite reflectance varies from 0.38% to 0.80% in the Southeast Kalimantan Basin, 0.40% to 0.75% in the Northwest Java Basin and between 0.36% and 0.76% in the South Sumatra Basin. Since these basins are all oil-producing, the above authors believed that the exsudatinite occurrence is related to petroleum generation in the basins, although the evidence is based solely on organic petrology.

The occurrence of solid bitumen in clastic rocks is considered to be a product of migrated hydrocarbons (Abraham, 1960; Hunt, 1979; Robert, 1981; Jacob, 1975; 1976; 1980; 1983; 1989). Bitumen was thought to occur in either or both the parent rock and the

reservoir rock within the rank range of lignite to graphite stage (Jacob, 1976; Hunt, 1979). However, at the lignite stage potential solid hydrocarbons only occur as ester gum, such as montan wax. In contrast, no chemical bitumen occurs at the graphite stage but has been replaced by high temperature derivatives (Jacob, 1976). The genesis of bitumen was stated by Jacob (1976) to result from disproportion reactions during resinite metamorphism that produced light hydrocarbons and solid bitumen, especially impositite. Jacob also thought that a similar process produced crude oil that infiltrates asphaltite and resin; gilsonite developed through the release of lighter hydrocarbons and glance pitch was produced at lower temperatures; bitumen containing many gas bubbles was interpreted to have undergone rapid heating. Wurtzilite and grahamite were produced after further heating. As the geothermal temperature increased, impositite will be formed.

Hunt (1979) suggested that bitumen is generated from fossil organic matter during diagenesis and catagenesis and the length of the migration route can vary from a fraction of a millimetre to several kilometres.

The above researchers have formed the foundation for assessing the significance of exsudatinite and bitumen in hydrocarbon generation and their work forms the basis for an assessment of the role of the two macerals in petroleum generation in the West Aceh Basin.

Using reflected light microscopy it is not possible to predict the parent maceral/s for the second type of exsudatinite found in West Aceh Basin samples. Quantitative fluorescence and infrared spectral analyses may serve to characterise the exsudatinite and parent



material and this could be the focus of another study.

Exsudatinite occurs in samples over a wide range of ranks (transitional peat/brown coal to high volatile bituminous coal), and opinions regarding the relationship between exsudatinite occurrence and petroleum generation are still open to discussion. The fact that many oil fields are found and characterised by immature chemical signatures suggests oil can be generated from resin-derived compounds at low rank, for example the study of Snowdon and Powell (1982), and that the conventional opinion that the oil window begins at sub-bituminous stage (0.5%  $R_{vmax}$ ) needs to be reassessed for certain type of organic matter.

The occurrence of exsudatinite in low rank coals, such as in West Aceh Basin where it occurs in coal as low as 0.25%  $R_{vmax}$ , possibly results from the expulsion of labile component during diagenesis (Boreham, pers. comm.). It is likely that the geological setting may also influence expulsion of labile components as the West Aceh Basin is a tectonically active forearc basin in which geothermal conditions have varied throughout geological time. The relatively close position of the magmatic arc (Barisan Mountains) to the basin, especially in the onshore area, is probably responsible for the increase in the geothermal gradient from the Middle Miocene until recent time. The role of rapid burial and compression due to the tectonic activity may also serve to foster the development of the exsudatinite in low rank coal since not only moisture will be expelled by increasing pressure but also volatile matter and labile components. The abundance of liptinite macerals, such as cutinite may also contribute to the occurrence of exsudatinite in low rank coal since cutinite contains soluble hydrocarbons and waxes on the surfaces of leaves

(Given, 1984).

Except for uneconomic pockets of methane gas, commercial petroleum has not yet been found in the West Aceh Basin. The question as to whether petroleum has been generated is partly answered if it is assumed that the small amounts of solid bitumen that have been recognised in most samples from the study area are a product of petroleum generation (as stated by many researchers, for example Abraham, 1960; Hunt, 1969; Jacob, 1976, 1989). Accepting this assumption, it is reasonable to say that petroleum generation has occurred in the West Aceh Basin.

Because the optical data appear to confirm the relationship between exsudatinitite and bitumen, the concept of immature petroleum generation, as suggested by Zhao *et al.* (1989), has to be considered for the sequences in the study area.

#### **8.5. CONCEPTUAL MODEL FOR HYDROCARBON GENERATION AND ACCUMULATION IN THE WEST ACEH BASIN**

This combined study of organic petrology and geochemistry indicates that West Aceh basin has the potential for hydrocarbon generation but as yet has not generated significant hydrocarbons because of the low maturation level of the sequence. Figure 8.3 summaries the maturation pattern and source rock potential of the Tertiary Formations in the West Aceh Basin and illustrates the potential for hydrocarbon generation and accumulation.

The model is modified from a geological cross section proposed by Union Oil Company

who used a combination of outcrop and seismic data to produce the section. The relative positions of selected offshore and onshore wells are projected onto the diagram and the rank ( $R_v$ max) isolines are plotted and correlated on the assumption that there is no thermal flux caused by magma activity. Where there is no subsurface reflectance data for a particular depth, a value was calculated using the vitrinite gradient of the respective well. The carbonate build-up is simplified and only plotted in the area in which Meulaboh and Tuba wells are located.

The model shows that in the depocentre of the offshore basin, as extrapolated from Tripa, Meulaboh and Meulaboh East wells, the vitrinite reflectance reaches a  $R_v$ max value of 0.5% at a depth of approximately 2000 to 2600 m. Thus assuming that the oil window commences at approximately 0.5%  $R_v$ max or slightly higher than 0.50%, all parts of the sequence above 2000 to 2600 m are immature and therefore should be disregarded as good potential source rock.

The maturation level increases onshore in all stratigraphic intervals and the mature zone or oil window in this area lies at shallower depths of less than 2000 metres which is significantly shallower than at the offshore depocentres. Pre-Miocene folds and faults occur in this area and thus there is a good potential for finding structural traps. In addition, the Oligo-Miocene unconformity surface can be regarded as potential seals for any such traps.

If the timing of the onset of oil generation had occurred in the Plio-Pleistocene period, as has been discussed and modelled in Chapter 6, this conceptual model predicts that any

hydrocarbon generated below the unconformity surface in the onshore area will be in structural traps below the unconformity or will have migrated upward through the fault zones or other zones of weaknesses. Any hydrocarbons that may have migrated through this unconformity would need to be in stratigraphic traps above the unconformity since there are no structurally-controlled traps above the Oligo-Miocene unconformity.

On the other hand, in the offshore depocentre area, the accumulations of hydrocarbon are likely to be in stratigraphic traps, for example, Miocene and Pliocene carbonate build-ups. Effective caprocks are reported to overly the carbonate build-ups in Keudapasi well and thus potential carbonate reservoirs can be expected. Good to excellent reservoir properties were reported in the Miocene limestone in Meulaboh and Keudapasi wells and methane gas was also reported in Meulaboh and Keudapasi wells. Meulaboh well penetrated a significant methane reservoir, with excellent flow characteristics over the period of drill stem test. The gas was suggested to have been generated in underlying and surrounding marine mudstone. In Keudapasi well, a gas zone in Miocene carbonate rocks was penetrated at depth of 1000 m. Both occurrences of methane gas was considered to be uneconomic at that time.

Minor shows of petroleum "vapour" were recorded in Eocene and pre-Tertiary sequences in Tuba well however all porous zones were reported to be water-saturated.

The above reported gas and oil shows indicate that hydrocarbons have been generated in the West Aceh Basin. However, in the case of Meulaboh and Keudapasi wells the shows of methane gas were possibly related either to diagenetic processes or thermogenic

degradation of organic matter. If it is from the latter, any methane gas trapped in the carbonates must have been derived from deeper sections since the temperature required for thermogenic methane generation are associated with vitrinite reflectance reported to be approximately 1.35% (Hunt, 1979)). This begs the possibility that the source of the methane is possibly Oligocene coal of the Tangla Formation.

Methane gas in the onshore area is likely to be at a lower stratigraphic level than for the depocentre because a vitrinite reflectance of 1.2%  $R_{\text{vmax}}$  occurs at the depth of approximately 1 km onshore. Given the volume of Oligocene coal in the onshore area and the suggested production rates of methane from coal in the Australian Permian situation, the quantity of methane gas could be expected to be as high as 15 cubic metres per tonne of coal (Faiz, pers. comm.). Considering the structural geology of the area, especially the potential for fractures and faults, onshore methane gas may have escaped from the coal and be in clastic reservoir rocks. No gas sorption tests or gas storage tests have been conducted for West Aceh Basin coals.

Diagenetic methane gas can be produced at ranks lower than 0.5%  $R_{\text{vmax}}$  and therefore the carbonates in the West Aceh Basin have potential as reservoir for the diagenetic methane. The occurrence of economically diagenetic methane was reported elsewhere. For example, economical methane gas resources has been found in the Apennine forearc basin of Italy where the geothermal gradient is 12 to 20°C/km. The methane was suggested to be a diagenetic gas because of the very high rate of subsidence and the gas was thought to have been generated early in the history of the sequence by bacteria or diagenetic processes. The gas was trapped in the overlying reservoir (Mattavelli and

Novelli, 1987). Unfortunately stable carbon isotope analysis was not carried out to assess the origin the methane gas.

The future exploration activity for the West Aceh Basin should concentrate on the additional evaluation of potential source rocks within the basin with special emphasis on the Tangla Formation. The onshore area should be viewed as a new prospect and given priority since the oil window is likely to be at shallower depths than in the offshore areas. The potential for traps that are necessary for the hydrocarbon accumulation is high because of the known regional and local geology. Subsurface geological investigations should be given priority work in order to gain a better understanding of the geological framework within the onshore area.

The discovery of economical, diagenetic methane gas elsewhere in the world, especially in the rapidly-formed, sedimentary forearc basins should open the opportunity for the West Aceh Basin and other forearc basins of Indonesia as locations for possible economic hydrocarbon accumulations. Finally, integration and evaluation of various techniques are necessary in order to gain the impetus for the discovery of hydrocarbons in forearc basin frontiers.

## CHAPTER 9

### CONCLUSIONS

The West Aceh Basin is one of several Indonesian Tertiary forearc basins which contains a thick sedimentary succession of coal-bearing rocks that were deposited during the Oligocene to Pliocene. The continued subduction of the Indo-Australian Plate under continental Sundaland was responsible for the development of this asymmetrical, tectonically-active forearc basin which is located along the west coast of the Aceh region of northwestern Sumatra. Significant petroleum discoveries have not been found in any Indonesian forearc basin and this study was initiated to assess the hydrocarbon generation potential of the West Aceh Basin and to formulate a model to aid future exploration in this and other forearc basins. West Aceh Basin is an ideal basin for a pilot study of petroleum generation in forearc basins because it contains Oligocene to Pliocene coals which contain abundant liptinite and vitrinite as well as numerous clastic units with abundant dispersed organic matter.

Indonesia relies heavily on petroleum both as a domestic energy resource and as an export commodity. Thus discoveries of liquid hydrocarbons in forearc basins, in which only minor gas shows and even less significant oil shows have previously been reported although the country has a long history of petroleum production, would be a major boost for future exploration and the present Indonesian economy. The results of this study should help future exploration strategies and encourage further studies of the organic

petrography and geochemistry of forearc sequences.

The primary objectives of this study were to obtain an understanding of the petroleum generation potential in the West Aceh Basin, with special reference to the organic petrology and geochemistry of coal and dispersed organic matter in the clastic interseam units. Specific aims were to determine regional variations in coal type and rank within the basin in order to assess the origin of the coal and the thermal history of the basin, to compare and integrate petrographic and geochemical data and to formulate a model for liquid hydrocarbon generation in the West Aceh Basin that may be applicable to other Indonesian forearc basins.

## 9.1. CONCLUSIONS

This combined study of organic petrology and geochemistry to assess the source rock potential of the various lithologies, indicates that West Aceh basin has the potential for hydrocarbon generation but as yet has not generated significant hydrocarbons because of the low maturation level of the sequence.

Specifically, the following conclusions were reached.

1. The organic matter in both coals and clastic rocks is derived from land plants with a minor algal component in some of the claystones and shales. The coals are dominated by vitrinite with lesser liptinite and only very minor inertinite. Vitrinite is dominantly detrovitrinite with desmocolinite dominant in the Oligocene and



Miocene coals and attrinite and densinite dominant in Pliocene coal. The Pliocene coal generally contains a higher proportion of telovitinite than either the Oligocene or Miocene coal.

A distinctive feature of the coals is the abundance of exsudatinite, resinite, suberinite and cutinite. Using optical properties and textural features, exsudatinite can be divided into two groups and much of this secondary maceral is derived from resinite and suberinite liptinite with lesser vitrinite and only minor inertinite.

In the clastic interseam shales and claystones, liptinite is dominant over vitrinite; inertinite is a minor maceral. Some of the liptinite appears to have been oxidized. The clastic rocks contain small but significant quantities of bitumen which indicates migration of hydrocarbons through the rocks or in situ generation of hydrocarbons.

2. The rank of the Oligocene to Pliocene coal as determined by vitrinite reflectance is equivalent to brown coal stage with a small number of samples in the high volatile bituminous rank range. The most obvious feature of the West Aceh Basin data is the overall increase in  $R_{\text{vmax}}$  with depth; reflectance gradients are generally around 0.2%/km. Maximum gradients occur onshore and this has resulted in a major difference in the maturation patterns between the offshore and onshore areas.

Some samples from the Kueh Formation have a reflectance value of up to 1.15%

but this is because of proximity to basaltic intrusions.

Regional reflectance data show a general increase towards the northwest within any given stratigraphic level. This pattern is relatively smooth and appears to be related directly to the geological age of the units as well as to the relative position of the sample location with respect to the magmatic arc beneath central Sumatra.

3. The average geothermal gradient in the West Aceh Basin is  $25^{\circ}\text{C}/\text{km}$  and this is lower than those of the backarc basins which is generally greater than  $35^{\circ}\text{C}/\text{km}$ .

The palaeothermal model for the study area is similar to models proposed for the other Tertiary Indonesian basins, such as the Southeast Kalimantan, Northwest Java, and South and Central Sumatra Basins. Present geothermal gradients in the offshore area show a lateral change from  $17^{\circ}\text{C}/\text{km}$  to  $39^{\circ}\text{C}/\text{km}$  but these are below the average for the other Tertiary basins of Indonesia, especially the backarc basins. The maturation history approximates the geothermal model and thus it can be assumed that coalification and maturation occurred during a phase of constant rapid burial, prior to a period of uplift and erosion. These subsidence and maturation histories of the West Aceh Basin suggest that the timing of any hydrocarbon generation is probably related to the subsidence and sedimentation during the Plio-Pleistocene.

The onshore vitrinite reflectance gradients, and interpreted palaeogeothermal gradients, are greater than those offshore and thus the oil window is predicted to

be shallower in the onshore areas.

4.  $T_{\max}$  data clearly show that the maturity level of the organic matter in the West Aceh Basin ranges from immature to marginally mature with a small portion extending into the mature zone.  $T_{\max}$  values increase as the vitrinite reflectance increases. However, the mature zone as determined from  $T_{\max}$  values, appears to fall at a vitrinite reflectance value of around 0.65% rather than 0.5%.

Mature samples with  $T_{\max}$  greater than 435°C are confined to the Tangla Formation, or its equivalent Oligocene samples, with some from the onshore Keuh Formation. The  $T_{\max}$  values are higher in samples from the onshore area for any given stratigraphic level and thus the oil window, using this parameter, is located within the Tangla Formation and partly in the Kueh Formation.

5. The coal and clastic rocks are potential source rocks but most are immature and have not produced significant liquid hydrocarbons. Use of a modified petrographic scoring system shows that of the clastic rocks, the Tangla Formation shales and to a lesser extent, the Kueh Formation, are the best source rocks. The Oligocene coal, and possibly the Miocene coal, have the best potential for hydrocarbon generation.

Using a 0.5% vitrinite reflectance for the commencement of the oil generation window, most of the West Aceh basin sequence is immature with only the deeper parts, below 2500 m, of the Tangla Formation marginally mature. However, the

presence of exsudatinite in most coal samples is interpreted as an indication of petroleum generation in an immature sequence; the quantities of hydrocarbons produced have not been significant.

6. Geochemical data confirms the source rock potential of the rocks although the organic matter is mostly Type III or transitional Type II/III using the 1984 classification of Tissot and Welte. Shale contains 1 to 5% Total Organic Carbon (TOC) which is above the threshold level for a good source rock.

Pyrolysis data from the Tertiary coals show that the Oligocene Tangla Formation coal has the best oil potential in terms of organic maturity and organic matter type and the Hydrogen Indices (HI) of the Tangla formation indicate that this Formation has both oil and gas potential ( $HI > 200$ ) whereas Tutut and Kueh Formations, characterised by hydrogen-poor organic matter, is only gas prone.

S<sub>2</sub> values are highest in the Tangla Formation but lowest in the Tutut Formation.

Samples from the Tangla Formation contain the highest extractable hydrocarbons (mgHC/gTOC) although some samples from the Kueh and Tutut Formations also have appreciable extractable hydrocarbons; petrographic data suggest that this is due to bitumen impregnation.

Gas chromatography data indicate that the Oligocene coal samples are mature as are a small number of Miocene coal samples. Some Oligocene samples have

similar normal hydrocarbon distributions as the Talang Akar delta plain coal, which is a proven oil source rock in the Northwest Java Basin.

Pyrolysis-GC traces of these Oligocene and Miocene coals are characterised by a high abundance of normal hydrocarbons. In many respects, the pyrograms are similar to those of the Talang Akar coal. The Pliocene coal is the most immature and the chemistry indicates it has the least hydrocarbon potential although appreciable amounts of waxy compounds were found in this coal.

7. Exploration in the West Aceh Basin has paralleled that in other Indonesian forearc basins in that targets have generally been reservoirs rather than source rocks. Following this study it is now possible to formulate a hydrocarbon generation model that uses petrographic and geochemical data to predict source rocks rather than reservoirs. The model shows that vitrinite reflectances of 0.5%, the onset of the oil window, are unlikely to be intersected at depths of less than 2500 m in the offshore areas and therefore sections shallower than this should be disregarded as source rock targets. Onshore, the oil window is likely to be shallower.

Hydrocarbons generated below the Oligo-Miocene unconformity, which is a good seal, are likely to be in structural traps in the onshore area but are likely to be in stratigraphic traps, such as carbonate build-ups, in the offshore area.

## 9.2 FUTURE WORK AND EXPLORATION STRATEGIES

This study confirmed that The Tangla Formation has a higher hydrocarbon potential than

either the Kueh or Tutut Formations although the Kueh Formation may also yet be a relatively good source rock because the maturation patterns within this formation vary considerably throughout the basin and the possibility of that it passes into the oil window onshore should not be overlooked. In contrast Tutut Formation should be discounted as good source rock potential since entirely of this Formation are immature.

Future exploration should be directed towards the onshore areas or those offshore areas where the sequence is thick and the potential for intersecting the oil window is greater.

One area for future research is the relationship between bitumen and exsudatinite and the significance of these macerals, if any, as indicators of petroleum generation. The literature on these macerals is at best ambivalent. It is suggested that quantitative fluorescence studies may be a useful avenue of research. The occurrence of exsudatinite in the coals, even at low rank levels, should encourage further research because such occurrences are currently believed to be an indicator of immature hydrocarbon generation by some researchers.

Finally, it is evident from this study that the high risk of unsuccessful exploration activity in forearc basins of Indonesia, commonly encountered in the past, can be reduced in the future by using, understanding and integrating organic petrographic and geochemical approaches to hydrocarbon exploration.

## REFERENCES

- AADLAND, A.J. and PHOA, R.S.K, 1981. Geothermal gradient map of Indonesia. Indonesian Petroleum Association, May 1981, Jakarta, Indonesia, 1-41.
- ABRAHAM, H., 1960. Asphalts and allied substances. Historical review and natural raw materials. Princeton, Van Nostrand, 1, 370 p.
- AHMED, M., KHAN, S.I. and SATTAR, M.A., 1991. Geochemical characterization of oils and condensates in the Bengal Foredeep, Bangladesh. Journal of Southeast Asian Earth Sciences, 5 (1-4), 391-399.
- AMIR, R.I., 1991. Coals, source rocks and hydrocarbon in the South-Basin, South Sumatra. Thesis Msc, University of Wollongong, Wollongong, (unpublished).
- AMMOSOV, I.I. and GORSHKOV, V.I., 1969. Vzaimosvyaz' katageneza i neftegazonosnosti otlozhenii Zapadno-Sibirskoy Nizmennosti (The relationship between catagenesis and petroleum content of strata in the West-Siberian lowland); in Rasseyannye vkladyeniya uglya v osadochnykh porodakh; Nauka Press, Moscow, 70-93.
- ANON, 1971. Completion report of Meulaboh well. Union Oil Company, 60p, (unpublished).
- BARBER, A.J., 1985. The relationship between the tectonic evolution of Southeast Asia and hydrocarbon occurrences. In: HOWELL, D.G. (editor), Tectonostratigraphic terranes of the Circum Pacific Region, Circum-Pacific Council for Energy and Mineral Resources Earth Sciences, 1, 523-527.
- BEAUDRY, D. and MOORE, G.F., 1985. Seismic stratigraphy and Cenozoic evolution of West Sumatra Forearc Basin. AAPG Bulletin, 5, 742-759.
- BEMMELEN, R.W. van, 1970. The Geology of Indonesia. Martinus Nijhoff, The Hague, 2 (2).
- BENNET, J.D.; BRIDGE, D.McC.; CAMERON, N.R., DJUNUDDIN, A.; GHAZALI, S.A.; JEFFERY, D.H.; KARTAWA, W.; KEATS, W.; ROCK, N.M.S. and THOMPSON, S.J., 1981. The Geology of the Calang Quadrangle, Sumatra. Geological Research and Development Centre, Bandung, Indonesia, 1-14.
- BILLMAN, HG., 1975. Indonesia Cenozoic correlation chart. Geological Survey of Indonesia.
- BINJIE, L., YOUXIAO, W., XINGHUA, Y., XINYU, L., GUODONG, Z. and ZHIYONG, W., 1991. Geochemical features and sedimentary environment of terrestrial crude oils. Journal of Southeast Asian Earth Sciences, 5 (1-4), 181-187.

BLACKWELL, D.D. and STEELE, L.J., 1989. Thermal conductivity of sedimentary rocks: Measurement and significance. In: Naeser, D.N. and Culloh, Mc.T.H. (editors), *Thermal history of Sedimentary Basins, Methods and Case Histories*, Springer-Verlag, New York Berlin Heidelberg, London Paris Tokyo, 13-36.

BOREHAM, C.J. and POWELL, T.G., 1987. Sources and preservation of organic matter in the cretaceous Tooleybuc Formation, Eastern Australia. *Organic Geochemistry*, **11** (6), 433-449.

BOREHAM, C.J., POWELL, T.G. and HUTTON, A.C., 1988. Chemical and petrographic characterisation of the Australian Tertiary Duaringa oil shale deposit. *FUEL*, **67**, 1369-1377.

BOREHAM, C.J., CRICK, I.H. and POWELL, T.G., 1988. Alternative Alternative calibration of the Methylphenanthrene Index against vitrinite reflectance: Application to maturity measurements on oils and sediments. *Organic Geochemistry*, **12** (3), 289-294.

BOREHAM, C.J. and POWELL, T.G., 1991. Variation in pyrolysate composition of sediments from the Jurassic Walloon Cool Measures, eastern Australia as a function of thermal maturation. *Organic Geochemistry*, **17** (6), 723-733.

BOSTICK, N.H., 1973. Time as a factor in thermal metamorphism of phytoclasts (coaly particles). *Compte Rendu 7th Congress International Stratigraphic et Geologie Carbonifere*, Krefeld, 1971, **7**, 183-193.

BOSTICK, N.H., 1974. Phytoclasts as indicators of thermal metamorphism, Franciscan assemblage and Great Valley sequence (upper Mesozoic), California. In *Carbonaceous Materials as Indicators of Metamorphism* (Edited by Dutcher R.R., Hacquebard, P.A., Schopf, J.M. and Simon, J.A.), *Geological Society of America, Special Paper*, **153**, 1-17.

BOSTICK, N.H., 1979. Microscopic measurements of the level of catagenesis of solid organic matter in sedimentary rocks to aid exploration for petroleum and to determine former burial temperatures - a review. *Society of Economic Palaeontologists and Mineralogists, Special Publication*, **26**, 17-43.

BROOKS, J.D. and SMITH, J.W., 1967. The diagenesis of plant lipids during the formation of coal, petroleum and natural gas - I. Changes in the n-paraffin hydrocarbons. *Geochimica Cosmochimica Acta*, **31**, 2389-2397.

BROOKS, J.D. and SMITH, J.W., 1969. The diagenesis of plant lipids during the formation of coal, petroleum and natural gas - I. Coalification and the formation of oil and gas in the Gippsland Basin. *Geochimica et Cosmochimica Acta*, **31**, 2389-2397.

BROOKS, J.D. and SMITH, J.W., 1969. The diagenesis of plant lipids during the formation of oil and gas in the Gippsland basin. *Geochimica et Cosmochimica Acta*, **33**, 1183-1194.



BROOKS, J.D., 1970. The use of coals as indicators of the occurrence of oil and gas. APEA Journal, 10 (2), 35-50.

BURGERS, J.D., 1974. Microscopic examination of kerogen (dispersed organic matter) in petroleum exploration. In: Dutcher R. R. et al., (editors): Carbonaceous Materials as Indicators of Metamorphism. Geological Society of America Special Paper 153, 19-52.

BURROUGH, H.C., and POWER, P.E., 1968. Field Survey, southern part of North West Sumatra Contract Area. Union R.G.E., (unpublished) 43.

BUSTIN, R.M., CAMERON, A.R., GRIEVE, D.A. and KALKREUTH W.D., 1983. Coal Petrology its principles, Methods, and applications. Geological Association of Canada, Victoria, British Columbia May 8-19, 1983, Short Course Notes, 3, 217p.

CAMERON, N.R.; CLARKE, M.C.G.; ALDISS, D.T.; ASPDEN, J.A. and DJUNUDDIN, A., 1980. The geological evolution of northern Sumatra. Proceeding Ninth Annual Convention, IPA, Jakarta, Indonesia, 149-187.

CAMERON N.R., BENNET, J.D., BRIDGE, D.McC., DJUNUDDIN, A., GHAZALI, S.A., HARAHAH, H., JEFFERY, D.H., KARTAWA, W., KEATS, W., ROCKS, N.M.S., and WHANDOYO, R., 1982. The Geology of the Tapaktuan Quadrangle Sumatra. Geological Research and Development Centre, Bandung, Indonesia, 1-19.

CAMERON, N.R., BENNETT, J.D., BRIDGE, D.McC., CLARKE, M.C.G., DJUNUDDIN, A., GHAZALI, S.A., HARAHAH, H., JEFFEREY, D.H., NGABITO, H., ROCKS, N.M.S., THOMPSON, S.J., 1983. The Geology of the Takengon Quadrangle, Sumatra. Geological Research and Development Centre, Bandung, Indonesia, 1-26.

CAMERON, A.R., KALKREUTH, W.D. and KOUKOUZAS, C., 1984. The petrology of Greek brown coals. International Journal of Coal Geology, 4, 173-207.

CAMERON, A.R., 1991. Regional patterns of reflectance in lignites of the Ravenscrag Formation, Saskatchewan, Canada. Organic Geochemistry, 17, 223-242.

CLEMENTZ, D.M., DEMAISON, G.J. and DALY, A.R., 1979. New pyrolysis device speeds on-site source bed evaluations. Oil Gas Journal, 77, 142-146.

CLEMENTZ, D.M., 1979. Effect of oil and bitumen saturation on source rock pyrolysis. AAPG, 60, 608-626.

CONNAN, J., 1974. Time temperature relation to oil genesis. AAPG Bulletin, 58, 2516-2521.

COOK, A.C., 1982. Organic facies in the Eromanga Basin. In Moore, P.J. and Mount, T.J. (compilers), Eromanga Basin Symposium, summary papers. Geological Society of Australia and Petrology Exploration Society of Australia, Adelaide, 234-257.

COOK, A.C. and STRUCKMEYER, H.I.M., 1986. The role of coal as a source rock for oil. In Second Southeastern Australia Oil Exploration Symposium (Edited by Glenie R.C.), Petroleum Exploration Society of Australia, Adelaide, 419-432.

COSTANO, J.R. and SPARKS, D.M., 1974. Interpretation of vitrinite reflectance measurements in sedimentary rocks and determination of burial history using vitrinite reflectance and authigenic minerals; in Dutcher, R.R., Hacquebard, P.A., Schopf, J.M., and Simon, J.A., editors, Carbonaceous Materials as Indicators of Metamorphism, Geological Society of America Special Paper, **163**, 31-52.

CRICK, I.H., BOREHAM, C.J., COOK, A.C. and POWELL, T.G., 1988. Studies of petroleum geology and geochemistry of the Middle Proterozoic McArthur Basin, northern Australia II: Assessment of source rocks. AAPG Bulletin. 156-164.

DAMBERGER, H.H., 1968. Ein Nachweis der Abhängigkeit der Ingkohlung von der Temperatur: Brennstoff-Chemie, **46**, 73-84

DAMBERGER, H.H., 1974. Coalification patterns of Pensylvanian coal basins of the United States. In: Carbonaceous Materials as Indicators of Metamorphism (Ed. by R.R. Dutcher *et al.*). Special Paper Geological Society of America, **153**, 53-74.

DAULAY, B., 1986. Petrology of some Indonesian Tertiary coals. Msc thesis, University of Wollongong, Wollongong, (unpublished).

DAULAY, B. and COOK, A.C., 1988. Petrology of some Indonesian coals. Journal of South East Asian Earth Sciences, **2** (2), 45-64.

DAVIES, P.R., 1987. Tectonics of North Sumatra. GEOSEA VI, Sixth Regional Congress on Geology, Mineral and Hydrocarbon Resources of Southeast Asia, July 1987, Papers 23-25, 1-16.

DICKINSON, W.R., 1970. Relations of andesites, granites, and derivative sandstones to arc-trench tectonisc. Rev. Geophysics Space Physics, **8**, 813-860.

DICKINSON, W.R. and SEELY, D.R., 1979. Structure and stratigraphy of forearc regions. AAPG Bulletin, **3** (1), 2-31.

DIDYK, B.M., SIMONEIT, B.R.T. and BRASSELL, S.C. & EGLINTON, 1978. Organic geochemical indicators of palaeoenvironmental conditions of sedimentation. Nature, **272**, 216-223.

DIESSEL, C.F.K., 1973. Coalification trends in the Sydney Basin, New South Wales. In: Campbell (editors) Gondwana Geology, Papers Presented at the Third Gondwana Symposium, Canberra, 295-309.

DIESSEL, C.F.K., 1985. Coal geology. Short course, Australian Mineral Foundation.

DIESSEL, C.F.K., 1986. The correlation between coal facies and depositional environments. In advances in the Study of the Sydney Basin. Proceedings of 20th Symposium, The University of Newcastle, 19-22.

DIESSEL, C.F.K., 1992. Coal composition and sequence stratigraphy. Geological Society of Australia, Abstract Number 32, Earth Sciences, Computers and the Environment, eleventh Australian Geological Convention, January 18-25, 1992, Ballarat University College, 118.

DOW, W.G., 1977. Kerogen studies and geological interpretation. Journal of Geochemical Exploration, 7, 79-99.

DURAND, B. and ESPITALIE, J., 1973. Evolution de la matiere organique au cours de l'enfouissement des sediments. C.R. Acad. Sci. Ser. D., 276, 2253-2255.

DURAND, B., (Editor), 1980. Kerogen. Techniz, Paris, 519 p. DURAND, B. and PARRATTE, M., 1982. Oil potential of coals, a geochemical approach. Institut Francais du petrole, Ref. 30560, 16 p.

DURAND, B. and PARATTE, M., 1983. Oil potential of coals - A geochemical approach. In Petroleum Geochemistry and Exploration of Europe (Edited by Brooks, J.) Blackwell Geology of Society Special Publication, 12, 255-266.

EJEDAWA, J.E., and COKER, S.J.L., 1984. Dynamic interpretation of organic matter maturation and evaluation of oil-generative window. Bulletin of American Association Petroleum Geologists, 68, 1024.

ESPITALIE, J., DURAND, B., ROUSSEL, J.C. and SOURON, C., 1973. Etude de la matiere organique insoluble (kerogene) des argiles du Toarcien du bassin de Paris. II. Etudes en spectrometrie infrarouge, en analyse thermique differentielle et en analyse thermogravimetrique. Rev. Inst. Fr. Petr., 28 (1), 37-66.

ESPITALIE, J., LAPORET, J.L, MADEC, M., MARQUIS, F., LEPLAT, P., PAULET, J., and BOUTEFEU, A., 1977. Methode rapide de caracterisation des roches meres, de leur potentiel petrolier et de leur degre d'evolution. Institut Francais du Petrole, Revue, 32, (1), 23-42.

ESPITALIE, J., MADEC, M. and TISSOT, B., 1980. Role of mineral matrix in kerogen pyrolysis: influence on petroleum generation and migration. AAPG Bulletin, 164, 59-66.

ESPITALIE, J., DEROO, G. and MARQUIS, F., 1985. La pyrolyse rock-eval et ses applications. Institute Francais du Petrole, Geologie, 272, 99, Projet B41 79008, 72p.

ESPITALIE, J., DEROO, G. and MARQUIS, F., 1985. Rock-Eval pyrolysis and its applications. Institute Francaies du Petrole Preprint, 33578, 72p.

ESTERLE, J.S. and FERM, J.C., 1986. Relationship between petrographic and chemical

properties and coal seam geometry, Hance Seam, Breathitt Formation, Southeastern Kentucky. International Journal Coal Geology, 6, 199-214.

ESTERLE, J.S., 1990. Trends in petrographic and chemical characteristics of tropical domed peats in Indonesia and Malaysia as analogues for coal formation . Ph.D. thesis, Lexington. University of Kentucky, (unpublished), 270p.

EUBANK, R.T. and MAKKI, A.Ch., 1981. Structural geology of the Central Sumatra Back-Arc Basin. Proceedings 10th Annual Convention, IPA, Jakarta, 153-196.

GIVEN, P.H., 1984. An essay on the organic geochemistry of coal. In: Coal Science (Edited by Gorbaty, M.L., Larsen, J.M. and Wender, I.), Academic Press, INC., Orlando, Florida, 3, 65-339.

GORDON, T.L., 1985. Talang Akar coals - Ardjuna Subbasin oil source. Proceedings Indonesian Petroleum Association. Fourteenth Annual Convention, October 1985, Jakarta, Indonesia, 91-97.

GROOT, P.F. de, 1946. Gold in Atjeh. Jaarb. Mijn. vet Delft (1941-6), 178-90.

GUIDISH, T.M., KENDALL, C.G.St.C., LERCHE, I., TOTH, D.J. and ARZAB, R.F., 1985. Basin evaluation using burial history calculations: An overview. AAPG Bulletin, 69, 92-105.

HACQUEBARD and DONALDSON, 1974. Rank studies of coals in the Rocky Mountains and inner foothills belt, Canada. In: Dutcher *et al.*, (editors), Carbonaceous materials as indicators of metamorphism. Geological Society of America, Special Paper 153, 75-93.

HADIYANTO and AMARULLAH, D., 1985. Eksplorasi Pendahuluan Endapan Batubara di Daerah Meulaboh-Aceh Barat. Laporan Kolokium Direktorat Sumberdaya Mineral Bagian I, 13-15 Mei, Bandung, Indonesia, 20 (1), 3-19, (unpublished).

HADIYANTO, HANIF, A., SUHARTA, K. and RISBANDI, 1986. Geologi endapan batubara di daerah Woyla, Kedue Aron dan Jeuram, Aceh Barat, Daerah Istimewa Aceh. Proyek Inventarisasi Batubara Tahun Anggaran 1985/1986, Departemen Pertambangan dan Energi, Direktorat Jenderal Geologi dan Sumberdaya Mineral, Direktorat Sumberdaya Mineral, Bandung, Indonesia, 1-12, (unpublished).

HADIYANTO, 1988. Coal measures sequences in a Forc-Arc Basin setting at Meulaboh, West Aceh, Sumatra. Abstract of Research, Research Student's Open Day, The University of Wollongong, 9th November, 1988.

HADIYANTO and FAIZ, M.M., 1990. Indonesia's Coal Export Potential and Its Prospects. Mineral Development in Asia and the Pacific. Proceeding of the Second Asia/Pacific Mining Conference and Exhibition, 14-17 March, 1990, Jakarta, Indonesia, 648-663.

- HADIYANTO and COOK, A.C., 1991. Plio-pleistocene coal resources in a forearc basin setting Meulaboh, West Aceh, Sumatra. Australian Society of Exploration Geophysicists 8th. Conference and Exhibition and The Geological Society of Australia Exploration Symposium, Exploration in a Changing Environment, Sydney, 1991, Abstracts **30**, 125.
- HADIYANTO, HUTTON, A.C. and BOREHAM, J.C., 1992. Petrology and geochemistry of Tertiary coals in West Aceh Basin, Sumatra, Indonesia. Geological Society of Australia, Earth Sciences, Computers and the Environment, Eleventh Australian Geological Convention, January 18-25, 1992, Ballarat University College, Abstracts **32**, 130-131.
- HAILE, N.S., 1979. Palaeomagnetic evidence for rotation and northward drift of Sumatra. Journal Geological Society of London, **136**, 541-546.
- HAMILTON, W.B., 1988. Plate tectonics and island arcs. Geological Society of America Bulletin, **100**, 1503-1527.
- HANDIQUE, G.K. and BHARALI, B., 1981. Temperature distribution and its relation to hydrocarbon accumulation in upper Assam Valley, India. AAPG Bulletin, **61**, 1633-1641.
- HARTMAN, C., and STROUP, 1987. The effect of organic matter type and organic carbon content on Rock-Eval hydrogen index in oil shales and source rocks. Organic Geochemistry, **11** (5), 351-367.
- HEROUX, Y., CHAGNON, A. and BERTRAND, R., 1979. Compilation and Correlation of Major Thermal Maturation Indicators. AAPG Bulletin, **63**, (12), 2128-2144.
- HOOD, A. and GUTJAHR, C.C.M., 1972. Organic metamorphism and the generation of petroleum. Annual Meeting Geology Society of America, Minneapolis, 1972.
- HOOD, A., GUTJAHR, C.C.M. and HEACOCK, R.L., 1975. Organic metamorphism and the generation of petroleum. Bulletin of the American Association of Petroleum Geologists, **59**, 986-996.
- HORSFIELD, B., YORDY, K.L. and CRELLING, J.C., 1988. Determining the petroleum-generating potential of coal using organic geochemistry and organic petrology. Organic Geochemistry, **13** (1-3), 121-129.
- HORSFIELD, B., 1989. Practical criteria for classifying kerogens: Some observations from pyrolysis-gas chromatography. Geochimica Cosmochimica Acta, **53**, 891-901.
- HUNT, J.M., 1979. Petroleum geochemistry and geology. W.H. Freeman and Company, San Francisco, 617 p.
- HUNT, J.W., BRAKEL, A.T. and SMYTH, M., 1986. Origin and distribution of the

Bayswater seam and its correlatives in the Permian Sydney and Gunnedah Basins, Australia. Australian Coal Geology, **6**, 59-75.

HUNT, J.M., 1991. Generation of gas and oil from coal and other terrestrial organic matter. Organic Geochemistry, **17** (6), 673-680.

HUTTON, A.C. and COOK, A.C., 1980. Influence of alginite on the reflectance of vitrinite from Joadja, NSW, and some other coals and oil shales containing alginite. Fuel, **59**, 711-714.

HUTTON, A.C., 1984. Petroleum generation and migration. Course Notes for Short Course F3, 7th Australian Geological Convention, The University of Wollongong, 25-26 August, 1984, 47-90.

ICCP International Committee for Coal Petrology, 1963. Handbook of coal petrography. 2nd Edition, Centre National de la Recherche Scientifique, Paris.

ICCP International Committee for Coal Petrology, 1971. International Handbook of Coal Petrography, 1st supplement to 2nd edition. Centre National de la Recherche Scientifique, Paris, France.

ICCP International Committee for Coal Petrology, 1975. Analysis subcommission fluorescence microscopy and fluorescence photometry and subcommission nomenclature. In: International Handbook of Coal Petrography, 2nd supplement to 2nd edition. Centre National de la Recherche Scientifique, Paris, France.

ISMAIL, M. and SHAMSUDDIN, A.H.M., 1991. Organic matter maturity and its relation to time, temperature and depth in the Bengal Foredeep, Bangladesh. Journal of Southeast Asian Earth Sciences, **5** (1-4), 381-390.

JACOB, H., 1966. Komplexuntersuchung zur Frage des bituminierungsprozesses in sedimenten. In: Advances in Organic Geochemistry 1964, Pergamon Press, Paris, 15-39.

JACOB, H., 1967. Petrologie von asphaltiten und asphaltischen pyrobitumina. Erdol Kohle, **20**, 393-400.

JACOB, H., 1975. Mikroskopphotometrische analyse naturlicher fester erdolbitumina. In Alpern, B. (Ed.), Petrographie de la matiere organique des sediments, relations avec la paleotemperature et le potentiel petrolier. Editions du Centre Nationale de la Recherche Scientifique, Paris, 103-113.

JACOB, H., 1976. Petrologie, Nomenklatur und genesis naturlicher, fester erdolbitumina. Gemeinschaftstagung OGEW/DGMK, **4** (6), 36-49.

JACOB, H., 1980. Die anwendung der mikrophotometrie in der organischen petrologie. Leitz-Mitt. Wiss. u. Techn. Bd., **VII** (7), 209-216.

- JACOB, H., 1981. Mikroskopphotometrische analyse disperser ferstbitumina in sedimenten. Erdol und Kohle-Edgas-Petrochemie vereinigt mit brenstoff-chemie, EKEP-Synopse 8133, 33 (11), 507.
- JACOB, H., 1983. Neuere untersuchungen zur genesis naturlicher, fester erdolbitumina. Geol. Jahrb. Hannover, **D59**, 61p.
- JACOB, H., 1989. Classification, structure, genesis and practical importance of natural solid oil bitumen ("migrabitumen"). International Journal of Coal Geology, **11**, 65-79.
- JAMAS, J.S., 1973. Penelitian micropaleontologi ulangan terhadap sumur Meulaboh - 1 (U.O.C.I). Pertamina Unit-1 Bagian Eksplorasi, Pangkalan Brandan, 1-11.
- JONES, B.G. and FACER, R.A., 1982. Corrmat/Prob, a program to create and test a correlation coefficient matrix from data with missing values. Computers in Geoscience, **8**, 191-198.
- JONES, J.M. and MURCHISON, D.G., 1963. The occurrence of resinite in bituminous coals. Economic Geology, **58**, 263-273.
- KALKREUTH, W., NAYLOR, R., PRATT, K. and SMITH, W., 1990. Fluorescence properties of alginite-rich oil shales from the Stellarton Basin, Canada. FUEL, **69**, 139-144.
- KALKREUTH, W., LANGENBERG, W., LECKIE, D. and MECHAN, Mc.M., 1990. Petrographic characteristics of lower cretaceous coals from the Canadian Rocky Mountain foothills and foreland -environments of deposition, coalification patterns and technological properties. Proceedings Southern and Western Coalfields of the Sydney Basin, Workshop, University of Wollongong, 15 February, 1990, 32-39.
- KANTSLER, A.J., SMITH, G.C. and COOK, A.C., 1978. Lateral and vertical rank variation: implications for hydrocarbon exploration. APEA Journal, **18**, 143-156.
- KANTSLER, A.J., COOK, A.C. and SMITH, G.C., 1978. Rank variation, calculated paleotemps in understanding oil, gas occurence. Oil and Gas Journal, **20**, 196-205.
- KANTSLER, A.J. and COOK, A.C., 1979a. Maturation patterns in the Perth Basin. Journal of Australia Petrology Exploration Association, **19**, 94-107.
- KARIG, D.E., SUPARKA, S., MOORE, G.F. and HEHANUSA, P., 1978. Structure and cenozoic evolution of the Sunda arc in the Central Sumatra Region. United Nations ESCAP, CCOP Technical Bulletin, **12**, 87-108.
- KARIG, D.E., SUPARKA, S., MOORE, G.F., and HEHANUSSA, P.E., 1979. Structure and Cenozoic Evolution of the Sunda Arc in the Central Sumatra Region. American Association of Petroleum Geologists Memoir, **29**, 223-236.

- KARIG, D.E., LAWRENCE, M.B., MOORE, G.F. and CURRAY, J.R., 1980. Structural Framework of the fore-arc basin, NW Sumatra. Journal Geological Society of London, **137**, 77-92.
- KARWEIL, J., 1956. Die metamorphose der kohlen vom Standpunkt der physikalischen Chemie. Zeltschrift Deutschen Geologischen Gesellschaft, **107**, 132-139.
- KATILI, J.A., 1973. Geochronology of West Indonesia and its implications on plate tectonics. Tectonophysics, **19**, 195-212.
- KATILI, A.J., 1984. Evolution of plate tectonic concepts and it's implication for the exploration of hydrocarbon and mineral deposits in Southeast Asia. Pangea, **3**, 5-18.
- KATILI, A.J. and ASIKIN, S., 1985. Hydrocarbon Prospects in Complex Paleo Subduction Zones. Proceedings Indonesian Petroleum Association, Fourteenth Annual Convention, Jakarta, Indonesia, 83-103.
- KATILI, J.A., 1989. Geologi Indonesia. Journal of the Indonesian Association of Geologists, J.A. Katili Commemorative Volume (60 Years), **12** (1), 113-143.
- KHORASANI, G.K. and MURCHISON, D.G., 1988. Order of generation of petroleum hydrocarbons from liptinitic macerals with increasing thermal maturity . FUEL, **67**, 1160-1162.
- KHORASANI, G.K. and MICHELSEN, J.K., 1991. Geological and laboratory evidence for early generation of large amounts of liquid hydrocarbons from suberinite and subereous components. Organic Geochemistry, **17** (6), 849-863.
- KISCH, H.J., 1969. Coal rank and burial-metamorphic mineral facies. In: Schenk, P.A., and Havenaar, I., (editors), Advances in organic geochemistry, 1968: Oxford, England, Pergamon Press, 407-426.
- KOESOEMADINATA, R.P., and HARDJONO, 1976. Kerangka sedimenter endapan batubara Tersier Indonesia. Ikatan Ahli Geologi Indonesia, Pertemuan Ilmiah Tahunan, 1-17.
- KURASH, G.E., 1967. Geology of Nias Island area, Indonesia. Union R.G.E. (unpublished), 33p.
- LANGFORD, F.F. and VALLERON, B.M.M., 1988. The interpretation of rock-eval pyrolysis data by the regression of the amount of generatable hydrocarbons against the total organic carbon. Department of Geological Science, University of Saskechewan, Saskaton S7N OWO, Canada, 1-18.
- LARTER, S.R., 1966. Application of analytical pyrolysis techniques to kerogen characterisation and fossil fuel exploration/exploitation. Proceedings of 3rd International Conference on Analytical Pyrolysis.



LEONARD, R., 1983. Geology and hydrocarbon accumulations, Columbus Basin, offshore Trinidad. American Association of Petroleum Geologists Bulletin, **6**, 1122-1140

LEYTHAEUSER, D. and SCHWARZKOPF, Th., 1986. The pristane/n-heptadecane ratio as an indicator for recognition of hydrocarbon migration effects. Organic Geochemistry, **10**, 191-197.

LEYTHAEUSER, D. and WELTE, D.H., 1969. Relation between distribution of heavy n-paraffins and coalification in carboniferous coals from the Saar district, Germany. In Advances in Organic Geochemistry, 1968, (editors P.A. Schenck and I.Havenaar), Pergamon Press, 429-440.

LIU, S., TAYLOR, G.H. and SHIBAOKA, M., 1982. Biochemical gelification and the nature of some huminite macerals. Geological Society of Australia, Proceedings Symposium Coal Resources, Origin Exploration and Utilization in Australia, Melbourne, 15-19 November 1982, Edited by C.W. Mallett, **4**, 145-152.

LOPATIN, N.V., 1971. Temperature and geologic time as factors in coalification. Akad. Nauka SSSR Izvestiya Ser. Geol., English Translation by N.H. Bostick, Illinois State Geological Survey, 1972, **3**, 95-106 (in Russian).

MATTAVELLI, L. and NOVELLI, L., 1988. Geochemistry and habitat of natural gases in Italy. Organic Geochemistry, **13** (1-3), 1-13.

MIDDLETON, M.F., 1982. Tectonic history from vitrinite reflectance. Geophysical Journal of the Royal Astronomical Society, **68**, 121-132.

MISHRA, H.K., 1984. A comparative study of the petrology of permian coals of India and Western Australia. Thesis PhD., University of Wollongong, Wollongong, (unpublished).

MISHRA, H.K. and COOK, A.C., 1992. Petrology and thermal maturity of coals in the Jharia Basin: Implications for oil and gas origins. International Journal of Coal Geology, **20**, 277-313.

MONTHIOUX, M., LANDAIS, P. and DURAND, B., 1985. Comparison between extracts from natural and artificial maturation series of Mahakam delta coals. Organic Geochemistry, **10**, 299-311.

MUKHOPADHYAY, P.K. and GORMLY, J.R., 1984. Hydrocarbon potential of two types of resinite. In: Advances in Organic Geochemistry 1983 (edited by Schenck P.A., De Leeuw, J.W. and Lijmbach, G.W.M.). Organic Geochemistry, Pergamon Press, Oxford, **6**, 439-454.

MUKHOPADHYAY, P.K., HATCHER, P.G. and CALDER, J.H., 1991. Hydrocarbon generation from deltaic and intermontane fluviodeltaic coal and coaly shale from the Tertiary of Texas and Carboniferous of Nova Scotia. Organic Geochemical, **17** (6), 765-

783.

MURCHISON, D.G., 1976. Resinite: its infrared spectrum and coalification pattern. FUEL, **55**, 79-83.

MURCHISON, D.G., COOK, A.C. and RAYMOND, A.C., 1985. Optical properties of organic matter in relation to thermal gradients and structural deformation. Royal Society of London, Philosophical Transactions Series A, Mathematical and Physical Sciences, **315**, 157-186.

NEWMAN, J., and NEWMAN, N.A., 1982. Reflectance anomalies in Pike River coals: Evidence of variability in vitrinite type, with implications for maturation studies and "Sugate-rank". New Zealand Journal of Geology and Geophysics, **25**, 233-243.

NOBLE, R.A. and WU, C.H., 1990. Geochemical characterization of Talang Akar coals and shales, Offshore N.W. Java, Indonesia. Organic Geochemistry (in press).

NOBLE, R.A., WU, C.H. and Atkinson, C.D., 1991. Petroleum generation and migration from Talang Akar coals and shales offshore N.W. Java, Indonesia. Organic Geochemistry, **17**, 363-374.

OPPENOORTH, W.F.F. and ZWIERZYCKI, J., 1918. Geomorphological and tectonic observations as a contribution to the explanation of the landforms of North Sumatra. Internal translation from Dutch of Jaarb. Ned. Oost-Indie Verh., 1917, **1**, 276-311.

ORR, W., 1983. Comments on pyrolytic hydrocarbon yields in source rock evaluation. In Advances in Organic Geochemistry 1981 (Edited by Bjoroy, M. *et al.*), 775-783.

PANGGABEAN, H., 1990. Tertiary source rocks, coals and reservoir potential in the Asem and Barito Basins, Southeastern Kalimantan, Indonesia. PhD Thesis, University of Wollongong, Wollongong, (unpublished).

PETERS, K.E., 1986. Guidelines for evaluating petroleum source rocks using programmed pyrolysis. AAPG Bulletin, **70**, 209-226.

POWELL, T.G. and McKIRDY, D.M., 1973. The effect of source material, rock type and diagenesis on the n-alkane content of sediments. Geochimica et Cosmochimica Acta, **37**, 623-633.

POWELL, T.G., 1978. An assessment of the hydrocarbon source rock potential of the Canadian Arctic Islands. Geological Survey of Canada, Paper 78-12, 82 p.

POWELL, T.G., 1988. Development in concepts of hydrocarbon generation from terrestrial organic matter. Bureau of Mineral Resources, Canberra City, Australia, 807-824.

POWELL, T.G., BOREHAM, C.J., SMYTH, M., RUSSELL, N. and COOK, A.C.,

1991. Petroleum source rock assessment in non-marine sequences: pyrolysis and petrographic analysis of Australian coals and carbonaceous shales. Organic Geochemistry, **17** (3), 375-394.

POWELL, T.G. and BOREHAM, C.J., 1991. Petroleum generation and source rock assessment in Terrigenous sequences: An update. APEA Journal, 297-309.

PRAMONO, H., CHARLIE, C.H.W. and NOBLE, R.A., 1990. A new oil kitchen and petroleum bearing subbasin in the offshore Northwest Java area. Proceeding Indonesian Petroleum Association, Nineteenth Annual Convention, October 1990, 90-167.

PRICE, L.C., 1982. Organic geochemistry of core samples from an ultra deep hot well (300°C; 7km). Chemical Geology, **37**, 215-228.

REMINTON, C.H. and PRANYOTO, U., 1985. A hydrocarbon generation analysis in the N.W. Java basin using Lopatin's method. Indonesian Petroleum Association, 4th Annual Convention, Jakarta 1985, Proceeding, **2**, 121-141.

RIMMER, S.M. and DAVIS, A., 1988. The influence of depositional environments on coal petrographic composition of the Lower Kittanning seam, western Pennsylvania. Organic Geochemistry, **12** (4), 375-387.

ROBERT, P., 1981. Classification of organic matter by means of fluorescence: application to hydrocarbon source rocks. Coal Geology, **1**, 101-137.

ROE, G.D. and POLITO, L.J., 1977. Source rocks for oils in the Ardjuna Sub-Basin of the Northwest Java Basin, Indonesia. Atlantic Richfield Company, Dallas, Texas, U.S.A., 180-193.

ROSE, R., 1983. Miocene Carbonate Rocks of Sibolga Basin, Northwest Sumatra. Proceedings Indonesian Petroleum Association, Twelfth Annual Convention, June, 1983, Jakarta, Indonesia, 107-124.

ROY, R.F., BLACKWELL, D.D., and BIRCH, F., 1968. Heat generation of pluton rocks and continental heat flow provinces. Earth and Planetary Science Letters, **5**, 1-12.

RUSSELL, N.J. and BAILLIE, P.W., 1989. Vitrinite palaeothermometry of offshore exploration wells, Tasmania. APEA, Journal, 130-151.

SCLATER, J.G. and CHRISTIE, P.A.F., 1980. Continental stretching - an explanation of the post-mid Cretaceous subsidence of the central North Sea basin. Journal of Geophysical Research, **85**, 3711-3739.

SHIBAOKA, M., 1978. Micrinite and exsudatinites in some Australian coals, and their relation to the generation of petroleum. FUEL, **57**, 73-77.

SHIBAOKA, M., 1978. Occurrence of oil 'exsudatinites' in brown coals. FUEL, **57**, 798

SMITH, G.C. and COOK, A.C., 1980. Coalification paths of exinite, vitrinite and inertinite. Fuel, **59**, 641-646.

SMITH, G.C. and COOK, A.C., 1984. Petroleum occurrence in the Gippsland basin and its relationship to rank and organic matter type. APEA Journal, **24**, 196-216.

SMITH, G.C., 1981. Tertiary and upper cretaceous coals and coal measure sediments in the Bass and Gippsland Basins. PhD Thesis, University of Wollongong, Wollongong, (unpublished).

SMITH, G.C., 1982a: A review of the Tertiary-Cretaceous Tectonic History of Gippsland Basin and its control on coal. In: Mallet, CW (editors) Measure Sedimentation. Proceedings Symposium on Coal Resources Origin Exploration and utilisation in Australia, Geological Society of Australia, Melbourne 15-19 November, 1982, **1**, 38 p.

SMITH, J.W., GILBERT, T.D. and BATTS, B.D., 1987. A quest for a new parameter in petroleum exploration geochemistry. APEA Journal, 98-105.

SMYTH, M., COOK, A.C. and PHILP, R.P., 1984. Birkhead revisited: petrological and geochemical studies of the Birkhead Formation, Eromanga Basin. APEA Journal, **24** (1), 196-216.

SMYTH, M., 1983. Nature of source material for hydrocarbons in Cooper Basin, Australia. AAPG Bulletin, **67** (9), 1422-1428.

SMYTH, M. and MASTALERZ, M., 1991. Organic petrological composition of Triassic source rocks and their clastic depositional environments in some Australian sedimentary basins. International Journal of Coal Geology, **18**, 165-186.

SNOWDON, L.R. and POWELL, T.G., 1982. Immature oil and condensate modification of hydrocarbon generation model for terrestrial organic matter. AAPG Bulletin, **66**, 775-788.

STACH, E., MACKOWSKY, M-TH., TEICHMULLER, M., TAYLOR, G.H., CHANDRA, D. and TEICHMULLER, R., 1982. Stach's Textbook of Coal Petrology, 3rd edition, Gebruder Borntraeger, Berlin, 535 p.

STACH, E., MACKOWSKY, M.Th., TEICHMULLER, M., TAYLOR, G.H., CHANDRA, D. and TEICHMULLER, R., 1982. Stach's Textbook of Coal Petrology. 3rd edn. Gebruder Borntraeger, Berlin.

STANDARDS ASSOCIATION OF AUSTRALIA, 1986. Australian Standard AS 2856: Coal maceral analysis. Standards Association of Australia, Sydney, 3-22.

SUKARDJO, 1989. Tertiary depositional environments with emphasis on Sawahlunto coal

distribution and quality in Waringin- Sugar area of the Ombilin Basin, West Sumatra, Indonesia. Project-B Geol. 951, Department of Geology, The University of Wollongong, 67p., (unpublished).

SUTRISMAN, A., 1991. Source rock distribution and evaluation in the Talang Akar Formation, Onshore Northwest Jawa Basin, Indonesia. Thesis Msc, University of Wollongong, Wollongong, (unpublished).

SUTTON, C., 1977. Depositional environments and their relation to chemical composition of Java Sea crude oils. Cities Services Company Exploration and Production Research, Box 50408, Tulsa , Oklahoma 74150, U.S.A., 162-179.

STRUCKMEYER, H.I., 1988. Source rock and maturation characteristics of the sedimentary sequence of the Otway Basin, Australia. Thesis PhD., University of Wollongong, Wollongong, (unpublished).

TEICHMULLER, M., 1950. Zum petrographischen aufbau und derdeyang der weichbraunkohle (mit biruksichtigung genetischer fragen der steinkohlenpetrographie). Zeitschrift der Deutschen Geologischen Gesellschaft, **64**, 429-488.

TEICHMULLER, M., 1954. Die stoffliche und strukturelle metamorphose der Kohle. Geologie Rundschau, **42**, 265-296.

TEICHMULLER, M., 1973. Zur petrographie und genese von naturkoksen im floz präsident/helene der zeche Friedrich Heinrich bei Kamp-Lintfort (Linker Niederrhein): Geol. Mitt. (Aachen), **12**, 219-254.

TEICHMULLER, M., 1974. Generation of petroleum-like substances in coal seams as seen under the microscope. In: Tissot, B., and Bienner, F. (eds.), Advances in Organic Geochemistry 1973, Editions Technip, Paris, 321-348.

TEICHMULLER, M., 1982. Application of petrological methods in geology including oil and gas prospecting. In Coal Petrology (Edited by Stach E.), 381-413.

TEICHMULLER, M., 1982. Fluorescence microscopical changes of liptinites and vitrinites during coalification and their relationship to bitumen generation and coking behaviour. Society for Organic Petrology Special Publication, **1**, 74p. (English translation by Neely Bostick, 1984).

TEICHMULLER, M. and TEICHMULLER, R., 1966. Geological Causes of Coalification, in Given, Peter, Chm., Coal Science: Washington, D.C., Advances in Chemistry Ser. 55, Am.Chem. Soc., p. 133-155.

TEICHMULLER, M. and TEICHMULLER, R., 1968. Geological aspects of coal metamorphism. In: MURCHISON, D.G. and WESTOLL, T.S (editors), Coal and coal-bearing strata, Oliver & Boyd, London, 233-267.

TEICHMULLER, M. and TEICHMULLER, R., 1981. The significance of coalification

studies to geology - a review. Bulletin de Centre de Recherches Exploration-Production Elf Aquitaine, **5**, 491-534.

TEICHMULLER, M. and TEICHMULLER, R., 1982. Fundamentals of coal petrography. In: E. Stach, M., Th. Mackowsky, M. Teichmuller, G.H. Taylor, D. Chandra and R. Teichmuller (Editors), *Stach's Textbook of Coal Petrology*, Gebruder Borntraeger, Berlin, 5-53.

TEICHMULLER, M. and WOLF, M., 1977. Application of fluorescence microscopy in coal petrology and oil exploration. Journal of Microscopy, **109**, 49-73.

TEICHMULLER, M. and DURAND, B., 1983. Fluorescence microscopical rank studies on liptinites and vitrinites in peat and coals; and comparison with results of the rock-eval pyrolysis. International Journal of Coal Petrology, **2**, 197-320.

THAMRIN, M., 1979. Heat flow in the Tertiary basin of South Sumatra, Indonesia. Proceedings 16th. Session, CCOP, Bandung, Indonesia, 250-271.

THAMRIN, M., 1985. An investigation of the relationship between the geology of Indonesian sedimentary basins and heat flow density. Tectonophysics, **121**, 45-62.

THOMAS, B.M., 1979. Geochemical analysis of hydrocarbon occurrences in northern Perth Basin, Australia. AAPG Bulletin, **63**, 1092-1107.

THOMPSON, S., COOPER, B.S., MORLEY, R.J. and BARNARD, P.C., 1985. Oil generating coals, in B.M. Thompson *et al.*, eds., *Petroleum geochemistry in exploration of the Norwegian shelf*. London, Graham and Trotman, Ltd., 59-73.

THOMPSON, S., MORLEY, R.J., BARNARD, P.C. and COOPER, B.S., 1985. Facies recognition of some Tertiary coals applied to prediction of oil source rock occurrence. Mar. Pet. Geol., **2**, 288-297.

TISSOT, B. and WELTE, D.H., 1978. *Petroleum Formation and Occurrence*. 1st. edition, Springer-Verlag, Berlin, 527 p.

TISSOT, B., DURAND, B., ESPITALIE, J. and COMBAZ, A., 1974. Influence of nature and diagenesis of organic matter in formation of petroleum. AAPG Bulletin, **58**, 499-506.

VAHRMANN, M. and WATTS, R.H., 1972. The smaller molecules obtainable from coal and their significance. 6. Hydrocarbons from coals heated in thin layers. Fuel, **51**, 235-241.

VAN HINTE, J.E., 1978. Geohistory analysis application of micropaleontology in exploration geology. AAPG Bulletin, **62**, 201-222.

VINCENT, P.W., MORTIMORE, I.R., and McKIRDY, D.M., 1985. Hydrocarbon

generation, migration and entrapment in the Jackson-Naccowlah area, Suthwestern Queensland. APEA Journal, **25**, 62-84.

WAPLES, D.W., 1980. Time and temperature in petroleum formation: application of Lopatin's method to petroleum exploration. AAPG Bulletin, **64**, 916-926.

WAPLES D.W., 1985. Geochemistry in Petroleum Exploration. D. Reidel Publishing Company, Dordrecht, 232p.

WHELAN, J.K, FARRINGTON, J.W. and TARAFA, M.E., 1986. Maturity of organic matter and migration of hydrocarbons in two Alaskan North Slope wells. Organic Geochemistry, **10**, 207-219.

WILKINS, R.W.T., RUSSELL N.J. and NINGNING, Z., 1991. The suppression of vitrinite reflectance - an important consideration in the determination of thermal maturity of organic matter for petroleum exploration in Australia. Australian Society of Exploration Geophysicists 8th Conference, 17-21 February, 1991, Sydney, Abstracts **30**, 61.

WILLIAMS, E.G. and KEITH, M.I., 1963. Relationship between sulfur in coals and the occurrences of marine roof beds. Economic Geology, **58**, 720-729.

WILSON, R.G., 1976. Estimating the potential of a coal basin. In: Coal Exploration. Miller Freeman, San Fransisco, 374- 400.

WINANS, R.E. and CRELLING, J.C., 1984. Chemistry and characterization of coal macerals: overview. In Chemistry and Cahracterization of Coal Macerals (Edited by Winans R.E. and Crelling J.C.). American Chemistry of Society Symposium, **252**, 1-20.

WU, C.H., 1987. Resource assessment of ARII offshore Northwest Java contract area. Atlantic Richfield Indonesia, Inc., 60p, (unpublished).

YALCIN, M.N. and WELTE, D.H., 1988. The thermal evolution of sedimentary basins and significance for hydrocarbon generation. Turkish Assoc. Pet. Geol. Bull., **1** (1), 12-26.

ZHAO, S.Q., ZHONG, N.N., XIONG, B., SIMONEIT, B.R.T. and WANG, T.G., 1989. Organic geochemistry and coal petrology of Tertiary brown coal in the Zhoujing mine, Base basin, South China - 1.Occurrence and significance of exsudatinite. FUEL, **69**, 4-20.

ZWIERZYCKI, J., 1922. Geological compilation map, Netherlands East Indies 1:1,000,000. Explanatory notes with sheet I (N. Sumatra). Internal translation from the Dutch of Jaarb. Mijnw. Ned. Oost-Indie Verh. (1919), **1**, 11-71.

## LIST OF FIGURES

1. 1 Geographic Map of Indonesia.
1. 2 Locality sketch map of Meulaboh area.
  
2. 1 Tertiary Basins Map of North and Central Sumatra Region.
2. 2 Geological Map of Meulaboh Area West Aceh Basin, Sumatra.
2. 3 Simplified Tertiary stratigraphy of West Aceh Basin.
2. 4 Structure Map of Meulaboh and surrounding area.
2. 5 Stratigraphic framework of West Aceh Basin and the surrounding area.
  
3. 1 Flow diagram of polishing samples.
4. 1 Maceral composition of Tertiary coals.
4. 2 Maceral composition of Oligocene coal.
4. 3 Maceral composition of Miocene coal.
4. 4 Maceral composition of Pliocene coal.
4. 5 Vitrinite reflectance of Tertiary coals.
4. 6 Correlation of vitrinite and bitumen reflectances for several countries.
4. 7 Triangular diagram showing maceral composition.
4. 8 Relationship between detrovitrinite and vitrinite reflectance of the Tertiary coals.
4. 9 Coal facies diagram for the Tertiary coal of West.
  
5. 1 Maturation indicators and hydrocarbon generation in relation to coal rank.
5. 2 Plots vitrinite reflectance against depth from offshore wells of West Aceh Basin.
5. 3 Maximum reflectance versus depth, Teunom well (a) linear; (b) semi-log.
5. 4 Maximum reflectance versus depth, Bubon well (a) linear; (b) semi-log.
5. 5 Maximum reflectance versus depth, Keudapasi well (a) linear; (b) semi-log.
5. 6 Maximum reflectance versus depth, Tuba well (a) linear; (b) semi-log.
5. 7 Maximum reflectance versus depth, Meulaboh well (a) linear; (b) semi-log.
5. 8 Maximum reflectance versus depth, Tripa well (a) linear; (b) semi-log.
5. 9 Maximum reflectance versus depth, Meulaboh East well (a) linear; (b) semi-log.
- 5.10 Maximum reflectance versus depth, Palumat well (a) linear; (b) semi-log.
- 5.11 Maximum vitrinite reflectance versus depth for onshore wells.
- 5.12 Maximum vitrinite reflectance versus depth for M10 and M1 wells.
- 5.13 Maximum vitrinite reflectance versus depth for M12 and M11 wells.
- 5.14 Maximum vitrinite reflectance versus depth for M15 and M13 wells.
- 5.15 Maximum vitrinite reflectance versus depth for M2 and M18 wells.
- 5.16 Maximum vitrinite reflectance versus depth for M4 and M3 wells.
- 5.17 Maximum vitrinite reflectance versus depth for M22 and M21 wells.
- 5.18 Depth versus  $T_{\max}$  (a) maximum vitrinite reflectance for offshore wells.
- 5.19 Isoreflectance contour map of West Aceh onshore area.
- 5.20 Isoreflectance profile showing rank gradients for onshore wells.
- 5.21 Isoreflectance profile for offshore wells of West Aceh Basin.
- 5.22 Vitrinite reflectance gradients for onshore and offshore wells, West Aceh Basin.
- 5.23 Vitrinite reflectance gradients for onshore and offshore wells, West Aceh Basin.
- 5.24 Offshore isorefectance gradient contour at 0.25% vitrinite reflectance level.
- 5.25 Offshore isorefectance gradient contour at 0.30% vitrinite reflectance level.
- 5.26 Offshore isorefectance gradient contour at 0.40% reflectance level.



6. 1 Karweil diagram.
6. 2 Plots T present versus T grad of the offshore wells, West Aceh Basin.
6. 3 Burial history diagram for Meulaboh well, West Aceh Basin.
6. 4 Burial history diagram for Tuba well, West Aceh Basin.
6. 5 Burial history diagram for Teunom well, West Aceh Basin.
6. 6 Burial history diagram for Bubon well, West Aceh Basin.
6. 7 Burial history diagram for Meulaboh East well, West Aceh Basin.
6. 8 Burial history diagram for Tripa well, West Aceh Basin.
6. 9 Burial history diagram for Keudapasi well, West Aceh Basin.
- 6.10 Burial history diagram for Palumat well, West Aceh Basin.
  
7. 1 Hydrogen index (a) oxygen index and (b)  $T_{max}$ , offshore samples.
7. 2 Hydrogen index (a) oxygen index and (b)  $T_{max}$ , onshore samples.
7. 3 TOC content and normalised hydrocarbon (mg/g TOC), (a) shale; (b) coal; (c) combined shale and coal.
7. 4 Vitrinite reflectance and normalised hydrocarbon (mg/g TOC), (a) shale; (b) coal.
7. 5 Vitrinite reflectance and ratio of saturates:aromatic fractions, (a) shale; (b) coal.
7. 6 N-alkane distribution, saturated fractions of shale extracts, Tutut Fm, BB6.
7. 7 N-alkane distribution, saturated fractions of shale extracts, Tutut Fm, BB10.
7. 8 N-alkane distribution, saturated fractions of shale extracts, Kueh Fm, BB25.
7. 9 N-alkane distribution, saturated fractions of shale extracts, Tutut Fm, TR9.
- 7.10 N-alkane distribution, saturated fractions of shale extracts, Kueh Fm, TR17.
- 7.11 N-alkane distribution, saturated fractions of shale extracts, Kueh Fm, TR27.
- 7.12 N-alkane distribution, saturated fractions of shale extracts, Kueh Fm, M10.
- 7.13 N-alkane distribution, saturated fractions of shale extracts, Kueh Fm, M16.
- 7.14 N-alkane distribution, saturated fractions of shale extracts, Tangla Fm, M21.
- 7.15 N-alkane distribution, saturated fractions of shale extracts, Tutut Fm, TN15.
- 7.16 N-alkane distribution, saturated fractions of shale extracts, Tutut Fm, TN18.
- 7.17 N-alkane distribution, saturated fractions, coal extracts, Pliocene coal, MBOI/1.
- 7.18 N-alkane distribution, saturated fractions, coal extracts, Pliocene coal, M22/2.
- 7.19 N-alkane distribution, saturated fractions, coal extracts, Pliocene coal, BB2.
- 7.20 N-alkane distribution, saturated fractions, coal extracts, Miocene coal, TR36.
- 7.21 N-alkane distribution, saturated fractions, coal extracts, Miocene coal, BB19.
- 7.22 N-alkane distribution, saturated fractions, coal extracts, Miocene coal, K20.
- 7.23 N-alkane distribution, saturated fractions, coal extracts, Miocene, K23.
- 7.24 N-alkane distribution, saturated fractions, coal extracts, Oligocene coal, M19.
- 7.25 N-alkane distribution, saturated fractions, coal extracts, Oligocene coal, L5.
- 7.26 N-alkane distribution, saturated fractions, coal extracts, Oligocene coal, L14.
- 7.27 N-alkane distribution, saturated fractions, coal extracts, Oligocene coal, L21.
- 7.28 N-alkane distribution, saturated fractions, coal extracts, Oligocene coal, L20.
- 7.29 Vitrinite reflectance and pristane to phytane ratios in (a) shale; (b) coal.
- 7.30 Vitrinite reflectance and (a) pristane/n-C17; (b) Ph/n-C18, shale samples.
- 7.31 Vitrinite reflectance and (a) pristane/n-C17; (b) Ph/n-C18, coal samples.
- 7.32 Pyrolysis gas chromatogram for Pliocene coal, sample PG 1.
- 7.33 Pyrolysis gas chromatogram for Pliocene coal, sample PG 2.
- 7.34 Pyrolysis gas chromatogram for Pliocene coal, sample PG 3.
- 7.35 Pyrolysis gas chromatogram for Pliocene coal, sample PG 4.
- 7.36 Pyrolysis gas chromatogram for Miocene coal, sample PG 5.

- 7.37 Pyrolysis gas chromatogram for Miocene coal, sample PG 7.
- 7.38 Pyrolysis gas chromatogram for Miocene coal, sample PG 11.
- 7.39 Pyrolysis gas chromatogram for Miocene coal, sample PG 14.
- 7.40 Pyrolysis gas chromatogram for Oligocene coal, sample PG 6.
- 7.41 Pyrolysis gas chromatogram for Oligocene coal, sample PG 13.
- 7.42 Pyrolysis gas chromatogram for Oligocene coal, sample PG 9.
- 7.43 Pyrolysis gas chromatogram for Oligocene coal, sample PG 10.
- 7.44 Pyrolysis gas chromatogram for Oligocene coal, sample PG 12.
- 7.45 Pyrolysis gas chromatogram for Oligocene coal, sample PG 8.
- 7.46 Ratio of normal hydrocarbons to aromatic versus (a) total hydrocarbons, and (b) vitrinite reflectance.
- 7.47 Compound classes of hydrocarbons, aromatics and phenol.
- 7.48 Hydrogen index versus (a) gas fraction, and (b) C7+ normal hydrogen.
- 7.49 R-mode dendogram, rock-eval and maceral composition.
- 7.50 R-mode dendogram, maceral composition and pyrolysis-GC products.
- 7.51 Maturation parameters and depth of the West Aceh offshore area
- 7.52 Maturation parameters with depth in Bubon well.
- 7.53 Maturation parameters with depth in Tripa well.
- 7.54 Maturation parameters with depth in Meulaboh well.
  
- 8. 1 Hydrocarbon occurrence map of Indonesia and the surrounding area.
- 8. 2 Idealised iso-reflectance profile versus age boundary and depth, offshore wells.
- 8. 3 Maturation pattern in the Tertiary Formations of West Aceh Basin.

## LIST OF TABLES

- |      |   |
|------|---|
| 4. 1 | Coal maceral classification (AS 2856, 1986).  |
| 4. 2 | Summary of the microscopic features of exsudatinite and bitumen.  |
| 4. 3 | Coal maceral classification (AS 2856, 1986).  |
| 4. 3 | Average maceral composition of Tertiary Coals, West Aceh Basin.   |
| 4. 4 | Average maceral composition, offshore Tangla Formation, West Aceh Basin.                                      |
| 4. 5 | Average maceral composition, offshore Kueh Formation, West Aceh Basin.  |
| 4. 6 | Average maceral composition, offshore Tutut Formation, West Aceh Basin.                                       |
| 4. 7 | Classification of the natural solid oil bitumens.   |
|      |   |
| 5. 1 | Maximum vitrinite reflectance ( $R_{v,max}$ ) values, offshore and onshore wells.                             |
| 5. 2 | Depth and reflectance gradient for given reflectance levels, West Aceh Basin.                                 |
|      |   |
| 6. 1 | Present-day geothermal gradients West Aceh Basin and other Sumatran Basins.                                   |
| 6. 2 | Thermal history data for various formations in the West Aceh Basin, Sumatra.                                  |
| 6. 3 | Correlation of vitrinite reflectance values with TTI values.  |
|      |   |
| 7. 1 | Scoring table for volume of DOM, vitrinite reflectance and volume of coal                                     |
| 7. 2 | Scoring table for volume of DOM, vitrinite reflectance and volume of coal,<br>Tertiary West Aceh Basin        |
| 7. 3 | Volume, type and rank of DOM and Coals in wells in the Tutut Formation.                                       |
| 7. 4 | Volume, type and rank of DOM and Coals in wells in the Kueh Formation.  |
| 7. 5 | Volume, type and rank of DOM and Coals in wells in the Tangla Formation.                                      |
| 7. 6 | Average formation scores for hydrocarbon-generating potential of the Tertiary<br>Formations, West Aceh Basin. |
| 7. 7 | Well scores for hydrocarbon generation potential, Tutut Formation based on<br>properties of the DOM.          |
| 7. 8 | Well scores for hydrocarbon generation potential, Tutut Formation based on<br>properties of coal and DOM.     |
| 7. 9 | Well scores for hydrocarbon generation potential, Kueh Formation based on<br>properties of the DOM.           |
| 7.10 | Well scores for hydrocarbon generation potential, Kueh Formation based on<br>properties of coal and DOM.      |
| 7.11 | Well scores for hydrocarbon generation potential, Tangla Formation based on<br>properties of the DOM.         |
| 7.12 | Well scores for hydrocarbon generation potential, Tangla Formation based on<br>properties of coal and DOM.    |
| 7.13 | Summary of Rock Eval/TOC and vitrinite reflectance analyses, offshore West<br>Aceh Basin.                     |
| 7.14 | Average of Rock Eval/TOC and vitrinite reflectance analyses for seven offshore<br>wells, West Aceh Basin.     |
| 7.15 | Rock eval extract data for samples.   |
| 7.16 | Rock eval, maceral composition and vitrinite reflectance data of onshore coals.                               |

- 7.17 Extraction results for shale samples, West Aceh Basin.
- 7.18 Extraction results for coal samples, West Aceh Basin.
- 7.19 Alkane parameters (source rock extract), West Aceh Basin.
- 7.20 Alkane parameters (coal extract), West Aceh Basin.
- 7.21 Significant values in P-M, matrix for Rock Eval and macerals.
- 7.22 Data matrix for pyrolysis-GC and coal petrology.
- 7.23 Significant values in P-M, matrix for pyrolysis-GC and coal petrology.
  
- 8.1 Geological factors controlling hydrocarbon generation and accumulation in forearc basins.

## LIST OF PLATES

- |           |  |
|-----------|--|
| PLATE I   | General microscopic features of exsudatinite and bitumen                             |
| PLATE II  | Vitrinite group of the Tertiary coals in West Aceh Basin                             |
| PLATE III | Liptinite macerals of the Tertiary coals in West Aceh Basin                          |
| PLATE IV  | Type I Exsudatinite in the Tertiary coals of West Aceh Basin                         |
| PLATE V   | Type II Exsudatinite in the Tertiary coals of West Aceh Basin                        |
| PLATE VI  | Solid bitumen in the clastic rocks of the Tertiary Formations of the West Aceh Basin |

## LIST OF APPENDICES

- |              |   |
|--------------|---|
| Appendix 1.  | Cuttings analysis form.   |
| Appendix 2.  | Quantitative method for demineralisation.   |
| Appendix 3.  | Procedure for gas chromatography analysis.  |
| Appendix 4.  | Maceral composition of Pliocene coal.   |
| Appendix 5.  | Maceral composition of Miocene coal.  |
| Appendix 6.  | Maceral composition of Oligocene coal.  |
| Appendix 7.  | Minerals content in Tertiary coals of West Aceh Basin, Sumatra.   |
| Appendix 8.  | Maceral and fluorescence colour data for all cutting samples from offshore wells of West Aceh Basin, Sumatra.         |
| Appendix 9.  | Vitrinite reflectance data for offshore wells vitrinite.  |
| Appendix 10. | Reflectance data for Pliocene coal from onshore wells.  |
| Appendix 11. | Rock-Eval and vitrinite reflectance data for Teunom, Bubon, Keudapasi, Meulaboh East, Meulaboh, Tripa, Palumat wells. |
| Appendix 12. | Product-moment, probability matrix for Rock Eval and macerals.  |
| Appendix 13. | Product-moment, probability matrix for pyrolysis-GC and coal petrology.   |

## FIGURES OF CHAPTER 1

Please see print copy for image

**Figure 1.1: Geographic Map of Indonesia.**



Please see print copy for image

## FIGURES OF CHAPTER 2

Please see print copy for image

Figure 2.1: Tertiary Basins Map of North and Central Sumatra Region (Modified from Cameron et al., 1980).

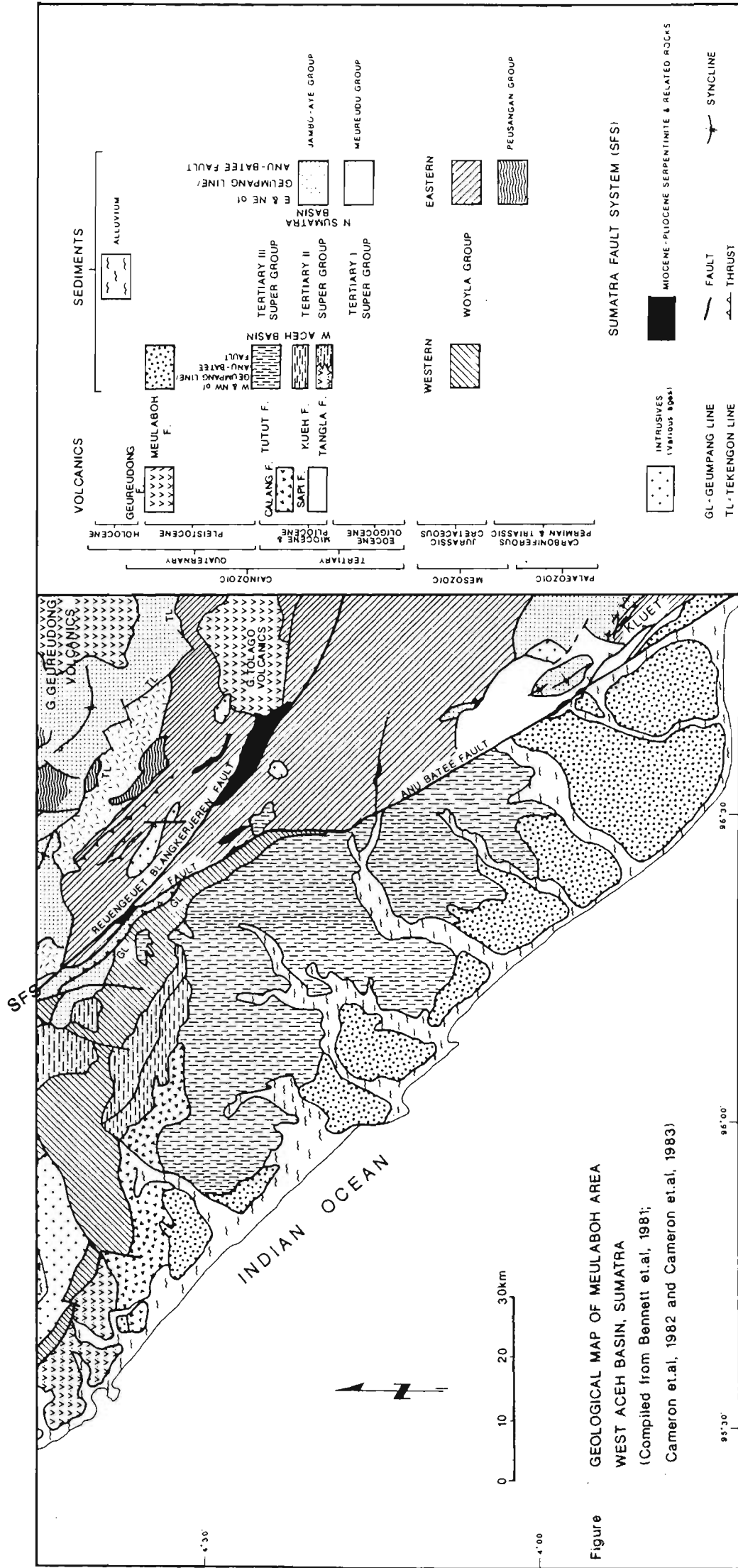


Figure 2.2: Geological Map of Meulaboh Area West Aceh Basin, Sumatra (Compiled from Bennett et al., 1981; Cameron et al., 1982 and Cameron et al., 1983).

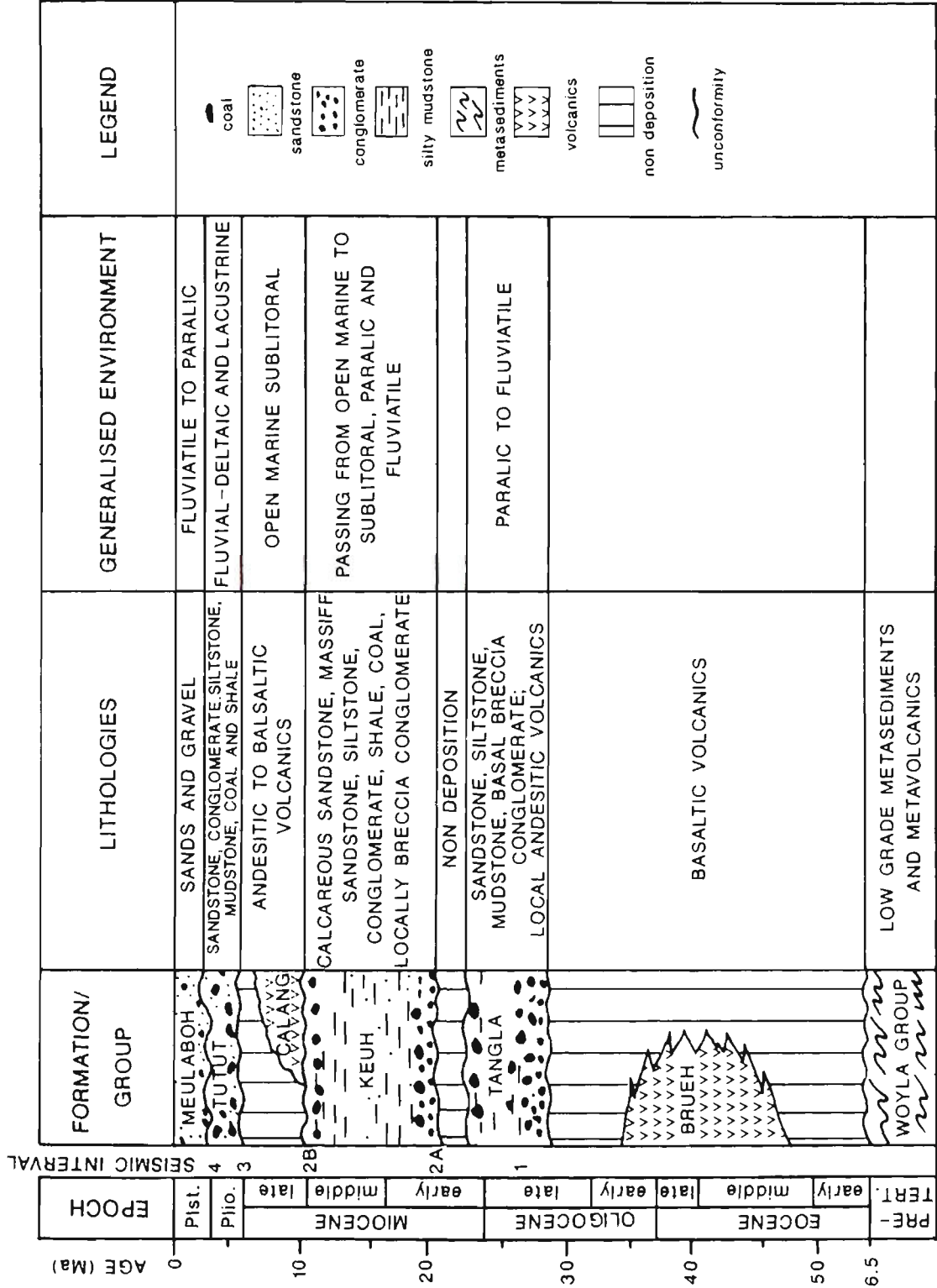


FIGURE 2.3 SIMPLIFIED TERTIARY STRATIGRAPHY OF WEST ACEH BASIN  
(MODIFIED FROM CAMERON ET.AL, 1980; BEAUDRY AND  
MOORE, 1985; HADIYANTO AND AMARULLAH, 1985)

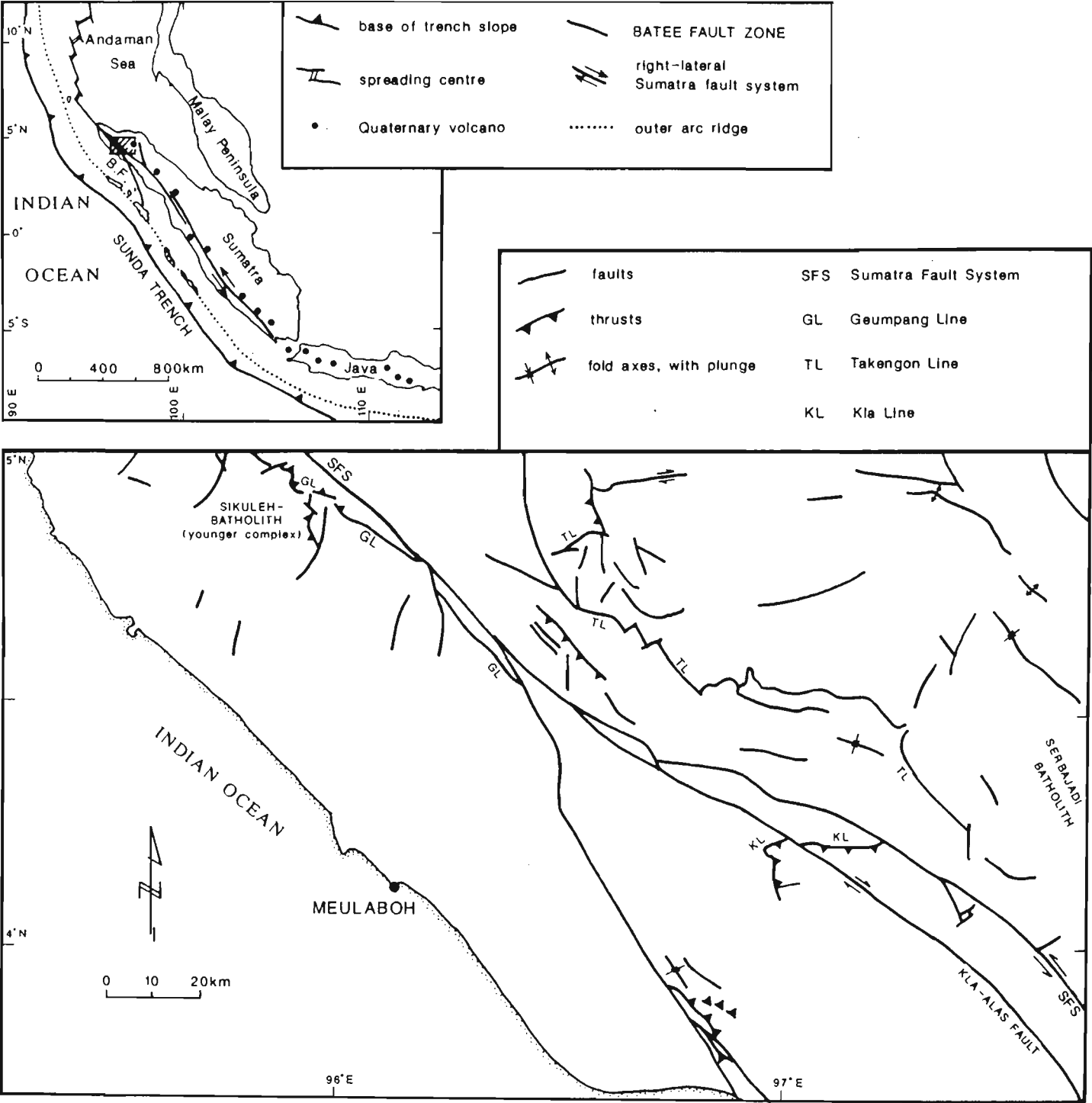


Figure 2.4: Structure Map of Meulaboh and surrounding area, Sumatra (Modified from Cameron et al., 1980 and Beaudry and Moore, 1985).

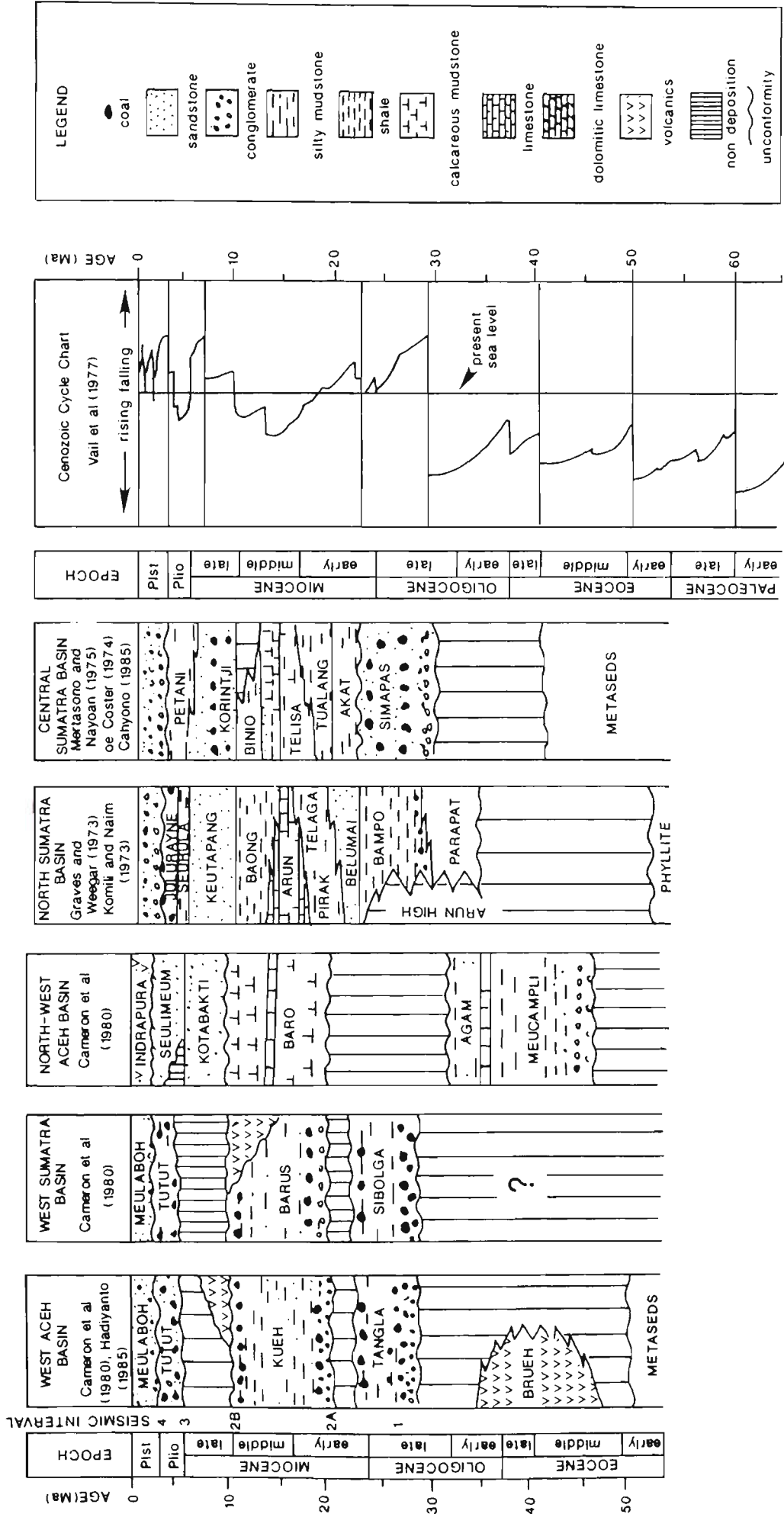


Figure 2.5: Stratigraphic framework of West Aceh Basin and the surrounding area.

## FIGURES OF CHAPTER 3

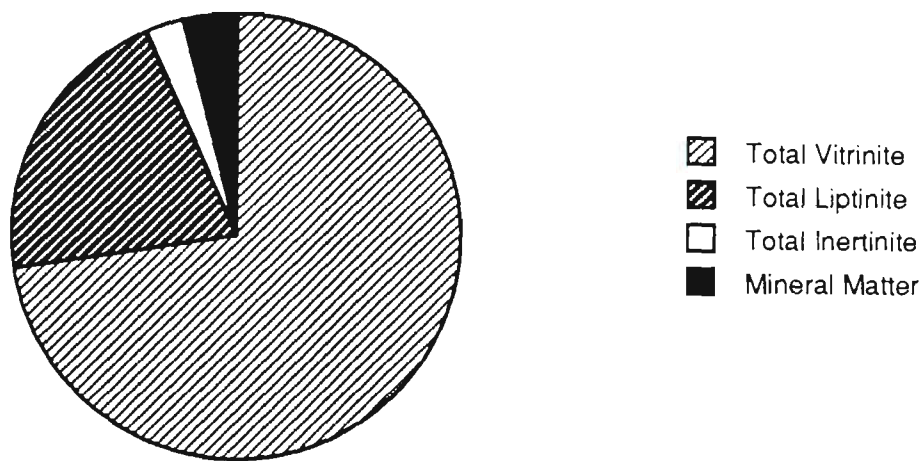


Please see print copy for image

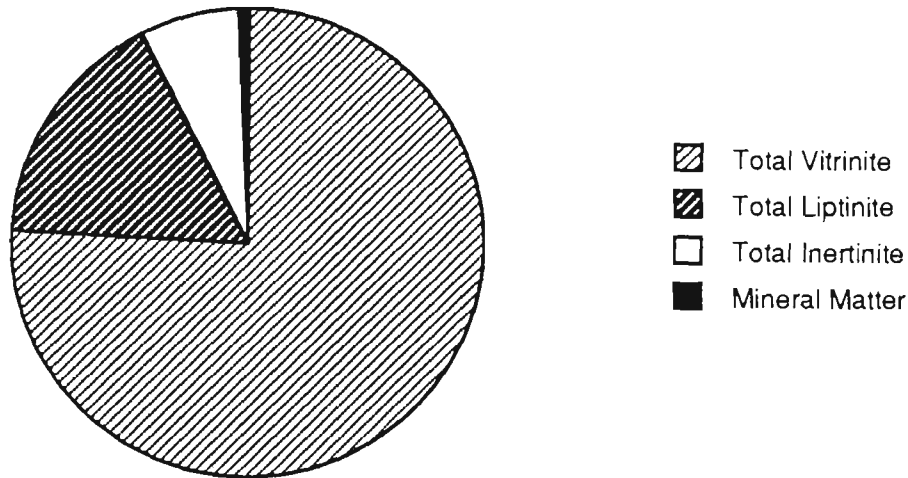
**FIGURE 3.1 FLOW DIAGRAM OF POLISHING SAMPLES**  
(Modified from Hutton, 1984)

FIGURES AND TABLES OF  
CHAPTER 4

Pliocene Coal



Miocene Coal



Oligocene Coal

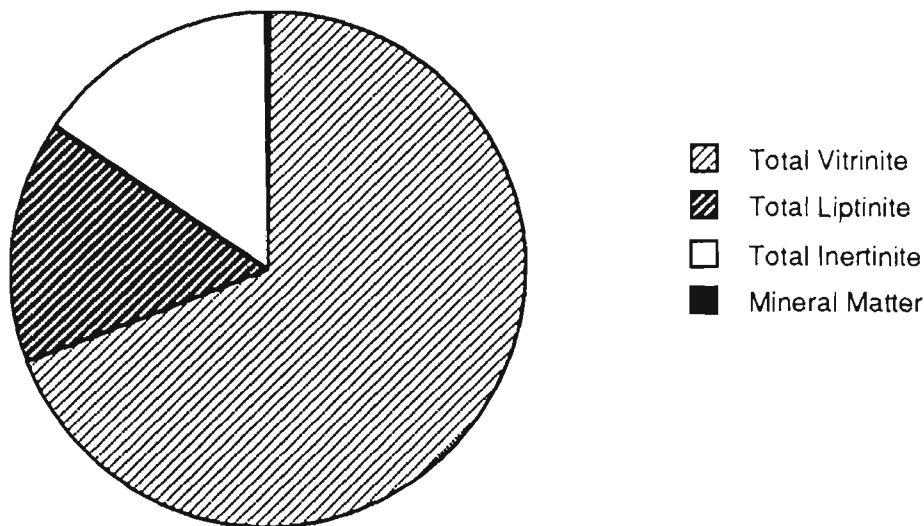


Figure 4.1: Maceral composition of Tertiary coals.

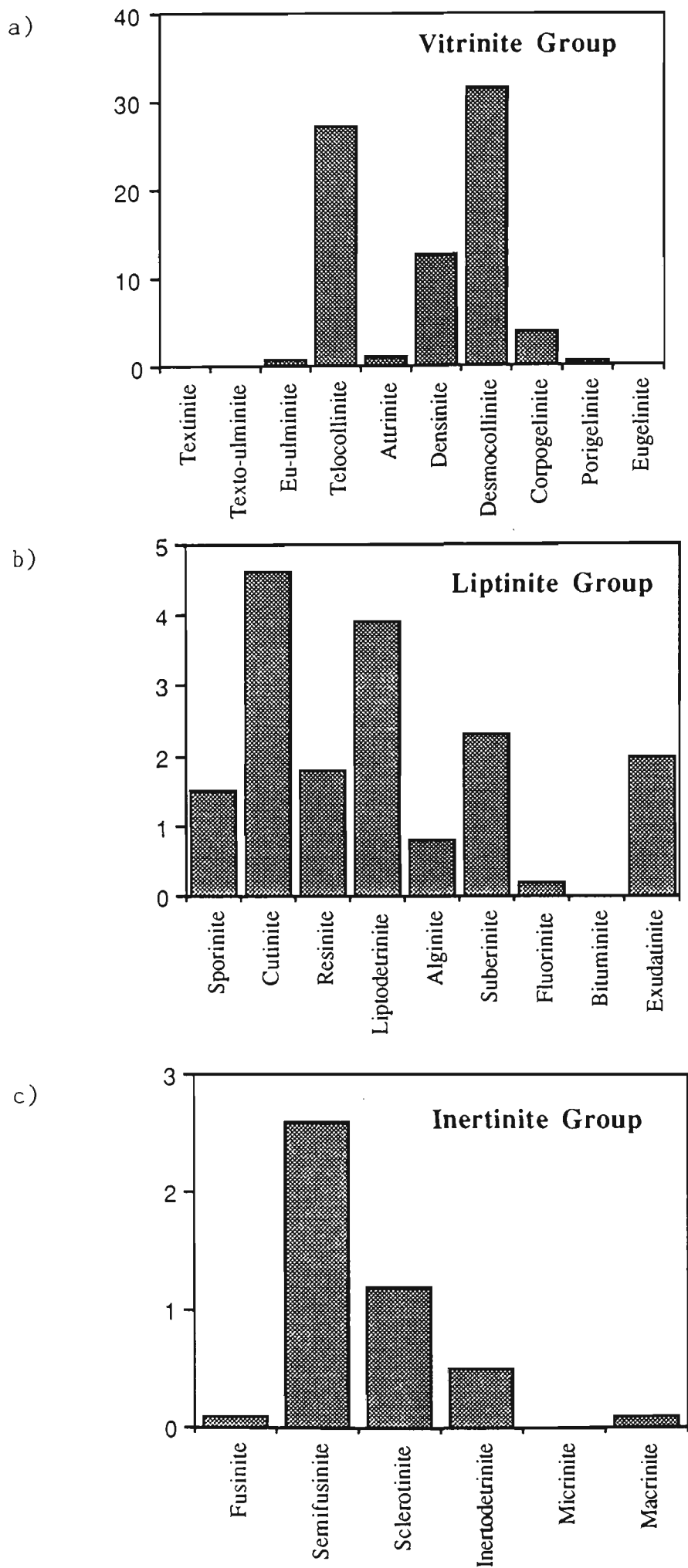


Figure 4.2: Maceral composition of Oligocene coal.

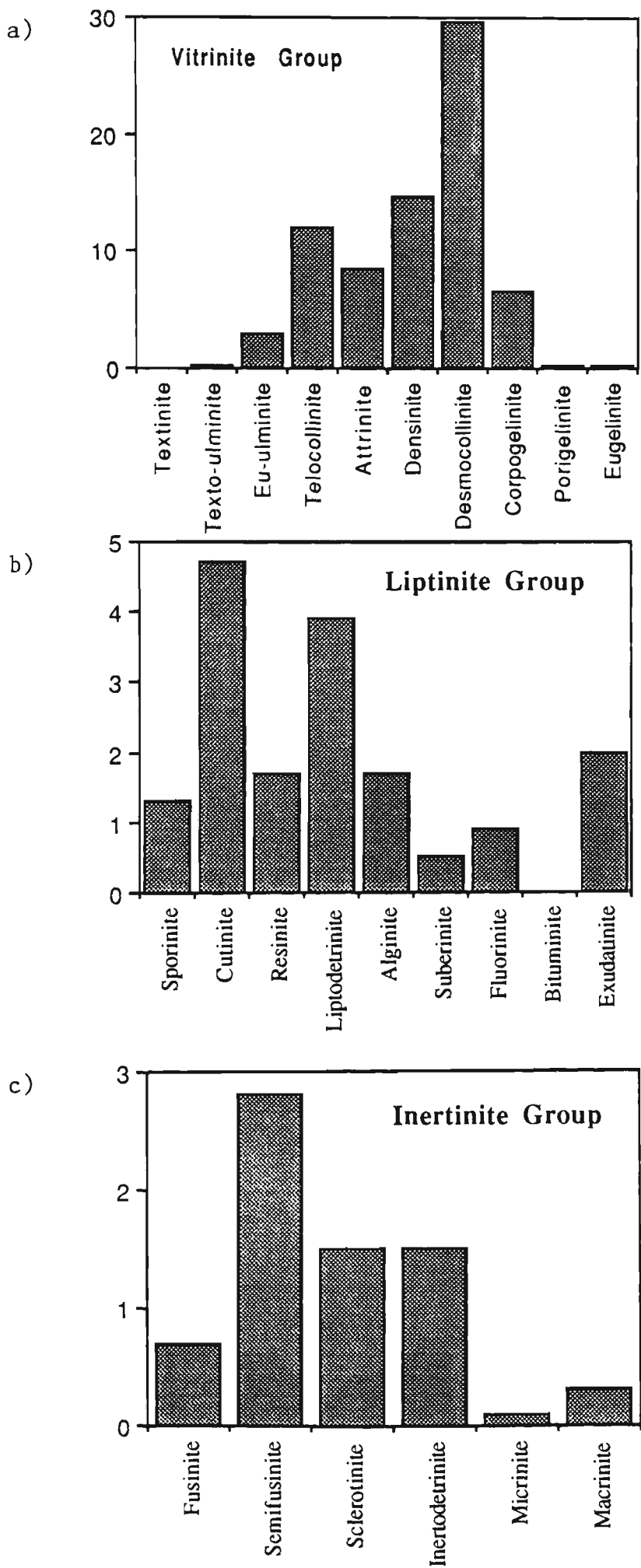


Figure 4.3: Maceral composition of Miocene coal.

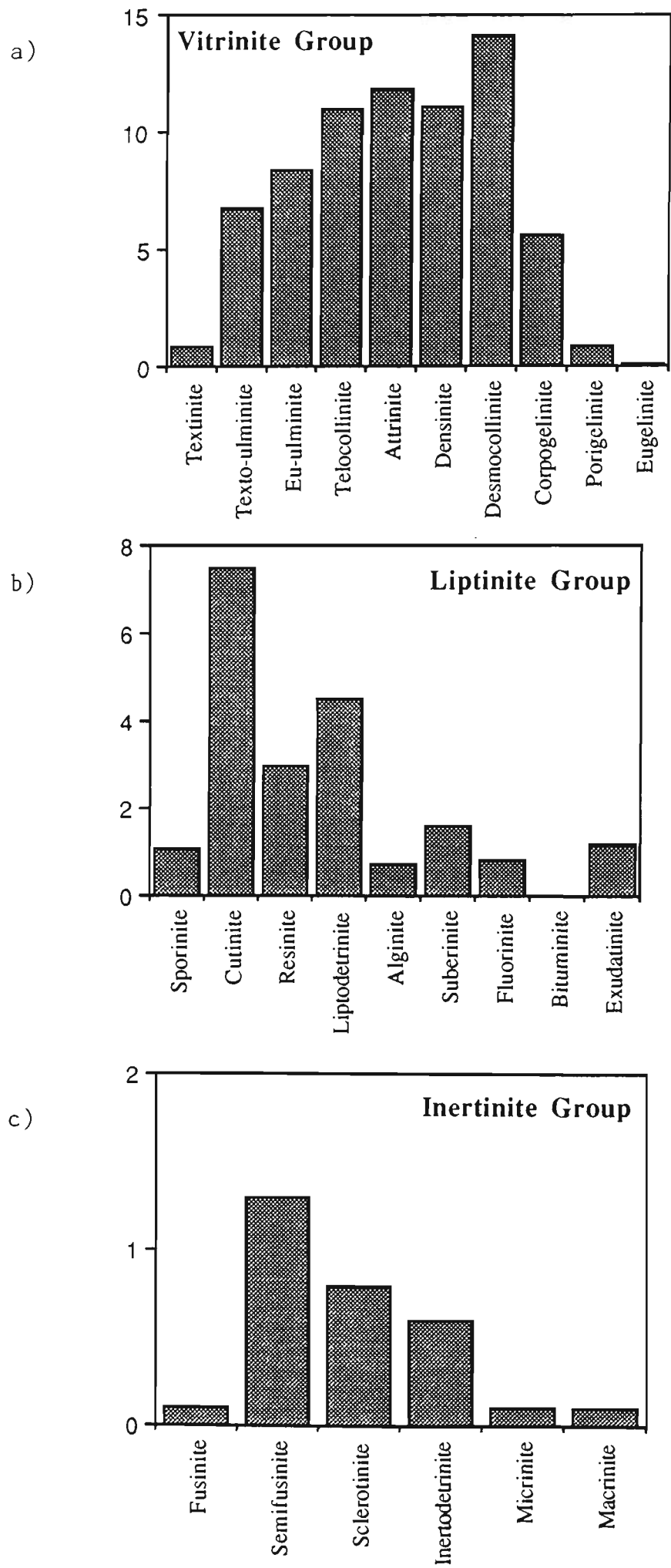


Figure 4.4: Maceral composition of Pliocene coal.

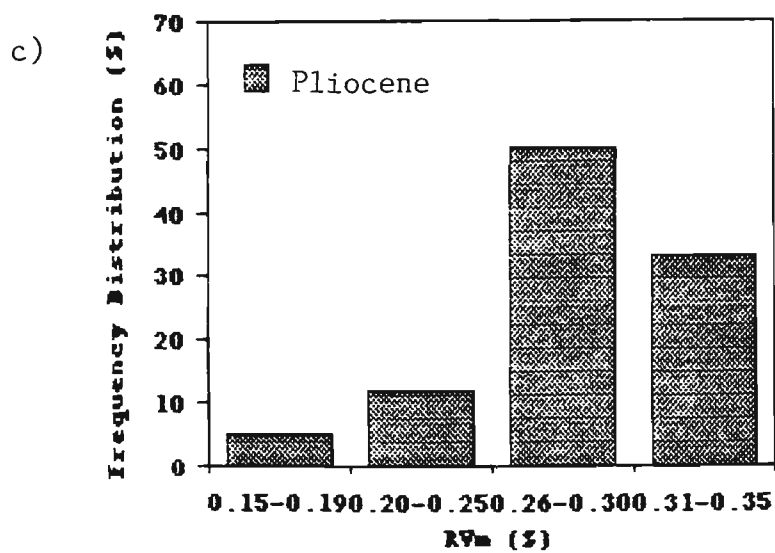
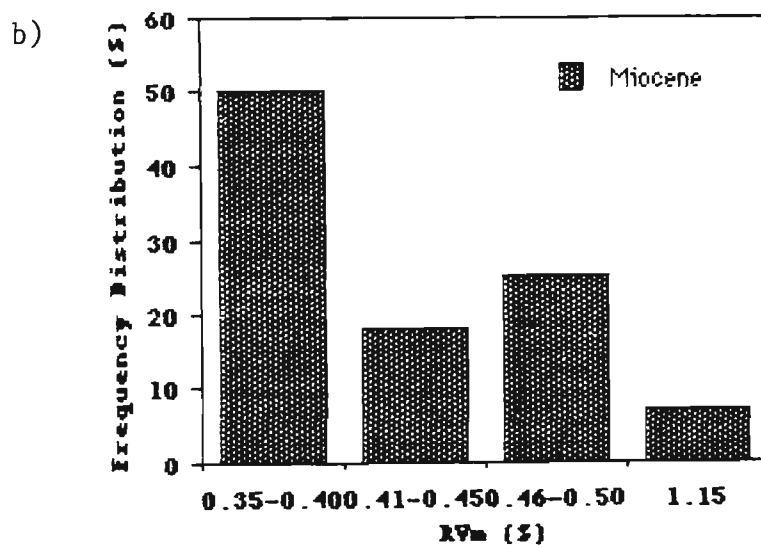
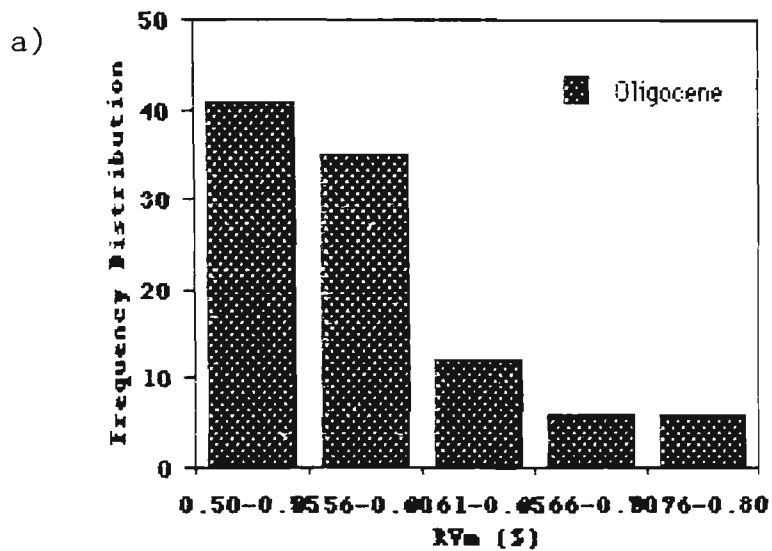


Figure 4.5: Vitrinite reflectance of Tertiary coals

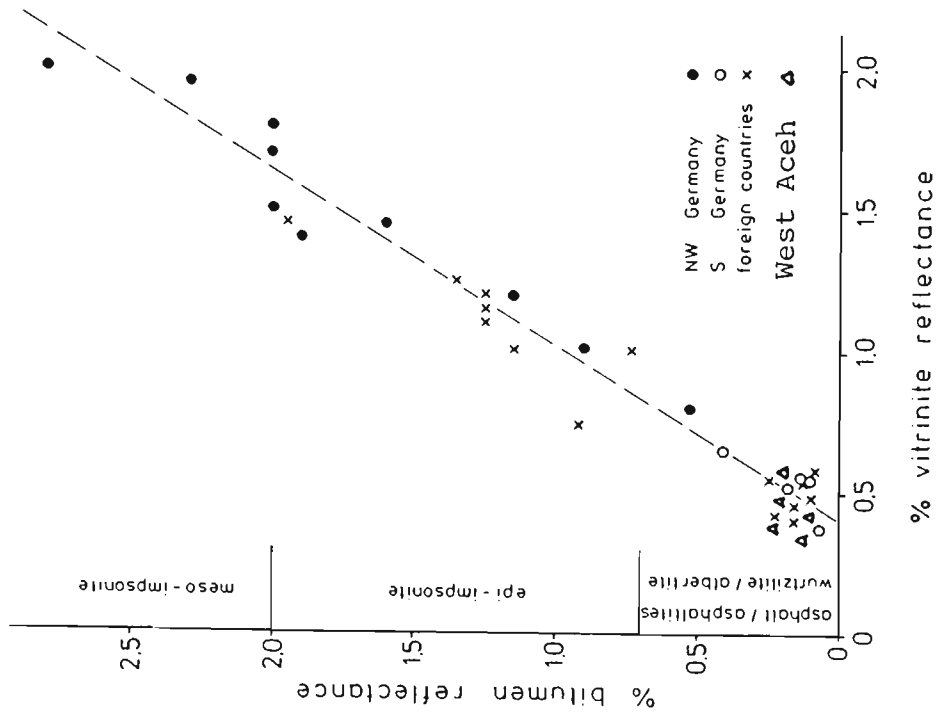


Figure 4.6: Correlation between vitrinite reflectance and bitumen reflectance from several countries (after Jacob, 1989).



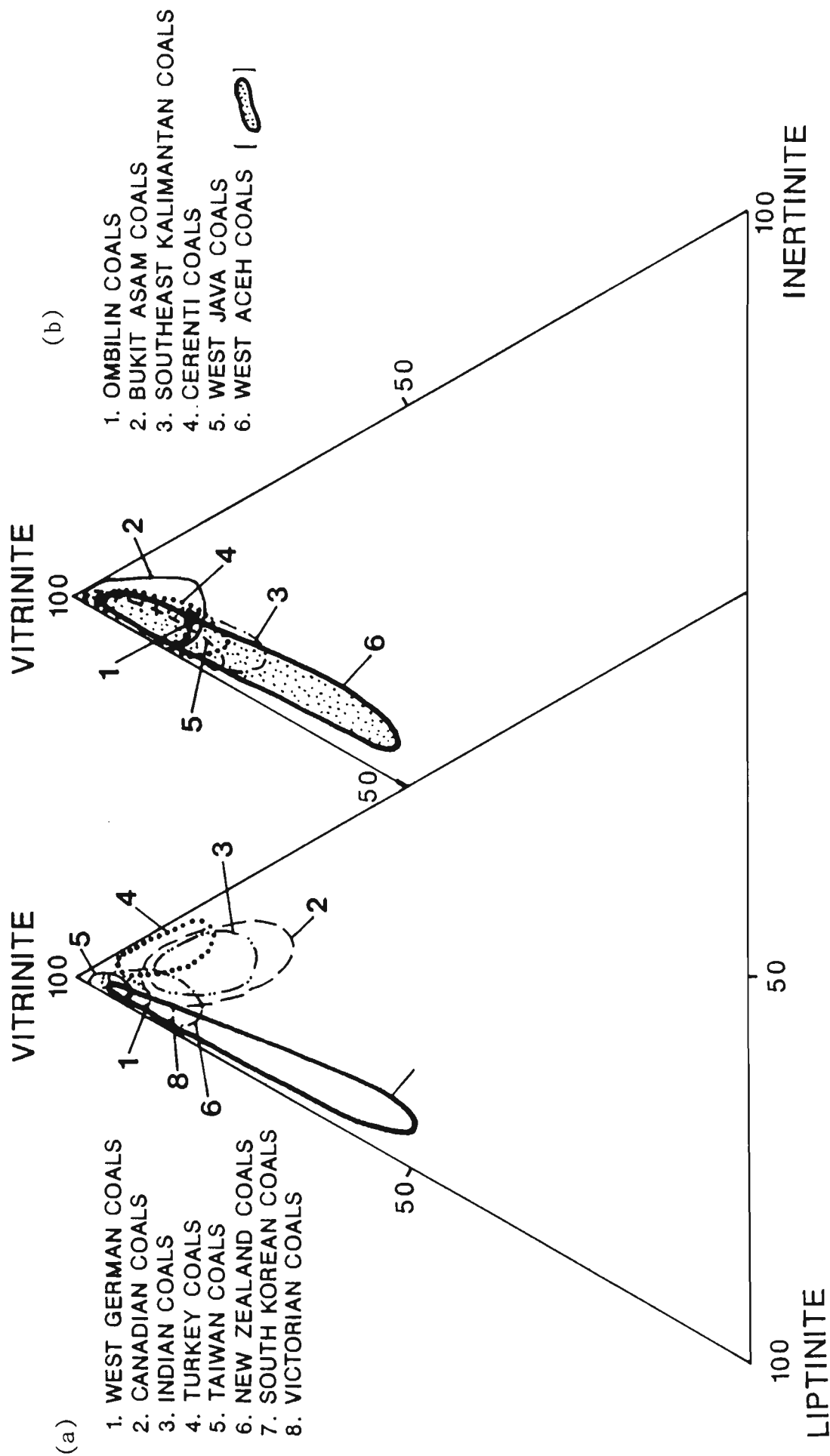


Figure 4.7: Triangular diagram showing maceral composition from several countries (a) and from some Tertiary Indonesia basin (b).

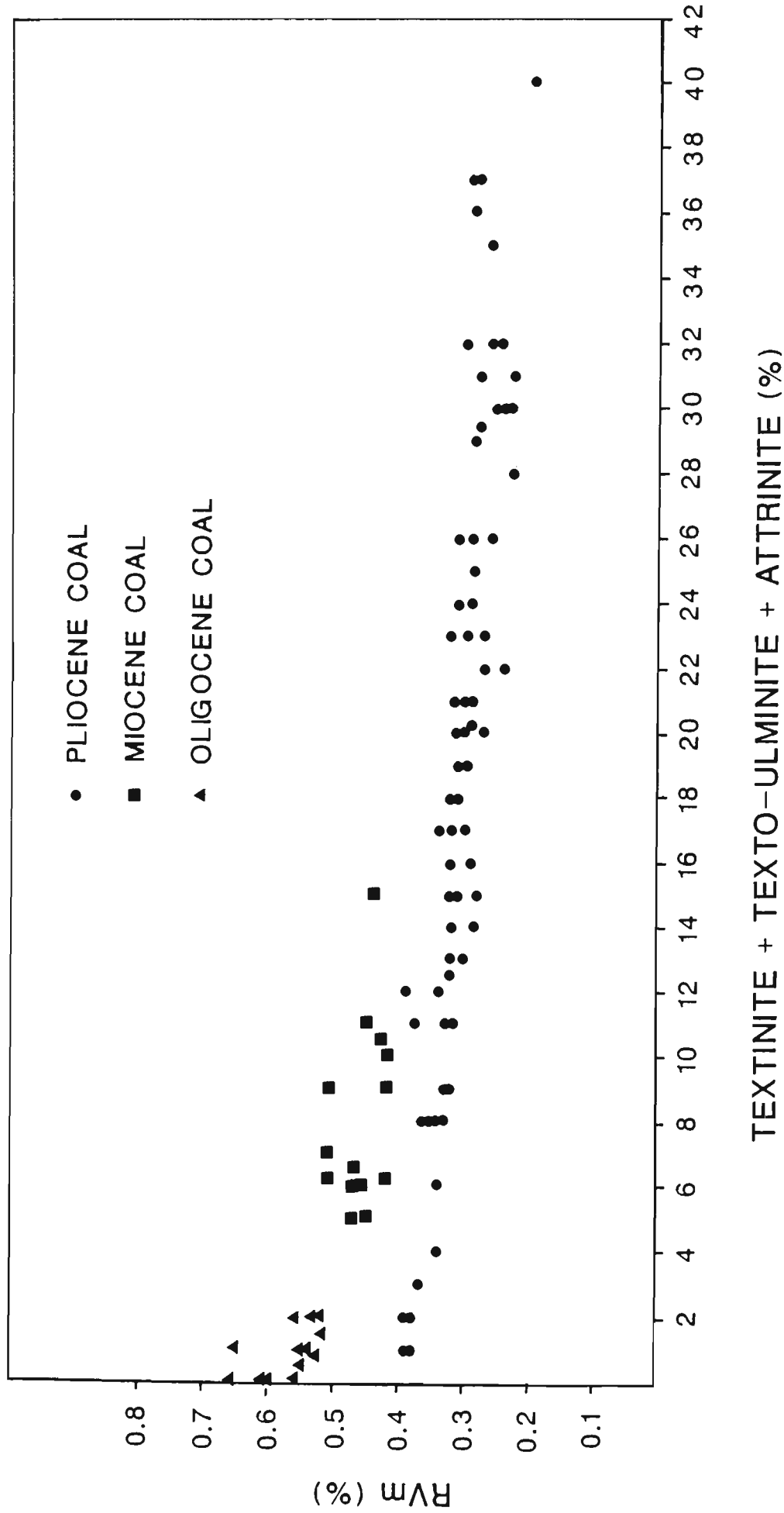
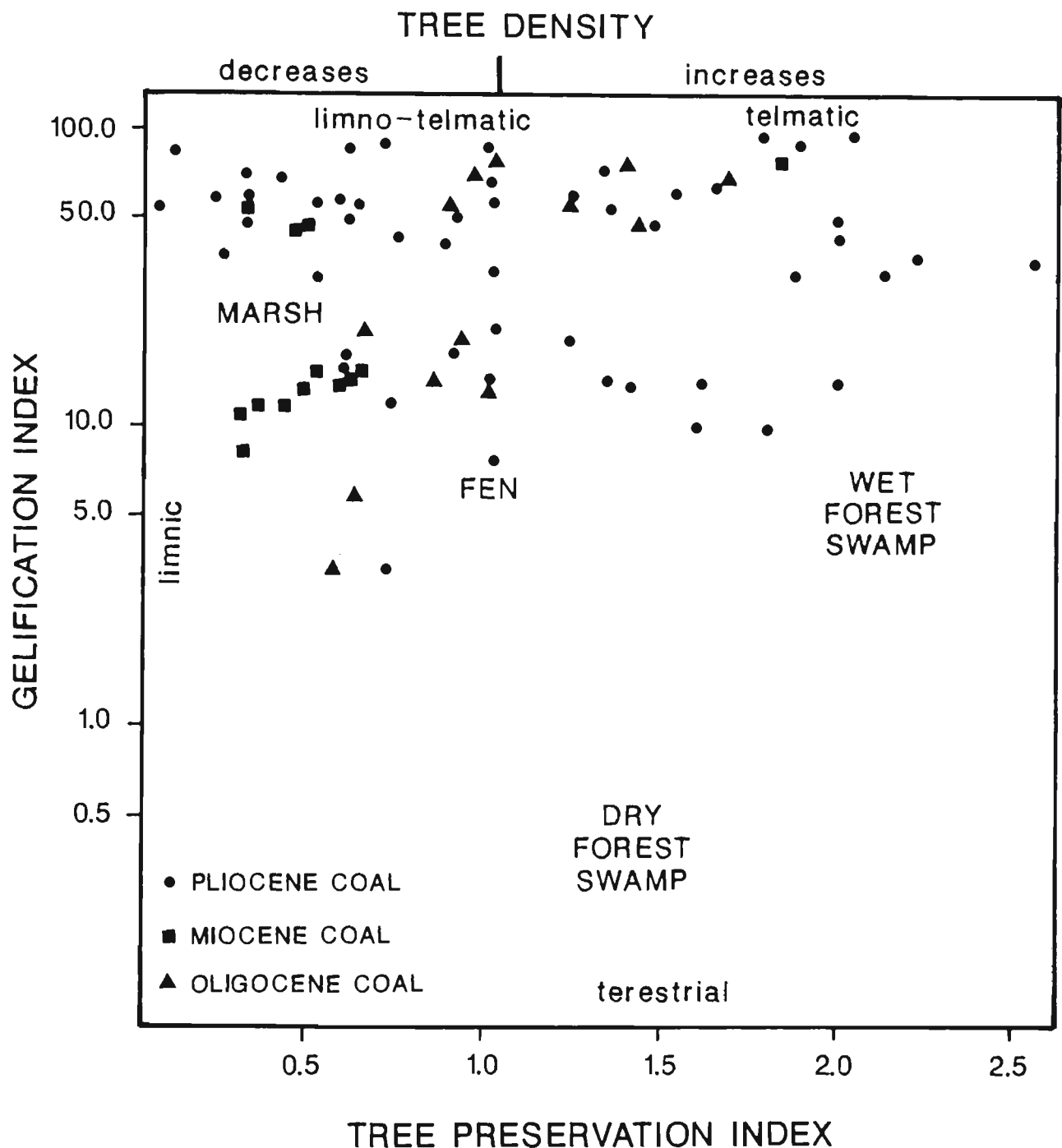


Figure 4.8: Relationship between detrovitrinite macerals and vitrinite reflectance of the Tertiary coals in West Aceh Basin.



$$GI = \frac{\text{vitrinite} + \text{macrinite}}{\text{semifusinite} + \text{fusinite} + \text{inertodetrinite}}$$

$$TPI = \frac{\text{telovitrinite} + \text{semifusinite} + \text{fusinite}}{\text{desmocollinite} + \text{macrinite} + \text{inertodetrinite}}$$

Figure 4.9: Coal facies diagram for the Tertiary coal of West Aceh Basin (after Diessel, 1986).

TABLE 4.1. COAL MACERAL CLASSIFICATION ( AS 2856, 1986 )

Please see print copy for image

Table 4.2. Summary of the microscopic features of exsudatinite and bitumen in coal

MICROSCOPIC FEATURES	EXSUDATINITE	BITUMEN
Morphology and occurrence	Filling cleats and cracks, commonly perpendicular to the bedding plane.	Globular, rounded, oval, cauliflower shaped or irregular bodies, also as cavity and crack fillings, discordant to the bedding plane.
Relief	Low to moderate, commonly equal to vitrinite.	Moderate to high, commonly higher than vitrinite.
Common association	Filling cracks or cleat in telocollinite; some associated with desmocollinite, resinite and cutinite.	Associated with the desmocollinite, densinite, porigellinite and porous sandstone or carbonate rocks; also associated with resinite; most forms show shrinkage cracks and vesicles.
Reflected colours	Transparent to grey	Grey to brown
Fluorescence colours	Moderate to high fluorescence intensity ranging from greenish-yellow to orange.	Low to moderate fluorescence intensity ranging from brownish-yellow to yellow.
Reflectance	0.05% - 0.1%	0.2% - 0.08%

Table 4.3. Calculated average maceral composition of Tertiary Coals in the West Aceh Basin

MACERAL	PLIOCENE COAL		MIOCENE COAL		OLIGOCENE COAL	
	AVERAGE (%)	RANGE (%)	AVERAGE (%)	RANGE (%)	AVERAGE (%)	RANGE (%)
Textinite	0.9	0.0 - 2.8	0.0	0.0	0.0	0.0
Texto-ulminite	6.7	0.0 - 18.4	0.1	0.0 - 0.6	<0.1	0.0 - 0.1
Eu-ulminite	8.4	0.0 - 30.0	2.9	1.5 - 12.0	0.7	0.0 - 1.5
Telocollinite	11.0	0.5 - 35.0	12.0	3.0 - 28.0	27.3	9.0 - 52.0
Attrinite	11.8	1.0 - 26.0	8.5	1.0 - 17.0	0.9	0.0 - 2.0
Densinite	11.1	0.6 - 35.0	14.8	8.0 - 21.0	12.6	3.1 - 24.0
Desmocollinite	14.1	2.0 - 22.6	29.6	20.0 - 40.0	31.5	21.0 - 42.5
Corpogelinite	5.6	0.0 - 20.0	6.5	0.0 - 20.0	3.8	0.0 - 8.5
Porigelinite	0.9	0.0 - 3.1	0.2	0.0 - 1.0	0.6	0.0 - 2.5
Eugelinite	0.1	0.0 - 1.0	<0.1	0.0 - 0.6	0.1	0.0 - 1.0
Total Vitrinite	71.0	43.6 - 91.5	75.4	60.0 - 98.0	77.7	64.0 - 92.2
Sporinite	1.1	0.0 - 4.2	1.3	0.0 - 3.7	1.5	0.4 - 3.3
Cutinite	7.5	0.8 - 24.0	4.7	0.4 - 18.1	4.6	1.0 - 9.8
Resinite	3.0	0.0 - 13.8	1.7	0.0 - 3.7	1.8	0.0 - 7.2
Liptodetrinite	4.5	0.0 - 14.3	3.9	0.0 - 6.0	3.9	0.0 - 9.8
Alginite	0.7	0.0 - 5.6	1.7	0.0 - 7.3	0.8	0.0 - 2.4
Suberinite	1.6	0.0 - 6.2	0.5	0.0 - 3.1	2.3	0.0 - 13.8
Fluorinite	0.8	0.0 - 4.9	0.9	0.0 - 2.6	0.2	0.0 - 1.8
Bituminite	0.0	0.0	0.0	0.0	0.0	0.0
Exsudatinite	1.2	0.0 - 4.1	2.0	0.0 - 18.0	2.0	0.0 - 9.0
Total Lipinite	20.4	6.6 - 50.0	16.7	2.0 - 29.0	17.1	5.7 - 26.1
Fusinite	<0.1	0.4 - 1.7	0.7	0.0 - 2.3	0.1	0.0 - 2.0
Semifusinite	1.3	0.0 - 5.0	2.8	0.0 - 14.7	2.6	0.0 - 10.8
Sclerotinite	0.8	0.0 - 4.3	1.5	0.0 - 3.0	1.2	0.0 - 4.0
Inertodetrinite	0.6	0.0 - 4.0	1.5	0.0 - 4.1	0.5	0.0 - 2.6
Micrinite	<0.1	0.0 - 0.9	0.1	0.0 - 1.8	0.0	0.0
Macrinite	<0.1	0.0 - 0.8	0.3	0.0 - 1.0	0.1	0.0 - 0.6
Total Inertinite	2.8	0.0 - 11.0	6.7	0.0 - 22.0	5.9	0.4 - 24.0
Mineral Matter	3.6	0.0 - 19.5	0.7	0.0 - 2.0	0.3	0.0 - 1.6



Table 4.5. Average abundance and maceral group composition

in the Kueh Formation at off-shores wells of West Aceh Basin.

DOM				Shaly Coal				Coal						
Well name	N	Abundance		Composition (%)		Abundance		Composition (%)		Abundance		Composition (%)		
		Vol. (%)		V	L	I	Vol. (%)	V	L	I	Vol. (%)	V	L	I
TEUNOH	6	1.3		15.0	83.0	2.0	0.5	81.0	19.0	0.0	2.9	15.0	83.0	2.0
BUBON	14	4.3		44.0	55.0	1.0	1.1	75.0	24.0	1.0	11.4	74.0	20.0	6.0
KEUDAPSI	4	1.9		31.0	69.0	0.0	-	-	-	-	0.0	-	-	-
MEULABOH EAST	6	2.7		48.0	52.0	0.0	20.0	82.0	18.0	0.0	3.0	93.0	7.0	-
TUBA	4	1.3		37.0	63.0	0.0	-	-	-	-	0.2	37.0	55.0	8.0
MEULABOH	8	2.0		52.0	48.0	0.0	0.6	80.0	20.0	0.0	11.2	85.0	11.0	4.0
TRIPA	17	2.1		49.0	51.0	0.0	1.5	40.0	60.0	0.0	4.1	88.0	10.0	2.0
PALUHAT	3	0.3		22.0	78.0	0.0	0.0	-	-	-	0.0	-	-	-



Table 4.6. Average abundance and maceral group composition in the Tutut Formation at offshore wells of West Aceh Basin.

DOM			Shaly Coal						Coal				
Well name	N	Abundance	Composition (%)			Abundance	Composition (%)			Abundance	Composition (%)		
		Vol. %	V	L	I	Vol. %	V	L	I	Vol. %	V	L	I
TEUNOM	6	6.0	43.0	54.0	3.0	1.2	80.0	16.0	4.0	13.8	90.0	8.0	2.0
BUBON	8	2.1	40.0	58.0	2.0	1.5	90.0	10.0	0.0	9.9	73.0	12.0	5.0
KEUDAPSI	9	1.9	33.0	67.0	0.0	0.0	-	-	-	3.2	89.0	11.0	0.0
MEULABOH EAST	8	3.5	42.0	58.0	0.0	0.0	-	-	-	5.2	90.0	8.0	2.0
TUBA	4	5.8	62.0	38.0	0.0	0.5	85.0	15.0	0.0	2.0	86.0	14.0	0.0
MEULABOH	8	1.2	38.0	61.0	1.0	0.0	-	-	-	6.3	86.0	13.0	1.0
TRIPA	14	0.7	56.0	44.0	0.0	0.8	70.0	28.0	2.0	1.4	67.0	20.0	13.0
PALUHAT	8	2.5	33.0	66.0	0.0	0.0	-	-	-	4.7	80.0	13.0	7.0

TABLE 4.7. Classification of the natural solid oil bitumens ( Jacob,1989)

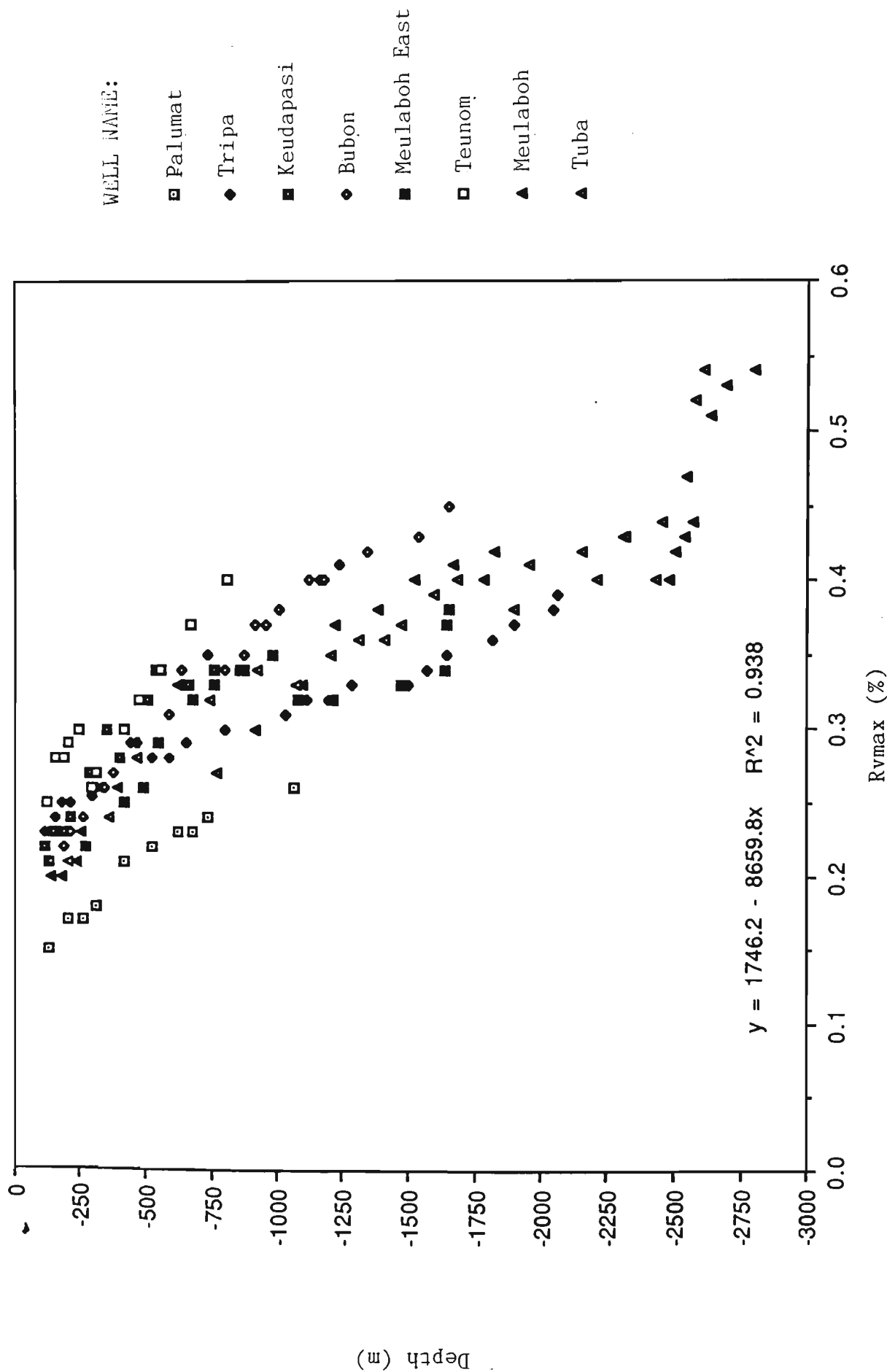


\* Anthraxolite as a synonym in part (e.g. Tomkeieff, 1954).

## FIGURES AND TABLES OF CHAPTER 5

Please see print copy for image

**Figure 5.1:** Maturation indicators and hydrocarbon generation in relation to coal rank (Heroux et al., 1979).



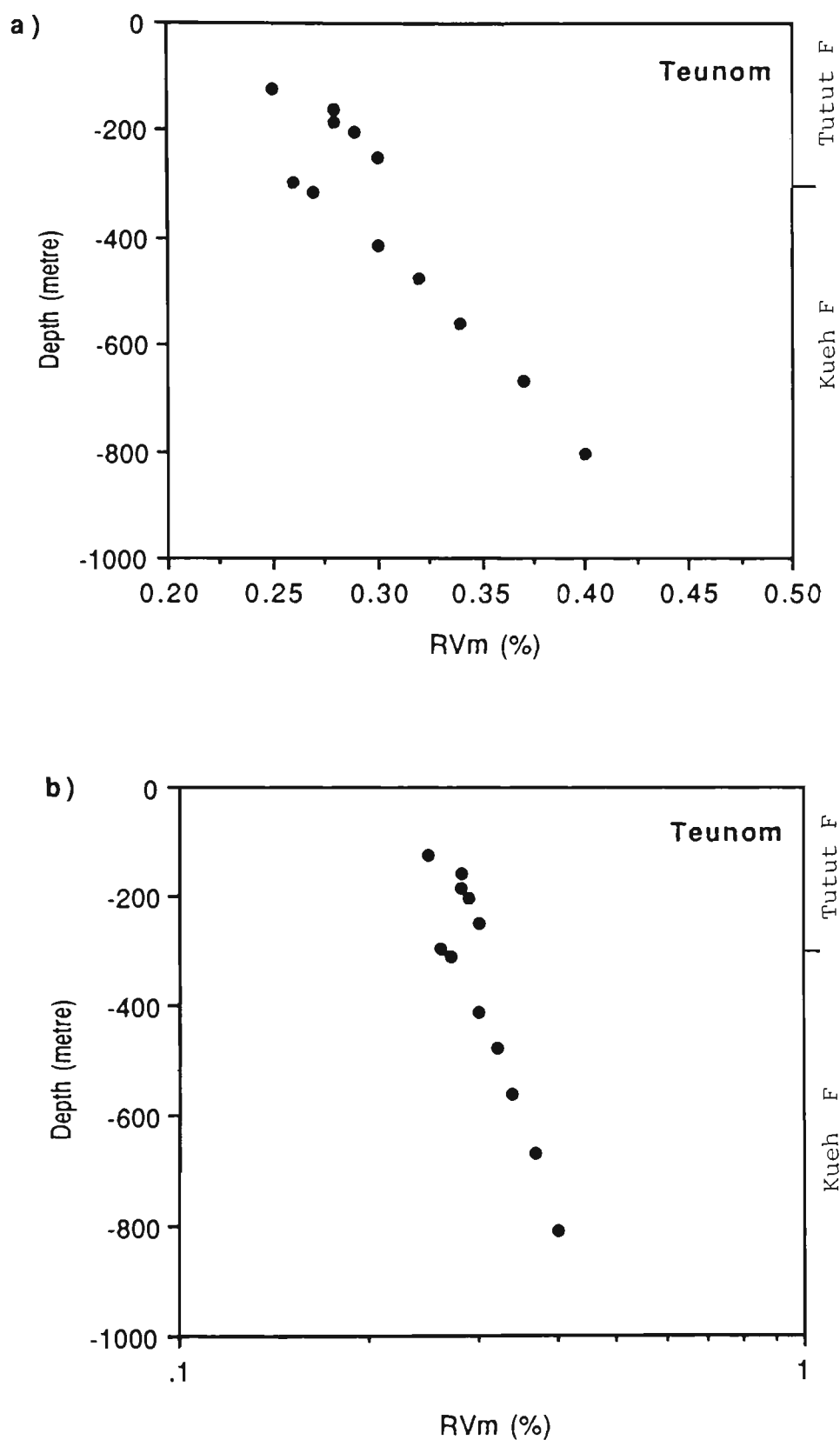


Figure 5.3: Maximum reflectance versus depth for Teunom well (a) linear plot; (b) semi-log plot.

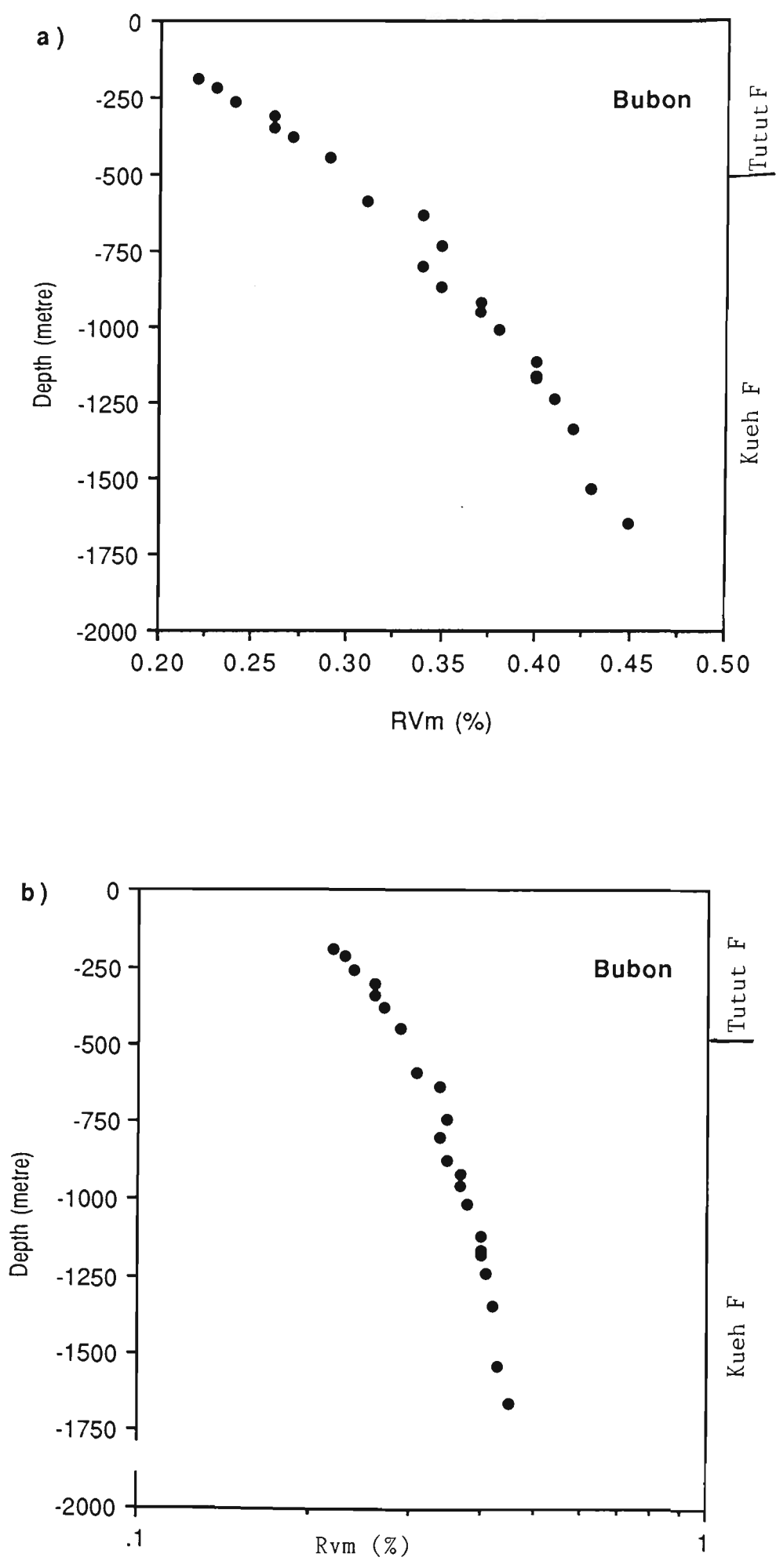


Figure 5.4: Maximum reflectance versus depth for Bubon well (a) linear plot; (b) semi-log plot.

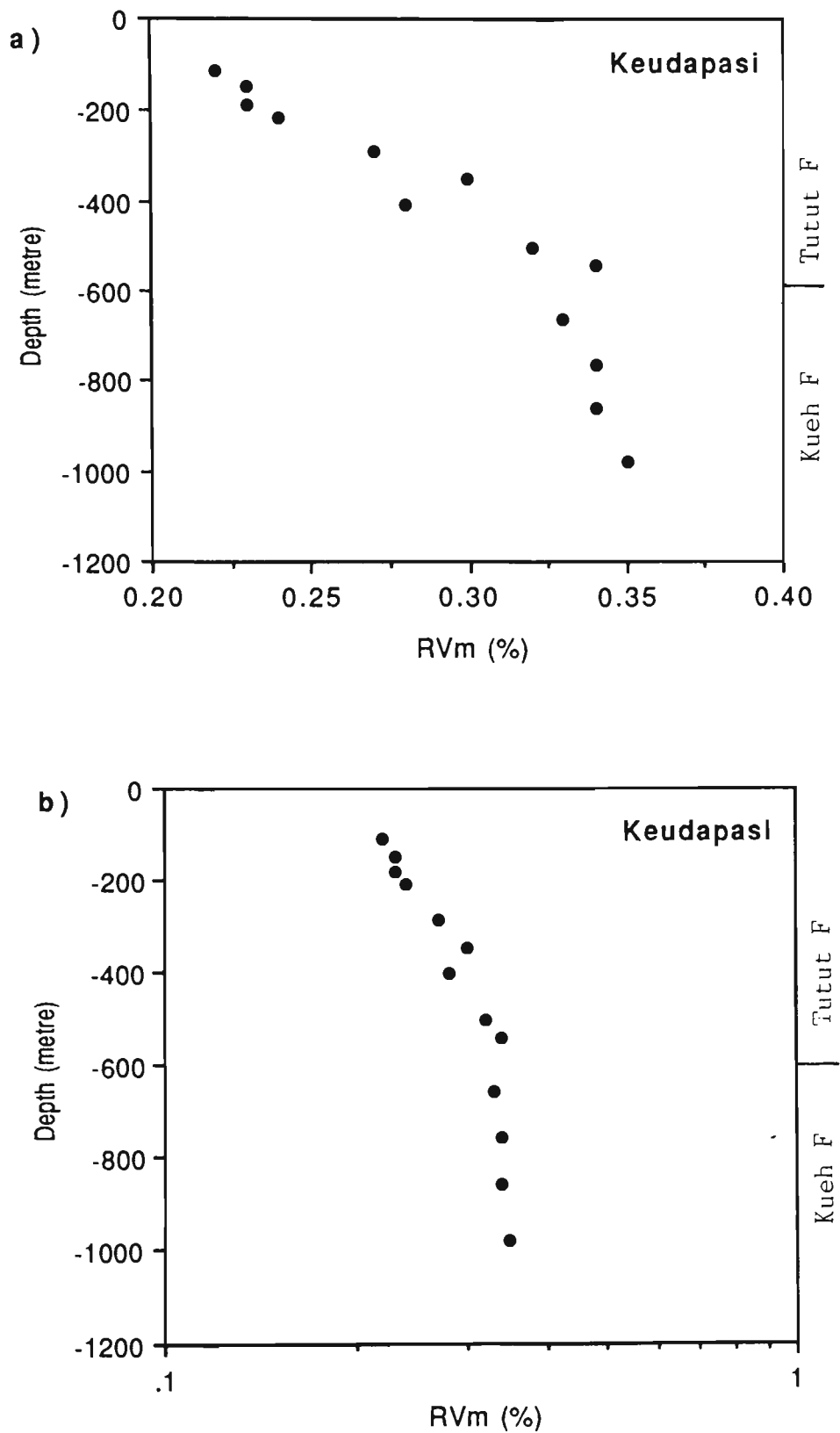


Figure 5.5: Maximum reflectance versus depth for Keudapasi well (a) linear plot; (b) semi-log plot.



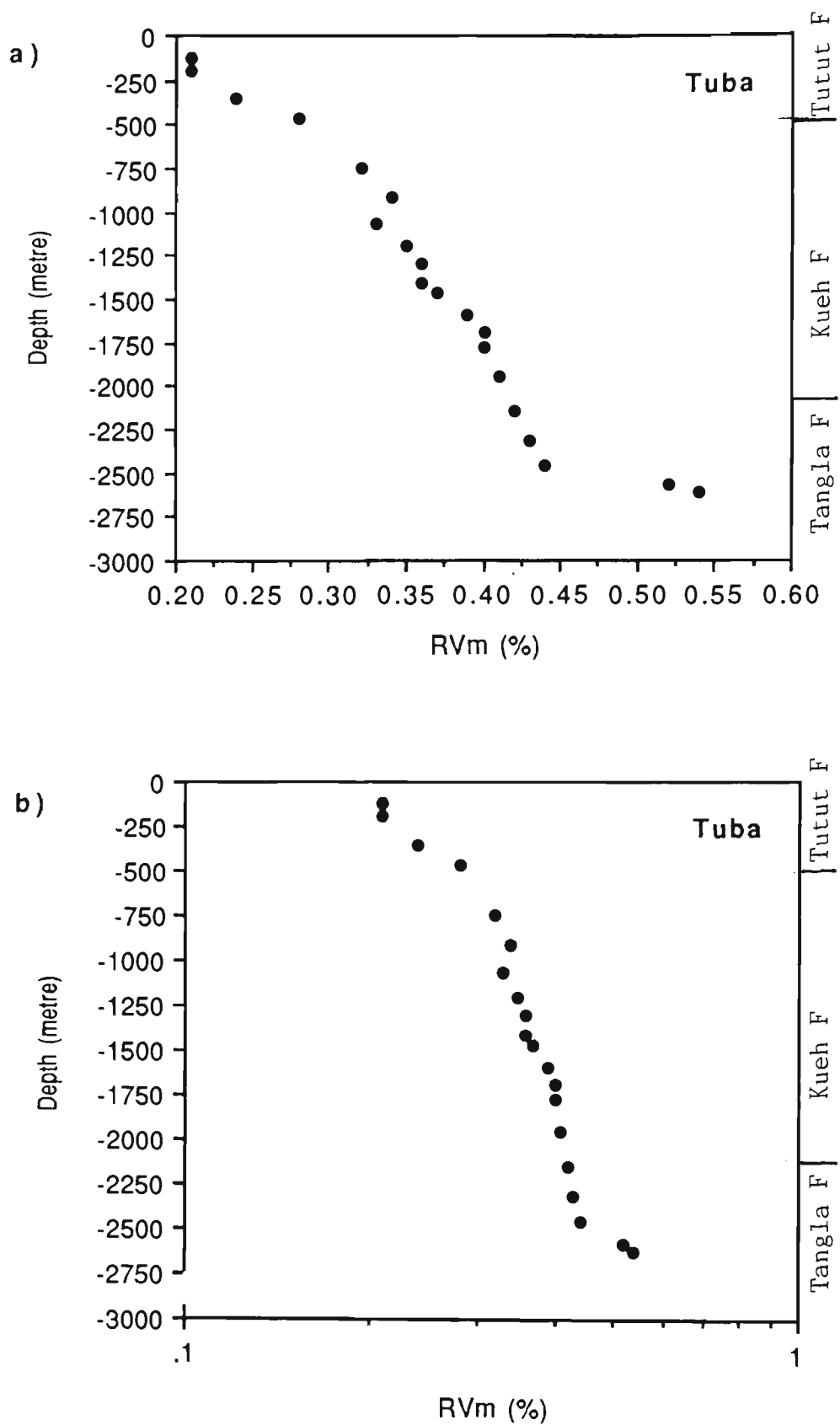


Figure 5.6: Maximum reflectance versus depth for Tuba well (a) linear plot; (b) semi-log plot.

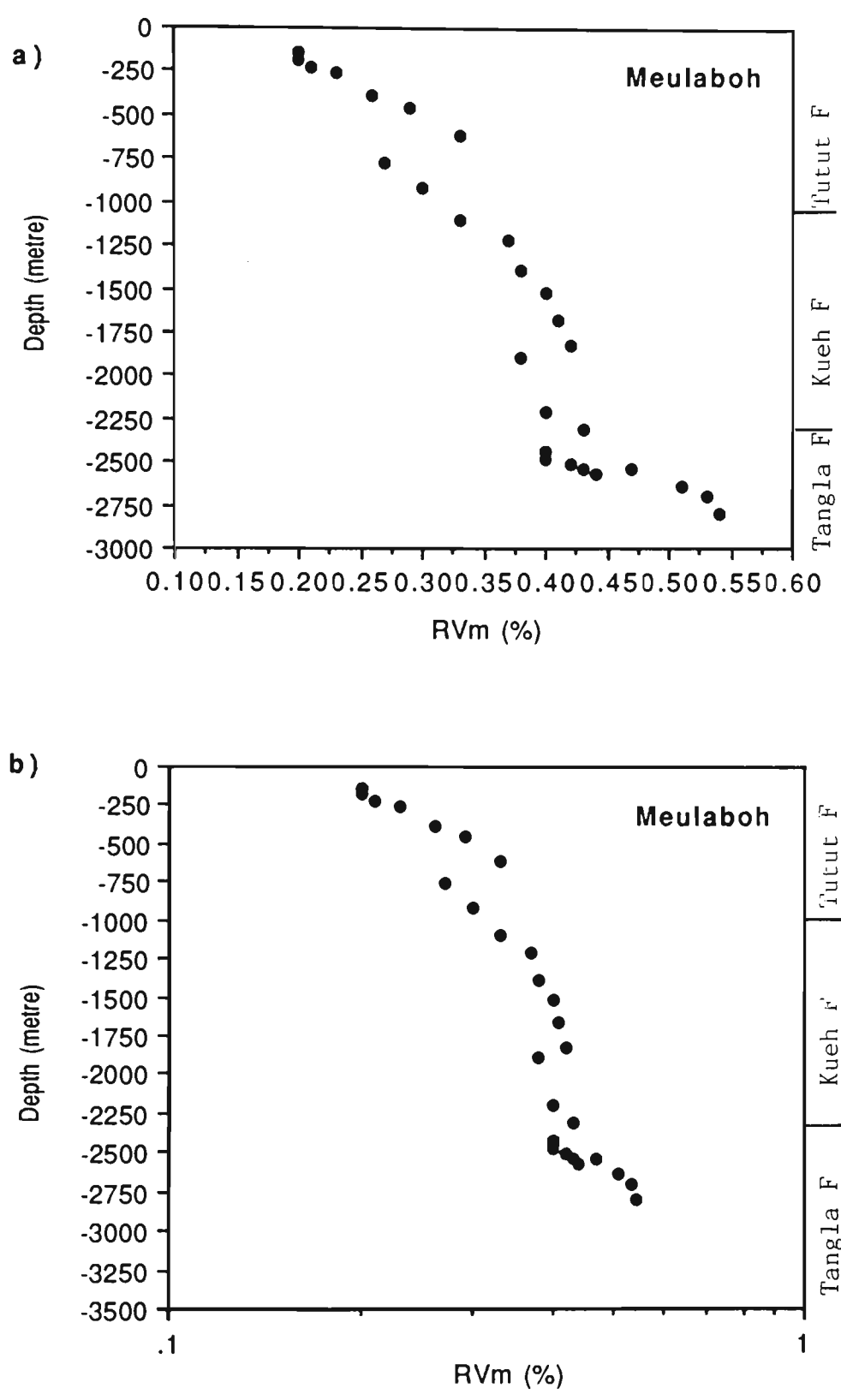


Figure 5.7: Maximum reflectance versus depth for Meulaboh well (a) linear plot ; (b) semi-log plot.

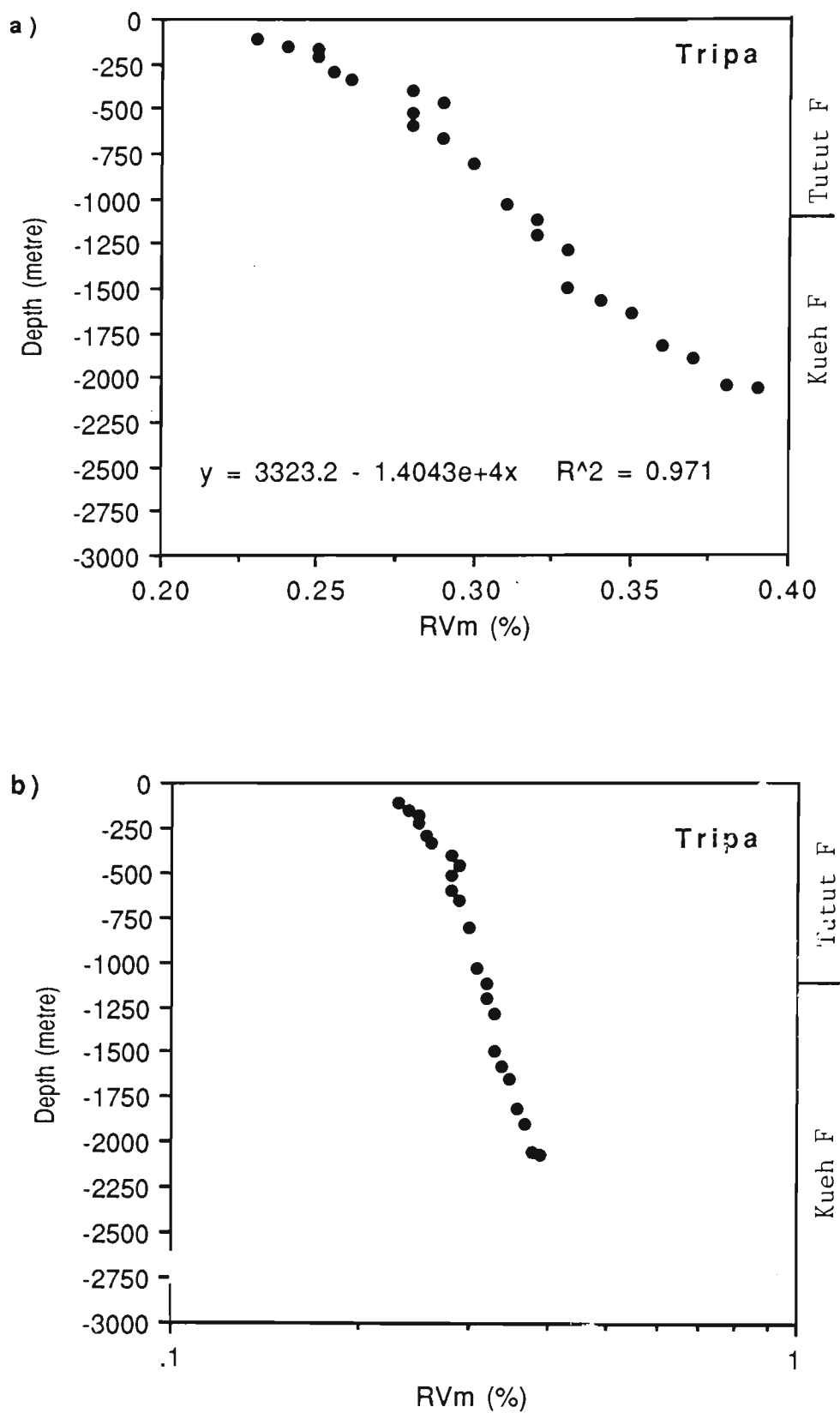


Figure 5.8: Maximum reflectance versus depth for Tripa well (a) linear plot; (b) semi-log plot.

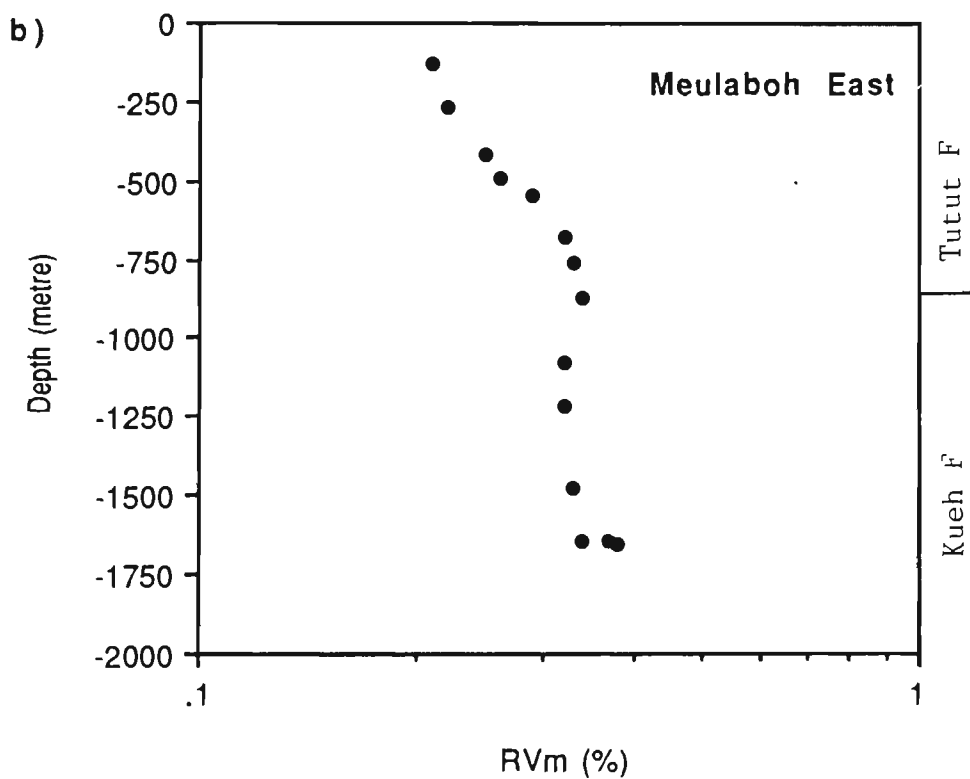
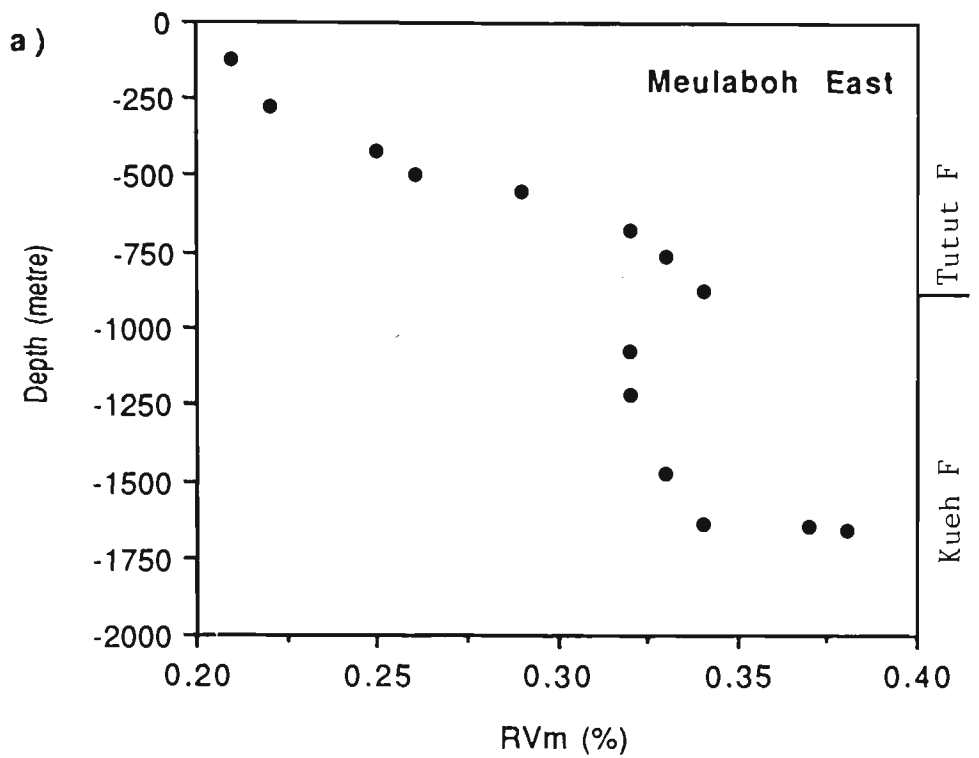


Figure 5.9: Maximum reflectance versus depth for Meulaboh East well (a) linear plot; (b) semi-log plot.

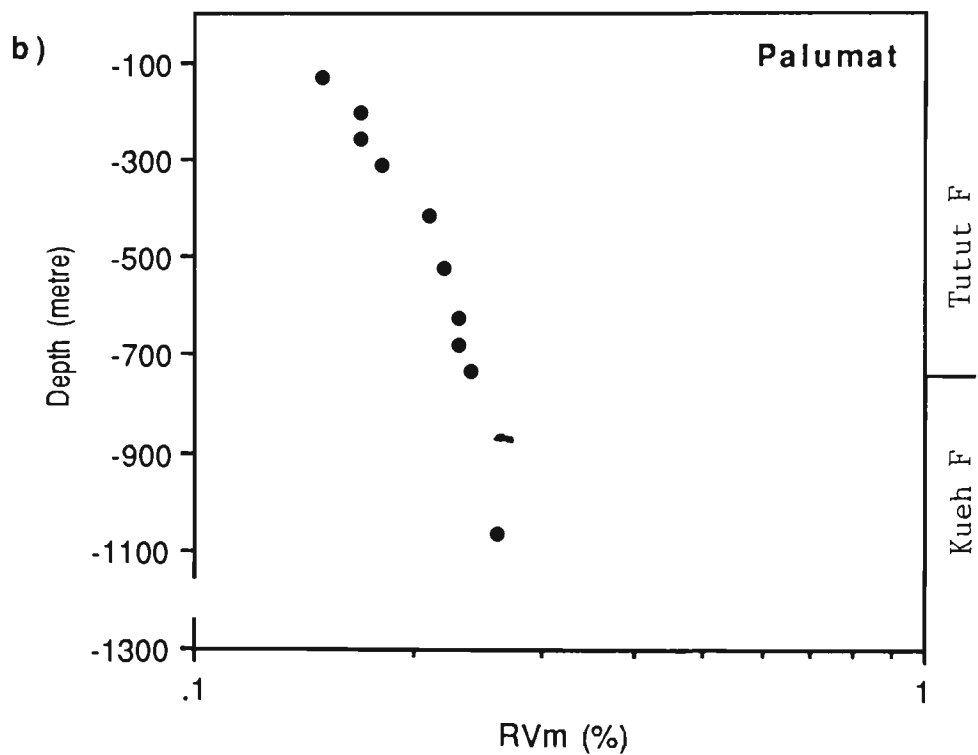
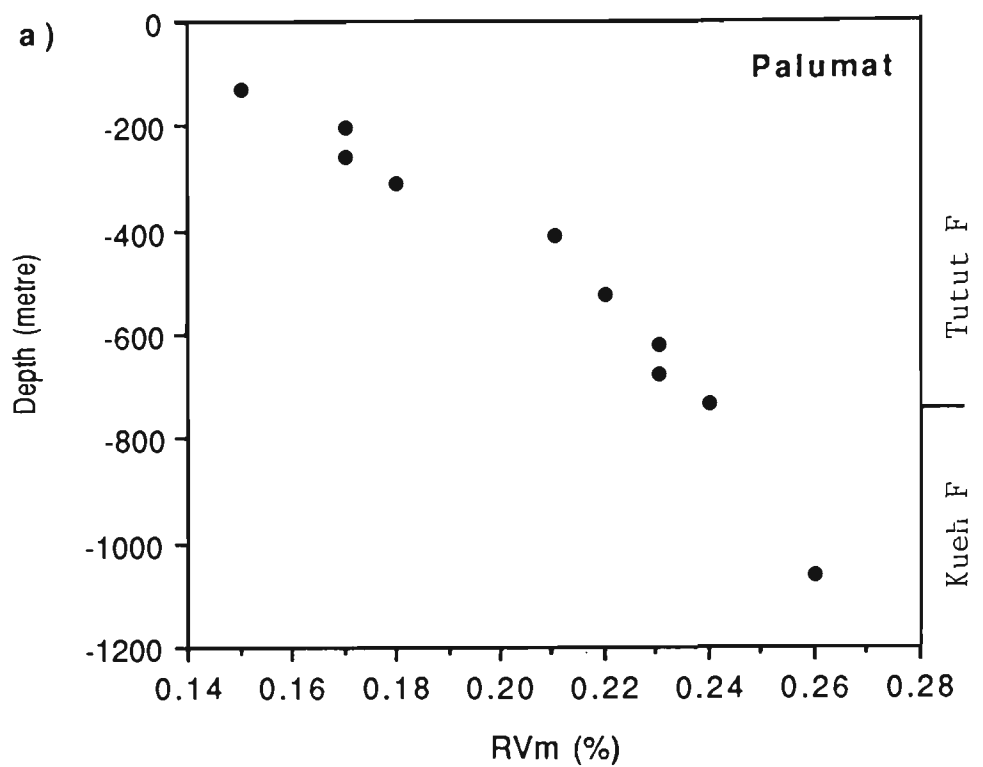


Figure 5.10: Maximum reflectance versus depth for Palumat well (a) linear plot; (b) semi-log plot.

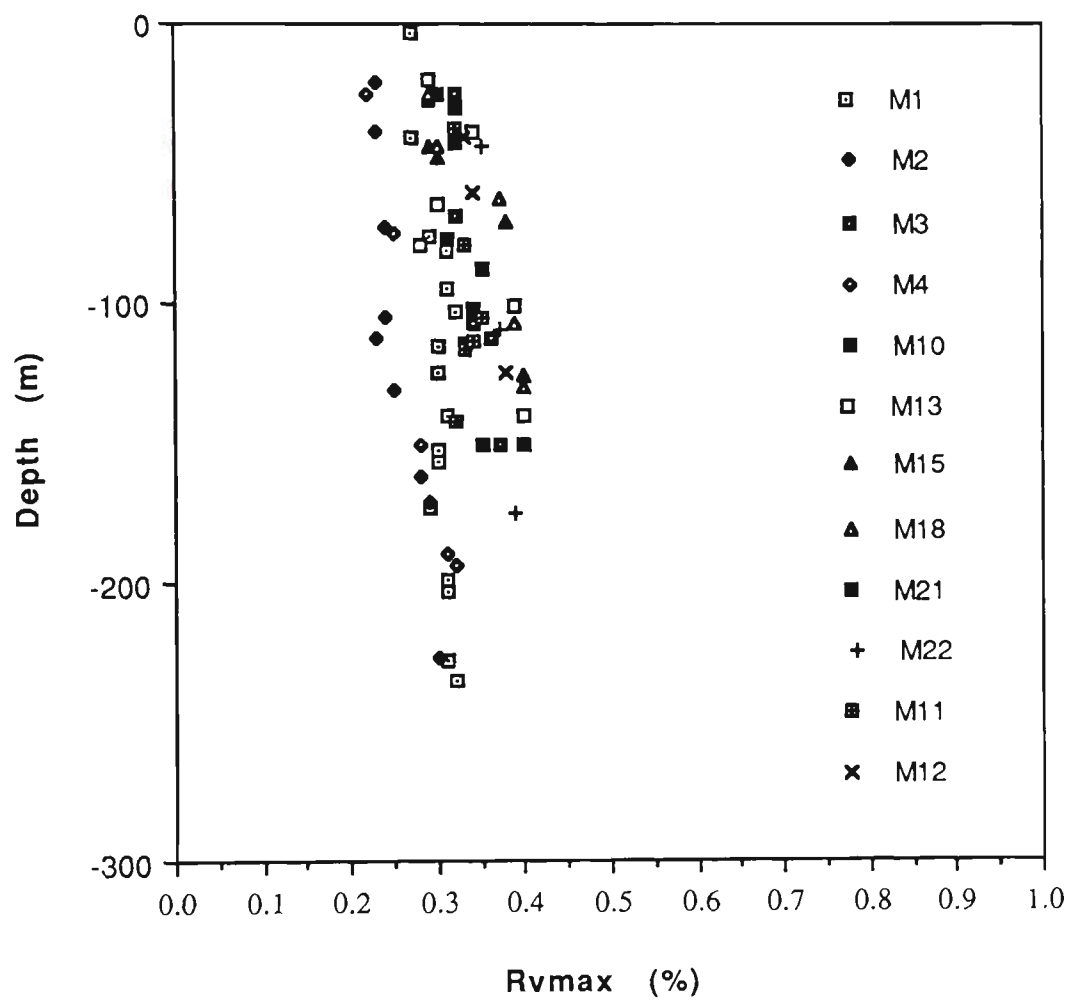


Figure 5.11: Maximum vitrinite reflectance versus depth for onshore wells.

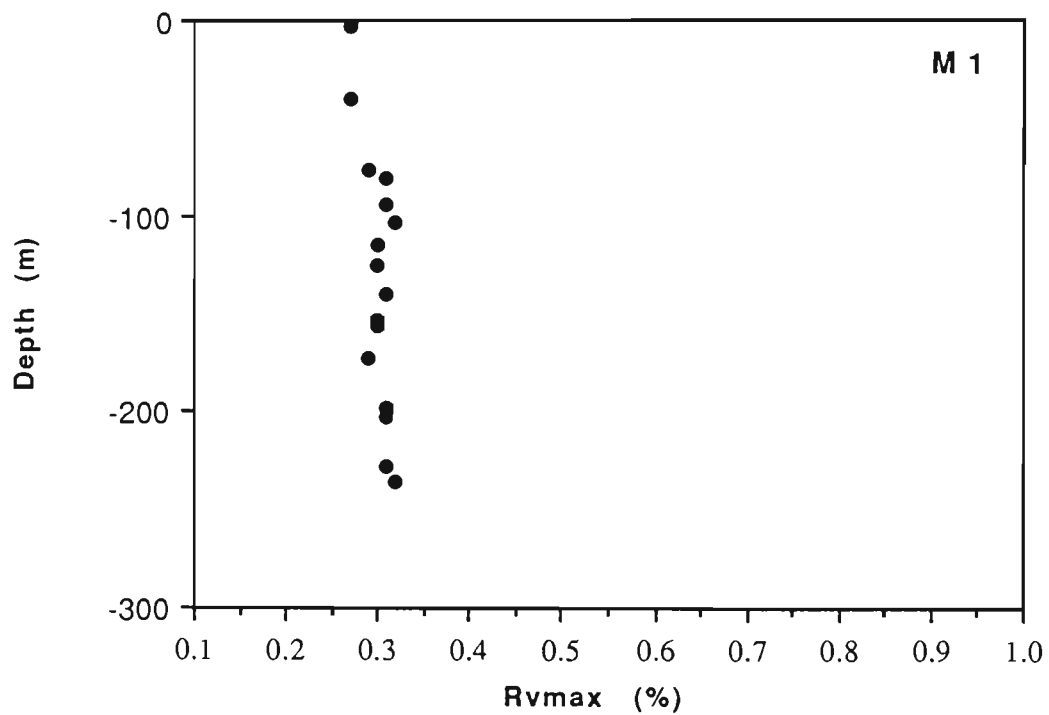
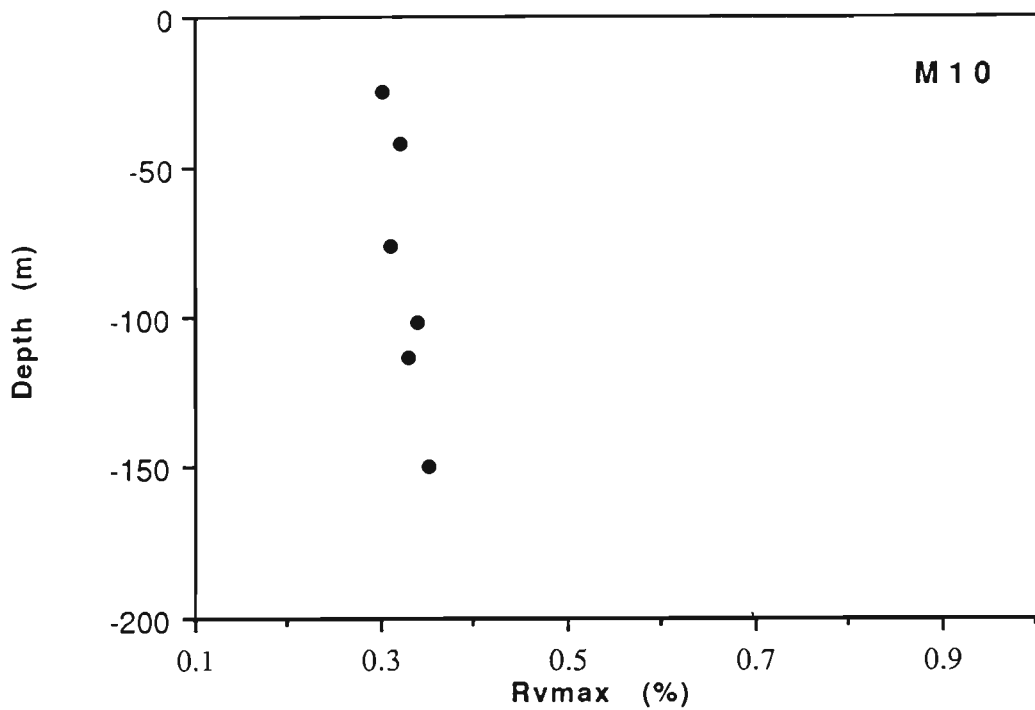


Figure 5.12: Maximum vitrinite reflectance versus depth for M10 and M1 wells.

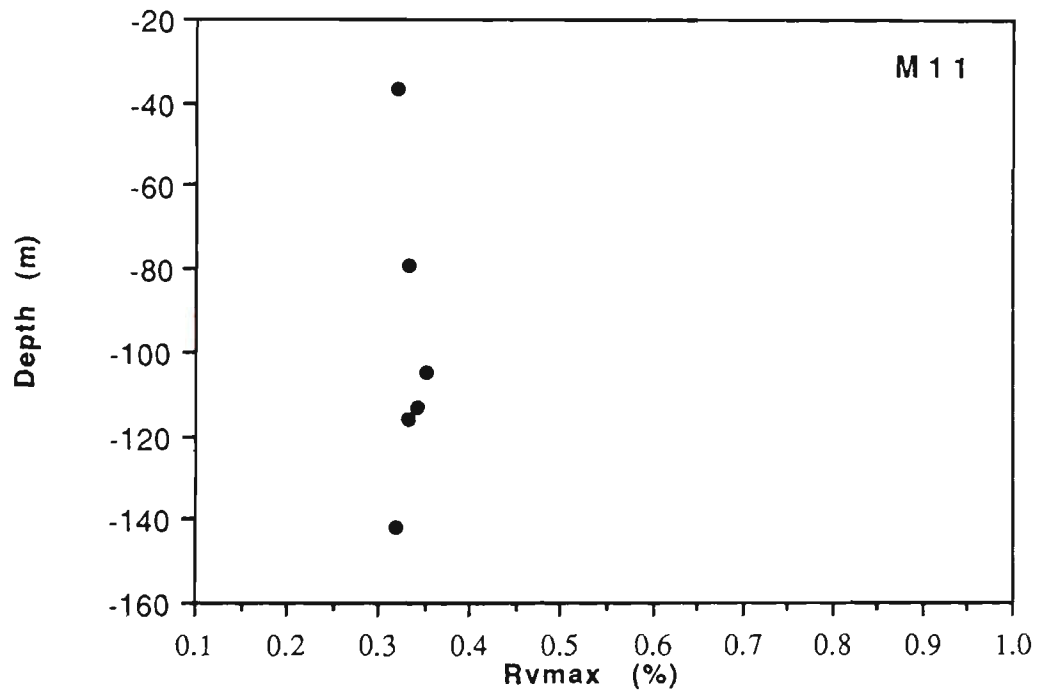
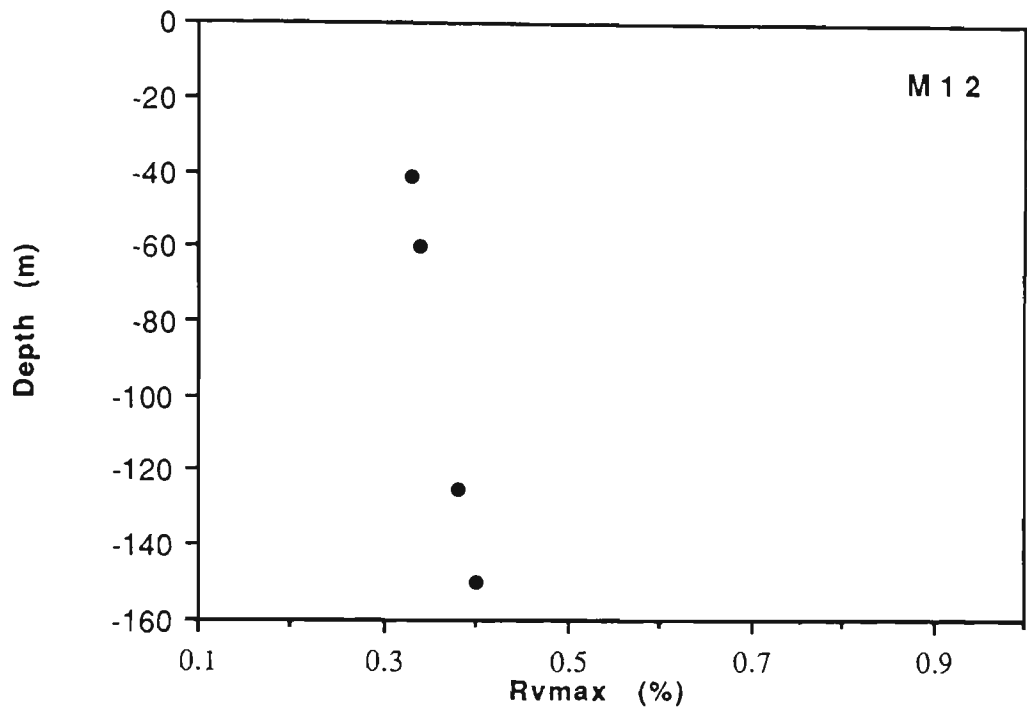


Figure 5.13: Maximum vitrinite reflectance versus depth for M12 and M11 wells.



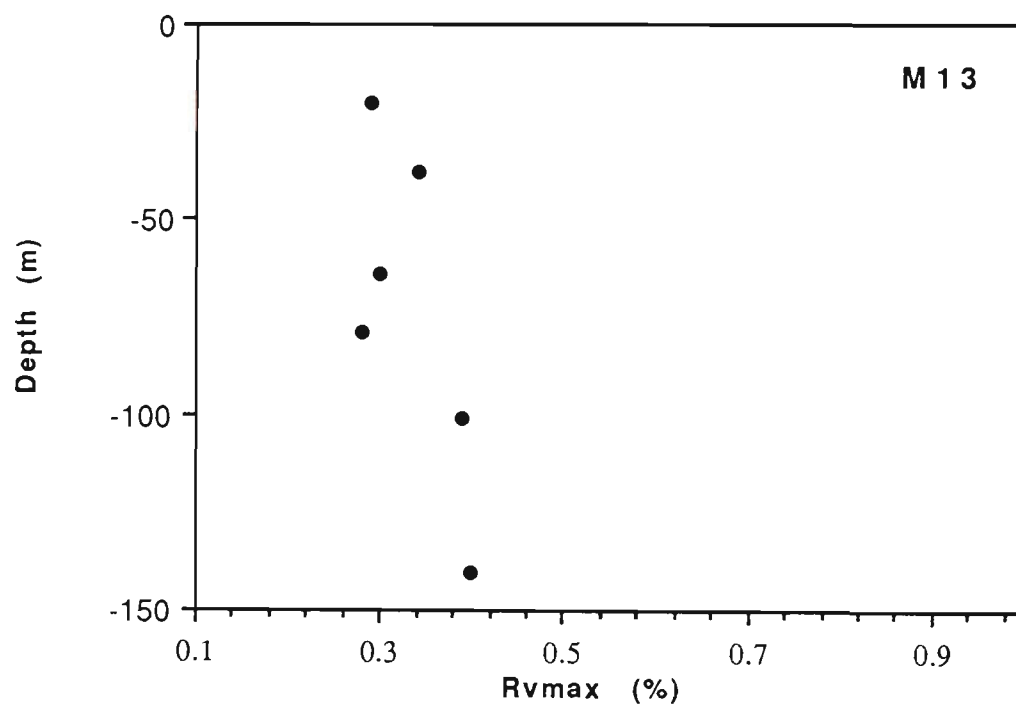
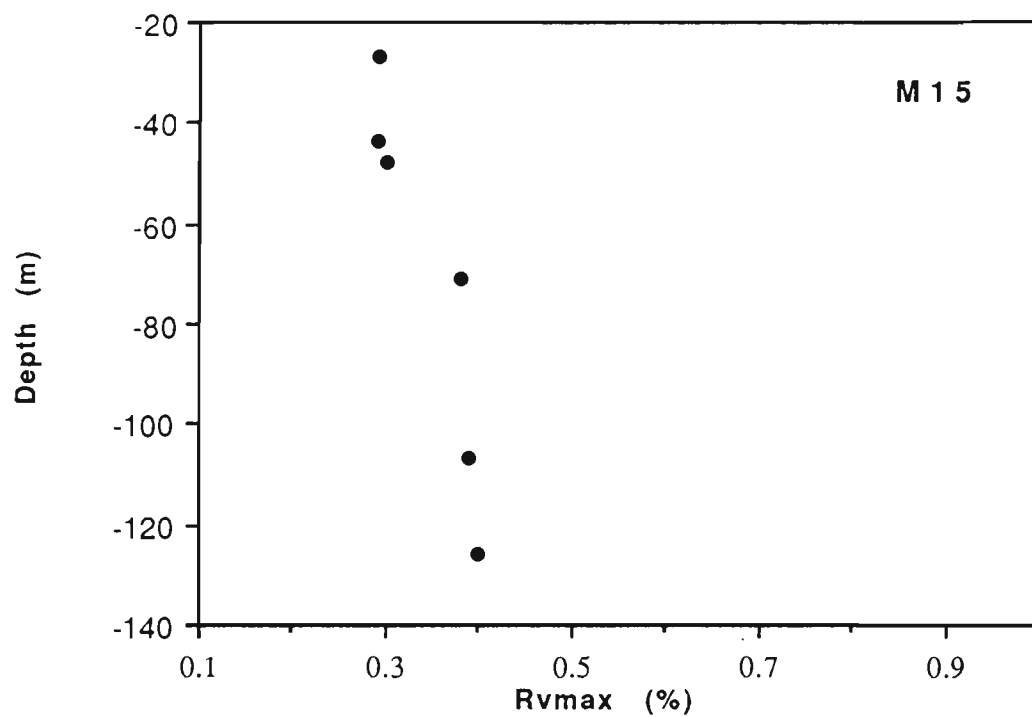


Figure 5.14: Maximum vitrinite reflectance versus depth for M15 and M13 wells.

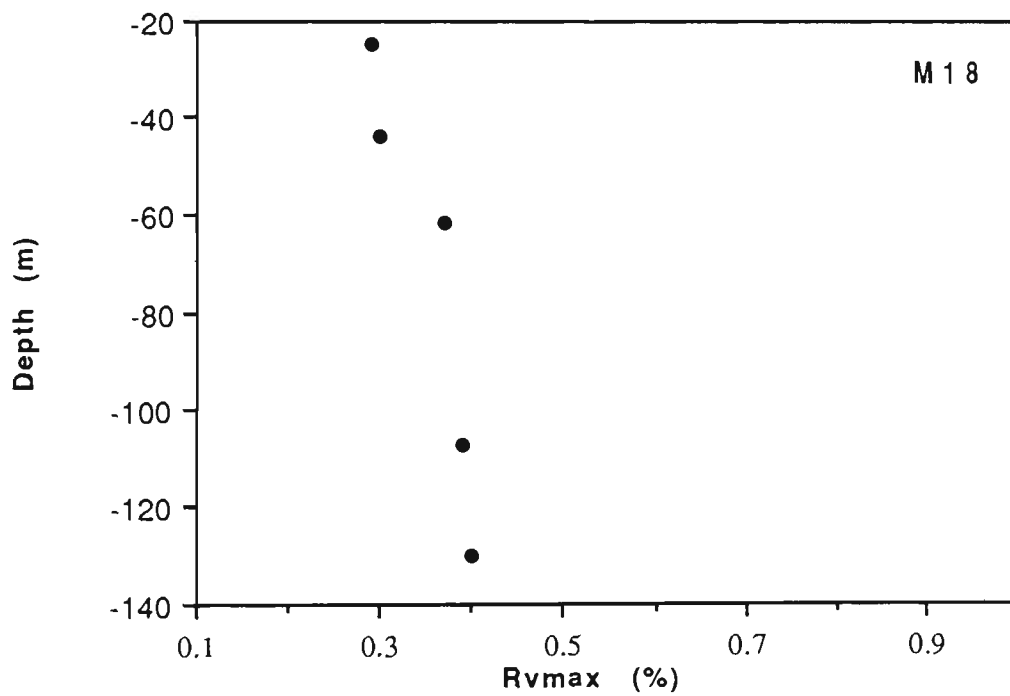
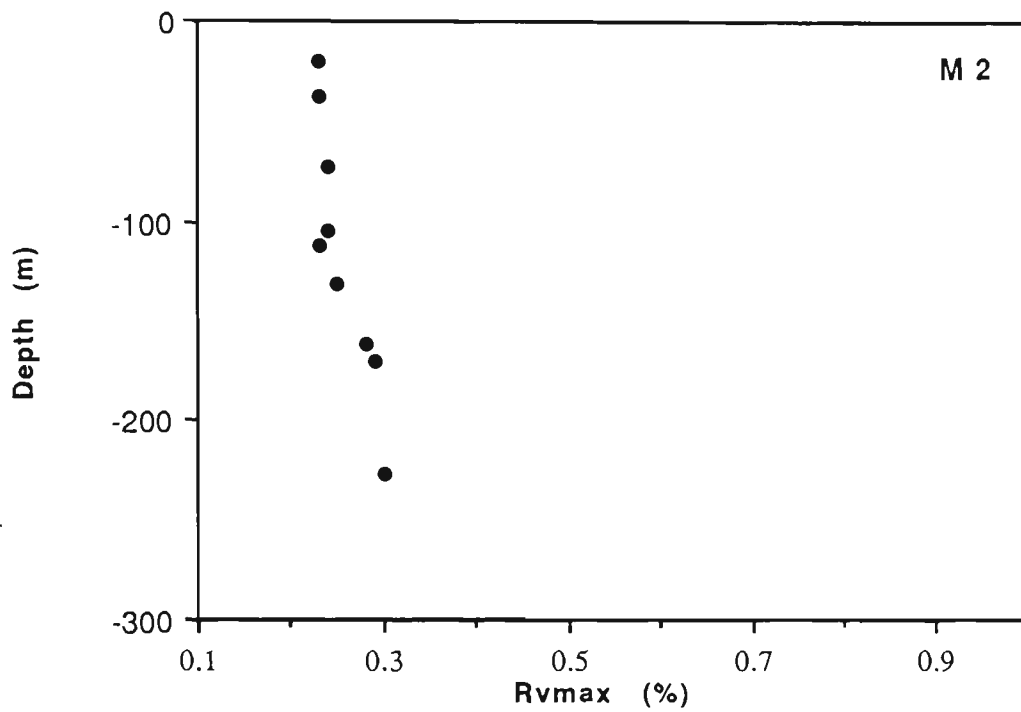


Figure 5.15: Maximum vitrinite reflectance versus depth for M2 and M18 wells.

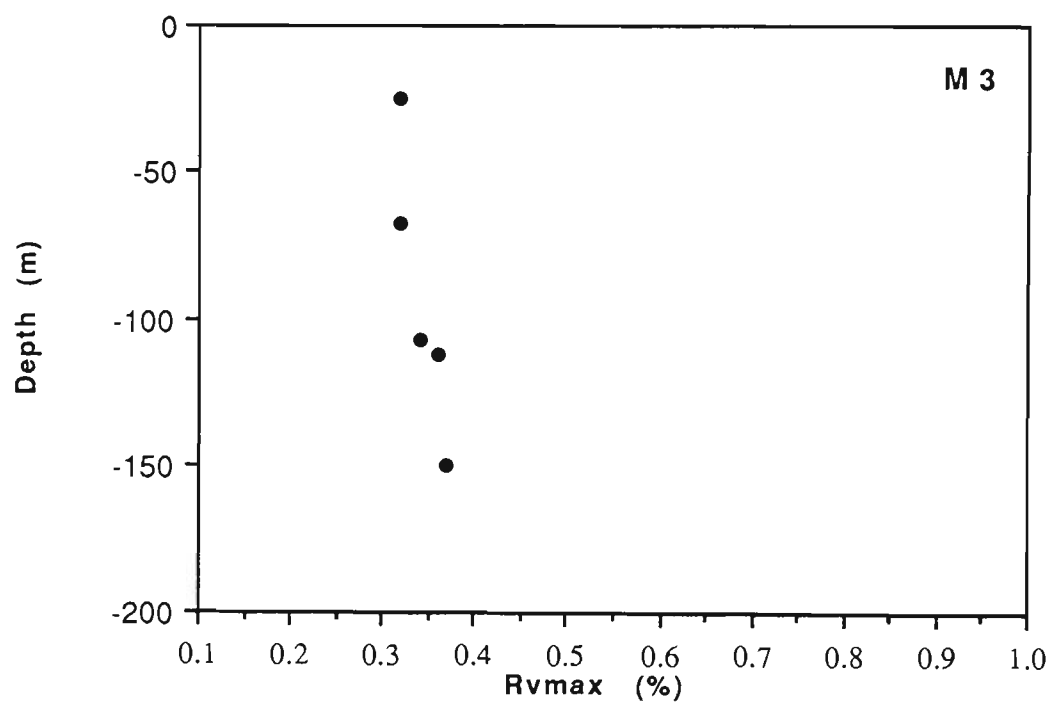
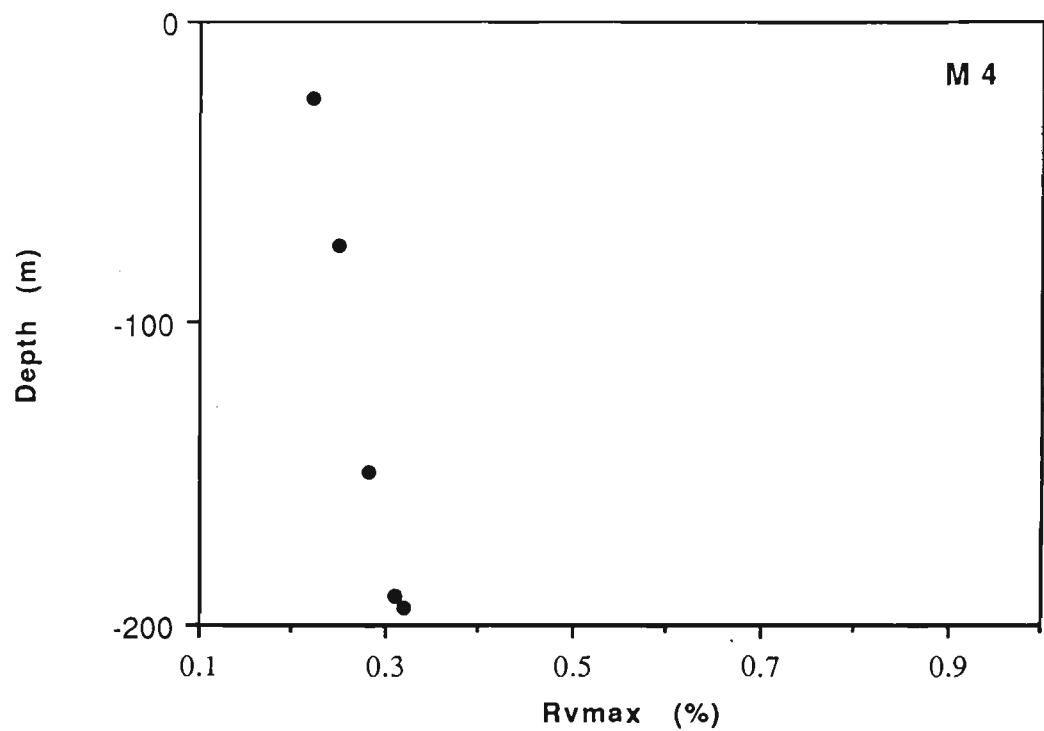


Figure 5.16: Maximum vitrinite reflectance versus depth for M4 and M3 wells.

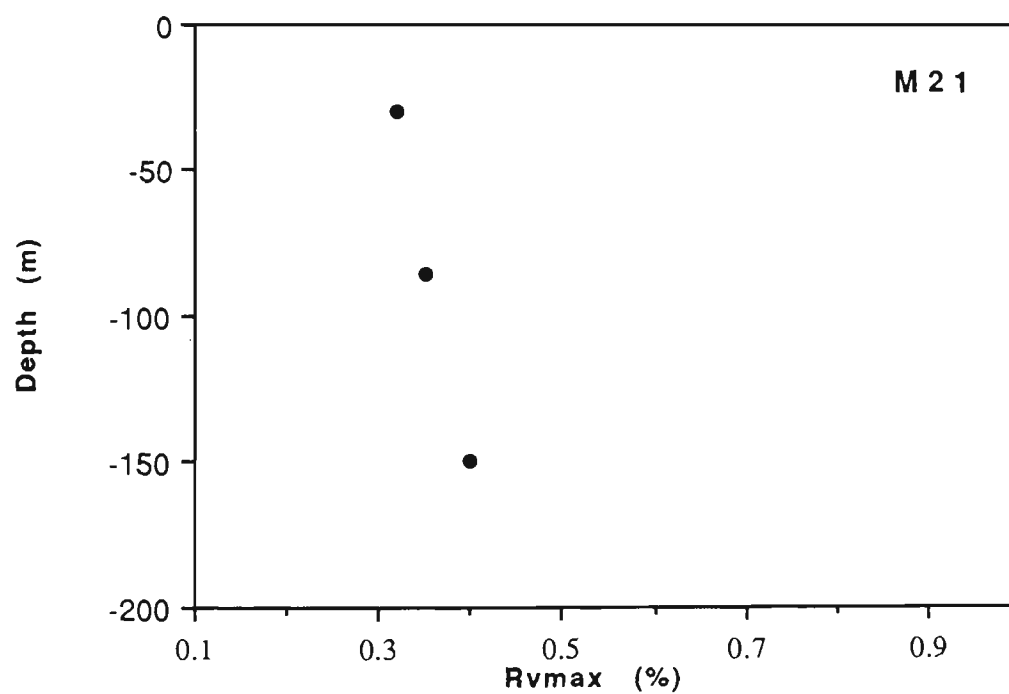
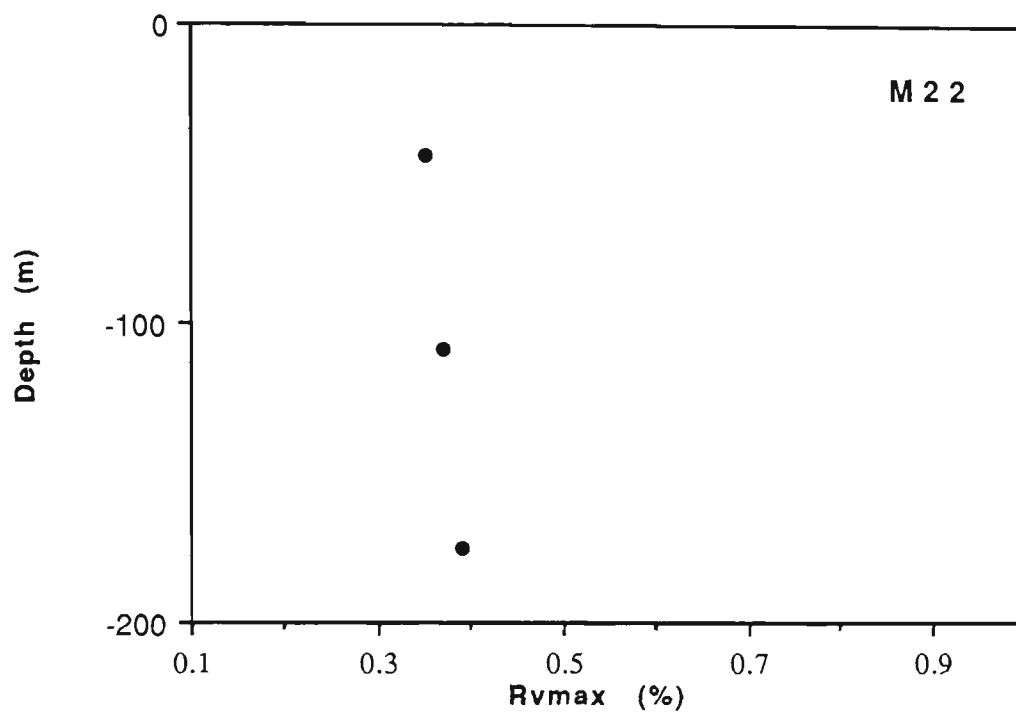


Figure 5.17: Maximum vitrinite reflectance versus depth for M22 and M21 wells.

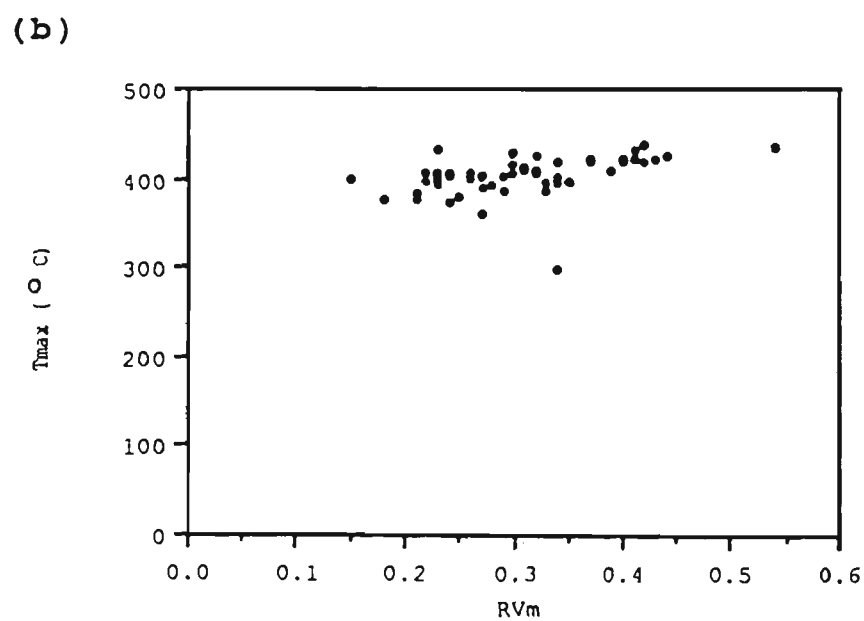
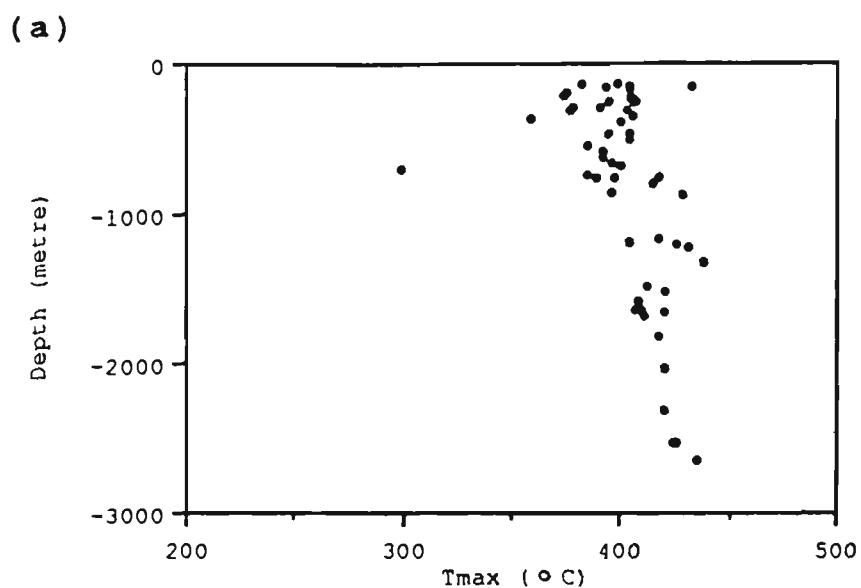


Figure 5.18: Depth versus Tmax (a) and Tmax versus maximum vitrinite reflectance (b) for offshore wells.

Please see print copy for image

Figure 5.19. Isoreflectance contour map of West Aceh Onshore area

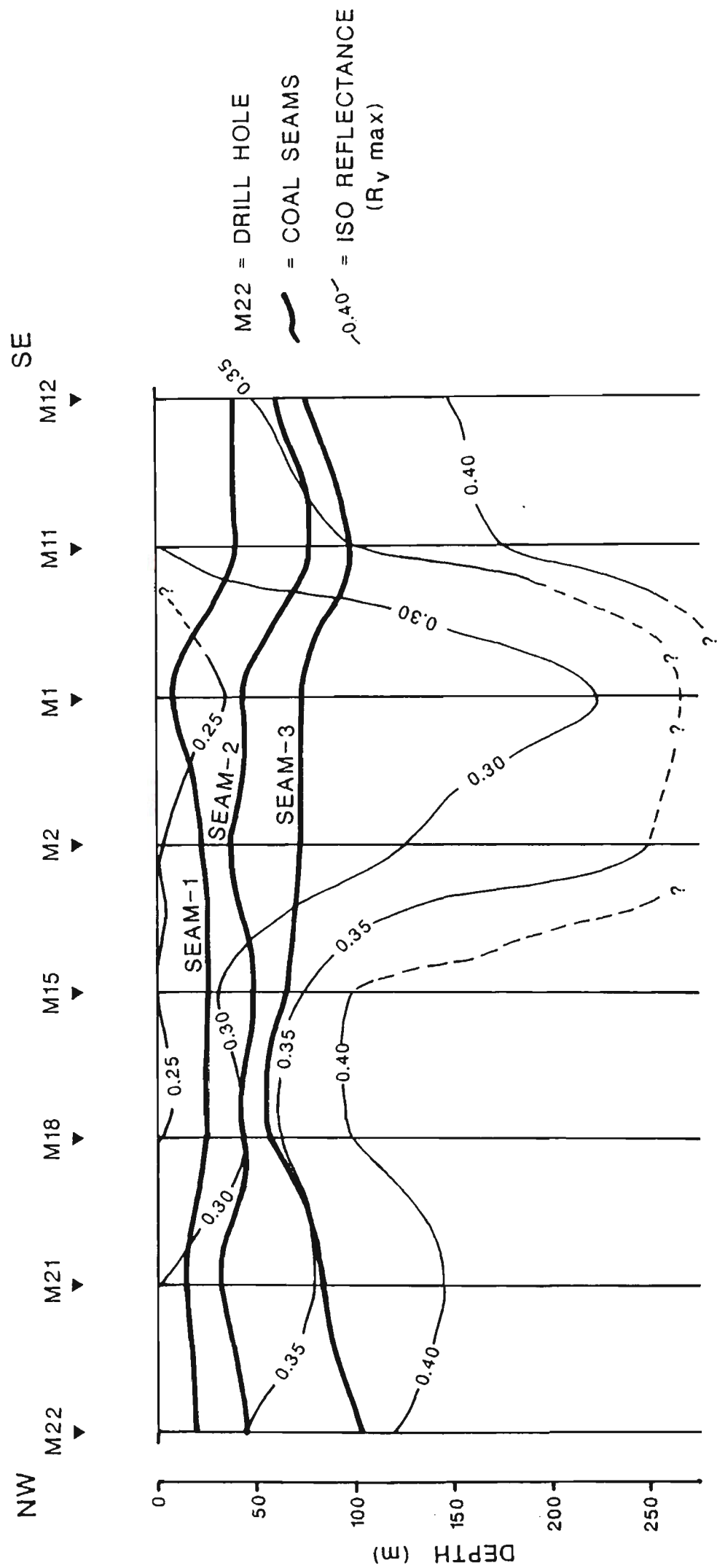


Figure 5.20: Isoreference profile showing rank gradients from some onshore wells of West Aceh Basin.

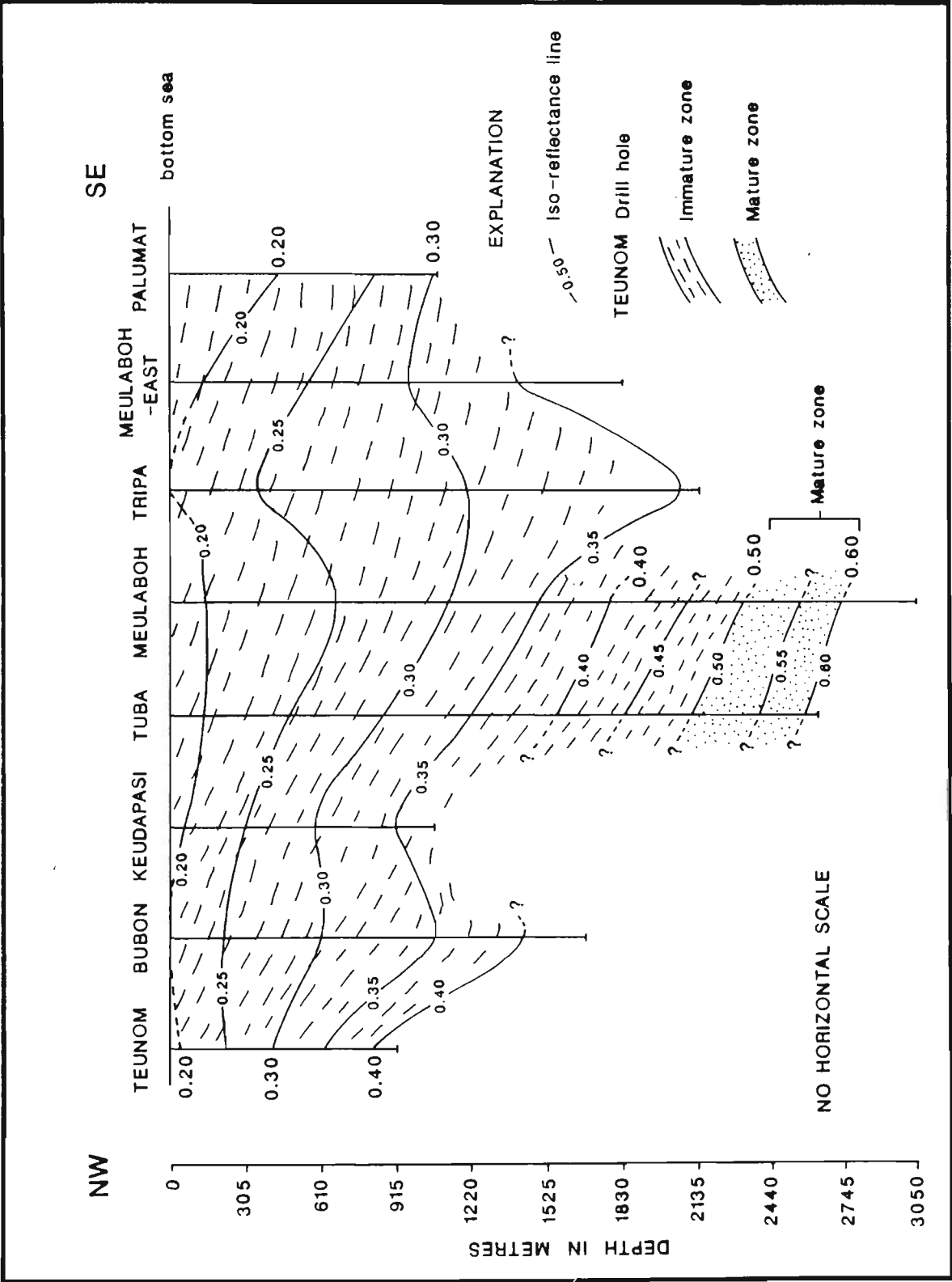


Figure 5.21: Isorefectance profile from offshore wells of West Aceh Basin.



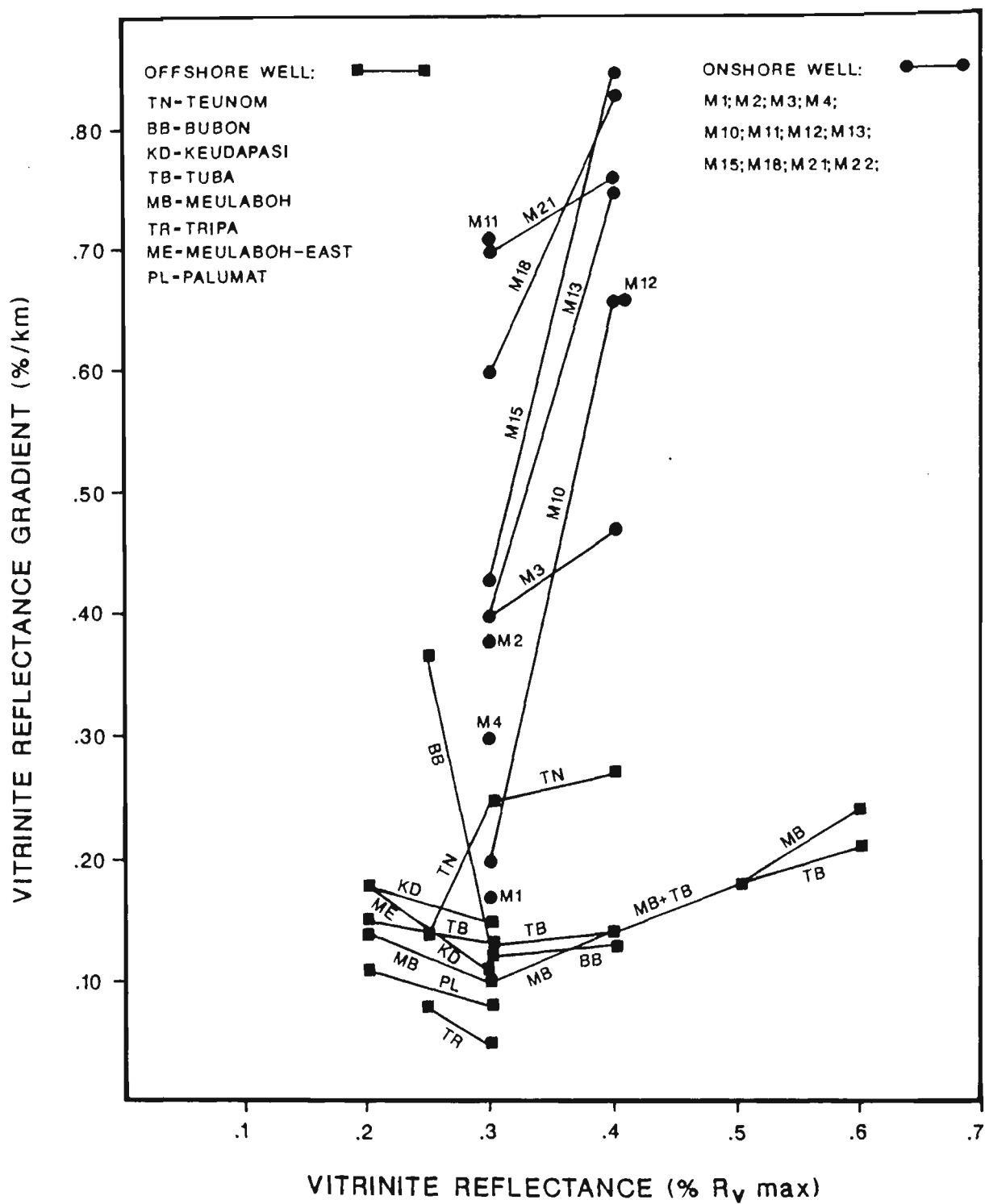


Figure 5.22: Vitrinite reflectance gradient at any given vitrinite reflectance level of the onshore and offshore wells of West Aceh Basin.

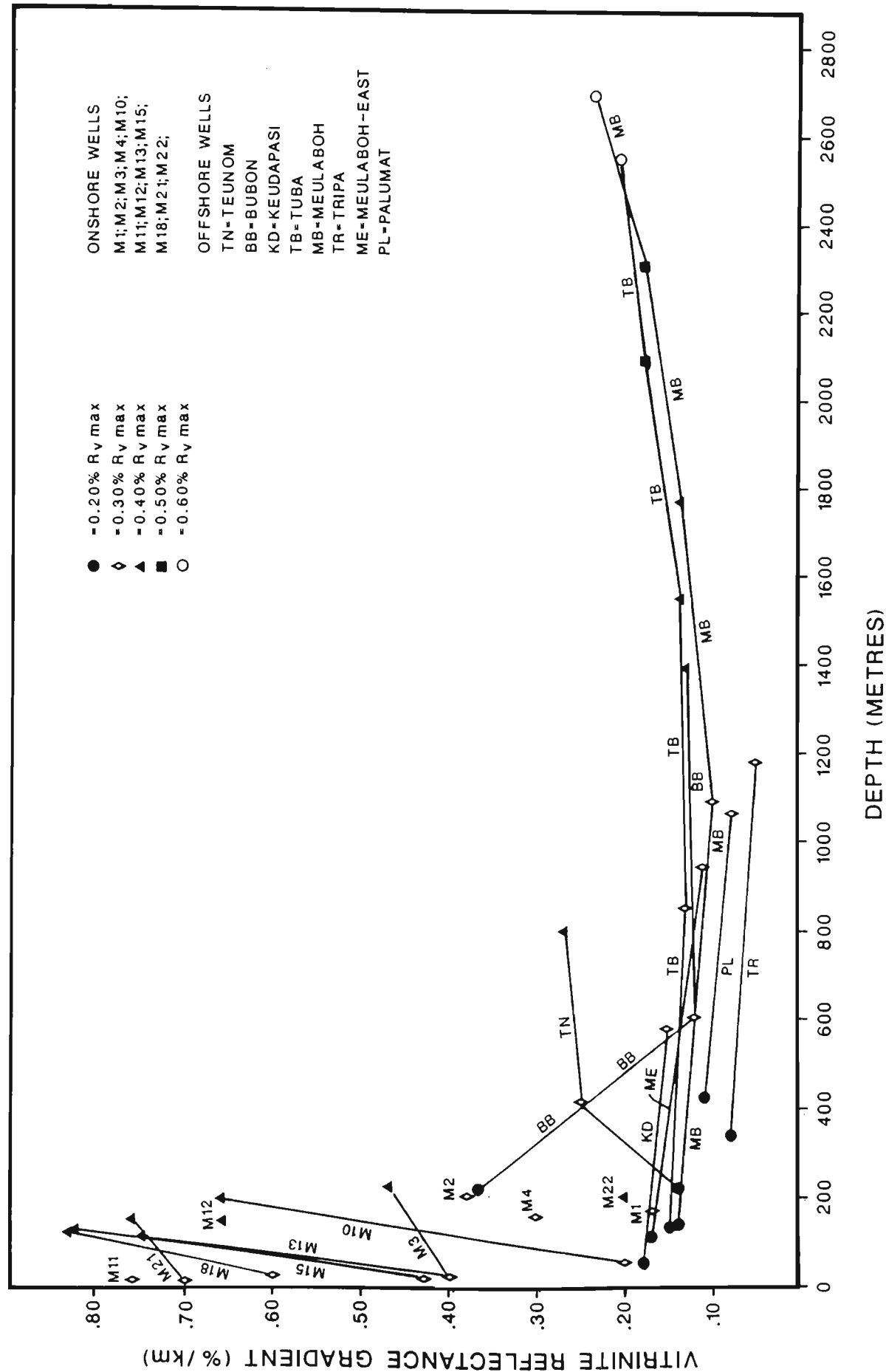


Figure 5.23: Vitrinite reflectance gradient at any depth intervals from the onshore and offshore wells of West Aceh Basin.

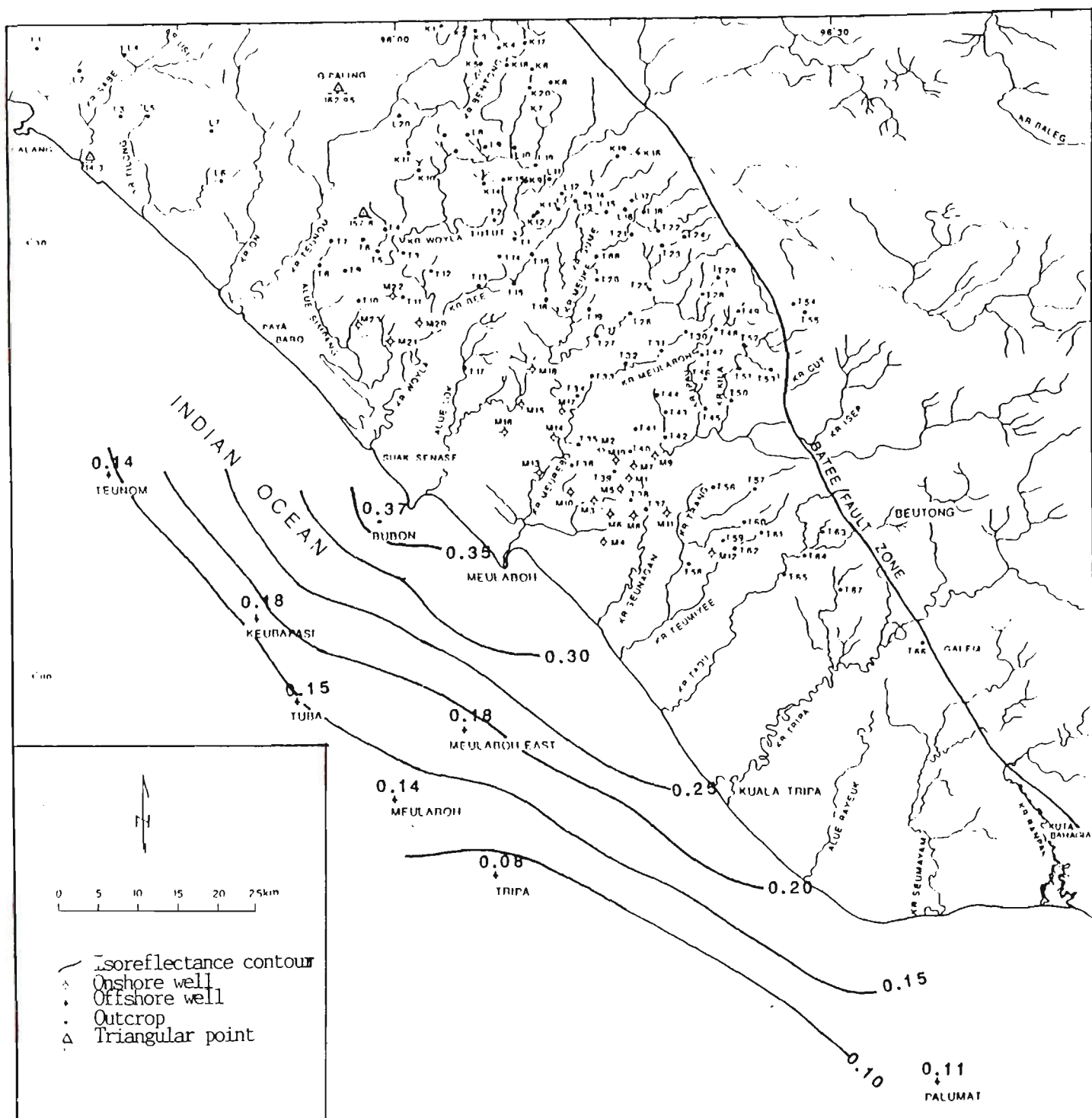


Figure 5.24. Isorefectance gradient contour at 0.25% vitrinite reflectance level at the offshore wells of West Aceh Basin.

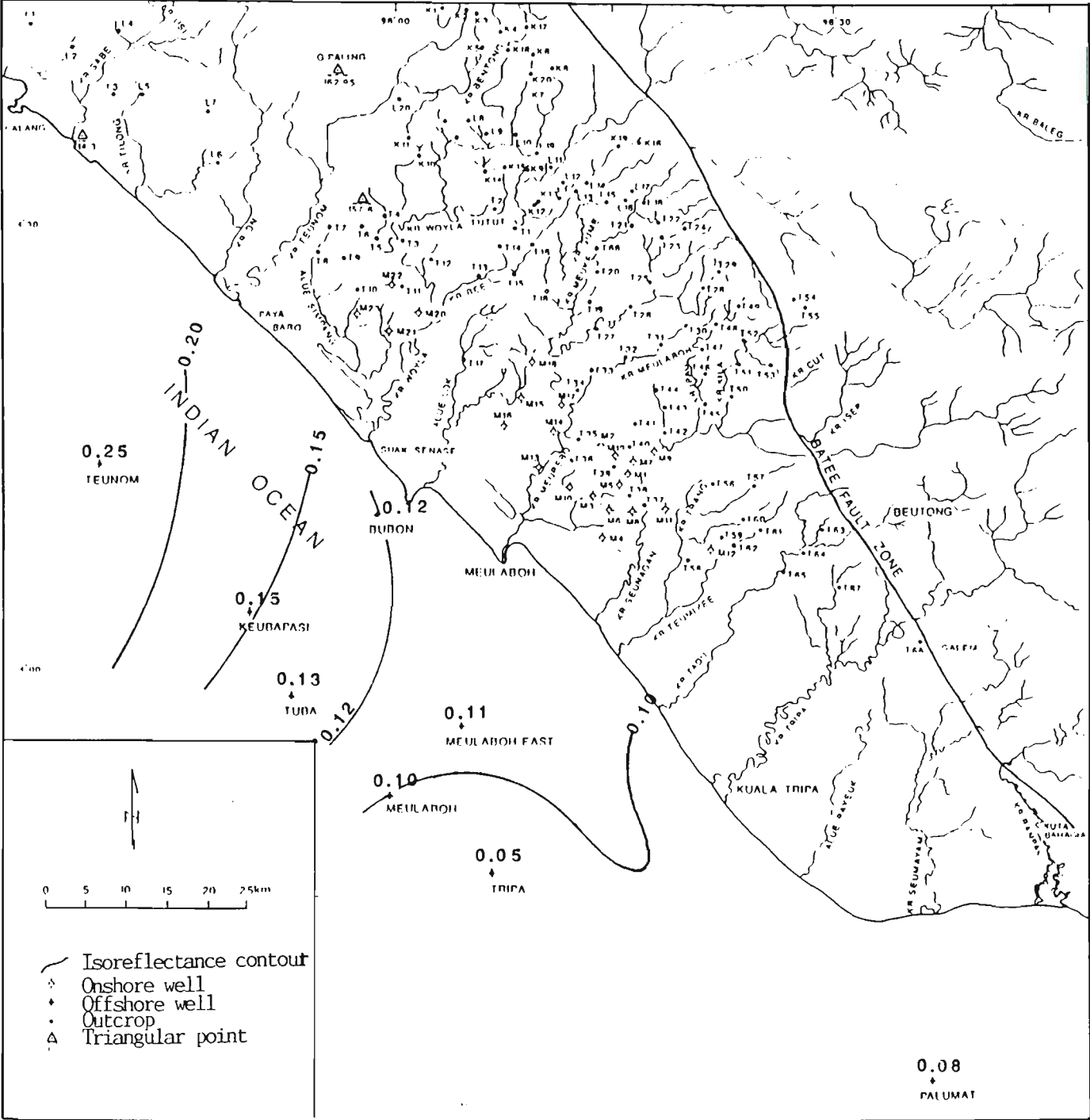


Figure 5.25. Isorefectance gradient contour at 0.30% vitrinite reflectance level at the offshore wells of West Aceh Basin.



Table 5.1. Range maximum vitrinite reflectance (R<sub>v</sub>max) values at the Tertiary Formations obtained from offshore and onshore wells

Well Name	Tutut Formation R <sub>v</sub> max range(%)	Kueh Formation R <sub>v</sub> max range(%)	Tangla Fomation R <sub>v</sub> max range(%)
<b>Offshore:</b>			
Teunom	0.25 - 0.30	0.25 - 0.40	-
Bubun	0.21 - 0.28	0.30 - 0.45	-
Keudapasi	0.22 - 0.30	0.30 - 0.35	-
Tuba	0.21 - 0.28	0.32 - 0.48	0.45 - 0.60
Meulaboh	0.18 - 0.30	0.32 - 0.42	0.40 - 0.60
Tripa	0.22 - 0.33	0.35 - 0.39	-
Meulaboh- East	0.20 - 0.34	0.31 - 0.38	-
Palumat	0.15 - 0.23	0.24 - 0.26	-
<b>Onshore :</b>			
M1	0.28 - 0.33	-	-
M2	0.21 - 0.32	-	-
M3	0.29 - 0.35	-	-
M4	0.20 - 0.35	-	-
M10	0.27 - 0.35	-	-
M11	0.30 - 0.38	-	-
M12	0.30 - 0.39	-	-
M13	0.27 - 0.40	-	-
M15	0.29 - 0.39	-	-
M18	0.27 - 0.40	-	-
M21	0.30 - 0.38	-	-

Table 5.2. Depth and reflectance gradient for given reflectance levels in well sections of onshore and offshore areas in the West Aceh Basin

Area	Well Name	0.20% R <sub>v</sub> max		0.30% R <sub>v</sub> max		0.40% R <sub>v</sub> max		0.50% R <sub>v</sub> max		0.60% R <sub>v</sub> max	
		Depth (m)	Gradient (%/Km)	Depth (m)	Gradient (%/Km)	Depth (m)	Gradient (%/Km)	Depth (m)	Gradient (%/Km)	Depth (m)	Gradient (%/Km)
Onshore	M1	-	-	175	0.17	-	-	-	-	-	-
	M2	-	-	210	0.38	-	-	-	-	-	-
	M4	-	-	162	0.30	-	-	-	-	-	-
	M3	-	-	25	0.40	237	0.47	-	-	-	-
	M10	-	-	50	0.20	200	0.66	-	-	-	-
	M13	-	-	25	0.40	112	0.75	-	-	-	-
	M15	-	-	23	0.43	127	0.85	-	-	-	-
	M18	-	-	25	0.60	132	0.83	-	-	-	-
	M21	-	-	13	0.70	150	0.76	-	-	-	-
	M22	-	-	-	-	200	0.20	-	-	-	-
	M11	-	-	13	0.76	-	-	-	-	-	-
	M12	-	-	-	-	150	0.66	-	-	-	-
Offshore	Teunom	217	0.14	412	0.25	803	0.27	-	-	-	-
	Bubon	217	0.37	607	0.12	1410	0.13	-	-	-	-
	Keudapasi	54	0.18	586	0.15	-	-	-	-	-	-
	Tuba	130	0.15	568	0.13	1562	0.14	2105	0.18	2560	0.21
	Meulaboh	141	0.14	1106	0.10	1779	0.14	2322	0.18	2734	0.24
	Tripa	347	0.08	1193	0.05	-	-	-	-	-	-
	Meulaboh- Bast	108	0.18	954	0.11	-	-	-	-	-	-
	Palumat	434	0.11	1085	0.08	-	-	-	-	-	-

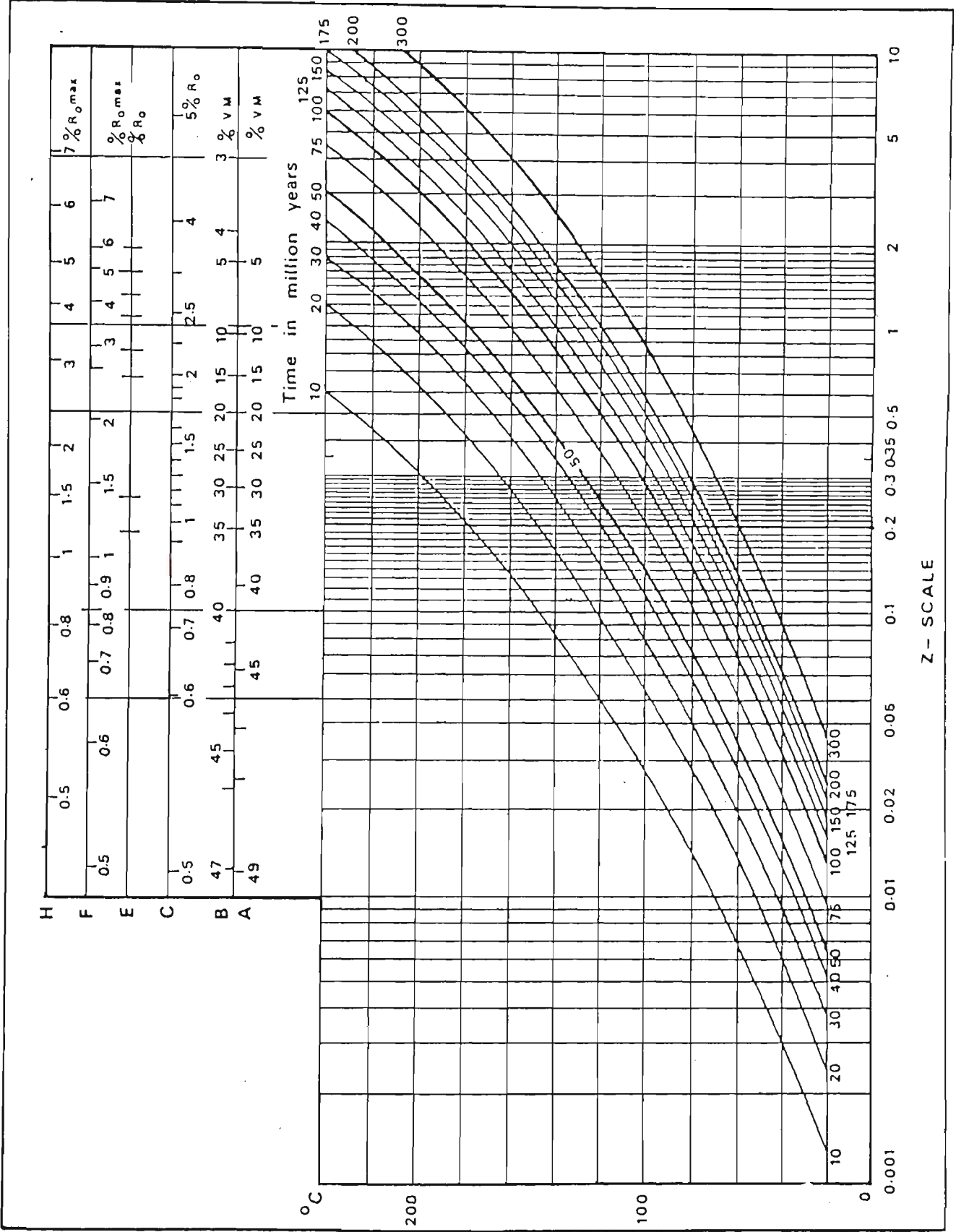


Figure 6.1: Karweil diagram (after Cook, A.C., 1982).



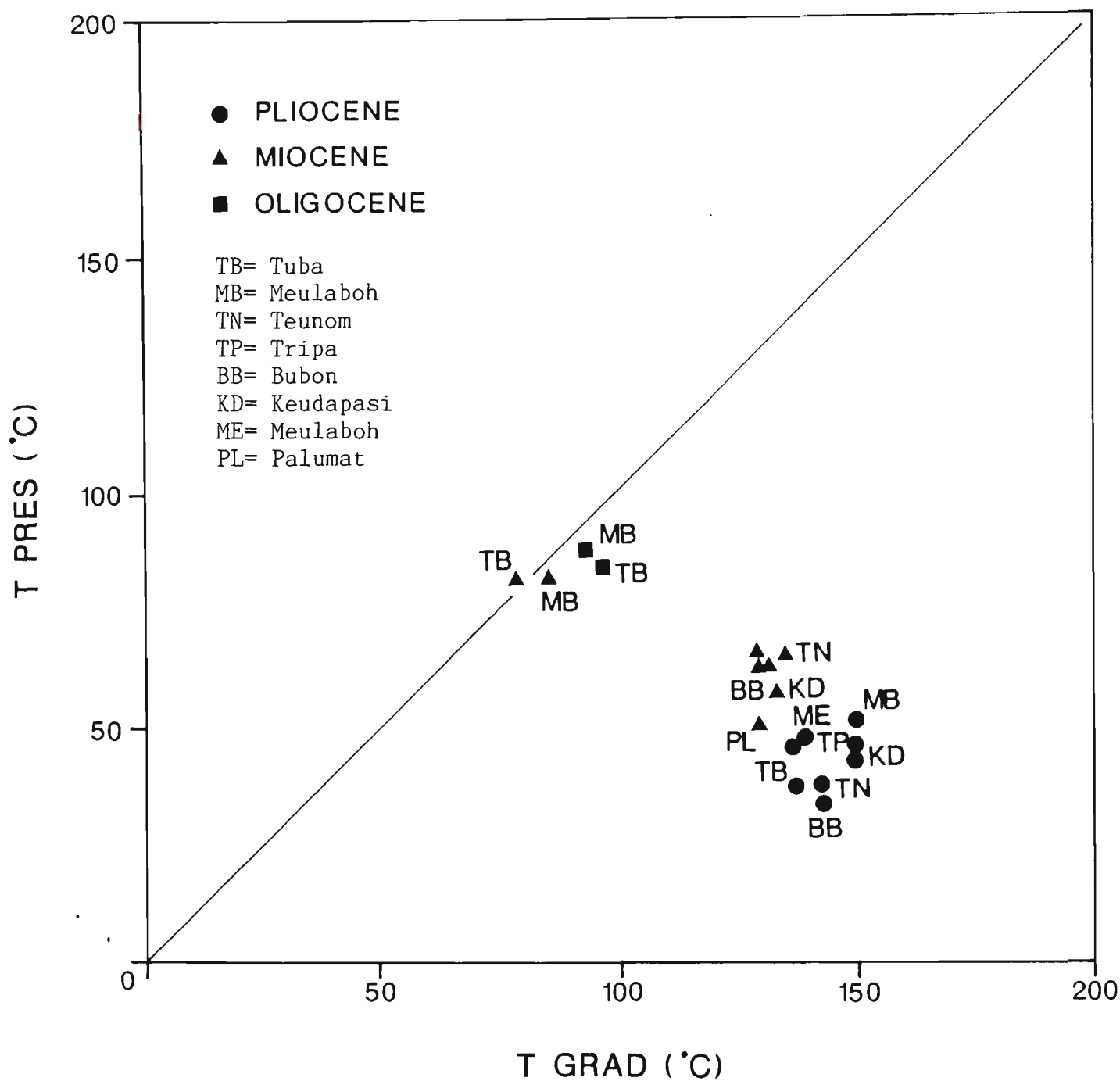


Figure 6.2: Plots T present versus T grad of the offshore wells, West Aceh Basin.

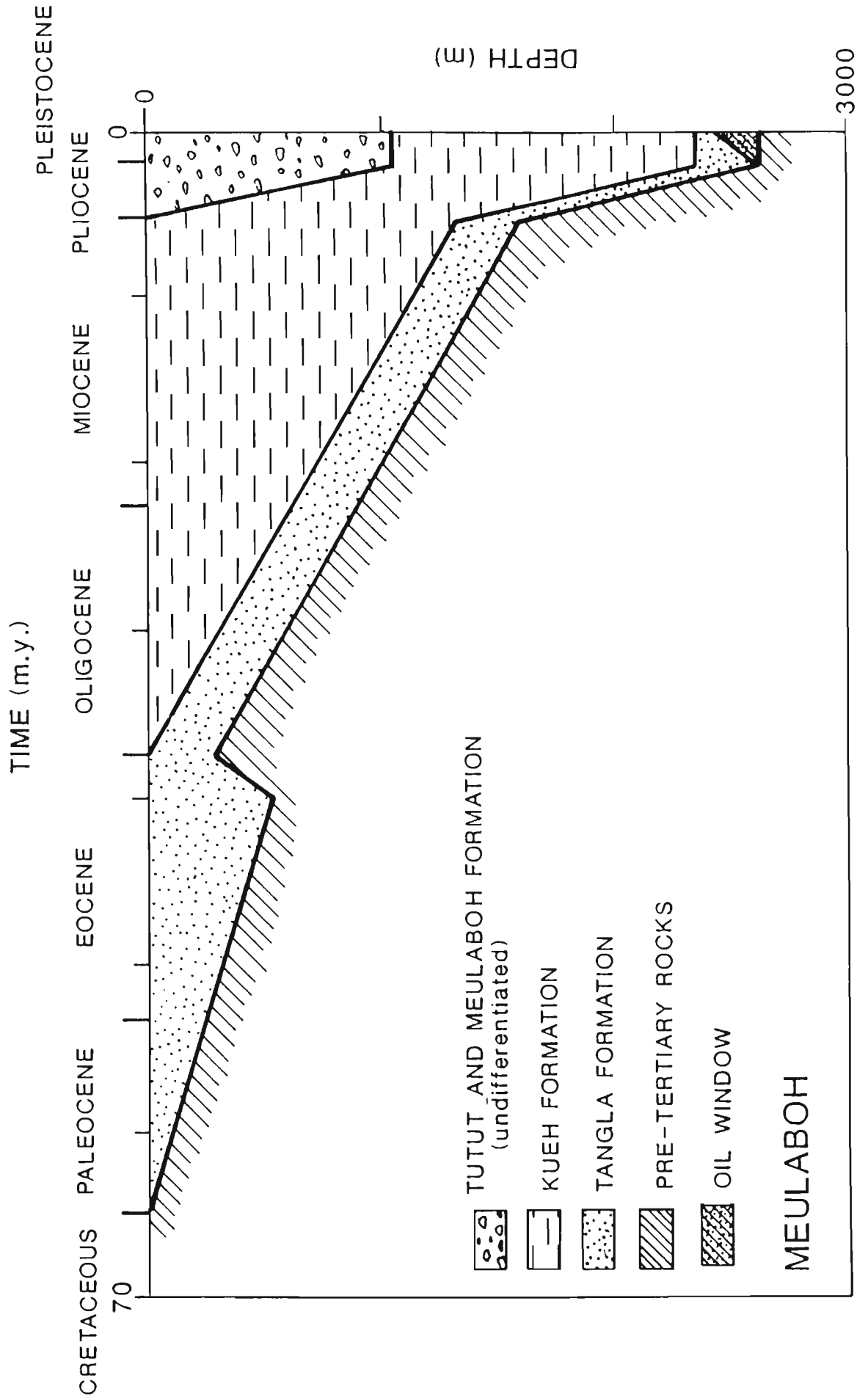


Figure 6.3: Burial history diagram at Meulaboh well, West Aceh Basin.

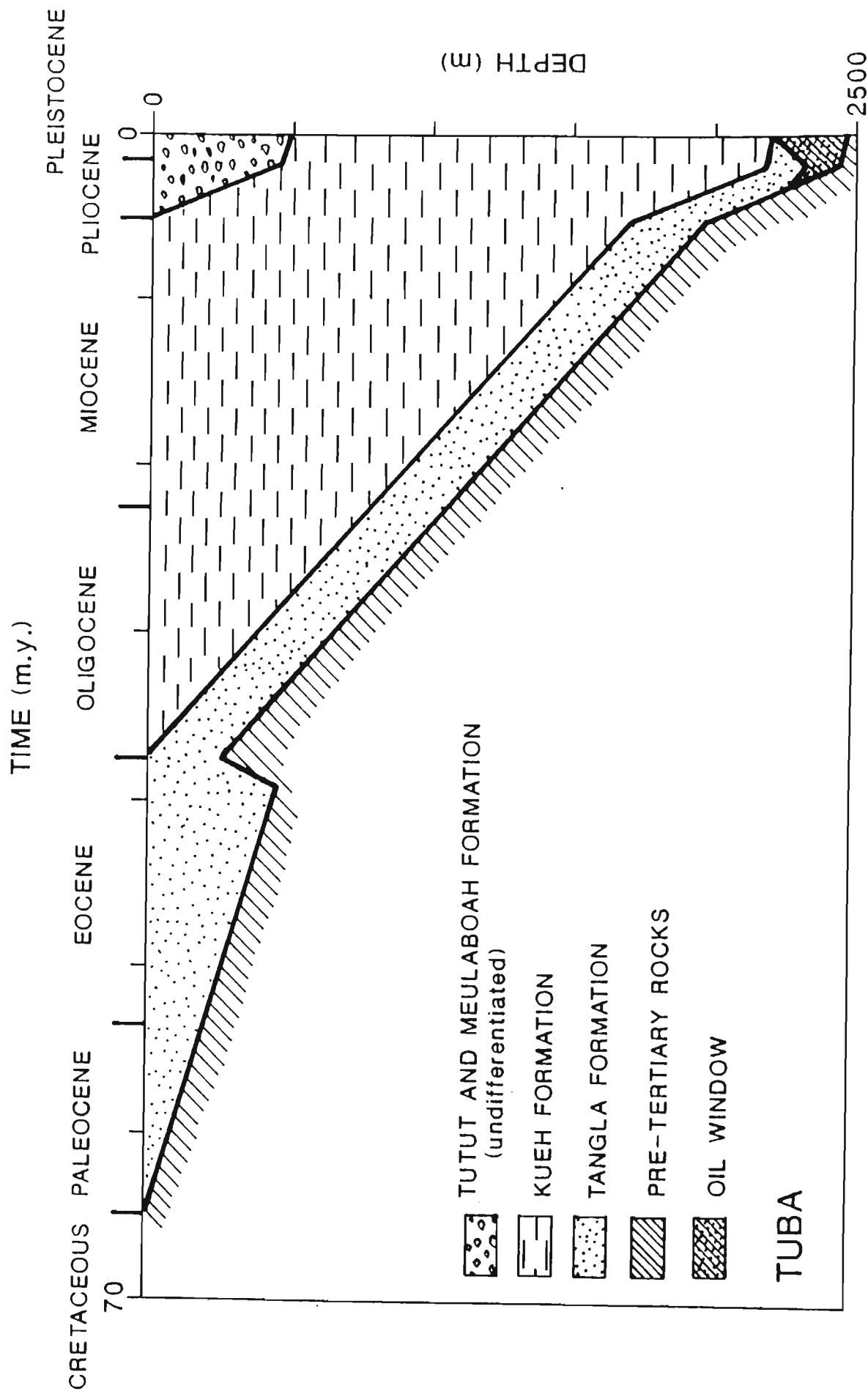


Figure 6.4: Burial history diagram at Tuba well, West Aceh Basin.

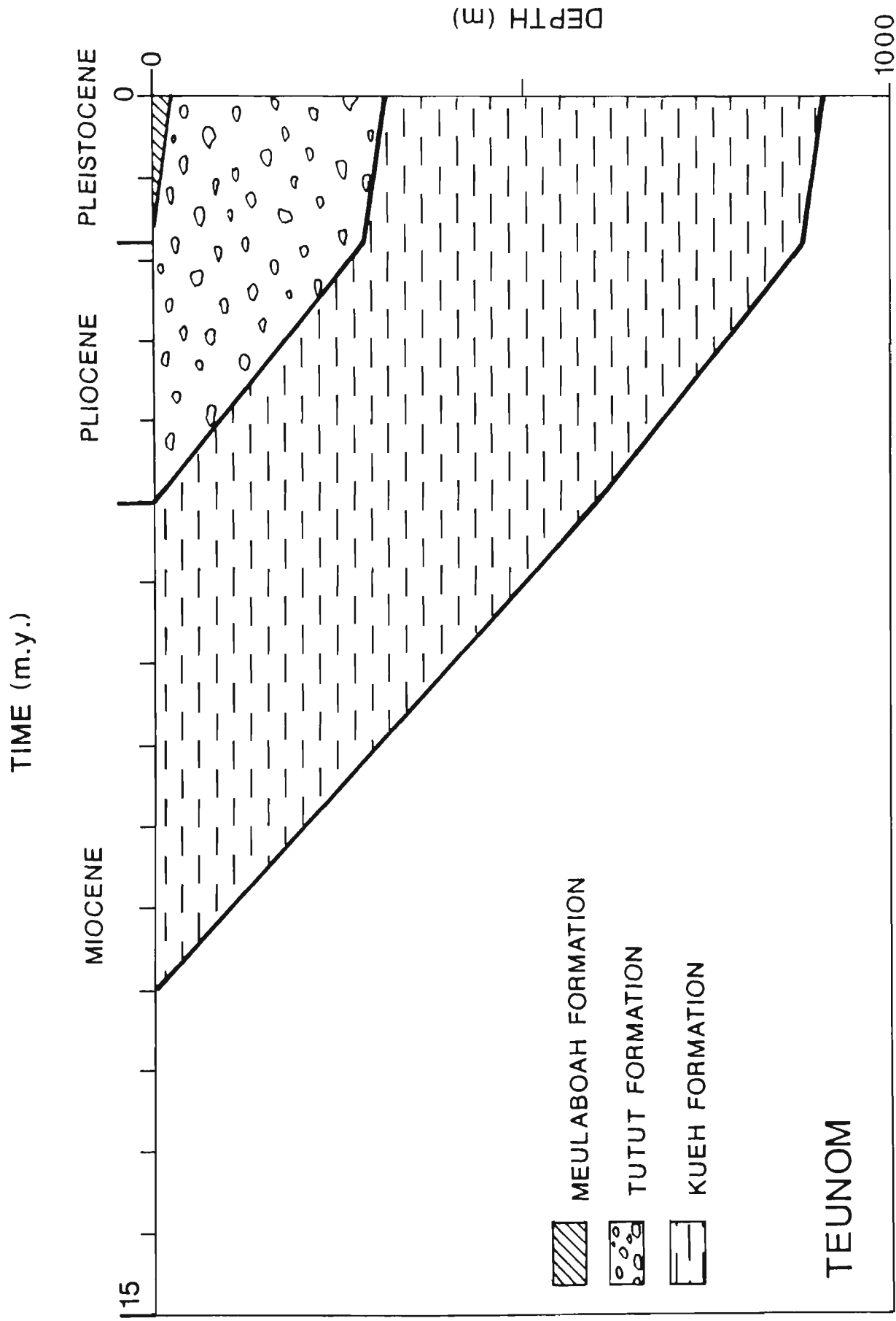


Figure 6.5: Burial history diagram at Teunom well, West Aceh Basin.

TIME (m.y.)

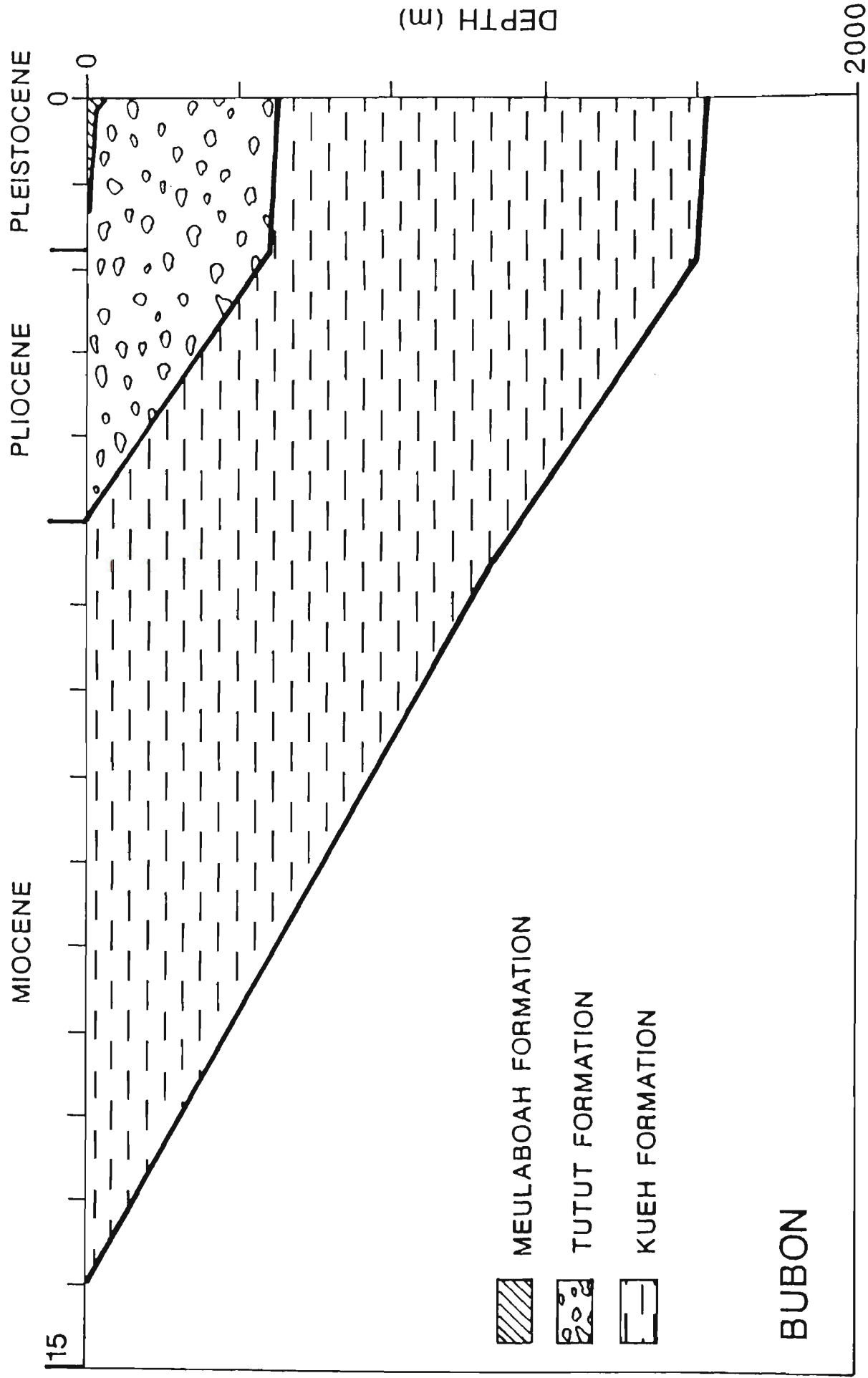


Figure 6.6: Burial history diagram at Bubon well, West Aceh Basin.

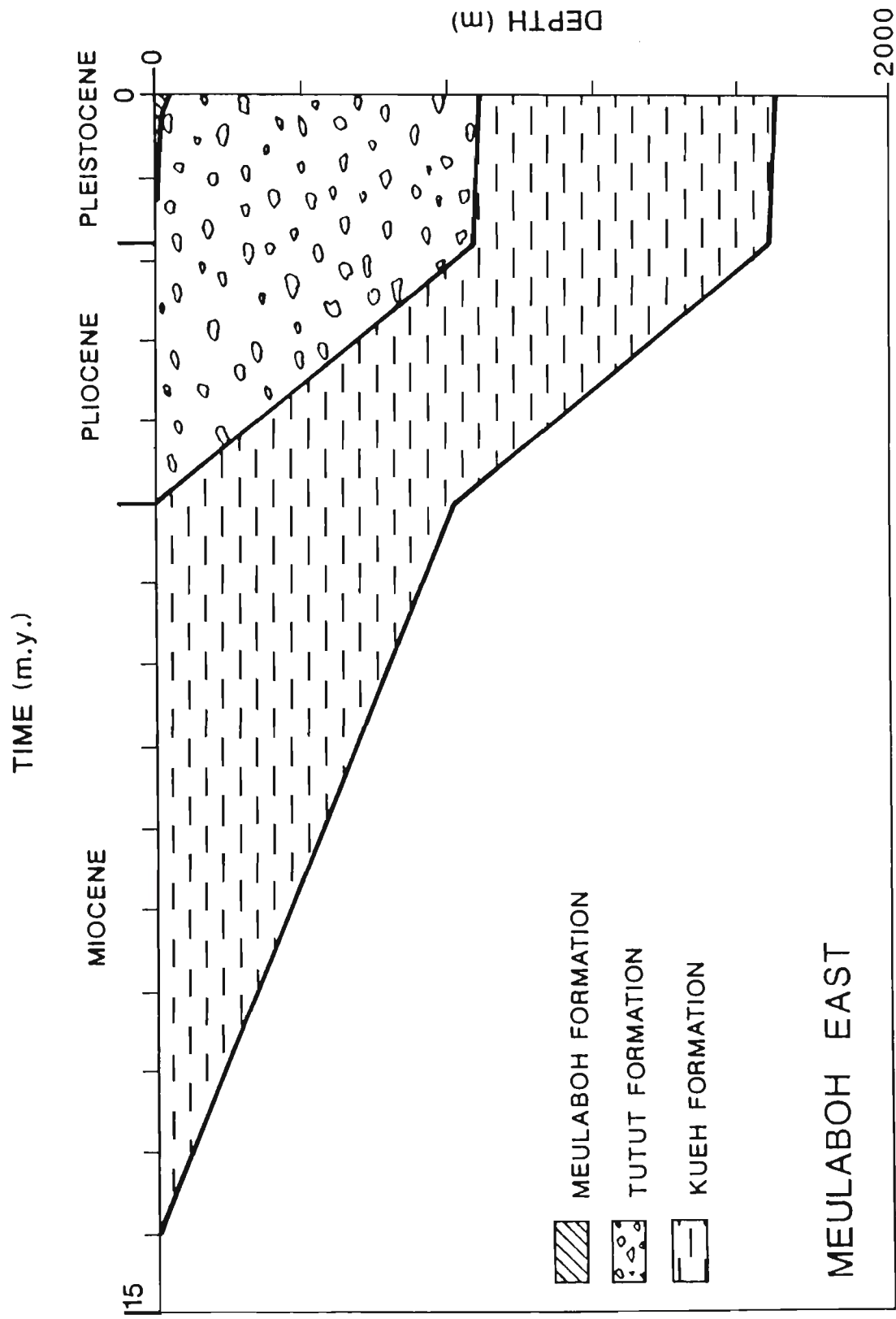


Figure 6.7: Burial history diagram at Meulaboh East well, West Aceh Basin.

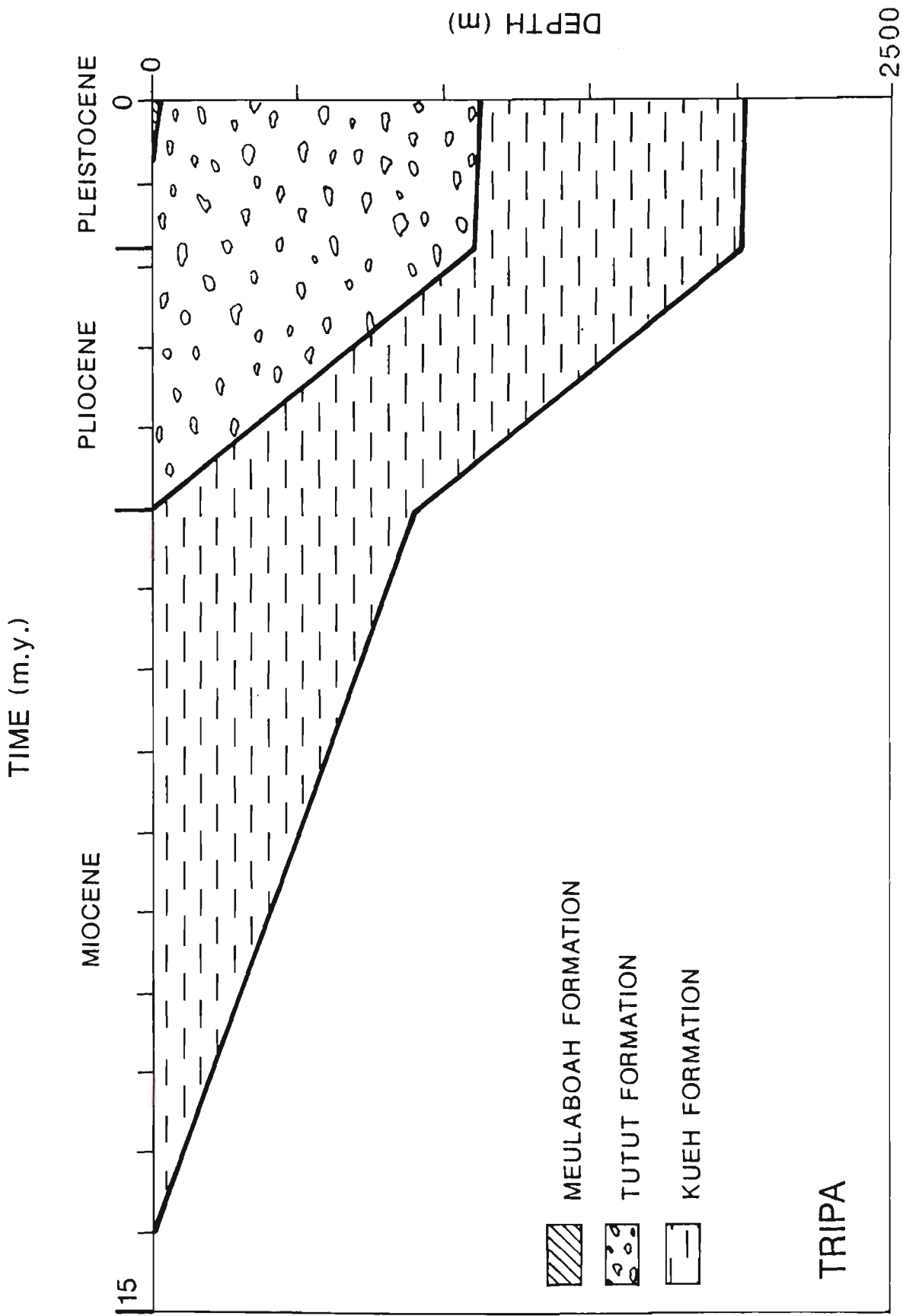


Figure 6.8: Burial history diagram at Tripa well, West Aceh Basin.

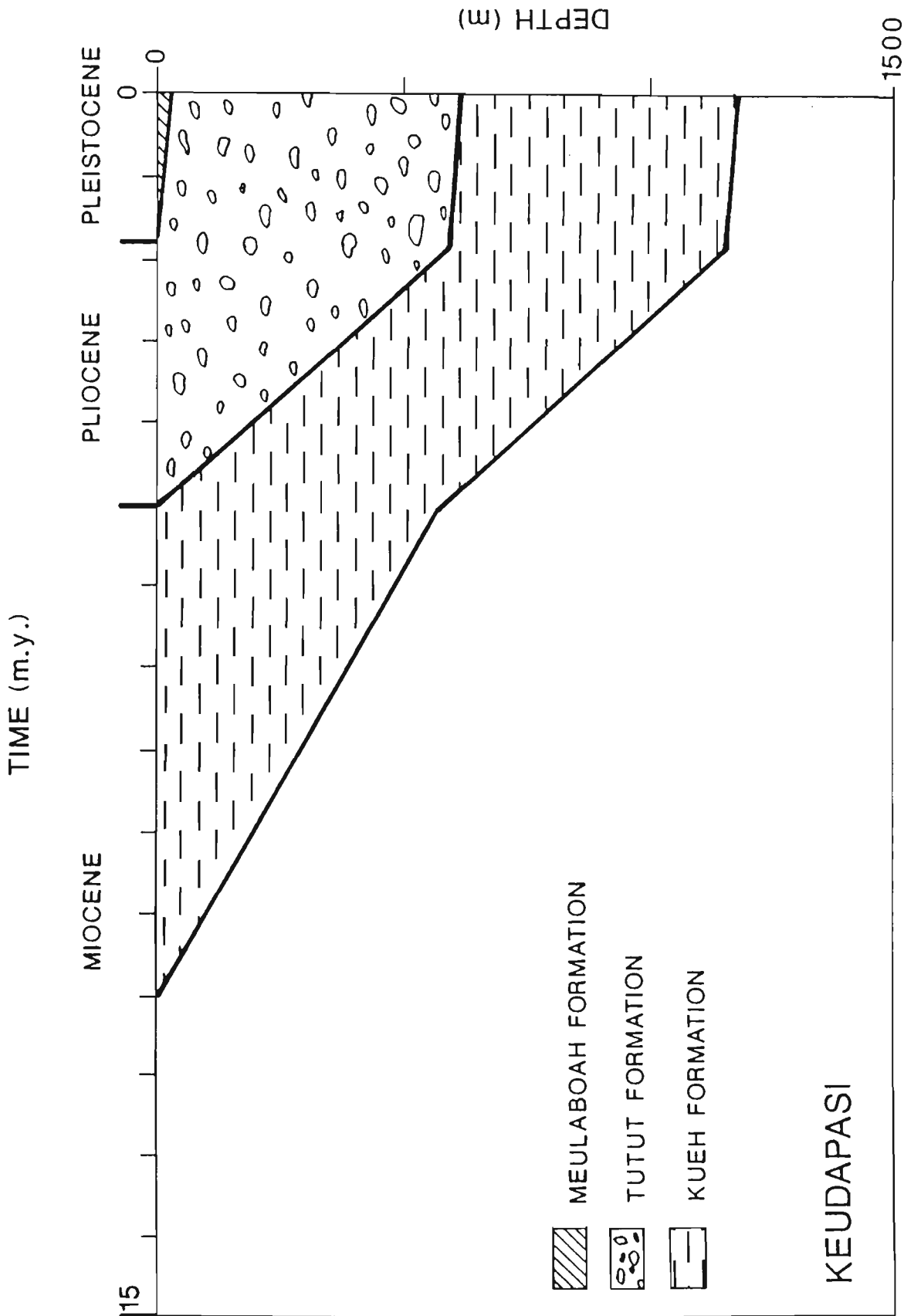


Figure 6.9: Burial history diagram at Keudapasi well, West Aceh Basin.



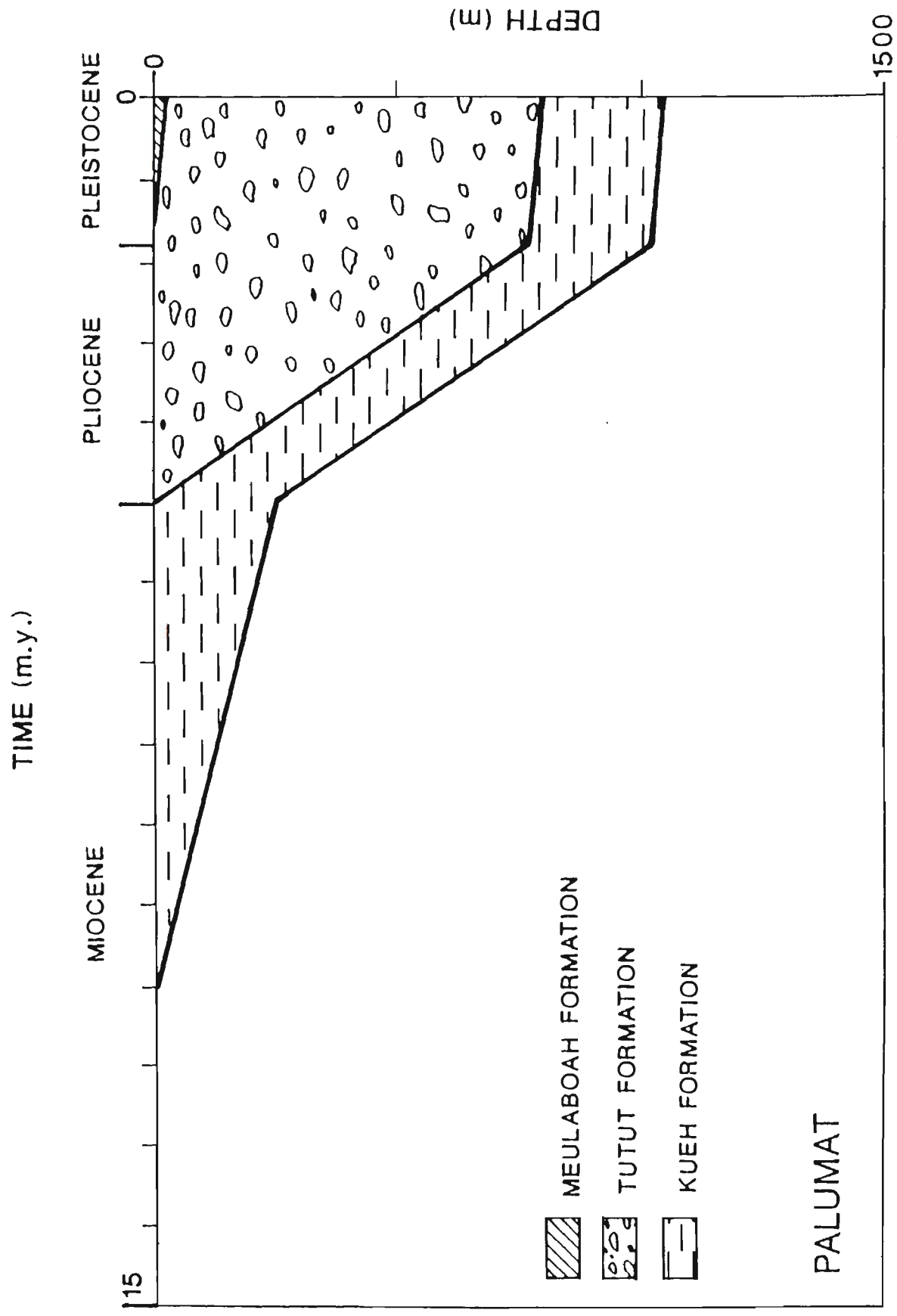


Figure 6.10: Burial history diagram at Palumat well, West Aceh Basin.

Table 6.1. Comparison present-day geothermal gradients in West Aceh Basin with the other Tertiary Sumatra Basins  
( bold indicate wells examined for this study; unbold adapted from Aadland and Phoa, 1981).

FORARC BASIN		BACKARC BASIN	
WELL NAME/BASIN	GEO THERMAL GRADIENT °C/Km	WELL NAME/BASIN	GEO THERMAL GRADIENT °C/Km
West Aceh Basin:		North West Aceh Basin	
<b>Teunom</b>	39	BAI - A1	29
<b>Bubon</b>	22	Sigli - B1	34
<b>Keudapasi</b>	25	Sigli - A1	32
<b>Tuba</b>	24		
<b>Meulaboh</b>	23	North Sumatra Basin	
<b>Tripa</b>	17	NSB - G1	66
<b>Meulaboh East</b>	24	NSB - H1	84
<b>Palumat</b>	23	Peudawa D - 1	45
<b>Raja</b>	27		
West Sumatra Basin:		Central Sumatra Basin	
<b>Singkel</b>	18	Kebun 1	82
<b>Telaga</b>	18	Lipai 1	58
		Tobat 1	70
Bengkulu Basin:		Kiri 1	53
<b>Aminol</b>	32	Bila 1	46

Table 6.2. Thermal history data for various formations in the West Aceh Basin, Sumatra.

WELL NAME	FORMATION	DEPTH (M)	AGE (Ma)	R <sub>v</sub> MAX (%)	T PRES °C	T ISO °C	T GRAD °C	GRAD:ISO
Teunom	Tutut	3100	5.0	0.27	39.0	92.5	142.0	-1.20
	Kueh	910	11.0	0.49	62.5	87.5	134.0	-0.50
Bubon	Tutut	450	5.0	0.48	37.0	93.0	142.8	-1.10
	Kueh	1610	14.0	0.45	62.5	85.0	130.0	-0.50
Keudapasi	Tutut	610	5.0	0.31	42.6	97.5	150.0	-1.00
	Kueh	1177	11.0	0.38	37.0	87.0	133.0	-0.60
Tuba	Tutut	462	5.0	0.25	38.0	90.0	138.0	-1.08
	Kueh	2184	37.0	0.40	79.3	55.0	82.0	0.90
	Tangla	2394	60.0	0.60	84.3	65.0	98.0	0.60
Meulaboh	Tutut	1050	5.0	0.30	51.3	97.5	150.0	-0.88
	Kueh	2373	37.0	0.50	81.5	57.5	86.0	0.84
	Tangla	2640	60.0	0.60	87.7	62.0	93.6	0.81
Tripa	Tutut	1100	4.5	0.30	45.8	97.3	149.6	-0.98
	Kueh	2000	14.0	0.35	61.2	82.5	126.0	-0.48
Meulaboh East	Tutut	880	5.0	0.30	48.5	97.5	150.0	-0.93
	Kueh	1700	14.0	0.35	68.6	82.5	126.0	-0.31
Palumat	Tutut	790	5.0	0.25	45.0	90.0	138.0	-0.93
	Kueh	1050	11.0	0.30	50.9	85.0	130.0	-0.75

Table 6.3. Correlation of vitrinite reflectance values with TTI values (after Waples, 1980).

TTI	Vitrinite Reflectance % R <sub>v</sub> max	TTI	Vitrinite Reflectance % R <sub>v</sub> max
< 1	0.40	180	1.35
3	0.50	300	1.50
10	0.60	900	2.00
20	0.70	2,700	2.50
50	0.90	6,000	3.00
100	1.10	23,000	4.00

FIGURES AND TABLES OF  
CHAPTER 7

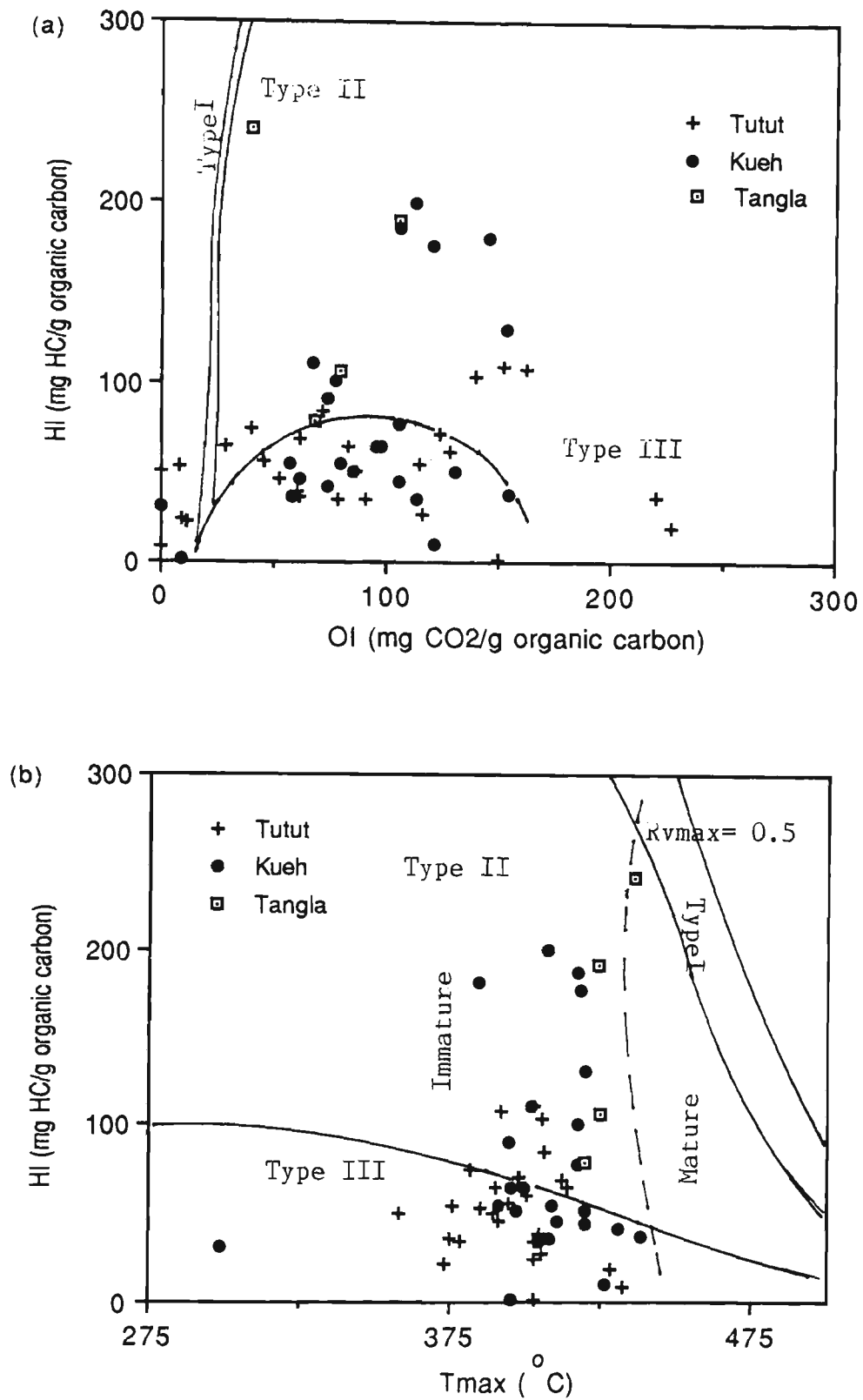


**Figure 7.1:** Crossplots of oxygen index vs hydrogen index (a) and Tmax vs hydrogen index (b) for offshore samples.

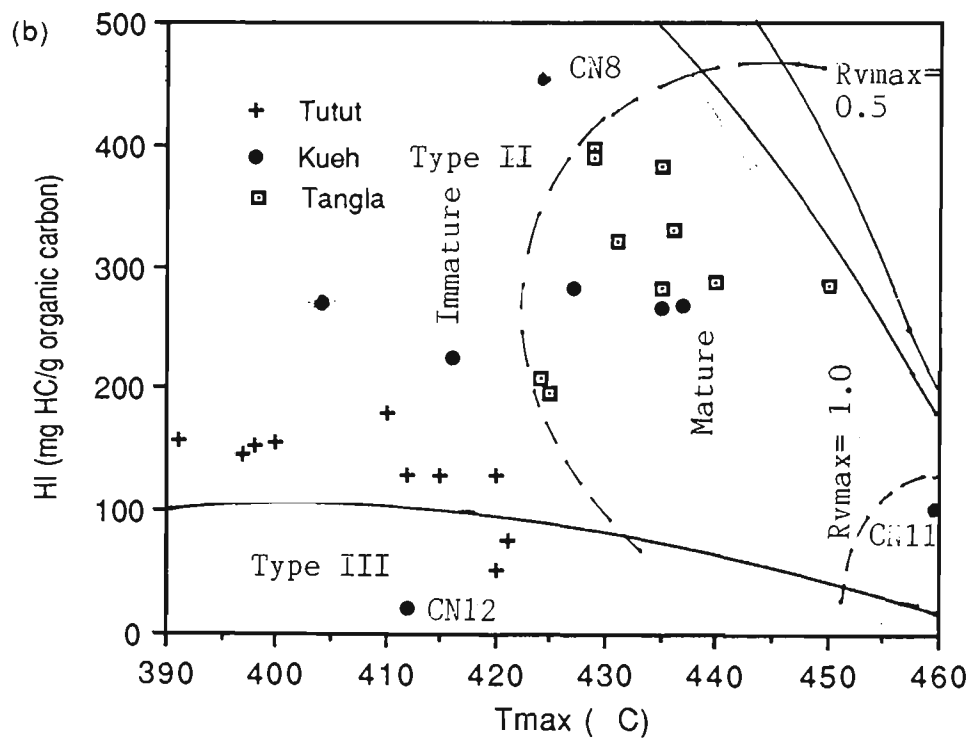
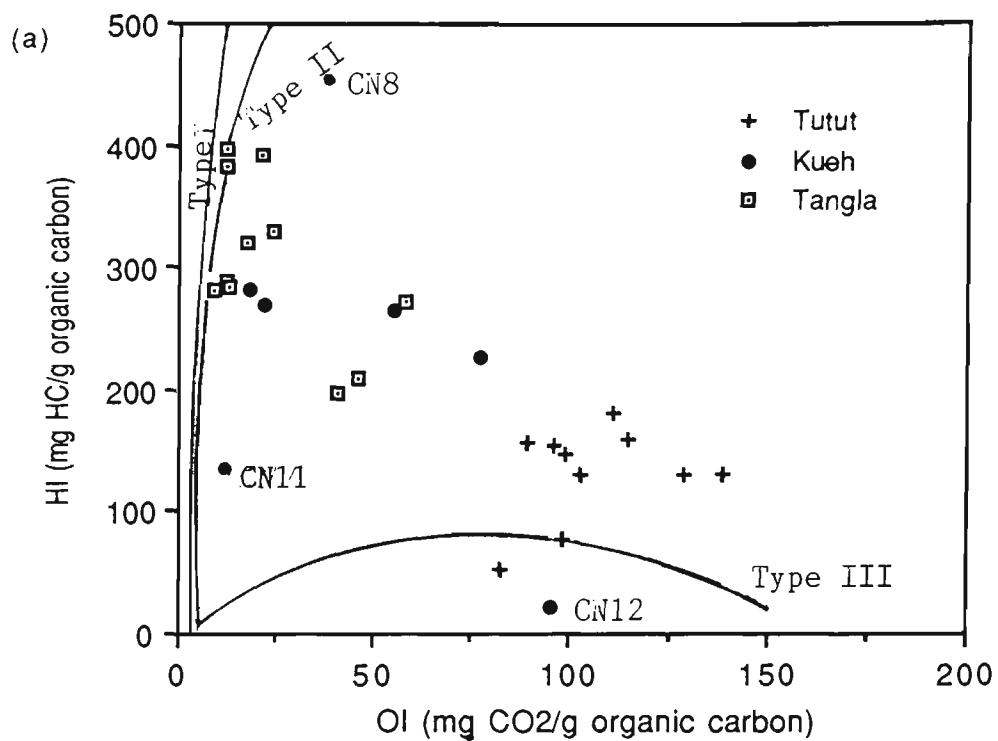


Figure 7.2: Crossplots of oxygen index vs hydrogen index (a) and Tmax vs hydrogen index (b) for onshore coal samples.

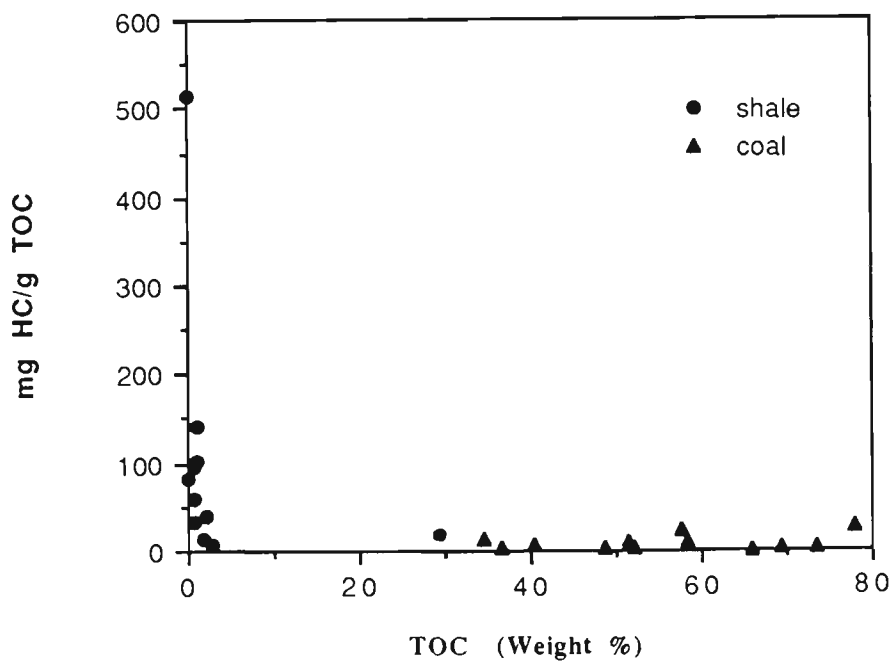
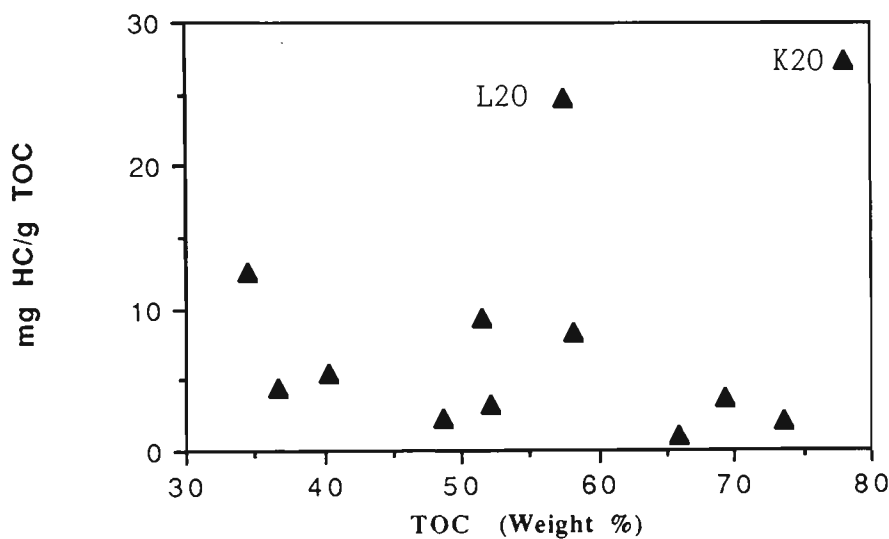
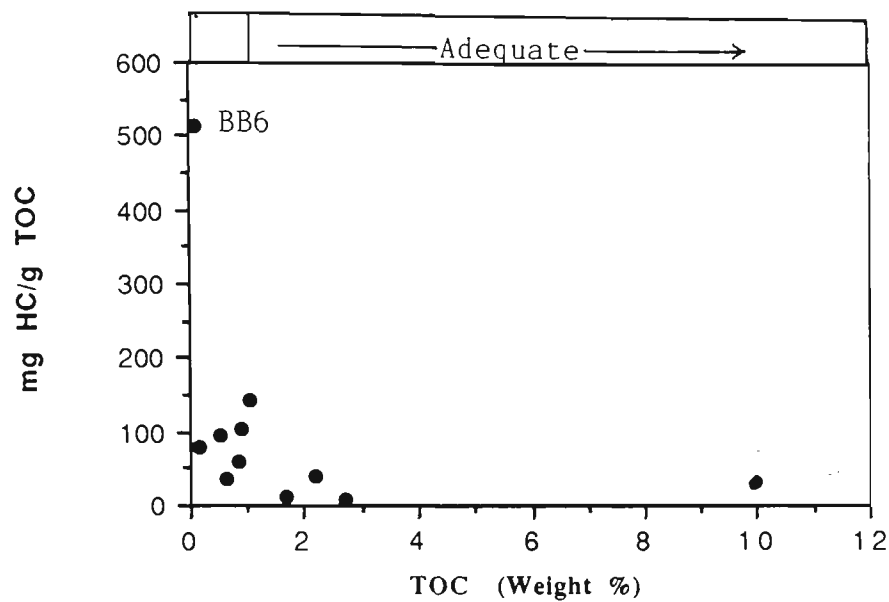


Figure 7.3: Relationship between the TOC content and normalised hydrocarbon (mg/g TOC), a. shale; b. coal; c. combined shale and coal.



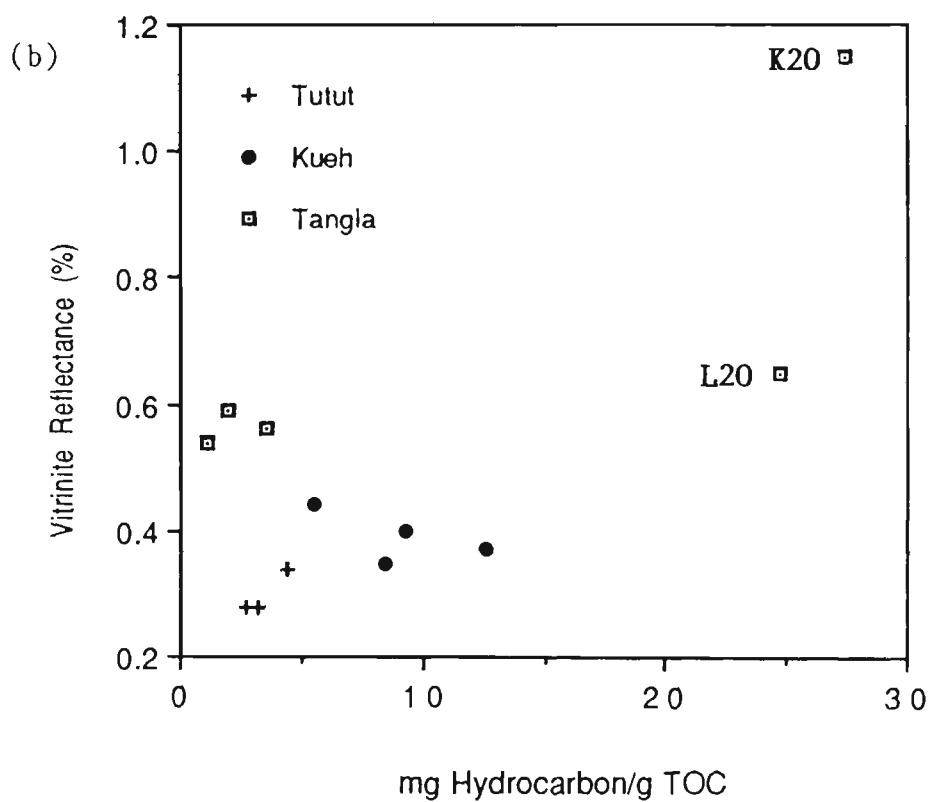
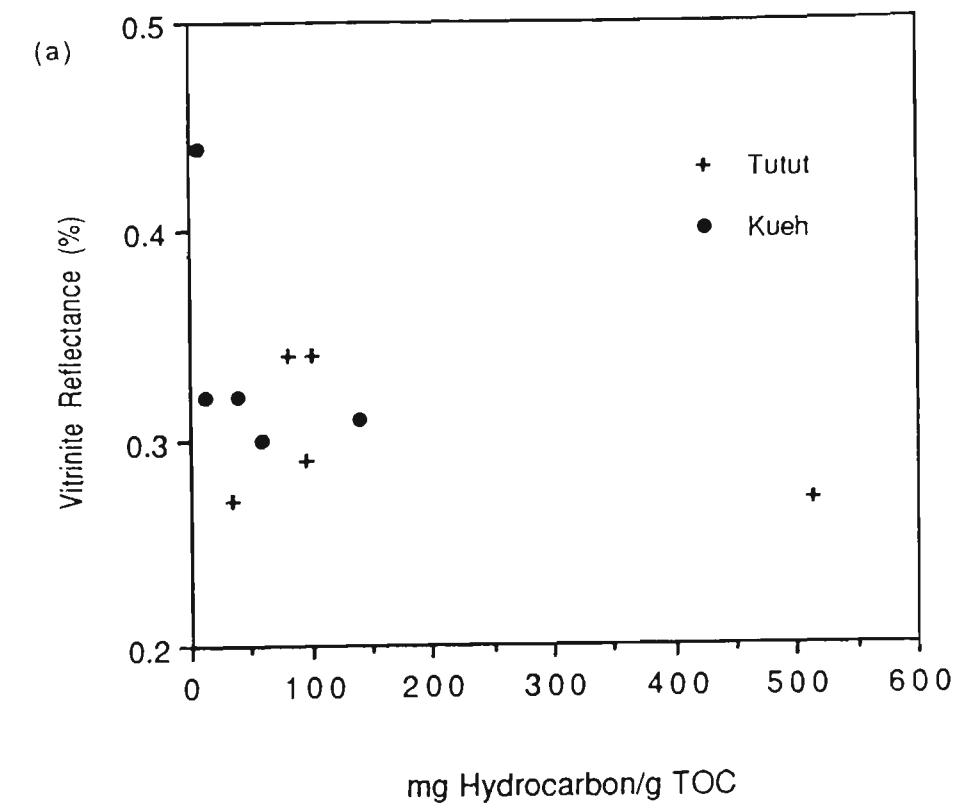


Figure 7.4: Relationship between the vitrinite reflectance normalised hydrocarbon (mg/g TOC). (a) shale; (b) coal.

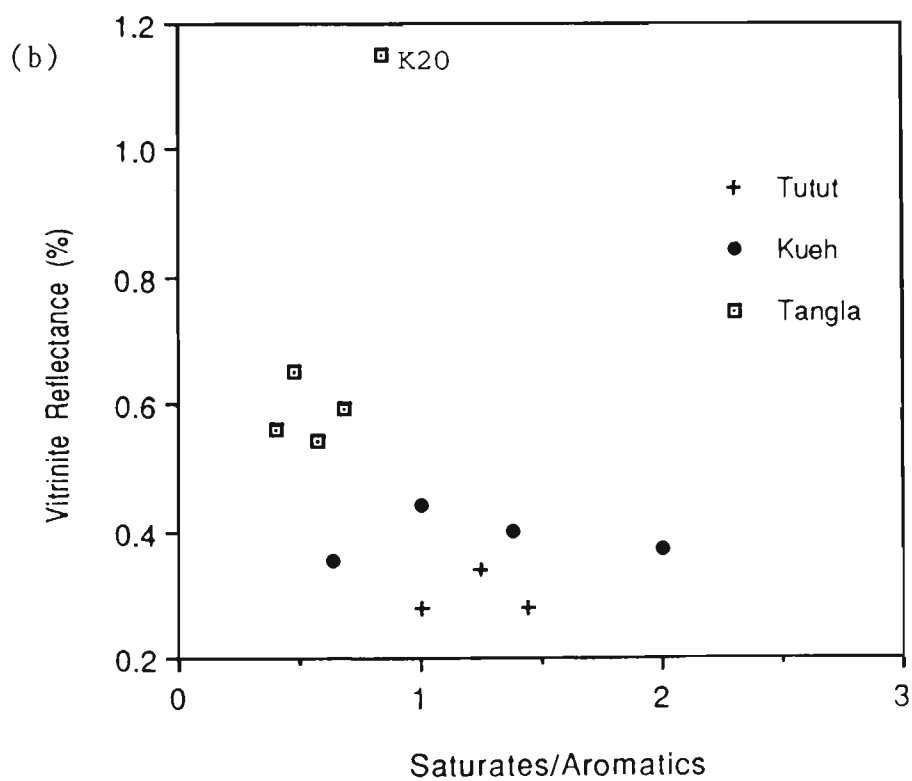
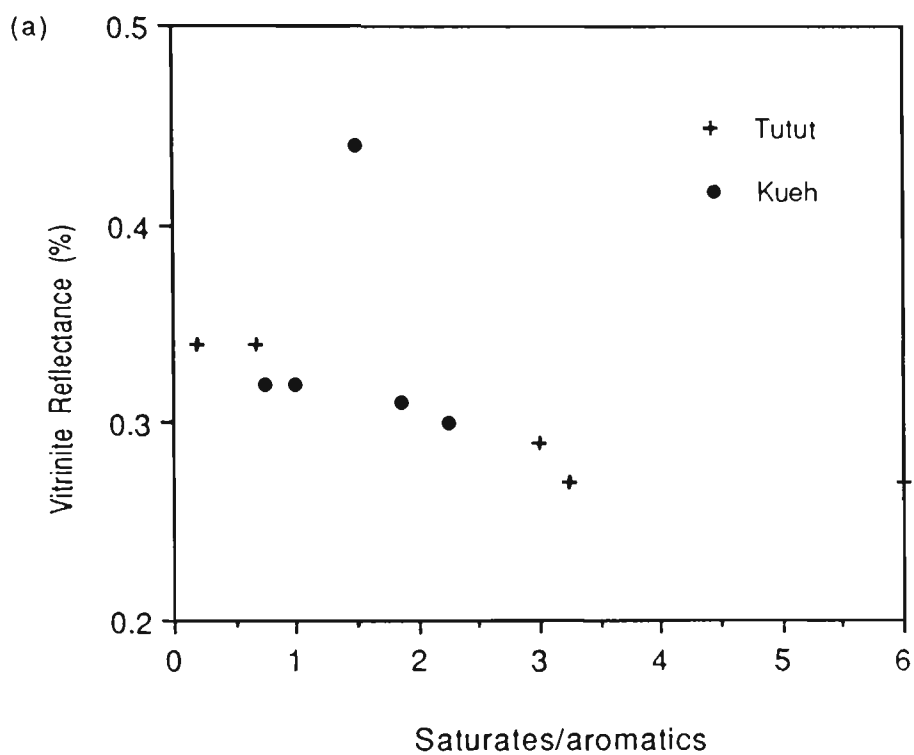


Figure 7.5: Relationship between the vitrinite reflectance and the ratio saturates to aromatic fractions, (a) shale; (b) coal.

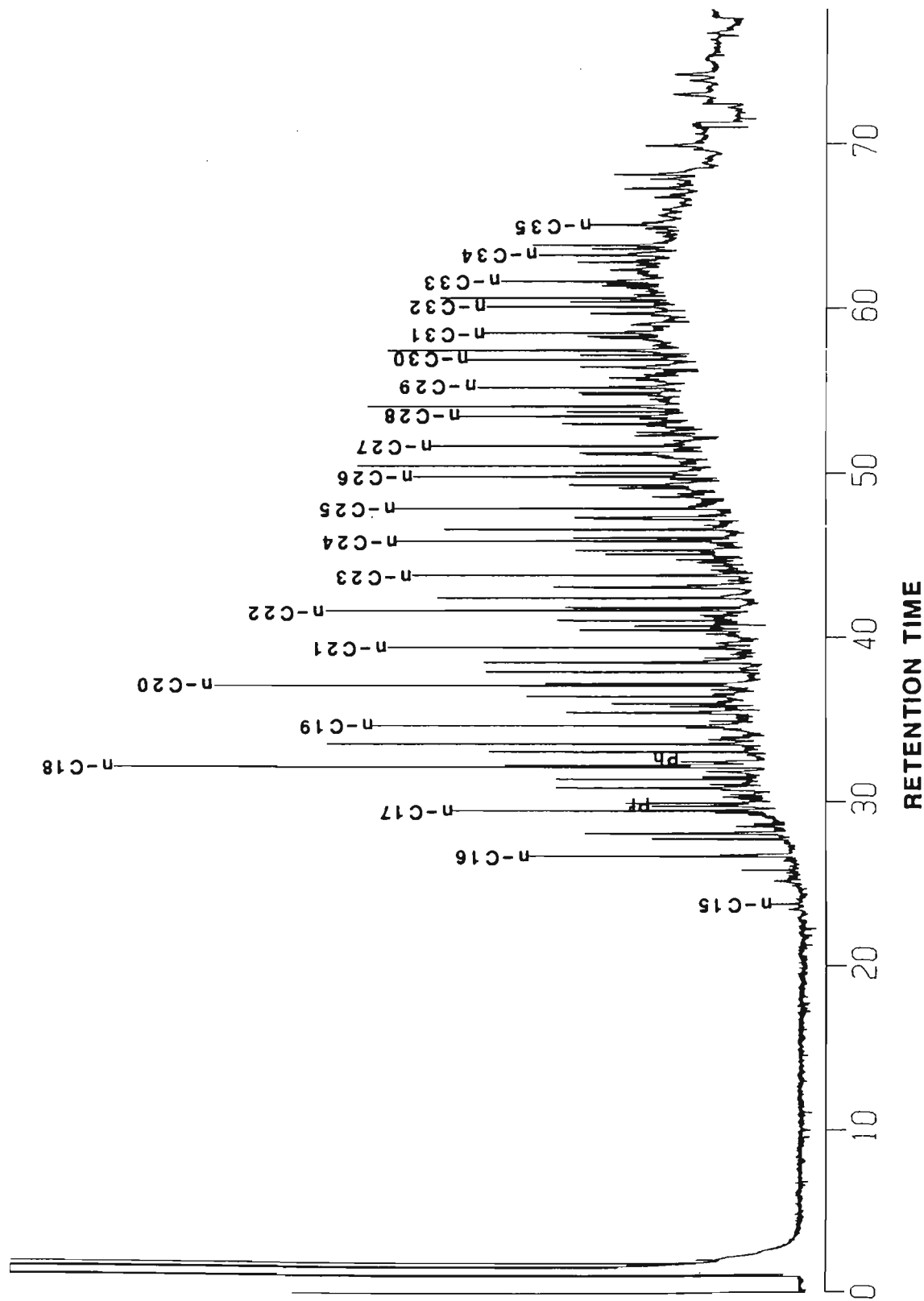


Figure 7.6: N-alkane distribution profiles in the saturated fractions in the extracts shale Tutut Formation, BB6

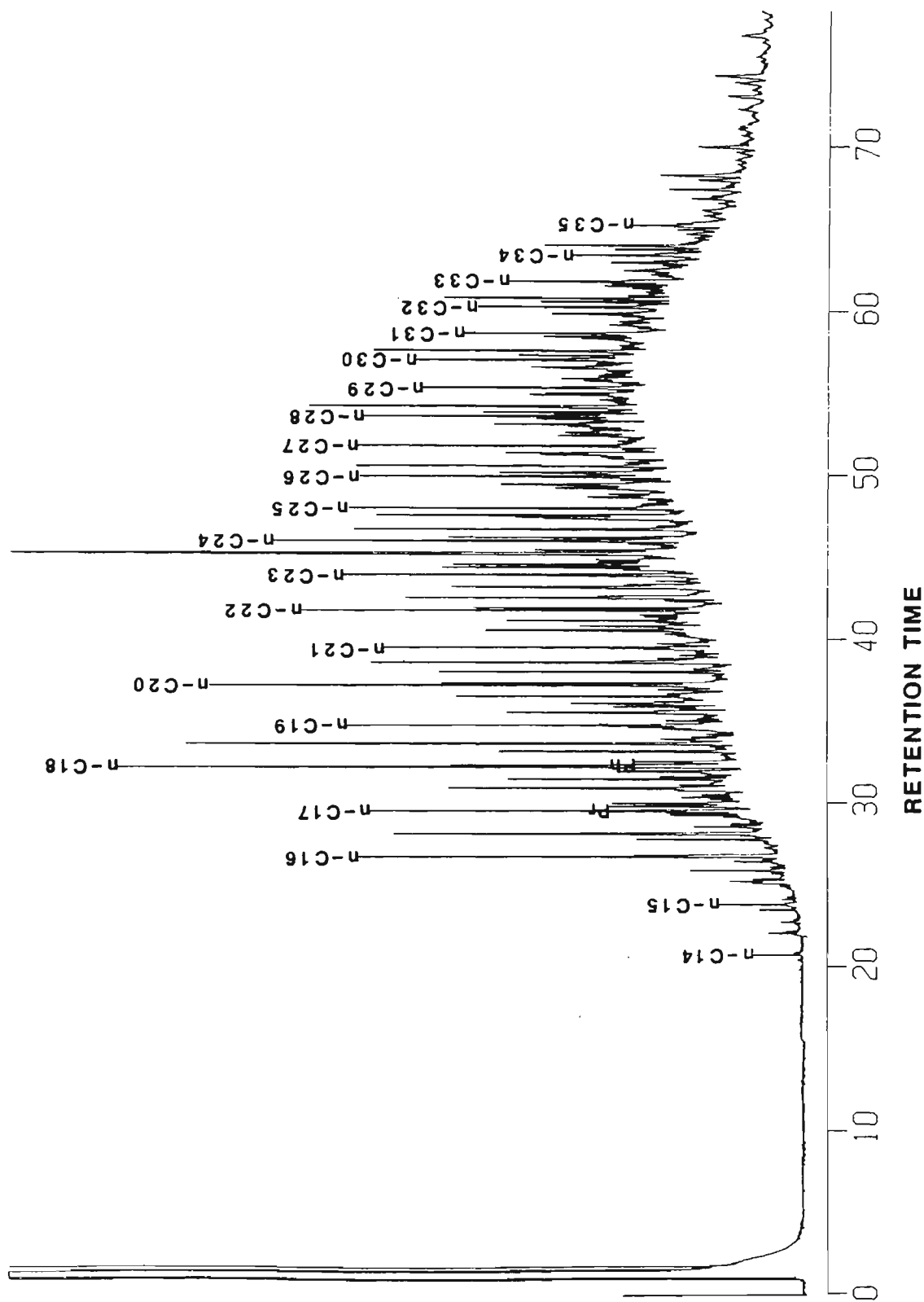


Figure 7.7: N-alkane distribution profiles in the saturated fractions in the extracts shale Tutut Formation, BB10

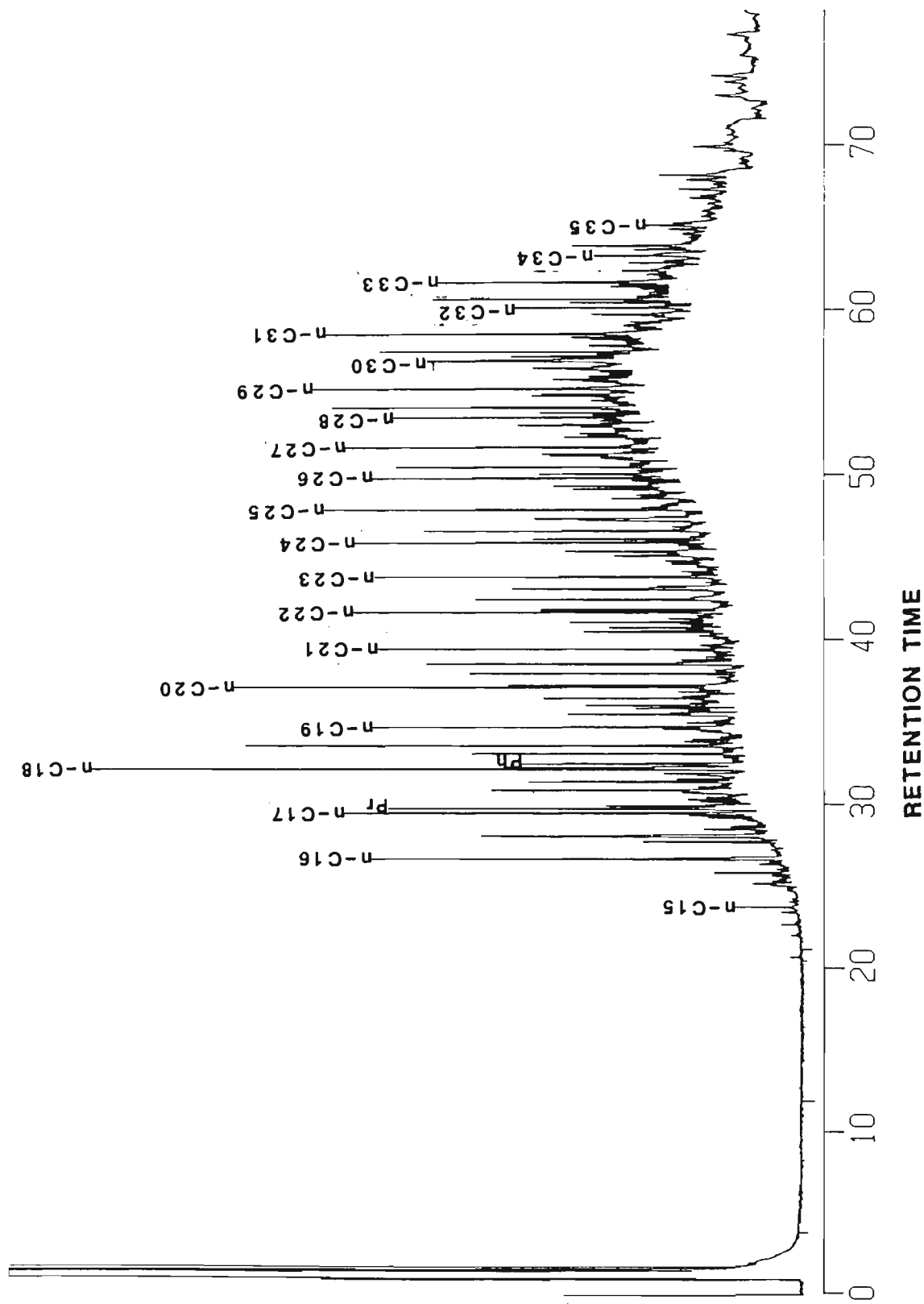


Figure 7.8: N-alkane distribution profiles in the saturated fractions in the extracts shale Kueh Formation, BB25.

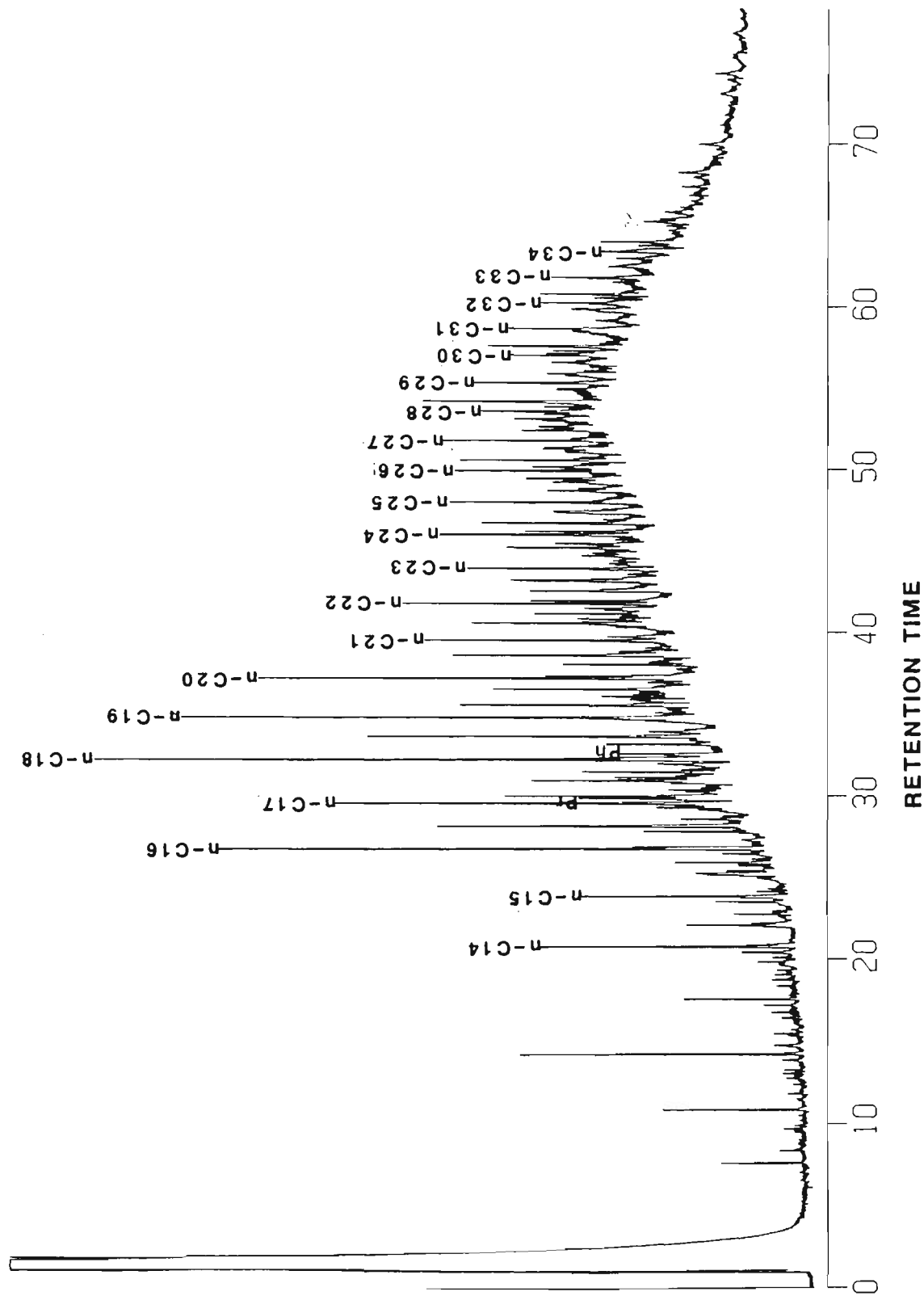


Figure 7.9: N-alkane distribution profiles in the saturated fractions in the extracts shale Tutut Formation, TR9.

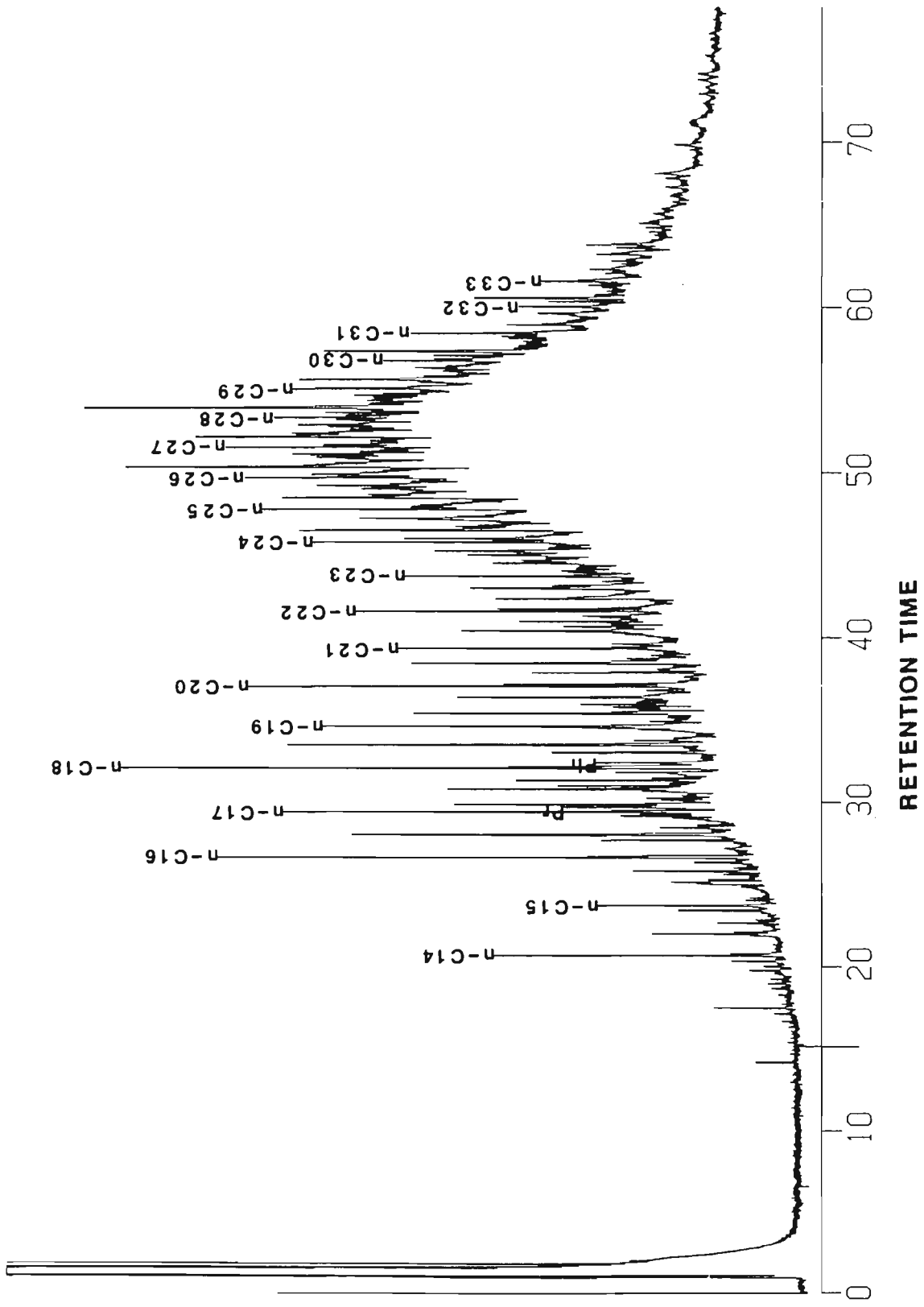


Figure 7.10: N-alkane distribution profiles in the saturated fractions in the extracts shale Kueh Formation, TR17.

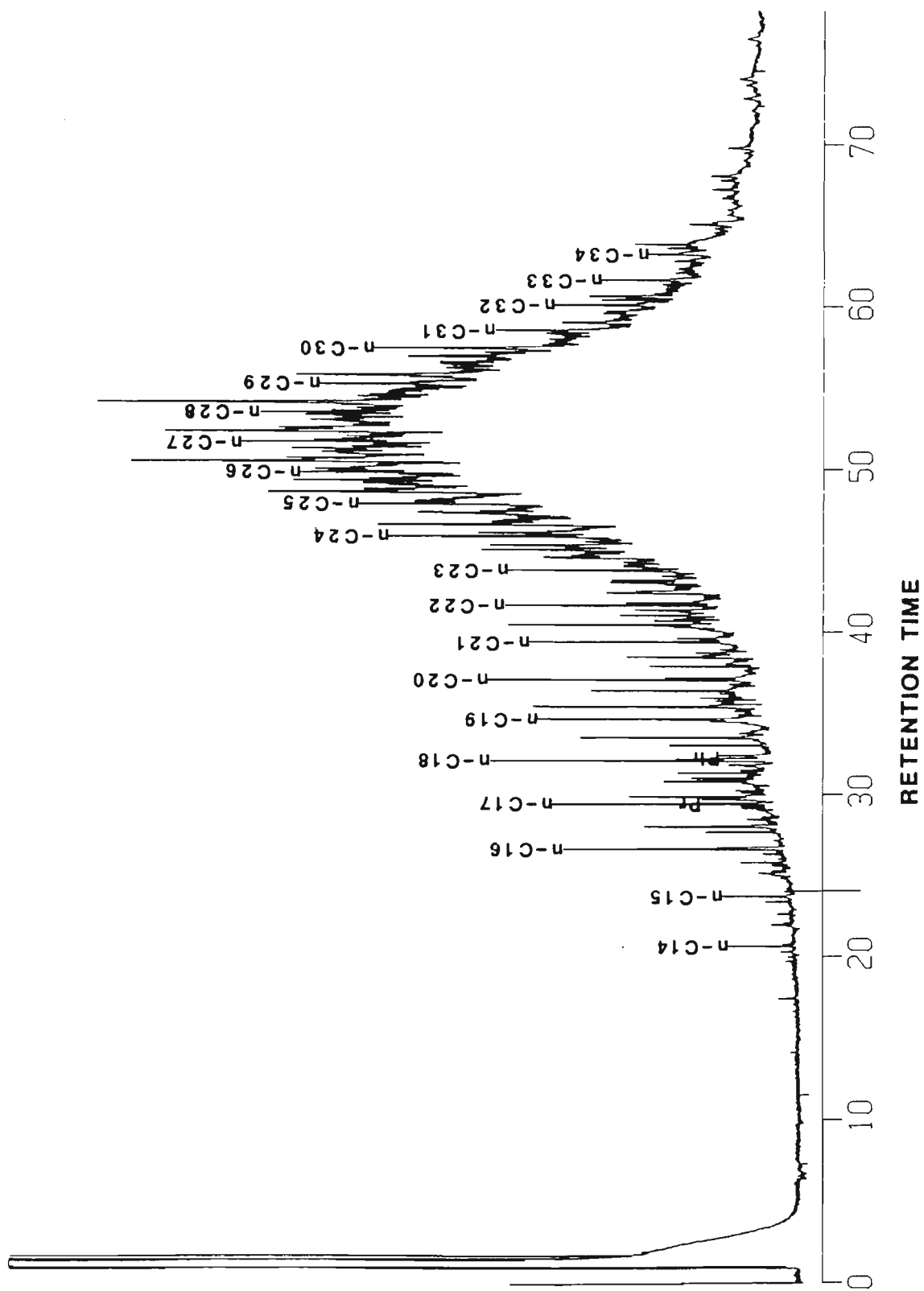


Figure 7.11: N-alkane distribution profiles in the saturated fractions in the extracts shale Kueh, TR27.



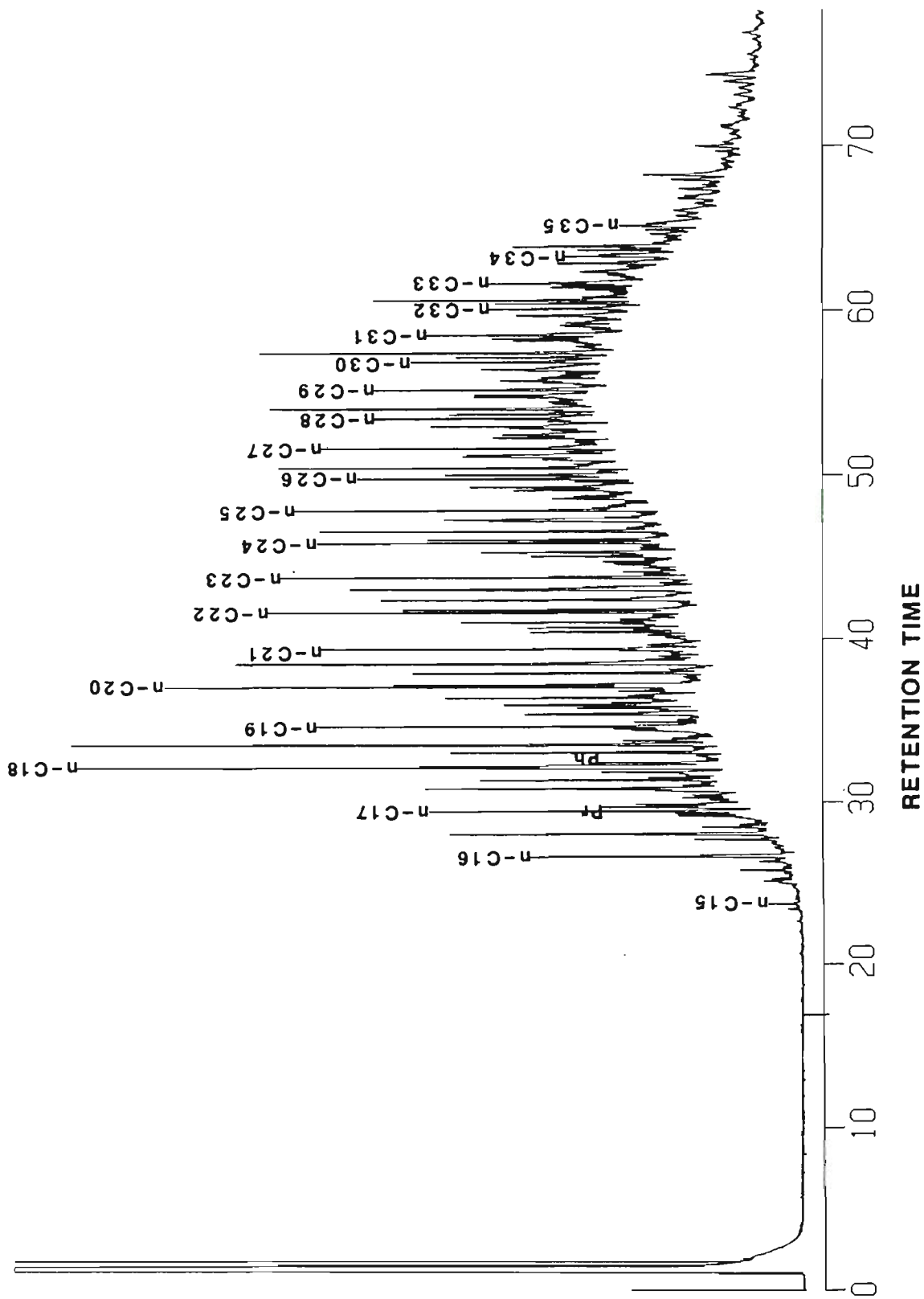


Figure 7.12: N-alkane distribution profiles in the saturated fractions in the extracts shale Kueh Formation, M10.

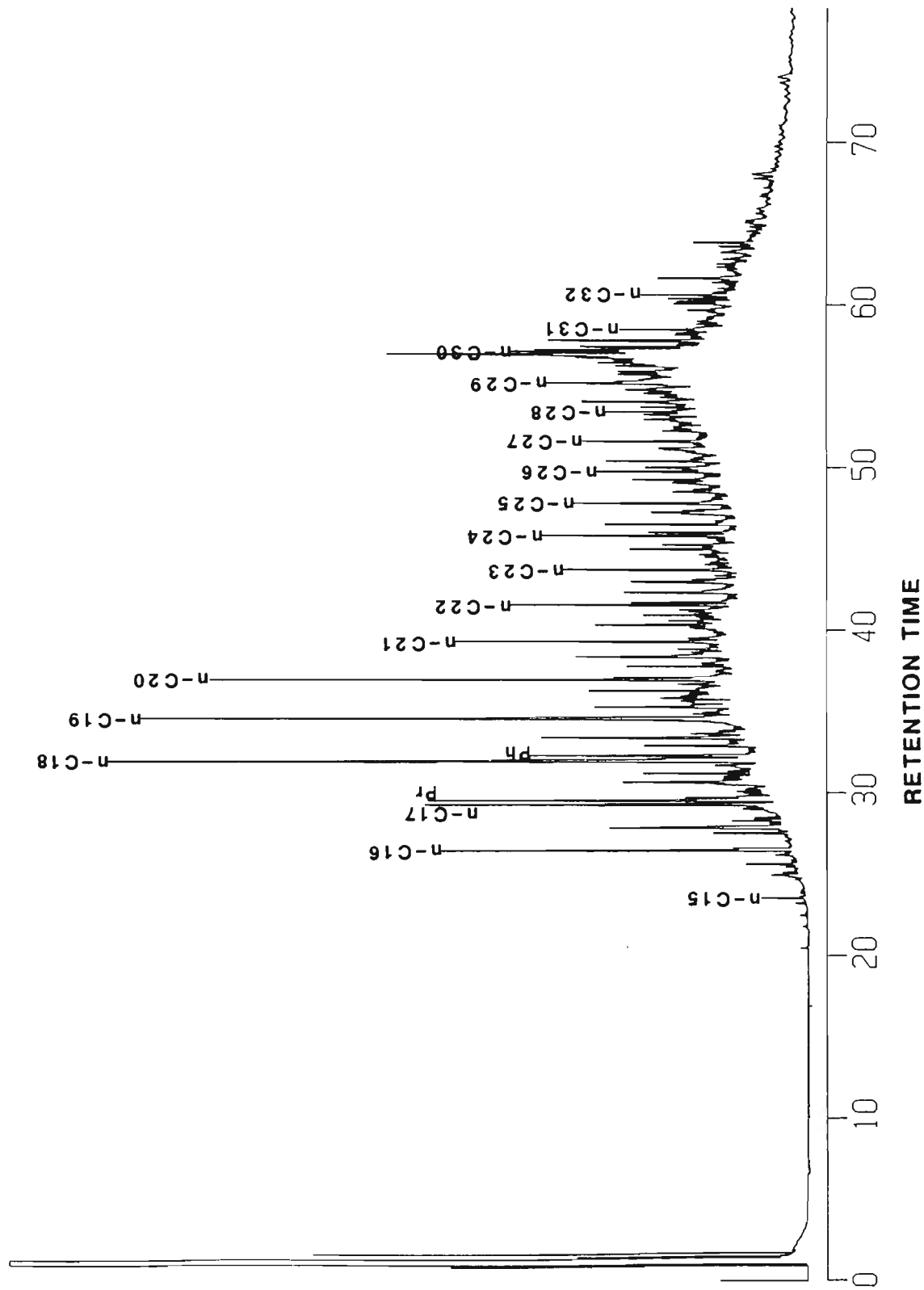


Figure 7.13: N-alkane distribution profiles in the saturated fractions in the extracts shale Kueh Formation, M16.

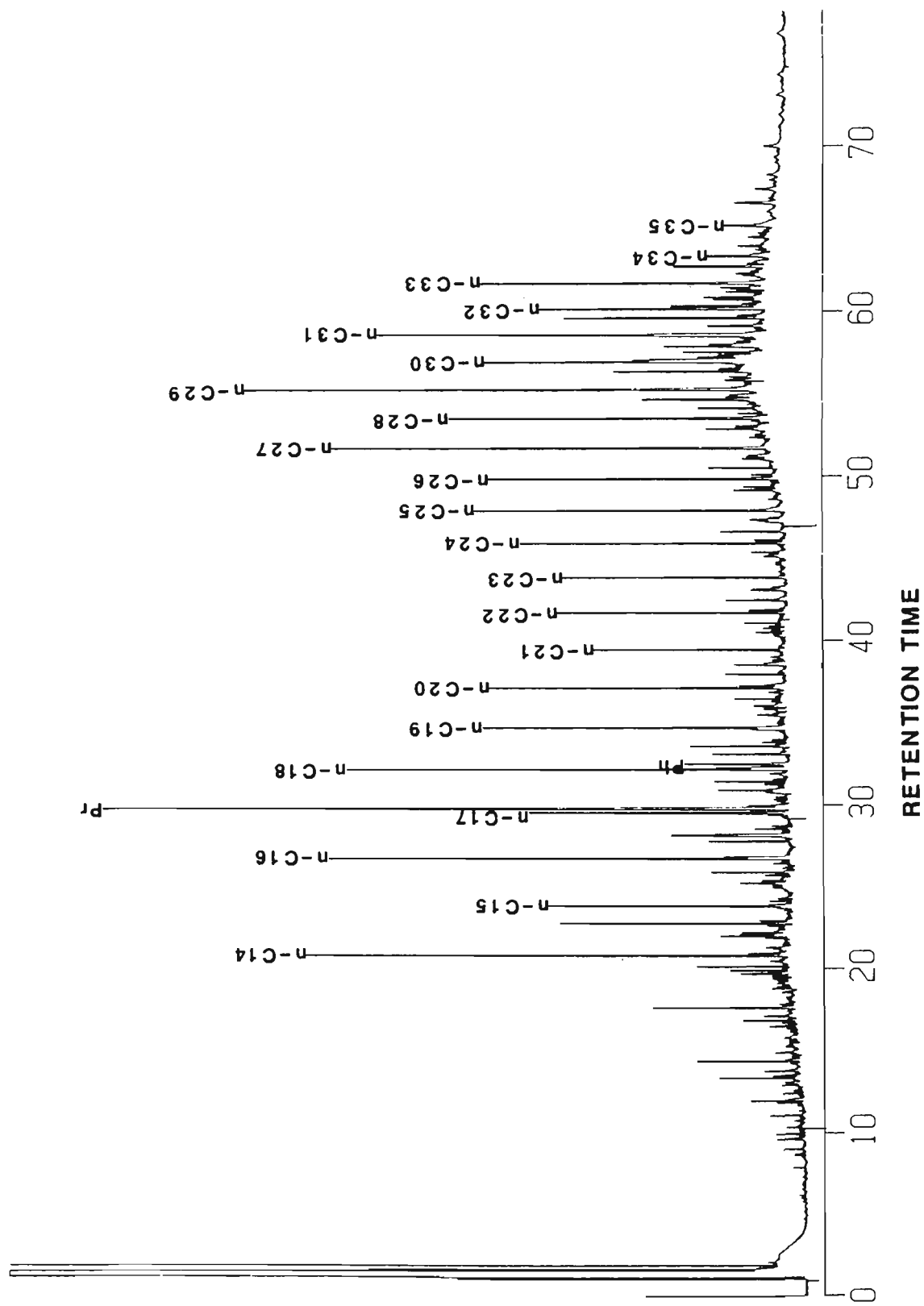


Figure 7.14: N-alkane distribution profiles in the saturated fractions in the extracts shale Tangla Formation, M21.

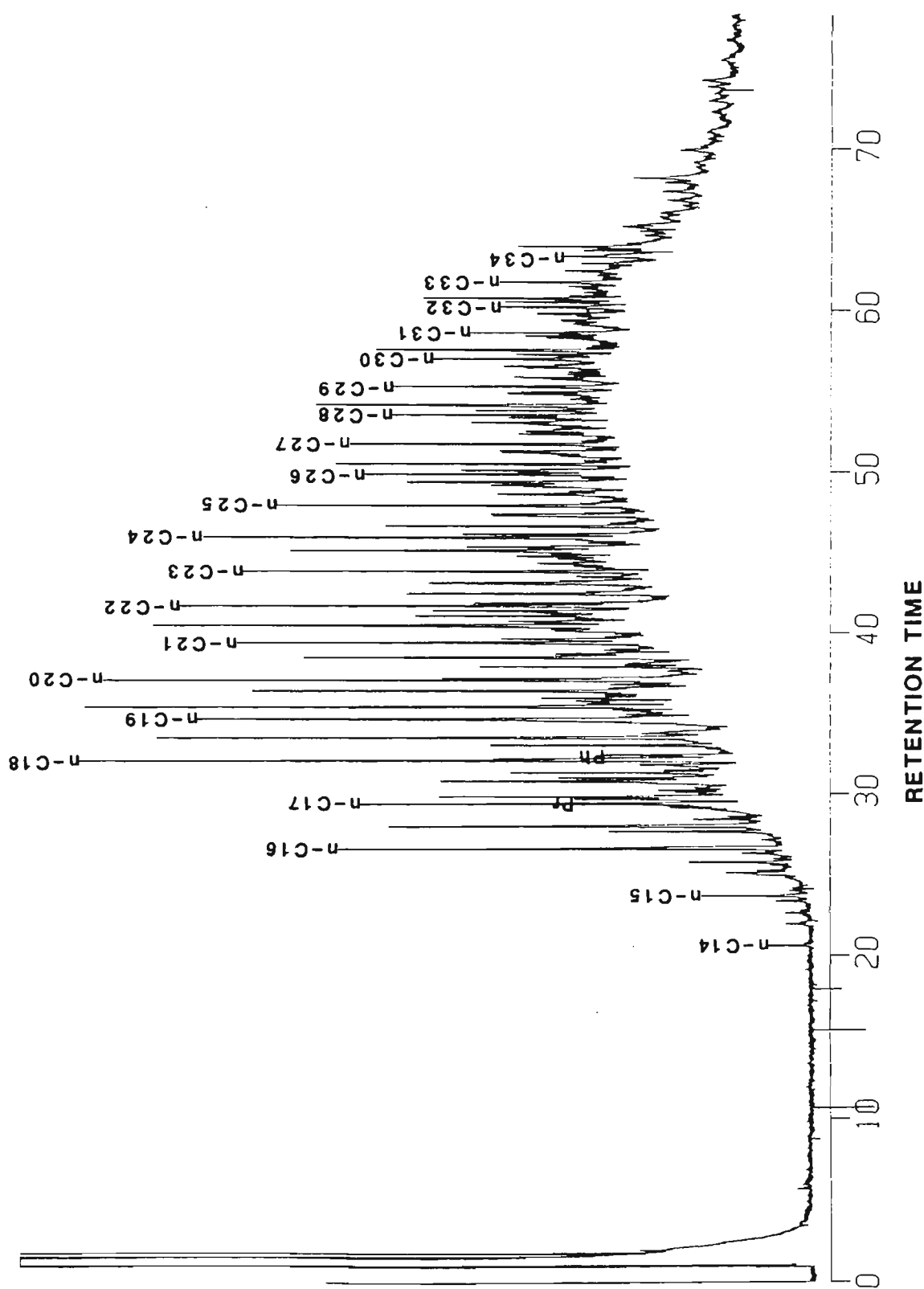


Figure 7.15: N-alkane distribution profiles in the saturated fractions in the extracts shale Tutut Formation, TN15.

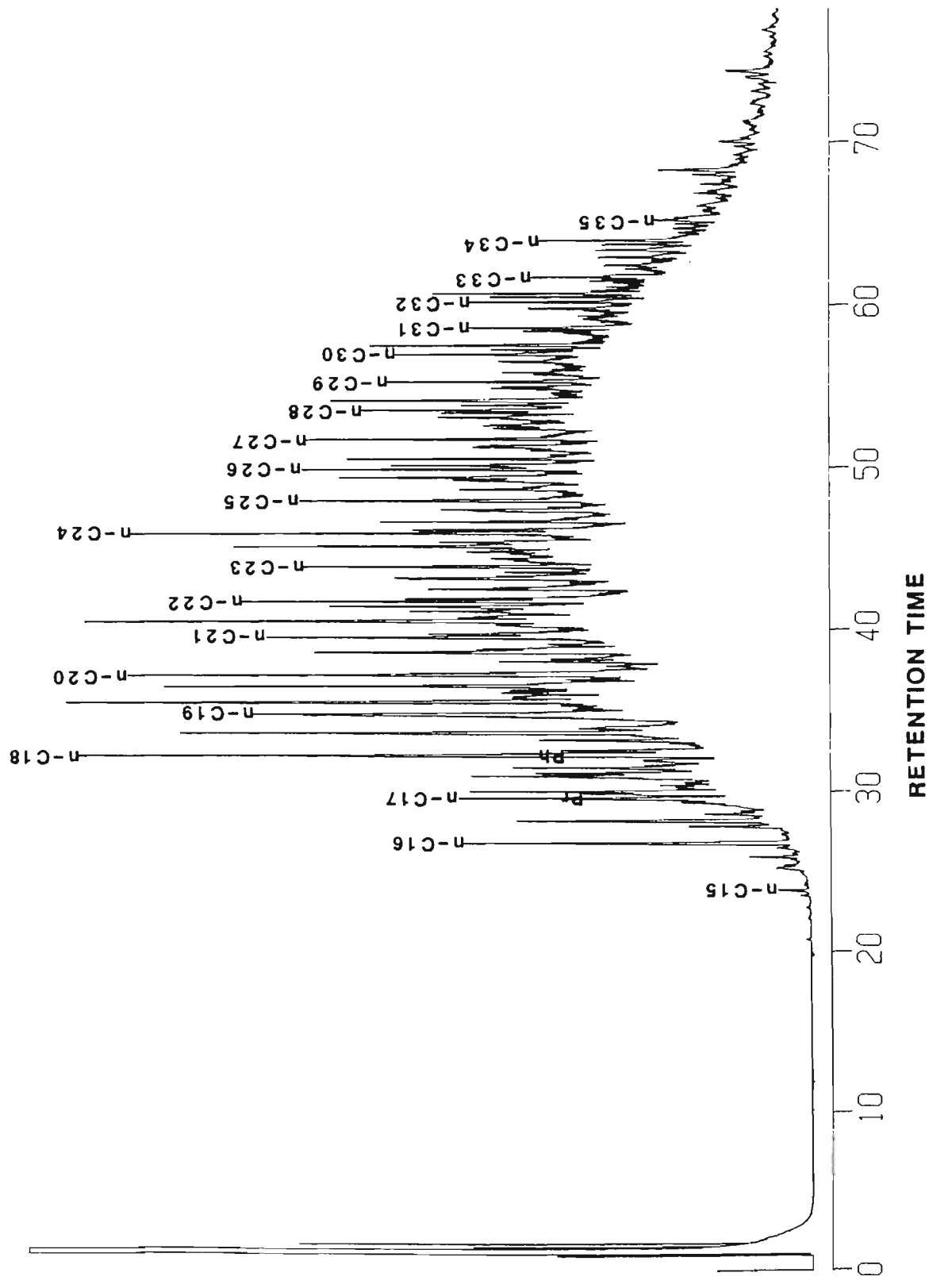


Figure 7.16: N-alkane distribution profiles in the saturated fractions in the extracts shale Tutut Formation, TN18.

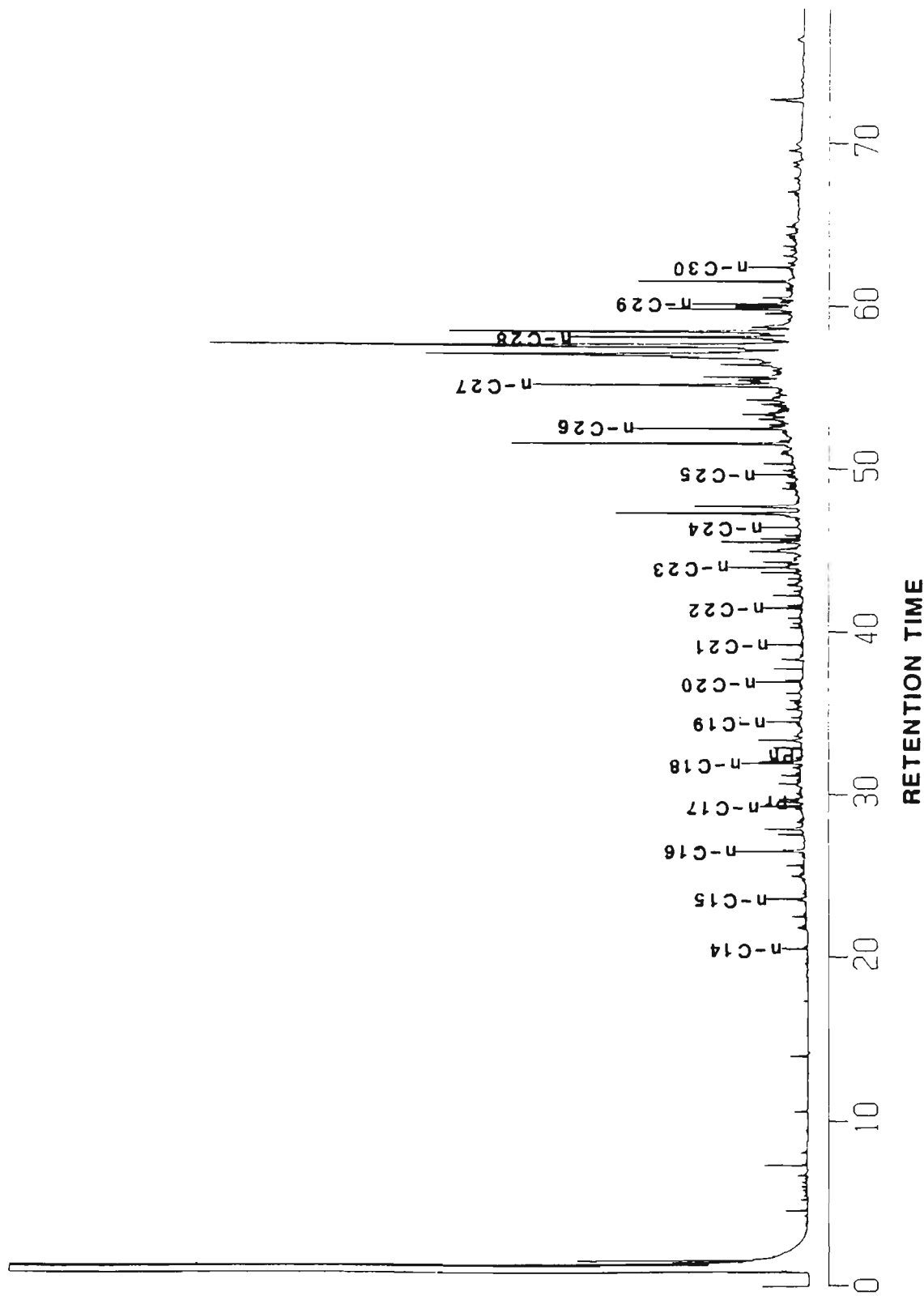


Figure 7.17: N-alkane distribution profiles in the saturated fractions in the extracts coal-Pliocene coal, MBOI/1.

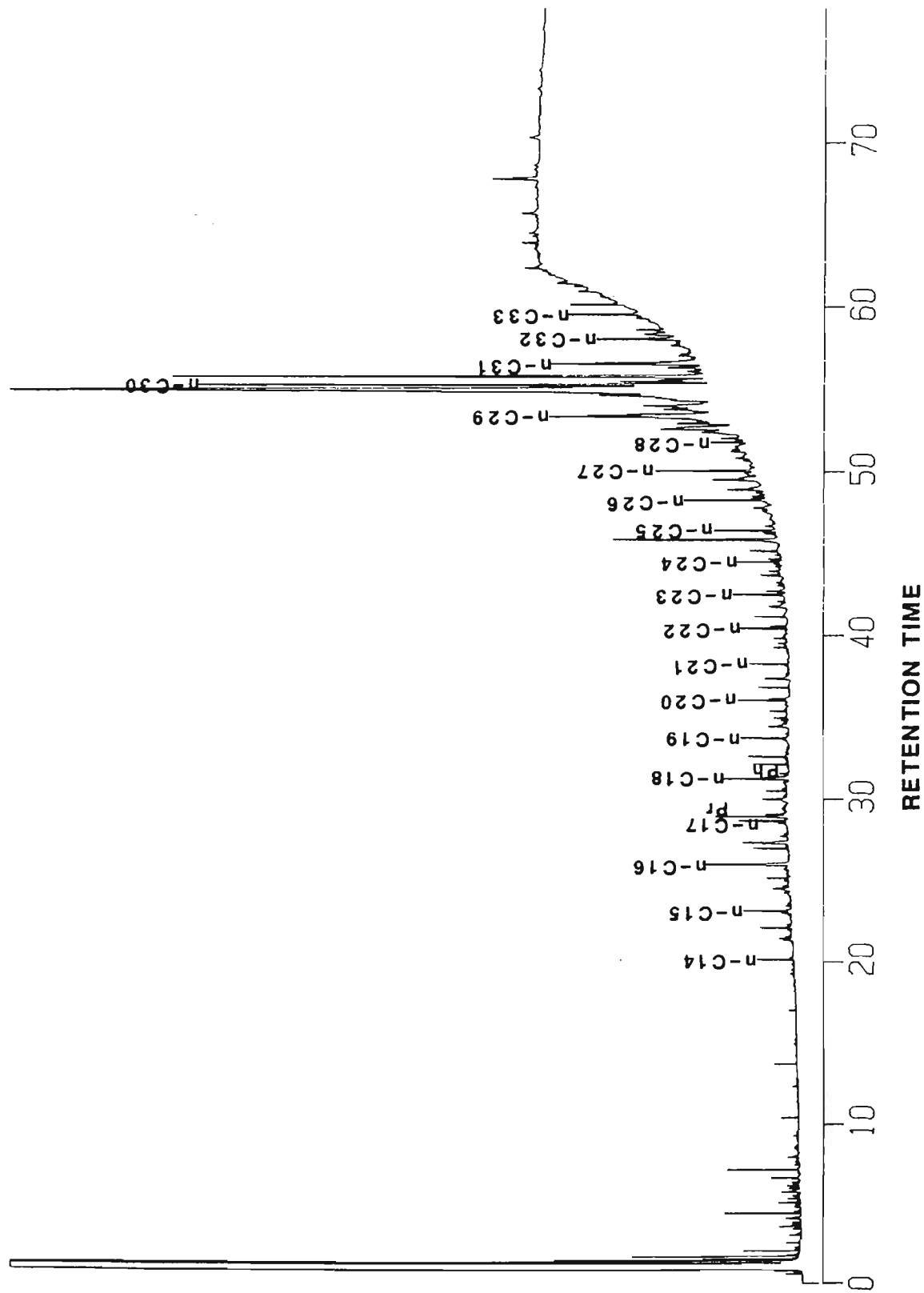


Figure 7.18: N-alkane distribution profiles in the saturated fractions in the extracts coal-Pliocene coal, M22/2

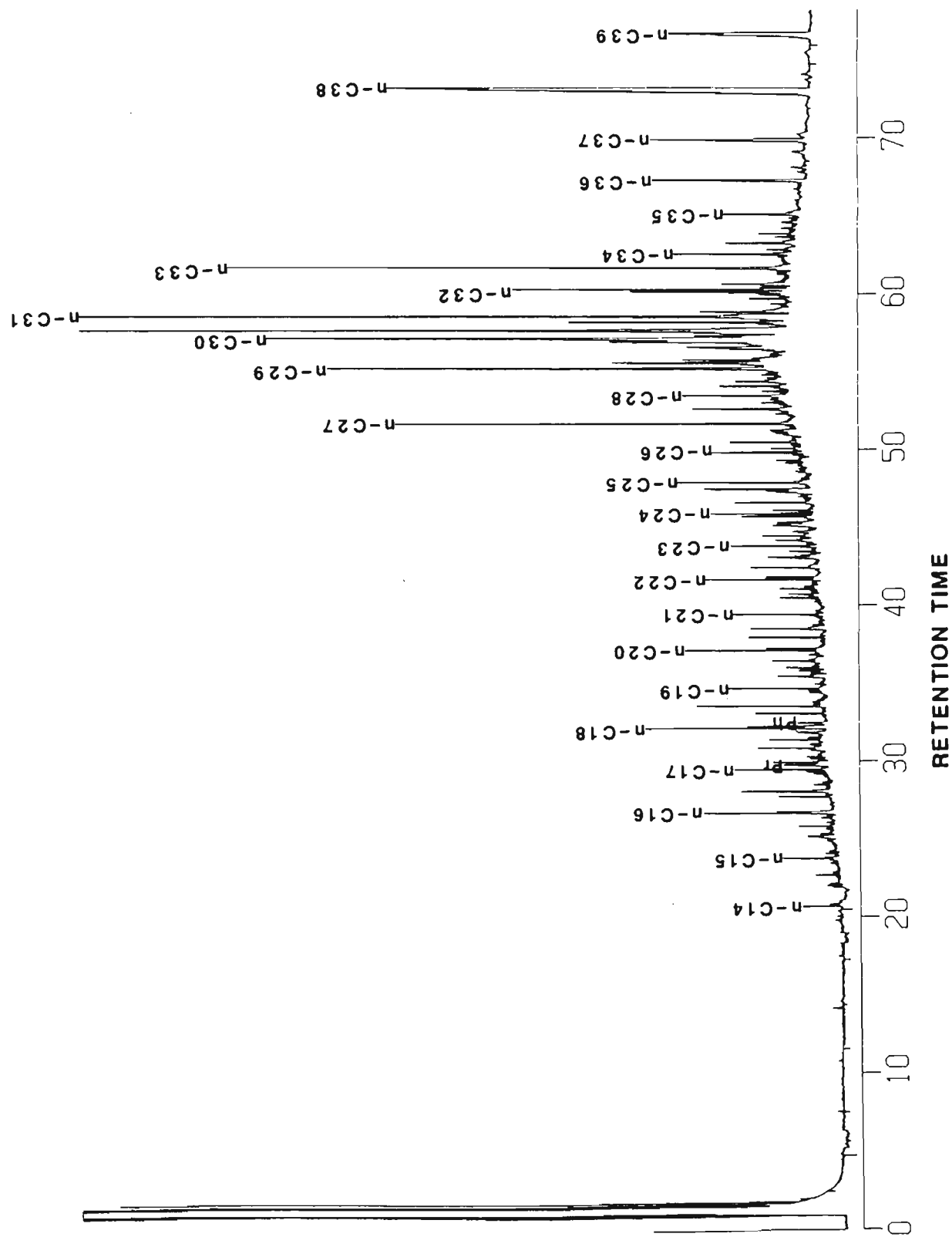


Figure 7.19: N-alkane distribution profiles in the saturated fractions in the extracts coal-Pliocene coal, BB2.



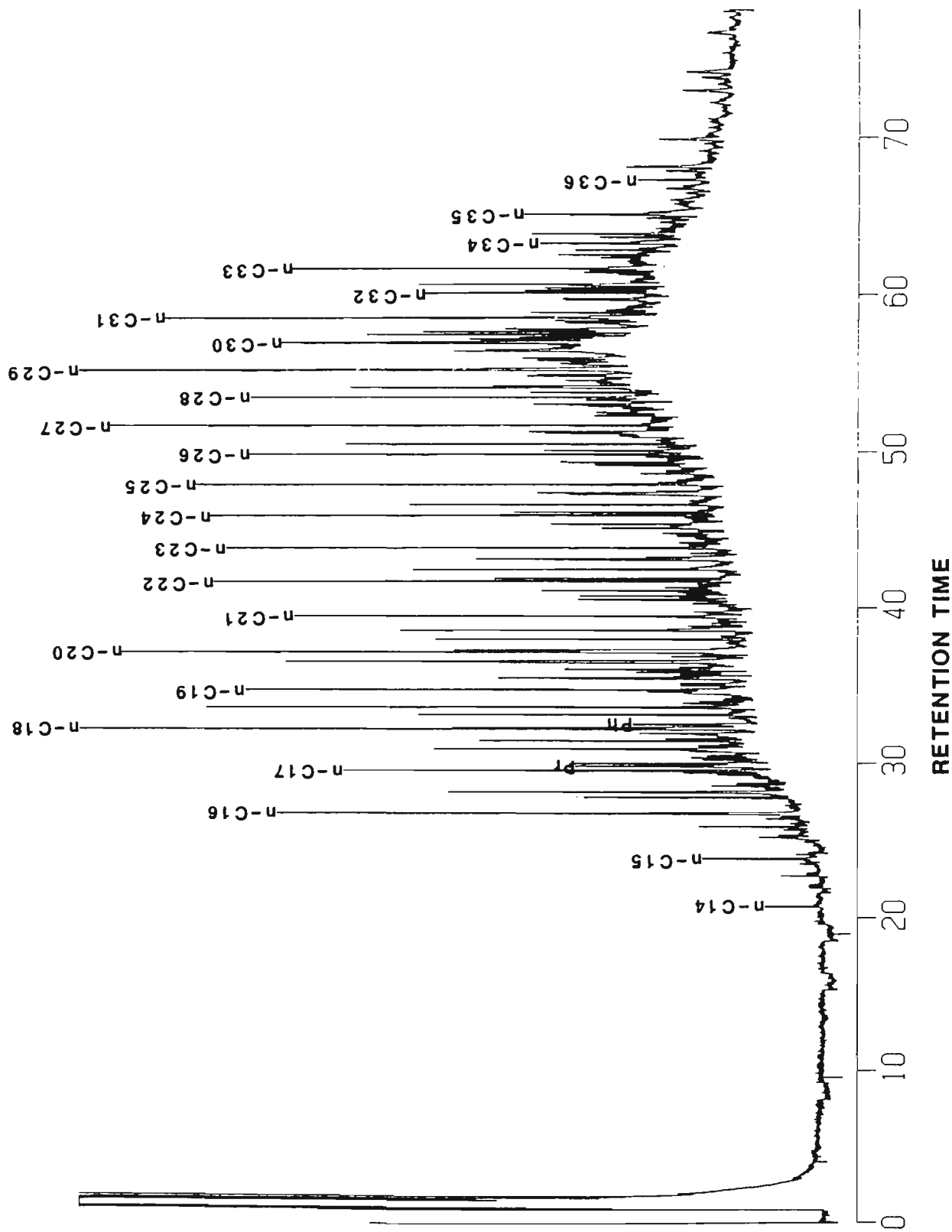


Figure 7.20: N-alkane distribution profiles in the saturated fractions in the extracts coal-Miocene coal, TR36.

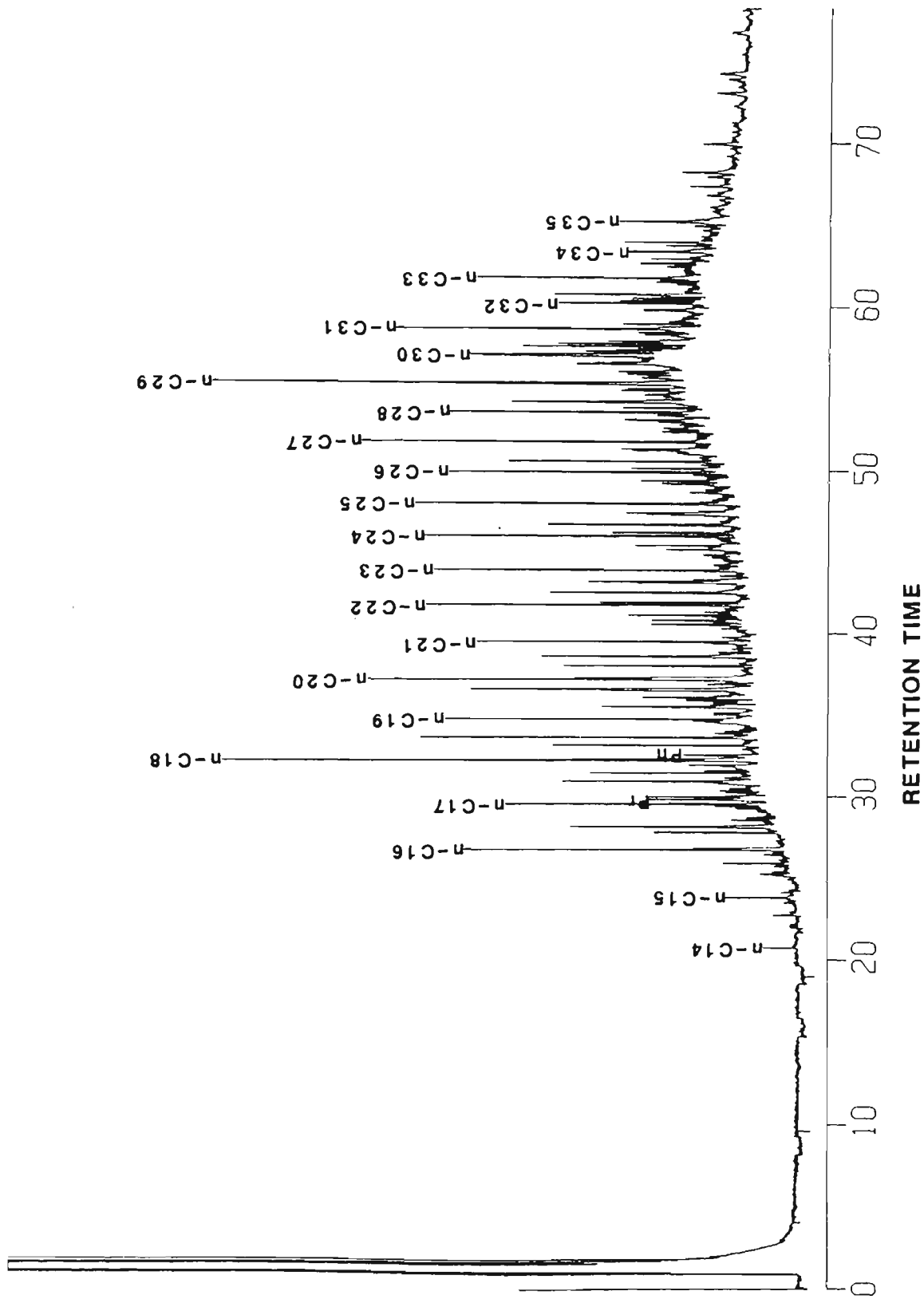


Figure 7.21: N-alkane distribution profiles in the saturated fractions in the extracts coal-Miocene coal, BB19.

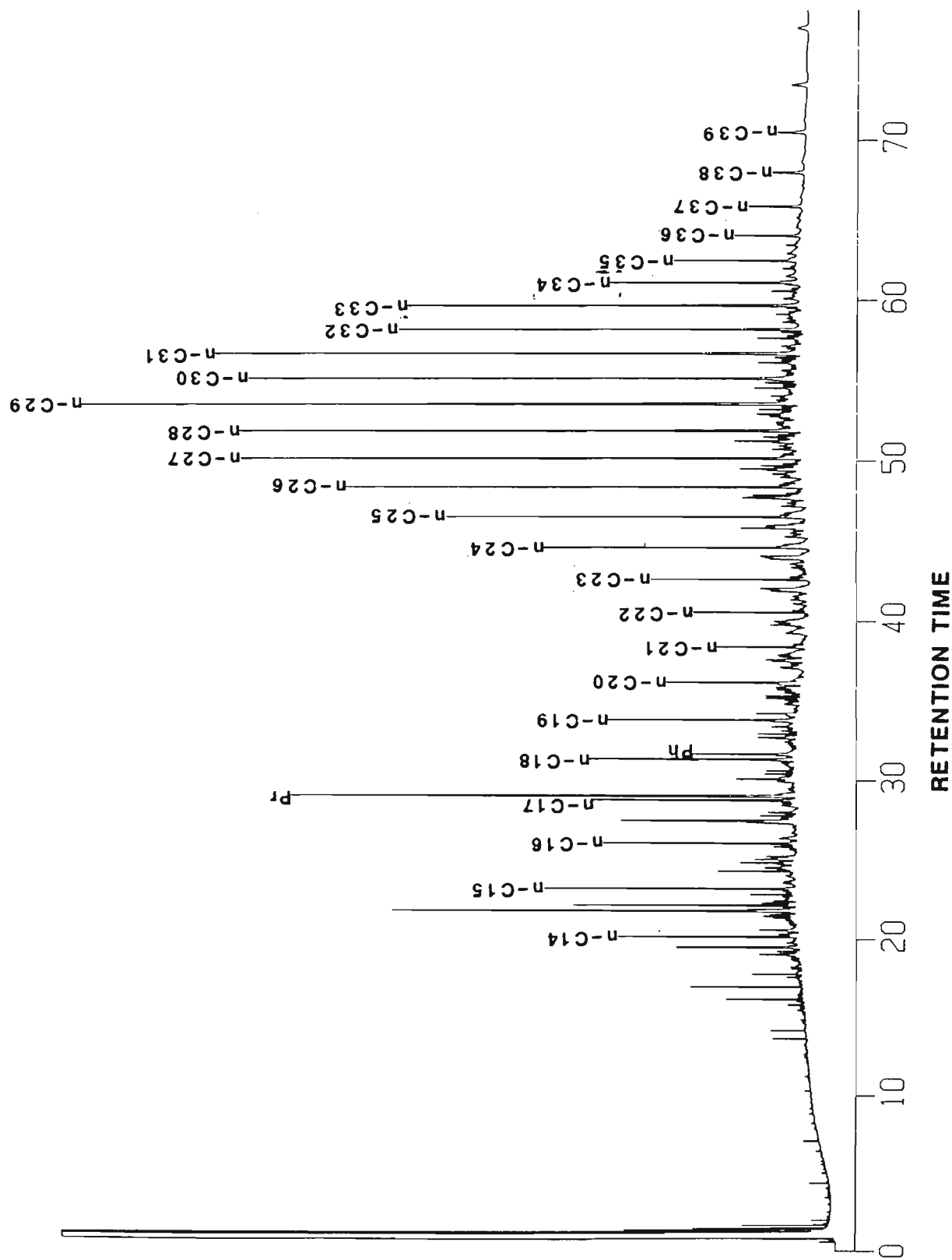


Figure 7.22: N-alkane distribution profiles in the saturated fractions in the extracts coal-Miocene coal, K20.

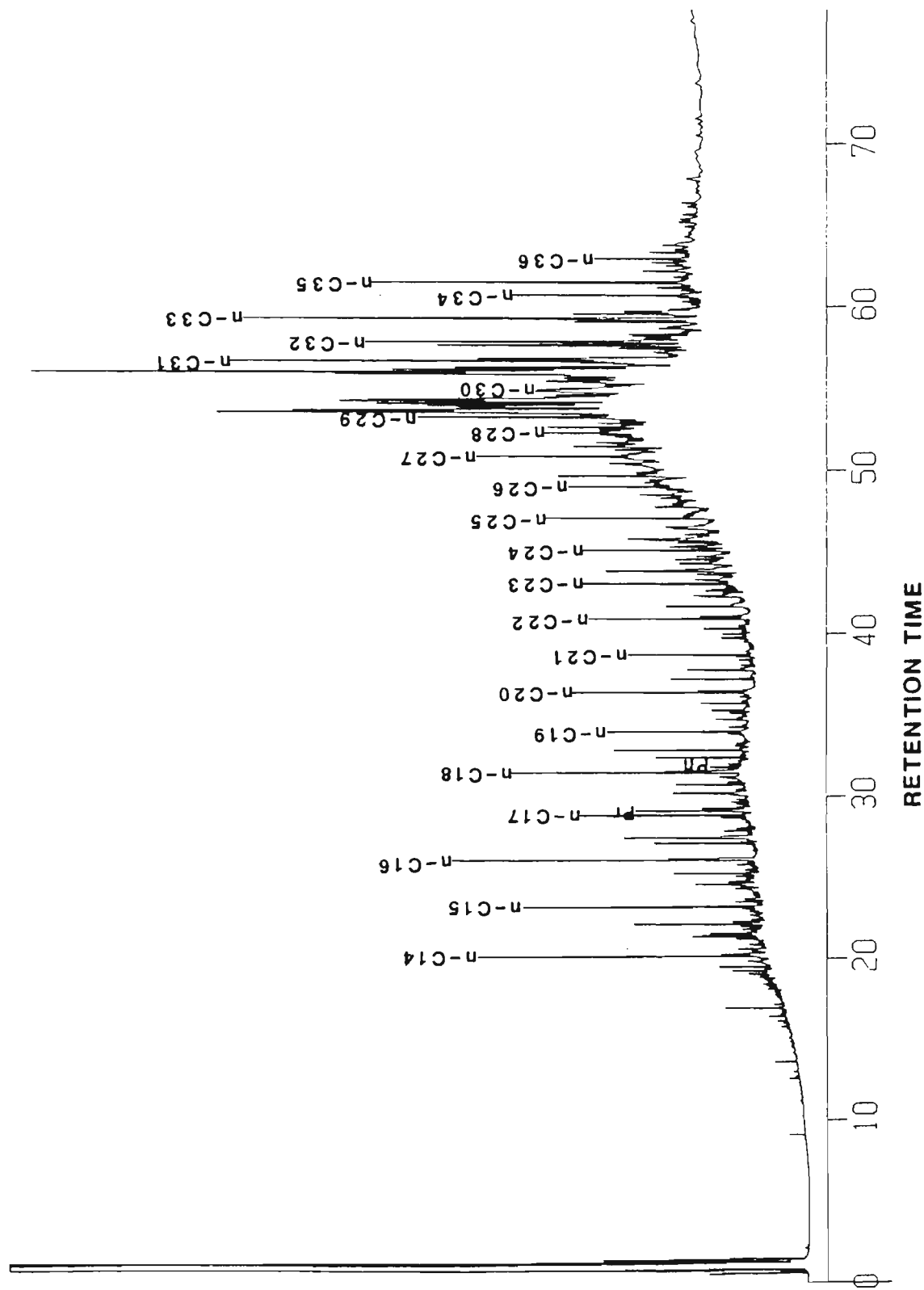


Figure 7.23: N-alkane distribution profiles in the saturated fractions in the extracts coal-Miocene coal, K23.

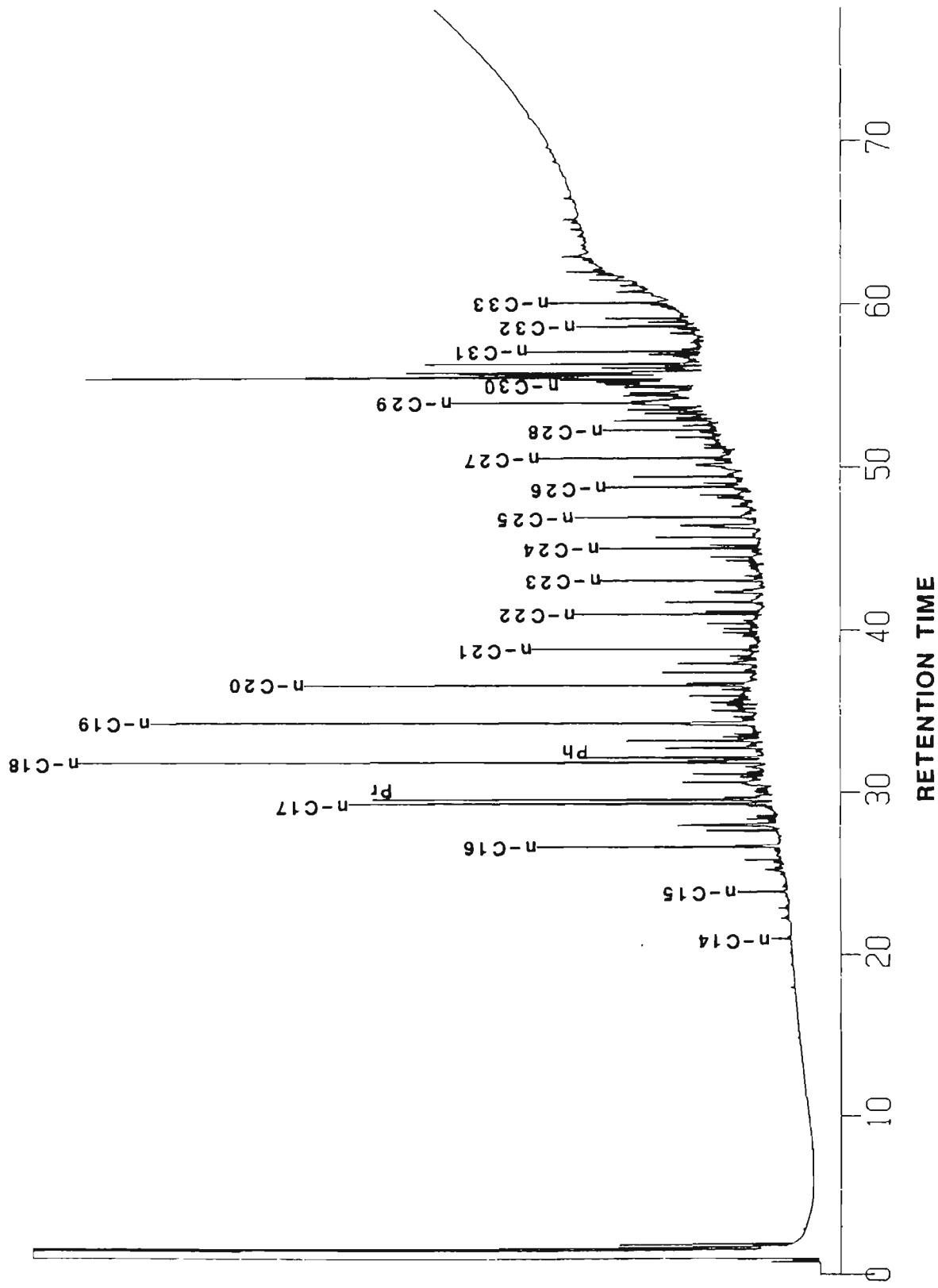


Figure 7.24: N-alkane distribution profiles in the saturated fractions in the extracts coal-Oligocene coal, M19.

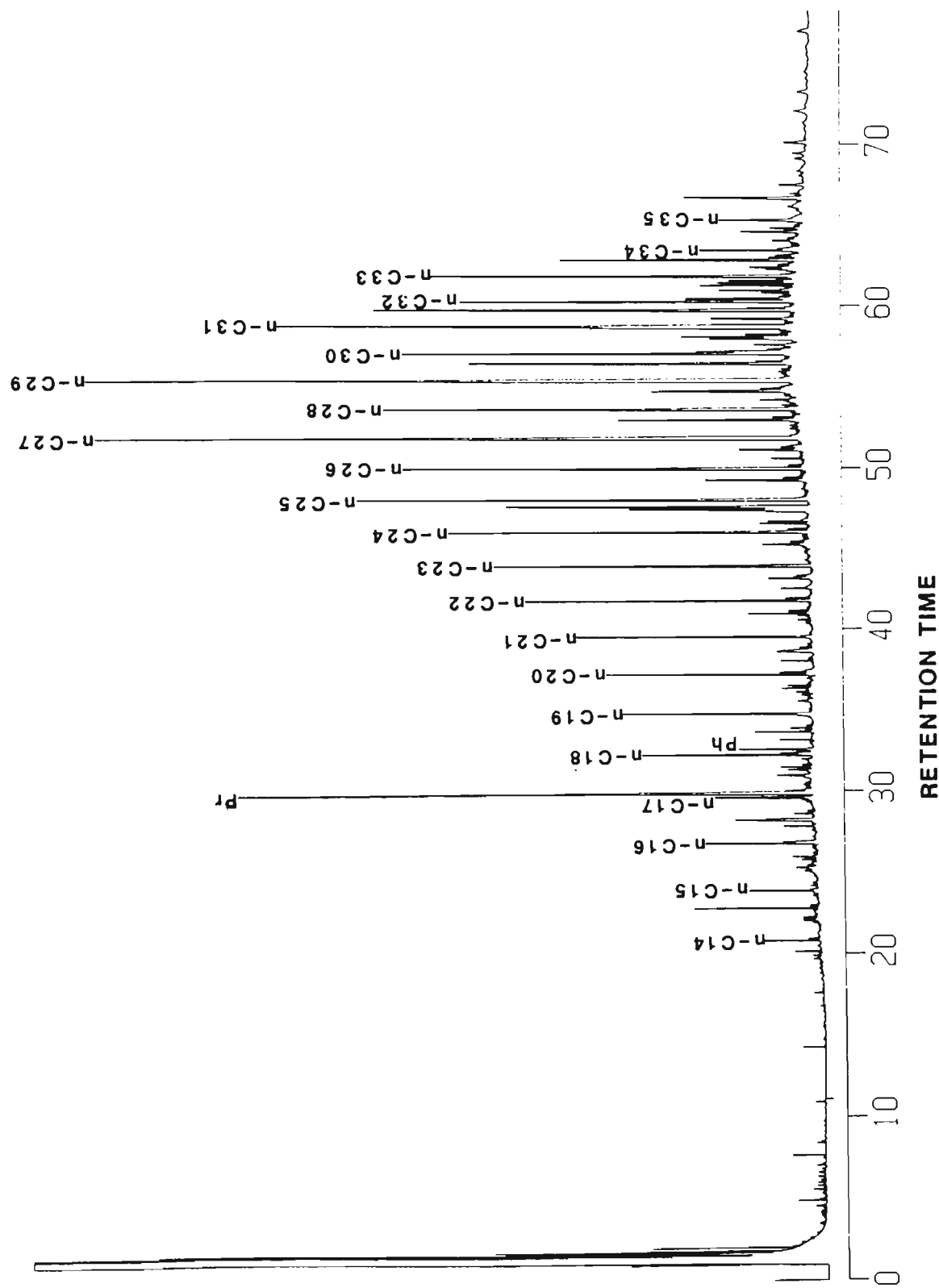


Figure 7.25: N-alkane distribution profiles in the saturated fractions in the extracts coal-Oligocene coal, L5.

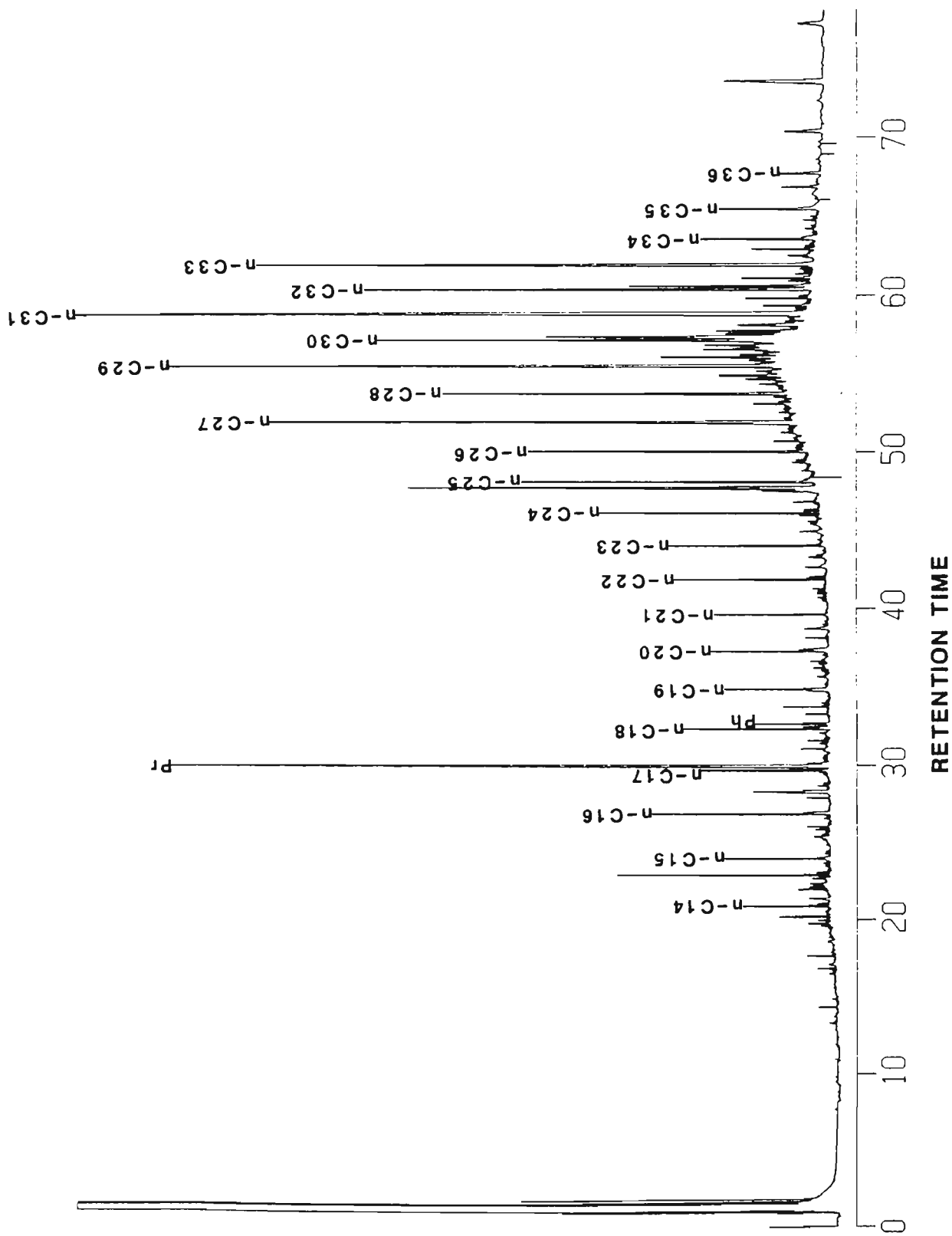


Figure 7.26: N-alkane distribution profiles in the saturated fractions in the extracts coal-Oligocene coal, L14.

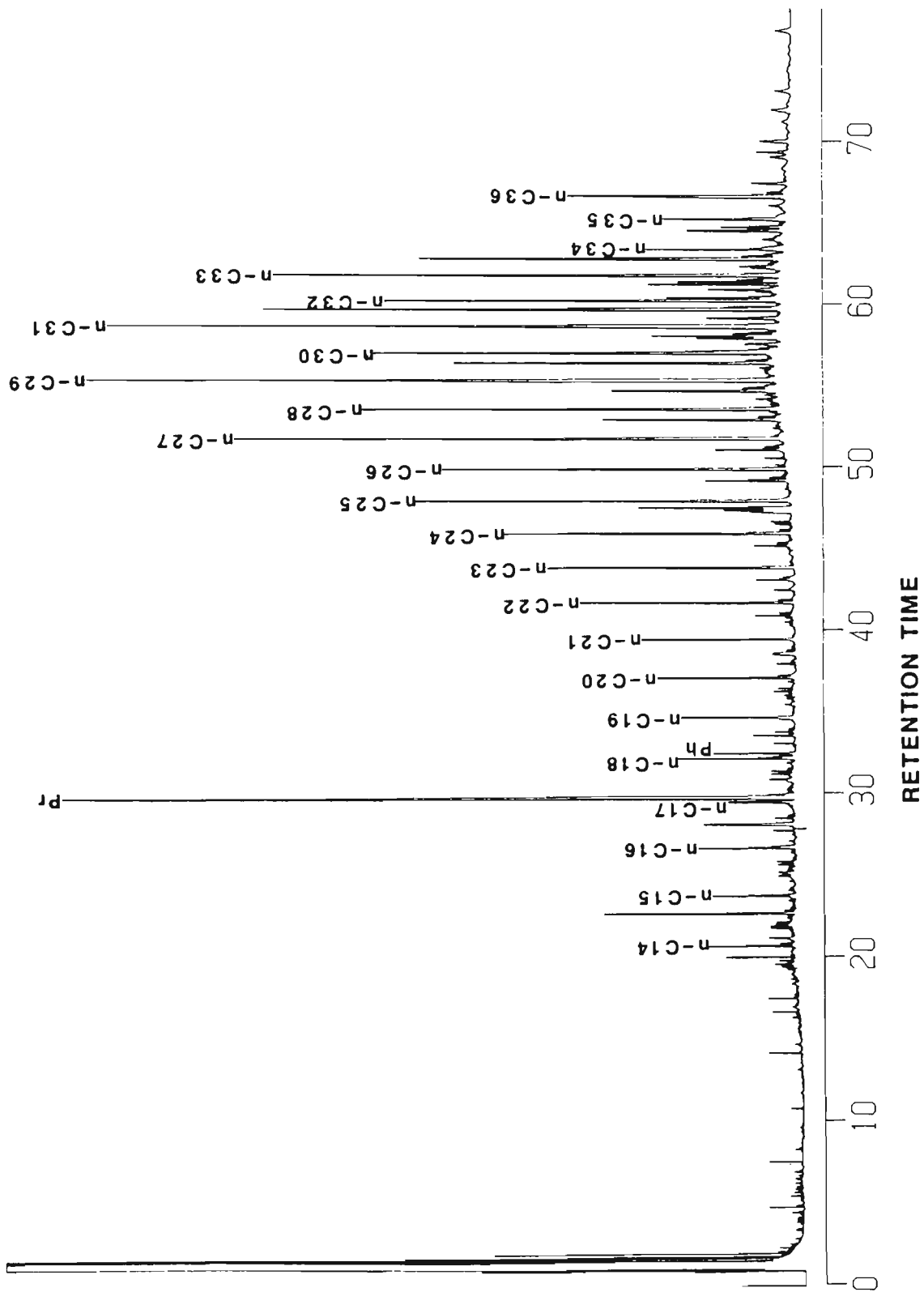


Figure 7.27: N-alkane distribution profiles in the saturated fractions in the extracts coal-Oligocene coal, L21.



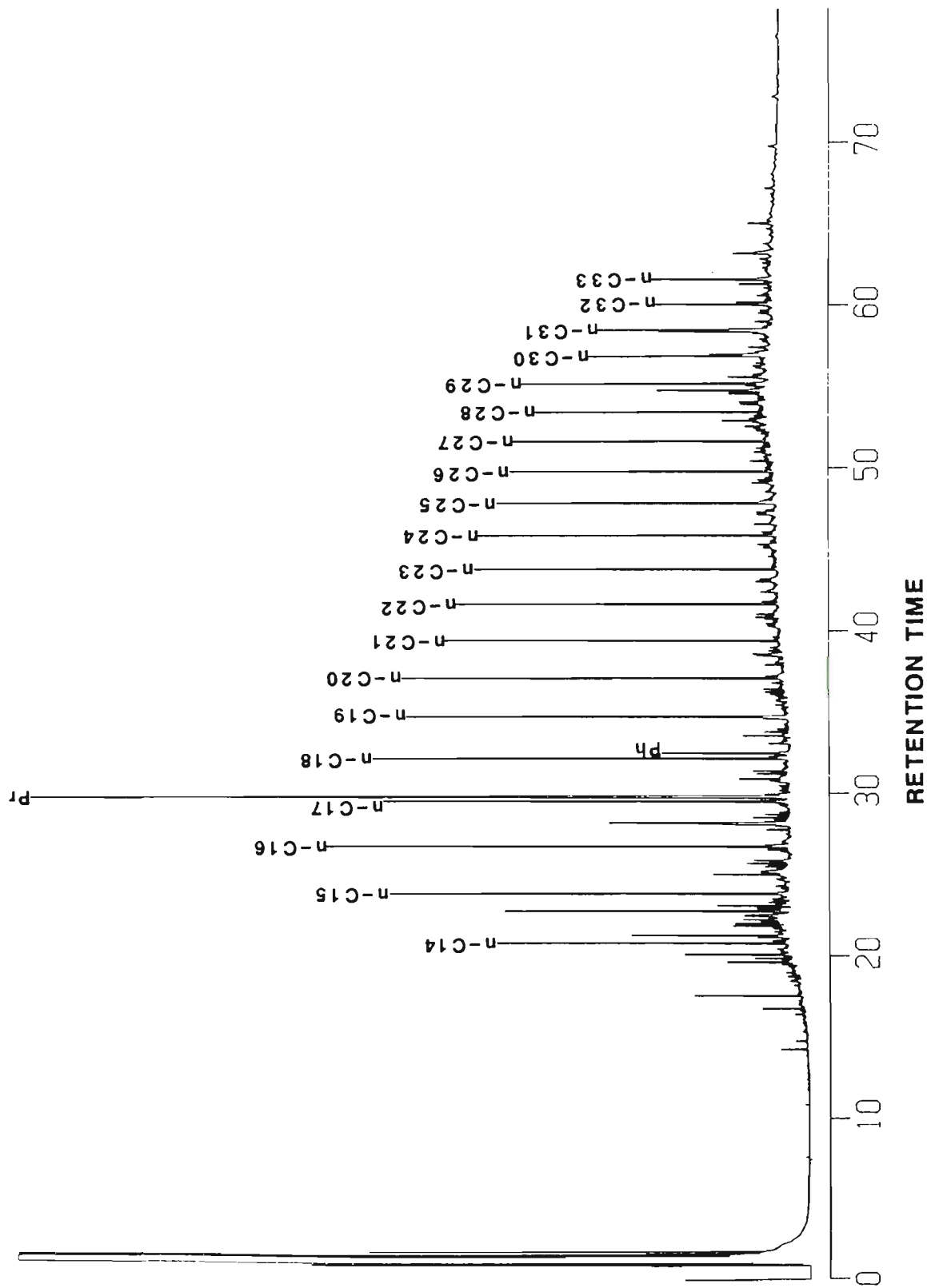


Figure 7.28: N-alkane distribution profiles in the saturated fractions in the extracts coal-Oligocene coal, L20.

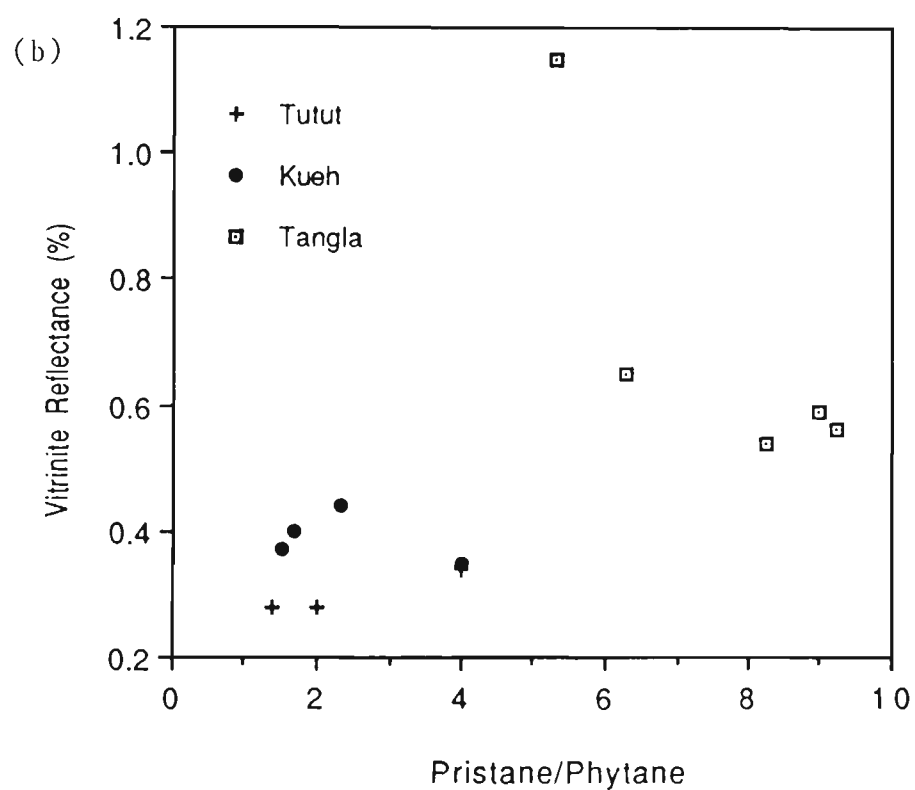
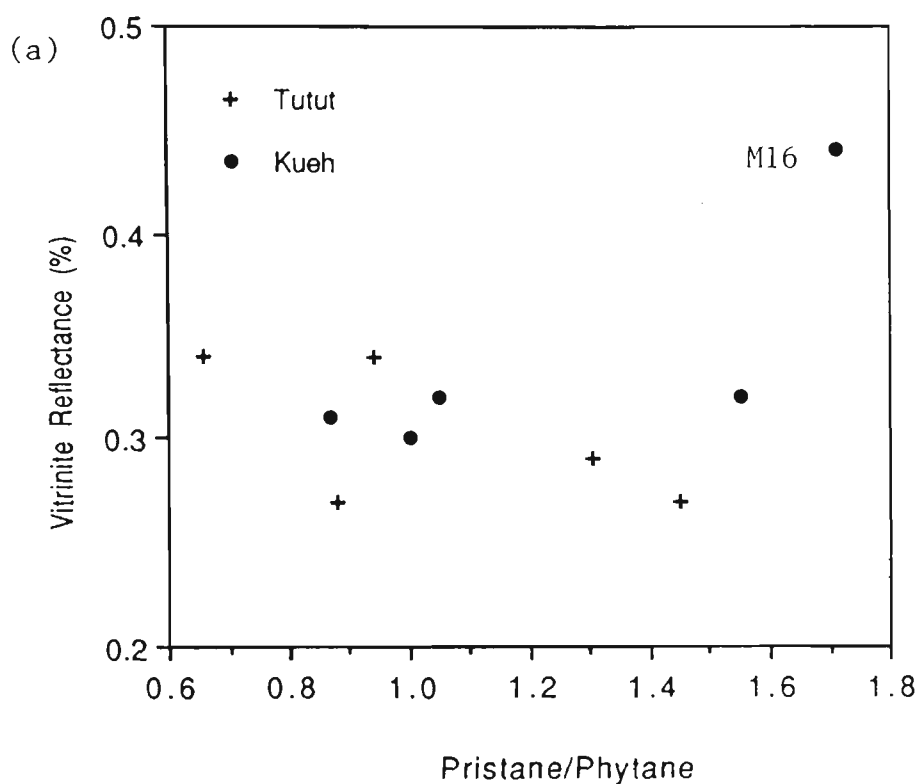


Figure 7.29: Relationship between the vitirinite reflectance and pristane to phytane ratios, (a) shale; (b) coal.

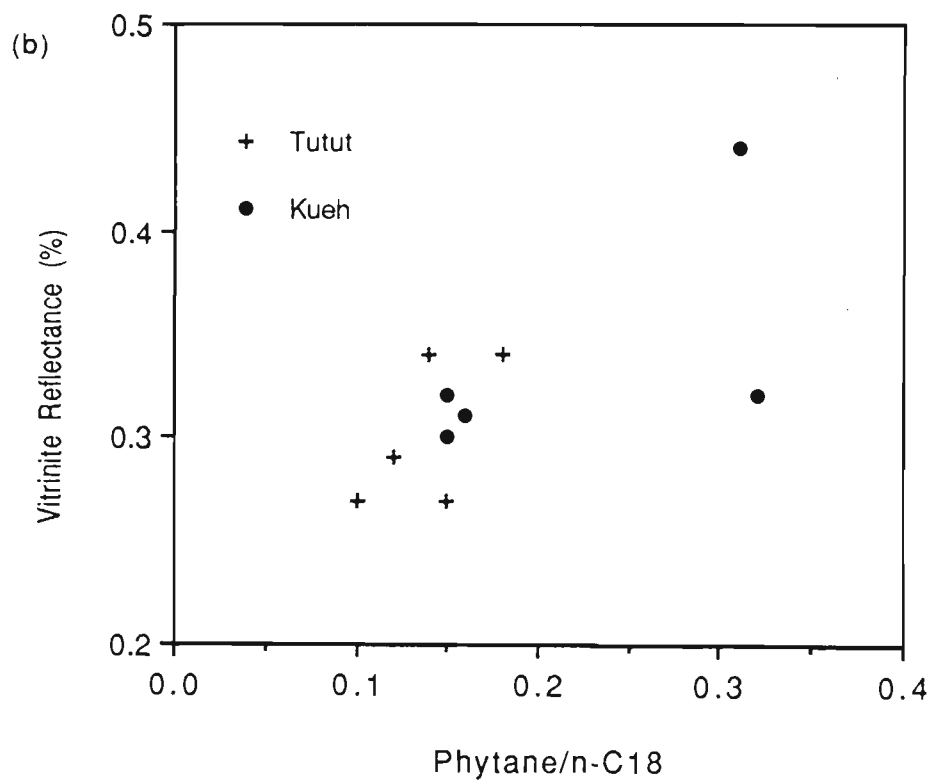
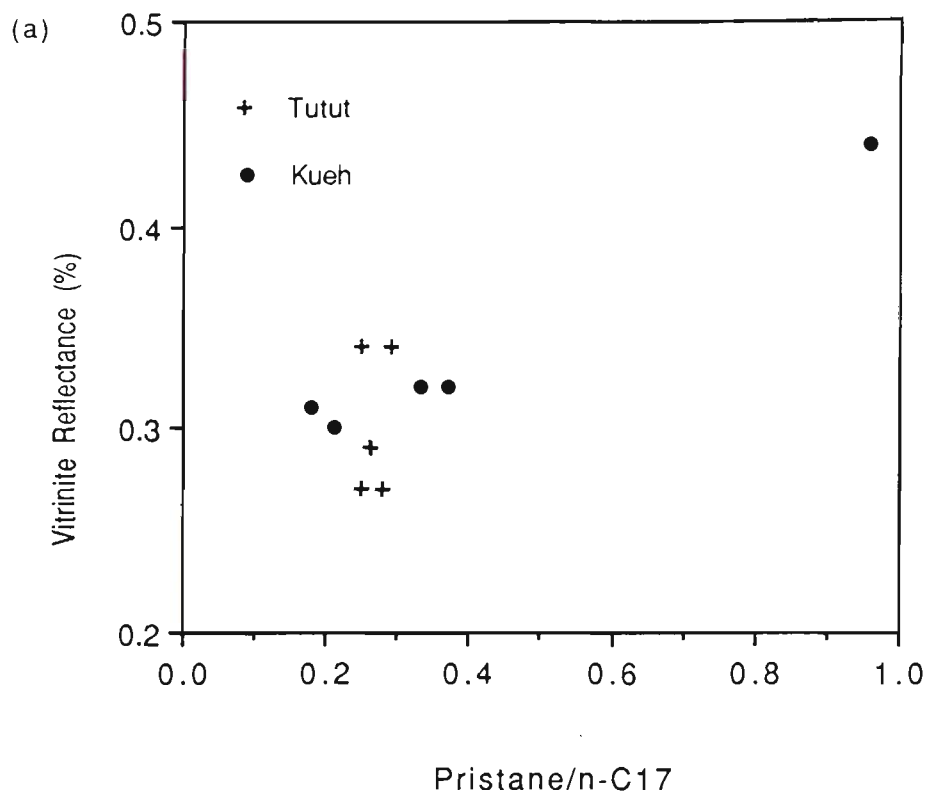


Figure 7.30: Relationship between (a) the vitrinite reflectance to pristane/n-C17; (b) the vitrinite reflectance and ph/n-C18 for shale samples.

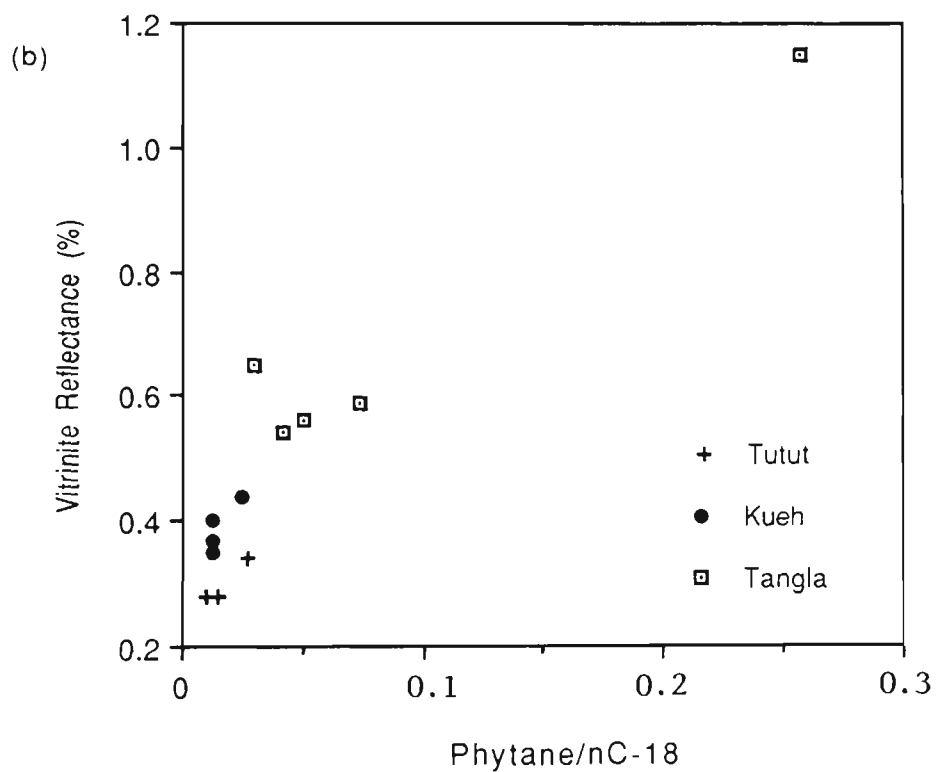
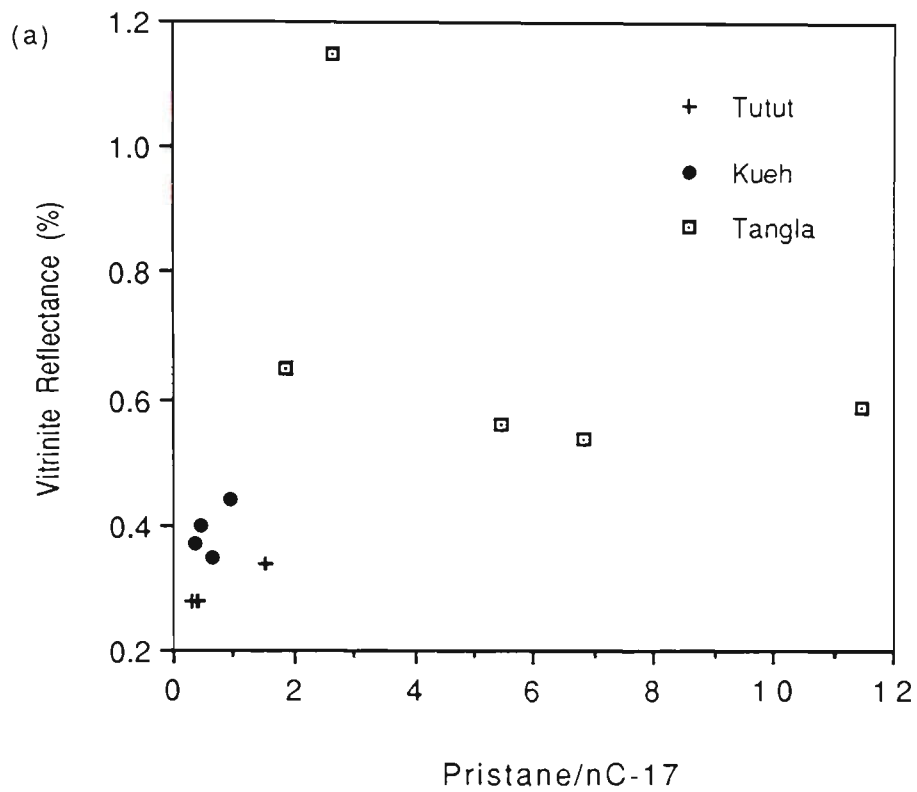


Figure 7.31: Relationship between (a) the vitrinite reflectance to pristane /n-C17; (b) the vitrinite reflectance and ph/n-C18 for coal samples.

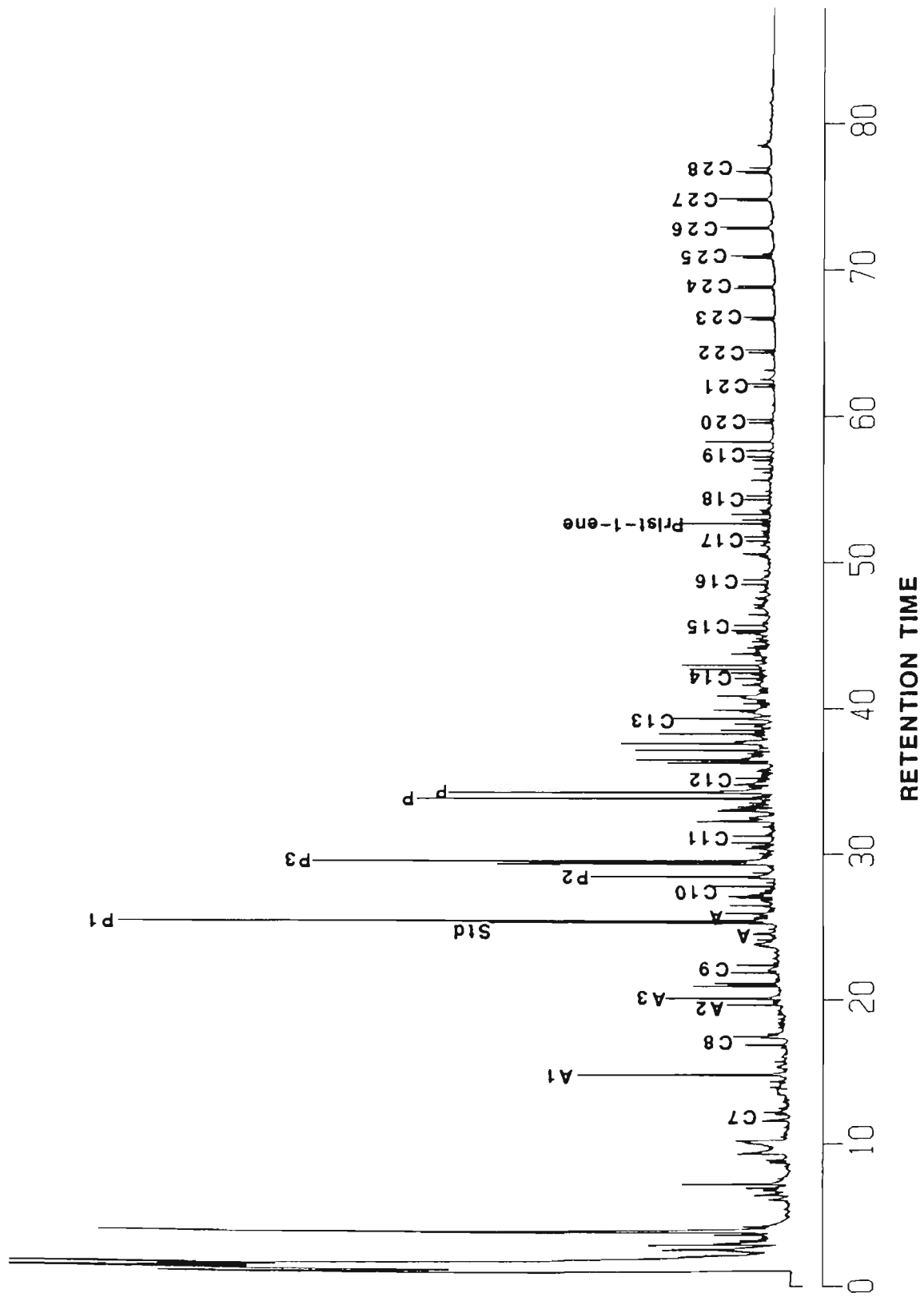


Figure 7.32: Pyrolysis gas chromatogram for Pliocene coal sample PG 1.

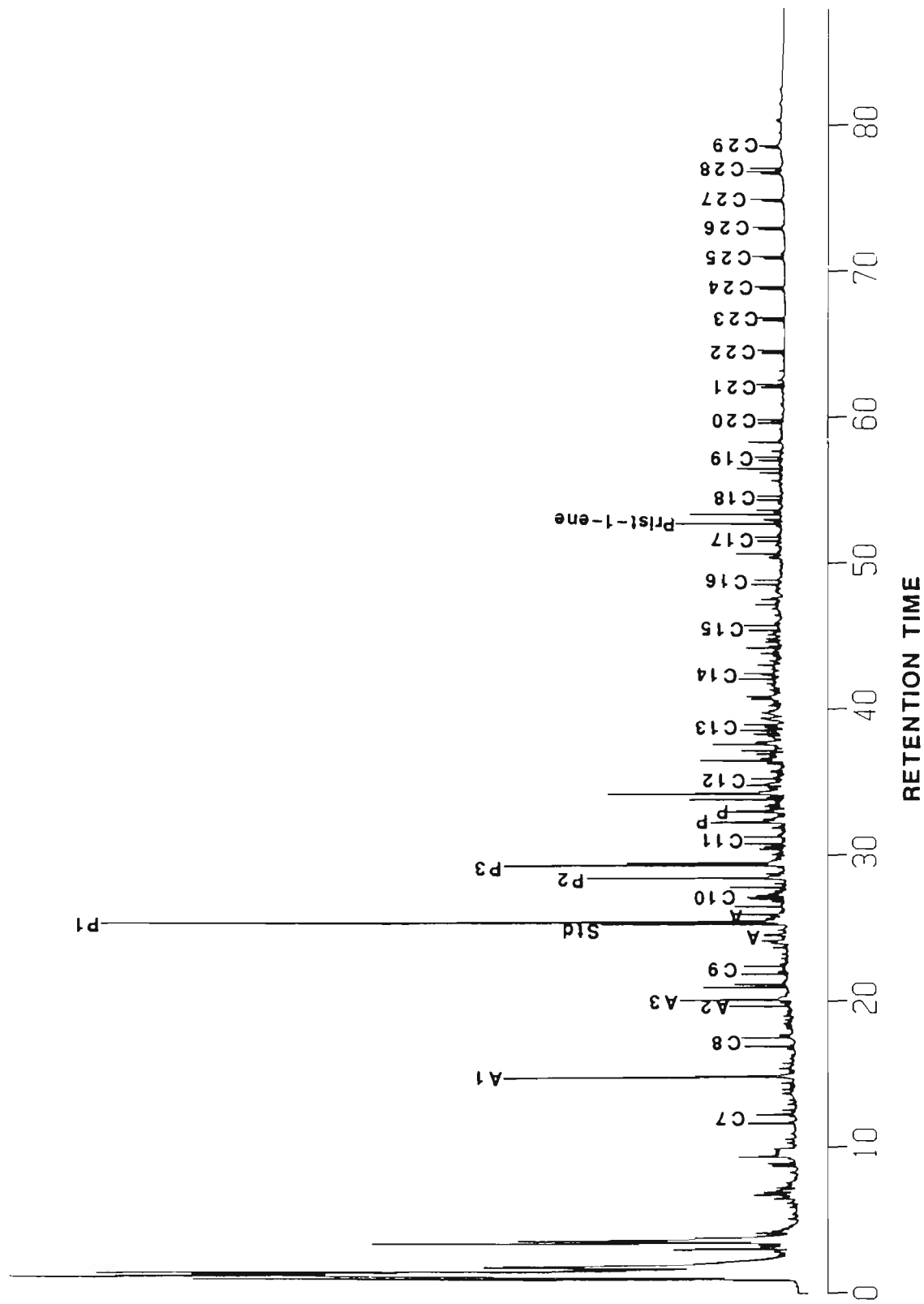


Figure 7.33: Pyrolysis gas chromatogram for Pliocene coal sample PG 2.

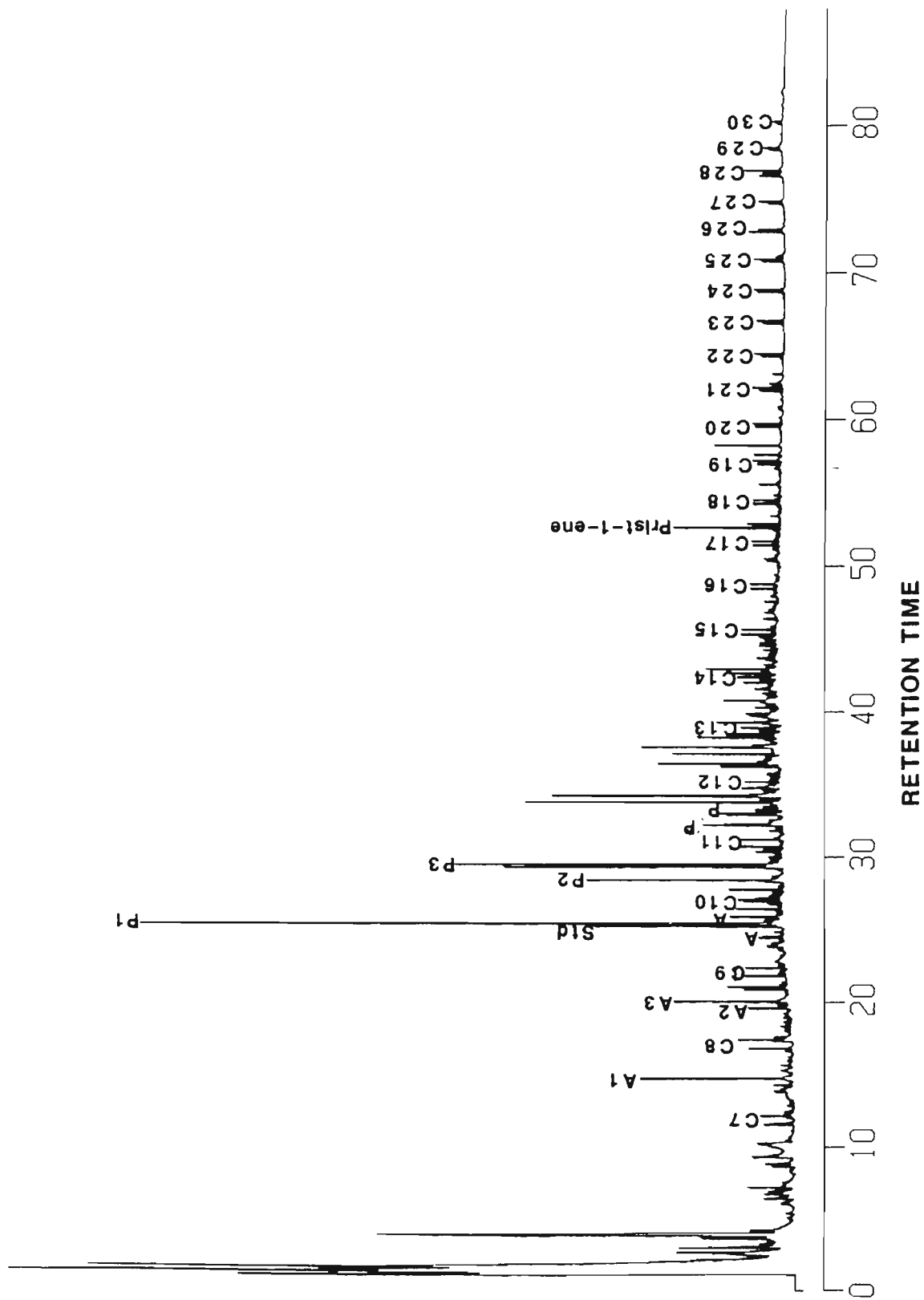


Figure 7.34: Pyrolysis gas chromatogram for Pliocene coal sample PG 3.

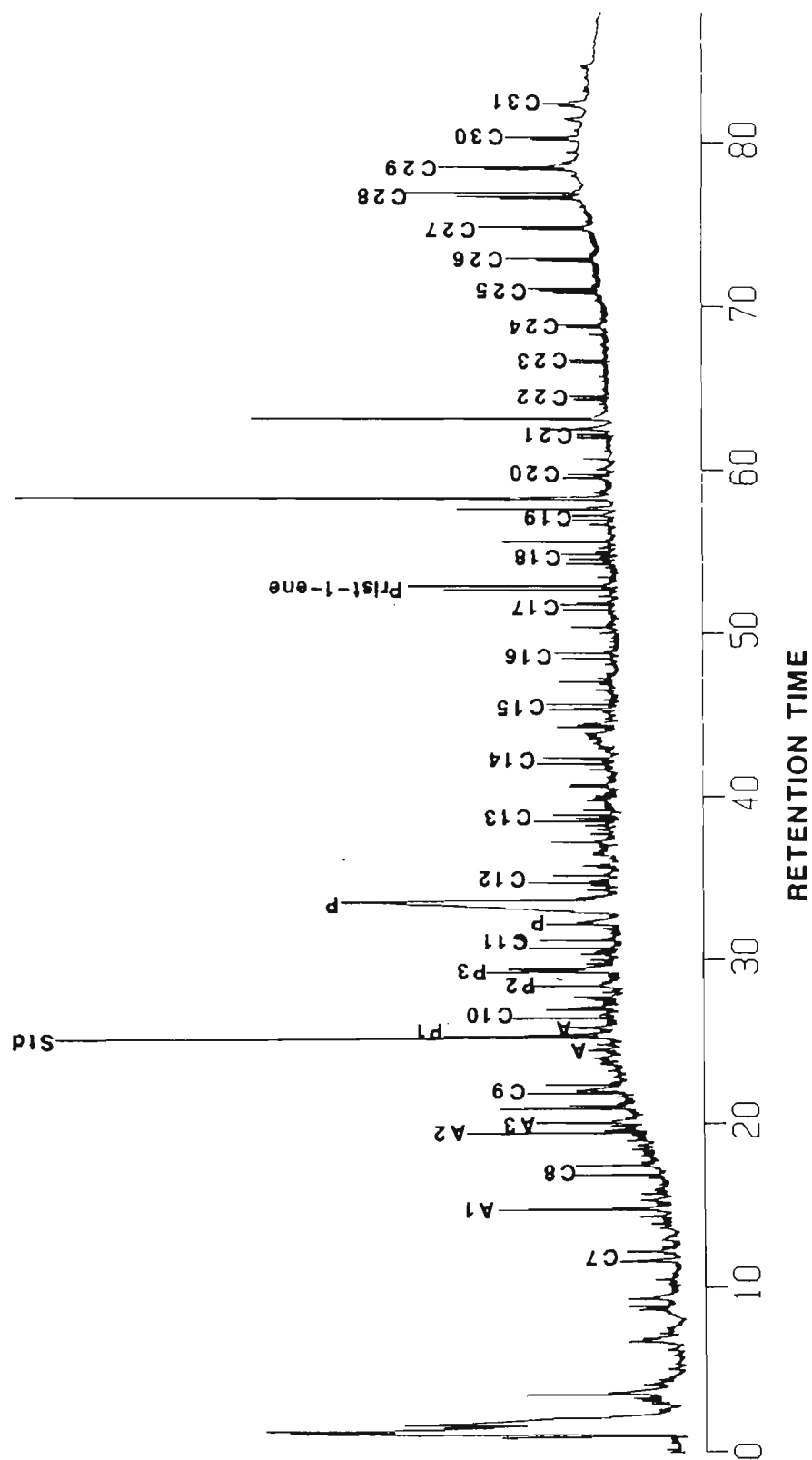


Figure 7.35: Pyrolysis gas chromatogram for Pliocene coal sample PG 4.



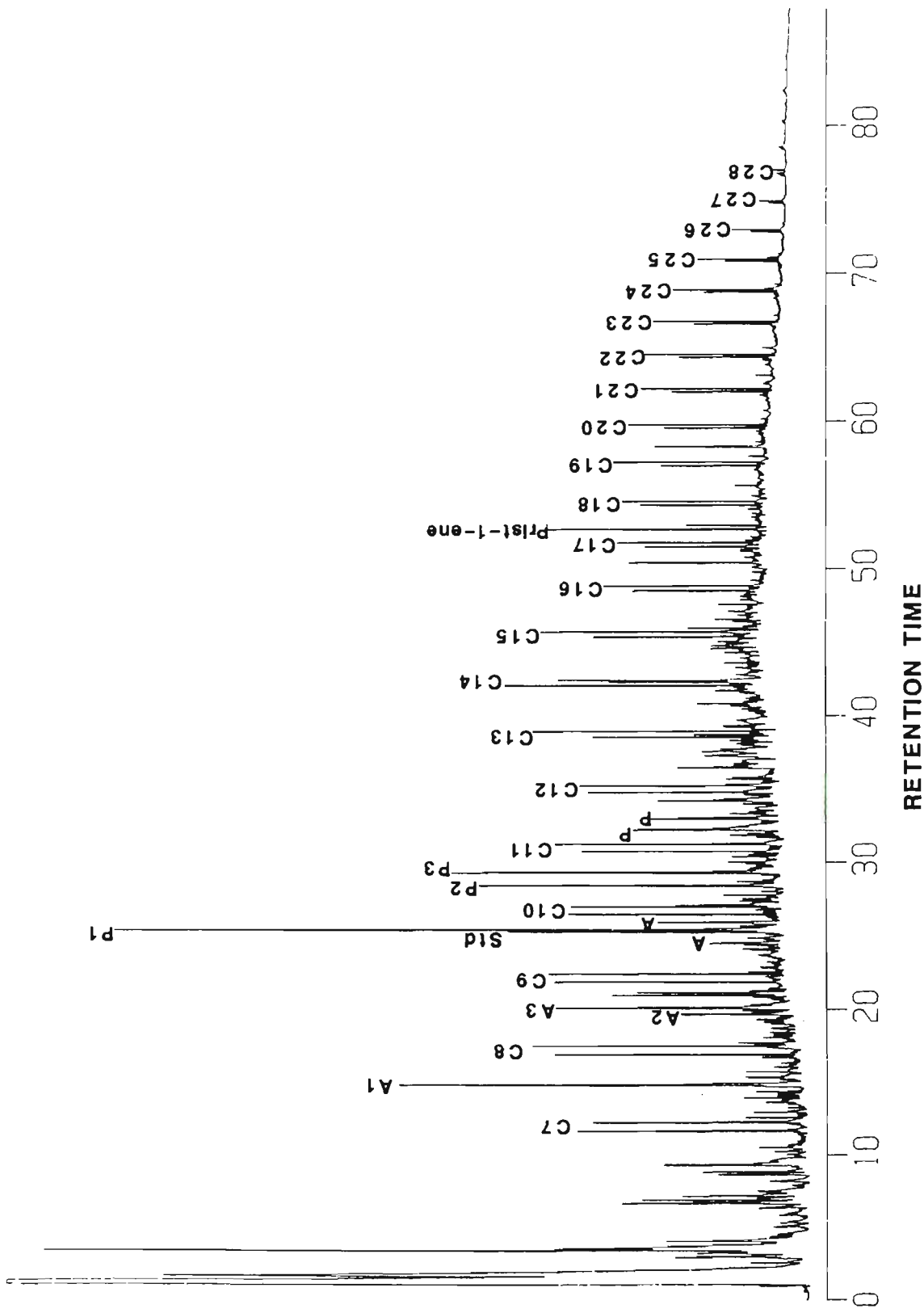


Figure 7.36: Pyrolysis gas chromatogram for Miocene coal sample PG 5.

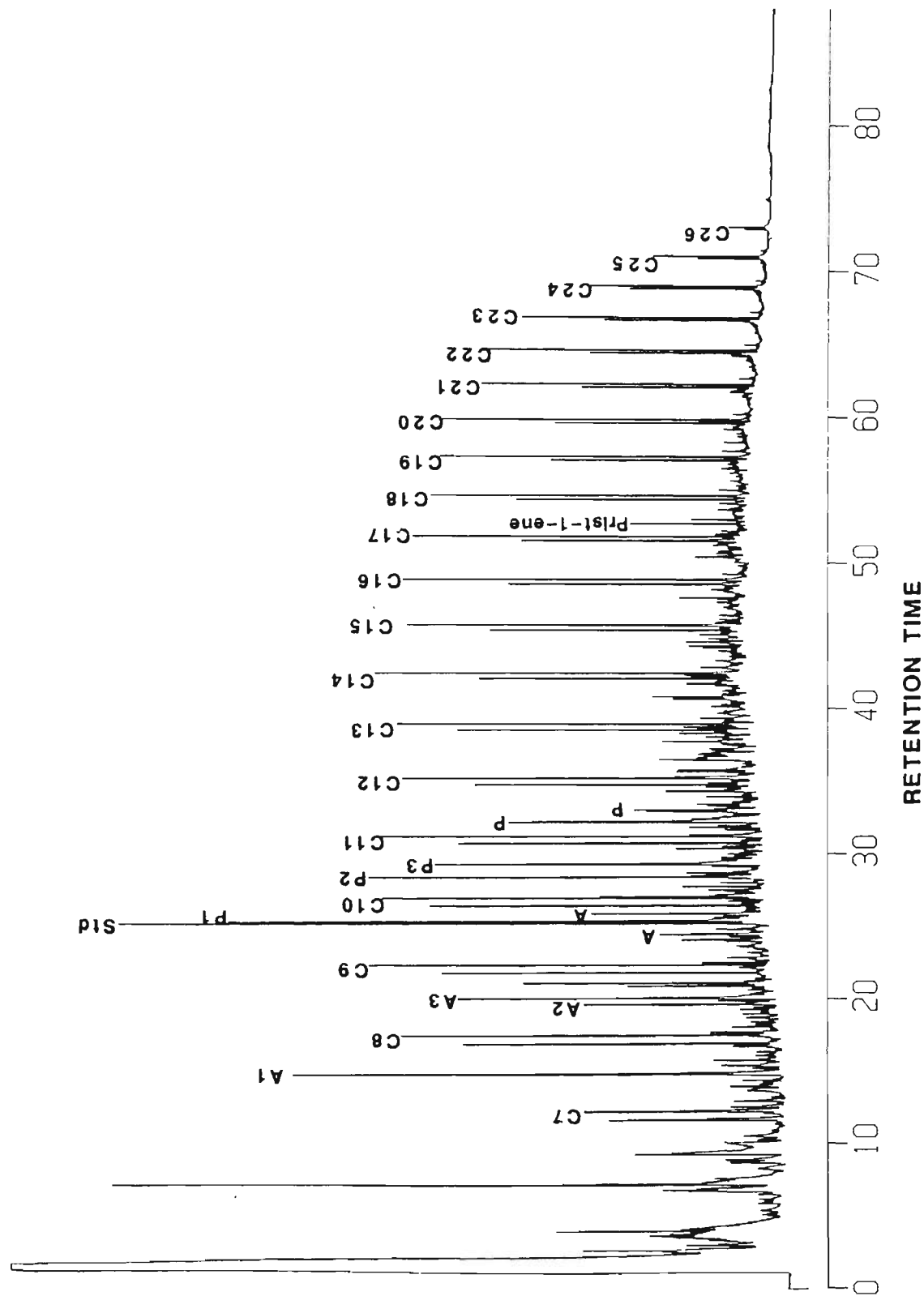


Figure 7.37: Pyrolysis gas chromatogram for Miocene coal sample PG 7.

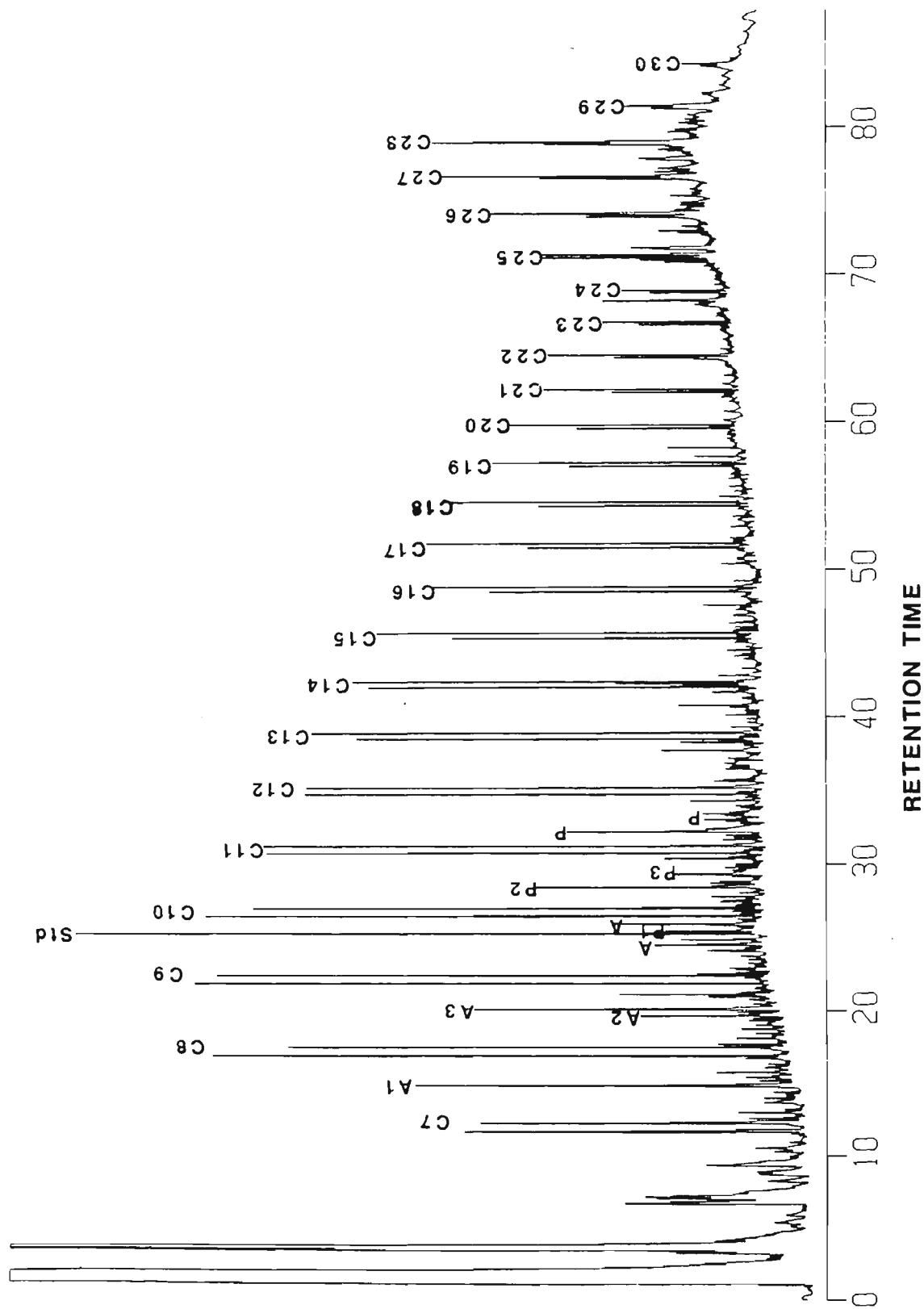


Figure 7.38: Pyrolysis gas chromatogram for Miocene coal sample PG 11.

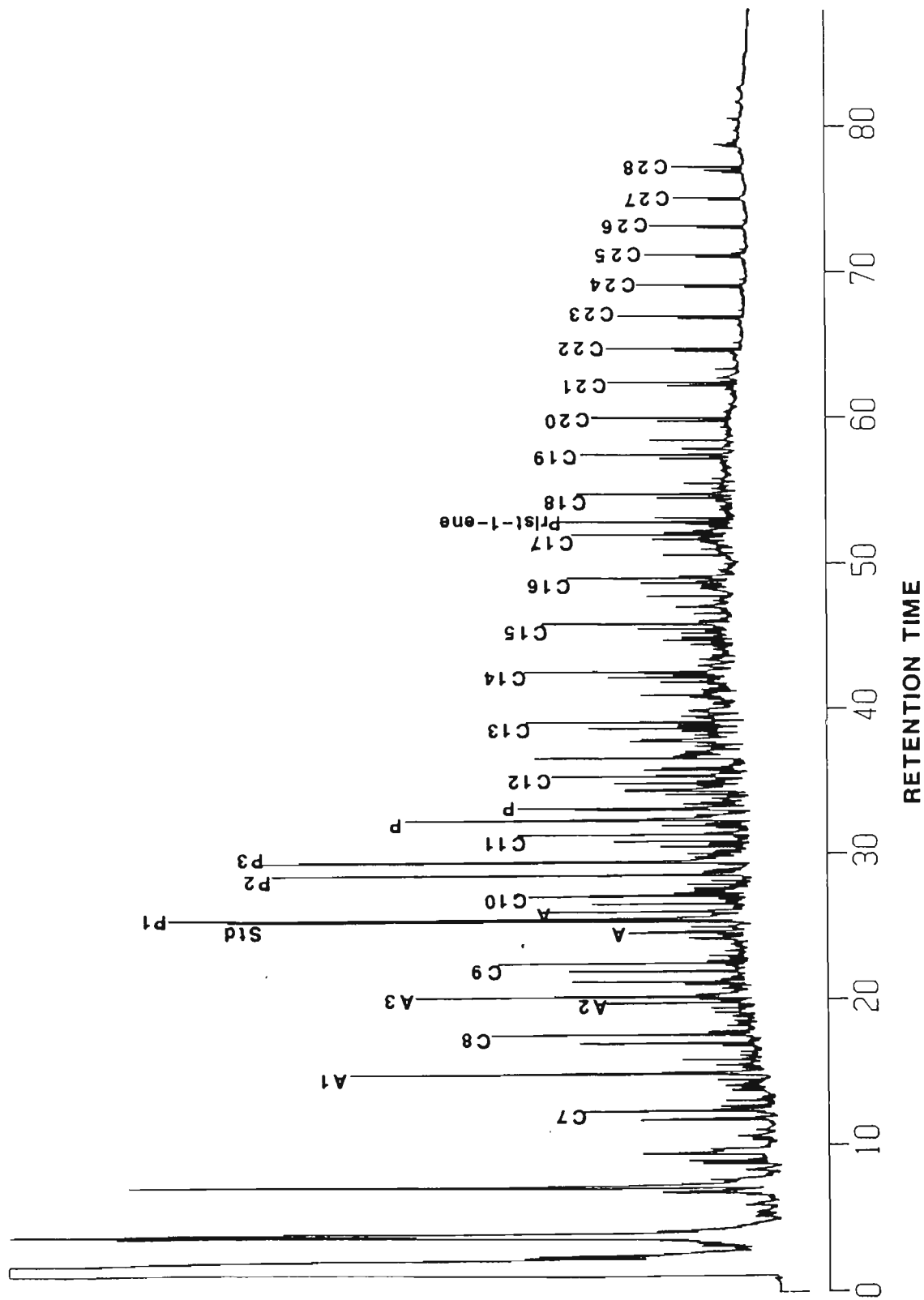


Figure 7.39: Pyrolysis gas chromatogram for Miocene coal sample PG 14.

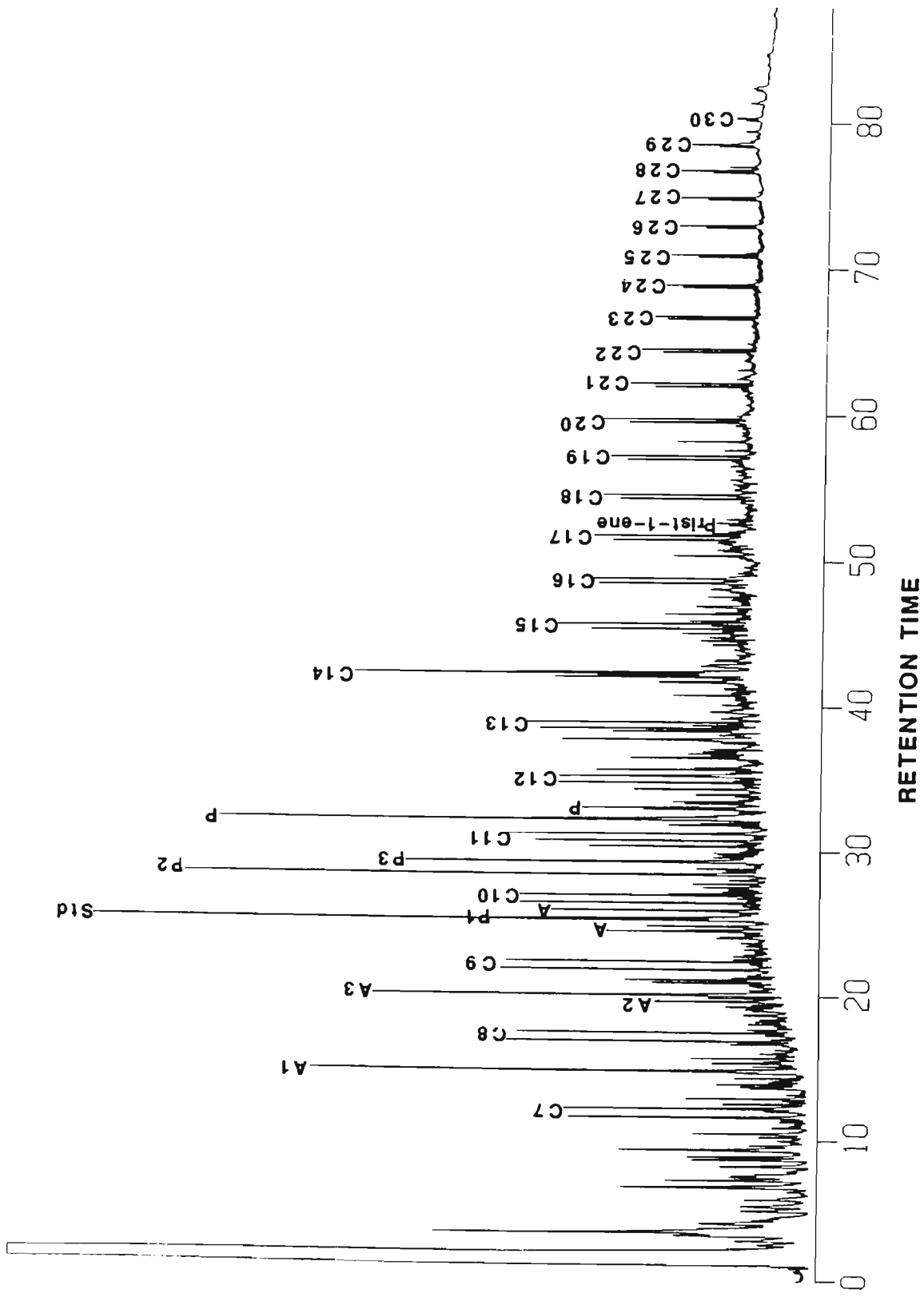


Figure 7.40: Pyrolysis gas chromatogram for Oligocene coal sample PG 6.

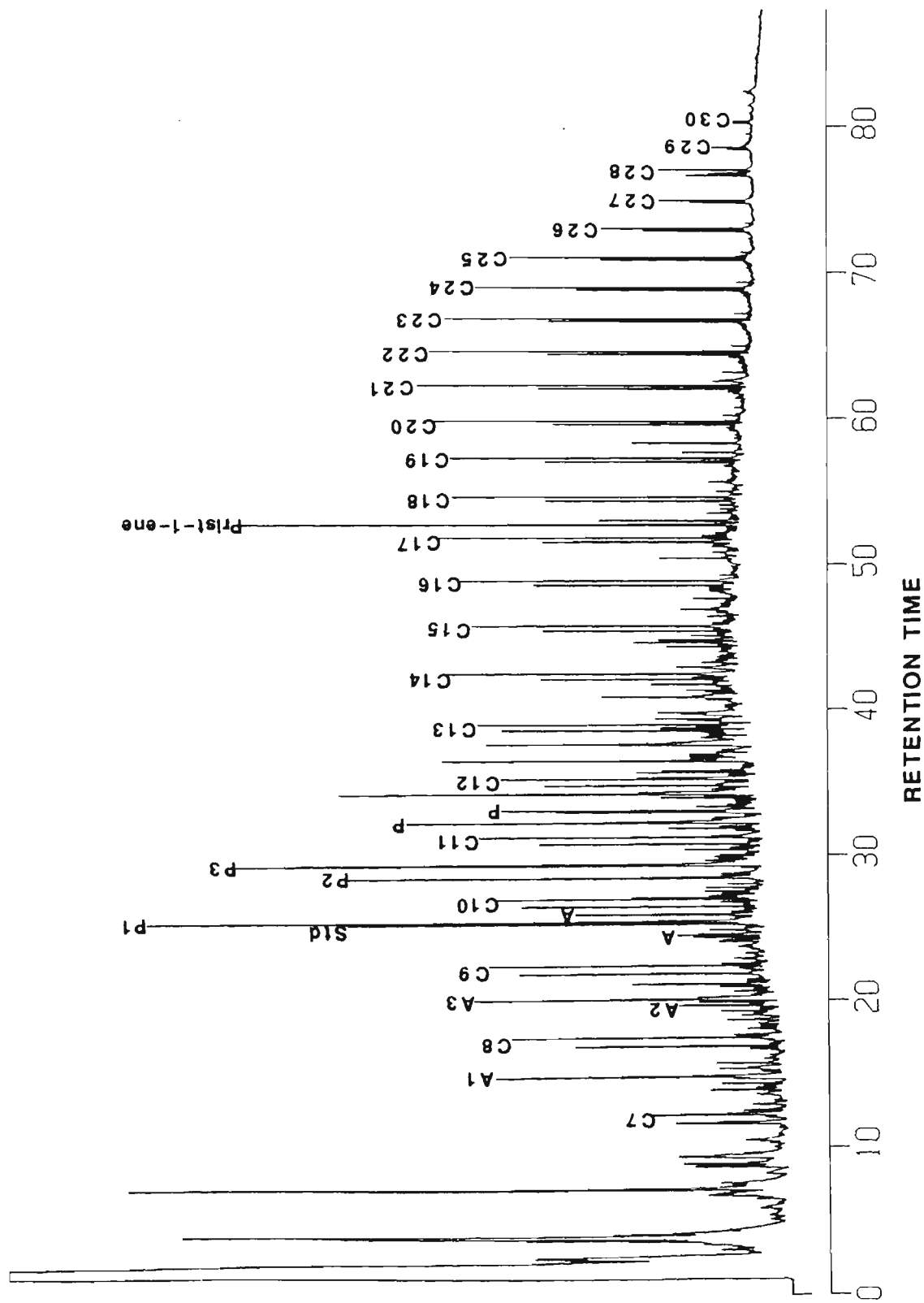


Figure 7.41: Pyrolysis gas chromatogram for Oligocene coal sample PG 13.

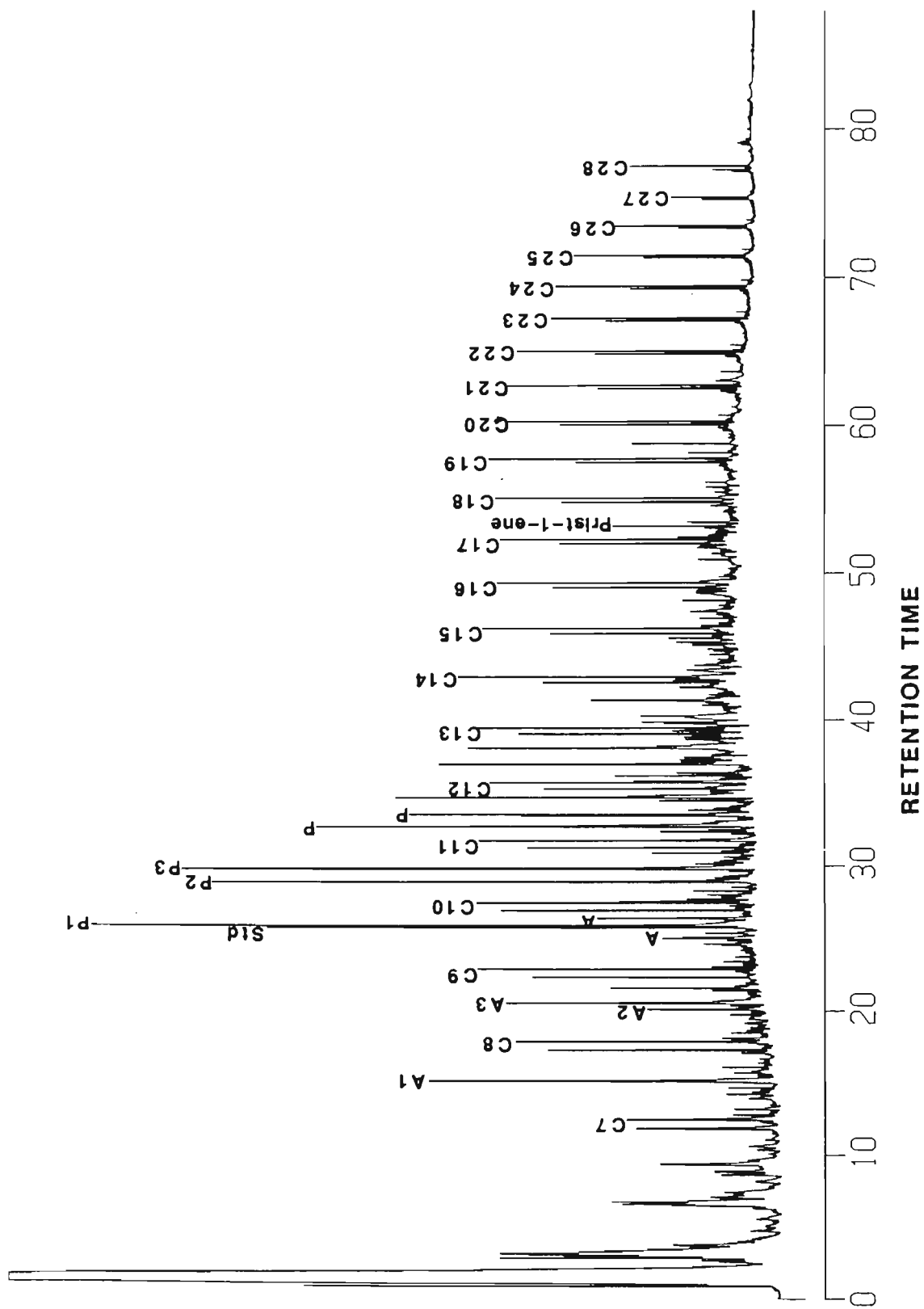


Figure 7.42: Pyrolysis gas chromatogram for Oligocene coal sample PG 9.

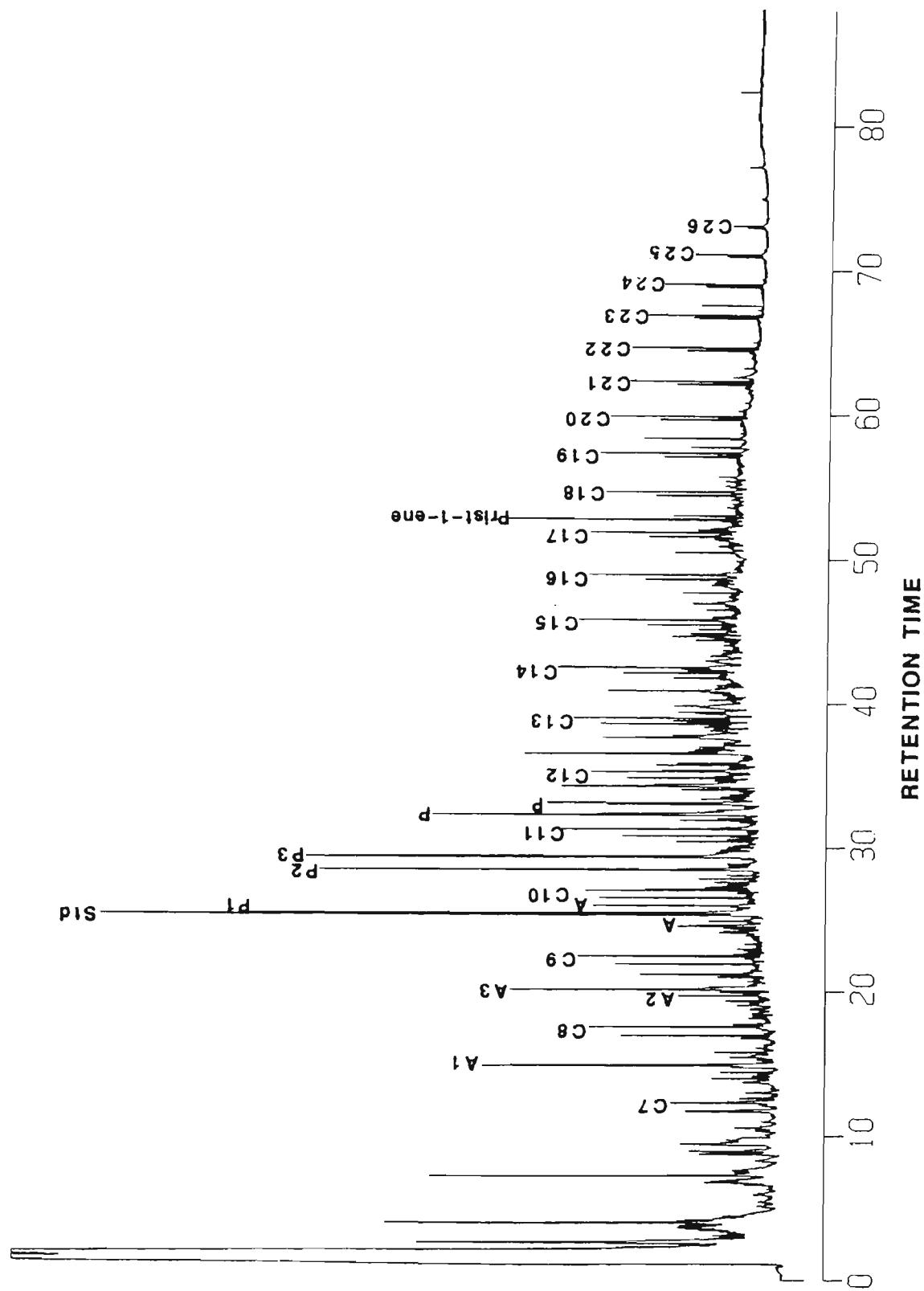


Figure 7.43: Pyrolysis gas chromatogram for Oligocene coal sample PG 10.



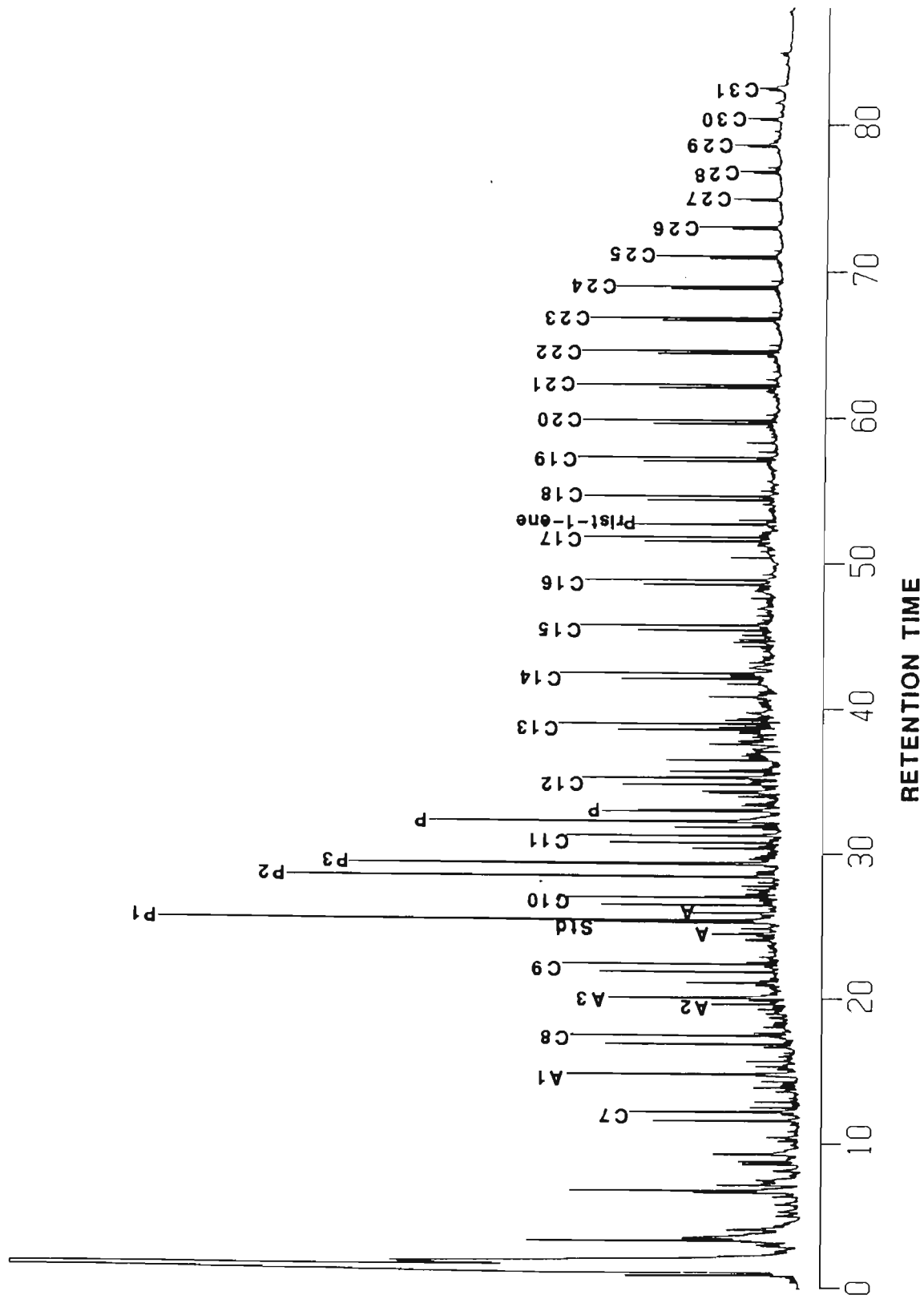


Figure 7.44: Pyrolysis gas chromatogram for Oligocene coal sample PG 12.

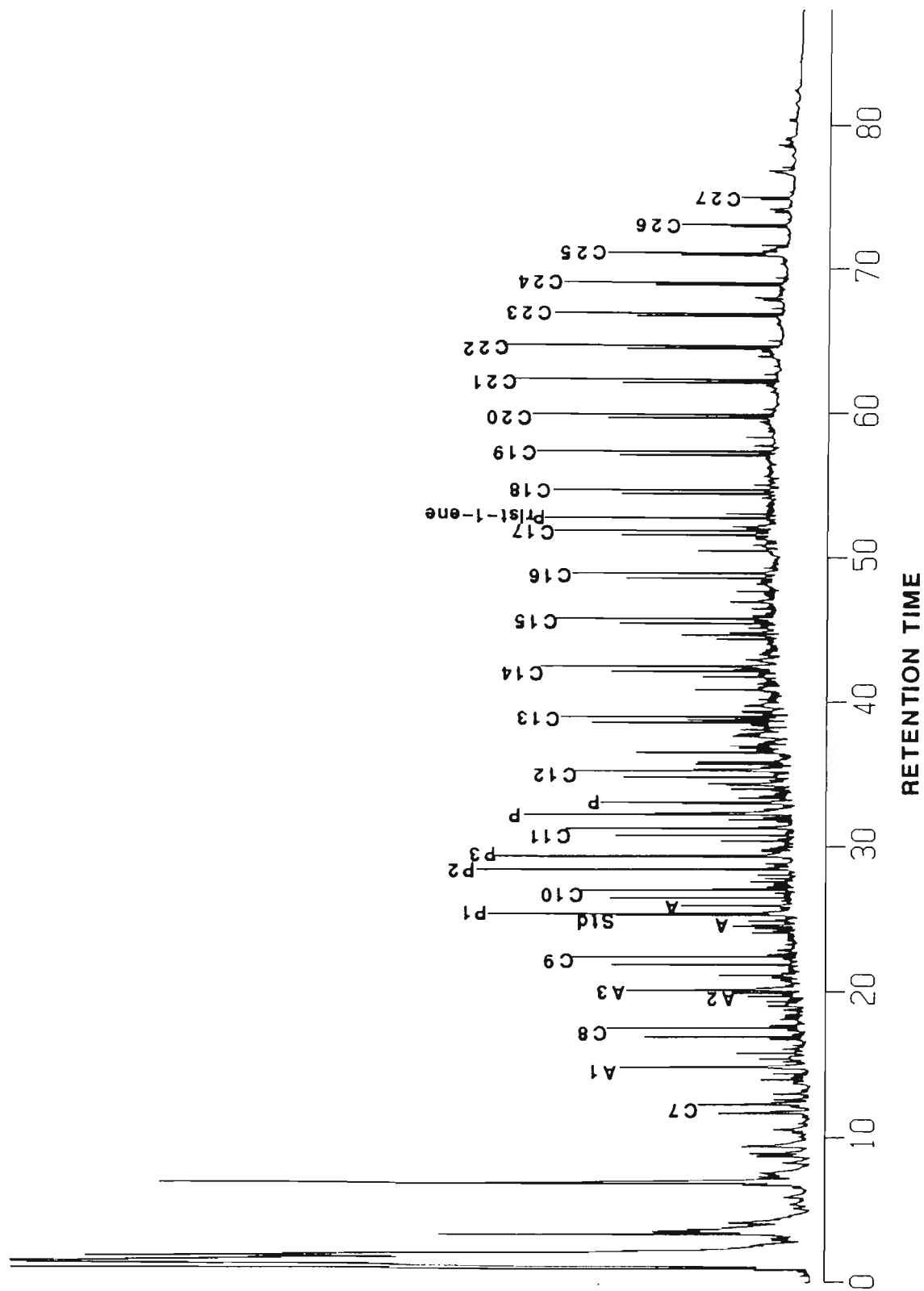


Figure 7.45: Pyrolysis gas chromatogram for Oligocene coal sample PG 8.

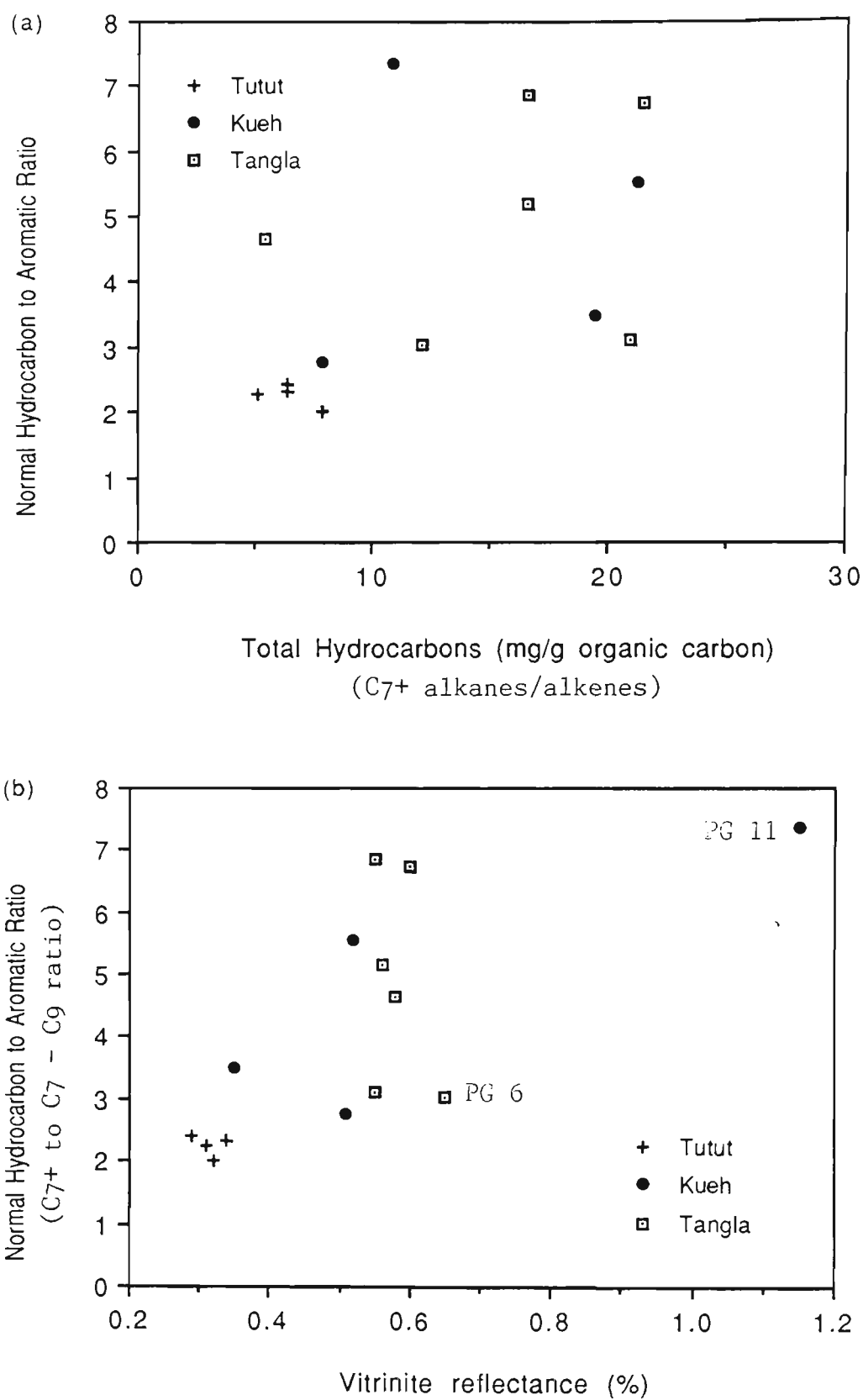


Figure 7.46: The relationships between total hydrocarbon and the ratio of normal hydrocarbon to aromatic (a) and between the vitrinite reflectance and the ratio of normal hydrocarbon to aromatic (b).

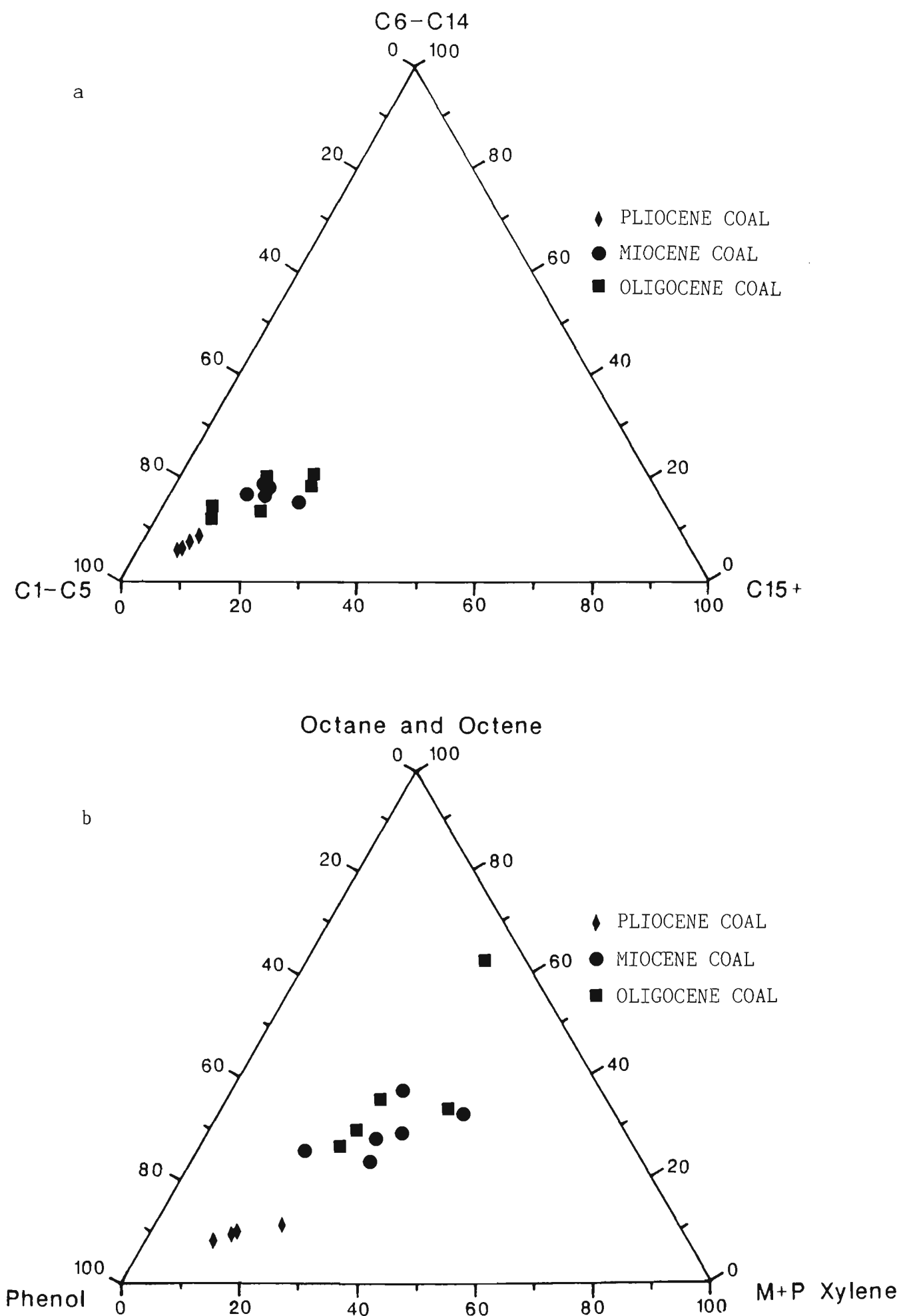


Figure 7.47: Triangular plots of various components in the compound classes of hydrocarbons, aromatics and phenols.

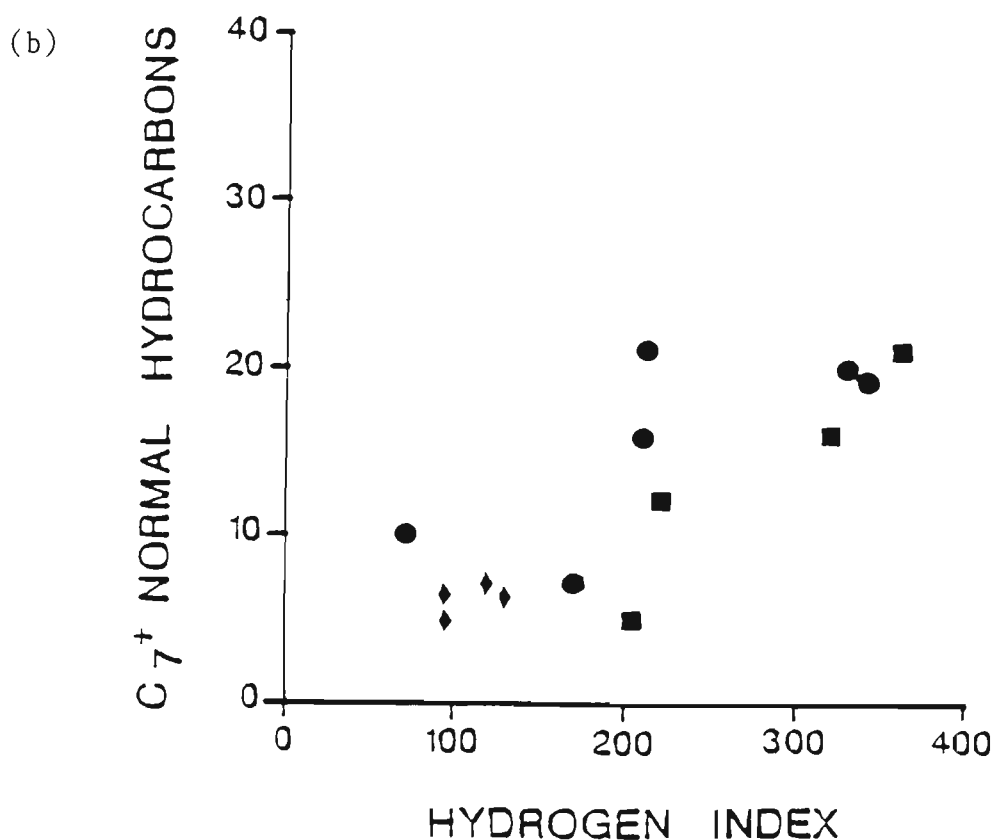
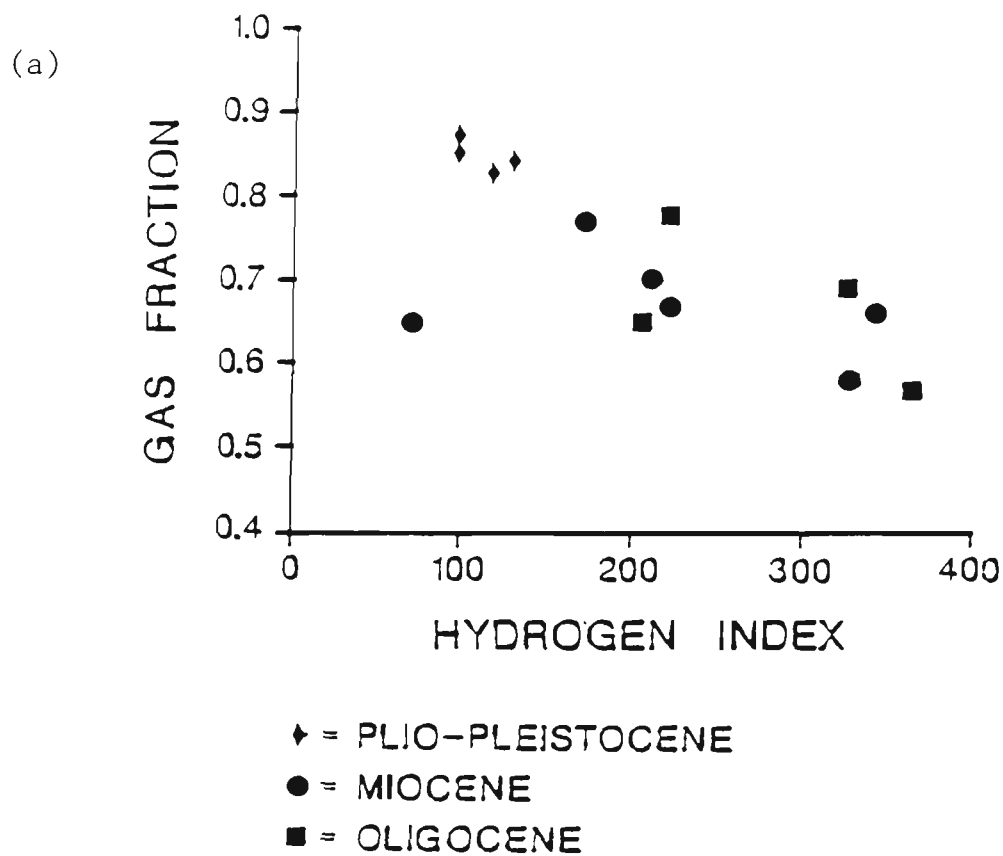
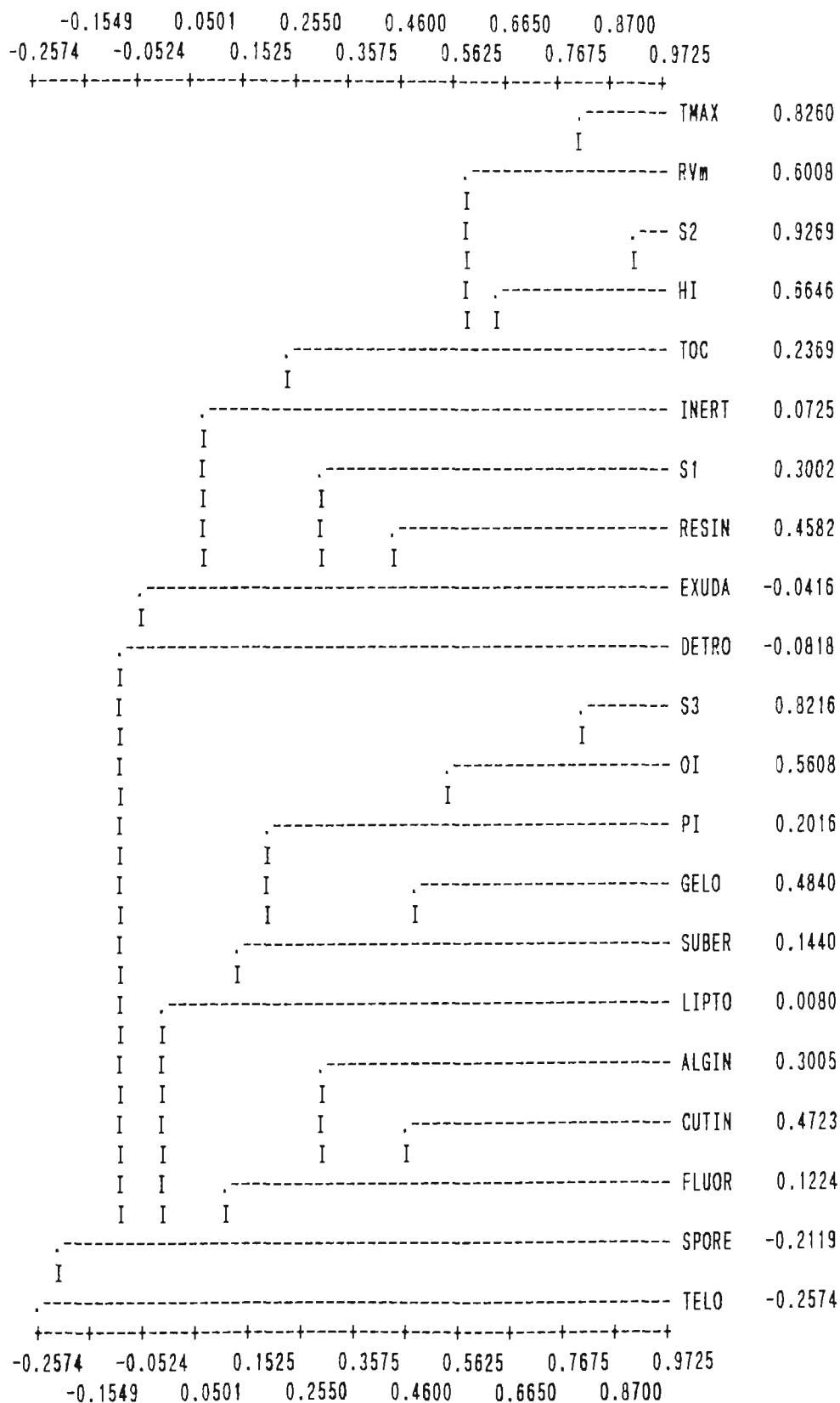
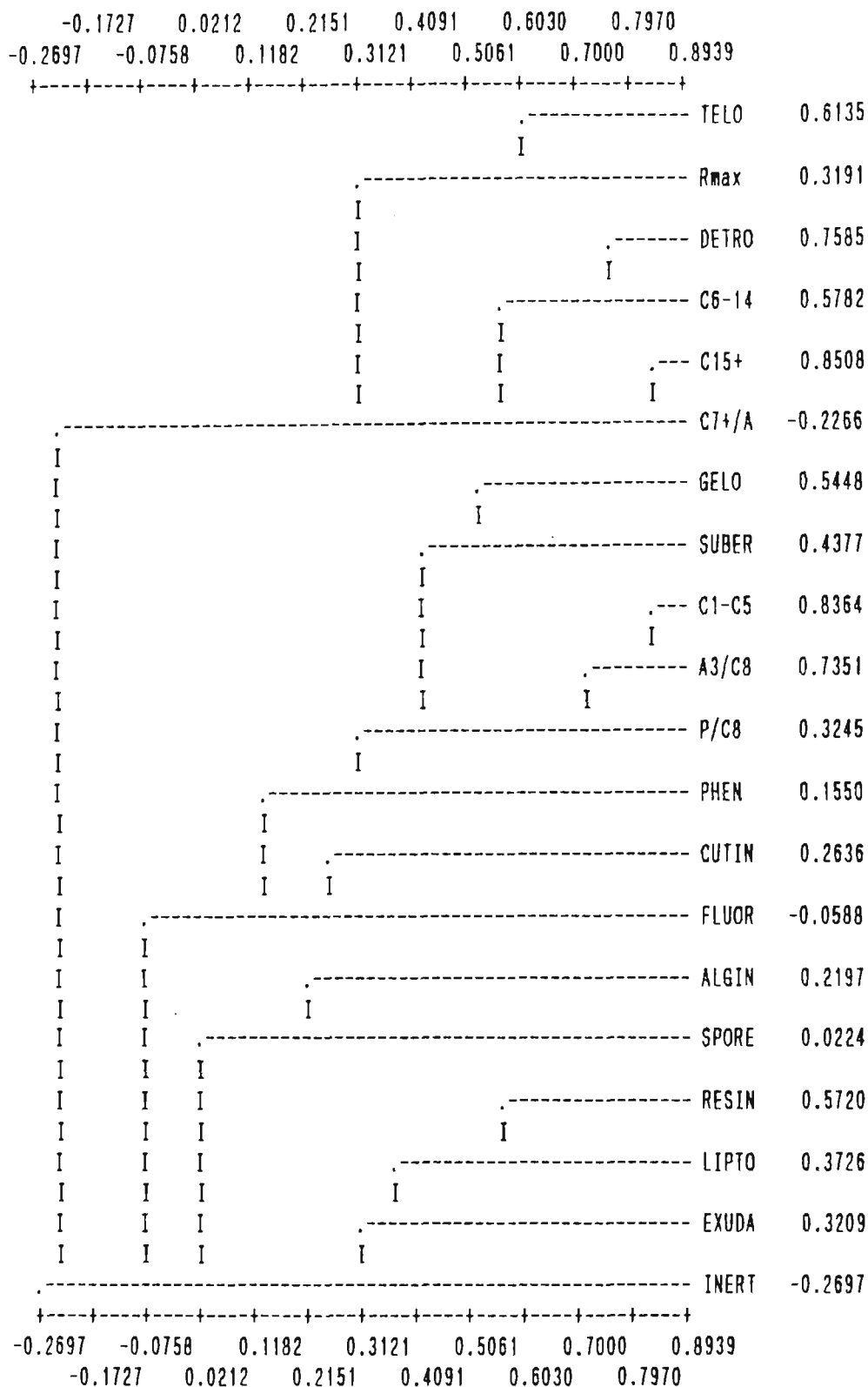


Figure 7.48: The relationships between hydrogen index and gas fraction (a) and between hydrogen index and C<sub>7</sub><sup>+</sup> normal hydrogen (b) of the Tertiary coals of West Aceh Basin.



DENDROGRAM - VALUES ALONG X-AXIS ARE SIMILARITIES

Figure 7.49: R-mode dendrogram of cluster analysis for rock-eval and maceral composition.



DENDROGRAM - VALUES ALONG X-AXIS ARE SIMILARITIES

Figure 7.50: R-mode dendrogram of cluster analysis for maceral composition and Pyrolysis-GC products of the Tertiary coals of West Aceh Basin.

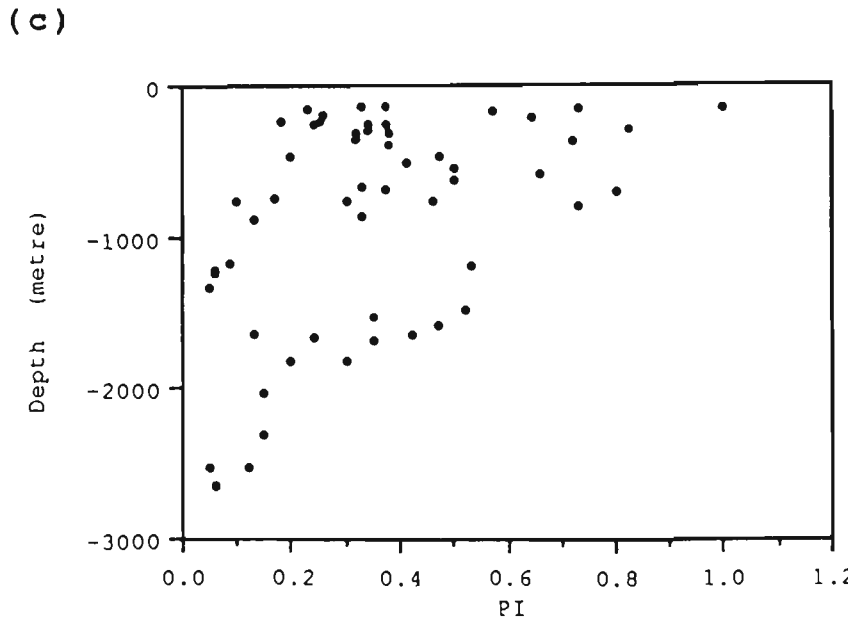
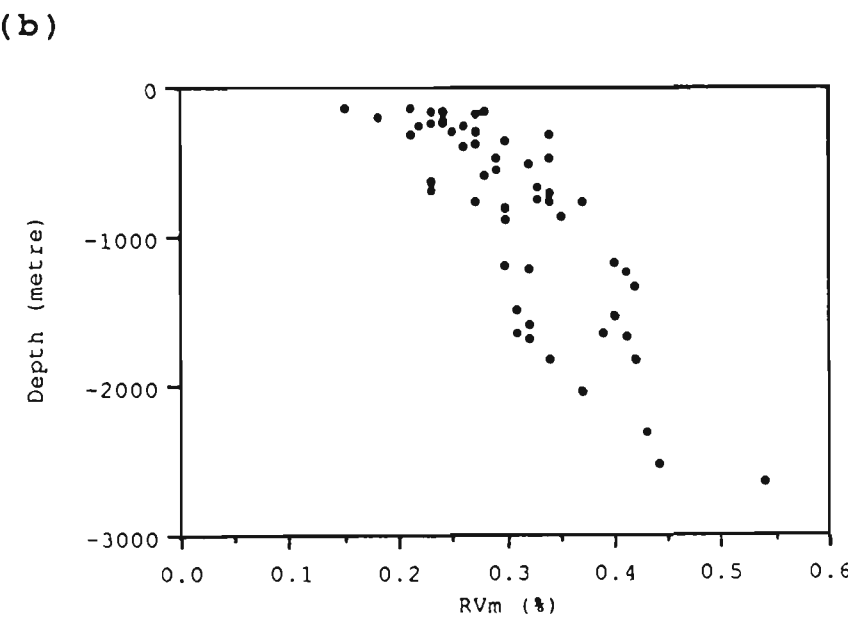
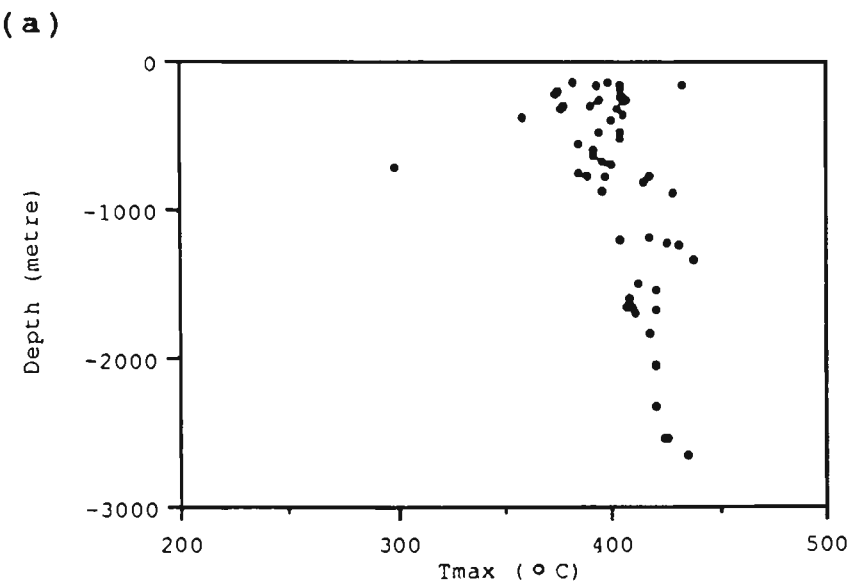
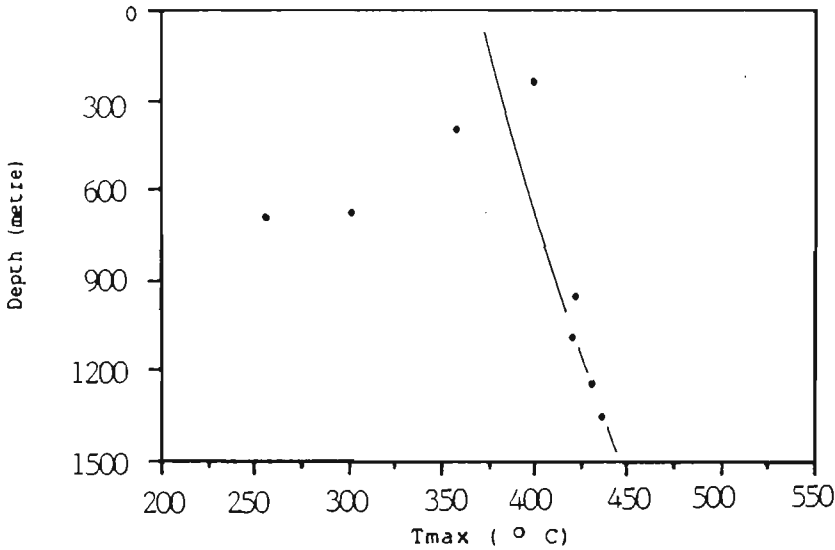


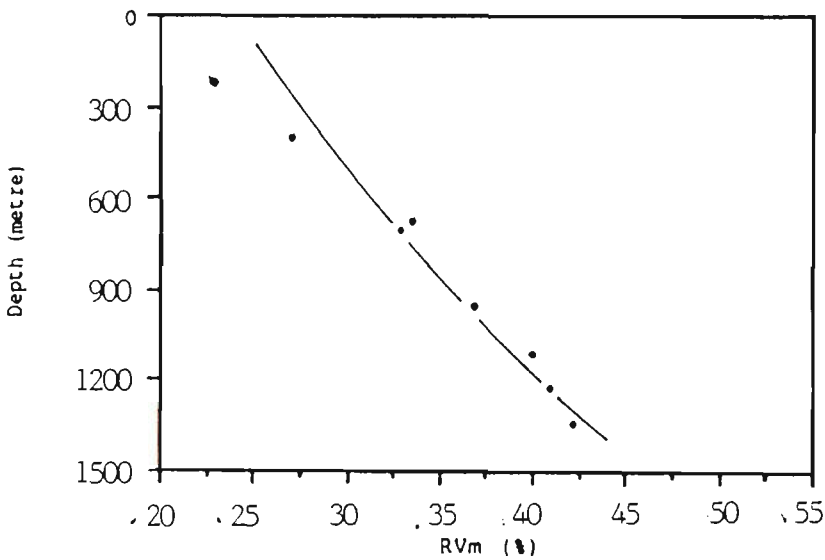
Figure 7.51: The relationship between maturation parameters and depth of the West Aceh offshore area.



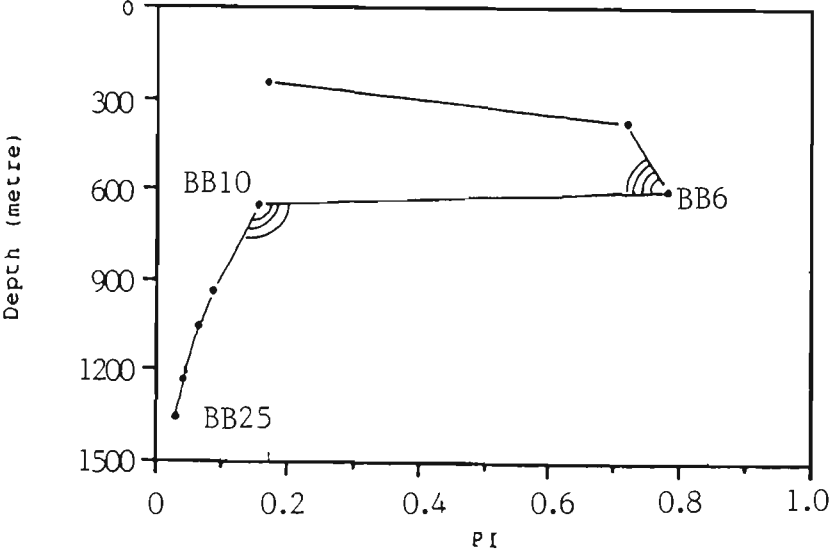
( a )



( b )



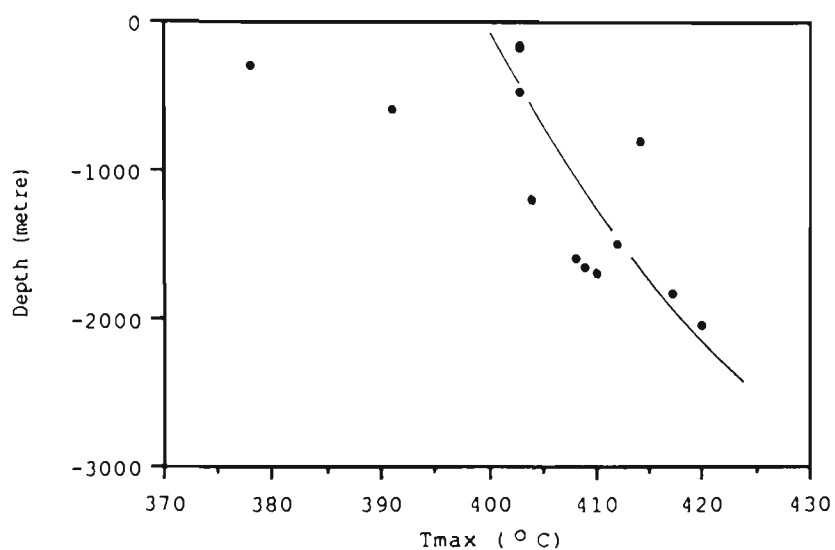
( c )



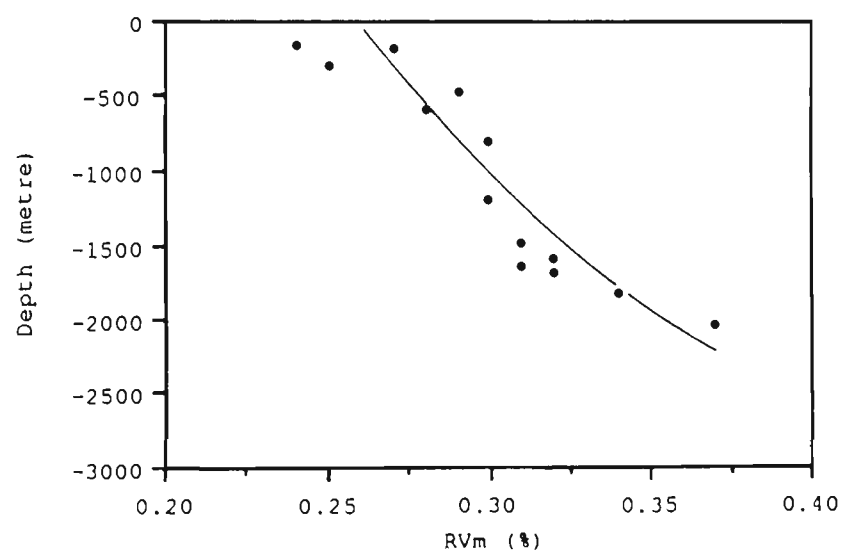
	TOC	mgHC/gTOC	Sat/Arom
BB6	0.10	514.20	3.20
BB10	0.16	80.80	0.70
BB25	2.20	38.20	1.47

Figure 7.52: The relationship between maturation parameters with depth in Bubon well at the offshore area of West Aceh Basin.

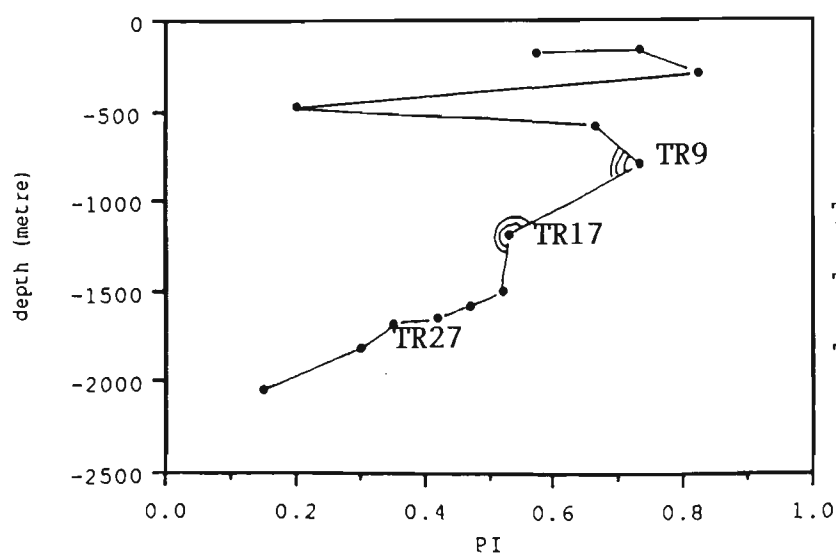
(a)



(b)



(c)



	TOC	mgHC/gTOC	Sat/Arom
TR9	0.54	96.10	0.17
TR17	0.83	58.80	2.33
TR27	1.04	140.80	1.87

Figure 7.53: The relationship between maturation parameters with depth in Tripa well at the offshore area of West Aceh Basin.

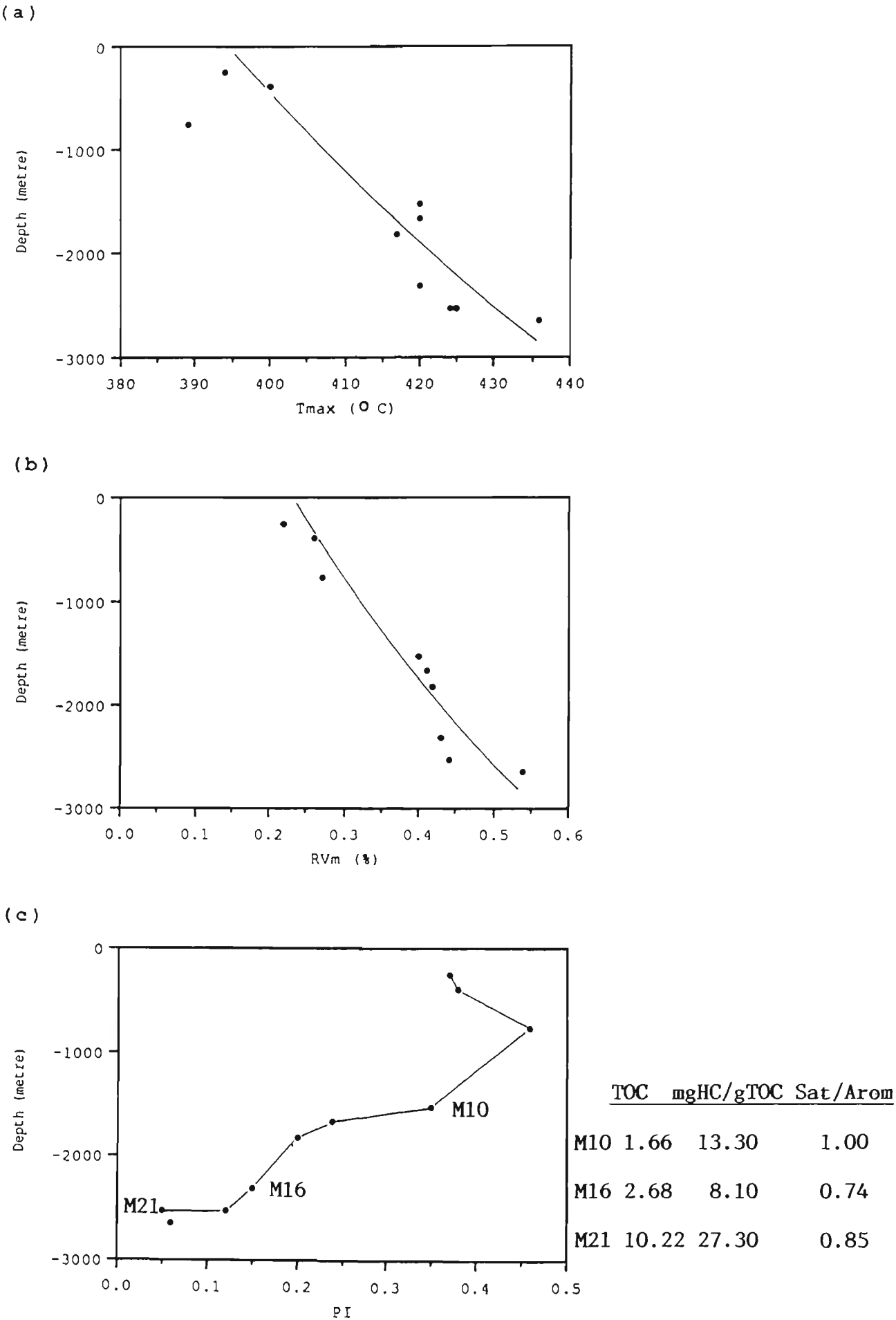


Figure 7.54: The relationship between maturation parameters with depth in Meulaboh well at the offshore area of West Aceh Basin.

Table 7.1.1. Scoring table for volume of DOM, vitrinite  
reflectance and volume of coal (Smyth et al., 1984)

Please see print copy for image

Table 7.2. Scoring table for volume of DOM, vitrinite reflectance and volume of coal of the Tertiary Formations in West Aceh Basin (modified from Smyth et al., 1984)

Please see print copy for image

Table 7.3. Volume, type and rank of DOM and Coals in wells in the Tutut Formation

Well name	No. of samples	Volume of DOM (%)	Composition of DOM			Volume of coal (%)	Composition of coal			Vitrinite reflectance (%)
			V	L	I		V	L	I	
Teunom	6	6.0	43.0	54.0	3.0	15.0	85.0	12.0	3.0	0.27
Bubon	8	2.1	40.0	58.0	2.0	11.4	82.0	11.0	7.0	0.27
Keudapasi	9	1.9	33.0	67.0	0.0	3.2	89.0	11.0	0.0	0.27
Meulaboh East	8	3.5	42.0	58.0	0.0	5.2	90.0	8.0	2.0	0.27
Tuba	4	5.8	62.0	38.0	0.0	2.5	86.0	14.0	0.0	0.26
Meulaboh	9	1.2	38.0	61.0	1.0	6.3	86.0	13.0	1.0	0.25
Tripa	14	0.7	56.0	44.0	0.0	2.2	69.0	24.0	7.0	0.27
Palumat	8	2.5	33.0	66.0	1.0	4.7	80.0	13.0	7.0	0.20

Table 7.4. Volume, type and rank of DOM and Coals in wells in the Kuch Formation

Well name	No. of samples	Volume of DOM (%)	Composition of DOM			Volume of coal (%)	Composition of coal			Vitrinite reflectance (%)
			V	L	I		V	L	I	
Teunem	6	1.3	15.0	83.0	2.0	3.4	48.0	51.0	1.0	0.20
Bubon	14	4.3	44.0	55.0	1.0	12.5	75.0	22.0	3.0	0.37
Keudapasi	4	1.9	31.0	69.0	0.0	0.0	0.0	0.0	0.0	0.34
Meulaboh East	6	2.7	48.0	52.0	0.0	23.0	87.0	13.0	0.0	0.33
Tuba	4	1.3	37.0	63.0	0.0	0.2	37.0	55.0	8.0	0.37
Meulaboh	8	2.0	52.0	48.0	0.0	11.8	83.0	16.0	1.0	0.36
Tripa	17	2.1	49.0	51.0	0.0	5.6	64.0	35.0	1.0	0.32
Palumat	3	0.3	22.0	78.0	0.0	0.0	0.0	0.0	0.0	0.24





Table 7.6. Average formation scores for hydrocarbon-generating potential of the Tertiary Formations in the West Aceh Basin, Sumatra

Formation	No of hole/ sample	Liptinite/ vitrinite for DOM	Well score for DOM	Liptinite/ vitrinite for coal	Well score for coal	Well score for DOM + coal
Tutut	8/66	1.38	3.73	0.18	0.24	3.96
Kueh	8/62	2.16	4.66	1.27	2.03	6.73
Tangla	2/18	1.45	8.52	0.35	0.95	9.45

Table 7.7. Well scores for hydrocarbon generation potential of the Tutut Formation based on properties of the DOM

Well	A Maturation Score	B DOM volume score	C <u>Liptinite</u> <u>Vitrinite</u>	D AxBxC	Well score for DOM $\frac{D}{5.95} \times 10$
Teunom	0.30	10.00	1.25	3.75	6.30
Bubon	0.30	7.00	1.45	3.04	5.10
Keudapasi	0.30	3.00	2.03	1.82	3.05
Meulaboh East	0.30	7.00	1.38	2.89	4.85
Tuba	0.30	10.00	0.61	1.83	3.07
Meulaboh	0.30	3.00	1.60	1.44	2.42
Tripa	0.30	1.00	0.78	0.23	0.38
Pulumat	0.20	7.00	2.00	2.80	4.70

\* 5.95\*: Highest value for DOM of the Tertiary Formation

Table 7.8. Well scores for hydrocarbon generation potential of the Tutut Formation based on properties of coal and DOM

Well	A Maturation score	B coal volume score	C Liptinite Vitrinite	D AxBxC	Well score for coal $\frac{D}{9.56} \times 10$	Well score for DOM + Coal (DOM values from table 7.7)
Teunom	0.30	5.00	0.28	0.42	0.43	6.73
Bubon	0.30	5.00	0.27	0.40	0.41	5.51
Keudapasi	0.30	3.50	0.12	0.12	0.12	3.17
Meulaboh East	0.30	5.00	0.08	0.12	0.12	4.97
Tuba	0.30	3.50	0.16	0.16	0.16	3.23
Meulaboh	0.30	5.00	0.15	0.22	0.23	2.65
Tripa	0.30	3.50	0.29	0.30	0.31	0.69
Pulumat	0.20	5.00	0.16	0.16	0.16	4.76

\* 9.56: highest value for coal of the Tertiary Formation

Table 7.9. Well scores for hydrocarbon generation potential of the Kueh Formation based on properties of the DOM

Well	A Maturation Score	B DOM volume score	C <u>Liptinite</u> Vitrinite	D AxBxCx	Well score for DOM $\frac{D}{5.95} \times 10$
Teunom	0.30	3.00	5.53	4.97	8.35
Bubon	0.40	10.00	1.25	5.00	8.90
Keudapasi	0.40	3.00	2.22	2.66	4.47
Meuluboh East	0.40	7.00	1.08	3.02	5.07
Tuba	0.40	3.00	1.70	2.04	3.42
Meuluboh	0.40	3.00	0.92	1.10	1.84
Tuipa	0.40	7.00	1.04	2.91	4.89
Pulumat	0.30	0.50	3.54	0.53	0.89

\* 5.95\*: highest value for DOM of the Tertiary Formation

Table 7.10. Well scores for hydrocarbon generation potential of the Kueh Formation based on properties of coal and DOM

Well	A Maturation score	B coal volume score	C <u>Liptinite</u> Vitrinite	D AxBxC	Well score for coal $\frac{D}{9.56} \times 10$	Well score for DOM + Coal (DOM values from table 7.9)
Teunom	0.30	3.50	5.76	9.56*	10.00	18.35
Bubon	0.40	5.00	0.59	1.18	1.21	6.61
Keudapasi	0.40	0.00	0.00	0.00	0.00	4.47
Meulaboh East	0.40	5.00	0.28	0.56	0.58	5.65
Tuba	0.40	0.25	1.48	0.14	0.14	3.56
Meulaboh	0.40	5.00	0.47	0.94	0.98	2.82
Tripa	0.40	5.00	1.61	3.22	3.36	8.55
Palumat	0.30	0.00	0.00	0.00	0.00	0.89

\* 9.56: highest value for coal of the Tertiary Formation

Table 7.11. Well scores for hydrocarbon generation potential of the Tangla Formation based on properties of the DOM

Well	A Maturation Score	B DOM volume score	C <u>Liptinite</u> Vitrinite	D AxExC	Well score for DOM $D \times 10$ 5.95*
Tuba	0.50	7.00	1.20	4.20	7.05
Meulaboh	0.50	7.00	1.70	5.95*	10.00

\*5.95: highest value for DOM

Table 7.12. Well scores for hydrocarbon generation potential of the Tangla Formation based on properties of coal and DOM

Well	A Maturation score	B coal volume score	C <u>Liptinite</u> Vitrinite	D AxBxC	Well score for coal $\frac{D}{9.56^*} \times 10$	Well score for DOM + Coal (DOM values from table 7.11)
Tuba	0.50	5.00	0.52	1.30	1.35	8.40
Meulaboh	0.50	5.00	0.19	0.47	0.49	10.49

\*9.56: highest value for coal of the Tertiary Formation

Table 7.13. Summary of results of rock-eval/TOC and vitrinite reflectance analyses of the Tertiary Formations in the West Aceh Basin (Offshore)

ROCK-EVAL; TOC; VITRINITE REFLECTANCE	TUPUT FORMATION		KUEH FORMATION		TANGLA FORMATION	
	AVERAGE	RANGE	AVERAGE	RANGE	AVERAGE	RANGE
T max (°C)	394.00	353.00 - 432.00	404.00	391.00 - 438.00	426.00	420.00 - 436.00
TOC (wt %)	6.92	0.10 - 48.60	8.59	0.77 - 52.50	14.13	3.22 - 40.40
S1 (mg HC/g rock)	1.96	0.62 - 13.92	2.22	0.01 - 15.20	1.69	0.36 - 4.46
S2 (mg HC/g rock)	2.86	0.05 - 8.91	14.13	0.38 - 52.50	26.87	1.33 - 42.66
S1 + S2 (mg HC/g rock)	4.79	0.32 - 11.65	16.32	0.96 - 60.06	28.56	2.48 - 81.59
S3 (mg CO2/g rock)	9.54	0.61 - 36.42	8.26	0.39 - 30.36	12.78	1.83 - 42.66
PI (S1/(S1 + S2))	0.41	0.28 - 0.61	0.30	0.09 - 0.43	0.09	0.05 - 0.15
HI (mg HC/g % TOC)	52.55	25.60 - 85.33	78.28	39.33 - 103.16	154.00	79.00 - 241.00
OI (mg CO2/g % TOC)	83.85	60.40 - 149.00	87.76	70.50 - 117.00	73.00	46.00 - 106.00
Rv max (%)	0.25	0.13 - 0.27	0.33	0.23 - 0.40	0.46	0.43 - 0.54





Table 7.15. Rock eval extracted coal samples

S.No	T <sub>max</sub>	S1	S2	S3	PI	S2/S3	PC	TOC	HI	Gi
CN7 433		9.03	106.53	11.34	0.08	9.39	9.63	61.70	172.00	18.00
CN10 435		3.52	123.03	11.17	0.03	11.01	10.54	59.90	205.00	18.00
CN11 436		3.49	148.86	13.01	0.02	11.44	12.69	67.70	219.00	19.00
CN20 432		4.95	127.47	30.77	0.04	4.14	11.03	60.60	210.00	50.00
CN9 403		7.50	50.10	57.40	0.13	0.87	4.80	50.90	98.00	112.00
CN13 415		5.90	57.60	52.60	0.09	1.09	5.29	48.80	118.00	107.00
CN24 413		6.97	68.16	52.47	0.09	1.29	6.26	51.80	131.00	101.00
CN2 429		5.55	187.67	10.90	0.03	17.21	16.10	57.30	527.00	19.00
CN3 434		5.41	226.78	9.26	0.02	24.49	19.34	63.10	359.00	14.00

TABLE 7.16. C.200 L.46L, MACERAL COMPOSITION AND VITRINITE REFLECTANCE DATA OF TERTIARY ONSHORE COALS

SAMPLE GR NO	T <sub>max</sub>	S1	S2	S3	PI	IOC	HI	QI	R <sub>max</sub>	TELO	DETRO	GELO	ALGIN	CUTIN FLUOR	SAMPLE	RESIN	SPORE	SUBST	LIFTS	EA.304	TELO	
CN1	23231	415.00	9.50	121.41	41.66	0.07	53.90	225.00	77.00	0.52	16.50	49.20	4.80	2.25	3.15	1.80	0.45	3.15	1.80	1.80	0.60	15.10
CN2	24585	436.00	11.41	17.68	0.05	72.60	329.00	24.00	0.57	26.80	43.60	5.40	1.20	8.40	0.60	8.00	0.50	0.60	0.60	0.60	3.90	0.00
CN3	22825	450.00	27.08	153.00	7.46	0.14	57.50	284.00	13.00	0.65	28.00	44.00	1.00	1.00	0.00	3.00	2.00	1.00	1.00	2.00	9.90	6.50
CN4	24584	440.00	4.51	177.01	7.27	0.02	61.50	288.00	12.00	0.62	30.00	50.00	8.00	0.00	1.00	0.00	0.40	0.80	0.50	0.50	1.50	6.00
CN5	23229	435.00	13.95	261.72	8.88	0.05	73.60	383.00	12.00	0.55	36.86	45.00	2.80	1.60	8.70	0.00	0.00	0.62	3.16	0.50	0.52	0.00
CN6	23244	429.00	8.98	233.71	12.82	0.04	59.70	391.00	21.00	0.43	3.70	59.00	2.50	1.88	3.76	0.00	6.50	13.17	0.00	0.00	2.50	0.50
CN7	23250	435.00	9.53	174.83	36.29	0.05	65.90	265.00	55.00	0.54	23.60	55.20	4.40	0.00	5.61	0.00	3.16	2.10	0.00	0.00	2.10	1.20
CN8	22826	424.00	20.33	264.10	22.25	0.07	58.20	454.00	38.00	0.35	8.14	40.60	1.30	0.90	0.90	0.00	11.72	0.90	1.80	11.72	18.00	4.00
CN9	24585	427.00	5.82	195.31	12.40	0.03	69.30	282.00	18.00	0.56	23.00	60.50	2.34	2.05	2.73	0.00	1.36	2.05	1.36	2.73	0.68	1.50
CN10	24580	437.00	4.25	180.87	14.81	0.02	67.30	269.00	22.00	0.59	11.00	52.00	1.00	2.40	1.20	1.20	1.20	1.20	0.00	3.60	1.20	24.00
CN11	22824	462.00	11.67	100.27	8.32	0.10	78.00	129.00	11.00	1.15	53.00	40.95	0.00	0.00	0.00	0.00	1.50	0.00	0.00	1.50	3.00	0.00
CN12	22053	412.00	0.19	11.89	50.98	0.02	53.50	22.00	95.00	0.40	51.40	46.60	0.60	0.00	0.00	0.00	0.00	0.00	0.00	0.00	0.00	1.40
CN13	22018	420.00	3.20	6.33	9.73	0.34	11.90	53.00	82.00	0.32	22.00	30.00	3.50	6.67	18.06	2.65	3.43	2.62	1.81	6.67	2.60	0.00
CN14	22849	415.00	9.53	58.95	46.40	0.14	45.20	130.00	103.00	0.35	19.23	35.70	6.00	0.51	15.91	0.51	7.70	2.05	0.51	13.75	0.00	1.10
CN15	22038	421.00	3.74	15.05	20.72	0.20	21.20	76.00	98.00	0.33	38.40	13.90	0.55	4.87	15.40	3.63	9.20	3.01	3.63	4.40	3.00	0.00
CN16	22009	400.00	16.93	73.66	42.13	0.19	47.30	156.00	89.00	0.29	11.00	54.90	9.20	0.84	5.30	1.60	1.70	1.50	3.85	7.31	0.20	1.70
CN17	22013	391.00	21.19	82.64	59.60	0.20	52.00	159.00	115.00	0.28	9.80	64.60	2.00	0.50	4.00	0.50	3.00	2.00	2.00	7.00	0.00	4.50
CN18	22019	412.00	5.56	34.83	34.83	0.14	27.10	129.00	129.00	0.32	17.30	57.00	8.60	0.70	3.50	1.55	0.70	0.35	1.05	7.50	1.05	0.50
CN19	22826	429.00	19.07	282.10	8.48	0.06	71.00	397.00	12.00	0.53	28.80	52.60	7.50	0.00	3.40	1.30	3.00	1.70	0.00	0.50	1.00	0.20
CN20	23237	435.00	9.33	153.37	4.70	0.06	54.40	282.00	9.00	0.70	23.30	44.40	9.24	0.00	9.23	0.00	0.40	0.80	1.10	5.70	0.00	5.70
CN21	23236	25.00	5.75	130.19	27.18	0.04	66.00	197.00	41.00	0.50	29.46	42.77	6.00	1.18	5.34	0.00	2.97	1.18	0.00	9.50	0.00	1.60
CN22	22039	404.00	1.73	33.66	7.13	0.05	12.40	271.00	58.00	0.30	25.00	48.00	5.00	2.90	4.30	0.00	1.00	1.00	1.30	7.00	1.50	1.70
CN23	22049	398.00	14.53	66.20	41.33	0.18	43.00	154.00	96.00	0.25	11.21	63.60	5.30	0.00	3.00	0.00	4.32	0.85	1.70	7.00	0.30	2.30
CN24	23242	424.00	3.15	123.55	27.03	0.02	59.10	209.00	46.00	0.52	7.19	62.00	2.50	0.00	2.76	0.92	2.78	3.71	1.85	4.64	2.78	8.50
CN25	21599	397.00	18.10	71.17	47.97	0.20	48.30	147.00	99.00	0.29	15.72	58.60	6.90	1.20	5.80	0.60	3.50	0.50	0.50	4.20	0.50	1.90
CN26	22382	410.00	12.80	56.80	35.20	0.18	31.60	180.00	111.00	0.30	23.30	48.30	5.20	0.00	5.70	2.30	1.70	2.50	1.70	7.00	0.00	2.30
CN27	21989	420.00	6.62	47.35	50.72	0.12	36.60	129.00	139.00	0.34	13.80	21.20	0.20	0.00	24.54	0.08	9.39	1.90	0.60	7.49	0.00	0.80
CN28	23518	431.00	6.00	142.53	7.40	0.04	44.60	320.00	17.00	0.80	28.60	44.70	8.00	0.00	5.40	0.00	0.40	0.80	1.10	5.70	0.50	5.00

Table 7.17. Extraction result on shale samples from West Aceh Basin

Borehole	Formation	Depth (M)	Sample No.	TOC (WT%)	EOM (mg)	SATS (%)	AROM (%)	POL (%)	MgHc/gTOC	R <sub>max</sub> (%)
BUBON	TUTUT	381	BB6	0.10	230.50	2.50	0.78	21.17	514.20	0.27
	KUEH	701	BB10	0.16	152.20	0.40	0.57	22.88	80.80	0.34
	KUEH	1341	BB25	2.20	16.00	2.00	2.70	70.66	38.20	0.42
TRIPA	TUTUT	594	TR9	0.54	68.00	3.00	17.60	2.40	90.10	0.29
	KUEH	1197	TR17	0.83	21.70	4.20	1.86	4.13	53.80	0.30
	KUEH	1645	TR27	1.04	21.20	6.20	3.31	52.60	140.80	0.31
MEULABOH	KUEH	1216	M10	1.66	0.80	12.50	12.50	25.00	13.30	0.32
	KUEH	2310	M16	2.68	17.30	1.70	1.15	8.09	8.10	0.43
	TANGLA	2639	M21	10.22	20.40	8.60	10.29	17.16	27.50	0.54
TEUNOM	TUTUT	295	TN5	0.61	25.20	2.40	0.39	7.20	34.20	0.27
	KUEH	473	TN3	0.90	8.70	1.20	5.88	3.50	101.30	0.34

Table 7.18. Extraction result on coal samples from West Aceh Basin

BOREHOLE	FORMATION	DEPTH ( M )	SAMPLE NO	TOC (Wt%)	EOM (mg)	SATS ( % )	AROM ( % )	POL (%)	MgHC/ g/TOC	R <sub>v</sub> max ( % )
M - 11	TUTUT	157	M1/11	52.00	58.20	2.60	0.90	35.20	3.20	0.28
M - 22	TUTUT	109	M22/2	36.60	113.60	1.90	1.53	16.34	4.40	0.34
MEULABOH	TANGLA	2529	M19	40.40	7.50	2.30	2.70	26.66	5.50	0.44
TRIPA	KUEH	2025	TR36	34.40	8.00	10.10	5.06	22.78	12.60	0.37
BUBON	TUTUT	225	BB2	48.60	36.20	3.60	3.61	33.05	2.30	0.28
BUBON	KUEH	1176	BB19	51.50	462.30	2.00	1.48	13.14	9.30	0.40
OUTCROP	KUEH	-	K20	78.00	82.80	25.90	30.98	36.66	27.40	1.15
OUTCROP	KUEH	-	K21	58.20	358.00	2.00	3.08	31.93	8.40	0.35
OUTCROP	TANGLA	-	L5	65.90	17.00	4.80	8.33	22.02	1.10	0.54
OUTCROP	TANGLA	-	L14	69.30	55.60	4.20	10.38	21.34	3.60	0.56
OUTCROP	TANGLA	-	L21	73.60	21.40	10.00	14.76	26.66	2.00	0.59
OUTCROP	TANGLA	-	L20	57.50	139.00	5.30	11.17	17.05	24.70	0.65

Table 7.20. Alkane parameters (coal extract) from West Aueh Basin

LOGHOLE	FORMATION	DEPTH ( m )	SAMPLE NO.	Pr/Ph	Pr/C17	Ph/C16	C11	MeHe g/TOC	S/A	Kolmaz ( % )
M - 11	TUTUT	157	M1/11	2.00	0.26	0.10	1.95	5.20	2.66	0.50
N - 22	TUTUT	103	M22/2	4.00	1.50	0.27	1.47	4.40	1.21	0.53
MEULABOH	TANGLA	2520	M19	2.33	0.94	0.25	1.88	5.50	0.85	0.44
TRIPA	KUEH	2025	TR36	1.50	0.35	0.12	2.74	12.60	1.99	0.37
BUEON	TUTUT	225	BR2	1.40	0.41	0.15	3.79	2.30	0.99	0.26
BUEON	KUEH	1170	BB19	1.66	0.44	0.12	2.93	9.50	1.35	0.40
OUTCROP	KUEH	-	K20	5.20	2.64	2.87	2.23	27.40	0.55	1.15
OUTCROP	KUEH	-	K21	9.00	11.45	0.73	2.87	3.00	0.67	0.53
OUTCROP	TANGLA	-	L5	3.25	6.60	0.42	2.65	1.10	0.67	0.54
OUTCROP	TANGLA	-	L14	3.23	5.45	0.50	3.00	3.60	0.40	0.50
OUTCROP	TANGLA	-	L21	6.00	11.45	0.73	2.87	2.00	0.67	0.53
OUTCROP	TANGLA	-	L20	6.28	1.33	0.23	2.16	21.70	0.47	0.15

Table 7.19. Alkane parameters (source rock extract) from West Aceh Basin

BOREHOLE	FORMATION	DEPTH ( M )	SAMPLE NO.	Pr/Ph	Pr/C17	Ph/C18	CPI	mgIic/ g/TOC	S/A	R <sub>V</sub> <sup>max</sup> ( % )
BUBON	TUTUT	381	BB6	1.45	0.28	0.10	0.87	514.20	3.20	0.27
	KUEH	701	BB10	0.94	0.29	0.18	1.88	80.80	0.70	0.34
	KUEH	1341	BB25	1.55	0.77	0.32	1.97	8.10	1.47	0.42
TRIPA	TUTUT	594	TR9	1.30	0.26	0.12	2.36	96.10	0.17	0.29
	KUEH	1197	TR17	1.00	0.21	0.15	1.44	58.80	2.33	0.30
	KUEH	1645	TR27	0.87	0.18	0.31	1.52	140.80	1.87	0.31
MEULABOH	KUEH	1216	M10	1.05	0.33	0.14	2.36	13.30	1.00	0.32
	KUEH	2310	M16	1.71	0.98	0.16	2.58	38.20	0.74	0.43
	TANGLA	2639	M21	9.75	2.60	0.15	2.82	530.40	0.85	0.54
TEUNOM	TUTUT	295	TN5	0.88	0.25	0.15	2.20	34.20	6.15	0.27
	KUEH	478	TN8	0.66	0.25	0.14	1.85	101.30	0.20	0.34





TABLE 2.2. DATA MATRIX FOR PYROLYSIS-60 : MACERAL AND VITRINITE REFLECTANCE

SAMPLE	GR NO	TELG	DETRO	GELO	KUGIN	CUTIN	FLUOR	RESIN	SPKRE	SUBER	LIPTO	EXUDA	INERT	R <sub>max</sub>	C1-C5	C6-14	C15+	C7+/A	PHEN	F/CB	A3/CB
P61	22039	40.00	20.82	13.00	0.00	5.20	0.78	0.78	0.00	11.96	6.76	0.00	0.70	0.30	87.18	6.19	6.63	2.27	4.94	7.54	1.46
P62	22018	18.39	44.53	11.83	0.50	2.64	1.44	2.85	1.44	3.81	7.66	1.00	2.53	0.32	82.32	8.93	8.75	2.02	9.35	10.09	1.43
P63	22009	26.50	17.20	7.50	0.00	11.20	0.70	13.30	0.70	8.40	7.00	0.00	7.50	0.29	84.34	7.50	7.96	2.41	7.25	8.54	1.56
P64	31509	13.80	21.20	0.20	0.00	24.54	0.08	9.39	1.90	0.60	7.49	0.00	0.80	0.34	86.43	6.52	7.05	2.33	5.50	5.42	1.76
P65	22826	8.14	40.60	1.30	0.90	0.90	0.00	11.72	0.90	1.80	11.72	18.00	4.00	0.35	66.34	19.09	14.57	3.50	6.77	1.90	0.90
P66	22825	28.00	44.00	1.50	1.00	1.00	0.00	3.00	5.00	1.00	2.00	9.90	6.60	0.65	78.63	12.14	9.23	3.03	4.48	0.80	1.29
P67	25231	23.80	43.30	5.40	1.20	8.40	0.60	7.20	0.60	0.60	1.20	4.20	0.00	0.52	70.33	16.84	12.84	5.55	4.85	1.08	0.78
P68	24585	27.20	34.00	4.50	0.60	10.90	0.00	0.00	1.80	13.80	4.20	0.00	2.00	0.56	69.55	13.00	16.90	5.18	5.06	1.54	1.03
P69	23239	11.55	56.00	1.50	1.00	18.12	2.62	2.17	0.70	0.72	3.62	0.00	2.00	0.55	67.33	16.69	15.98	4.67	5.46	1.53	0.64
P610	24523	23.60	60.54	2.00	2.05	2.73	0.00	1.36	2.05	1.36	2.73	0.66	1.50	0.58	65.36	20.17	14.47	3.12	2.84	1.95	1.30
P611	22824	53.00	40.95	0.00	0.00	0.00	0.00	1.50	0.00	0.00	1.50	3.10	0.00	1.15	65.88	18.79	15.32	7.37	4.68	0.11	0.46
P612	24583	36.86	45.00	2.80	1.60	8.70	0.00	0.00	0.62	3.18	0.62	0.62	0.00	0.56	58.47	16.57	22.96	6.74	8.09	2.16	0.73
P613	24584	24.41	44.20	8.80	0.00	9.20	0.00	0.40	0.80	1.20	5.60	0.00	5.30	0.61	57.11	20.62	22.27	6.67	5.12	0.92	0.75
P614	22826	29.20	47.15	3.20	7.02	1.31	0.80	1.75	1.31	0.00	2.63	3.05	2.40	0.51	77.24	14.38	8.37	2.78	4.04	1.75	1.14

TABLE 7.23

SIGNIFICANT VALUES IN P-M. MATRIX FOR PYROLYSIS GC AND COAL PETROLOGY

UPPER HALF OF MATRIX EQUALS PROBABILITY AT 95% CONFIDENCE LEVEL  
 LOWER HALF OF MATRIX EQUALS PROBABILITY AT 99% CONFIDENCE LEVEL

SAMPLE	TELO	DETRO	GELO	ALGIN	CUTIN	FLUOR	RESIN	SPORE	SUBER	LIPTO	EXUDA	INERT	Rmax	C1-C5	C6-14	C15+	C7+/A	PHEN	P/C8	A3/C8
TELO	*****	0.0000	0.0000	0.0000	0.0000	0.0000	0.0000	0.0000	0.0000	-0.5689	0.0000	0.0000	0.6135	0.0000	0.0000	0.0000	0.0000	0.0000	0.0000	0.0000
DETRO	0.0000*****	*****	0.0000	0.0000	0.0000	0.0000	0.0000	0.0000	-0.5709	0.0000	0.0000	0.0000	0.0000	-0.6490	0.7585	0.0000	0.0000	0.0000	-0.5680	0.0000
GELO	0.0000	0.0000*****	*****	0.0000	0.0000	0.0000	0.0000	0.0000	0.5448	0.0000	0.0000	0.0000	0.0000	0.0000	0.0000	0.0000	0.0000	0.0000	0.6893	0.6600
ALGIN	0.0000	0.0000	0.0000*****	*****	0.0000	0.0000	0.0000	0.0000	0.0000	0.0000	0.0000	0.0000	0.0000	0.0000	0.0000	0.0000	0.0000	0.0000	0.0000	0.0000
CUTIN	0.0000	0.0000	0.0000	0.0000*****	*****	0.0000	0.0000	0.0000	0.0000	0.0000	0.0000	0.0000	0.0000	0.0000	0.0000	0.0000	0.0000	0.0000	0.0000	0.0000
FLUOR	0.0000	0.0000	0.0000	0.0000	0.0000*****	*****	0.0000	0.0000	0.0000	0.0000	0.0000	0.0000	0.0000	0.0000	0.0000	0.0000	0.0000	0.0000	0.0000	0.0000
RESIN	0.0000	0.0000	0.0000	0.0000	0.0000	0.0000*****	*****	0.0000	0.0000	0.5720	0.0000	0.0000	0.0000	0.0000	0.0000	0.0000	0.0000	0.0000	0.0000	0.0000
SPORE	0.0000	0.0000	0.0000	0.0000	0.0000	0.0000	0.0000*****	*****	0.0000	0.0000	0.0000	0.0000	0.0000	0.0000	0.0000	0.0000	0.0000	0.0000	0.0000	0.0000
SUBER	0.0000	0.0000	0.0000	0.0000	0.0000	0.0000	0.0000	0.0000*****	*****	0.0000	0.0000	0.0000	0.0000	0.0000	0.0000	0.0000	0.0000	0.0000	0.0000	0.0000
LIPTO	0.0000	0.0000	0.0000	0.0000	0.0000	0.0000	0.0000	0.0000	0.0000*****	*****	0.0000	0.0000	0.0000	0.0000	0.0000	0.0000	0.0000	0.0000	0.0000	0.0000
EXUDA	0.0000	0.0000	0.0000	0.0000	0.0000	0.0000	0.0000	0.0000	0.0000	0.0000*****	*****	0.0000	-0.6418	0.0000	0.0000	0.0000	0.0000	0.0000	0.5414	0.0000
INERT	0.0000	0.0000	0.0000	0.0000	0.0000	0.0000	0.0000	0.0000	0.0000	0.0000*****	*****	0.0000	0.0000	0.0000	0.0000	0.0000	0.0000	0.0000	0.0000	0.0000
Rmax	0.0000	0.0000	0.0000	0.0000	0.0000	0.0000	0.0000	0.0000	0.0000	0.0000	0.0000*****	*****	0.0000	-0.5324	0.5733	0.0000	0.0000	0.0000	0.0000	0.0000
C1-C5	0.0000	0.0000	0.0000	0.0000	0.0000	0.0000	0.0000	0.0000	0.0000	0.0000	0.0000	0.0000	0.0000*****	*****	-0.9455	-0.9522	0.7183	0.0000	-0.6883	-0.6922
C6-14	0.0000	0.7585	0.0000	0.0000	0.0000	0.0000	0.0000	0.0000	0.0000	0.0000	0.0000	0.0000	0.0000	0.0000	0.0000	0.0000	-0.8262	0.0000	0.7305	0.8584
C15+	0.0000	0.0000	0.0000	0.0000	0.0000	0.0000	0.0000	0.0000	0.0000	0.0000	0.0000	0.0000	0.0000	-0.9455*****	*****	0.8011	0.7130	0.0000	-0.7897	-0.8252
C7+/A	0.0000	0.0000	0.0000	0.0000	0.0000	0.0000	0.0000	0.0000	0.0000	0.0000	0.0000	0.0000	0.0000	0.0000	0.8011	*****	0.8508	0.0000	-0.5966	-0.7637
PHEN	0.0000	0.0000	0.0000	0.0000	0.0000	0.0000	0.0000	0.0000	0.0000	0.0000	0.0000	0.0000	0.7183	-0.8262	0.7130	0.8508*****	*****	0.0000	-0.6710	-0.8945
P/C8	0.0000	0.0000	0.0000	0.0000	0.0000	0.0000	0.0000	0.0000	0.0000	0.0000	0.0000	0.0000	-0.6883	0.7305	-0.7897	0.0000	0.0000*****	*****	0.6028	0.0000
A3/C8	0.0000	0.0000	0.0000	0.0000	0.0000	0.0000	0.0000	0.0000	0.0000	0.0000	0.0000	0.0000	-0.6922	0.8364	-0.8252	-0.7637	-0.8945	0.0000	0.7396*****	*****

FIGURES AND TABLES OF  
CHAPTER 8

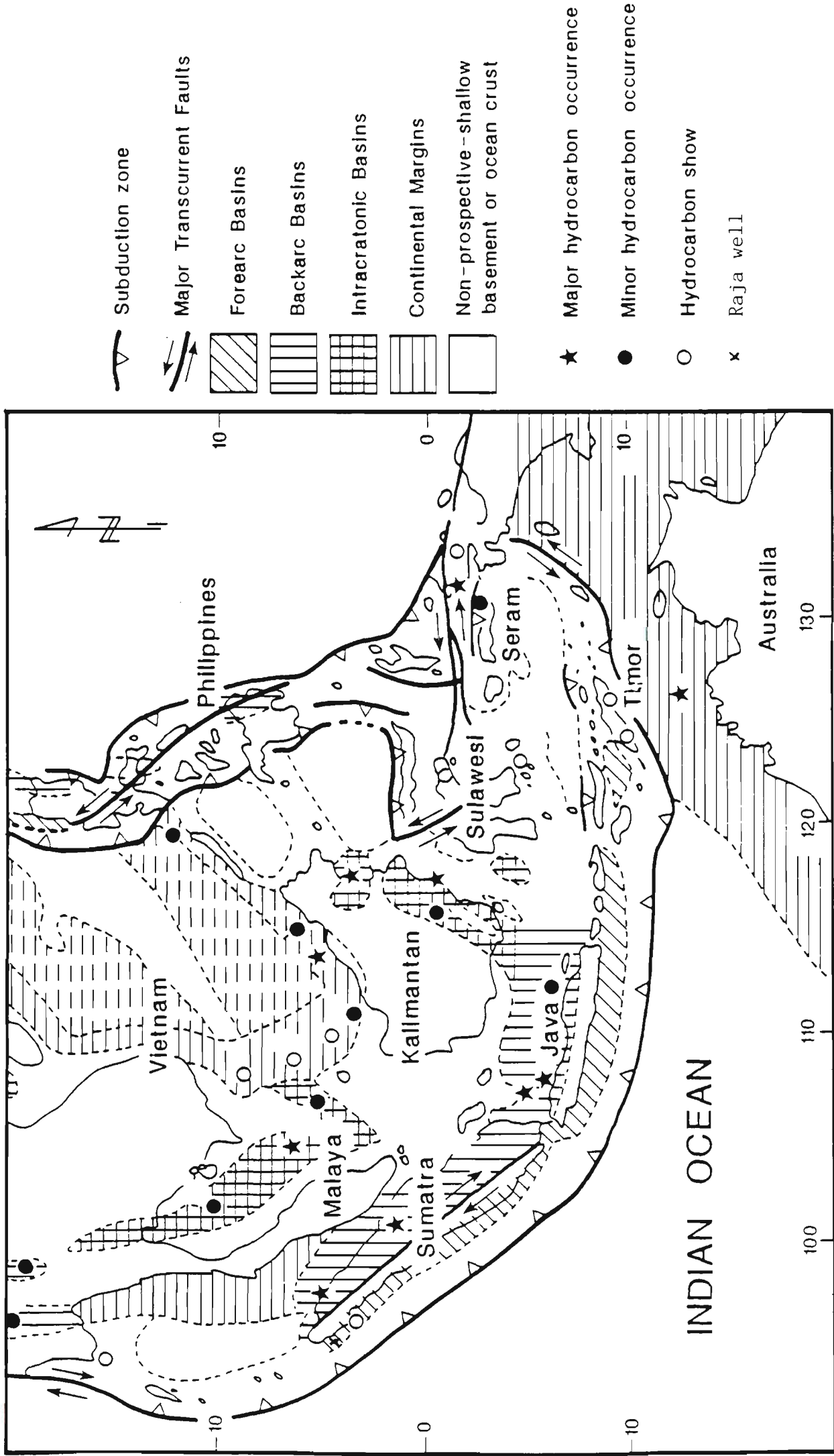


Figure 8.1: Hydrocarbon occurrence Map of Indonesia and the surrounding area (after Barber, 1985).

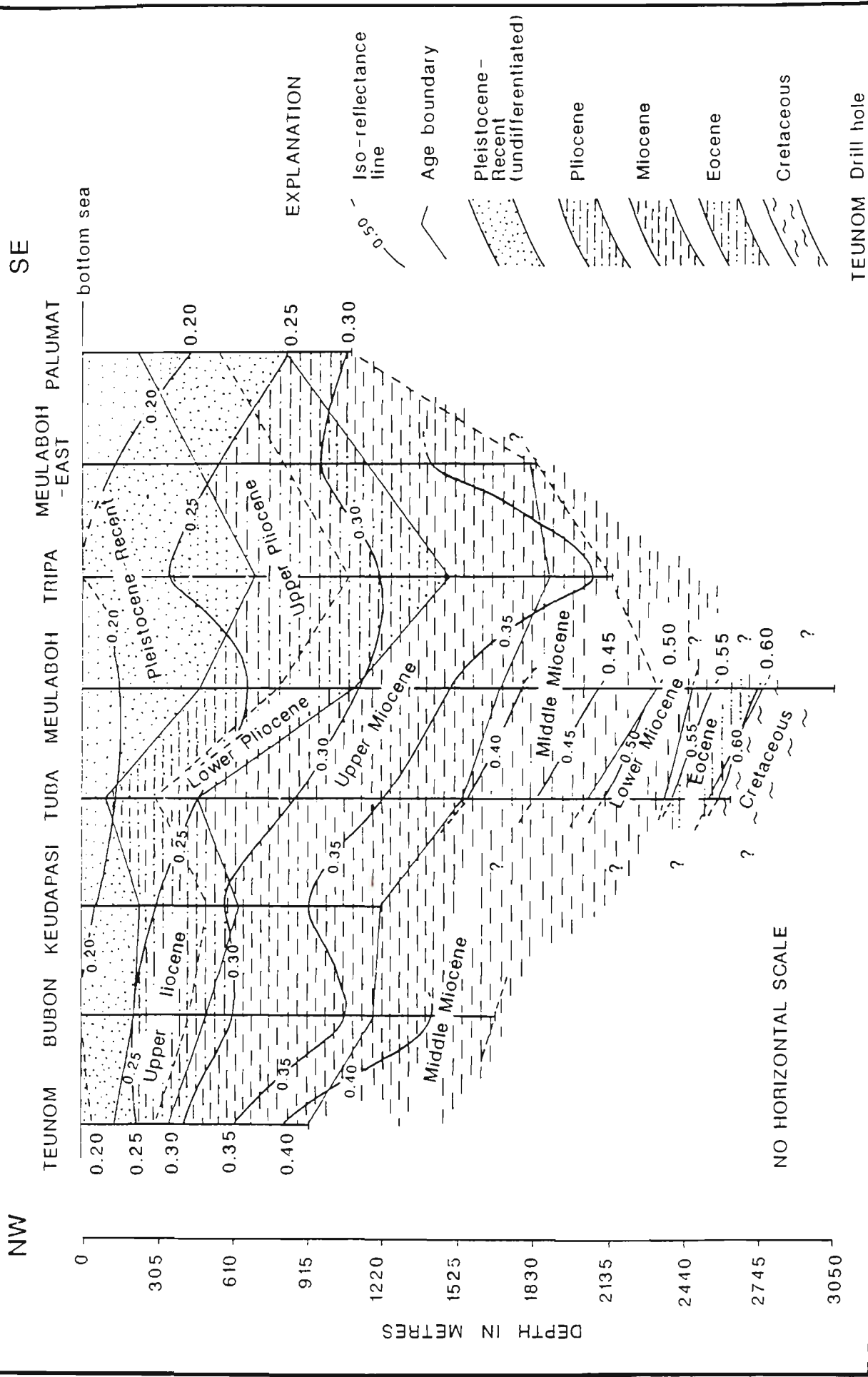


Figure 8.2: Idealized iso-reflectance profile versus tentative Age Boundary and depth at the offshore wells of West Aceh Basin.

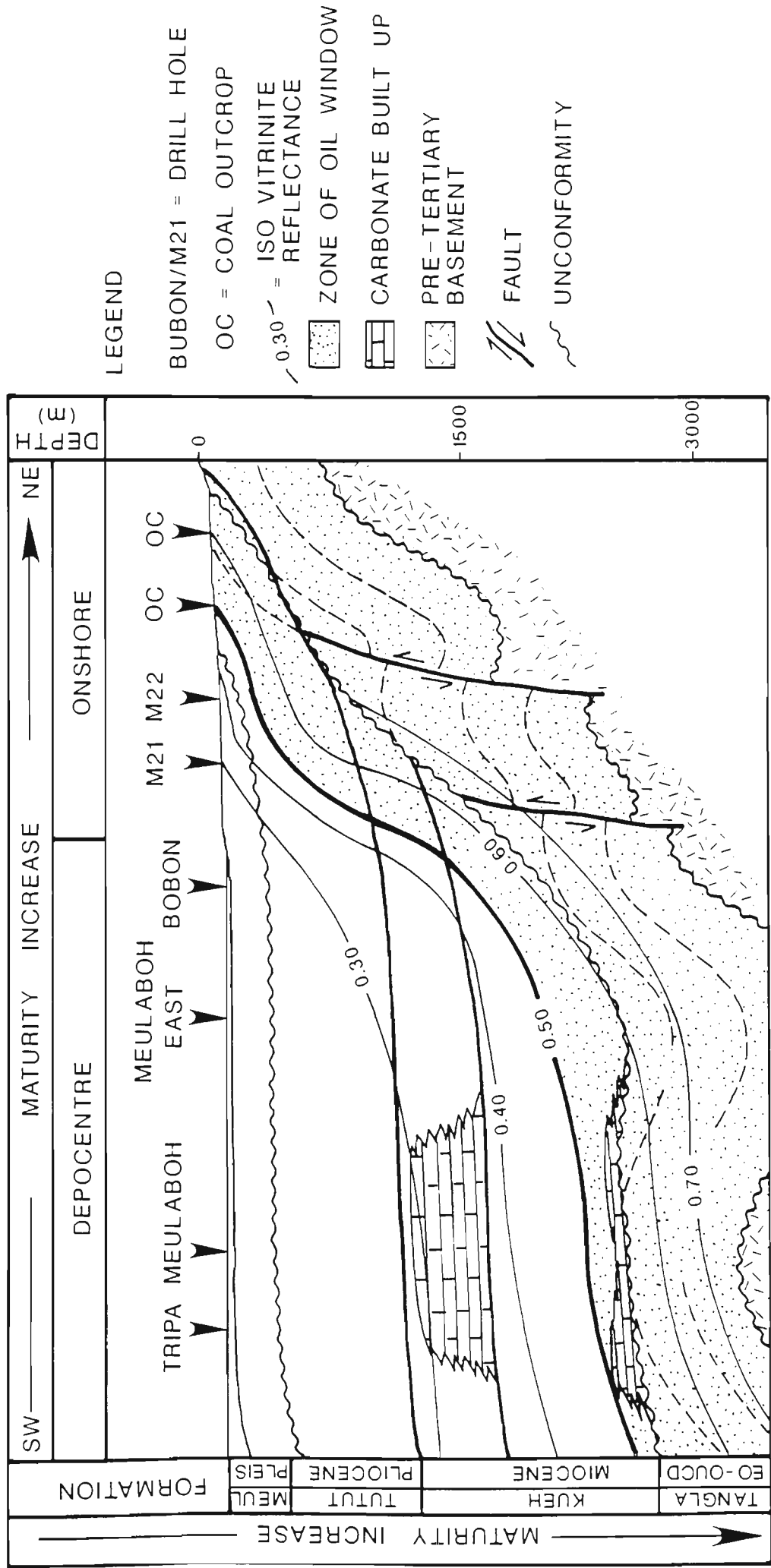
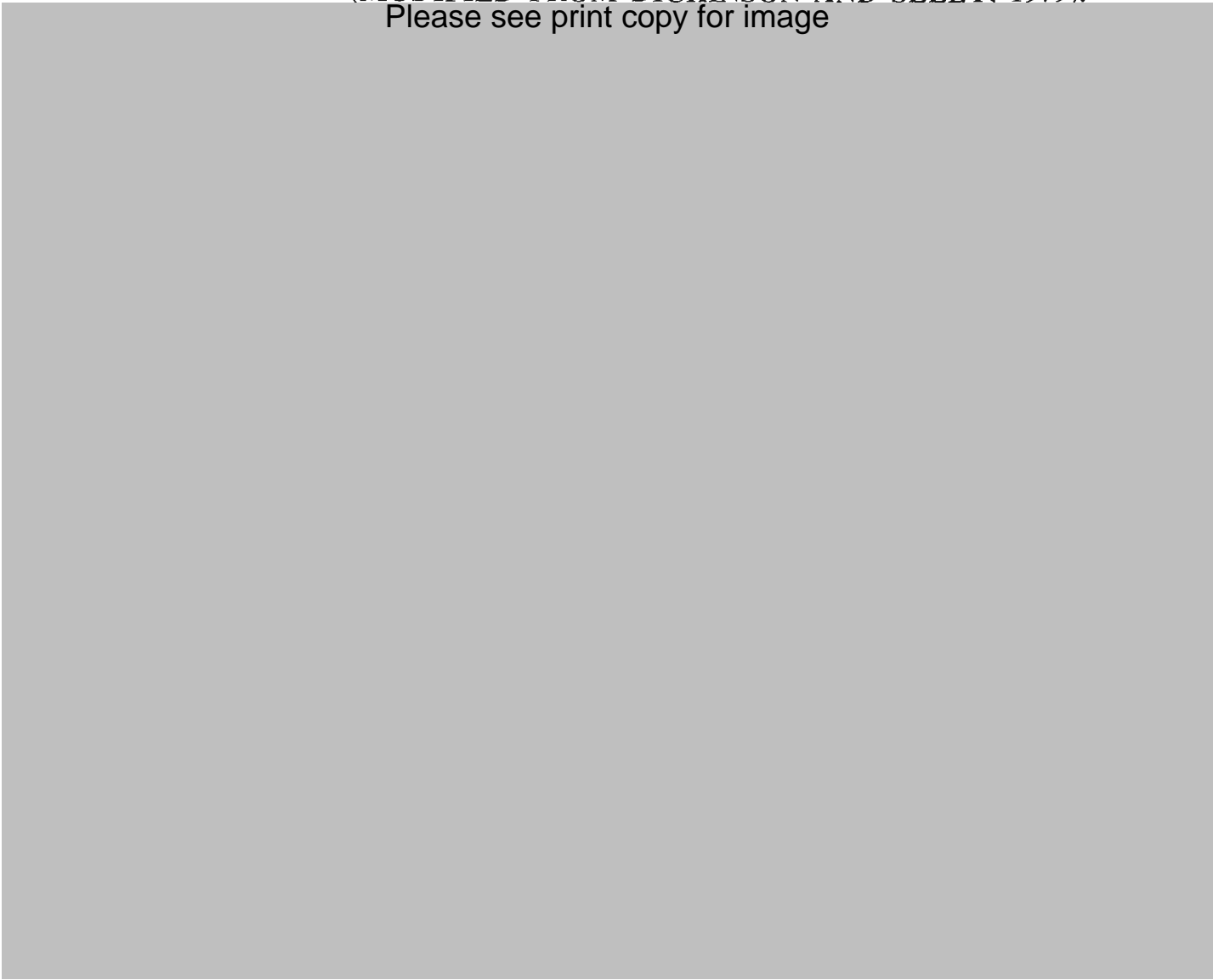


Figure 8.3: Maturation pattern in the Tertiary Formations of West Aceh Basin.

**TABLE 8.1. THE POSSIBILITY GEOLOGICAL FACTORS  
CONTROLLING HYDROCARBON GENERATION AND  
ACCUMULATION IN THE FOREARC BASIN SETTING  
(MODIFIED FROM DICKINSON AND SEELY, 1979).**  
Please see print copy for image



# PLATES

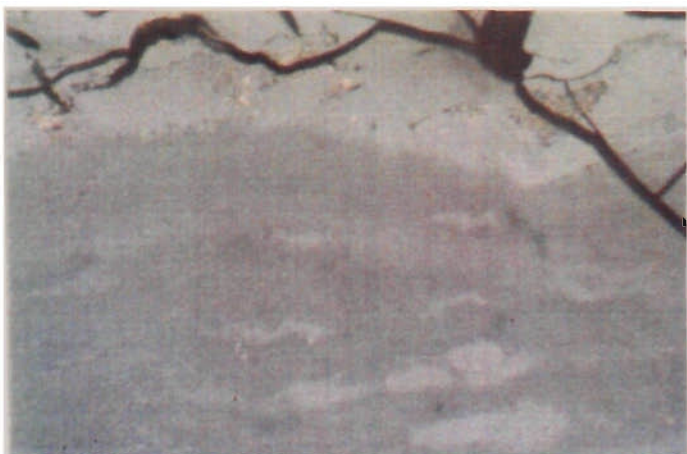


## PLATE I

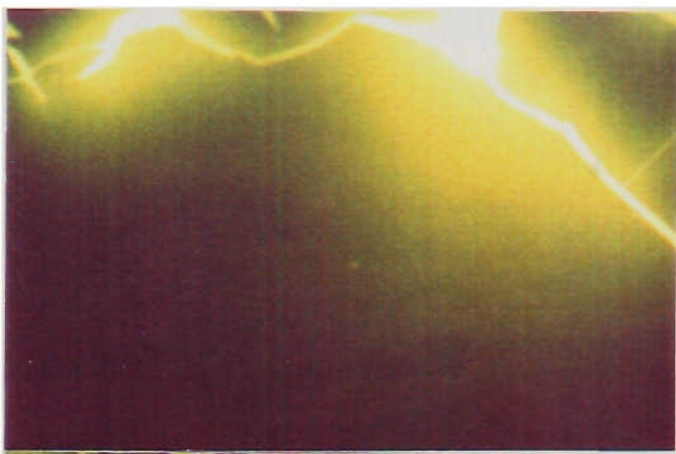
General microscopic features of exsudatinite and bitumen.

- 1a. Perpendicular and parallel exsudatinite to the desmocollinite bands. Sample GM 23233, Miocene coal,  $R_{\max}=0.51\%$ , field with 0.33mm.
- 1b. As for plate 1a, but in fluorescence mode with bright-yellow oil haze.
- 2a. Exsudatinite perpendicular to the detrovitrinite. Sample GM 23319, Pliocene coal,  $R_{\max}=0.27\%$ , field width 0.29mm.
- 2b. As for plate 2a, but in fluorescence mode.
- 3a. Exsudatinite with the shrinkage cracks and vesicle associated with detrovitrinite groundmass. Sample GM 21992, Pliocene coal,  $R_{\max}=0.31\%$ , field width 0.33mm.
- 3b. As for plate 3a, but in fluorescence mode.
- 4a. Globular solid bitumen in calcareous sandstone with shrinkage cracks. Sample GM 22386, Tutut Formation. Keudapasi well,  $R_{\max}=0.24\%$ , field width 0.53mm.
- 4b. As for plate 4a, but in fluorescence mode.
- 5a. Flat body solid bitumen associated with calcite grain. Sample GM 22469, Kueh Formation. Bubon well,  $R_{\max}=0.41\%$ , field width 0.43mm.
- 5b. As for plate 5a, but in fluorescence mode

# PLATE I



1a



1b



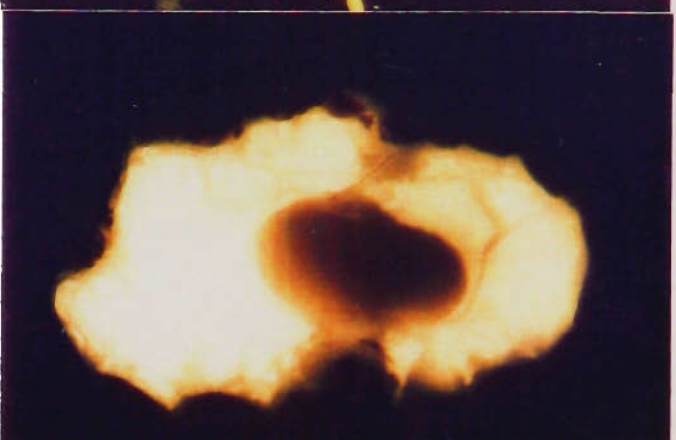
2a



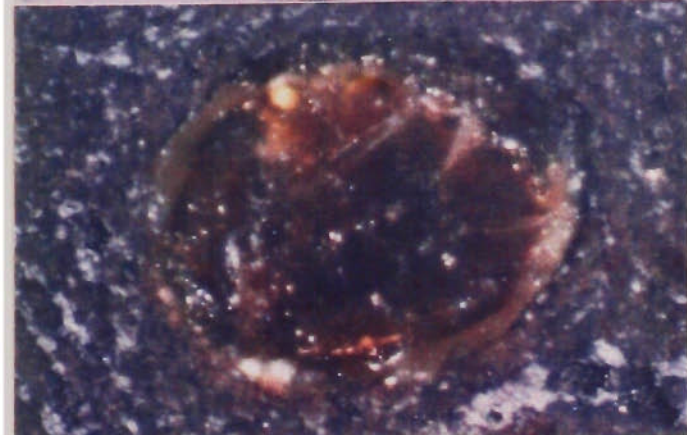
2b



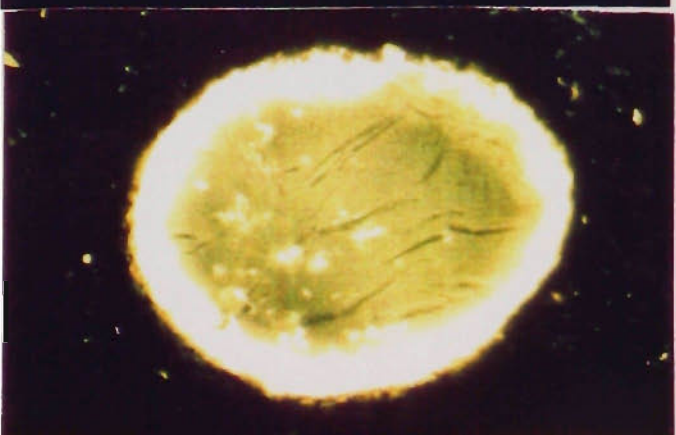
3a



3b



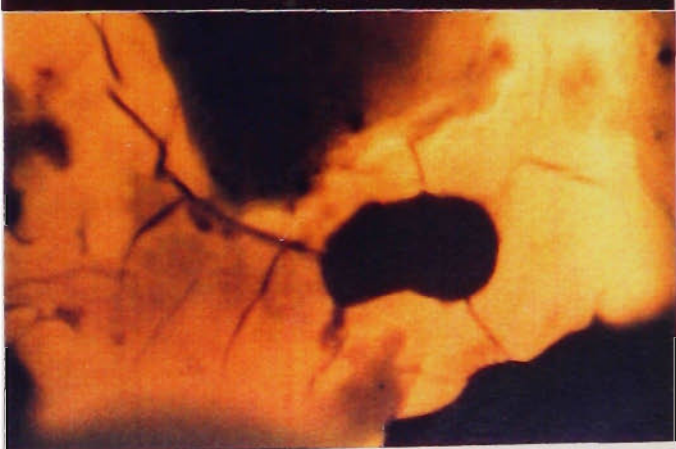
4a



4b



5a



5b

## PLATE II

### Photomicrographs of vitrinite group of the Tertiary coals in West Aceh Basin

1. Telocollinite band associated with corpogelinite and semifusinite. Sample GM 24290, Oligocene coal,  $R_{\max}=0.55\%$ , field width 0.60mm.
2. Desmocollinite and attrinite band. Sample GM 23231, Oligocene coal,  $R_{\max}=0.52\%$ , field width 0.53mm.
3. Alternation between densinite (Dn) and desmocollinite (Ds). Sample GM 23241, Miocene coal,  $R_{\max}=0.47\%$ , field width 0.60mm.
4. Corpogelinite in the densinite groundmass. Sample GM 23238, Miocene coal,  $R_{\max}=0.51\%$ , field width 0.53mm.
5. Various type of fungal sclerotia associated with cutinite and desmocollinite bands. Sample GM23243, Miocene coal,  $R_{\max}=0.42\%$ , field width 0.51mm.
6. Oval body of macrinite associated with cutinite and desmocollinite bands. Sample GM 22832, Miocene coal,  $R_{\max}=0.44\%$ , field width 0.56mm.
7. Attrinite associated with inertodetrinite. Sample GM 22826, Pliocene coal,  $R_{\max}=0.35\%$ , field width 0.61mm.
8. Porigelinite filling in textinite cell lumens. Sample GM 22034, Pliocene coal,  $R_{\max}=0.40\%$ , field width 0.51mm.



PLATE II

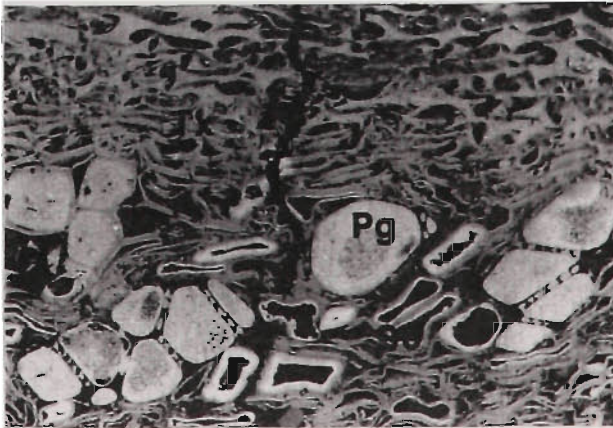
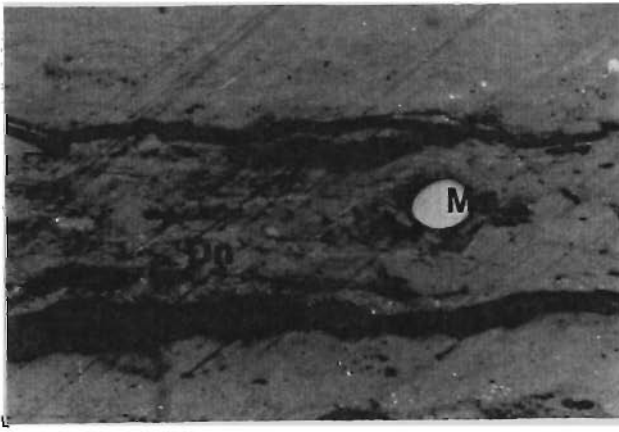
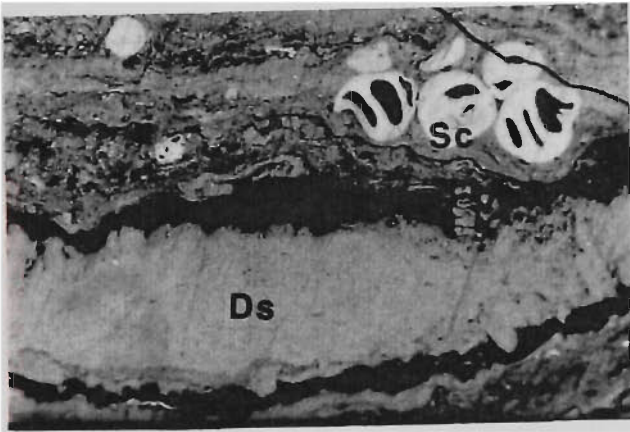
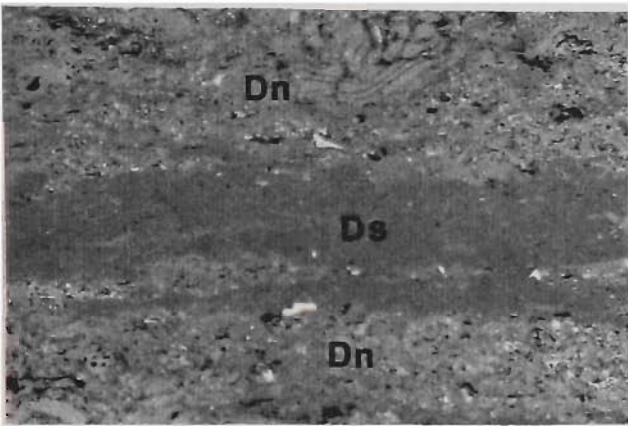
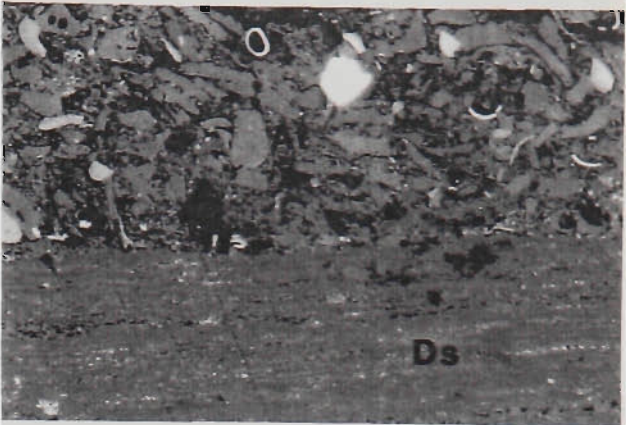
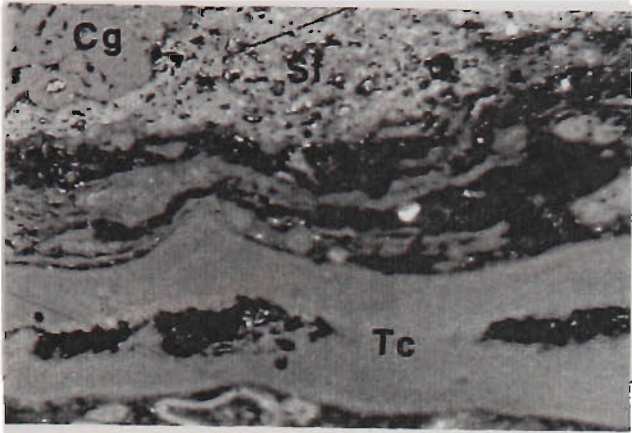
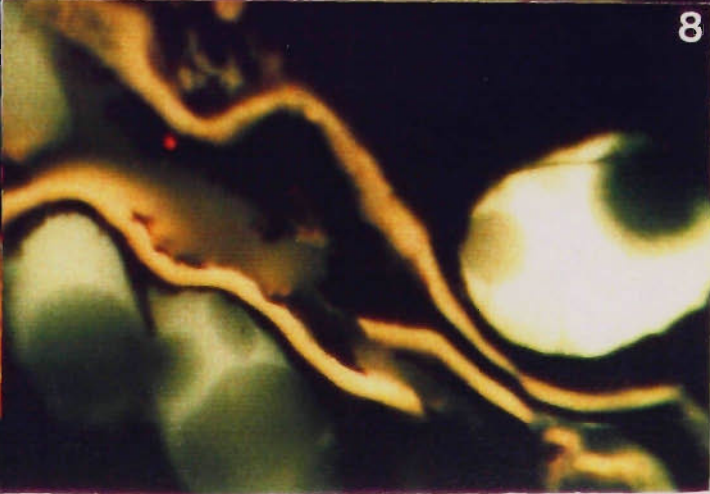
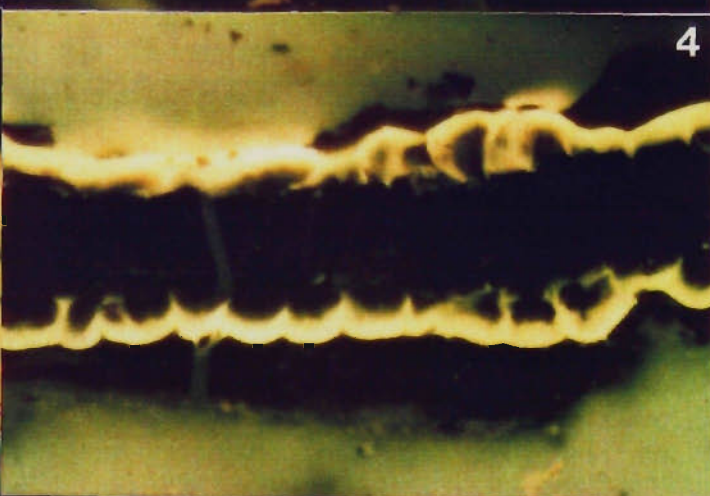
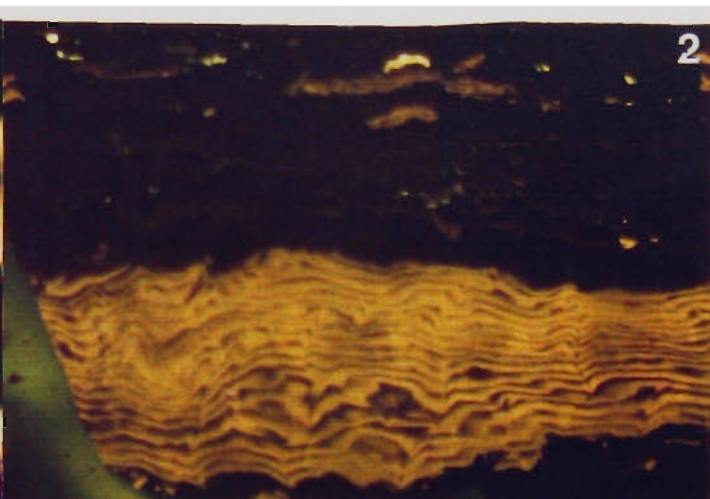




PLATE III



### PLATE III

Fluorescence photomicrographs of liptinite macerals of the Tertiary coals in West Aceh basin.

1. Fragmented crassicutinite in detrovitrinite groundmass. Sample GM 24583, Oligocene coal,  $R_{\max}=0.56\%$ , field width 0.32mm.
2. Thick wall suberinite bands associated with clarite. Sample GM 23239,  $R_{\max}=0.55\%$ , field width 0.45mm.
3. *Botryococcus*-derived telalginite in Oligocene coal, sample GM 23237,  $R_{\max}=0.53\%$ , field width 0.53mm.
4. Cutinite in vitrinite bands of Miocene coal. Sample GM 23240,  $R_{\max}=0.45\%$ , field width 0.45mm.
5. Cell-filling resinite associated with clarite. Sample GM 22826, Miocene coal,  $R_{\max}=0.35\%$ , field width 0.44mm.
6. Soluble exsudatinitite expelled from clarite layer. Sample GM 22826, Miocene coal,  $R_{\max}=0.35\%$ , field width 0.51mm.
7. Sporangium in Pliocene coal. Sample 22032,  $R_{\max}=0.29\%$ , field width 0.35mm.
8. Globular fluorinite associated with fragmented cutinite. Sample GM 22845, Pliocene coal,  $R_{\max}=0.29\%$ , field width 0.44%.

## PLATE IV

### Type I exsudatinite in the Tertiary coals of West Aceh basin.

1. Exsudatinite-derived resinite, filling vitrinite cavities. Sample GM 23242, Miocene coal,  $R_{\max}=0.42\%$ , field width 0.30mm.
2. Exsudatinite expell from resinite body. Sample GM 22826, Miocene coal,  $R_{\max}=0.35\%$ , field width 0.33mm.
3. Exsudatinite associated with sporinite-rich clarite. Sample GM 23487,  $R_{\max}=0.30$ , field width 0.29mm.
4. Exsudatinite-derived from clarite band. Sample GM 23355, Pliocene coal,  $R_{\max}=31\%$ , field width 0.33mm.
5. Soluble exsudatinite expell from suberinite. Sample 22003, Pliocene coal,  $R_{\max}=0.31\%$ , field width 0.35mm.
6. Soluble exsudatinite expelled from megaspore. Sample GM 22825, Oligocene coal,  $R_{\max}=0.65\%$ , field width 0.30mm.
7. Exsudatinite and oil haze associated with cutinite. Sample GM 21995, Pliocene coal,  $R_{\max}=0.29\%$ , field width 0.29mm.
8. Soluble exsudatinite expelled from desmocollinite. Sample GM 23244, Miocene coal,  $R_{\max}=0.43\%$ , field width 0.35mm.



PLATE IV

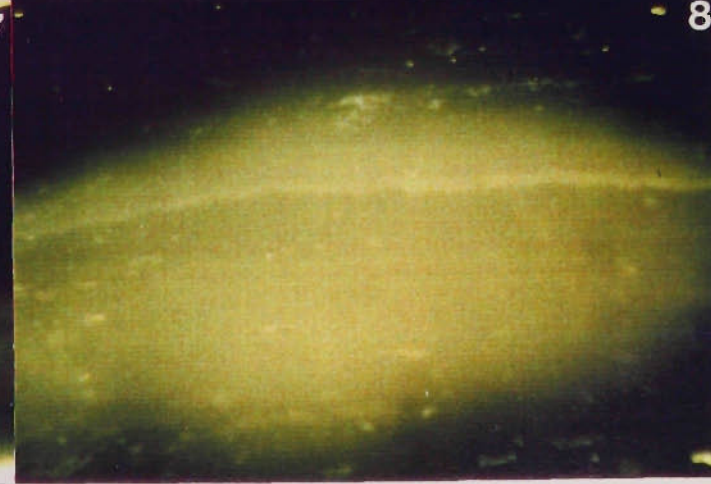
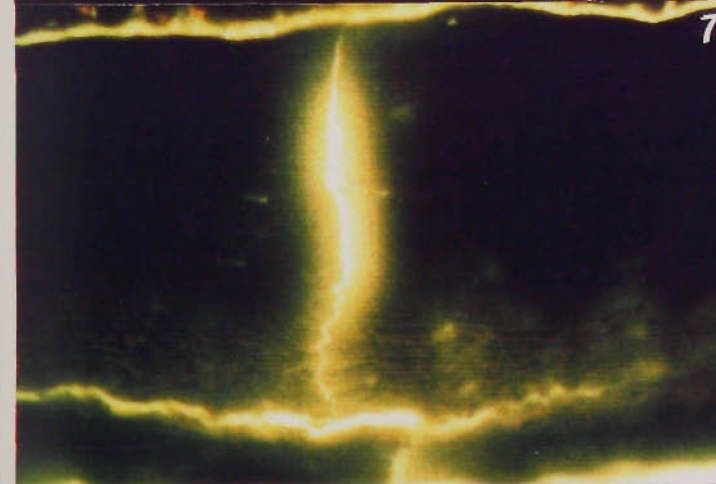
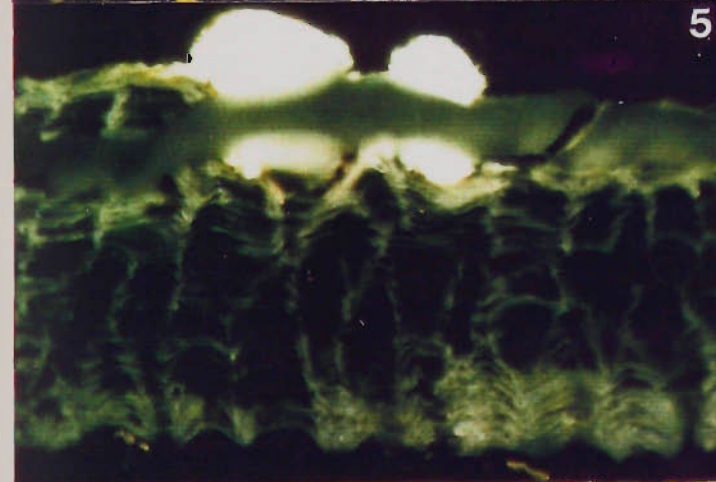
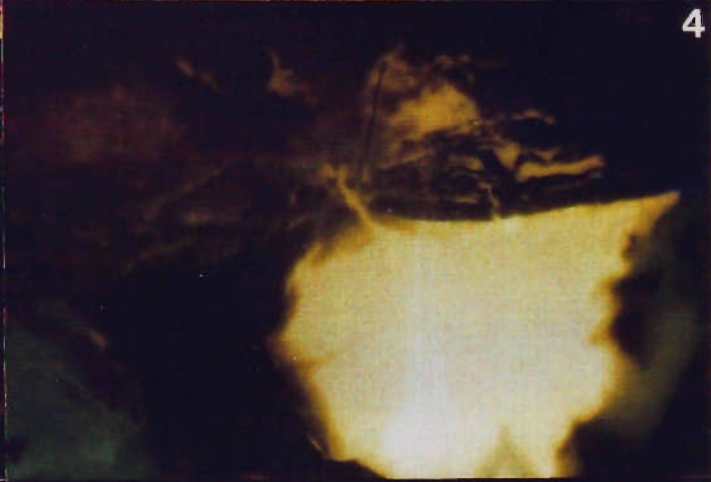
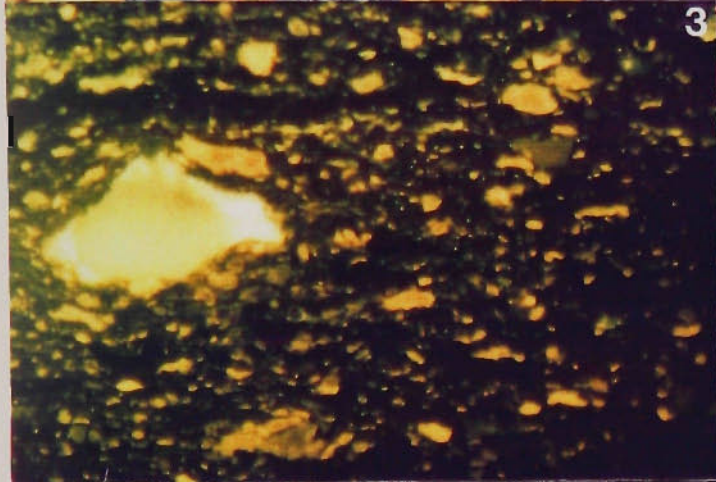
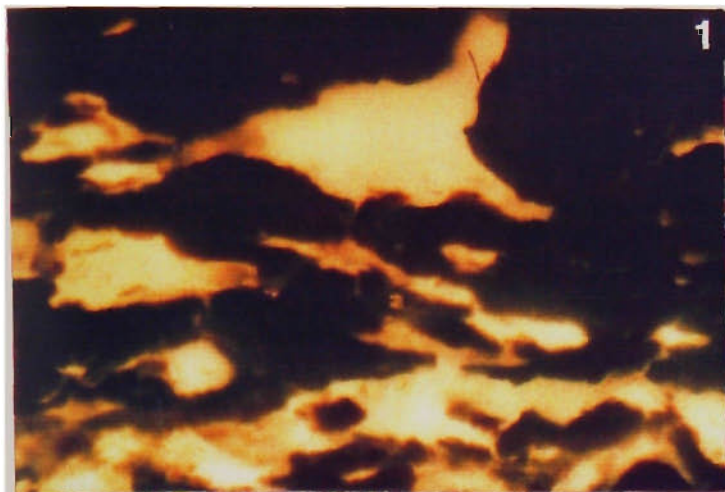




## PLATE V

### Type II Exsudatinite in the Tertiary coals of West Aceh basin

1. Exsudatinite filling vitrinite cracks and associated with framboidal pyrite. Sample GM 24590, Oligocene coal,  $R_{\max}=0.65\%$ , field width 0.33mm.
2. Cauliflower exsudatinite associated with sporinite showing different colour and intensity. Sample GM 23416, Pliocene coal,  $R_{\max}=0.32\%$ , field width 0.33mm.
3. Exsudatinite with shrinkage cracks in clarite layer. Sample GM 23241, Miocene coal,  $R_{\max}=0.47\%$ , field width 0.35%.
4. Exsudatinite associated with detrovitrinite in Pliocene coal. Sample GM 22051,  $R_{\max}=0.26\%$ , field width 0.30mm.

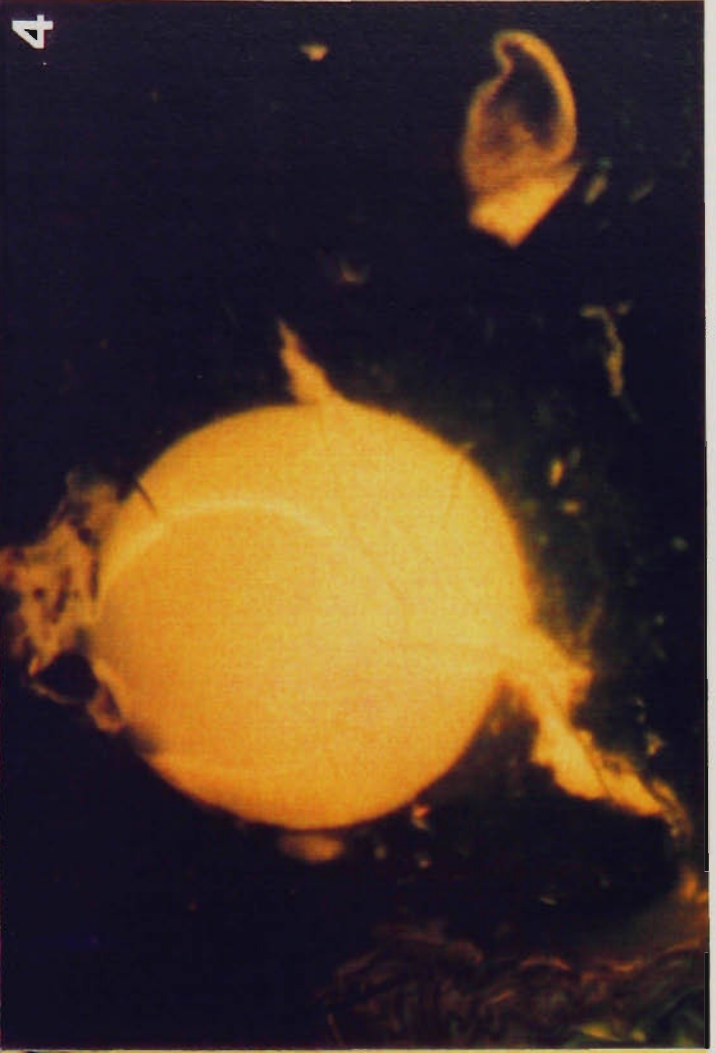
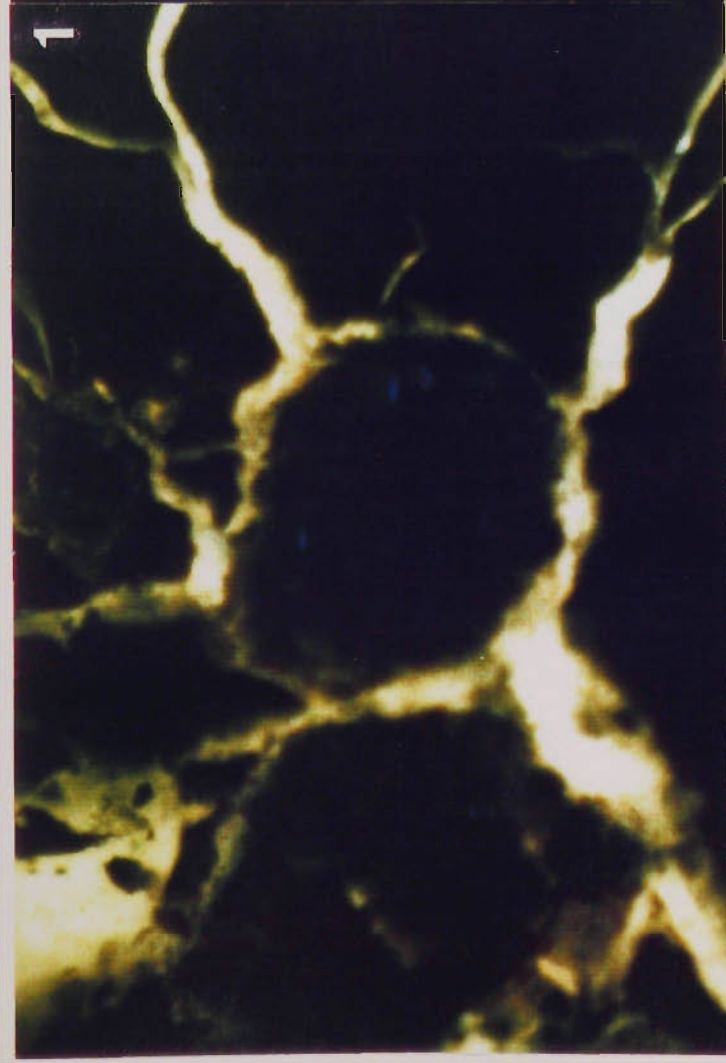


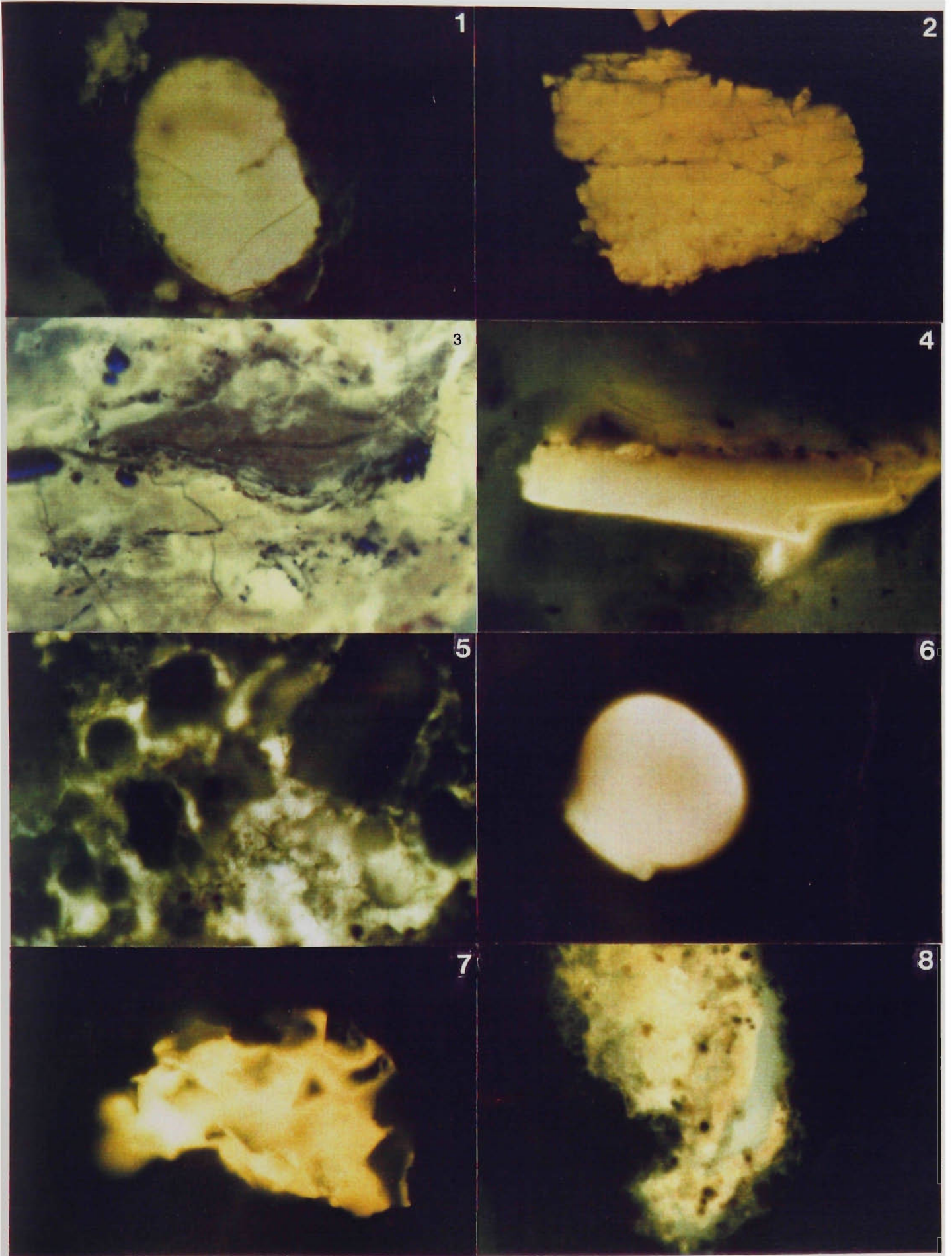
## PLATE VI

Solid bitumen in the clastic rocks of the Tertiary Formations of West Aceh Basin.

1. Globular bitumen occurs in siltstone of Tutut Formation. Sample GM 22350, Meulaboh well,  $R_{\max}=0.27\%$ , field width 0.34mm.
2. Bitumen with frequent shrinkage cracks in the Tangla siltstone. Sample GM 22354, Meulaboh well,  $R_{\max}=0.37\%$ , field width 0.34mm.
3. Impregnated bitumen in carbonate rock. Sample GM 22414, Kueh Formation, Meulaboh East well.  $R_{\max}=0.32\%$ , field width 0.45mm.
4. Bitumen in siltstone. Tutut Formation in Meulaboh East well, GM 22416,  $R_{\max}=0.30\%$ , field width 0.30mm.
5. Bitumen impregnated in sandstone pore. Sample GM 22363, Tutut Formation, Teunom well,  $R_{\max}=0.23\%$ , field width 0.35mm.
6. Bitumen in carbonate pore. Sample GM 22451, Tutut Formation, Bubon well,  $R_{\max}=0.22\%$ , field width 0.33mm.
7. Bitumen occurs in fossil chamber. Sample GM 22467, Kueh Formation, Bubon well.  $R_{\max}=0.40\%$ , field width 0.29%.
8. Bitumen associated with carbonate rock at Tripa well, Tutut Formation.  $R_{\max}=0.30\%$ , field width 0.30mm.



PLATE VI



## APPENDICES

Appendix 1. Cuttings analysis form.

SAMPLE NO	PROJECT	FORMATION	DEPTH M FT	TYPE	OPERATOR	DATE

REFLECTANCE SUMMARY			
	MEAN MAX.	RANGE	N
V			

[illegible]

**REMARKS:**

FLUORESCENCE ANALYSIS						
LIPTINITE	G	Y	O	OO	B	ABUNDANCE
SPORINITE						
CUTINITE						
RESINITE						
LIPTODETRINITE						
TELALGINITE						
LAMALGINITE						
SUBERINITE						
FLUORINITE						
EXSUDATINITE						
BITUMINITE						
OTHERS						
BITUMEN						
OIL CUTS						
OIL DROPS						
THUCHOLITE						
VITRINITE						

REMARKS:

DOM SUMMARY								
	V		I		L		DOM	
	%	cum.	%	cum.	%	cum.	%	cum.
MAJOR								
ABUNDANT								
COMMON								
SPARSE								
RARE								
DOM	TOTAL		TOTAL		TOTAL		TOTAL	
>	>							

OTHERS SUMMARY		
	COAL	SHALY COAL
V		
I		
L		
MICRO - LITHOTYPES		
TOTAL		

VITRINITE TYPES		
	N	%
1		
2		
3		
4		
5		
6		

100

COAL	DOM	
1 TELOVITRINITE	3 ASSOC./INERTINITE	5 NO IDENTIFICATION
2 DETROVITRINITE	4 ASSOC./LIPINITE	6 LEAF TISSUE

REMARKS:

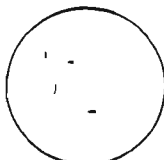
Appendix 1. Cuttings analysis form.

CUTTINGS ANALYSIS																					
Sandstone				Siltstone				Claystone				Limestone/ Carbonate		Others		Coal		Shaly Coal			
V	I	L	O	V	I	L	O	V	I	L	O	V	I	L	O	V	I	L	V	I	L
5																					
10																					
15																					
20																					
25																					
30																					
	%				%				%				%				%			%	

KEY	
• Major	10-40%
x Abundant	2-10%
! Common	0.5-2%
- Sparse	0.1-0.5%
- Rare	<0.1%
0 Absent	0

Dominant	> 40%
Shaly Coal	40-80%
Coal	> 80%

OTHER COMPONENTS		
Pyrite	Mud additive	Other
Foraminifera	Shell fragments	
REMARKS:		



0.5%



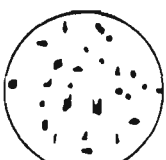
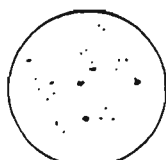
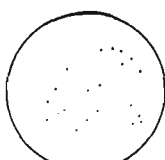
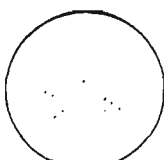
1.0%



2.0%



10%



## APPENDIX. 2.

### QUANTITATIVE METHOD OF DEMINERALISATION

#### I. HYDROCHLORIC ACID (HCL) TREATMENT

1. Crush sample to a fine powder (approximately 10 microns) in the Tema mill.
2. Make about 400 ml of 3N HCL by adding 120 ml of 10N HCL to 280 ml of distilled water.
3. Decant 100 ml of the 3N HCL into each of 4 beaker.
4. Place a watch glass over each beaker and warm them over a steam bath until a condensate forms on the under surface of the watch glass.
5. Weigh out exactly 10 gram of sample into a small beaker (100 - 150 ml size). Slowly add each of the samples to one of the beakers of warm 3N HCL whilst stirring .
6. Place watch glasses on each beaker and heat for 1 hour and stir occasionally. Wash any residue from the stirring rod into the beaker with 3N HCL and wash any residue adhering into the sides back into the solution.
7. Allow samples to coll for 15 minutes.
8. Pour HCL-residue mixture down a glass rod into a centrifuge tube. Equalise the weights of the four tubes using distilled H<sub>2</sub>O.
9. Centrifuge for 10 minutes at 3000 r.p. m. If the residue fails to settle add a few drops of acetone.
10. Pipette the supernatant; add more acid-residue mixture to the centrifuge tube and repeat step 8 and 9. Repeat until all mixture is centrifuged.
11. After centrifuging, wash the organic extract until all HCL has been removed. Then, add distilled water to the tube after pouring off excess liquid; equalise the weight; centrifuge until the pH is neutral.
12. Dry at 50° C and under mercury vacuum of 500 millibars until dry or alternatively dry overnight.
13. Crush the sample with a mortar and pastle, weigh and



record. If greater than 5% weight loss, repeat the HCL treatment (Steps 3 to 12).

## II. HYDROFLUORIC ACID (HF) TREATMENT

1. Do HF treatment as HCL treatment above.
2. Make HF solution asfollow :
  - 100 mls 10N HCL
  - 100 mls distilled water
  - 200 mls HF from bottle
2. Cover the beaker and heat on a steam bath for about for 2 hours. Stir occasionally. Let sample cool for about 30 minutes.
3. Centrifuge as for HCL treatment stage. Wash until the solution is neutral.
4. Dry under a vacuum of 500 millibars and at 50 - 60° C until dry.
5. Weight and grind to a powder.
6. If the weight loss is more than 5%, repeat the HF treatment until weight loss is less than 5%.

Note: All steps for either HCL or HF treatment must be carried out in a fume cupboard except when weighing sample.

## APPENDIX 3.

### PROCEDURE ON GAS CHROMATOGRAPHY ANALYSIS:

#### I. Soxhlet Extraction

1. 400 ml of HCL3/MeOH (87/13) is placed in 500 ml round-bottomed flask and the empty soxhlet apparatus and thimble washed for 24 hours.
2. Clean CHCL3/MeOH (87/13) is added to the round-bottomed flask. Prewieghed rock is added to the thimble and extracted for 48 hours.
3. The chloroform/methanol solution is rotavaped to near dryness and filtered through a 0.2um Anotop disposable syringe filter, into a preweighed vial.

#### II. Asphaltene Removal

##### Short method - Sep-Pak

1. A sep-pak alumina N Cartridge is attached to a glass luer lock syringe. This will take up to 50 mg of EOM. If more needed to be processed then the cartridge may be joined to another cartridge by a connecting piece of teflon tubing.
2. The E.O.M. is then dissolved in 1:1 pet. ether/dichloromethane and carefully transfered to the top of the Sep-Pak.
3. For each 50 mg of EOM., 6 mls. of 1:1 pet. ether/dichloro methane is added to the syringe. The solvent may than be slowly forced through with a plunger or allowed to drip under gravity. The eluent, containing the saturates and aromatics is collected in a clean scintillation vial and becomes the asphaltene free fraction, or polar free fraction. The base of the Sep-Pak should be washed into the vial in case evaporation of the sample onto the outside of the Sep-Pak has occurred during elution. This can than be dried down under a stream of nitrogen, with gentle heating (  $<40^{\circ}\text{C}$  ).
4. The asphaltenes and polars are then eluted off the Sep-Pak with 6 mls. of 1:1 chloroform/methanol, followed by 4 mls. of chloroform, for each 50 mg of E.O.M. The fraction is collected in a clean scintillation vial. The base of the Sep-Pak should be washed again. This sample can than be dried down under a stream of nitrogen with gentle heating.

5. The weight of the fractions may be determined using pre-weighed scintillation vials, or by transferring the samples, afterwards, to pre-weighed sample vials.

### III. Chromatography On Silica Gel

1. Only distilled solvents are used.
2. Merck 40(70-230 mesh) silica gel is activated at 150° C until dry or overnight.
3. The column is plugged with non-absorbent cotton wool and is then washed using 2 column volumes of methanol, followed by 2 column volumes of chloroform and 1 column volume of petroleum ether. The column is then filled with petroleum ether until the bulb is approximately half full.
4. 12 grams of the activated silica gel is then slowly added to the column and allowed to settle. Gentle tapping helps to remove any bubbles from the column. The solvent is then passed through the column until it is about 1 - 2 mm from the column surface.
5. The asphaltene (1+2) free fraction ( <100mg ) is then dissolved in petroleum ether and carefully added to the top column. The surface should be disturbed as little as possible during the column run. The samples should then be run on to the column.
6. The column is then eluted sequentially using:
  - 40 mls pet. ether/dichloromethane (Saturates Fraction)
  - 50 mls 1:1 pet. ether/dichloromethane (Aromatic Fraction).The fractions should be collected in clean 100 ml round bottom flasks.
7. Rotor-vap each fraction to almost complete dryness (about 1-2 mls left) and then transfer them to pre-weighted sample vials. The flask should be thoroughly washed to remove all the sample (3-4 washes with one pipette full of dichloromethane, or chloroform is usually sufficient). They are then be dried under a stream of nitrogen with gentle heating.

APPENDIX 4 . MACERAL COMPOSITION OF PLIOCENE COAL

S.NO	GW.NO	DEPTH	IX	TXU	EUU	TEL	AT	DEN	DES	COR	POR	EU	T.VIT	SP	CT	RS	LD	AL	SR	FL	BT	EX	T.LIP	FS	SC	ID	MIC	MAC	T.INT	MM	R <sub>v</sub> me			
M1/1	23319	3	2.0	2.0	2.0	1.0	20.0	34.0	10.6	1.0	1.0	-	72.6	2.0	5.0	4.0	7.0	0.5	2.0	0.5	-	1.8	22.8	-	3.5	0.6	0.5	-	-	4.6	-	0.27		
M1/2	23338	41	1.0	-	0.6	-	19.0	35.0	11.6	10.0	2.3	-	79.5	1.0	3.0	3.0	3.0	1.5	3.5	1.0	-	1.5	18.5	-	2.0	-	-	-	2.0	-	0.27			
M1/3	23342	76	1.5	3.1	6.0	5.0	17.0	10.0	11.0	1.6	3.0	-	58.2	1.0	5.0	2.0	10.0	1.0	1.0	1.5	-	0.5	23.0	0.6	-	0.3	-	-	0.9	17.5	0.29			
M1/4	23351	81	0.7	0.7	-	1.3	14.0	16.1	32.0	8.6	-	1.0	74.4	0.3	6.0	1.0	1.0	1.5	3.5	-	-	-	13.3	-	-	-	1.1	-	-	1.1	11.2	0.31		
M1/5	23355	94	1.5	5.0	4.6	2.8	14.0	18.0	16.0	4.0	3.0	1.0	67.3	0.3	3.5	3.5	7.8	0.7	1.0	1.5	-	1.0	17.3	-	0.4	0.4	-	-	0.8	14.6	0.31			
M1/6	23361	103	0.3	4.0	4.4	3.0	13.0	25.0	20.6	5.6	0.8	0.5	77.2	0.5	5.8	3.5	3.5	1.5	0.5	0.8	-	0.5	16.5	-	1.0	0.9	-	-	1.9	4.6	0.32			
M1/7	23376	115	1.2	2.5	2.0	2.0	14.0	30.0	19.4	4.3	0.8	0.3	76.5	0.8	3.0	4.5	7.0	-	1.5	-	-	0.5	17.3	-	0.3	1.1	0.8	-	2.3	3.9	0.30			
M1/8	23382	125	1.1	2.9	1.5	2.5	14.5	1.5	16.5	3.0	-	0.1	43.6	1.8	1.8	0.4	4.0	0.9	0.5	-	-	-	9.4	-	-	-	-	-	0.2	46.8	0.30			
M1/9	23389	140	0.6	5.0	3.0	2.1	14.0	20.0	19.9	7.2	1.0	1.0	73.8	1.5	4.9	1.7	7.3	1.0	3.3	1	-	0.2	20.9	-	-	1.1	0.8	-	-	1.9	3.4	0.31		
M1/10	23393	153	1.5	4.8	9.0	8.0	14.0	11.3	15.0	4.0	-	0.3	68.9	2.6	5.8	1.8	7.0	-	1.7	2.3	-	-	21.3	-	-	1.1	0.6	0.6	-	2.3	7.5	0.30		
M1/11	23397	157	1.5	5.0	8.0	9.7	14.0	8.0	20.7	3.0	2.0	0.3	72.2	1.2	4.8	5.7	7.5	-	0.7	1.6	-	0.8	22.3	-	-	0.3	1	-	-	1.3	4.2	0.30		
M1/12	23402	173	1.4	3.2	5.6	5.0	17.0	27.2	11.0	7.0	0.2	-	77.6	2.8	5.0	2.6	0.9	1.2	3.4	0.5	-	-	16.4	-	-	5.0	1.0	-	-	6.0	-	0.29		
M1/13	23406	199	0.6	5.9	6.0	2.9	13.3	14.3	16.0	4.0	0.3	2.0	65.3	1.0	7.5	3.0	6.0	0.6	5.1	1.6	-	0.3	25.1	-	-	1.0	1.0	-	-	2.0	7.6	0.31		
M1/14	23411	203	0.5	9.5	11.7	5.6	14.2	19.0	18.6	3.3	0.8	-	87.2	0.4	3.9	0.4	1.3	0.7	1.6	0.4	-	0.7	9.4	-	-	1.7	0.9	-	-	2.6	0.8	0.31		
M1/15	23416	228	0.6	12.7	10.0	5.5	13.0	14.6	15.0	2.0	1.0	0.4	74.8	1.5	3.0	3.0	0.5	-	-	1.0	-	1.0	10.0	-	-	-	0.2	-	-	0.2	15.0	0.31		
M1/16	23420	236	0.4	2.9	9.0	7.0	12.0	8.2	21.0	-	0.3	-	60.8	-	1.6	0.4	2.5	-	0.8	0.8	-	0.5	6.6	-	-	-	1.0	-	-	1.0	32.4	0.32		
M2/1	23427	21	2.8	3.2	1.0	8.0	22.0	30.0	9.0	2.0	-	0.6	78.6	3.5	3.5	4.6	2.0	1.0	2.0	-	-	-	16.6	-	-	2.4	1.6	-	-	4.0	0.8	0.23		
M2/2	23452	38	2.5	0.2	-	0.5	25.5	35.1	9.0	3.0	2.0	0.2	78.0	1.7	5.1	3.4	2.3	1.2	4.5	0.5	-	0.5	19.2	-	-	0.9	0.4	1.4	-	-	2.8	-	0.23	
M2/3	23464	73	2.3	3.5	0.2	1.2	24.0	24.4	10.0	4.0	3.5	0.9	74.0	1.0	8.6	5.5	4.5	0.5	1.5	0.5	-	1.5	23.6	-	-	1.6	0.8	-	-	2.4	-	0.24		
M2/4	23467	105	2.3	6.0	5.0	1.2	24.0	21.0	10.5	4.0	-	-	74.0	0.8	7.7	5.5	7.1	1.6	1.6	0.7	-	-	25.0	-	-	-	-	1.0	-	-	-	0.24		
M2/5	23474	112	2.5	4.5	5.5	1.0	25.0	19.5	9.0	4.5	0.2	0.3	72.0	0.6	7.3	4.5	6.1	0.5	2.4	1.1	-	0.5	23.0	-	-	0.7	1.8	-	-	2.5	2.5	0.23		
M2/6	23477	131	2.1	7.0	8.0	1.4	23.0	14.5	11.0	11.5	0.5	-	79.0	0.8	6.0	2.9	2.9	0.7	0.7	-	-	-	14.0	-	-	2.5	1.5	-	-	4.0	3.0	0.25		
M2/7	23487	162	1.6	9.5	9.5	4.4	18.0	14.8	10.2	4.5	5.5	-	78.0	-	3.6	2.7	-	1.8	6.2	-	-	2.7	17.0	-	-	0.5	0.5	0.5	-	-	1.5	3.5	0.28	
M2/8	23496	171	1.4	10.0	9.5	5.0	19.5	18.0	12.0	4.4	0.6	0.9	81.3	1.3	3.4	4.2	1.6	1.6	3.2	0.6	-	-	15.9	-	-	1.6	0.5	-	-	2.2	0.6	0.29		
M2/9	23493	227	1.7	3.3	2.0	8.4	14.1	24.0	20.0	3.2	0.8	-	77.5	1.7	3.4	1.7	0.9	-	2.5	0.8	-	0.8	11.8	-	-	1.6	1.6	-	0.8	4.0	6.7	0.30		
M3/1	21985	25	0.5	6.5	4.5	20.5	11.0	1.0	20.3	4.3	3.3	-	71.9	1.3	4.5	4.5	12.4	1.1	-	-	-	-	23.8	-	-	2.6	-	0.9	-	-	0.8	4.3	-	0.32
M3/2	21988	68	0.5	1.0	2.0	12.1	11.0	1.3	20.0	12.0	0.6	-	60.5	1.5	11.8	3.5	6.5	5.5	2.5	-	-	0.3	31.6	-	-	2.8	0.9	1.8	-	0.1	5.6	2.3	0.32	
M3/3	21999	107	-	7.0	3.1	14.0	10.0	16.0	15.0	10.0	0.4	-	75.5	4.5	9.6	1.3	2.6	1.3	0.7	2.0	-	-	22.1	-	-	-	-	0.4	-	-	0.4	2.0	0.24	
M3/4	21990	111	-	1.2	2.0	21.0	7.0	0.8	23.0	10.0	0.4	-	64.4	0.4	9.6	0.8	11.1	-	3.0	1.9	-	-	26.8	-	-	1.9	0.4	1.9	-	0.4	4.8	3.4	0.36	
M4/1	21991	190	0.6	12.7	9.5	5.5	13.0	19.0	15.0	0.4	0.6	-	76.3	0.5	8.2	1.9	3.4	-	0.5	2.7	-	1.4	18.6	-	-	-	-	-	-	-	5.5	0.31		
M4/2	21992	191	0.6	7.0	6.0	5.4	13.0	13.0	15.0	1.0	2.5	-	63.5	-	16.0	1.0	6.4	-	5.8	2.4	-	2.4	34.0	-	-	0.8	0.8	0.7	-	-	2.5	-	0.31	
M4/3	21993	194	0.5	5.0	4.0	12.0	11.0	5.5	20.0	3.0	0.5	-	61.5	0.8	8.9	0.8	4.7	-	-	-	-	3.8	19.0	-	-	-	-	-	-	-	19.5	0.32		

Continued

APPENDIX 4 (Continued)

S.NO	GM.NO	DEPTH (M)	TX	TXU	TEL	AI	DEN	DES	COR	POR	EU	I.VIT	SP	CT	RS	LD	AL	SR	FL	BT	EX	T.LIP	FS	SF	SC	ID	MIC	HAC	T.INT	MM	R <sub>v</sub> max(%)	
M10/1	22034	25	1.2	7.0	7.7	10.0	15.0	5.3	20.0	4.2	3.0	0.2	73.6	0.5	3.8	3.4	8.6	-	1.9	2.9	-	1.4	22.5	-	1.0	1.2	-	-	-	2.2	1.7	0.30
M10/2	22035	43	-	0.5	6.0	20.0	12.0	6.9	12.0	6.0	-	-	63.4	1.9	1.3	1.3	14.4	-	0.6	0.6	-	-	20.2	-	0.9	-	-	-	-	0.9	15.5	0.32
M10/3	22036	77	0.4	15.1	10.0	3.5	4.0	19.0	21.0	3.0	1.0	-	77.0	0.9	4.7	2.3	4.7	-	2.8	-	-	0.9	16.5	-	2.1	1.4	-	-	-	3.5	3.0	0.31
M10/4	22037	102	-	2.0	2.0	10.0	10.0	12.5	25.0	2.0	3.0	-	67.5	0.6	5.9	1.3	16.3	-	0.6	1.3	-	1.9	28.0	-	-	1.5	-	-	-	1.5	3.0	0.34
M10/5	22038	114	-	-	10.0	18.0	10.0	9.0	25.0	1.6	1.0	-	74.6	0.8	6.3	1.5	2.3	-	-	2.4	-	3.2	16.6	-	-	0.6	-	-	-	0.6	8.2	0.33
M13/1	22844	20	1.0	23.0	20.6	20.0	5.0	1.0	11.3	5.6	-	-	91.5	0.4	1.5	3.7	1.1	-	-	0.3	-	-	7.0	-	-	-	0.6	-	-	0.6	0.9	0.29
M13/2	22845	38	-	4.0	10.0	22.0	2.0	4.0	9.0	8.5	-	-	59.5	2.1	18.6	5.8	5.8	-	-	0.7	-	-	33.0	-	1.0	-	1.0	-	-	2.0	5.5	0.34
M13/3	22846	64	1.0	29.0	20.0	20.0	2.0	2.0	5.0	7.3	-	-	86.3	0.9	6.7	1.5	0.9	-	-	-	-	-	10.0	-	1.7	-	0.8	-	-	2.6	1.1	0.30
M13/4	22847	79	-	3.0	9.0	30.0	1.0	1.0	5.0	12.0	0.5	0.5	62.0	0.7	21.1	3.5	4.2	1.4	-	-	-	31.0	-	1.8	0.6	0.6	-	-	3.0	4.0	0.38	
M13/5	22032	101	-	2.0	8.0	30.0	2.0	1.0	6.0	12.0	-	-	61.0	1.7	21.1	3.5	4.4	1.4	-	-	-	32.0	-	-	1.8	1.6	0.6	-	4.0	3.0	0.39	
M15/1	22033	27	0.9	30.0	20.0	14.1	10.0	4.0	3.0	6.5	-	-	88.5	0.5	1.4	4.7	2.1	-	-	0.3	-	-	10.0	-	-	0.5	-	-	0.5	1.0	0.29	
M15/2	22034	44	0.7	20.0	6.3	13.0	5.0	1.0	3.0	8.0	-	-	59.0	3.0	19.0	5.8	5.7	-	-	0.2	-	-	33.5	-	1	0.5	0.5	-	2.0	5.5	0.29	
M15/3	22029	48	0.6	18.4	30.0	20.0	4.0	2.0	4.0	7.0	-	-	86.0	1.0	6.8	1.3	1.5	-	-	-	-	10.3	-	1	0.5	0.5	-	-	2.0	1.7	0.30	
M15/4	21984	71	-	-	10.0	30.0	1.0	2.0	6.0	12.5	0.5	-	62.0	0.8	21.6	3.1	4.2	1.4	-	-	-	31.0	-	-	1.0	1.5	-	-	3.0	4.0	0.38	
M15/5	21983	107	-	-	7.0	31.0	1.0	3.0	7.0	11.5	0.5	-	61.0	1.7	24.0	0.5	5.0	4.3	-	-	-	35.5	-	0.5	1.5	0.5	-	-	2.5	1.0	0.39	
M18/1	22044	25	0.8	20	20.0	20.2	5.0	9.0	5.0	6.0	-	-	86.0	0.5	1.4	5.7	3.1	-	-	0.8	-	-	12.5	-	0.5	0.5	0.5	-	1.5	-	0.29	
M18/2	22045	44	0.6	8.4	10.0	20.0	4.0	2.0	4.0	9.5	-	0.5	59.0	3.5	19.0	5.8	5.7	-	-	0.2	-	-	33.0	-	0.5	1.0	0.5	-	2.0	6.0	0.30	
M18/3	22046	62	-	-	30.0	37.0	3.0	2.0	5.0	9.0	-	-	86.0	1.0	6.5	1.3	1.5	-	-	-	-	10.0	-	0.5	1.5	1.0	-	-	3.0	1.0	0.37	
M18/4	22047	107	-	-	8.0	32.0	2.0	1.0	6.0	12.0	-	-	61.0	1.0	21.6	3.1	5.0	1.4	-	-	-	32.0	-	1.0	1.5	0.5	-	-	3.0	4.0	0.39	
M21/1	22840	30	-	-	3.0	18.0	9.0	10.0	10.0	1.0	1.5	-	52.2	1.6	17.0	2.5	5.6	5.6	0.81	1.6	-	1.6	36.5	-	-	-	-	-	-	11.0	0.32	
M21/2	22841	87	-	2.0	9.0	25.0	1.0	1.5	9.0	-	-	-	47.5	0.6	13.0	6.8	1.7	2.5	1.2	1.2	-	-	36.0	-	-	-	-	-	-	16.5	0.35	
M22/1	22842	44	-	-	1.0	14.0	5.0	10.7	20.0	6.0	-	-	56.7	2.0	16.0	7.7	10.8	0.6	0.5	0.5	-	-	38.0	-	0.3	0.8	-	-	1.1	4.2	0.35	
M22/2	22843	109	-	-	7.0	7.8	3.0	-	20.2	1.2	-	-	39.2	1.9	26.6	9.5	9.5	1.9	0.6	-	-	50.0	-	0.3	0.5	-	-	-	0.8	10.0	0.37	
M11/1	22848	37	0.3	5.0	8.0	15.3	8.0	10.0	10.0	9.5	-	-	67.0	2.4	11.9	2.9	5.3	0.6	1.2	1.8	-	-	26.1	-	1.6	2.7	2.2	-	6.6	0.3	0.32	
M11/2	22307	79	-	1.0	8.0	20.0	7.0	6.5	15.0	9.2	-	0.3	67.0	2.0	10.9	2.9	5.7	0.6	1.2	1.8	-	-	25.0	-	1.0	2.0	1.0	-	4.0	2.6	0.33	
M11/3	22049	105	-	5.0	15.5	24.0	3.0	3.2	16.0	5.4	-	-	72.1	0.6	4.8	6.6	-	-	1.8	-	0.6	15.0	-	3.6	0.5	3.5	-	-	8.1	4.8	0.35	
M11/4	23308	109	-	1.0	19.5	22.0	3.0	2.2	17.0	5.0	-	0.4	70.7	0.6	4.4	6.6	0.6	-	-	1.8	-	0.6	15.4	-	2.5	0.5	3.5	-	7.0	5.1	0.34	
M11/5	23310	114	0.2	9.0	10.8	20.0	2.0	5.0	15.0	5.0	-	-	67.0	1.3	8.4	3.4	0.6	-	-	2.4	-	0.6	20.1	-	2.5	1.5	3.5	-	8.1	4.8	0.33	
M11/6	22850	142	0.3	9.0	1.0	15.0	2.0	3.0	13.0	7.6	-	-	50.6	2.5	12.8	13.8	6.9	2.5	2.5	1.9	-	-	43.0	-	2.3	-	3.6	-	0.3	6.4	-	0.32
M12/1	22851	41	-	5.0	5.0	15.0	4.0	4.0	14.0	20.0	-	-	67.0	1.6	6	1.6	4.8	0.8	8.8	-	-	24.0	-	1.0	2.4	4.0	1.1	-	0.8	9.4	-	0.33
M12/2	22852	60	-	4.0	5.6	15.0	4.0	5.0	13.0	19.5	0.5	-	66.6	1.6	6.4	1.6	4.8	0.8	8.8	-	-	24.0	-	1.7	1.7	4.3	0.8	-	0.8	9.4	-	0.34

Continued

APPENDIX 4 (Continued)

S.NO	GM.NO	DEPTH (M)	TX	TXU	EUU	TEL	AT	DEN	DES	COR	POR	EU	T.VIT	SP	CT	RS	LD	AL	SB	FL	BT	EX	T.LIP	FS	SF	SC	ID	MIC	MAC	T.INT	MM	R <sub>max</sub> (%)	
I 1	21994	O/C	2.4	3.0	3.4	5.0	25.9	9.8	9.0	2.0	1.3	-	60.9	3.9	10.4	1.8	9.3	1.2	1.2	1.2	1.2	-	1.0	30.0	-	-	3.3	-	1.1	-	4.4	4.7	0.23
I 2	21995	O/C	1.6	2.0	0.7	5.0	26.0	11.3	18.0	2.0	1.3	-	77.9	1.2	4.7	2.4	-	-	3.5	1.3	-	3.5	16.6	-	1.8	1.8	-	0.9	-	4.6	0.9	0.29	
I 7	21996	O/C	1.6	10.2	9.0	5.5	26.0	11.2	17.8	5.0	3.1	5.0	89.9	-	3.3	3.2	0.8	0.8	0.5	-	-	-	8.6	-	0.5	0.5	-	-	0.5	1.5	1.5	0.29	
I 9	21997	O/C	1.7	2.5	1.3	5.5	25.5	18.7	18.0	3.2	0.1	-	76.5	-	4.0	1.5	1.5	-	-	-	-	-	-	7.0	-	0.3	-	-	-	0.3	16.2	0.29	
I13	21998	O/C	1.6	10.2	7.5	5.0	26.0	6.4	18.0	2.7	2.0	-	79.4	-	3.9	2.6	1.9	-	-	1.3	-	2.6	11.3	-	0.8	-	-	-	-	0.8	9.5	0.29	
I14	21999	O/C	1.7	10.2	11.2	5.5	25.5	6.2	5.9	6.0	0.3	-	72.5	-	2.1	1.7	9.0	-	0.9	2.6	-	-	8.3	-	0.2	0.1	-	-	-	0.3	18.9	0.29	
I15	22000	O/C	1.5	5.3	5.0	9.7	14.4	10.6	20.0	10.5	3.0	0.5	80.5	-	4.0	0.7	-	-	12.5	-	-	-	12.5	-	0.5	0.5	0.5	-	-	1.5	5.5	0.30	
I17	22003	O/C	0.6	5.0	13.9	2.8	14.5	17.5	22.0	5.3	0.8	0.2	82.6	0.6	2.6	3.0	2.6	-	2.0	1.3	-	0.8	13.0	-	4	-	0.4	-	-	4.4	-	0.31	
I18	22005	O/C	0.5	6.5	3.0	7.0	11.0	19.5	22.0	9.5	3.0	0.5	82.5	-	2.5	4.3	5.4	-	-	-	-	1.7	14.0	-	2.2	1.3	-	-	-	3.5	-	0.32	
I20	22006	O/C	0.5	2.0	1.1	8.0	12.0	26.0	22.0	6.0	1.6	-	79.2	0.3	1.2	1.4	0.3	-	4.4	-	-	-	7.6	-	-	-	-	-	-	9.6	3.7	0.32	
I21	22009	O/C	1.6	10.5	8.4	5.0	14.0	1.0	2.0	5.5	1.0	-	48.0	0.7	11.2	14.0	6.0	2.4	7.0	0.7	-	-	42.0	-	2.7	2.0	2.0	-	0.7	7.5	2.5	0.29	
I22	22011	O/C	2.2	20.0	18.0	1.4	23.0	1.4	10.0	3.4	1.0	-	80.4	1.9	3.4	1.9	3.4	-	3.4	0.5	-	1.4	18.4	-	0.6	0.2	0.2	-	0.2	1.2	-	0.25	
I24	22013	O/C	1.6	15.7	15.0	4.5	18.0	9.2	10.0	4.4	-	-	78.4	1.6	7.5	1.2	7.5	-	1.2	1.2	-	-	20.4	-	0.8	0.4	-	-	-	1.2	-	0.28	
I25	22015	O/C	1.7	15.8	16.0	45.0	18.0	1.8	10.2	6.1	1.0	-	75.1	4.8	7.7	1.6	10.1	2.6	1.6	0.9	-	1.2	32.3	-	-	-	0.4	0.9	-	0.4	5.5	0.28	
I27	22016	O/C	-	5.0	22.0	3.0	14.0	1.2	9.0	4.2	0.5	-	58.9	1.4	7.6	1.7	6.3	-	0.6	1.1	-	-	19.0	-	-	-	-	-	-	1.4	7.5	0.31	
I28	22017	O/C	0.6	17.0	22.0	3.4	4.0	0.6	21.0	1.0	2.0	0.4	71.4	0.5	13.5	1.1	2.2	-	-	1.1	-	5.9	24.3	0.4	0.4	0.4	0.5	-	0.2	-	1.7	2.6	0.31
I30	22018	O/C	-	5.0	15.0	20.0	2.0	2.0	12.0	2.0	-	-	68.0	-	10.1	2.0	5.3	0.9	0.9	0.9	-	-	21.0	-	1.0	-	1.0	-	-	2.0	9.0	0.32	
I32	22019	O/C	-	-	1.0	26.0	1.0	2.0	19.0	4.0	3.0	-	56.0	2.9	13.9	0.8	5.6	-	1.9	3.9	-	3.9	33.0	-	1.5	-	2.5	-	-	3.5	7.5	0.38	
I34	22021	O/C	-	-	6.0	30.0	2.0	1.5	29.0	0.5	2.0	-	71.0	2.9	13.9	0.8	5.6	-	1.9	4.9	-	3.0	25.0	-	2.0	-	1.5	-	-	0.5	3.5	0.38	
I37	22030	O/C	1.7	10.0	13.3	6.0	5.0	6.3	10.0	11.4	0.9	-	64.4	0.8	7.6	2.0	2.4	-	4.0	2.4	-	0.8	20.0	-	4.6	0.3	6.0	-	-	11	4.4	0.29	
I38	22031	O/C	1.7	7.0	7.9	21.0	6.0	14.0	4.3	13.0	-	-	74.9	0.9	5.4	1.8	3.7	-	0.4	0.9	-	-	13.0	0.4	2.7	0.1	4.0	-	-	7.3	4.8	0.28	
I39	22039	O/C	0.7	1.3	1.0	9.0	15.0	17.8	20.0	4.8	-	-	69.6	-	3.5	4.2	1.4	1.4	3.5	0.7	-	-	13.2	-	3.1	0.5	0.5	-	-	4.8	12.4	0.30	
I41	22040	O/C	0.8	4.0	2.8	10.0	17.0	13.0	20.0	4.6	-	-	72.2	0.6	-	0.5	1.5	-	-	0.5	-	0.5	3.6	-	3.8	0.6	-	-	-	4.3	19.9	0.30	
I44	22041	O/C	-	15.0	6.6	4.0	3.6	19.0	21.0	6.3	-	-	75.5	0.5	4.0	0.5	2.0	-	1.0	-	-	-	8.3	-	0.8	0.4	0.4	-	-	1.6	14.6	0.31	
I45	22042	O/C	0.8	10.7	6.2	4.0	8.0	19.0	21.0	10.0	-	-	79.7	-	1.5	2.2	1.9	0.4	-	-	-	-	6.0	-	1.4	1.3	-	-	-	2.7	11.6	0.31	
I49	22043	O/C	1.7	2.8	13.0	6.0	20.0	27.0	10.0	9.8	-	0.2	88.5	-	3.3	-	-	0.8	4.9	-	-	-	9.0	-	2.5	-	-	-	-	2.5	-	0.29	
I53	22047	O/C	-	5.0	4.0	17.0	18.0	16.0	22.0	6.3	-	-	88.3	1.2	2.3	1.4	0.6	1.4	0.6	1.2	-	-	9.7	0.4	1.2	0.4	-	-	-	2.0	-	0.30	
I55	22049	O/C	2.5	5.0	18.0	1.5	23.0	2.0	11.0	4.5	2.0	-	69.5	0.5	7.0	7.0	6.5	-	1.6	1.0	-	2.2	26.0	-	-	-	-	-	-	4.5	-	0.25	
I57	22050	O/C	2.0	2.3	15.0	2.0	22.0	9.3	10.0	2.8	2.5	-	67.9	1.5	8.9	4.3	3.6	1.5	0.8	1.5	-	3.8	26.0	-	-	-	-	-	-	2.0	-	0.26	
I61	22051	O/C	2.0	20.0	16.0	2.0	10.0	6.0	7.0	2.3	3.0	-	68.3	1.0	5.1	3.1	5.1	2.0	2.0	-	-	4.0	22.6	-	1.0	1.0	1.3	-	-	3.3	-	0.26	
I64	22052	O/C	1.9	4.0	3.0	2.4	9.0	27.0	10.0	0.1	0.5	-	57.9	2.6	5.2	1.3	10.4	3.9	-	-	-	2.6	26.0	-	0.6	-	-	-	-	0.6	14.5	0.28	
I66	22053	O/C	1.0	27.5	20.0	15.0	8.0	7.0	11.5	0.3	0.2	-	99.0	-	0	0	0	0	0	-	0	-	0	0	-	-	0.5	0.5	-	1.0	-	0.40	

APPENDIX 5. MACERAL COMPOSITION OF MIOCENE COAL

S.NO	GM.NO	DEPTH ( M )	TX	TXU	TUU	TEL	AT	DEN	DES	COR	POR	EU	T.VIT	SP	CT	RS	LD	AL	SB	FL	BT	EX	T.LIP	FS	SF	SC	ID	MIC	MAC	T.INT	HM	R <sub>max</sub> (%)
K 1	23233	O/C	-	-	2.0	7.0	7.0	10.0	30.0	3.5	-	0.5	60.0	1.3	1.3	1.7	2.6	7.3	-	0.8	-	3.0	18.0	-	14.7	2.3	2.8	1.8	0.4	22.0	-	0.51
K 2	23238	O/C	-	-	10.5	28.0	9.5	10.0	20.0	20.0	-	-	98.0	-	0.4	0.8	-	-	-	-	-	0.8	2.0	-	-	-	-	-	-	-	-	0.51
K 3	23241	O/C	-	0.1	3.9	9.0	6.0	15.0	35.0	-	1.0	-	70.0	1.5	2.5	3.5	3.5	1.5	-	1.5	-	6.0	20.0	0.5	6.6	1.0	1.4	-	0.5	10.0	-	0.47
K 4	23239	O/C	-	0.2	4.3	7.0	6.0	15.0	40.0	5.2	0.8	-	78.5	0.6	6.4	3.7	1.8	1.2	-	0.6	-	4.2	18.5	-	1.5	0.5	-	0.5	2.5	0.5	0.45	
K 5	22826	O/C	-	-	2.3	20.0	6.1	10.0	30.0	11.0	0.2	-	79.5	-	2.2	-	5.5	3.8	-	-	-	-	11.5	0.7	0.6	2.1	4.0	-	-	7.4	1.5	0.51
K 6	22827	O/C	-	0.1	4.0	18.0	5.0	10.0	31.0	11.0	-	-	79.0	0.2	2.0	0.5	5.0	3.8	-	0.5	-	-	12.0	0.7	0.2	2.1	4.0	-	-	7.0	1.9	0.47
K 7	22828	O/C	-	0.5	3.5	17.0	6.0	12.0	35.0	14.0	-	-	80.0	-	2.0	0.2	5.0	3.0	-	0.8	-	-	11.0	0.2	0.5	2.1	4.0	-	0.6	7.4	1.5	0.45
K 8	23243	O/C	-	0.2	2.3	3.0	5.5	10.0	20.0	2.0	0.5	-	70.0	3.7	2.7	2.7	5.0	-	1.8	0.9	-	2.7	19.5	2.3	3.5	2.3	0.4	-	0.5	8.5	2.0	0.42
K 9	23244	O/C	-	0.5	0.5	4.0	10.0	17.0	35.0	2.4	0.6	-	70.0	3.0	2.9	2.7	5.0	-	-	0.9	-	2.7	19.0	2.0	4.0	2.0	0.7	-	0.6	8.5	2.0	0.43
K10	23240	O/C	-	0.6	4.1	6.8	11.0	20.0	25.0	1.5	-	-	69.0	0.7	18.1	2.1	3.6	1.2	0.7	2.6	-	-	29.0	-	1.5	0.5	-	-	-	2.0	-	0.45
K12	24588	O/C	-	-	12.0	23.0	9.0	15.0	20.0	8.4	-	0.6	88.0	1.5	4.9	0.7	3.1	-	3.1	0.7	-	-	11.0	-	1.0	-	-	-	-	1.0	-	0.42
K15	22820	O/C	-	-	1.0	11.0	6.0	20.0	30.0	2.0	-	-	70.0	0.7	17.0	2.2	3.6	1.2	0.7	2.6	-	-	28.0	0.5	1.0	0.5	-	-	-	2.0	-	0.46
K17	22828	O/C	-	-	3.0	18.0	5.0	8.0	32.0	12.8	0.1	0.1	79.0	0.5	2.0	0.5	5.0	3.5	-	0.5	-	-	12.0	0.5	0.4	2.0	4.1	-	-	7.0	-	0.47
K18	22832	O/C	-	-	1.0	6.0	15.0	21.0	24.0	2.2	-	0.3	70.0	3.5	4.4	3.5	6.7	-	-	0.9	-	-	19.0	2.0	3.0	3.0	0.5	-	1.0	8.5	2.5	0.44
K19	22823	O/C	-	0.2	1.8	4.0	17.0	20.0	25.0	3.0	-	-	70.0	3.7	2.7	2.7	6.0	-	1.8	0.9	-	-	20.0	2.0	3.5	2.0	0.7	-	0.8	8.0	-	0.42
K20	22824	O/C	-	-	-	53.0	-	-	40.95	-	-	-	93.9	-	-	1.5	1.5	-	-	-	-	3.0	6.0	-	-	-	-	-	-	-	-	1.15
K21	22826	O/C	-	-	2.14	6.0	15.0	15.0	10.60	1.3	-	-	51.0	0.9	0.9	11.7	11.7	0.9	1.8	-	-	18.0	49.0	1.5	1.5	1.0	-	-	-	4.0	-	0.35

APPENDIX 6. MACERAL COMPOSITION OF OLIGOCENE COAL

S.NO	CM.NO	DEPTH (M)	TX	TXU	EUU	TEL	AT	DEN	DES	COR	POR	BU	T.VIT	SP	CT	RS	LD	AL	SB	FL	BT	EX	T.LIP	FS	SP	SC	ID	MIC	HAC	T.INT	NH	R <sub>y</sub> max(X)	
L 3	24590	O/C	-	-	-	36.6	-	15.0	26.8	8.5	0.9	0.9	88.7	0.4	4.4	0.4	1.2	0.8	1.2	-	-	-	-	8.4	-	1.9	1.0	-	-	-	2.9	-	0.65
L 4	23229	O/C	-	-	-	1.0	52.0	1.0	6.2	21.0	1.0	0.8	1.0	84.0	0.6	8.8	-	0.6	-	3.1	-	-	0.6	14.0	-	-	0.4	-	-	-	0.4	1.6	0.55
L 5	23230	O/C	-	-	-	0.6	23.0	1.0	24.0	30.0	4.4	-	83.0	2.1	5.9	3.1	2.6	-	-	-	-	2.1	15.8	-	-	-	1.2	-	-	1.2	-	0.54	
L 7	23231	O/C	-	-	-	0.8	26.0	1.5	12.0	30.1	5.1	0.5	76.0	0.6	8.4	7.2	1.2	1.2	0.6	0.6	-	4.2	24.0	-	-	-	-	-	-	-	-	0.52	
L 8	23232	O/C	-	0.1	0.9	20.5	0.9	10.1	31.0	4.2	-	-	67.0	2.2	2.8	3.4	6.6	1.1	3.9	0.5	-	5.6	26.1	-	0.6	3.2	2.6	-	0.6	6.9	-	0.53	
L 9	23234	O/C	-	-	-	0.5	16.0	2.0	7.5	40.0	4.6	0.2	70.5	3.3	3.1	0.4	1.8	2.2	1.8	1.8	-	-	14.4	-	10.8	3.0	1.3	-	-	15.1	-	0.52	
L10	23235	O/C	-	-	-	21.5	0.5	10.5	42.5	-	0.5	-	75.5	1.3	4.3	2.0	4.7	1.3	6.7	-	-	2.7	23.0	-	0.4	0.7	-	-	0.4	23.0	-	0.55	
L11	23236	O/C	-	-	-	1.0	22.0	2.0	21.0	37.5	1.9	0.1	85.5	2.4	2.7	1.3	2.7	2.0	1.3	-	-	0.6	13.0	-	-	1.2	-	-	0.3	1.5	-	0.53	
L12	23237	O/C	-	-	-	2.0	9.0	11.0	11.0	40.0	0.5	0.5	64.0	1.2	1.2	1.2	3.6	2.4	-	1.2	-	1.2	12.0	-	16.6	4.0	2.4	-	1.0	24.0	-	0.53	
L13	23242	O/C	-	-	-	2.6	2.7	2.0	10.0	30.0	6.0	-	77.6	1.1	5.3	2.9	9.8	1.1	-	-	-	0.6	20.8	-	0.5	0.5	0.6	-	-	1.6	-	0.52	
L14	24583	O/C	-	-	-	27.0	2.0	14.0	20.0	3.0	1.5	-	65.5	1.8	10.9	-	4.4	0.6	13.8	-	-	-	31.5	-	1.0	2.0	-	-	-	3.0	-	0.56	
L15	24584	O/C	-	-	-	0.9	28.1	-	23.0	30.0	2.0	25.0	86.5	1.0	2.0	1.0	1.0	-	2.5	-	-	2.5	10.0	-	1.0	1.0	-	-	-	2.0	1.5	0.61	
L16	24585	O/C	-	-	-	1.5	35.8	0.1	10.6	25.0	5.0	-	78.0	3.0	5.0	2.0	9.0	-	1.0	-	-	-	20.0	-	0.7	0.6	-	-	-	1.3	0.7	0.56	
L17	24586	O/C	-	-	-	0.3	30.4	0.9	31.0	36.0	7.3	-	78.0	1.5	3.0	1.5	9.0	-	0.3	-	-	-	15.3	-	5.0	-	-	-	-	5.0	1.5	0.61	
L18	24587	O/C	-	-	-	39.2	0.6	14.5	31.8	4.1	1.6	0.4	92.2	0.9	1.0	0.8	1.0	-	2.0	-	-	-	5.7	-	1.5	-	-	-	-	1.5	0.6	0.66	
L19	24589	O/C	-	-	-	23.4	-	14.7	29.4	6.0	2.8	-	76.4	0.8	9.8	0.4	5.8	-	1.2	-	-	-	18.0	-	3.6	2.0	-	-	-	5.6	-	0.60	
L20	22825	O/C	-	-	-	28.0	1.0	8.0	35.0	1.0	-	-	73.5	2.0	1.0	3.0	2.0	1.0	1.0	-	-	9.9	19.9	2.0	2.0	1.0	1.0	-	0.6	6.6	-	0.65	



APPENDIX 7. MINERALS CONTENT IN TERTIARY COALS OF WEST ACEH  
BASIN, SUMATRA.

GM NO	FORMATION	CLAY (%)	PYRITE (%)	CARBONATE (%)	QUARTZ (%)
23342	Tutut	17.9	-	-	-
23351	Tutut	11.2	-	-	-
23355	Tutut	14.6	-	-	-
23361	Tutut	4.6	-	-	-
23376	Tutut	3.9	-	-	-
23382	Tutut	46.8	-	-	-
23389	Tutut	3.4	-	-	-
23393	Tutut	7.5	-	-	-
23397	Tutut	4.2	-	-	-
23406	Tutut	7.6	-	-	-
23411	Tutut	0.8	-	-	-
23416	Tutut	15.0	-	-	-
23420	Tutut	32.4	-	-	-
23427	Tutut	0.8	-	-	-
23474	Tutut	2.5	-	-	-
23477	Tutut	3.0	-	-	-
23487	Tutut	3.5	-	-	-
23492	Tutut	0.6	-	-	-
23493	Tutut	6.7	-	-	-
21988	Tutut	2.0	0.3	Trace	-
21989	Tutut	-	2.0	-	-
21990	Tutut	3.0	0.4	-	-
21991	Tutut	4.0	1.1	-	-
21993	Tutut	19.0	0.5	-	-
21994	Tutut	3.3	1.4	-	-
21995	Tutut	0.9	-	Trace	-
21997	Tutut	14.6	1.6	-	-
21998	Tutut	8.5	1.0	-	-
21999	Tutut	18.9	-	-	-
22000	Tutut	3.5	2.0	-	-
22006	Tutut	3.7	-	-	-
22009	Tutut	2.5	-	-	-
22015	Tutut	4.7	0.8	-	-
22016	Tutut	6.5	0.9	-	Trace
22017	Tutut	2.6	-	-	-
22018	Tutut	4.5	4.5	-	-
22019	Tutut	2.0	5.5	-	-
22021	Tutut	2.5	-	-	-
22030	Tutut	4.4	-	-	-
22031	Tutut	2.6	2.2	-	Trace
22034	Tutut	1.1	0.6	-	-
22035	Tutut	12.0	3.5	-	-
22036	Tutut	1.5	1.5	-	-

Appendix 7 cont'd

Cont'd Appendix 7

22037	Tutut	2.5	0.5	-	-
22038	Tutut	6.9	1.3	-	-
22039	Tutut	12.4	-	-	-
22040	Tutut	19.0	-	-	Trace
22041	Tutut	14.6	-	-	-
22042	Tutut	11.6	-	-	-
22050	Tutut	4.1	-	-	-
22051	Tutut	5.8	-	-	-
22052	Tutut	0.5	14.0	-	-
22053	Tutut	-	0.5	-	-
22844	Tutut	-	0.9	-	-
22845	Tutut	3.5	2.0	-	-
22846	Tutut	-	1.1	-	-
22847	Tutut	1.0	3.0	-	-
22032	Tutut	-	3.0	Trace	-
22033	Tutut	-	1.0	-	-
22034	Tutut	3.0	2.5	-	-
22029	Tutut	0.6	1.1	-	-
21984	Tutut	1.0	3.0	-	-
21983	Tutut	-	1.0	-	-
22045	Tutut	3.0	3.0	-	-
22046	Tutut	1.0	-	-	-
22047	Tutut	1.0	3.0	-	-
22840	Tutut	6.0	5.0	-	-
22841	Tutut	9.5	7.0	-	-
22842	Tutut	2.3	1.9	-	-
22843	Tutut	5.2	4.8	-	-
22848	Tutut	0.3	-	-	-
23307	Tutut	2.6	-	-	-
22849	Tutut	4.0	0.8	-	Trace
23308	Tutut	5.1	-	-	-
23310	Tutut	4.8	-	-	-
23239	Kueh	0.5	-	-	-
22826	Kueh	1.5	-	-	-
22827	Kueh	1.9	-	-	-
22828	Kueh	1.5	-	-	-
23243	Kueh	-	2.0	-	-
23244	Kueh	2.0	-	-	-
22828	Kueh	1.9	-	-	-
22822	Kueh	0.5	2.5	-	-
22823	Kueh	2.0	-	-	-
23229	Kueh	1.6	-	-	-
24584	Tangla	-	1.5	-	-
24585	Tangla	-	0.7	-	-
24586	Tangla	-	1.5	-	-
24587	Tangla	-	0.6	-	-

APPENDIX 8. MACERAL AND FLUORESCENCE COLOUR DATA OF ALL CUTTING SAMPLES FROM OFFSHORE WELLS OF WEST ACEH BASIN, SUMATRA.

Meulaboh

Sample No	Depth (m)	Formation	Description
22344	143	Tutut	Calcareous claystone > sandstone > coal. Coal major, V=98%, L=2%; vitrite>>; vitrinite mostly detrovitrinite; liptinite chiefly resinite, yellow, sporinite and liptodetrinite, common, dull brown, bitumen rare - sparse, greenish-yellow with cracks; pyrite disseminated. DOM abundant, V > L > I (V=94%; L=5%; I=1%); vitrinite common to abundant; liptinite rare to common, chiefly yellow liptodetrinite and some acritarchs; inertinite rare. R <sub>y</sub> max= 0.20%.
22345	179	Tutut	Claystone > siltstone > coal. Coal abundant, V=98%, L=2%; vitrite > clarite; resinous vitrinite common; cutinite > resinite, yellow-brown; pyrite disseminated. DOM common, L > V (L=92%; V=8%), vitrinite rare to common; liptinite rare to abundant mostly greenish yellow liptodetrinite and brown cutinite. R <sub>y</sub> max= 0.20%
22346	234	Tutut	Coal > siltstone > claystone. Coal major, V=56%, L=43%, I=1%; vitrite > clarite; vitrinite mostly detrovitrinite, resinous vitrinite common; sporinite > suberinite > liptodetrinite, dark brown. DOM abundant, L > V (L=62%, V=38%); vitrinite rare to common; liptinite rare to common, chiefly dull brown liptodetrinite. R <sub>y</sub> max= 0.21%
22347	252	Tutut	Siltstone > claystone > coal. Coal major, V=86%, L=13%, I=1%; vitrite > clarite; resinous vitrinite abundant, brownish yellow; sporinite > suberinite, dark brown. DOM abundant, L > V > I (L=74%, V=24%, I=2%); vitrinite rare to common; liptinite rare to abundant, mostly brown sporinite; inertinite rare to sparse, inertodetrinite >; acritarch, green. R <sub>y</sub> max= 0.26%.
22365	393	Tutut	Siltstone > coal > claystone > shaly coal. Coal major, V=97%, L=2%, I=1%; vitrinite > clarite; resinous vitrinite abundant; cutinite and sporinite common, brownish yellow; framboidal pyrite. Shaly coal, common; clarite > vitrite; Dom abundant L > V (V=18%, L=82%), vitrinite rare to common; liptinite sparse to common, chiefly cutinite, brownish yellow, bitumen rare, yellow, shrinkage cracks. R <sub>y</sub> max= 0.20%.
22348	457	Tutut	Siltstone > limestone > sandstone. DOM common, L > V (V=45%, L=55%); vitrinite rare to common; liptinite rare to common, chiefly liptodetrinite and cutinite, yellow to brown. R <sub>y</sub> max= 0.33%.
22349	621	Tutut	Claystone > siltstone > coal abundant, V=86%, L=12%, I=2%; vitrite > clarite; resinous vitrinite common; liptodetrinite abundant, brownish yellow; inertodetrinite common; framboidal pyrite. Dom common, L > V (V=43%, L=57%), vitrinite rare to common; liptinite rare to common, chiefly liptodetrinite, yellow, some acritarch, green. R <sub>y</sub> max= 0.33%

Appendix 8 cont'd

Conn't Appendix 3

22350	768	Tutut	Siltstone > limestone > sandstone. DOM common, L > V (V=33%, L=57%); vitrinite rare to common; liptinite sparse to common, dominantly liptodetrinite and sporinite, brown to yellow, shrinkage cracks, R= 0.03%. R <sub>y</sub> max= 0.27%.
22351	917	Tutut	Limestone > claystone > siltstone. DOM common, L > V (V=23%, L=77%); vitrinite rare to common; liptinite rare to abundant, chiefly liptodetrinite, dull yellow, bitumen in carbonate, yellow, sparse. R <sub>y</sub> max= 0.30%.
22352	1100	Kueh	Claystone > siltstone > limestone. DOM sparse, L > V (V=42%, L=58%); vitrinite rare-common; liptinite rare to common, mostly liptodetrinite, yellow, <u>Botryococcus</u> rare, yellow, bitumen, yellow in carbonate pore; framboidal pyrite. R <sub>y</sub> max= 0.32%.
22353	1222	Kueh	Siltstone > limestone. DOM common, V > L (V=56%, L=44%); vitrinite rare to common; liptinite rare to common, chiefly sporinite, brownish yellow, <u>Botryococcus</u> rare, brownish yellow. R <sub>y</sub> max= 0.37%
22354	1368	Kueh	Limestone > siltstone. DOM sparse, V > L (V=63%, L=37%); vitrinite rare to sparse; liptinite rare to sparse, mostly liptodetrinite, yellow, oil drop in siltstone, greenish yellow. R <sub>y</sub> max= 0.37%.
22355	1527	Kueh	Limestone > siltstone. DOM common, V>L (V=68%, L=38%); vitrinite rare to common; liptinite rare to common, chiefly cutinite, greenish yellow-brown. R <sub>y</sub> max= 0.38%
22356	1673	Kueh	Limestone > siltstone > sandstone. DOM common, L>V (V= 45%; L= 55%); vitrinite rare to common, liptinite rare sparse, chiefly liptodetrinite with minor cutinite and sporinite, yellow, lamalginites in siltstone, rare, greenish yellow. R <sub>y</sub> max= 0.39%
22357	1825	Kueh	Siltstone > sandstone > limestone. DOM abundant V > L (V=75%, L=25%); vitrinite rare to abundant; liptinite rare to common, mostly cutinite and liptodetrinite, yellow, bitumen in sandstone, rare, yellow. R <sub>y</sub> max= 0.40%
22358	1898	Kueh	Calcareous siltstone > limestone. DOM common, L > V (V=46%, L=54%); vitrinite rare to common; liptinite rare to abundant, mostly cutinite, yellow, bitumen in carbonate, sparse, yellow, shrinkage cracks, R 0.04%. R <sub>y</sub> max= 0.38%
22359	2209	Kueh	Siltstone > coal > sandstone. Coal major, V=85%, L=11%, I=4%; vitrinite mostly detrovitrinite; liptinite chiefly sporinite and resinite, yellow-brown, bitumen associated with detrovitrinite, yellow, cracks, R 0.003%, exsudatinite in telio vitrinite, greenish yellow; inertinite mostly sclerotinite and semifusinite; framboidal pyrite abundant. DOM abundant, L > V (V=30%, L=70%); vitrinite rare to abundant; liptinite rare to major, chiefly cutinite and sporinite, yellow, bitumen in siltstone, rare, yellow. R <sub>y</sub> max= 0.40%.

Appendix 8 cont'd

cont'd Appendix 3

22360	2310	Kueh	Siltstone > claystone. DOM common, V > L (V=85%, L=15%); vitrinite rare-sparse; liptinite rare-common, cutinite common, yellow; pyrite desseminated. $R_{\text{vmax}} = 0.43\%$ .
22361	2438	Tangla	Siltstone > limestone. DOM abundant, V > L (V=55%, L=45%); vitrinite rare to abundant; liptinite rare to abundant, chiefly sporinite, yellow, liptodetrinite and resinite sparse, brown; pyrite desseminated. $R_{\text{vmax}} = 0.40\%$ .
22362	2484	Tangla	Coal > siltstone > claystone > shaly coal. Coal major, V=93%, L=7%; vitrite > clarite; vitrinite mostly detrovitrinite; liptinite chiefly cutinite, yellow, resinite and sporinite sparse, brownish yellow, bitumen as with detrovitrinite, brownish yellow, cracks, R 0.05%, exsudatinite yellow, oil haze, <u>Botryococcus</u> rare; framboidal pyrite. DOM major, L > V (V=16%, 84%); vitrinite rare to abundant; liptinite rare to major, dominantly cutinite, yellow to brown. $R_{\text{vmax}} = 0.40\%$ .

TEUNOM

22363	2502	Tangla	Coal > claystone > siltstone. Coal abundant, V=89%, L=11%; vitrite > clarite; vitrinite chiefly detrovitrinite; liptinite mostly cutinite, yellow, sporinite and resinite rare, yellow-brown, exsudatinite yellow; framboidal pyrite. DOM abundant, V > L (V=54%, L=46%); vitrinite rare to abundant; liptinite rare to abundant, chiefly cutinite and sporinite, yellow. $R_{\text{vmax}} = 0.47\%$ .
22364	2511	Tangla	Claystone > coal > siltstone. Coal, abundant, V=90%, L=10%; vitrite > clarite; vitrinite chiefly detrovitrinite; liptinite chiefly resinite, yellow to brown; framboidal pyrite. DOM abundant, L > V (V=45%, L=55%); vitrinite rare to abundant; liptinite sparse to abundant, mostly sporinite, brownish yellow. $R_{\text{vmax}} = 0.42\%$ .
22366	2529	Tangla	Coal > shaly coal > claystone > siltstone. Coal V=92%, L=8%; vitrite > clarite; vitrinite chiefly detrovitrinite; liptinite mostly resinite, brown to yellow, cutinite rare, bright yellow. Shaly coal, abundant, V=85%, L=15%, I=5%); clarite > vitrite; vitrinite common to abundant; liptinite common to abundant, mostly cutinite, yellow. DOM abundant, L > V (V=40%, L=60%), vitrinite sparse to abundant; liptinite rare to abundant, mostly cutinite, yellow. $R_{\text{vmax}} = 0.44\%$
22474	2557	Tangla	Siltstone > coal > sandstone. Coal major, V=93%, L=7%; vitrite > clarite; vitrinite mostly telovitrinite; liptinite chiefly sporinite, brownish yellow, bitumen, yellow, associated with detrovitrinite, shrinkage cracks, R 0.05%. DOM abundant, L>V (V= 40%, L=60%); vitrinite rare to abundant; liptinite abundant, dull orange sporinite. $R_{\text{vmax}} = 0.51\%$ .
22475	2639	Tangla	Siltstone > coal > sandstone. Coal major, V=90%, L=10%; vitrite > clarite; vitrinite mostly

Cont'd Appendix 3

detrovitrite; liptinite dominantly cutinite, brownish yellow. DOM abundant, L > V (L=78%, V=22%); vitrinite rare to abundant; liptinite abundant, mostly brownish yellow cutinite. R<sub>max</sub>= 0.54%.

22476	2804	Tangla	Siltstone > claystone > coal. Coal abundant, V=91%, L=9%; vitrite > clarite; vitrinite mostly telovitrinite; liptinite chiefly brownish yellow cutinite. DOM abundant, V > L (V=65%, L=45%); vitrinite rare to abundant; liptinite rare to abundant, chiefly cutinite, brownish yellow. R <sub>max</sub> = 0.60%.
22363	124	Tutut	Siltstone > claystone > coal > sandstone. Coal major, V=66%, L=32%, I=2%; vitrite > clarite > duroclarite; vitrinite mostly detrovitrinite, liptinite chiefly crassicutinite, greenish yellow, resinite rare, brown, bitumen associated with detrovitrinite R 0.04%, yellow, cracks and vesiculars, oil drop rare, greenish yellow; framboidal pyrite. DOM abundant, L > V > I (V=32%, L=60%, I=8%); vitrinite rare to sparse; liptinite rare to abundant, chiefly cutinite, greenish yellow, bitumen rare in sandstone, yellow. R <sub>max</sub> = 0.23%.
22364	158	Tutut	Siltstone > sandstone > claystone > coal. Coal abundant, V=37%, L=63%; clarite > vitrite; vitrinite mostly detrovitrinite, resinous vitrinite common; liptinite chiefly crassicutinite, greenish yellow, sporinite rare, dull brown. DOM abundant V > L > I (V=60%, L=39%, I=1%); vitrinite rare to abundant; liptinite sparse to abundant, chiefly cutinite, greenish yellow, bitumen in siltstone, greenish yellow R=0.03%, cracks; pyrite disseminated. R <sub>max</sub> = 0.28%.
22365	185	Tutut	Coal > shaly coal > siltstone. Coal major, V=86%, L=9%, I=5%; vitrite > clarite > duroclarite; vitrinite mostly detrovitrinite, resinous vitrinite common; liptinite chiefly sporinite, brownish yellow, crassicutinite sparse, greenish yellow, suberinite sparse, greenish yellow, inertinite rare-sparse, chiefly sclerotinite. Shaly coal abundant, V=40%, L=55%, I=5%; clarite > vitrite > duroclarite; Vitrinite rare to common, mostly detrovitrinite, inertinite rare to sparse mostly inertodetrinite, liptinite rare to abundant, dominantly sporinite and cutinite (crassicutinite), greenish yellow. DOM abundant, V > I (V=60%, L=40%), vitrinite rare to major; liptinite rare to major, chiefly sporinite and cutinite, greenish yellow; inertinite rare to sparse, mostly inertodetrinite. R <sub>max</sub> = 0.28%.
22366	204	Tutut	Coal > shaly coal > claystone. Coal major, V=69%, L=31%; vitrite > clarite; vitrinite mostly detrovitrinite, resinous vitrinite common; liptinite chiefly crassicutinite, greenish yellow, sporinite sparse greenish yellow, resinite sparse, brown, fluorinite sparse, green. Shaly coal abun-

			dant, V=80%, L=20%; vitrinite mostly detrovitrinite; liptinite chiefly detrital cutinite, greenish yellow, sporinite sparse, dull brown, vitrite > clarite. DOM abundant, L > V (V=33%, L=67%), vitrinite rare to abundant, liptinite sparse to abundant, chiefly cutinite, yellow. $R_{\text{max}} = 0.29\%$ .
22367	249	Tutut	Coal > claystone > siltstone > sandstone. Coal major, V=91%, L=6%, I=3%; vitrite > clarite, vitrinite mostly detrovitrinite, resinous vitrinite common; liptinite chiefly resinite; brownish yellow, sporinite and cutinite rare, yellow, oil cut in resinite, greenish yellow; inertinite dominantly sclerotinite; framboidal pyrite common. DOM abundant, L > V (V=43%, L=57%), vitrinite rare to abundant; liptinite sparse to abundant, mostly cutinite, yellow. $R_{\text{max}} = 0.28\%$ .
22368	295	Tutut	Siltstone > claystone > coal. Coal abundant, V=93% L=3%, I=4%; vitrite abundant; vitrinite mostly detrovitrinite, resinous vitrinite common, liptinite chiefly sporinite, yellow, oilcut associated with sporinite, bright yellow; framboidal pyrite abundant. DOM abundant, L > V (V=63%, L=37%), vitrinite rare to major; liptinite sparse to abundant, chiefly cutinite, yellow, resinite sparse, dull brown, bitumen in siltstone, yellow, cracks, R 0.03%. $R_{\text{max}} = 0.26\%$ .
22369	313	Kueh	Siltstone > claystone > coal > sandstone. Coal abundant, V > L > I (V=93%, L=5%, I=2%), vitrinite > clarite, vitrinite dominantly detrovitrinite, liptinite chiefly sporinite, yellow, inertinite mostly inertodetrinite, framboidal pyrite common. DOM abundant, L > V (V=30%, L=70%), vitrinite rare to abundant, liptinite sparse to abundant, chiefly sporinite, yellow, detrital cutinite common, yellow. $R_{\text{max}} = 0.27\%$ .
22370	414	Kueh	Siltstone > claystone > shaly coal. Shaly coal common, V > L (V=81%, L=19%), vitrinite mostly detrovitrinite, liptinite chiefly detrital cutinite, yellow, sporinite rare, yellow. DOM abundant, L > V (V=24%, L=76%), vitrinite rare to abundant, liptinite mostly cutinite, yellow, acritarch sparse, greenish yellow. $R_{\text{max}} = 0.30\%$ .
22371	478	Kueh	Claystone > siltstone > shaly coal > limestone. Shaly coal abundant, V > L (V=81%, L=19%), vitrite > clarite, vitrinite mostly detrovitrinite, liptinite chiefly sporinite, yellow, framboidal pyrite abundant. DOM abundant, L > V (V=3%, L=97%), vitrinite rare, liptinite rare to abundant, chiefly sporinite, yellow, bitumen in limestone pore yellow, cracks, R 0.04%. $R_{\text{max}} = 0.34\%$ .
22372	560	Kueh	Limestone > siltstone > claystone. DOM common, L > I > V (V=5%, L=86%, I=9%), vitrinite rare to sparse, liptinite sparse to abundant, chiefly cutinite, yellow, bitumen common, in limestone, cracks, yellow, R 0.04% acritarch rare, green; inertinite chiefly inertodetrinite. $R_{\text{max}} = 0.34\%$ .

Cont'd Appendix 3

22373	670	Kueh	Siltstone > claystone > limestone. DOM sparse, L > V (V=20%, L=80%), vitrinite rare to sparse, liptinite rare to sparse, chiefly detrital cutinite, yellow acritarch sparse, greenish yellow. R <sub>v</sub> max= 0.37%.
22374	807	Kueh	Claystone > sandstone. DOM sparse, L > V (V=30%, L=70%), vitrinite rare to sparse, liptinite rare to sparse, chiefly liptodetrinite, yellow, acritarch sparse, greenish yellow. R <sub>v</sub> max= 0.40%.
<b>BUBON</b>			
22451	192	Tutut	Claystone > siltstone > sandstone > coal. Shaly coal common, V > L > I (V=48%, L=34%, I=18%), vitrite, vitrinite mostly detrovitrinite, liptinite chiefly resinite, yellow, fluorinite sparse, greenish yellow. DOM abundant, L > V > I (V=50%, L=40%, I=10%), vitrinite rare to abundant, mostly oxidised, liptinite sparse to abundant, chiefly liptodetrinite, greenish yellow, bitumen in siltstone, yellow, cracks, R 0.04%. R <sub>v</sub> max= 0.22%.
22452	216	Tutut	Coal > siltstone > sandstone > claystone. Coal major, V > L > I (V=81%, L=18%, I=1%), vitrinite > clarite, vitrinite mostly detrovitrinite, liptinite chiefly sporinite and liptodetrinite, brownish yellow, crassicutinite common, greenish yellow, telalcinite sparses, yellow. Inertinite mostly inertodetrinite. DOM abundant, L > V > I (V=32%, L=60%, I=8%), vitrinite rare to common, liptinite sparse to abundant, chiefly liptodetrinite, yellow, sporinite sparse, brownish yellow. R <sub>v</sub> max= 0.28%.
22453	262	Tutut	Siltstone > coal > shaly coal > claystone. Coal major, V > L (V=90%, L=10%), vitrite, vitrinite mostly telovitrinite, liptinite chiefly liptodetrinite, greenish yellow, cutinite common, greenish yellow, suberinite rare, greenish yellow. Shaly coal abundant, V > L (V=85%, L=15%), vitrite > clarite, vitrinite mostly detrovitrinite, liptinite mostly detrital cutinite, greenish yellow. DOM abundant, L > V (V=40%, L=60%), vitrinite rare to common, liptinite sparse to abundant, chiefly cutinite, greenish yellow, liptodetrinite common, dull brown. R <sub>v</sub> max= 0.29%.
22454	307	Tutut	Coal > claystone > siltstone. Coal major, V > L (L=70%, L=30%), vitrinite chiefly detrovitrinite, liptinite mostly sporinite and liptodetrinite, brownish yellow, telalginite sparse, bright yellow, bitumen associated with detrovitrinite, yellow, cracks, R 0.04%. DOM abundant, V > L (V=68%, L=32%), vitrinite rare to abundant, liptinite chiefly sporinite, yellow. R <sub>v</sub> max= 0.28%.
22455	345	Tutut	Siltstone > coal > claystone > sandstone. Coal major, V > I (V=90%, L=10%), vitrinite, vitrinite



Cont'd Appendix 3

			chiefly detrovitrinite, liptinite dominated by sporinite and resinite, brownish yellow, framboidal pyrite in vitrinite. DOM common, L > V (V=44%, L=56%), vitrinite rare to common, liptinite sparse to common, chiefly cutinite, greenish yellow, pyrite disseminated in claystone. $R_{v,max}$ = 0.26%.
22456	381	Tutut	Claystone > siltstone > sandstone. DOM common, L > V (V=47%, L=53%), vitrinite rare to sparse, liptinite rare to abundant, chiefly liptodetrinite, yellow, sporinite rare, brownish yellow. $R_{v,max}$ = 0.27%. Bitumen common, in sandstone pore, shrinkage cracks.
22457	445	Tutut	Siltstone > Claystone > sandstone > coal > limestone. Coal abundant, V > L (V=83%, L=17%), vitrite, vitrinite mostly telovitrinite, liptinite chiefly resinite, brown to yellow, bitumen common associated with detrovitrinite, yellow, cracks, R 0.03%, framboidal pyrite abundant in vitrinite. DOM abundant, L > V (V=20%, L=80%), vitrinite rare to abundant, liptinite chiefly cutinite, greenish yellow, acritarch sparse, greenish blue, bitumen in sandstone pore, cracks, R 0.4%. $R_{v,max}$ = 0.29%.
22458	591	Tutut	Claystone > siltstone > sandstone > limestone. DOM abundant, L > V (V=23%, L=77%), vitrinite rare to abundant, chiefly cutinite, yellow, acritarch common in claystone, greenish yellow. $R_{v,max}$ = 0.31%.
22459	637	Kueh	Claystone > siltstone > sandstone > limestone. DOM common, L > V (V=27%, L=63%), vitrinite rare to sparse, liptinite sparse to abundant, chiefly resinite, dull brown, lamacinite in coal, greenish yellow, bitumen common in sandstone and carbonate, yellow, cracks, R 0.04%. $R_{v,max}$ = 0.34%.
22460	701	Kueh	Coal > shaly coal > Claystone > siltstone. Coal major, V > L > I (V=82%, L=17%, I=1%), vitrite > clarite, vitrinite chiefly detrovitrinite, liptinite mostly cutinite, yellow, resinite sparse, brown, fluorinite, green; inertinite mostly inertodetrinite. Shaly coal abundant, V > L (V=90%, L=10%), vitrite > clarite, vitrinite mostly detrovitrinite, liptinite chiefly cutinite, yellow. DOM common L > V (V=37%, L=63%), vitrinite rare to common, liptinite rare to common, chiefly cutinite, yellow. $R_{v,max}$ = 0.34%. Cauliflower bitumen common in siltstone.
22461	737	Kueh	Coal > siltstone > sandstone > claystone > limestone. Coal major, V > L > I (V=90%, L=90%, I=1%), vitrite > clarite, vitrinite mostly detrovitrinite, liptinite chiefly liptodetrinite, yellow, telalginite sparse, bright yellow, inertodetrinite sparse. DOM common, V > L (V=55%, L=45%), vitrinite rare to common, liptinite rare to common, chiefly cutinite, yellow. $R_{v,max}$ = 0.33%.

Cont'd Appendix 3

22462	801	Kueh	Claystone > siltstone > coal > sandstone. Coal abundant, $V > L$ ( $V=93\%$ , $L=75\%$ ), vitrinite chiefly detrovitrinite, liptinite mostly liptodetrinite, yellow, cutinite and sporinite sparse, yellow, framboidal pyrite in vitrinite. DOM common, $V > L$ ( $V=69\%$ , $L=31\%$ ), vitrinite rare to common, liptinite rare to common, chiefly liptodetrinite, yellow, oil cut expelled from resinite. $R_{\text{max}}= 0.34\%$ .
22463	874	Kueh	Siltstone > sandstone > claystone. DOM abundant, $L > V$ ( $V=44\%$ , $L=56\%$ ), vitrinite rare to abundant, liptinite sparse to abundant, chiefly cutinite, yellow, bitumen in sandstone, yellow, cracks, $R_{\text{max}}= 0.32\%$ .
22464	920	Kueh	Shaly coal > siltstone > claystone > sandstone. Shaly coal major, $V > L$ ( $V=90\%$ , $L=10\%$ ), vitrite clarite, vitrinite mostly detrovitrinite, liptinite chiefly liptodetrinite, yellow, cutinite common, yellow, telalginite sparse, yellow, bitumen in detrovitrinite, yellow, cracks. DOM abundant, $L > V$ ( $V=47\%$ , $L=53\%$ ), vitrinite rare to common, liptinite sparse to abundant, chiefly detrital cutinite, yellow. $R_{\text{max}}= 0.37\%$ .
22465	957	Kueh	Claystone > siltstone > coal > limestone. Coal abundant, $V > L$ ( $V=84\%$ , $L=16\%$ ), clarite, vitrinite mostly detrovitrinite, liptinite chiefly resinite and liptodetrinite, brownish yellow, sporinite rare, yellow, exsudatinite, green, bitumen in detrovitrinite, yellow, $R_{\text{max}}= 0.04\%$ . DOM abundant, $L > V$ ( $V=47\%$ , $L=53\%$ ), vitrinite rare to common, liptinite rare to abundant, chiefly liptodetrinite, yellow. $R_{\text{max}}= 0.37\%$ .
22466	1011	Kueh	Siltstone > coal > claystone > limestone. Coal major, $V > L$ ( $V=60\%$ , $L=40\%$ ), vitrinite > clarite, vitrinite mostly detrovitrinite, liptinite chiefly resinite, brown, cutinite sparse, yellow, exsudatinite in telovitrinite, green, bitumen in detrovitrinite, yellow, cracks, $R_{\text{max}}= 0.04\%$ . DOM abundant, $L > V$ ( $V=36\%$ , $L=64\%$ ), vitrinite rare to sparse, liptinite rare to major, chiefly detrital cutinite, yellow. $R_{\text{max}}= 0.35\%$ .
22467	1121	Kueh	Siltstone > coal > shaly coal. Coal major, $V > L$ ( $V=94\%$ , $L=6\%$ ), vitrite, vitrinite mostly telovitrinite, liptinite dominantly liptodetrinite, yellow, cutinite common, dark orange-brown, sporinite sparse, brown. Shaly coal abundant, $L > V$ ( $V=40\%$ , $L=60\%$ ), clarite > vitrite, vitrinite dominated by detrovitrinite, liptinite chiefly detrital cutinite, yellow, spore common, dark brown, bitumen in shale, greenish yellow. DOM abundant, $L > V$ ( $V=49\%$ , $L=51\%$ ), vitrinite rare to abundant, liptinite rare to major, chiefly cutinite and sporinite, yellow and brown. $R_{\text{max}}= 0.40\%$ .

Cont,d Appendix 8

22468	1167	Kueh	Coal > claystone > siltstone > sandstone. Coal major, V > L (V=85%, L=15%), vitrite > clarite, vitrinite mostly detrovitrinite, liptinite dominated by liptodetrinite and resinite, yellow, fluorinite sparse, green, sporinite and cutinite sparse, brown and yellow. DOM abundant, L > V (V=44%, L=56%), vitrinite rare to abundant, liptinite sparse to abundant, chiefly liptodetrinite, brownish yellow, oil drop in sandstone, yellow. $R_{v,max}$ = 0.40%.
22469	1176	Kueh	Coal > siltstone > claystone > limestone. Coal major, V > L (V=89%, L=11%) vitrite > clarite, vitrinite mostly detrovitrinite, liptinite dominated by liptodetrinite and resinite, brown, sporinite and cutinite sparse. DOM abundant, L > V (V=37%, L=63%), vitrinite rare-sparse, liptinite sparse to abundant, chiefly liptodetrinite and detrital cutinite, brown and dark orange-brown, bitumen in carbonate, yellow, cracks, R 0.05%. $R_{v,max}$ = 0.40%.
22470	1240	Kueh	Siltstone > shaly coal > sandstone > claystone. Shaly coal major vitrite > clarite, V > L (V=86%, L=14%), vitrinite mostly detrovitrinite, liptinite dominated by liptodetrinite, brown, detrital cutinite common, yellow, resinite and fluorinite sparse, brown and greenish yellow. DOM abundant, L > V (V=32%, L=68%), vitrinite rare to sparse, liptinite rare to abundant, chiefly detrital cutinite, yellow. $R_{v,max}$ = 0.41%.
22471	1341	Kueh	Claystone > siltstone > sandstone. DOM abundant, L > V (V=33%, L=67%), vitrinite rare to abundant, liptinite sparse to major, chiefly liptodetrinite, brownish yellow, detrital sporinite sparse, brown, bitumen in claystone, green. $R_{v,max}$ = 0.41%.
22472	1539	Kueh	Limestone > siltstone > claystone. DOM common, L > V (V=10%, L=90%), vitrinite rare to sparse, liptinite rare to common, chiefly liptodetrinite, yellow-crown, bitumen in limestone, yellow, cracks, R 0.05%. $R_{v,max}$ = 0.41%.
22473	1655	Kueh	Limestone, dom sparse, L > V (V=85, L=92%), vitrinite rare, liptinite rare to sparse, chiefly liptodetrinite, yellow to brown, oil drop in limestone, green. $R_{v,max}$ = 0.42%.

KEUDAPASI

22383	112	Tutut	Sandstone > siltstone > claystone. DOM rare, L > V (V=80%, L=90%), vitrinite rare, liptinite rare, liptinite rare-sparse, chiefly cutinite (crassicutinite), greenish yellow, acritarch rare, green. $R_{v,max}$ = 0.23%.
22384	149	Tutut	Siltstone > claystone > sandstone > limestone > coal. Coal abundant, V > L (V=88%, L=12%), vi-

Cont'd Appendix 8

trite, vitrinite mostly telovitrinite, resinous vitrinite common, brownish yellow, liptinite chiefly resinite and crassicutinite, brown and yellow. DOM abundant, L > V (V=37%, L=63%), vitrinite sparse to abundant, liptinite sparse to abundant, chiefly cutinite, greenish yellow, liptodetrinite common, brownish yellow.  $R_{v,max} = 0.23\%$ .

22385                      185                      Tutut                      Siltstone > sandstone > claystone > limestone. DOM common, L > V (V=21%, L=79%), vitrinite rare to common, liptinite rare to common, chiefly cutinite, greenish yellow, liptodetrinite sparse, brownish yellow.  $R_{v,max} = 0.22\%$ .

22386                      213                      Tutut                      Siltstone > sandstone > coal > limestone. Coal abundant, V > L > I (V=91%, L=7%, I=2%), vitrite > clarite, vitrinite mostly detrovitrinite, resinous vitrinite common, brown, liptinite chiefly crassicutinite, greenish yellow, liptodetrinite common, yellow, inertodetrinite common, framboidal pyrite in vitrinite. DOM abundant, L > V (V=13%, L=87%), vitrinite rare to abundant, liptinite sparse to major, chiefly cutinite, greenish yellow, liptodetrinite common, yellow, oil drops in siltstone, green, bitumen in sandstone, yellow, cracks,  $R_{v,max} = 0.24\%$ .

22387                      289                      Tutut                      Siltstone > carbonate > coal > sandstone. Coal abundant, V > L > I (V=91%, L=5%, I=4%), vitrite > clarite > duroclarite, vitrinite mostly detrovitrinite, resinous vitrinite common, brownish yellow, liptinite chiefly crassicutinite, greenish yellow, liptodetrinite and resinite sparse, brown, sclerotinite sparse, framboidal pyrite in vitrinite. DOM abundant, L > V (V=36%, L=64%), vitrinite rare to abundant, liptinite sparse to major, chiefly cutinite, greenish yellow, dynoflagellate sparse in siltstone.  $R_{v,max} = 0.27\%$ .

22388                      350                      Tutut                      Siltstone > claystone > sandstone > limestone > coal. Coal common, V > L (V=94%, L=65%), vitrite > clarite, vitrinite mostly detrovitrinite, resinous vitrinite common, liptinite chiefly resinite, brown, cutinite common, framboidal pyrite in vitrinite. DOM common, V > L (V=52%, L=48%), vitrinite rare to abundant, liptinite rare to common, chiefly cutinite, greenish yellow, sporangium in siltstone, acritarch sparse in claystone, oil drop in siltstone, green, bitumen in sandstone, yellow, cracks.  $R_{v,max} = 0.30\%$ .

22389                      405                      Tutut                      Limestone > siltstone > sandstone. DOM sparse, L > V (V=14%, L=86%), vitrinite rare-sparse, liptinite rare-sparse, mostly cutinite, yellow acritarch sparse, green.  $R_{v,max} = 0.28\%$ .

22390                      505                      Tutut                      Siltstone > claystone > limestone > sandstone. DOM abundant, L > V (V=49%, L=51%), vitrinite

Cont'd Appendix 8

			rare to abundant, liptinite rare to major, chiefly cutinite, greenish yellow, liptodetrinite, yellow, sporinite sparse, yellow, acritarch in siltstone, green, bitumen in limestone, yellow, cracks, R 0.03%. R <sub>v</sub> max= 0.32%.
22391	542	Tutut	Siltstone > sandstone > claystone > limestone. DOM abundant, V > L (V=51%, L=49%), vitrinite rare to abundant, liptinite rare to abundant, chiefly detrital crassicutinite, greenish yellow, acritarch common in claystone, bitumen in sandstone, sparse. R <sub>v</sub> max= 0.34%.
22392	661	Kueh	Claystone > sandstone > limestone. DOM abundant, L > V (V=30%, L=70%), vitrinite rare to abundant, liptinite rare to abundant, chiefly liptodetrinite, yellow, cutinite common, yellow. R <sub>v</sub> max= 0.33%.
22393	762	Kueh	Siltstone > claystone > limestone. DOM abundant, L > V (V=40%, L=60%), vitrinite rare to abundant, liptinite rare to major, mostly cutinite, yellow, detrital suberinite, brownish yellow, bitumen in limestone, yellow. R <sub>v</sub> max= 0.34%.
22394	862	Kueh	Limestone > siltstone. DOM sparse, L > V (V=23%, L=77%), vitrinite rare to sparse, liptinite chiefly liptodetrinite, yellow, bitumen in carbonate pore, yellow. R <sub>v</sub> max= 0.34%.
22394a	981	Kueh	Limestone > siltstone. DOM common, L > V (V=28%, L=72%), vitrinite rare to common, liptinite sparse to common, mostly liptodetrinite, yellow, bitumen in carbonate, yellow, cracks, R 0.04%. R <sub>v</sub> max= 0.35%.
TUBA			
22375	131	Tutut	Claystone > sandstone > coal. Coal common, V > L (V=69%, L=31%) vitrite, vitrinite mostly detrovitrinite, resinous vitrinite common, brownish yellow, liptinite chiefly oxidized cutinite, brownish yellow-dull black, sporinite sparse, brownish yellow. DOM major, V > L (V=75%, L=25%), vitrinite sparse to major, oxidized vitrinite common, liptinite rare to sparse, chiefly liptodetrinite, brownish yellow. R <sub>v</sub> max= 0.21%.
22376	201	Tutut	Limestone > claystone > siltstone. DOM common, V > L (V=94%, L=6%), vitrinite rare to abundant, liptinite rare to common, chiefly liptodetrinite yellow, acritarchs, common in siltstone, green. R <sub>v</sub> max= 0.21%.
22377	356	Tutut	Sandstone > siltstone > limestone > coal. Coal common, V > L (V=99%, L=1%), vitrite, vitrinite mostly telovitrinite, resinous vitrinite common, brownish yellow, liptinite chiefly sporinite, yellow. DOM abundant, L > V (V=23%, L=77%), vitrinite rare to abundant, liptinite rare to

Cont'd Appendix 8

			abundant, chiefly detrital cutinite, greenish yellow, lamalginite in siltstone, sparse, green, acritarch in siltstone, greenish yellow. $R_{\text{max}} = 0.24\%$ .
22378	466	Tutut	Siltstone > limestone > sandstone. DOM common, $V > L$ ( $V=45\%$ , $L=55\%$ ), vitrinite rare to common, liptinite rare to common, mostly oxidized cutinite, dark brown, bitumen in sandstone, brownish yellow. $R_{\text{max}} = 0.28\%$ .
22379	749	Tutut	Siltstone > limestone > sandstone. DOM sparse, $V > L$ ( $V=56\%$ , $L=44\%$ ), vitrinite rare to sparse, liptinite rare to sparse, chiefly liptodetrinite, brownish yellow, pyrite disseminated in siltstone. $R_{\text{max}} = 0.35\%$ .
22380	923	Kueh	Siltstone > limestone. DOM abundant, $L > V$ ( $V=31\%$ , $L=69\%$ ), vitrinite rare to common, liptinite rare to abundant, chiefly liptodetrinite, yellow, lamalginite in siltstone, sparse, green, bitumen in sandstone pore, yellow. $R_{\text{max}} = 0.34\%$ .
22381	1069	Kueh	Claystone > siltstone > sandstone. DOM abundant, $L > V$ ( $V=40\%$ , $L=60\%$ ), vitrinite rare to abundant, most oxidized, dark brown, liptinite sparse to abundant, chiefly liptodetrinite, yellow, sporinite common, most oxidized, brownish black. $R_{\text{max}} = 0.33\%$ .
22382	1207	Kueh	Claystone > siltstone > coal. Coal common, $L > V > I$ ( $V=37\%$ , $L=55\%$ , $I=8\%$ ) vitrite, vitrinite mostly detrovitrinite, liptinite chiefly sporinite, yellow, resinite sparse, brown, pyrite disseminated in vitrinite, inertodetrinite sparse. DOM abundant, $L > V$ ( $V=30\%$ , $L=70\%$ ), vitrinite sparse to abundant, liptinite sparse to abundant, chiefly sporinite and cutinite, yellow, <u>Botryococcus</u> in siltstone, sparse, yellow, pyrite disseminated. $R_{\text{max}} = 0.35\%$ .
23259	1037	Kueh	Siltstone > limestone. DOM common, $V > L$ ( $V=57\%$ , $L=43\%$ ), vitrinite rare to common, liptinite sparse to common, chiefly sporinite, brownish yellow, <u>Botryococcus</u> , yellow. $R_{\text{max}} = 0.36\%$ .
23260	1411	Kueh	Limestone > siltstone. DOM common, $V > L$ ( $V=68\%$ , $L=32\%$ ), vitrinite rare to common, liptinite rare to common, mostly cutinite, yellow. $R_{\text{max}} = 0.36\%$ .
23261	1472	Kueh	Limestone > siltstone > sandstone. DOM sparse $V > L$ ( $V=64\%$ , $L=36\%$ ), vitrinite rare to sparse, liptinite rare to sparse, mostly liptodetrinite, yellow, bitumen in limestone, yellow. $R_{\text{max}} = 0.37\%$ .
23262	1600	Kueh	Limestone > siltstone > sandstone. DOM common, $L > V$ ( $V=45\%$ , $L=55\%$ ), vitrinite rare to common, liptinite rare to common, chiefly liptodetrinite, yellow, cutinite and sporinite sparse, yellow, lamalginite in siltstone, rare, greenish yellow. $R_{\text{max}} = 0.39\%$ .

Appendix 8 cont'd

Cont'd Appendix 3

23263	1691	Kueh	Siltstone > limestone > sandstone. DOM common, L > V (V=48%, L=52%), vitrinite sparse, liptinite common, chiefly liptodetrinite, yellow. $R_{vmax}$ = 0.40%.
23264	1783	Kueh	Siltstone > sandstone > limestone. DOM abundant, V > L (V=76%, L=24%), vitrinite rare to abundant, liptinite rare to common, mostly cutinite and liptodetrinite, yellow, bitumen in sandstone, yellow. $R_{vmax}$ = 0.40%.
23265	1956	Kueh	Calcareous siltstone > limestone. DOM common, L > V (V=45%, L=55%), vitrinite rare to common, liptinite sparse to abundant, chiefly cutinite, yellow. $R_{vmax}$ = 0.41%.
23266	2158	Kueh	Siltstone > coal > sandstone. Coal major, V > L > I (V=85%, L=12%, I=3%), vitrite > clarite, vitrinite dominantly detrovitrinite, liptinite chiefly sporinite and resinite, brownish yellow, bitumen in detrovitrinite, yellow, cracks, R 0.03%, inertinite mostly senifusinite and sclerotinite, framboidal pyrite in vitrinite. DOM abundant, L > V (V=30%, L=70%), vitrinite rare to abundant, liptinite sparse to major, chiefly cutinite and sporinite, yellow. $R_{vmax}$ = 0.42%.
23267	2322	Tangla	Siltstone > claystone. DOM common, V > L (V=86%, L=14%), vitrinite rare to sparse, liptinite rare to common, chiefly cutinite, yellow, pyrite disseminated. $R_{vmax}$ = 0.43%.
23268	2459	Tangla	Coal > siltstone > claystone > shaly coal. Coal major, V > L (V=92%, L=8%), vitrite > clarite, vitrinite mostly detrovitrinite, liptinite dominantly cutinite, yellow, resinite and sporinite sparse, brownish yellow, bitumen in detrovitrinite, yellow, cracks, R 0.05%, framboidal pyrite in vitrinite. Shaly coal abundant, V > L (V=85%, L=15%), vitrite > clarite, vitrinite mostly detrovitrinite, liptinite chiefly cutinite, yellow, sporangium sparse, bright yellow, pyrite disseminated. DOM abundant, V > L (V=55%, L=45%), vitrinite rare to abundant, chiefly sporinite, yellow, liptodetrinite sparse, brown. $R_{vmax}$ = 0.41%.
23269	2578	Tangla	Coal > claystone > siltstone. Coal abundant, V > L (V=88%, L=12%), vitrite > clarite, vitrinite chiefly detrovitrinite, liptinite mostly cutinite, yellow, sporinite and resinite rare, yellow-brown. DOM abundant, V > L (V=54%, L=46%), vitrinite rare to abundant, liptinite rare to abundant, chiefly cutinite and sporinite, yellow. $R_{vmax}$ = 0.52%.
23270	2618	Tangla	Siltstone > coal > sandstone. Coal major, V > L (V=90%, L=10%), vitrite > clarite, vitrinite mostly detrovitrinite, liptinite mostly cutinite, brownish yellow. DOM abundant, L > V (V=23%, L=77%), vitrinite rare-abundant, liptinite

Cont'd Appendix 3

abundant, mostly cutinite, brownish yellow.  
R<sub>y</sub>max= 0.54%.

TRIPA

22419	118	Tutut	Limestone > claystone > siltstone > sandstone. DOM common, L > V (V=29%, L=71%), vitrinite rare detrital resinous vitrinite, brown, liptinite rare to abundant, chiefly sporinite, dull brown. R <sub>y</sub> max= 0.23%.
22420	155	Tutut	Siltstone > sandstone > coal. Coal abundant, I > L (V=42%, L=11%, I=47%), vitrite > inertite > duroclarite, vitrinite mostly detrovitrinite, resinous vitrinite common, liptinite chiefly cutinite, greenish yellow, sporinite, bright yellow, liptodetrinite sparse, yellow, inertinite dominantly semifusinite and inertodetrinite. DOM abundant, V > L (V=40%, L=60%), vitrinite rare to common, liptinite sparse to abundant, chiefly fine grained liptodetrinite, yellow, bitumen in siltstone, yellow. R <sub>y</sub> max= 0.24%.
22421	176	Tutut	Calcareous > sandstone > siltstone > claystone. DOM common, V > L (V=55%, L=45%), vitrinite rare rare to common, mostly oxidized detrovitrinite, brown-black, liptinite sparse-common, chiefly teinuspore, brown, thick wall cutinite sparse, oxidized, brownish black. R <sub>y</sub> max= 0.27%.
22422	216	Tutut	Siltstone > sandstone > claystone > shaly coal. Shaly coal abundant, V > L > I (V=70%, L=28%, I=2%), vitrite > clarite, vitrinite mostly detrovitrinite, resinous vitrinite common, brownish yellow, liptinite chiefly thick wall cutinite, yellow, inertodetrinite sparse. DOM abundant, L > V (V=46%, L=54%), vitrinite rare to common, liptinite sparse to abundant, chiefly thick wall cutinite, greenish yellow, pyrite disseminated in vitrinite. R <sub>y</sub> max= 0.25%.
22423	292	Tutut	Siltstone > sandstone > coal. Coal common, V > L > I (V=87%, L=12%, I=1%). vitrinite mostly detrovitrinite, resinous vitrinite sparse, brown, liptinite chiefly liptodetrinite, yellow, inertodetrinite sparse. DOM common, V > L (V=60%, L=40%), vitrinite rare to common, liptinite sparse to common, chiefly liptodetrinite, yellow, acritarch in siltstone sparse, greenish yellow. R <sub>y</sub> max= 0.25%.
22424	338	Tutut	Siltstone > sandstone > claystone. DOM sparse, L > V (V=40%, L=60%), vitrinite rare to sparse, liptinite sparse, chiefly detrital thick wall cutinite, greenish yellow, acritarchs in siltstone, sparse-common, green-blue. R <sub>y</sub> max= 0.26%.
22425	402	Tutut	Siltstone > claystone > limestone. DOM abundant, L > V (V=41%, L=59%), vitrinite rare to abundant, liptinite sparse-abundant, mostly liptodetrinite, yellow, thick wall cutinite sparse, greenish yellow. R <sub>y</sub> max= 0.29%.



22426	466	Tutut	Limestone > siltstone > sandstone. DOM sparse, V > L (V=90%, L=10%), vitrinite rare to common, liptinite rare common, chiefly fine-grained liptodetrinite, greenish yellow, lamalginite in siltstone, rare, greenish yellow. $R_{\text{max}} = 0.30\%$ .
22427	521	Tutut	Limestone > claystone > siltstone > sandstone. DOM sparse, V > L (V=54%, L=46%), vitrinite rare to common, most oxidised, brown-black, liptinite rare-sparse, chiefly liptodetrinite, yellow. $R_{\text{max}} = 0.28\%$ .
22428	594	Tutut	Siltstone > sandstone > claystone > coal. Coal sparse, V > L (V=60%, L=40%), vitrinite mostly oxidized detrovitrinite, dark brown, liptinite chiefly tennospore, dull brown. DOM abundant, V > L (V=85%, L=15%), vitrinite rare to abundant, mostly oxidised, brown, liptinite sparse to abundant, chiefly detrital cutinite, greenish yellow, lamalginite in siltstone, sparse, green, acritarch in siltstone, green. $R_{\text{max}} = 0.26\%$ . Bitumen common in sandstone pore, shrinkage cracks.
22429	658	Tutut	Siltstone > sandstone > coal. Coal abundant, V > L > I (V=78%, L=21%, I=1%), vitrinite mostly detrovitrinite, resinous vitrinite sparse, brownish yellow, liptinite chiefly cutinite, greenish yellow, tennospore, dark brown, resinite rare, brown, sclerotinite sparse. DOM abundant, V > L (V=80%, L=20%), vitrite, vitrinite sparse to abundant, liptinite rare to abundant, chiefly cutinite, greenish yellow, bitumen in sandstone, yellow. $R_{\text{max}} = 0.29\%$ .
22430	804	Tutut	Siltstone > sandstone. DOM common, V > L (V=60%, L=40%), vitrinite sparse to common, liptinite rare to common, chiefly liptodetrinite, yellow, acritarch in siltstone common, green. $R_{\text{max}} = 0.30\%$ .
22431	1033	Tutut	Siltstone > claystone > sandstone. DOM common, L > V (V=46%, L=54%), vitrinite rare to abundant, mostly oxidised, dark brown, liptinite sparse to common, chiefly lamalginite in siltstone, green, sporinite rare, brown, acritarch in siltstone, green. $R_{\text{max}} = 0.32\%$ .
22432	1115	Tutut	Siltstone > claystone > shaly coal. Shaly coal common, V > L (V=90%, L=10%), vitrite, vitrinite mostly detrovitrinite, liptinite chiefly sporinite, brown. Dom abundant, L > V (V=48%, L=52%), vitrinite rare to abundant, liptinite sparse to abundant, chiefly lamalginite, green, acritarch in acritarch in siltstone, sparse, green, bitumen in siltstone, yellow. $R_{\text{max}} = 0.28\%$ .
22433	1197	Kueh	Calcareous siltstone > coal. Coal abundant, V > L (V=83%, L=17%), vitrite, vitrinite mostly detrovitrinite, liptinite chiefly sporinite, yellow, liptodetrinite common yellow, bitumen in detrovitrinite, yellow, cracks, $R = 0.03\%$ . DOM abundant, L > V (V=41%, L=59%), vitrinite rare to abundant, liptinite sparse to abundant, chiefly cutinite, yellow, lamalginite in siltstone, greenish yellow. $R_{\text{max}} = 0.31\%$ .

Cont'd Appendix 8

22434	1289	Kueh	Siltstone > claystone > shaly coal. Shaly coal common, L > V (V=40%, L=60%), clarite > vitrite, vitrinite mostly telovitrinite, some oxidized, brow. DOM abundant, V > L (V=50%, L=40%), vitrinite rare to abundant, liptinite sparse to abundant, chiefly liptodetrinite, yellow, lamalginite in siltstone, yellow. $R_{\text{vmax}} = 0.31\%$ .
22435	1499	Kueh	Siltstone > claystone. DOM abundant, V=L (V=50%, L=50%), vitrinite rare to abundant, liptinite rare to abundant, chiefly detrital cutinite, yellow, lamalginite in siltstone, greenish yellow. $R_{\text{vmax}} = 0.31\%$ .
22436	1572	Kueh	Siltstone > shaly coal. Shaly coal major, L > V (V=40%, L=60%), clarite > vitrite, vitrinite mostly detrovitrinite, liptinite dominantly cutinite and sporinite, yellow, resinite sparse, brownish yellow. DOM sparse, L > V (V=40%, L=60%), vitrinite rare to sparse, liptinite sparse, chiefly cutinite, yellow. $R_{\text{vmax}} = 0.34\%$ .
22437	1581	Kueh	Siltstone > coal. Coal major, V > L > I (V=83%, L=16%, I=1%), vitrinite mostly detrovitrinite, liptinite chiefly sporinite, yellow, liptodetrinite common, yellow, semifusinite sparse. DOM abundant, V > L (V=53%, L=47%), vitrinite rare to abundant, liptinite sparse to abundant, chiefly sporinite, yellow. $R_{\text{vmax}} = 0.31\%$ .
22438	1591	Kueh	Siltstone > coal > sandstone. Coal major, V > L > I (V=77%, L=21%, I=2%), vitrite > clarite > du-roclarite, vitrinite mostly detrovitrinite, liptinite chiefly sporinite, yellow, exsudatinitite in telovitrinite, greenish yellow. DOM abundant, V=L (V=50%, L=50%), vitrinite rare to abundant, liptinite sparse to abundant, chiefly sporinite yellow, liptodetrinite, yellow. $R_{\text{vmax}} = 0.34\%$ .
22439	1600	Kueh	Siltstone > coal. Coal major, V > L > I (V=86%, L=8%, I=6%), vitrite > clarite, vitrinite mostly detrovitrinite, liptinite chiefly sporinite, yellow, liptodetrinite sparse, yellow, exsudatinitite in telovitrinite, yellow, semifusinite and sclerotinitite sparse. DOM abundant, L > V (V=40%, L=60%), vitrinite rare to common, liptinite sparse to abundant, chiefly sporinite and liptodetrinite, yellow. $R_{\text{vmax}} = 0.31\%$ .
22440	1609	Kueh	Siltstone > shaly coal > sandstone. Shaly coal abundant, V > l (V=65%, L=45%), vitrite, vitrinite mostly detrovitrinite, liptinite dominantly sporinite and liptodetrinite, yellow. DOM abundant, V > L (V=75%, L=25%), vitrinite rare to common, liptinite sparse to abundant, chiefly sporinite, yellow, liptodetrinite sparse, yellow. $R_{\text{vmax}} = 0.31\%$ .

Cont'd Appendix 8

22441	1645	Kueh	Siltstone > sandstone > shaly coal. Shaly coal common, V > L (V=90%, L=10%), clarite, vitrinite mostly detrovitrinite, liptinite chiefly liptodetrinite, yellow. DOM, common, L > V (V=42%, L=58%), vitrinite rare to common, liptodetrinite and sporinite, yellow, bitumen in sandstone pore, sparse, yellow, cracks, R <sub>v</sub> max= 0.04%. R <sub>v</sub> max= 0.31%.
22442	1682	Kueh	Siltstone > sandstone. Dom abundant, V > L (V=55%, L=45%), vitrite, vitrinite mostly detrovitrinite, liptinite chiefly, liptodetrinite yellow, lamalginite sparse, green, bitumen in sandstone, yellow. R <sub>v</sub> max= 0.32%.
22443	1746	Kueh	Siltstone > coal. Coal abundant, V > L > I (V=88%, L=8%, I=4%), vitrite, vitrinite mostly detrovitrinite, liptinite dominantly liptodetrinite, yellow, inertodetrinite common. Dom abundant, L > V (V=30%, L=70%), vitrinite rare to abundant, liptinite sparse to abundant, chiefly liptodetrinite, yellow, cutinite sparse, yellow, bitumen in siltstone, rare, yellow. R <sub>v</sub> max= 0.32%.
22444	1783	Kueh	Siltstone > shaly coal, sandstone. Shaly coal abundant, L > V (V=30%, L=70%), liptite > vitrite, vitrinite mostly telovitrinite, liptinite chiefly sporinite, yellow to orange, cutinite sparse, yellow to orange, bitumen common, yellow. Dom abundant, L > V (V=40%, L=60%), vitrinite rare to sparse, liptinite sparse to abundant, chiefly detrital sporinite and cutinite, yellow to orange. R <sub>v</sub> max=0.31%.
22445	1792	Kueh	Siltstone > coal > sandstone. Coal major, V > L > I (V=96%, L=3%, I=1%), vitrite, vitrinite mostly detrovitrinite, liptinite dominantly sporinite and cutinite, yellow-orange, exsudatinitite in telovitrinite cleat, yellow. DOM abundant, L > V (V=20%, L=80%), vitrinite sparse to common, liptinite sparse to abundant chiefly liptodetrinite, yellow to orange. R <sub>v</sub> max= 0.33%.
22446	1891	Kueh	Siltstone > claystone > sandstone > shaly coal. Shaly coal abundant, L > V (V=30%, L=70%), clarite > vitrite, vitrinite mostly telovitrinite, liptinite chiefly cutinite, brown orange, sporinite sparse, brown, bitumen, yellow, cracks, R 0.03%. DOM abundant, V > L (V=55%, L=45%), vitrinite sparse to abundant, liptinite rare to abundant, chiefly cutinite, brown. R <sub>v</sub> max= 0.31%.
22447	1901	Kueh	Siltstone > coal. Coal abundant, V > I > L (V=97%, L=1%, I=2%), vitrite, vitrinite mostly detrovitrinite, liptinite chiefly liptodetrinite, yellow, inertodetrinite common. DOM abundant, V > L (V=55%, L=45%), vitrinite rare to abundant, liptinite sparse to abundant, chiefly liptodetrinite, yellow-orange. R <sub>v</sub> max= 0.33%.

Cont'd Appendix 8

22448	2048	Kueh	Limestone > siltstone. DOM common, $V > L$ ( $V=30\%$ , $L=20\%$ ), vitrinite rare to common, liptinite rare to common, chiefly cutinite yellow, bitumen in carbonate rare, yellow. $R_{\text{max}}=0.36\%$ .
22449	2057	Kueh	Limestone > siltstone. DOM sparse, $L > V$ ( $V=38\%$ , $L=62\%$ ), vitrinite rare-sparse, liptinite sparse, mostly liptodetrinite, yellow, bitumen in limestone, sparse, yellow. $R_{\text{max}}=0.37\%$ .
22450	2066	Kueh	Limestone > siltstone, DOM sparse, $L > V$ ( $V=40\%$ , $L=60\%$ ), vitrinite rare-sparse, liptinite sparse, chiefly liptodetrinite, yellow, $R_{\text{max}}=0.34\%$ .

MEULABOH EAST

22405	128	Tutut	Siltstone > limestone > sandstone > coal. Coal abundant, $V > L$ ( $V=69\%$ , $L=31\%$ ), vitrite, clarite, vitrinite mostly detrovitrinite, resinous vitrinite common, brownish yellow, liptinite chiefly thick wall cutinite (crassicutinite), greenish yellow, sporinite sparse, dark brown, framboidal pyrite in vitrinite cleats. DOM abundant, $L > V$ ( $V=41\%$ , $L=59\%$ ), vitrinite rare to abundant, liptinite sparse to abundant, chiefly detrital cutinite, greenish yellow. $R_{\text{max}}=0.20\%$ .
22406	274	Tutut	Siltstone > coal > sandstone. Coal major, $V > L$ ( $V=93\%$ , $L=7\%$ ), vitrite, vitrinite mostly detrovitrinite, liptinite chiefly cutinite, greenish yellow, liptodetrinite abundant, yellow, framboidal pyrite filling vitrinite cracks. DOM common, $L > V$ ( $V=41\%$ , $L=59\%$ ), vitrinite rare to common, liptinite sparse to common, chiefly detrital thick wall cutinite, greenish yellow, sporinite sparse, brown. $R_{\text{max}}=0.21\%$ .
22407	420	Tutut	Claystone > sandstone > coal. Coal common, $V > I$ ( $V=96\%$ , $I=4\%$ ), vitrite, vitrinite mostly detrovitrinite, resinous vitrinite common, brownish yellow, inertodetrinite sparse. DOM common, $L > V$ ( $V=40\%$ , $L=60\%$ ), vitrinite rare to sparse, liptinite sparse to common, mostly liptodetrinite, yellow. $R_{\text{max}}=0.25\%$ .
22408	493	Tutut	Claystone > coal > sandstone. Coal abundant $V > I > L$ ( $V=86\%$ , $L=3\%$ , $I=11\%$ ), vitrite > duroclarite, vitrinite mostly detrovitrinite, resinous vitrinite common, brownish yellow, liptinite chiefly liptodetrinite, greenish yellow, bitumen in detrovitrinite, vesicular, yellow, semifusinite and inertodetrinite common, framboidal pyrite in vitrinite cleats. DOM abundant, $L > V$ ( $V=20\%$ , $L=80\%$ ), vitrinite rare, liptinite sparse to abundant, chiefly detrital cutinite, greenish yellow. $R_{\text{max}}=0.25\%$ .
22409	548	Tutut	Claystone > siltstone > coal > coal abundant, $V > L > I$ ( $V=81\%$ , $L=15\%$ , $I=4\%$ ), vitrinite mostly detrovitrinite, resinous vitrinite

			common, brownish yellow, liptinite chiefly cutinite, bright yellow, resinite common, brown, sclerotinite and inerstodetrinite sparse, framboidal pyrite in vitrinite. DOM abundant, V > L (V=60%, L=40%), vitrinite rare to common, liptinite sparse to abundant, chiefly cutinite, greenish yellow. R <sub>y</sub> max= 0.29%.
22410	676	Tutut	Siltstone > claystone > coal. Coal common, V > L (V=99%, L=1%), vitrite, vitrinite mostly detrovitrinite, resinous vitrinite sparse, brown, inertodetrinite sparse, pyrite disseminated in vitrinite. DOM common, L > V (V=40%, L=60%), vitrinite rare to common, liptinite sparse to common, mostly liptodetrinite, yellow, acritarch in claystone, green. R <sub>y</sub> max= 0.32%.
22411	759	Tutut	Siltstone > sandstone. DOM common, V=L (V=50%, L=50%), vitrinite rare to common mostly detrovitrinite, oxidized vitrinite common, liptinite rare to common mostly liptodetrinite, bright yellow, acritarch in siltstone, greenish yellow. R <sub>y</sub> max= 0.32%.
22412	877	Tutut	Siltstone > coal > sandstone. Coal major, V > L (V=97%, L=3%), vitrite, vitrinite dominantly detrovitrinite, liptinite chiefly sporinite, brown, liptodetrinite common, yellow, telalginites sparse in vitrinite, yellow. DOM abundant, L > V (V=45%, L=55%), vitrinite rare to common, liptinite sparse to abundant, chiefly detrital sporinite, brown, bitumen in sandstone, yellow, cracks, R 0.003%. R <sub>y</sub> max= 0.30%.
22413	1079	Kueh	Sandstone > siltstone. DOM common, V > L (V=55%, L=45%), vitrinite rare to common, oxidized vitrinite common, black, liptinite sparse to common, chiefly liptodetrinite, yellow-brown, sporinite sparse, brown. R <sub>y</sub> max= 0.30%.
22414	1216	Kueh	Siltstone > sandstone. DOM abundant, L > V (V=43%, L=57%), vitrinite rare to common, liptinite rare to major, chiefly liptodetrinite, brownish yellow, cutinite rare, yellow, sporinite sparse, yellow, lamalginites in siltstone, green, bitumen in siltstone, yellow, cracks, R 0.03%. R <sub>y</sub> max= 0.32%.
22415	1475	Kueh	Siltstone > sandstone > limestone. DOM common, L > V (V=49%, L=51%), vitrinite rare to sparse, liptinite sparse to common, chiefly liptodetrinite and sporinite, yellow, oil drop in siltstone, green, bitumen in sandstone, yellow, cracks R 0.03%. R <sub>y</sub> max= 0.33%.
22416	1642	Kueh	Coal > siltstone > claystone. Coal major, V > L (V=70%, L=30%), vitrite > clarite, vitrinite mostly detrovitrinite, liptinite chiefly sporinite, yellow, suberinite common, exsudatinite in telovitrinite crack, common, greenish yellow, fluorinite sparse, cell

filling green, bitumen in porigelinite, yellow, cracks. DOM abundant, L > V (V=40%, L=60%), vitrinite rare to abundant, liptinite sparse to abundant, chiefly sporinite, yellow, bitumen in siltstone, green. R<sub>max</sub>= 0.34%.

22417                      1645                      Kueh                      Coal > siltstone > sandstone. Coal major, V > L > I (V=70%, L=20%, I=10%), vitrite > clarite, vitrinite mostly detrovitrinite, liptinite chiefly sporinite, dark brown-orange, suberinite common dark brown, liptodetrinite sparse, yellow, exsudatinite in telovitrinite cracks, common, greenish yellow, bitumen in detrovitrinite, dark yellow, cracks, cauliflower, R 0.03%, sclerotinite and semifusinite common. DOM abundant, V > L (V=80%, L=20%) vitrinite sparse to abundant, liptinite rare to common, mostly detrital sporinite, dark orange, bitumen in sandstone pore, yellow. R<sub>max</sub>= 0.32%.

22418                      1658                      Kueh                      Siltstone > coal > claystone. Coal major, V > L (V=93%, L=7%), vitrite, vitrinite mostly detrovitrinite, liptinite chiefly sporinite, brown-orange, suberinite sparse, yellow-brown, liptodetrinite, yellow, exsudatinite in telovitrinite cracks, common, yellow. Dom abundant, L > L (V=45%, L=55%), vitrinite rare to common, liptinite sparse to abundant, chiefly liptodetrinite, yellow, bitumen in siltstone, yellow. R<sub>max</sub>= 0.36%.

# PALUMAT

22395                      131                      Tutut                      Siltstone > claystone > sandstone > limestone. DOM abundant, L > V (V=33%, L=67%), vitrinite rare to common, liptinite sparse to abundant mostly liptodetrinite and bitumen, liptodetrinite, yellow, bitumen in sandstone and limestone, dark yellow, cracks, R 0.02%. R<sub>max</sub>= 0.15%.

22396                      204                      Tutut                      Siltstone > sandstone > claystone > coal. Coal abundant, V > L > I (V=82%, L=17%, I=1%), vitrite > clarite, vitrinite mostly detrovitrinite, resinous vitrinite common, brown, liptodetrinite chiefly thick wall cutinite, greenish yellow, resinite common, brown, liptodetrinite sparse, yellow, framboidal pyrite common in vitrinite cracks inertodetrinite sparse. DOM common, V > L (V=87%, L=13%) vitrinite rare to abundant, chiefly cutinite, greenish yellow. R<sub>max</sub>= 0.18.

22397                      259                      Tutut                      Coal > siltstone > sandstone > limestone. Coal major, V > L > V (V=73%, V=24%, I=3%), vitrite, vitrinite dominated by detrovitrinite, resinous vitrinite abundant, brownish yellow, liptinite chiefly cutinite, thick wall

Cont'd Appendix 3

			greenish yellow, liptodetrinite common, yellow, sclerotinite rare, framboidal pyrite in vitrinite crack. DOM abundant, L > V (V=16%, L=84%), vitrinite rare-abundant, liptinitite sparse-major, chiefly detrital cutinite, greenish yellow. R <sub>v</sub> max= 0.22%.
22398	313	Tutut	Claystone > coal > siltstone > sandstone. Coal major, V > I > L (V=86%, L=5%, I=9%), vitrite > clarite, vitrinite mostly detrovitrinite, resinous vitrinite abundant, brownish yellow, liptinitite chiefly thick wall cutinite, greenish yellow, suberinite sparse, yellow, spore rare, dull brown, framboidal pyrite in vitrinite cleats. DOM abundant, L > V (V=32%, L=70%), vitrinite rare to abundant, liptinitite sparse to abundant, chiefly cutinite, greenish yellow, fluorinite sparse, green. R <sub>v</sub> max= 0.18%.
22399	414	Tutut	Siltstone > claystone > sandstone > coal. Coal abundant, V > L > I (V=81%, L=13%, I=6%), vitrite, vitrinite mostly detrovitrinite, resinous vitrinite common, brown, liptinitite chiefly cutinite and suberinite, greenish yellow, inertodetrinite common, framboidal pyrite in vitrinite cleats. DOM abundant, L > V (V=23%, L=77%), vitrinite rare to abundant, liptinitite rare to abundant, chiefly cutinite, greenish yellow, acritarch in siltstone, green. R <sub>v</sub> max= 0.21%.
22400	524	Tutut	Siltstone > sandstone > claystone. DOM common L > V (V=45%, L=55%), vitrinite rare to common, liptinitite rare to abundant, chiefly cutinite, greenish yellow. R <sub>v</sub> max= 0.22%.
22401	624	Tutut	Siltstone > sandstone > claystone > limestone. DOM common, L > V (V=31%, L=69%), vitrinite rare to sparse, liptinitite rare to common, chiefly cutinite, greenish yellow, pyrite disseminated in siltstone. R <sub>v</sub> max= 0.23%.
22402	679	Tutut	Siltstone > sandstone > coal. Coal abundant, V > L (V=75%, L=25%) vitrite, vitrinite mostly detrovitrinite, resinous vitrinite common, liptinitite chiefly cutinite, greenish yellow, resinite rare, brown. DOM sparse, L > V (V=5%, L=95%), vitrinite rare, liptinitite rare to sparse, chiefly detrital cutinite, yellow. R <sub>v</sub> max= 0.23%.
22403	734	Kueh	Limestone > siltstone. Dom rare, L > V (V=45%, L=55%), vitrinite rare, liptinitite rare, chiefly liptodetrinite, yellow, R <sub>v</sub> max= 0.23%.
22404	1063	Kueh	Limestone > siltstone. DOM common, L > V (V=13%, L=87%), vitrinite rare, liptinitite rare to common, chiefly cutinite, yellow, acritarch in siltstone, sparse, green. R <sub>v</sub> max= 0.26%.

APPENDIX 9. VITRINITE REFLECTANCE DATA OF OFFSHORE WELLS VITRINITE

WELL NAME: TEUNOM                      TOTAL DEPTH: 816.80 METRE

NO.	GM. NO	FORMATION	DEPTH (M)	N	R <sub>v</sub> max (%)		
					Average	Range	STD
1.	22363	Tutut	124	5	0.23	0.19-0.23	0.04
2.	22364	Tutut	158	25	0.28	0.25-0.34	0.03
3.	22365	Tutut	185	31	0.28	0.20-0.36	0.04
4.	22366	Tutut	204	15	0.29	0.24-0.36	0.03
5.	22367	Tutut	249	32	0.28	0.22-0.32	0.04
6.	22368	Tutut	295	14	0.26	0.20-0.31	0.04
7.	22369	Kueh	313	14	0.27	0.22-0.32	0.03
8.	22370	Kueh	414	3	0.30	0.30-0.31	0.00
9.	22371	Kueh	478	20	0.34	0.21-0.38	0.05
10.	22372	Kueh	560	3	0.34	0.30-0.40	0.05
11.	22373	Kueh	670	3	0.37	0.31-0.40	0.08
12.	22374	Kueh	807	3	0.40	0.39-0.41	0.01

WELL NAME: BUBON                      TOTAL DEPTH: 1674.26 METRE

NO.	GM. NO	FORMATION	DEPTH (M)	N	R <sub>v</sub> max (%)		
					Average	Range	STD
1.	22451	Tutut	192	10	0.22	0.12-0.29	0.06
2.	22452	Tutut	216	54	0.28	0.20-0.35	0.05
3.	22453	Tutut	262	60	0.29	0.22-0.52	0.06
4.	22454	Tutut	307	100	0.28	0.17-0.38	0.04
5.	22455	Tutut	345	45	0.26	0.20-0.36	0.04
6.	22456	Tutut	381	4	0.27	0.20-0.34	0.03
7.	22457	Tutut	445	10	0.29	0.25-0.34	0.03
8.	22458	Tutut	591	3	0.31	0.29-0.37	0.05
9.	22459	Kueh	637	6	0.34	0.29-0.39	0.04
10.	22460	Kueh	701	50	0.34	0.25-0.42	0.04
11.	22461	Kueh	737	30	0.33	0.27-0.44	0.04
12.	22462	Kueh	801	10	0.34	0.30-0.41	0.03
13.	22463	Kueh	874	20	0.32	0.24-0.45	0.06
14.	22464	Kueh	920	40	0.37	0.30-0.44	0.04
15.	22465	Kueh	957	60	0.37	0.29-0.37	0.03
16.	22466	Kueh	1011	22	0.35	0.30-0.47	0.06
17.	22467	Kueh	1121	25	0.40	0.35-0.45	0.03
18.	22468	Kueh	1167	50	0.40	0.35-0.45	0.05
19.	22469	Kueh	1176	60	0.40	0.36-0.46	0.06
20.	22470	Kueh	1240	5	0.40	0.40-0.45	0.02
21.	22471	Kueh	1341	45	0.41	0.30-0.50	0.05
22.	22472	Kueh	1539	6	0.41	0.40-0.42	0.05
23.	22473	Kueh	1655	9	0.42	0.39-0.44	0.02

WELL NAME: KEUDAPASI                      TOTAL DEPTH: 1219.20 METRE

NO.	GM. NO	FORMATION	DEPTH (M)	N	R <sub>v</sub> max %		
					Average	Range	STD
1.	22383	Tutut	112	4	0.23	0.18-0.32	0.06
2.	22384	Tutut	149	14	0.23	0.20-0.31	0.03



Cont'd Keudapasi

3.	22385	Tutut	185	7	0.22	0.16-0.28	0.04
4.	22386	Tutut	213	19	0.24	0.16-0.39	0.06
5.	22387	Tutut	289	18	0.27	0.18-0.36	0.06
6.	22388	Tutut	350	13	0.30	0.20-0.45	0.08
7.	22389	Tutut	405	6	0.28	0.24-0.37	0.05
8.	22390	Tutut	505	11	0.32	0.28-0.43	0.05
9.	22391	Tutut	542	14	0.34	0.18-0.54	0.06
10.	22392	Kueh	661	19	0.33	0.20-0.48	0.02
11.	22393	Kueh	762	21	0.34	0.20-0.49	0.04
12.	22394	Kueh	862	8	0.34	0.19-0.50	0.05
13.	22394a	Kueh	981	15	0.35	0.20-0.48	0.05

WELL NAME: TUBA

TOTAL DEPTH: 2625.85 METRE

NO.	GM. NO	FORMATION	DEPTH (M)	N	R <sub>v</sub> max %		
					Average	Range	STD
1.	22375	Tutut	131	5	0.21	0.15-0.25	0.04
2.	22376	Tutut	201	5	0.21	0.16-0.28	0.05
3.	22377	Tutut	356	10	0.24	0.18-0.35	0.06
4.	22378	Tutut	466	16	0.28	0.16-0.46	0.08
5.	22379	Tutut	749	15	0.35	0.23-0.50	0.08
6.	22380	Kueh	923	27	0.34	0.24-0.51	0.04
7.	22381	Kueh	1069	21	0.33	0.25-0.45	0.07
8.	22382	Kueh	1207	16	0.35	0.29-0.42	0.04
9.	23259	Kueh	1307	21	0.36	0.27-0.58	0.05
10.	23260	Kueh	1411	23	0.36	0.28-0.55	0.04
11.	23261	Kueh	1472	20	0.37	0.29-0.50	0.04
12.	23262	Kueh	1600	37	0.39	0.25-0.56	0.04
13.	23263	Kueh	1691	21	0.40	0.28-0.45	0.04
14.	23264	Kueh	1783	28	0.40	0.29-0.50	0.05
15.	23265	Kueh	1956	29	0.41	0.27-0.55	0.05
16.	23266	Kueh	2158	12	0.42	0.37-0.44	0.05
17.	23267	Tangla	2322	14	0.43	0.33-0.56	0.05
18.	23268	Tangla	2459	11	0.41	0.30-0.34	0.05
19.	23269	Tangla	2578	25	0.52	0.43-0.64	0.04
20.	23270	Tangla	2618	21	0.54	0.48-0.61	0.05

WELL NAME: MEULABOH

TOTAL DEPTH: 3073.07 METRE

NO.	GM. NO	FORMATION	DEPTH (M)	N	R <sub>v</sub> max %		
					Average	Range	STD
1.	22344	Tutut	143	53	0.20	0.20-0.55	0.08
2.	22345	Tutut	179	30	0.20	0.28-0.53	0.08
3.	22346	Tutut	234	51	0.21	0.16-0.55	0.08
4.	22347	Tutut	252	22	0.26	0.20-0.35	0.04
5.	22348	Tutut	457	34	0.33	0.20-0.65	0.10
6.	22349	Tutut	621	35	0.33	0.20-0.64	0.13
7.	22350	Tutut	768	16	0.27	0.21-0.32	0.04
8.	23251	Tutut	917	20	0.30	0.27-0.58	0.09
9.	23252	Kueh	1100	25	0.32	0.28-0.59	0.12
10.	22353	Kueh	1222	16	0.37	0.27-0.58	0.07
11.	23254	Kueh	1368	19	0.37	0.26-0.59	0.08
12.	23255	Kueh	1527	30	0.38	0.29-0.55	0.01
13.	23256	Kueh	1673	37	0.39	0.25-0.57	0.02
14.	22357	Kueh	1825	42	0.40	0.29-0.65	0.03

Cont't Meulaboh

15.	22358	Kueh	1898	10	0.38	0.29-0.45	0.04
16.	22359	Kueh	2209	40	0.40	0.30-0.53	0.04
17.	22360	Kueh	2310	20	0.43	0.30-0.57	0.01
18.	22361	Tangla	2438	11	0.40	0.39-0.65	0.10
19.	22362	Tangla	2484	10	0.40	0.37-0.42	0.04
20.	22363	Tangla	2511	12	0.42	0.37-0.45	0.04
21.	22364	Tangla	2538	50	0.43	0.33-0.45	0.04
22.	22365	Tangla	393	10	0.20	0.30-0.48	0.04
23.	22366	Tangla	2502	41	0.47	0.30-0.51	0.04
24.	22367	Tangla	2529	30	0.44	0.39-0.45	0.03
25.	22474	Tangla	2557	40	0.51	0.42-0.65	0.05
26.	22475	Tangla	2639	20	0.54	0.48-0.62	0.05
27.	22476	Tangla	2804	25	0.53	0.48-0.71	0.05

WELL NAME: TRIPA

TOTAL DEPTH: 2075.55 METRE

NO.	GM. NO	FORMATION	DEPTH (M)	N	R <sub>v</sub> max (%)		
					Average	Range	STD
1.	22419	Tutut	118	33	0.23	0.19-0.29	0.04
2.	22420	Tutut	155	40	0.24	0.17-0.32	0.04
3.	22421	Tutut	176	12	0.27	0.21-0.41	0.06
4.	22422	Tutut	216	28	0.25	0.18-0.36	0.05
5.	22423	Tutut	292	26	0.25	0.19-0.33	0.04
6.	22424	Tutut	338	22	0.26	0.19-0.38	0.04
7.	22425	Tutut	402	20	0.29	0.20-0.37	0.07
8.	22426	Tutut	466	4	0.30	0.26-0.36	0.04
9.	22427	Tutut	521	5	0.28	0.24-0.31	0.02
10.	22428	Tutut	594	20	0.26	0.22-0.31	0.03
11.	22429	Tutut	658	40	0.29	0.23-0.42	0.04
12.	22430	Tutut	804	31	0.30	0.21-0.46	0.07
13.	22431	Tutut	1033	26	0.32	0.22-0.41	0.06
14.	22432	Tutut	1115	30	0.28	0.22-0.41	0.06
15.	22433	Kueh	1197	30	0.31	0.24-0.42	0.06
16.	22434	Kueh	1289	20	0.31	0.23-0.40	0.05
17.	22435	Kueh	1499	21	0.31	0.23-0.43	0.06
18.	22436	Kueh	1572	28	0.34	0.25-0.45	0.06
19.	22437	Kueh	1581	9	0.31	0.28-0.36	0.03
20.	22438	Kueh	1591	30	0.34	0.26-0.46	0.04
21.	22439	Kueh	1600	30	0.31	0.25-0.36	0.04
22.	22440	Kueh	1609	20	0.31	0.22-0.40	0.05
23.	22441	Kueh	1645	12	0.31	0.25-0.36	0.04
24.	22442	Kueh	1682	16	0.32	0.26-0.38	0.04
25.	22443	Kueh	1746	25	0.32	0.26-0.45	0.05
26.	22444	Kueh	1783	30	0.31	0.24-0.36	0.04
27.	22445	Kueh	1792	25	0.33	0.25-0.46	0.05
28.	22446	Kueh	1819	20	0.31	0.23-0.36	0.05
29.	22447	Kueh	1901	18	0.33	0.24-0.41	0.05
30.	22448	Kueh	2048	6	0.36	0.24-0.44	0.07
31.	22449	Kueh	2057	12	0.37	0.30-0.47	0.06
32.	22450	Kueh	2066	10	0.34	0.29-0.45	0.05

WELL NAME: MEULABOH EAST

TOTAL DEPTH: 1660.55 METRE

NO.	GM.NO	FORMATION	DEPTH (M)	N	R <sub>v</sub> max %		
					Average	Range	STD
1.	22405	Tutut	128	30	0.20	0.13-0.29	0.06
2.	22406	Tutut	274	26	0.21	0.13-0.28	0.10

Cont'd Meulaboh East

3.	22407	Tutut	420	22	0.25	0.14-0.35	0.07
4.	22408	Tutut	493	18	0.25	0.19-0.38	0.04
5.	22409	Tutut	548	11	0.29	0.24-0.35	0.13
6.	22410	Tutut	676	20	0.32	0.22-0.45	0.09
7.	22411	Tutut	759	25	0.32	0.23-0.40	0.10
8.	22412	Tutut	877	25	0.30	0.25-0.45	0.04
9.	22413	Kueh	1079	3	0.30	0.25-0.42	0.11
10.	22414	Kueh	1216	20	0.32	0.26-0.45	0.06
11.	22415	Kueh	1475	8	0.33	0.30-0.42	0.04
12.	22416	Kueh	1642	45	0.34	0.25-0.47	0.05
13.	22417	Kueh	1645	32	0.39	0.35-0.44	0.02
14.	22418	Kueh	1658	30	0.36	0.32-0.52	0.09

WELL NAME: PALUMAT

TOTAL DEPTH: 1071.35 METRE

NO.	GM. NO	FORMATION	DEPTH (M)	N	R <sub>v</sub> max (%)		
					Average	Range	STD
1.	22395	Tutut	131	7	0.15	0.11-0.25	0.05
2.	22396	Tutut	204	10	0.18	0.14-0.23	0.02
3.	22397	Tutut	259	27	0.22	0.16-0.27	0.03
4.	22398	Tutut	313	22	0.18	0.14-0.27	0.05
5.	22399	Tutut	414	21	0.21	0.16-0.31	0.04
6.	22400	Tutut	524	8	0.22	0.14-0.30	0.06
7.	22401	Tutut	624	13	0.23	0.18-0.33	0.04
8.	22402	Tutut	679	12	0.23	0.18-0.29	0.04
9.	22403	Kueh	734	3	0.23	0.23-0.24	0.00
10.	22404	Kueh	1063	2	0.26	0.25-0.30	0.00

APPENDIX 10. REFLECTANCE DATA OF PLIOCENE COAL FROM ONSHORE WELLS

WELL NAME: M-1		TOTAL DEPTH: 250.70 M					
SAMPLE NO.	DEPTH (m)	FORMATION	LITHOLOGY	N	REFLECTANCE (%)		
					Average	Range	STD
23319	3.00	TUTUT	COAL	50	0.27	0.21 - 0.28	0.03
23338	41.00	TUTUT	COAL	50	0.27	0.21 - 0.28	0.02
23342	76.00	TUTUT	COAL	50	0.29	0.20 - 0.30	0.01
23351	81.00	TUTUT	COAL	50	0.31	0.24 - 0.32	0.03
23355	94.00	TUTUT	COAL	50	0.31	0.25 - 0.31	0.04
23361	103.00	TUTUT	COAL	50	0.32	0.26 - 0.33	0.03
23376	115.00	TUTUT	COAL	50	0.30	0.25 - 0.32	0.04
23382	125.00	TUTUT	COAL	50	0.30	0.28 - 0.31	0.02
23389	140.00	TUTUT	COAL	50	0.31	0.29 - 0.32	0.01
23393	153.00	TUTUT	COAL	50	0.30	0.27 - 0.31	0.01
23397	157.00	TUTUT	COAL	50	0.30	0.29 - 0.32	0.01
23402	173.00	TUTUT	COAL	50	0.29	0.28 - 0.30	0.02
23406	199.00	TUTUT	COAL	50	0.31	0.29 - 0.32	0.02
23411	203.00	TUTUT	COAL	50	0.31	0.27 - 0.33	0.04
23416	228.00	TUTUT	COAL	50	0.31	0.28 - 0.32	0.03
23420	236.00	TUTUT	COAL	50	0.32	0.20 - 0.33	0.04

WELL NAME: M-2		TOTAL DEPTH: 250.70 M					
SAMPLE NO.	DEPTH (m)	FORMATION	LITHOLOGY	N	REFLECTANCE (%)		
					Average	Range	STD
23427	21.00	TUTUT	COAL	50	0.23	0.19 - 0.24	0.04
23452	38.00	TUTUT	COAL	50	0.23	0.20 - 0.24	0.03
23464	73.00	TUTUT	COAL	50	0.24	0.22 - 0.25	0.04
23467	105.00	TUTUT	COAL	50	0.24	0.22 - 0.25	0.04
23474	112.00	TUTUT	COAL	50	0.23	0.20 - 0.24	0.01
23477	131.00	TUTUT	COAL	50	0.25	0.23 - 0.27	0.02
23487	162.00	TUTUT	COAL	50	0.28	0.26 - 0.30	0.05
23496	171.00	TUTUT	COAL	50	0.29	0.27 - 0.31	0.04
23493	227.00	TUTUT	COAL	50	0.30	0.28 - 0.32	0.03

WELL NAME: M-3		TOTAL DEPTH: 148.70 M					
SAMPLE NO.	DEPTH (m)	FORMATION	LITHOLOGY	N	REFLECTANCE (%)		
					Average	Range	STD
21985	25.00	TUTUT	COAL	50	0.32	0.30 - 0.33	0.01
21988	68.00	TUTUT	COAL	50	0.32	0.31 - 0.33	0.01
21989	107.00	TUTUT	COAL	50	0.34	0.30 - 0.35	0.02
21990	111.00	TUTUT	COAL	50	0.36	0.35 - 0.37	0.03

WELL NAME: M-4		TOTAL DEPTH: 205.75 M					
SAMPLE NO.	DEPTH ( m )	FORMATION	LITHOLOGY	N	REFLECTANCE (%)		
					Average	Range	STD
21991	190.00 - 190.70	TUTUT	COAL	50	0.31	0.29-0.33	0.02

Cont'd M-4

21992	191.00 - 194.40	TUTUT	COAL	50	0.31	0.29-0.34	0.02
21993	194.00 - 195.20	TUTUT	COAL	50	0.32	0.30-0.33	

WELL NAME: M-10                      TOTAL DEPTH:

SAMPLE NO.	DEPTH ( m )	FORMATION	LITHOLOGY	N	REFLECTANE (%)		
					Average	Range	STD
22034	25	TUTUT	COAL	50	0.30	0.29-0.31	0.02
22035	43	TUTUT	COAL	50	0.32	0.30-0.34	0.03
22036	77	TUTUT	COAL	50	0.31	0.30-0.35	0.04
22037	102	TUTUT	COAL	50	0.34	0.32-0.35	0.03
22038	114	TUTUT	COAL	50	0.33	0.31-0.35	0.02

WELL NAME: M-13                      TOTAL DEPTH: 235.00 M

SAMPLE NO.	DEPTH (m)	FORMATION	LITHOLOGY	N	REFLECTANCE (%)		
					Average	Range	STD
22844	20	TUTUT	COAL	50	0.29	0.28 - 0.30	0.03
22845	38	TUTUT	COAL	50	0.34	0.33 - 0.35	0.03
22846	64	TUTUT	COAL	50	0.30	0.29 - 0.31	0.02
22847	79	TUTUT	COAL	50	0.38	0.37 - 0.39	0.03
22032	101	TUTUT	COAL	50	0.39	0.38 - 0.40	0.04

WELL NAME: M-15                      TOTAL DEPTH: 249.00 M

SAMPLE NO.	DEPTH (m)	FORMATION	LITHOLOGY	N	REFLECTANCE (%)		
					Average	Range	STD
22033	27	TUTUT	COAL	50	0.29	0.28 - 0.30	0.03
22034	44	TUTUT	COAL	50	0.29	0.28 - 0.31	0.03
22029	48	TUTUT	COAL	50	0.30	0.29 - 0.32	0.02
21984	71	TUTUT	COAL	50	0.38	0.37 - 0.39	0.03
21983	107	TUTUT	COAL	50	0.39	0.38 - 0.40	0.04

WELL NAME: M-18                      TOTAL DEPTH: 235.00 M

SAMPLE NO.	DEPTH (m)	FORMATION	LITHOLOGY	N	REFLECTANCE (%)		
					Average	Range	STD
22044	25	TUTUT	COAL	50	0.29	0.28 - 0.30	0.03
22045	44	TUTUT	COAL	50	0.30	0.29 - 0.31	0.03
22046	62	TUTUT	COAL	50	0.37	0.36 - 0.38	0.04
22047	107	TUTUT	COAL	50	0.39	0.38 - 0.40	0.03

WELL NAME: M-21                      TOTAL DEPTH:

SAMPLE NO.	DEPTH (m)	FORMATION	LITHOLOGY	N	REFLECTANCE (%)		
					Average	Range	STD
22840	30	TUTUT	COAL	50	0.32	0.31 - 0.33	0.03
22841	87	TUTUT	COAL	50	0.35	0.34 - 0.36	0.04

WELL NAME: M-22                      TOTAL DEPTH: 250.00 M

SAMPLE NO.	DEPTH (m)	FORMATION	LITHOLOGY	N	REFLECTANCE (%)		
					Average	Range	STD
22842	44	TUTUT	COAL	50	0.35	0.34 - 0.36	0.03
22843	109	TUTUT	COAL	50	0.37	0.36 - 0.38	0.04

WELL NAME: M-11                      TOTAL DEPTH: 250.00 M

SAMPLE NO.	DEPTH (m)	FORMATION	LITHOLOGY	N	REFLECTANCE ( % )		
					Average	Range	STD
22848	37	TUTUT	COAL	50	0.32	0.31 - 0.33	0.03
23307	79	TUTUT	COAL	50	0.33	0.32 - 0.34	0.04
22849	105	TUTUT	COAL	50	0.35	0.34 - 0.36	0.04
23308	109	TUTUT	COAL	50	0.34	0.33 - 0.35	0.03
23310	114	TUTUT	COAL	50	0.33	0.32 - 0.34	0.03
22850	142	TUTUT	COAL	50	0.32	0.30 - 0.33	0.03

WELL NAME: M-12                      TOTAL DEPTH: 250.00 M

SAMPLE NO.	DEPTH (m)	FORMATION	LITHOLOGY	N	REFLECTANCE (%)		
					Average	Range	STD
22851	41	TUTUT	COAL	50	0.33	0.32 - 0.34	0.03
22852	60	TUTUT	COAL	50	0.34	0.33 - 0.35	0.03

Appendix 11. Rock-Eval and Vitrinite Reflectance Data of Teunom Well

Sample	GM No	Depth (m)	Litho- logy	Form- ation	Tmax	S1	S2	S3	P1	S2/S3	PC	TGc	R1	Rmax (%)
TN2	22364	158.50	Coaly shale	Tutut	392.00	7.71	25.68	38.30	0.23	0.67	2.78	23.70	108.00	0.28
TN4	22366	249.10	Shale	Tutut	406.00	0.33	0.66	0.57	0.34	1.16	0.08	0.79	84.00	0.26
TN5	22367	295.65	Shale	Tutut	390.00	0.20	0.39	0.17	0.34	2.29	0.04	0.61	64.00	0.27
TN7	22369	313.90	Shale	Kueh	402.00	0.85	1.42	0.86	0.38	1.65	0.18	1.28	111.00	0.34
TN8	22370	478.50	Shale	Kueh	394.00	0.74	0.82	0.67	0.47	1.22	0.13	0.90	91.00	0.34

Appendix II. Rock Eval and Vitrinite Reflectance Data of Buoon Well

Sample	GM No	Depth (m)	Litho- logy	Form- ation	Tmax	S1	S2	S3	FI	S2/S3	PC	TOC	HI	OI	R <sub>max</sub> (%)
BB2	22352	225.50	Coal	Tutut	403.00	13.97	65.49	72.84	0.18	0.90	6.62	48.60	1.35	150.00	0.22
BB6	22456	581.00	Shale	Tutut	339.00	0.13	0.05	0	0.72	0	0.01	0.01	50.00	0	0.27
BB10	22460	701.00	Shale	Kueh	299.00	0.16	0.05	0	0.80	0	0.01	0.16	31.00	0	0.34
BB11	22461	737.60	Carb shale	Kueh	384.00	6.34	31.73	25.32	0.17	1.25	3.17	17.50	181.00	145.00	0.33
BB15	22465	957.10	Coal	Kueh	413.00	9.17	82.40	56.70	0.10	1.45	7.63	45.80	176.00	121.00	0.39
BB19	22469	1176.45	Coal	Kueh	417.00	9.60	96.26	54.53	0.09	1.77	8.82	51.50	187.00	106.00	0.40
BB24	22470	1240.50	Shale	Kueh	421.00	0.05	0.82	1.44	0.06	0.57	0.07	1.95	42.00	74.00	0.41
BB25	22471	1341.10	Shale	Kueh	426.00	0.04	0.84	3.79	0.05	0.25	0.07	2.20	38.00	154.00	0.42





Appendix 11. Rock-Eval and Vitrinite Reflectance Data of Meulaboh East Well

Sample	GM No	Depth (m)	Litho- logy	Form- ation	Tmax	S1	S2	S3	PI	S2/S3	PC	TGC	H1	DI	R.m.a: (%)
ME2	22405	128.00	Shale	Tutut	382.00	0.38	0.66	0.36	0.37	1.83	0.08	0.89	74.00	40.00	0.21
ME4	22406	249.10	Shale	Tutut	406.00	0.33	0.66	0.57	0.34	1.16	0.08	0.79	84.00	72.00	0.26
ME5	22409	548.60	Shale	Tutut	385.00	0.19	0.20	0.03	0.50	6.67	0.03	0.38	53.00	8.00	0.29
ME8	22412	877.80	Shale	Tutut	429.00	0.07	0.45	5.39	0.13	0.08	0.04	2.37	19.00	277.00	0.30
ME10	22414	1216.15	Shale	Kueh	426.00	0.01	0.17	2.02	0.06	0.08	0.01	1.66	10.00	122.00	0.32
ME13	22417	1645.90	Coal	Kueh	407.00	15.12	105.25	58.70	0.13	1.79	10.03	52.50	200.00	112.00	0.39

Appendix 11. Rock-Eval and Vitrinite Reflectance Data of Neulaboh Well

Sample	GR No	Depth (m)	Litho- logy	Form- ation	T <sub>max</sub>	S1	S2	S3	PI	S2/S3	FC	IOC	HI	OI	R <sub>max</sub> (%)
M4	22347	252.95	Silt	Tutut	394.00	0.20	0.35	0.28	0.37	1.25	0.04	0.62	56.00	45.00	0.22
M5	22365	393.20	Shale	Tutut	400.00	0.50	0.81	1.55	0.38	0.52	0.10	1.21	61.00	128.00	0.23
M7	22350	768.10	Shale	Tutut	389.60	0.44	0.53	0.90	0.46	0.59	0.08	1.05	50.00	86.00	0.20
M11	23255	1527.00	Shale	Kueh	420.00	0.33	0.61	1.01	0.35	0.60	0.07	1.19	51.00	85.00	0.04
M12	23256	1673.35	Shale	Kueh	420.00	0.19	0.60	1.41	0.24	0.43	0.60	1.33	45.00	106.00	0.41
M15	23257	1825.75	Shale	Kueh	417.00	0.38	1.52	1.20	0.20	1.27	0.16	1.56	101.00	77.00	0.42
M16	22360	2310.40	Shale	Tangla	420.00	0.36	2.12	1.83	0.15	1.16	0.20	2.68	79.00	68.00	0.43
M19	22367	2529.80	Coal	Tangla	424.00	4.46	77.13	42.66	0.05	1.81	6.79	40.40	191.00	106.00	0.44
M20	22474	2538.90	Shale	Tangla	425.00	0.47	3.45	2.60	0.12	1.33	0.32	3.22	106.00	80.00	0.44
M21	22475	2639.60	Carb shale	Tangla	456.00	1.48	24.65	4.04	0.06	6.10	2.17	10.22	241.00	40.00	0.54

Appendix II. Rock Eval and Vitrinite Reflectance Data of Tripa Well

Sample	GM No	Depth (m)	Litho- logy	Form- ation	Tmax	SI	S2	S3	PI	S2/S3	PC	TOC	HI	GI	R <sub>max</sub> (%)
TR2	22420	155.45	Shale	Tutut	403.00	1.24	0.47	1.23	0.73	0.38	0.14	1.35	35.00	91.00	0.24
TR3	22421	176.80	Shale	Tutut	403.00	0.17	0.14	0.05	0.57	2.80	0.02	0.58	24.00	9.00	0.27
TR7	22423	292.60	Shale	Tutut	378.00	0.67	0.16	0.36	0.82	0.44	0.06	0.46	35.00	78.00	0.25
TR8	22426	466.30	Coal	Tutut	403.00	8.80	36.35	50.12	0.20	0.73	3.76	33.00	110.00	152.00	0.29
TR9	22428	594.35	Shale	Tutut	391.00	0.46	0.25	0.28	0.66	0.89	0.05	0.54	46.00	52.00	0.28
TR14	22430	804.65	Shale	Tutut	414.00	1.43	0.53	0.68	0.73	0.78	0.16	0.82	65.00	83.00	0.30
TR17	22433	1197.85	Shale	kueh	404.00	0.35	0.32	0.50	0.53	0.64	0.05	0.83	39.00	60.00	0.30
TR18	22435	1499.60	Shale	Kueh	412.00	0.72	0.66	0.59	0.52	1.12	0.11	0.96	69.00	61.00	0.31
TR23	22438	1591.00	Shale	Kueh	408.00	0.30	0.35	0.57	0.47	0.61	0.05	0.98	36.00	58.00	0.32
TR27	22441	1645.00	Shale	kueh	409.00	0.48	0.66	0.96	0.42	0.69	0.09	1.21	55.00	79.00	0.31
TR28	22442	1682.00	Shale	Kueh	410.00	0.26	0.48	0.63	0.35	0.76	0.06	1.04	46.00	61.00	0.32
TR32	22446	1819.65	Shale	Kueh	417.00	0.98	2.27	3.10	0.30	0.73	0.27	2.93	77.00	106.00	0.34
TR36	22448	2045.25	Coal	Kueh	420.00	8.14	44.56	52.59	0.15	0.85	4.39	34.40	130.00	153.00	0.37

Appendix II. Rock-Eval and Vitrinite Reflectance Data of Palumat Well

Sample	GM No	Depth (m)	Litho- logy	Form- ation	Tmax	S1	S2	S3	PI	S2/S3	PC	IUC	HI	OI	K <sub>max</sub> (%)
P1	22395	131.05	Silt	Tutut	398.00	0.12	0.24	0.42	0.33	0.57	0.03	0.34	71.00	124.00	0.15
P2	22396	204.20	Coaly shale	Tutut	375.00	2.62	7.43	45.00	0.26	0.17	0.83	20.50	36.00	220.00	0.18
P3	22397	259.05	Shale	Tutut	405.00	1.66	5.25	7.03	0.24	0.75	0.57	5.03	104.00	140.00	0.22
P4	22398	313.95	Shale	Tutut	376.00	0.50	1.04	2.21	0.32	0.47	0.12	1.92	54.00	115.00	0.21
P7	22401	624.25	Shale	Kueh	391.00	0.38	0.38	0.39	0.50	0.97	0.06	0.69	55.00	57.00	0.20
P8	22402	679.70	Shale	Kueh	399.00	0.40	0.68	1.10	0.37	0.68	0.09	1.05	65.00	95.00	0.23

APPENDIX 12  
PRODUCT-MOMENT MATRIX FOR ROCKEVAL AND MACERALS

SAMPLE	TMAX	S1	S2	S3	PI	TOC	HI	OI	RVm	TELO	DETRO	GELO	ALGIN	CUTIN	FLUOP
TMAX	*****	0.0467	0.6337	-0.6736	-0.6274	0.5606	0.5464	-0.8437	0.3260	0.2404	-0.1301	-0.2398	0.1813	-0.0576	-0.0756
S1	0.0467*****	0.3216	0.0804	0.2242	0.2650	0.3088	-0.1066	0.0177	-0.1372	0.1306	0.0411	-0.1541	-0.2577	-0.1262	
S2	0.6337	0.3216*****	-0.5809	-0.6523	0.7755	0.9269	-0.7813	0.5472	-0.0362	0.0971	-0.1414	-0.0317	-0.1513	-0.2242	
S3	-0.6736	0.0804	-0.5809*****	0.4209	-0.2952	-0.6242	0.2216	-0.6463	-0.2711	0.0471	0.3609	-0.4160	0.0737	-0.0292	
PI	-0.6274	0.2242	-0.6523	0.4209*****	-0.6926	-0.6305	0.7007	-0.5801	-0.0224	-0.0777	0.0758	0.1405	0.1500	0.2836	
TOC	0.5606	0.2650	0.7755	-0.2952	-0.6926*****	0.5538	-0.7094	0.5465	0.0370	0.0755	-0.1520	-0.1045	-0.1754	-0.2260	
HI	0.5464	0.3088	0.9269	-0.6242	-0.6305	0.5538*****	-0.7410	0.4649	-0.1375	0.1340	-0.0599	-0.0340	-0.0060	-0.2732	
OI	-0.8437	-0.1066	-0.7813	0.3216	0.7007	-0.7410*****	-0.7603	-0.1457	0.0460	0.0971	0.0932	-0.0590	-0.0854	-0.1510	
RVm	0.3260	0.0177	0.5472	-0.6463	-0.5801	0.4649	-0.7603*****	0.3792	-0.0202	-0.0219	-0.0016	-0.0006	-0.0294	-0.0365	
TELO	0.2404	-0.1372	-0.0362	-0.0224	0.0370	-0.1375	-0.1457	0.3792*****	-0.2896	-0.0300	0.1036	-0.1040	-0.0366		
DETRO	-0.1301	0.1306	0.0971	0.0471	-0.0777	0.0758	0.1340	0.0460	-0.0202	-0.2896*****	0.0300	-0.2894	-0.0574	-0.0162	
GELO	-0.2398	0.0411	-0.1414	0.3600	0.0758	-0.1520	-0.0599	0.2574	-0.0219	-0.0300	0.0932*****	-0.0590	-0.0854	-0.1510	
ALGIN	0.1813	-0.1541	-0.0317	-0.4160	0.1405	-0.1345	-0.0342	-0.2672	-0.0016	0.1006	-0.2294	-0.0590*****	0.1464	0.4546	
CUTIN	-0.0576	-0.2577	-0.1613	0.0737	0.1500	-0.1754	-0.2660	0.1150	-0.2010	-0.0406	-0.0574	-0.0954	0.1464*****	0.4703	
FLUOP	-0.0756	-0.1262	-0.2242	-0.0292	0.2896	-0.2260	-0.2732	0.0675	-0.2123	-0.0592	-0.0312	-0.1513	0.4546	0.4703*****	
RESIN	0.0777	0.1774	0.1106	0.0444	0.0296	0.0620	0.0850	-0.0524	-0.0729	-0.0975	-0.3231	-0.2676	0.1307	0.4038	0.1923
SPORE	0.0309	-0.0105	0.1675	-0.0793	-0.0335	-0.0097	0.2679	-0.0729	-0.0915	-0.3231	0.1195	-0.2043	0.1310	0.0413	0.0365
SUPER	-0.2372	-0.0274	-0.1893	0.3173	0.1181	-0.2027	-0.1232	0.2946	-0.2336	-0.2747	-0.1460	0.4840	-0.1963	-0.0512	-0.1072
LIPTO	-0.2936	0.0046	-0.1936	0.2550	0.1117	-0.2569	-0.0653	0.1914	-0.3337	-0.4393	-0.2031	0.2090	-0.0406	0.0366	0.1178
EXUDA	0.2975	0.4231	0.3625	-0.2692	-0.0690	0.1678	0.4047	-0.2861	0.1303	-0.0512	-0.1265	-0.0212	0.1632	-0.1811	-0.0528
INERT	0.2214	-0.0094	0.2340	-0.1714	-0.2966	0.2573	0.2239	-0.2957	0.2399	-0.1749	0.0221	-0.1632	0.0511	-0.1795	0.1073

SAMPLE	RESIN	SPORE	SUPER	LIPTO	EXUDA	INERT
TMAX	0.0777	0.0309	-0.2372	-0.2835	0.2975	0.2214
S1	0.1774	-0.0105	-0.0274	0.0943	0.4231	-0.0094
S2	0.1106	0.1675	-0.1893	-0.1936	0.3625	0.2340
S3	0.0444	-0.0793	0.3173	0.2550	-0.2692	-0.1714
PI	0.0296	-0.0335	0.1181	0.1117	-0.0690	-0.2966
TOC	0.0620	-0.0097	-0.2027	-0.2569	0.1678	0.2573
HI	0.0850	0.2679	-0.1232	-0.0653	0.4047	0.2239
OI	-0.0524	-0.0729	0.2946	0.1914	-0.2861	-0.2957
RVm	-0.1702	-0.0815	-0.2336	-0.3337	0.1303	0.2399
TELO	-0.0975	-0.3231	-0.2747	-0.4393	-0.0512	-0.1749
DETRO	-0.6301	0.1195	-0.1460	-0.2031	-0.1265	0.0221
GELO	-0.2676	-0.2043	0.4840	0.2090	-0.0212	-0.1632
ALGIN	0.1307	0.1910	-0.1962	-0.0406	0.1632	0.0511
CUTIN	0.4038	0.0413	-0.0512	0.0366	-0.1811	-0.1795
FLUOP	0.1923	0.0366	-0.1072	0.1178	-0.0528	0.1073
RESIN*****	0.1517	-0.1166	0.2986	0.4582	-0.0354	
SPORE	0.1817*****	-0.0942	0.1251	0.0412	-0.0046	
SUPER	-0.1186	-0.0942*****	0.0323	-0.1520	-0.1402	
LIPTO	0.2986	0.1251	0.0323*****	0.0991	-0.0320	
EXUDA	0.4582	0.0412	-0.1520	0.0991*****	0.0550	
INERT	-0.0354	-0.0046	-0.1402	-0.0620	0.0550*****	

APPENDIX 12  
PROBABILITY MATRIX FOR ROCKEVAL AND MACEPAIS

UPPER HALF OF MATRIX EQUALS PROBABILITY AT 95% CONFIDENCE LEVEL  
LOWER HALF OF MATRIX EQUALS PROBABILITY AT 99% CONFIDENCE LEVEL

SAMPLE	TMAX	S1	S2	S3	PI	TOC	HI	OI	RVW	TELO	DETRO	GELO	ALGIN	CUTIN	FLUOR
TMAX	*****	0.2841	0.2841	0.2841	0.2841	0.2841	0.2841	0.2841	0.2841	0.2841	0.2841	0.2841	0.2841	0.2841	0.2841
S1	0.3662*****	0.2841	0.2841	0.2841	0.2841	0.2841	0.2841	0.2841	0.2841	0.2841	0.2841	0.2841	0.2841	0.2841	0.2841
S2	0.3662	0.3662*****	0.2841	0.2841	0.2841	0.2841	0.2841	0.2841	0.2841	0.2841	0.2841	0.2841	0.2841	0.2841	0.2841
S3	0.3662	0.3662	0.3662*****	0.2841	0.2841	0.2841	0.2841	0.2841	0.2841	0.2841	0.2841	0.2841	0.2841	0.2841	0.2841
PI	0.3662	0.3662	0.3662	0.3662*****	0.2841	0.2841	0.2841	0.2841	0.2841	0.2841	0.2841	0.2841	0.2841	0.2841	0.2841
TOC	0.3662	0.3662	0.3662	0.3662	0.3662*****	0.2841	0.2841	0.2841	0.2841	0.2841	0.2841	0.2841	0.2841	0.2841	0.2841
HI	0.3662	0.3662	0.3662	0.3662	0.3662	0.3662*****	0.2841	0.2841	0.2841	0.2841	0.2841	0.2841	0.2841	0.2841	0.2841
OI	0.3662	0.3662	0.3662	0.3662	0.3662	0.3662	0.3662*****	0.2841	0.2841	0.2841	0.2841	0.2841	0.2841	0.2841	0.2841
RVW	0.3662	0.3662	0.3662	0.3662	0.3662	0.3662	0.3662	0.3662*****	0.2841	0.2841	0.2841	0.2841	0.2841	0.2841	0.2841
TELO	0.3662	0.3662	0.3662	0.3662	0.3662	0.3662	0.3662	0.3662	0.3662*****	0.2841	0.2841	0.2841	0.2841	0.2841	0.2841
DETRO	0.3662	0.3662	0.3662	0.3662	0.3662	0.3662	0.3662	0.3662	0.3662	0.3662*****	0.2841	0.2841	0.2841	0.2841	0.2841
GELO	0.3662	0.3662	0.3662	0.3662	0.3662	0.3662	0.3662	0.3662	0.3662	0.3662	0.3662*****	0.2841	0.2841	0.2841	0.2841
ALGIN	0.3662	0.3662	0.3662	0.3662	0.3662	0.3662	0.3662	0.3662	0.3662	0.3662	0.3662	0.3662*****	0.2841	0.2841	0.2841
CUTIN	0.3662	0.3662	0.3662	0.3662	0.3662	0.3662	0.3662	0.3662	0.3662	0.3662	0.3662	0.3662	0.3662*****	0.2841	0.2841
FLUOR	0.3662	0.3662	0.3662	0.3662	0.3662	0.3662	0.3662	0.3662	0.3662	0.3662	0.3662	0.3662	0.3662	0.3662*****	0.2841
RESIN	0.3662	0.3662	0.3662	0.3662	0.3662	0.3662	0.3662	0.3662	0.3662	0.3662	0.3662	0.3662	0.3662	0.3662	0.3662
SPORE	0.3662	0.3662	0.3662	0.3662	0.3662	0.3662	0.3662	0.3662	0.3662	0.3662	0.3662	0.3662	0.3662	0.3662	0.3662
SUPER	0.3662	0.3662	0.3662	0.3662	0.3662	0.3662	0.3662	0.3662	0.3662	0.3662	0.3662	0.3662	0.3662	0.3662	0.3662
LIPTO	0.3662	0.3662	0.3662	0.3662	0.3662	0.3662	0.3662	0.3662	0.3662	0.3662	0.3662	0.3662	0.3662	0.3662	0.3662
EXUDA	0.3662	0.3662	0.3662	0.3662	0.3662	0.3662	0.3662	0.3662	0.3662	0.3662	0.3662	0.3662	0.3662	0.3662	0.3662
INERT	0.3662	0.3662	0.3662	0.3662	0.3662	0.3662	0.3662	0.3662	0.3662	0.3662	0.3662	0.3662	0.3662	0.3662	0.3662

SAMPLE	RESIN	SPORE	SUPER	LIPTO	EXUDA	INERT
TMAX	0.2841	0.2841	0.2841	0.2841	0.2841	0.2841
S1	0.2841	0.2841	0.2841	0.2841	0.2841	0.2841
S2	0.2841	0.2841	0.2841	0.2841	0.2841	0.2841
S3	0.2841	0.2841	0.2841	0.2841	0.2841	0.2841
PI	0.2841	0.2841	0.2841	0.2841	0.2841	0.2841
TOC	0.2841	0.2841	0.2841	0.2841	0.2841	0.2841
HI	0.2841	0.2841	0.2841	0.2841	0.2841	0.2841
OI	0.2841	0.2841	0.2841	0.2841	0.2841	0.2841
RVW	0.2841	0.2841	0.2841	0.2841	0.2841	0.2841
TELO	0.2841	0.2841	0.2841	0.2841	0.2841	0.2841
DETRO	0.2841	0.2841	0.2841	0.2841	0.2841	0.2841
GELO	0.2841	0.2841	0.2841	0.2841	0.2841	0.2841
ALGIN	0.2841	0.2841	0.2841	0.2841	0.2841	0.2841
CUTIN	0.2841	0.2841	0.2841	0.2841	0.2841	0.2841
FLUOR	0.2841	0.2841	0.2841	0.2841	0.2841	0.2841
RESIN*****	0.2841	0.2841	0.2841	0.2841	0.2841	0.2841
SPORE	0.3662*****	0.2841	0.2841	0.2841	0.2841	0.2841
SUPER	0.3662	0.3662*****	0.2841	0.2841	0.2841	0.2841
LIPTO	0.3662	0.3662	0.3662*****	0.2841	0.2841	0.2841
EXUDA	0.3662	0.3662	0.3662	0.3662*****	0.2841	0.2841
INERT	0.3662	0.3662	0.3662	0.3662	0.3662*****	0.2841

## APPENDIX 12

COLUMNS 1 AND 2 - OBSERVATIONS COMBINED INTO CLUSTERS  
 COLUMN 3 - SIMILARITY LEVEL OF CLUSTERING

TMAX	PVM	0.62881
S2	HIT	0.62882
S3	OI	0.62168
GELO	SUBER	0.48336
CUTIN	FLUOR	0.47237
RESIN	EXUDA	0.46824
S2	TOC	0.66460
S3	PI	0.66084
ALGIN	CUTIN	0.60047
TMAX	S2	0.60079
S1	RESIN	0.60026
S3	GELO	0.20166
TMAX	INERT	0.23689
S3	LIPTO	0.14404
TMAX	S1	0.07262
ALGIN	SPORE	0.12243
S3	ALGIN	0.00804
TMAX	DETRO	-0.04159
TMAX	S3	-0.08175
TMAX	TELO	-0.21166



# APPENDIX 13

## PRODUCT-MOMENT MATRIX FOR PYROLYSIS GC AND COAL PETROLOGY

SAMPLE	TELO	DETRO	GELO	ALGIN	CUTIN	FLUOR	RESIN	SPORE	SUPER	LIPTO	EXUDA	INERT	Rmax	C1-C6	C6-14
TELO	*****	-0.1482	0.1064	-0.0007	-0.4039	-0.3163	-0.4594	-0.4945	0.1870	-0.5669	-0.2746	-0.2997	0.6135	-0.0725	0.0440
DETPO	-0.1482	*****	-0.3312	0.4132	-0.3346	0.1911	-0.4729	0.2082	-0.5709	-0.4557	0.1326	-0.1700	0.4060	-0.6490	0.7555
GELO	0.1064	-0.3312	*****	-0.2175	-0.1241	0.2469	-0.1303	-0.2359	0.5446	0.3010	-0.3483	0.1450	-0.4770	0.3330	-0.4317
ALGIN	-0.0007	0.4132	-0.2175	*****	-0.3092	0.0966	-0.2061	0.2197	-0.3046	-0.3236	0.0751	-0.0942	0.0047	-0.0411	0.1275
CUTIN	-0.4039	-0.3346	-0.1241	-0.3092	*****	0.2638	0.2359	0.1157	0.0753	0.1152	-0.4760	-0.1155	-0.3156	0.1556	-0.3159
FLUOR	-0.3163	0.1911	0.2469	0.0966	0.2638	*****	-0.0361	-0.2136	-0.0257	0.0524	-0.2743	-0.0434	-0.2603	0.2334	-0.2163
RESIN	-0.4594	-0.4729	-0.1303	-0.2061	0.2359	-0.0361	*****	0.0191	-0.0516	0.5720	0.4121	0.3739	-0.4699	0.3517	-0.2353
SPORE	-0.4945	0.2082	-0.2359	0.2197	0.1157	-0.2136	0.0191	*****	-0.0999	0.0314	0.0600	0.2359	-0.2016	0.1550	-0.1217
SUPER	0.1870	-0.5709	0.5446	-0.3046	0.0753	-0.0257	-0.0516	-0.0999	*****	0.2447	-0.2317	0.0723	-0.3556	0.3209	-0.5026
LIPTO	-0.5669	-0.4557	0.3010	-0.0942	0.1155	0.0524	0.5720	0.0314	0.2447	*****	0.3330	0.3446	-0.6418	0.3555	-0.2653
EXUDA	-0.2746	0.1326	-0.3483	0.0751	-0.4760	-0.2743	0.4121	0.0600	-0.2317	0.3330	*****	0.2800	-0.0031	-0.1103	0.2669
INERT	-0.2997	-0.1700	0.1450	-0.0942	-0.1155	-0.0434	0.3739	0.2359	0.0723	0.3446	0.2800	*****	-0.2446	0.1586	-0.1497
Rmax	0.6135	0.4060	-0.4770	0.0047	-0.3156	-0.2603	-0.4699	-0.2016	-0.3556	-0.6418	-0.0031	-0.2446	*****	-0.5324	0.5730
C1-C6	-0.0725	-0.6490	0.3330	-0.0411	0.1556	0.2334	0.3517	0.1550	0.3238	0.3556	-0.1103	0.1586	-0.5324	*****	-0.9455
C6-14	0.0440	0.7555	-0.4317	0.1275	-0.3159	-0.2163	-0.2353	-0.1217	-0.5026	-0.3555	0.2669	-0.1497	0.5730	-0.9455	*****
C15-	0.0924	0.4819	-0.2135	-0.1103	0.0122	-0.2214	-0.4164	-0.1630	-0.1356	-0.3162	-0.0439	-0.1501	0.4386	-0.9822	0.8011
CT-14	0.4293	0.3169	-0.2555	-0.1621	-0.0224	-0.2462	-0.2392	-0.4273	-0.1964	-0.5130	-0.0918	-0.2943	0.7193	-0.8262	0.7100
PHEN	-0.2544	-0.2444	0.3770	-0.2600	0.1212	0.2471	0.3357	-0.1445	0.1910	0.4197	0.0210	0.1476	-0.4314	0.1327	-0.2690
P106	-0.1090	-0.6560	0.6690	-0.2659	0.1524	0.3160	0.3239	-0.0343	0.4409	0.5414	-0.3066	0.1524	-0.6560	0.7305	-0.7397
AG103	-0.3310	-0.3165	0.3034	-0.3593	0.3769	0.0744	0.3478	0.4905	0.3159	0.4574	-0.1969	0.2905	-0.6922	0.5384	-0.3252

SAMPLE C15- CT-14 PHEN P106 AG103

TELO	0.0924	0.4293	-0.2544	-0.1090	-0.3310
DETRO	0.4819	0.3169	-0.2444	-0.6560	-0.3165
GELO	-0.2135	-0.2555	0.3770	0.6690	0.3034
ALGIN	-0.1103	-0.1621	-0.2600	-0.2659	-0.3593
CUTIN	0.0122	-0.0224	0.1212	0.1524	0.3769
FLUOR	-0.2214	-0.2462	0.2471	0.3160	0.0744
RESIN	-0.4164	-0.3392	0.2357	0.3239	0.3478
SPORE	-0.1630	-0.4273	-0.1445	-0.0343	0.4905
SUPER	-0.1356	-0.1964	0.1910	0.4409	0.3159
LIPTO	-0.3162	-0.5130	0.4197	0.5414	0.4574
EXUDA	-0.0439	-0.0918	0.0210	-0.3066	-0.1969
INERT	-0.1501	-0.2943	0.1476	0.1524	0.2905
Rmax	0.4386	0.7193	-0.4314	-0.6560	-0.6922
C1-C6	-0.9822	-0.8262	0.1327	0.7305	0.8354
C6-14	0.8011	0.7100	-0.2590	-0.7397	-0.3252
C15-	*****	0.6503	0.0349	-0.5966	-0.7657
CT-14	0.6503	*****	-0.1237	-0.6710	-0.6945
PHEN	0.0349	-0.1237	*****	0.6023	0.3413
P106	-0.5966	-0.6710	0.6023	*****	0.7336
AG103	-0.7657	-0.6945	0.3413	0.7336	*****

# APPENDIX 13

PROBABILITY MATRIX FOR PYROLYSIS GC AND COAL PETROLOGY  
UPPER HALF OF MATRIX EQUALS PROBABILITY AT 95% CONFIDENCE LEVEL  
LOWER HALF OF MATRIX EQUALS PROBABILITY AT 99% CONFIDENCE LEVEL

SAMPLE	TELO	DETRO	GELO	ALGIN	CUTIN	FLUOP	RESIN	SPORE	SUPER	LIPTO	EXUDA	INERT	Rmax	C1-C5	C6-14
TELO	*****	0.5306	0.5306	0.5306	0.5306	0.5306	0.5306	0.5306	0.5306	0.5306	0.5306	0.5306	0.5306	0.5306	0.5306
DETRO	0.6508*****	0.5306	0.5306	0.5306	0.5306	0.5306	0.5306	0.5306	0.5306	0.5306	0.5306	0.5306	0.5306	0.5306	0.5306
GELO	0.6508	0.6508*****	0.5306	0.5306	0.5306	0.5306	0.5306	0.5306	0.5306	0.5306	0.5306	0.5306	0.5306	0.5306	0.5306
ALGIN	0.6508	0.6508	0.6508*****	0.5306	0.5306	0.5306	0.5306	0.5306	0.5306	0.5306	0.5306	0.5306	0.5306	0.5306	0.5306
CUTIN	0.6508	0.6508	0.6508	0.6508*****	0.5306	0.5306	0.5306	0.5306	0.5306	0.5306	0.5306	0.5306	0.5306	0.5306	0.5306
FLUOP	0.6508	0.6508	0.6508	0.6508	0.6508*****	0.5306	0.5306	0.5306	0.5306	0.5306	0.5306	0.5306	0.5306	0.5306	0.5306
RESIN	0.6508	0.6508	0.6508	0.6508	0.6508	0.6508*****	0.5306	0.5306	0.5306	0.5306	0.5306	0.5306	0.5306	0.5306	0.5306
SPORE	0.6508	0.6508	0.6508	0.6508	0.6508	0.6508	0.6508*****	0.5306	0.5306	0.5306	0.5306	0.5306	0.5306	0.5306	0.5306
SUPER	0.6508	0.6508	0.6508	0.6508	0.6508	0.6508	0.6508	0.6508*****	0.5306	0.5306	0.5306	0.5306	0.5306	0.5306	0.5306
LIPTO	0.6508	0.6508	0.6508	0.6508	0.6508	0.6508	0.6508	0.6508	0.6508*****	0.5306	0.5306	0.5306	0.5306	0.5306	0.5306
EXUDA	0.6508	0.6508	0.6508	0.6508	0.6508	0.6508	0.6508	0.6508	0.6508	0.6508*****	0.5306	0.5306	0.5306	0.5306	0.5306
INERT	0.6508	0.6508	0.6508	0.6508	0.6508	0.6508	0.6508	0.6508	0.6508	0.6508	0.6508*****	0.5306	0.5306	0.5306	0.5306
Rmax	0.6508	0.6508	0.6508	0.6508	0.6508	0.6508	0.6508	0.6508	0.6508	0.6508	0.6508	0.6508*****	0.5306	0.5306	0.5306
C1-C5	0.6508	0.6508	0.6508	0.6508	0.6508	0.6508	0.6508	0.6508	0.6508	0.6508	0.6508	0.6508	0.6508*****	0.5306	0.5306
C6-14	0.6508	0.6508	0.6508	0.6508	0.6508	0.6508	0.6508	0.6508	0.6508	0.6508	0.6508	0.6508	0.6508	0.6508*****	0.5306
C15+	0.6508	0.6508	0.6508	0.6508	0.6508	0.6508	0.6508	0.6508	0.6508	0.6508	0.6508	0.6508	0.6508	0.6508	0.6508
C7+/A	0.6508	0.6508	0.6508	0.6508	0.6508	0.6508	0.6508	0.6508	0.6508	0.6508	0.6508	0.6508	0.6508	0.6508	0.6508
PHEN	0.6508	0.6508	0.6508	0.6508	0.6508	0.6508	0.6508	0.6508	0.6508	0.6508	0.6508	0.6508	0.6508	0.6508	0.6508
P/C6	0.6508	0.6508	0.6508	0.6508	0.6508	0.6508	0.6508	0.6508	0.6508	0.6508	0.6508	0.6508	0.6508	0.6508	0.6508
A3/C8	0.6508	0.6508	0.6508	0.6508	0.6508	0.6508	0.6508	0.6508	0.6508	0.6508	0.6508	0.6508	0.6508	0.6508	0.6508

SAMPLE	C15+	C7+/A	PHEN	P/C6	A3/C8
TELO	0.5306	0.5306	0.5306	0.5306	0.5306
DETRO	0.5306	0.5306	0.5306	0.5306	0.5306
GELO	0.5306	0.5306	0.5306	0.5306	0.5306
ALGIN	0.5306	0.5306	0.5306	0.5306	0.5306
CUTIN	0.5306	0.5306	0.5306	0.5306	0.5306
FLUOP	0.5306	0.5306	0.5306	0.5306	0.5306
RESIN	0.5306	0.5306	0.5306	0.5306	0.5306
SPORE	0.5306	0.5306	0.5306	0.5306	0.5306
SUPER	0.5306	0.5306	0.5306	0.5306	0.5306
LIPTO	0.5306	0.5306	0.5306	0.5306	0.5306
EXUDA	0.5306	0.5306	0.5306	0.5306	0.5306
INERT	0.5306	0.5306	0.5306	0.5306	0.5306
Rmax	0.5306	0.5306	0.5306	0.5306	0.5306
C1-C5	0.5306	0.5306	0.5306	0.5306	0.5306
C6-14	0.5306	0.5306	0.5306	0.5306	0.5306
C15+	*****	0.5306	0.5306	0.5306	0.5306
C7+/A	0.6508*****	0.5306	0.5306	0.5306	0.5306
PHEN	0.6508	0.6508*****	0.5306	0.5306	0.5306
P/C6	0.6508	0.6508	0.6508*****	0.5306	0.5306
A3/C8	0.6508	0.6508	0.6508	0.6508*****	0.5306

# APPENDIX 13

COLUMNS 1 AND 2 - OBSERVATIONS COMBINED INTO CLUSTERS

COLUMN 3 - SIMILARITY LEVEL OF CLUSTERING

PESIN	LIPTO	0.57205
C1-C5	43/C8	0.33636
C15+	37+/A	0.35085
TELO	Rmax	0.51346
DETPO	C6-14	0.75354
C1-C5	9/C3	0.73506
DETPO	C15+	0.57220
GELO	SUBER	0.54480
CUTIN	FLUOR	0.26362
TELO	DETPO	0.31915
GELO	C1-C5	0.43771
PESIN	EXUDA	0.37256
GELO	PHEN	0.32451
RESIN	INERT	0.32093
GELO	CUTIN	0.15502
ALGIN	SPORE	0.21974
ALGIN	RESIN	0.02239
GELO	ALGIN	-0.05663
TELO	GELO	-0.22662